Cold nuclear fusion reactor

And new modern physics

Huang Zhenqiang Huang Yuxiang

Modern physics classical particle quantization Orbital motion model general solution

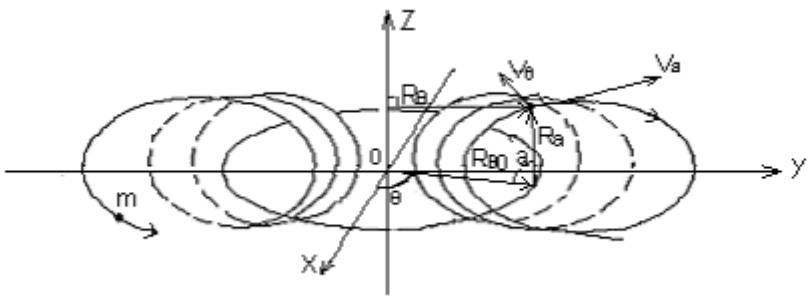

($X^2 + Y^2 = R_{\theta 0}^2$ Is round question)

$$\begin{cases} \vec{R}_\alpha \times m\vec{v}_\alpha = \dfrac{\vec{h}}{2\pi} \quad (\dfrac{\vec{h}}{2\pi} \text{Is moment of momentum wave vector}) & (1.2-1) \\ \vec{R}_\theta \times m\vec{v}_\theta = \dfrac{\vec{h}}{2\pi} & (1.2-2) \\ \vec{R}_\theta = \vec{R}_{\theta 0} - \vec{R}_\alpha \cos\alpha & (1.2-3) \\ \alpha = N_\alpha \theta & (1.2-4) \\ \dfrac{\oint \vec{R}_\theta d\theta}{\vec{v}_\theta} = \dfrac{N_\alpha \int_0^{2\pi} \vec{R}_\alpha d\alpha}{\vec{v}_\alpha} & (1.2-5) \end{cases}$$

January 2005 in Fuzhou, China

Book summary

The mainstream of modern physics research status

Nearly 100 years to the birth of quantum physics, relativity and cosmic physics, has become the three pillars of Building propped modern physics. However, the international mainstream of modern physics research areas, there are still many aspects of the scientific community a hundred years to trying to explore not be resolved, they have to face the problem, such as:

1.Why decades in collision experiments in high-energy particle accelerators ejected freedom of all debris particles, all particles to split the decay of the whole process all transitional product particles, including the final stable protons, electrons, neutrinos, photons, not electrically neutral , is only charged particles with a unit?

2. What is the elementary particles basic composition unit? Why 36 of the so-called mixed fraction charge "quark" (including antiparticles) turned out to be all incarcerated? If it does exist, then the confinement of the reasons is it? Why infinitesimal point charges have been no energy "divergence"?

3. Why all the microscopic particles have wave-particle duality? So far, we still do not know the laws of their formation principles and specific sports! Why nuclear energy is $E = mc^2$? What causes within the nucleus and the quality of all the particles missing?

4. Why the proton, neutron, electron, and hundreds of nuclei prime fixed rest mass, magnetic moment value and the corresponding electromagnetic field spatial distribution of range? How their energy, magnetic moment is formed? How accurate calculation?

5. Why protons, neutrons, there are strong, weak, electrical, magnetic interactions within all of the elementary particles and nuclei? What is the relationship between? How each interaction forming principle? How accurate calculation of strength?

6. Why natural radioactive series starting nuclear ${}^{232}_{90}Th$、${}^{235}_{92}U$、${}^{238}_{92}U$, and the total number of nucleons are close to 234? Why that has synthetic nuclear charge number 114 heavy nuclei is still very unstable? What causes nuclides stable island prophecy fails? Why the end of nuclear stability is that ${}^{206}_{82}Pb$、${}^{207}_{82}Pb$、${}^{208}_{82}Pb$? Why that nuclear in the face of high energy fast neutron was actually completely "transparent"? Inside them in the end was what kind of structure?

7. Why nuclei emit electrons $\beta^{\pm}$ and rays γ ? They originally existed within the nucleus? Or later transformed form? How they are transformed? How to calculate their energy spectrum, intensity?

8. Why electrons in atomic surface will form a so-called "S, P, D, F type electron cloud"? Characteristics of each electron in the electron cloud movement, how the law? How accurate calculation of electronic excitation transition spectroscopy (especially surface multi-electron atom)? If the electron is indeed based on the probability of the state distribution, how to interpret the fixed orbital moment and emission and absorption spectra level?

9. How to analyze the energy calculation of heavy atoms lining K L layer many characteristics of the movement of electrons and X fluorescence-ray spectrum?

10. Why is there the 2.73K microwave blackbody background radiation in the universe? It is what? The photons are electrically neutral particles, why the characteristics of electromagnetic waves? Why is the speed of light c exactly 299792458m/s? What relationship exists between them? Why thermodynamics experiment to get ultra-low temperature of 0.0K is quite difficult?

11. Since the larger mass of the neutron star is bound to lead to gravitational collapse to form a black hole, the black hole shrinks gravitational collapse will inevitably lead to the gravitational potential energy tends to infinity, is the black hole mass is bound tends to infinity. This will inevitably lead to the gravitational field strength; gravitational sphere of "divergence" phenomenon tends to infinity. Why we found all galaxies within the central galactic nuclei have a great mass of the black hole, but have never seen the quality and strength of the gravitational field, the gravitational sphere "divergence" phenomenon?

12. Since we already know that all galaxies are large nebula contraction. Well, from the cosmic hot big bang full expansion diffusion to form thin large nebula to nebula to split the process of contraction as the galaxy density and gravitational force, should the changes? Why some form elliptical galaxies, some form spiral galaxy and some formation of barred spiral-shaped galaxy? How the spiral arms of the galaxy formation and evolution? These galaxies in formation the process of evolution, is gradually shrinking? Or gradually spread?

13. Now mainstream astronomical community unanimously found that the age of the universe is 13.7 billion years old. The age of stellar age, ancient globular cluster

surface stellar age, the age of the galactic nuclei of the central black hole, or the entire galaxy age how to contact? Accounted for more than 90% of the dark matter in the universe, dark energy in the end is what? They count as a principal member of the universe? How is more than 90% of dark matter, dark energy ages?

14. Universe really is expanding it? Universe really is formed by a hot big bang? If true, then the so-called mathematical singularity before the Big Bang is what? How it is formed? A second before the Big Bang excitation mechanism, what is it?

15. Is how the formation of ultra-high energy r-ray burst in the depths of the universe? The ultra-high-energy proton beam is formed? The so-called strength and size observed in recent years after the Big Bang creation of the universe and how it formed?

16. Why quasars have the unthinkably large energy radiation? Within it should have what kind of structure? Part quasars exceptional value red shift in the end is what causes it? All celestial spectral red shift ， is Doppler red shifts?

17. How to solve the relativity twin paradox, clock problems between different time and space? Newton's absolute time and space and what relationship exists between Einstein's relative time and space? Light bending phenomenon, should understand the role of the gravitation field to track the movement of the photon bending it? Or the so-called space curved?

18. The gravitation is how it formed? The graviton, dark matter and dark energy in the end are what? Is what causes the solar neutrino missing? Internal neutrino was what structural features? How did they constitute all other elementary particles?

19. All the basic laws of physics in quantum physics, cosmology and physics and the theory of relativity between how unified? The role of the strong, weak, electrical, magnetic interactions of gravitational force between modern physics and classical physics is how unified? Modern physics and all the basic physical laws of classical physics, how unified? ……。

The 19 aspects of the problem, basically outlines the main challenges facing the international mainstream of modern physics community and the current research. One out by taxpayers spent heavily dependent, as the core foundation of natural science theory doctrine, but still there are so many contradictory nature of the problem, at least that it was still in the exploratory stage hypothesis. Thus not only lead to a large number of non-mainstream scholars questioned and re-discover, even sober sense of

social responsibility and conscience mainstream scholars are waiting to look forward to the advent of new doctrine. So the trend of the times, the scientific community there is any reason to continue to adhere to the "one-man" does not allow the new doctrine?

The new research progress of modern physics

The author of his life admired Einstein, convinced that he stubbornly adhere to the orbital theory of quantum physics is. According to the author of an intuitive understanding of the physics, thereby establishing a set of classical particle fluctuations, spin along the vertical double elliptical orbit movement model equations (see the cover of the particles along the orbital motion of the models and equations). Newtonian mechanics, classical electrodynamics, the Track of quantum mechanics and particle energy relativistic combination that can solve the issues of the universality of classical physics, but also the system to accurately solve all above the mainstream of modern physics faces 19 problems. After 14 years of hard work, repeated algorithmic verification, and finally completed modern physics classical particle the quantum orbital motion model general solution monographs, referred to as "the new modern physics. Manuscript sub-particle physics, nuclear physics, atomic physics, the infinite eternal cosmology and the time and space relativistic questioned five parts and 29 chapters, about 0.4 million words. Points are as follows:

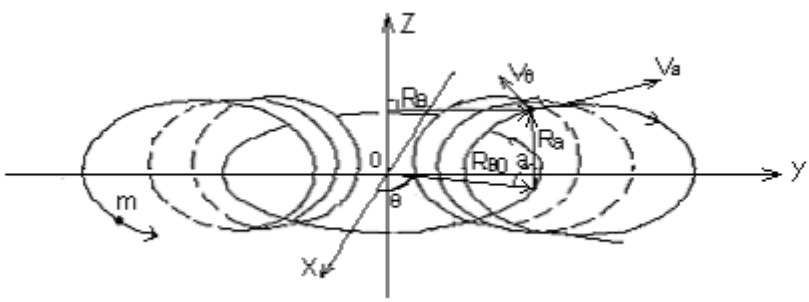

$$(X^2 + Y^2 = R_{\theta 0}^2 \text{ Is round question})$$

Figure 1.1 still elementary particle fluctuations, spin vertical double oval track movement diagram

1. Has established the macro still elementary particles orbital motion model, as shown in Figure 1.1, equations (1.2). Only the introduction of two quantum numbers N_a N_θ (N_a fluctuations orbital quantum number used in particle physics and nuclear physics; N_θ spin orbital quantum number, only used atomic physics), elementary particle fluctuations deduced The spin quantum steady state vertical double elliptical

orbit motion model, see equation (1.3). Fluctuations, spin, when the macro still elementary particles accelerated by foreign energy, it is converted into a combination of orbital precession cylindrical helix, as shown in Figure 1.2.

$$\begin{cases} \vec{R}_\alpha \times m\vec{v}_\alpha = \dfrac{\vec{h}}{2\pi} \quad (\dfrac{\vec{h}}{2\pi} \text{Is moment of momentum wave vector}) & (1.2-1) \\ \vec{R}_\theta \times m\vec{v}_\theta = \dfrac{\vec{h}}{2\pi} & (1.2-2) \\ \vec{R}_\theta = \vec{R}_{\theta 0} - \vec{R}_\alpha \cos\alpha & (1.2-3) \\ \alpha = N_\alpha \theta & (1.2-4) \\ \dfrac{\oint \vec{R}_\theta d\theta}{\vec{v}_\theta} = \dfrac{N_\alpha \int_0^{2\pi} \vec{R}_\alpha d\alpha}{\vec{v}_\alpha} & (1.2-5) \end{cases}$$

$$\begin{cases} \vec{R}_\alpha = \dfrac{\vec{R}_{\theta 0} E_{\alpha\theta}}{1 + E_{\alpha\theta} \cos\alpha} & (1.3-1) \\ \vec{R}_\theta = \dfrac{\vec{R}_{\theta 0}}{1 + E_{\alpha\theta} \cos\alpha} \qquad (E_{\alpha\theta} = \dfrac{\vec{v}_\theta}{\vec{v}_\alpha} = \dfrac{1}{\sqrt{N_\alpha}}) & (1.3-2) \end{cases}$$

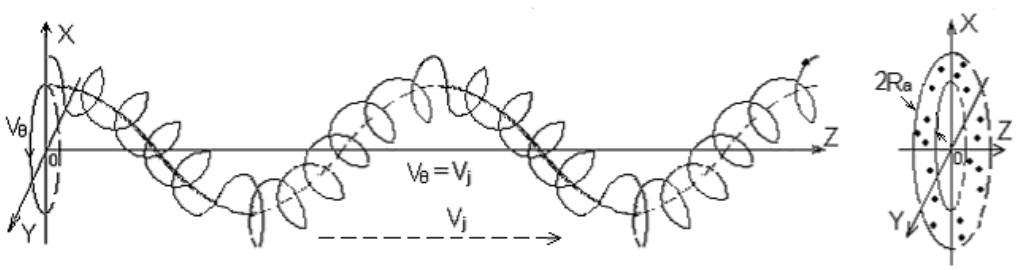

Figure 1.2 elementary particles along fluctuations, the spin precession of the orbital motion characteristics of the formation of wave-particle duality diagram

2. The crash test data based on decades of high-energy particle accelerator, the model system to validate the calculation, that form the most basic unit of all elementary particles with a unit of electricity charged particles. Load of electric particles composed of electric dipole; electrically neutral particles by n electric dipole, different particle n is a natural number; charged particles only bring to charged particles.

Classical Newtonian mechanics, electrodynamics, energy theory of relativity (Einstein's theory of relativity in the high-speed movement of particles of energy, charged particles electric, magnetic field strength and movement speed relation) introduced into the model, export the fine-structure constant; prove elementary particle

energy fluctuations in the direction of motion of charged electromagnetic field energy particle aggregates formed nearly the speed of light c sports; internal, weak, electrical, magnetic interactions are electromagnetic field interactions; deduced particle separatist, the average life expectancy in the decay process with the electromagnetic field radiation $W_{e\|i}$, relationship, see (4.13); projections of the internal structure of protons, neutrons instance is shown in Figure 6.5, table 6.2.

$$W_{e\|i}\overline{T} = \frac{h}{8}\left(1+\frac{2.16}{N_{\alpha i}}+\frac{3.35}{N_{\alpha i}^2}\right) \qquad (4.13)$$

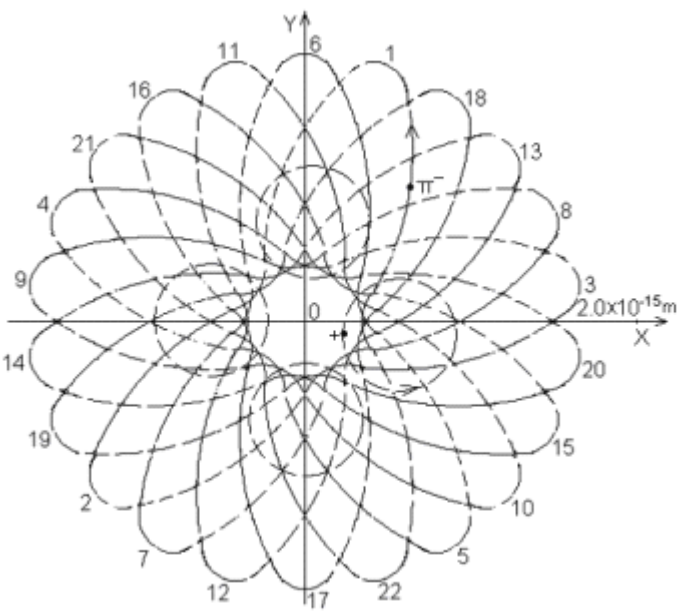

Fluctuations of the Figure 6.5 neutrons internal two electrically charged elementary particles spin motion track In XOY plane projection diagram

Points 1 to 2, can solve the aspects puzzle of the above 1 to 5.

3. By the model of Figure 1.1, the "dismantling" of protons, neutrons within nuclei into high-, low-energy meson. A certain number, fluctuating quantum number, the same energy, low energy meson composed of a pair of particles spiral ring, the composition of the particles spiral ring track the nucleus internal structure of Figure 7.2, as shown in Figure 11.4 determine the nuclear force is the nuclear field force and the track at the point of tangency with the ampere force between the magnetic field to track current element. Each high and low energy particles spiral ring and lateral orbital nuclear force at the point of tangency accurate calculation of the examples of results are shown in Table 11.3.

The neutron internal structure parameter simulation results exemplar 6.2

Analog value	N_{a2}=2	N_{a2}=12/5	N_{a2}=22/9	N_{a2}= 5/2	N_{a2}=3
Parameters and use number of the formula	$m_{\pi 2}\times10^{-28}$ Kg				
	6.632975	6.247308	6.215628	6.178265	5.924168
β_2 (4.9)	0.9990883	0.99901523	0.99900886	0.9990013	0.9989473
$m_1\times10^{-28}$ Kg (6.1)	10.116311	10.501978	10.533658	10.571021	10.825118
$R_{\theta 20}\times10^{-15}$m (1.6)	0.530816	0.666891	0.680851	0.698022	0.840622
$R_{\theta 2(0)}\times10^{-15}$m (6.2-1)	0.310945	0.405282	0.415254	0.427590	0.532933
$R_{\theta 2(\pi)}\times10^{-15}$m (6.2-2)	1.812317	1.881201	1.889164	1.899149	1.988934
$R_{a1}\times10^{-15}$m (1.2-1)	0.348172	0.335386	0.334377	0.333195	0.325374
$U_n\times10^{-26}$J/ T (6.12)	-0.966114	-0.9661144	-0.9661136	-0.966114	-0.9661143

Note: m_1 to the core particle mass, β_2 coefficient for π^- meson fluctuations in the direction of movement of the speed of light c, U_n neutron magnetic moment.

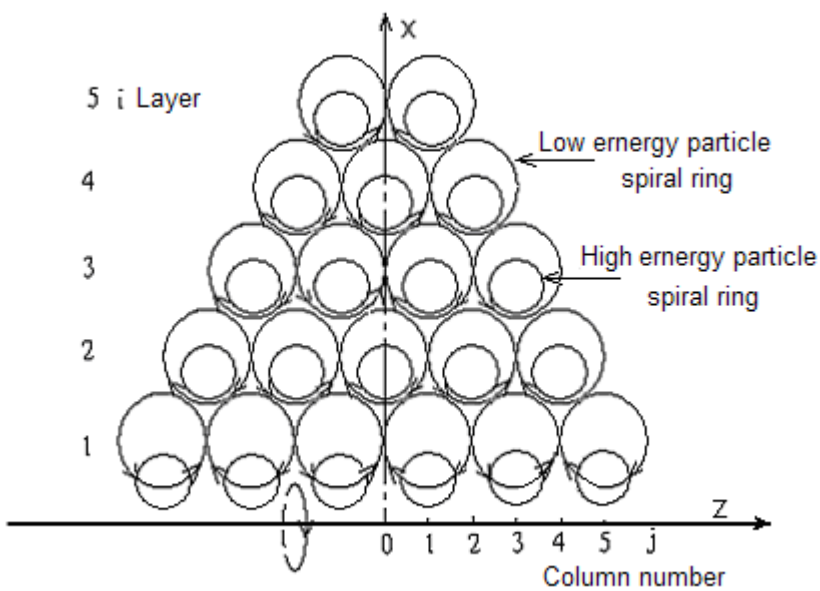

Figure 7.2 B nuclei internal low energy particles spiral ring combination schematic cross sectional view

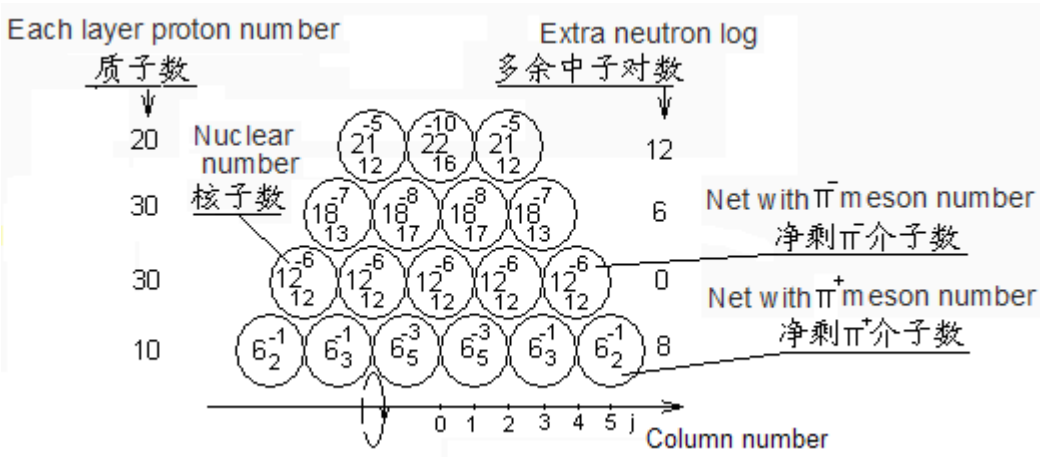

Figure 11.4 $^{232}_{90}Th$ nucleus kernel sub、net surplus $\pi^{\pm}$ meson assigned to schematic diagram

$$\underset{10}{Va}\ \underset{-6}{\overset{10}{Vb}}\ \underset{6}{\overset{4}{Vc}}\ \underset{-2}{\overset{10}{Vd}}\ \underset{12}{\overset{8}{Ve}}\ \underset{-6}{\overset{20}{Vf}}\ \underset{4}{\overset{14}{Vg}}\ \underset{24}{\overset{18}{Vh}}\ \underset{-2}{\overset{42}{Vi}}\ \underset{-12}{\overset{40}{Vj}}\ \underset{24}{\overset{28}{Vk}}\ \underset{34}{\overset{52}{Vl}}$$

$$\underset{-12}{\overset{86}{Vm}}\ \underset{-16}{\overset{74}{Vn}}\ \underset{26}{\overset{58}{Vo}}\ \underset{-14}{\overset{84}{Vp}}\ \underset{16}{\overset{70}{Vq}}\ \underset{24}{\overset{86}{Vr}}\ \underset{-10}{\overset{110}{Vs}}\ \underset{-10}{\overset{100}{Vt}}$$

$$W_e = 1.817530386\times10^{-27}\,Kg,\ldots W_b = 1.437800649\times10^{-29}\,Kg$$

$$\sum {}^{232}_{90}ThW_1 = 3.85240599\times10^{-25}\,Kg$$

Note: Figure 11.4, the figures of the middle of the ring is the total number of nucleons in the particles spiral ring, the superscript negative value is left π⁻meson number of low-energy particles spiral ring net subscript value is high-energy particles spiral ring net the left π^+ meson number. Nuclear power, magnetic energy, the total energy calculated on the left.

By the model to expand export within the nucleus the β± electronics ray, γ ray $\pi^{\pm}$ meson split decay, each high and low energy particles spiral ring orbit between meson position adjustments, causing the entire nucleus the excess electromagnetic field energy release due. Classical electrodynamics, energy relativistic energy equations, each level of the different nuclei beam electron ray β±, γ ray energy, adjusts the position computing for accurate simulation.

The points can solve the problem of the foregoing the 5 to 7.

4. The Figure 1.1, Figure 1.2 model extended to atomic physics, by the combined effects of the nucleus of the repulsive force of the electric field between the attractiveness of the electric field of the electron and electronic export the surface various electronics around the nuclear spin, additional rotational ellipsoid track surface motions "s, p, d, f" electron cloud of the overall model, as shown in Figure 18.2, Figure

18.6. Based on the experimental determination of an atomic energy level variation, you can export the electronic orbital motion equations. To combined with the electric field energy equations, accurate simulation of the atoms of each of the various electronic orbital parameters and energy levels.

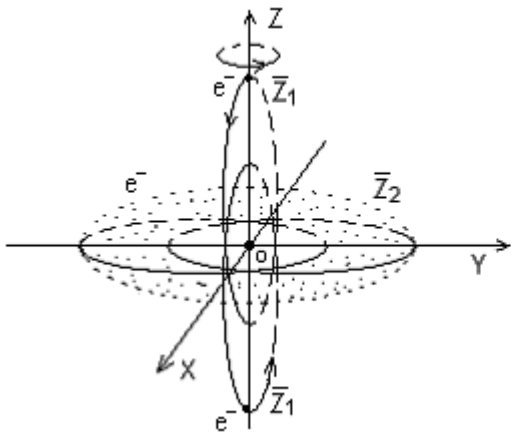

Figure 18.2 atomic surface 3 electron electron cloud" to form a schematic diagram

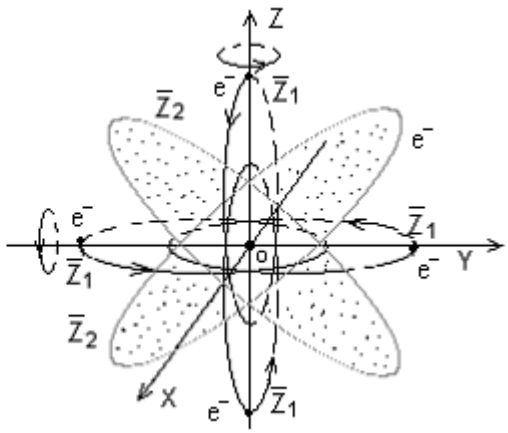

Figure 18.6 atomic surface 5 "s+p-type "s+p-type electron cloud" to form a schematic diagram

$^{232}_{90}Th$ Nucleus kernel force balance validate the calculation results table (Figure 11.4, unit: Newton) Table 11.3

J / N_a	1	2	3	4	5	Nuclear magnetic force accumulated
58 $F_{e\theta}$		t.769.3464576				65.54948748
$F_{b\theta}$		-742.46066				
34 $F_{e\theta}$	n.935.7967665		p.1242.139919			38.66368988
$F_{b\theta}$	-1222.642838		-1069.812483			
16 $F_{e\theta}$		j.1177.523759		m.332.5403438		-133.663746
$F_{b\theta}$		-943.7382432		-943.7382432		
$F_{e\theta}$	b.474.7645659		d.360.3313781		i.-30.5202085	243.7486375
34/13 $F_{b\theta}$	128.3900218		-42.79667394		-14.26555798	
$\Delta F_{\theta b}$	107.2499555		-153.2142222		-114.9106666	

Note: Table 11.3 $F_{e\theta}$ for every high, low energy particles spiral ring spin the axial nuclear field force, $F_{b\theta}$ for side-by-side low energy particles spiral ring orbit tangent point at the current element magnetic field Ampere force, $\Delta F_{\theta b}$ side by side, the two pairs of particles spiral ring. The track overall current between the magnetic field force.

n-bar position spiral ring on excess magnetic forces on the lower outside of space mosaic restricting, so I do not participate in the nuclear force balance accumulated.

The combined energy theory of relativity, the points can solve the aforementioned 8 to 9 aspect problems.

5. Figure 4.2 elementary particle wave-particle duality model confirm photons, neutrinos are composed only by a pair of electric dipole motion orbits are cylindrical helix, as shown in Figure 2.4. The difference between the two is the electric dipole around fluctuations N_γ N_v the precession orbit rotation frequency photons N_γ=1 the neutrinos 343323≥Nv≥5991. Thermodynamic energy relativistic introduce the model of Figure 2.4, export 2.73K blackbody microwave background radiation field in space of the universe is the neutrino venue neutrino average energy $\overline{W}_v$:

$$\overline{W}_v = 1.5KT = 5.653794510 \times 10^{-23} J = 6.290694778 \times 10^{-40} Kg \quad (5.1)$$

Bohr Tsz Man (wherein K is a constant)

High frequency electromagnetic field can be part of the neutrino in the neutrino field excitation photon, the photon energy loss to close neutrino background field energy into neutrinos. Exported by the laws of thermodynamics neutrino propagation longitudinal wave speed vj coincides with the speed of light c, thus proving that the electromagnetic waves such as sound waves as longitudinal waves, not transverse wave!

$$v_j = \sqrt{\frac{1.5RT}{u}} = 299792436 \text{ m/s} \quad (c=299792458 \text{ m/s !}) \quad (5.4)$$

(Wherein 1.5 is the adiabatic exponent of the gas molecules, R is the universal gas constant, u neutrino field atoms).

By the model and the calculation results based on the total energy conservation law, inferences 2.73K blackbody microwave background radiation in the universe, space must be the long-term energy consumption in from After all frequency spectrum trace absorption of the supplement in order to maintain balance; spectrum in which the long-distance spread because the energy has been trace loss will inevitably lead to the red shift. With Olbeth paradox simultaneous, overall as a unlimited eternal universe on key basis. Derived by the Hubble constant Ho, the spectral red shift $\sum K_{zi}$ with propagation distance R relation (22.10):

$$R = \sum K_{zi} \Big/ H_0 \qquad \begin{pmatrix} It \cdot will \cdot be \cdot the \cdot field \cdot of \cdot astronomy \\ a \cdot rare \cdot precise \cdot range \cdot ruler \end{pmatrix} \qquad (22.10)$$

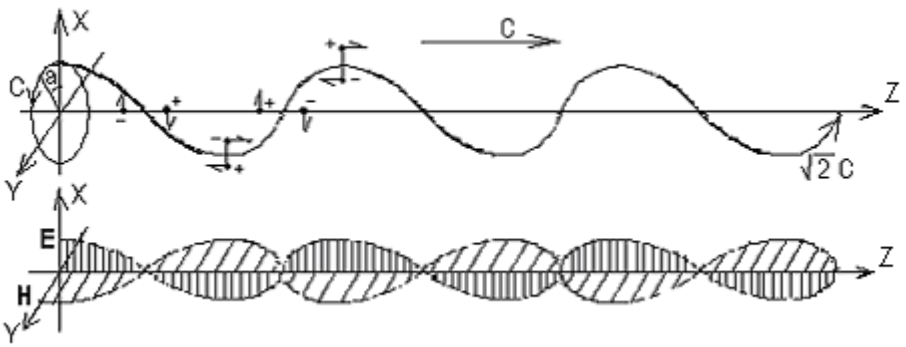

Figure 2.4 photons along fluctuations precession of the orbital motion of the medium wave-particle duality and electromagnetic waves forming principle schematic diagram

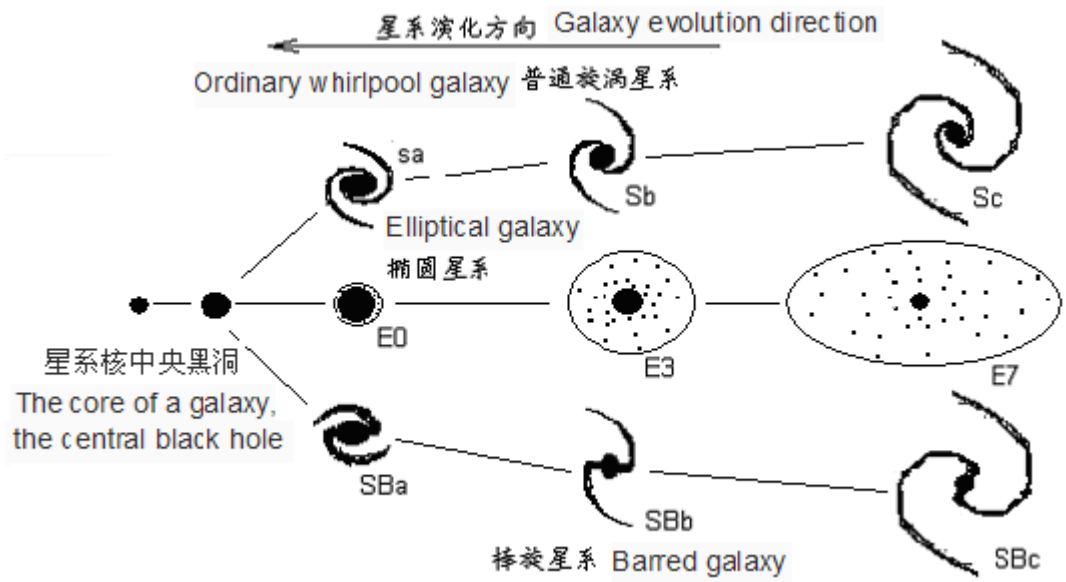

Figure 26.1 galaxy Hubble classification, evolution direction diagram

6. Inferences the Ming substances optical galaxy evolution is gradual contraction by the observed characteristics of different types of galaxy evolution, according to the law of gravity and the viral theorem, see Figure 26.1, and thus determine the stellar accounted for more than 90% of the dark matter in the universe have died globular clusters, galaxies, and even the wreckage of the entire group of galaxies. According to Figure 7.2, the nuclei of the internal structure of the model of Figure 11.4, the design inside the massive black hole were stable the neutron matter ring structure can be shown in Figure 24.5, thus avoiding the gravitational collapse led to the energy, the

strength of the gravitational field, the gravitational sphere of influence trends form a "singularity" at infinity "divergence" problem. And thus achieve a balance in the black hole the internal gravitation and strong, weak, electrical, magnetic interaction between grand unified.

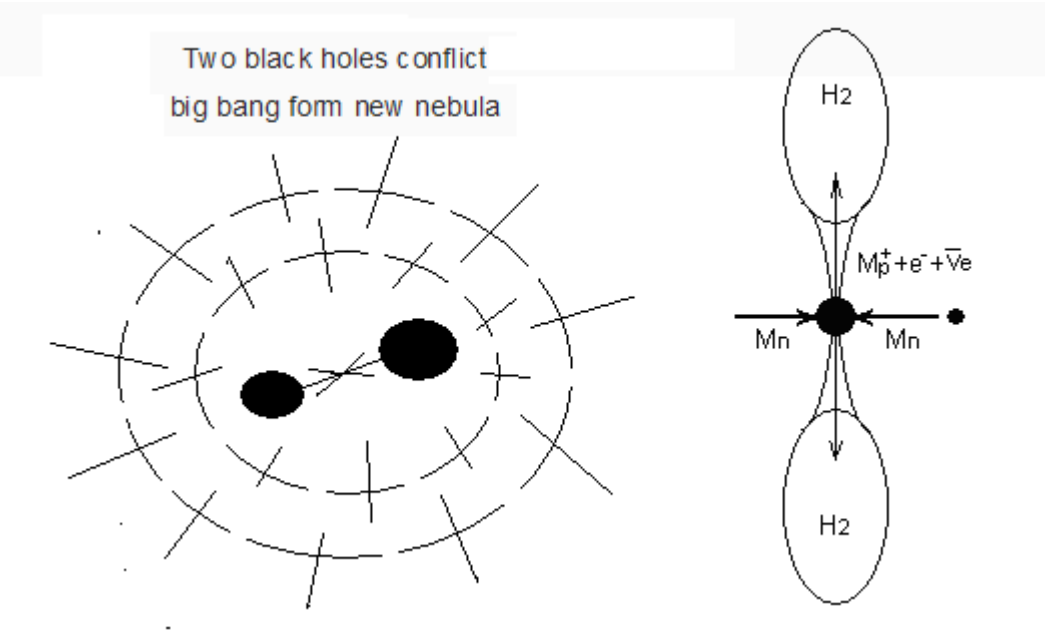

Figure 26.3 Two black holes conflict big bang form new nebula and Devour process polar axis radio nebula group forming principle diagram

7. When two black holes are near to each other in their respective field of gravitation winding movement due to phagocytes neutron can turn to the polar jet formation newborn nebula, and the emergence of symmetrical compact source of radio lobes, as shown in Figure 26.3. When the two qualities close to the black hole collision, will undermine the stability of the ring structure of neutron matter will be thoroughly large explosion, can be completely converted to form a large group of freshmen nebula.

8. All globular clusters and galaxies we have observed, on the basis of the original material, the original role of universal gravitation field through the newborn nebulae along the track-by-phase adsorption newborn nebula to grow and develop. Therefore, the cosmological constant term in Einstein's equations, must maintain the dynamic gravitational equilibrium of galaxy clusters that dark matter overall average density is infinite and eternal universe model.

9. The extraordinary value of the energy of the quasar radiation and spectral the

extraordinary value red shift, indeed the so the cosmic hot Big Bang Theory overwhelmed. Chapter 27 in the use of the black hole to suck the energy release of the accretion disk light pressure on the peripheral fullerene stellar black holes clouds bracketing principle the design the quasars internal structure model, spectrum extraordinary value red shift caused by gravitation places.

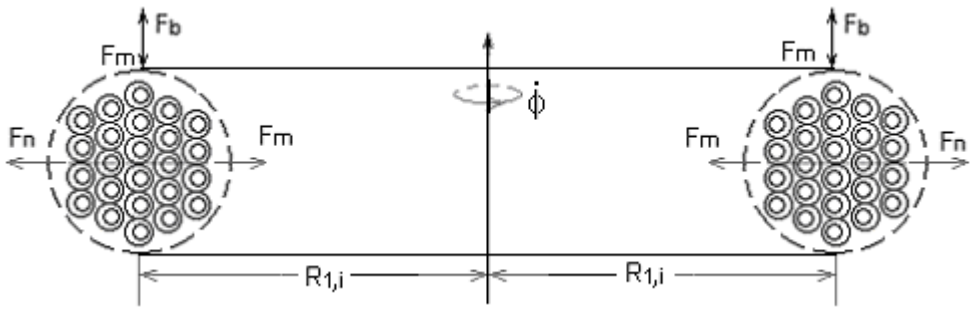

Figure 24.5 massive black hole internal neutron matter ring structure and gravitational F_m, the centrifugal force of the F_n nuclear force F_b balance diagram

Points 5 to 8, and can solve the aforementioned 10 to 16 regard problems.

10. By the wave-particle duality of the photon and the energy equation, Newtonian mechanics can also prove: photon as a particle grazed the surface of the sun from a distance, in the gravitation field effect, the precession of the orbit bending angle is 1.75//! Means to determine the relative space in the relativistic high-speed movement of the object relative the relative space in the moving direction of the neutrino; relative time is defined as electromagnetic waves in the direction of movement of the relative speed of light through the high-speed moving objects relative neutrino field required when spatial propagation relative time. The relative space and time is only on the fast moving objects have any meaning. Absolute spatial location coordinates to determine when the object began to accelerate from a standstill, the final deceleration to stationary; it corresponds to the relative space and time, is Newton's infinite, eternal cosmology and unified eternal time. By the spectral Doppler frequency shift effect, and further demonstrated the so-called relative spatial spectral frequency shift change the direction of the track along the precession wavelength; relative time is the speed of light through the spectral frequency shift change when the wavelength of the direction of the track along the precession required time. The argument inference: the gravitation field of light bending is the photon orbit precession bending, rather than the so-called space bending!

11. Based on the neutrino energy shock exists fact, demonstrated the principle of

the neutrino form a quantum gravitational field. For solar neutrino disappearance deduced neutrino energy density. Further inference is dark matter, neutrino lucky enough to answer with a simple and intuitive physical model, including four graviton and dark matter problem.

Element 9 to 11, and can be systematically solve the aforementioned 17-19 aspects puzzle.

In summary, the manuscript by the classical Newtonian mechanics, electrodynamics, thermodynamics, energy relativistic astronomy and particle physics, nuclear physics, atomic physics eight interdisciplinary basic, has been completely conclusive evolution of the classical laws of physics too. The book established the orbital theory of quantum physics and the infinite eternal universe theory model proved weak interaction is electric, magnetic field interactions; demonstrated in the field of Macrocosm the gravitation field dominated nebulae, galaxies and dark matter in the microscopic field loop transformation between the Ming, dark matter and states of matter by the electromagnetic field; final analysis, determine the relativistic relative space and time relationship with Newton's absolute space and time; the final settlement gravitation forming principle and the mystery of dark matter. System to solve the problem of the 19 aspects; raise the overall three disciplines to accurately calculate the level of the orbital parameters; complete micro, macro, and the Macrocosm field between strong and weak, electricity, magnetic interactions and the role of gravity unified to achieve the grand unification of all the basic physical laws of classical physics and modern physics.

Fluctuations spin motion detection and detection of particles. the existing experimental detection level, the scientific community of the particle, nuclear, atomic energy, magnetic moments, electromagnetic energy radiation understand in more detail. Nuclei atoms and nuclei outer electron cloud "shape, size also have a certain understanding. However, the overall composition of the two and more than two hundreds proton, neutron and electron atomic systems, analysis calculated the specific orbital motion characteristics of each particle and many other relevant parameters, due to the complexity of the mutual influence of various parameters, and simply can not do；estimated that difficult to do in the future for a long time. Because of this, the reader's attention, the book is different from the conventional quantum mechanics research methods, the overall research program are as follows:

1. Start with the most simple of electrons, photons, neutrinos fluctuations,

spin-orbit motion feature to start exporting all particles follow fluctuations, spin quantum steady state vertical double oval or circular helix orbital motion equations.

2. Reveal the internal structure of elementary particles, momentum, moment of momentum, energy forming principle; strong, weak, power, the magnetic interactions unity principles and related orbital parameters calculation method.

3. Combined with each other between two or more elementary particles vertical double elliptical motion orbit on the space, and the formation of a large number of elementary particles, protons, neutrons, nuclei and atoms of the orbital motion of the electrons in a combination of the overall model.

4. Each particle fluctuations, quantum between the spin-orbit motion cycle of multiples N_a N_θ and many other parameters, the correlation, export particle momentum equations of each respective elliptical orbit, the moment of momentum, electric, magnetic field strength, the electromagnetic field energy and the original fluctuation energy, particle velocity, elliptical orbit eccentricity, radius parameters all quantum numbers N_a N_θ related.

5. Finally, the N_a, N_θ is a natural number, or a simple fraction to simulation. The final calculated particle energy, momentum, moment of momentum, magnetic moment, the radiation characteristics of electromagnetic energy, electricity, magnetic field strength of the spatial distribution of the particles and atomic nuclei within the strong, weak, electrical, magnetic interaction strength, the morphology of the particles, nuclei, atoms the size of the outer nuclear layer of "electron cloud" shape, size, all consistent with the experimentally determined value.

Thus proving that has the overall success of the model in the field of quantum physics.

The track on the success of the model theory of quantum physics, the basis of theoretical support for the study of the physics of the universe. Looking at the Modern Astrophysics development history, whether the medium of propagation of electromagnetic waves "Ethernet" really exist directly around the scientific community of the spectral red shift reason, Hubble's law and Lobbers paradox explained. Only found 2.73K blackbody microwave background radiation in the universe, I demonstrated in Chapter 5, 21 to 22 2.73K blackbody microwave background radiation is caused by the neutrino, the neutrino is the propagation of electromagnetic waves "Ethernet field the electromagnetic waves are longitudinal wave spectral red shift,

Lobbers paradox and 2.73K blackbody background microwave radiation, the law of conservation of total energy photons trip overall argument for infinitely eternal cosmological key basis. The formation and evolution of stars, galaxies, the infinitely eternal cosmological model, trend, and determine the entire galaxy formation in the neonatal nebulae complemented the process of evolution is gradual contraction. Inferred that the uneven distribution of the universe, and accounted for more than 90% of the dark matter is the death of stars, galaxies, and even the wreckage of the entire group of galaxies. Be resolved according to the orbital theory of quantum physics point charge energy "divergence" of experience, the author designed a huge black hole of galactic nuclei Center internal the Global hollow structure of neutron matter, successfully overcome the gravitational collapse, the total energy of the gravitational field strength of the gravitational sphere of influence tends to infinity "divergence" difficult. The black hole by attracting outside dark matter collisions Big Bang, or turn to the polar injection process in the accretion disk, the successful completion of the dark matter into the prescribed substance nebula cycle process; successfully resolved quasars internal structure, energy radiation mechanisms and spectral extraordinary value of the red shift of the problem, so infinitely eternal cosmological model to be fully demonstrated. Further demon started that the relationship of Newton's absolute space and time and the Einstein relative space and time.

Finally, in the interior of a black hole structure and force analysis, simulation, so as to realize the neutrino field as medium, in microscopic and macroscopic and space in the field of view of strong, weak, electrical, magnetic and gravitational interaction effect between the unified field balance grand unified. The results indicated: classical physics and modern physics as overall comprehensive study has been to achieve unity and success.

So, even though the book has more than one high-order equation, implicit function, irrational numbers, equations, a large number of the original function of integral equations can not be obtained directly. We can use a modern high-performance calculator; many equations compiled continuous calculation procedures, different N_a N_θ values into the simulation solving. As long as the reader has Newton's mechanics, electrodynamics, thermodynamics, energy relativistic quantum mechanics, astronomy and calculus basics, it like the physical model is simple and intuitive, logical and mathematical calculation to learn popular science books alone a high-performance calculator can whole book to read and review. Similarly, if the book was adapted into ordinary physics textbooks for high schools and institutions of higher

education, it will be for the benefit of society and the entire human immeasurable merit.

The reader is advised to read the audit book before reading and thinking seriously Introduction and summary. It will help you overcome School prejudice, and make it easy for you to master the quantum model of the orbital motion of the classical particle of modern physics, the general solution of the basic physical conceptual model and practical knowledge of the system. To explored and promote the future of mankind a new era of science and civilization.

Published cold nuclear fusion reactor and the meaning of the new modern physics

This book reveals the universe, space, and all of the basic law of motion of celestial things and a variety of material elements from visible optical galaxy Ming substances, into the dark matter of the circular ring of black holes, the spray injection electricity from the polar axis of the black hole or the collision of black holes thorough the Big Bang, and the formation of the elements of the Ming substances nebula phase transition reincarnation evolution of the whole process of the objective laws of physics, for mankind modern and future of the many applications of science and technology engineering areas of innovation, the quantum to classical orbits expressed in mathematical physics equations, the precise analysis of the theoretical basis for the calculation of the relevant parameters of all particles, nuclei, atoms and molecules. Book chapters 15 to 20 atomic physics part, derived atomic surface electron orbital motion law model and the corresponding mathematical physics equations, if appropriate expand, will be able to directly and accurately analyze the chemical bond between the calculation of atomic and molecular relevant parameters. Thus eliminating the need to reverse estimates rely on a large number of the cumbersome experimental determination data, trouble chemically related parameters. The book theoretical system, in the research areas of biology, chemistry, nonsocial materials science, electronics and information science, aviation and astronautics and many applications of science and technology innovation to it as the core foundation of theoretical and analytical calculations based on have a multiplier effect.

That thank God for many years frequently on the author's special care given to the author "the cold nuclear force constraints inertial guidance nuclear direct hit fusion reactor and ion speed dc transformer" subject (the subject has applied for national defense patent). Present invention patents referred to as "cold fusion reactor" core

basic theory from book 1 to 14 of Chapter particles and nuclei internal strong, weak, and the principle of the unity of the interaction of the electric and magnetic. Wherein: set the specific combination of the electromagnetic field of the space in the room temperature within the vacuum duct, linear from 0.6 to 1 million volts electrostatic particle accelerator according to the intrinsic magnetic moment and the internal electric field of the light nuclei, the first jet out of the bunches to be fusion of light nuclei constraints with a segment of the "pipeline"; recycling light nuclei intrinsic spin moment of momentum vector formed near the speed of light spin characteristics of super-strong rotation gyro inertial guidance, to overcome the bias of the Coulomb strong barrier repulsion, active guidance aimed at directly hit fusion. The biggest advantage of this device is lightweight structure, the process is simple, easy to manufacture, reliable and stable operation. Existing manufacturing large generators, high-voltage transmission grid system equipment's ability to be competent, and you can use as an aircraft or spacecraft engine power.

Fusion of through this atomic nucleus of, access to safe, clean and environmentally friendly, inexhaustible, huge nuclear energy! Completely eliminate the carbon dioxide emissions of the greenhouse gas! So that once and for all, completely solve the energy and environmental problems of our country still face to all mankind! Will human from the current earth science in the age of cradle of civilization, and promote the future space science in the age of the universe civilization!

All the basic theory of natural science research, services are to advance the science of mankind civilization. Practice is the sole criterion for testing truth. I believe that in the next three to five years, if the author is able to complete the support of the relevant departments of the state and people of insight in their "nuclear force constraints the cold nuclear inertial guidance direct collision of the fusion reactor and ion speed dc transformer" This experiment the research topics of modern physics community at home and abroad quantum model of the orbital motion of the classical particle of modern physics is the general solution of the set of physical models and theoretical system should eventually will understand and accept.

The research results at one's own expenses "cold fusion reactor and new modern physics published, they show that the mainstream of

nuclear fusion reactor engineering circles and modern physics circles of subsequent research has no meaning. If will continue to adhere to the school's point of view, will be spent all his life and tax payers a lot after the hard-earned money nothing. Such as dozens of years searching for quark, dark matter particles, graviton and Higgs boson are missing. Dozens of years all the nuclear fusion research, including the ITER international cooperation research progress is slow, hope is frail. Continue will increase historic jokes, in the face of the tax payers and severity of later generations' question, please let your careful consideration.

Authors: Huang Zhenqiang Huang Yuxiang

January 2005 in Fuzhou, China

Table of Contents

Particle Physics

Nuclear physics

New modern physics meaning

References

1 Elementary particle fluctuations spin quantum orbital Motion of the steady-state vertical double elliptic Equations and parameters characteristic answer

1.1 Elementary particle fluctuations. Established based On spin quantum physical model of steady-state Vertical double ellipse

1.1.1 Elementary particles essential characteristics

After nearly a century of experiments, the scientific community has confirmed that: the end product of all baryon decay electrons, neutrinos and photons in addition to proton; final product of all mesons and leptonic decay electrons, neutrinos and photons; neutrino accompanied forward to the weak interaction of electrons and photons can be transformed into each other under certain conditions.

In the entire process of particle decay, its energy, momentum, angular momentum, charge, baryon number conservation, and the direction towards energy decreases spontaneous. Reaction unit charge is always the most basic human science experiment can achieve the highest energy particle collisions, can be freely separated stable charged units. Find also much larger than the energy of the daughter mixed numbers charged "quark" is unwise as the idea of the most elementary particles in high-energy particle accelerator by particle collisions reaction. After decades of effort, and ultimately find some meager circumstantial evidence, still can not be separated, and stable presence. The face of such an outcome, we should reconsider the definition of the elementary particles? Like substance composed of molecules, molecules are made of atoms, atoms, electronics, nuclear composition, the spontaneous separatist decay, the final stable energy minimum, widespread electronic, photons, neutrinos truly the most elementary particles.

The $U^{\pm}$ lepton In addition to protons, neutrons, electrons, photons, neutrinos, particles longest average life, but 2.197×10^{-6} seconds. They can only exist as an instant energy group. Therefore, as long as we clarify the internal structure of the electrons, photons, neutrinos, protons, neutrons, energy of origin, momentum, moment of momentum and nuclear forces forming principle, parameter calculation

method and the relationship between particle physics is equivalent to solve the main problem.

1.1.2 Elementary particle fluctuations spin quantum steady-state Orbital motion characteristics

Proposed by de Broglie early descendants confirmed microscopic particles exist volatility, its wavelength $\vec{\lambda}$, particle momentum $\vec{P}$ is Planck's constant h relationship:

$$\vec{\lambda} = \frac{h}{\vec{P}} \qquad (1.1)$$

Modern physics experiments have confirmed: microscopic particles, elementary particles to existed fluctuations, spin two movements, and follow the momentum, moment of momentum and mean the law of conservation of energy. Just two movement's orbital quantum, Figure 1.1 and (1.1), we have:

$$\begin{cases} \vec{R}_\alpha \times m\vec{v}_\alpha = \dfrac{\vec{h}}{2\pi} \\ \vec{R}_\theta \times m\vec{v}_\theta = \dfrac{\vec{h}}{2\pi} \end{cases} \qquad \begin{cases} \vec{\lambda}_\alpha = \int_0^{2\pi} \vec{R}_\alpha d\alpha \\ \vec{\lambda}_\theta = \oint \vec{R}_\theta d\theta \end{cases} \qquad \begin{cases} \vec{P}_\alpha = m\vec{v}_\alpha \\ \vec{P}_\theta = m\vec{v}_\theta \end{cases}$$

The m represents the elementary particles along fluctuations; the $\vec{R}_\alpha$ quality of the moment in the movement $\vec{v}_\alpha$ of spin-orbit is variable. The $\vec{R}_\theta$、$\vec{v}_\theta$ said elementary particles to tend to the speed of light for the orbital radius vector of the wave motion; said and $\vec{v}_\alpha \perp \vec{R}_\alpha$、$\vec{v}_\theta \perp \vec{R}_\theta$、$\vec{v}_\alpha \perp \vec{v}_\theta$。$\vec{\lambda}_\alpha$ orbital radius vector of the spin motion energy relativistic velocities; Represents elementary particles along the wave direction of movement in the in each fluctuation movement cycle T_α, rail length; that $\vec{\lambda}_\theta$ each spin motion cycle T_θ in the length of the track along the spin direction of movement;, respectively, the $\vec{P}_\alpha$、$\vec{P}_\theta$ said elementary particles along fluctuations, spin the direction of movement of the moment of momentum. They are below standard "α, θ" distinction (following the same).

Note: book fluctuations, spin refers elementary particle along two vertical twin elliptical orbital motion of the two directions mutually perpendicular velocity component, the fluctuation of the elementary particles of the specified long-term human and academia spin different concepts.

Two orbital motions simultaneous three-dimensional Cartesian coordinate system, centered at the origin, still elementary particle fluctuations shown in the steady-state spin quantum orbital motion in Figure 1.1. Like a spring bent into a closed spiral rings, wire line on behalf of elementary particle fluctuations, spin the orbits. Fluctuations, the prerequisites for the establishment of the steady-state spin quantum orbital motion: orbital period of the spin motion must be fluctuations motion orbital period T_α N_α times T_θ! ($N_\alpha \geq 1$ is a natural number or a relatively simple Score). Thus, according to the wave equation and momentum moments conservation law still elementary particle internal orbital motion equations:

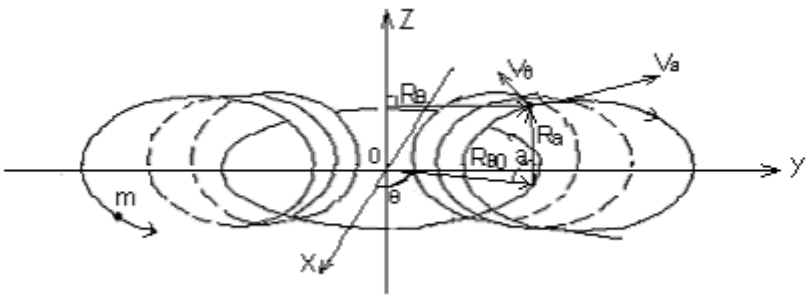

($X^2 + Y^2 = R_{\theta 0}^2$ Is round question)

Figure 1.1 still elementary particle internal fluctuations, the steady-state spin quantum the vertical double oval track movement diagram

$$\begin{cases} \vec{R}_\alpha \times m\vec{v}_\alpha = \dfrac{\vec{h}}{2\pi} \quad (\dfrac{\vec{h}}{2\pi} \text{Is moment of momentum wave vector}) & (1.2-1) \\ \vec{R}_\theta \times m\vec{v}_\theta = \dfrac{\vec{h}}{2\pi} & (1.2-2) \\ \vec{R}_\theta = \vec{R}_{\theta 0} - \vec{R}_\alpha \cos\alpha & (1.2-3) \\ \alpha = N_\alpha \theta & (1.2-4) \\ \dfrac{\oint \vec{R}_\theta d\theta}{\vec{v}_\theta} = \dfrac{N_\alpha \int_0^{2\pi} \vec{R}_\alpha d\alpha}{\vec{v}_\alpha} & (1.2-5) \end{cases}$$

1. 2 Orbit equations parameters characteristic answers

1.2.1 Orbit equations parameters characteristic answers

We first define the equations (1.2), the θ is a constant denoting the position fluctuations track projection plane, Z = 0 represents the projection plane of the

spin-orbit. The （1.2-1）、(1.2-2) into the （1.2-3） type, which $\vec{v}_\theta / \vec{v}_\alpha = E_{\alpha\theta} \le 1$ is constant, so:

$$\begin{cases} \vec{R}_\alpha = \dfrac{\vec{R}_{\theta 0} E_{\alpha\theta}}{1 + E_{\alpha\theta} \cos\alpha} & (1.3-1) \\ \vec{R}_\theta = \dfrac{\vec{R}_{\theta 0}}{1 + E_{\alpha\theta} \cos\alpha} & (1.3-2) \end{cases}$$

Two movement orbits are elliptical orbit, and perpendicular to each other! (Hereinafter, for convenience, always omitted $\vec{R}_\alpha$、$\vec{R}_\theta$、$\vec{v}_\alpha$、$\vec{v}_\theta$、$\vec{h}$ vector "→" symbol). Let fluctuations, the direction of the spin motion track of the total length respectively L_α, L_θ, equations obtained by the (1.2-5), (1.3):

$$\begin{cases} L_\alpha = N_\alpha \int_0^{2\pi} \dfrac{R_{\theta 0} E_{\alpha\theta}}{1 + E_{\alpha\theta} \cos\alpha} d\alpha & (1.4-1) \\ L_\theta = N_\alpha \int_0^{2\pi/N\alpha} \dfrac{R_{\theta 0}}{1 + E_{\alpha\theta} \cos\alpha} d\theta & (1.4-2) \end{cases}$$

Substituting (1.4) equations (1.2-3), (1.2-5), we obtain:

$$E_{\alpha\theta} = \frac{1}{\sqrt{N_\alpha}} \qquad (1.5)$$

Equations (1.2), (1.3) compared with the elliptical orbit of the celestial planetary motion can be seen: the elementary particles along the fluctuations, spin quantum stationary state vertical twin elliptical orbital motion is, in fact, along the circumferential line $X^2 + Y^2 = R_{\theta 0}^2$ and Z the orbital movement of the shaft two rotary axis angular momentum conservation. The v_α speed v_θ constant R_α R_θ is a variable, so m the state of motion of the two tracks are the same, for the same variables. With the fluctuations in the radius of the orbit of the spin motion, the basic particles in which the coordinates of the position varies. Laboratory determination of the quality of elementary particles should be for each of the fluctuations, the average mass $\overline{m}$ of the the spin orbital motion cycle. (1.2-1), (1.3-1), (1.4-1), (1.5), we have:

$$\overline{m} = \int_0^{2\pi} \frac{m R_\alpha}{L_\alpha} d\alpha = \frac{h}{2\pi v_\alpha} \int_0^{2\pi} \frac{1}{L_\alpha} d\alpha = \frac{h\sqrt{N_\alpha - 1}}{2\pi v_\alpha R_{\theta 0}} \qquad (1.6)$$

1. 2. 2 The importance of the orbit equations

Because of the fluctuations, the spin quantum steady state vertical double elliptic orbit motion model of elementary particle fluctuations equation, derived in the classic basic laws of physics of elementary particles inherent wave-particle duality, Quantum momentum, angular momentum, and the average energy conservationout equations (1.2) - (1.6) are all still elementary particles, nuclei, atoms, even microscopic particles in the entire universe physics parameters to calculate the basic equation. Classical Newtonian mechanics, electrodynamics, thermodynamics, quantum fluctuations in the orbit of the movement mechanics and energy relativistic combine accurate simulation answer the Preface proposed quantum physics, cosmic physics and relativistic field problems. Because all the parameters calculated ultimately comes down to the method of classical physics, elementary particle quantum orbital motion model of elementary particles orbiting moment of momentum, charge number and average energy and momentum are completely conserved under conditions only with the orbital parameters m, $N_{\alpha i}$ related calculations. Everyone else to specify a variety of quantum number, parity, isospin, strangeness ..... and laboratory observations of the parameters of the amendment, the abolition of all, in addition to the baryon number, charge number reserved!

Seen from the equations of Figure 1.1 and (1.3): When us still elementary particles the internal moving orbit calibration coordinate system, after the start time and the initial position, the coordinates of the elementary particle at any time t is located in orbit, energymomentum, moment of momentum parameter on all uniquely identified. Coordinates of elementary particles can be expressed as follows:

$$\begin{cases} \alpha = \dot{\alpha}\ t + \alpha_0 & (1.7-1) \\ X = (R_{\theta 0} - R_\alpha \cos\alpha)\cos\theta & (1.7-2) \\ Y = (R_{\theta 0} - R_\alpha \cos\alpha)\sin\theta & (1.7-3) \\ Z = R_\alpha \sin\alpha & (1.7-4) \end{cases}$$

However, measurement techniques available to the scientific community can not be precise, measured directly. Because the spray-type particles as a probe itself also exist fluctuations spin motion along the track. (2 to 4 will prove that they are also along the cylindrical helix orbital precession), as shown in Figure 1.2.

Elementary particles are much smaller than the radius of the fluctuations of its own entity, the spin-orbit radius R_α, R_θ fluctuations sports track intersection area, so

the two can only very small probability of a random collision occurred. And the collision point of the particle energy, momentum, orbital radius and coordinates of the location are variables; this is academia long debate how to understand the microscopic particles of uncertainty phenomenon reason. However, the distribution state of the spin motion along tracks fluctuations from the electrically charged elementary particles, the performance out of the magnetic moments, the average mass, charge density, elementary particle fluctuations, the size of the spin motion orbit distribution range shown by the appearance of the elementary particles, particles inside and outside , within the nucleus, and the weak, electrical, magnetic interaction force strength, the laboratory can be directly measured and estimated data for the book's physical model validation and accurate simulation proved.

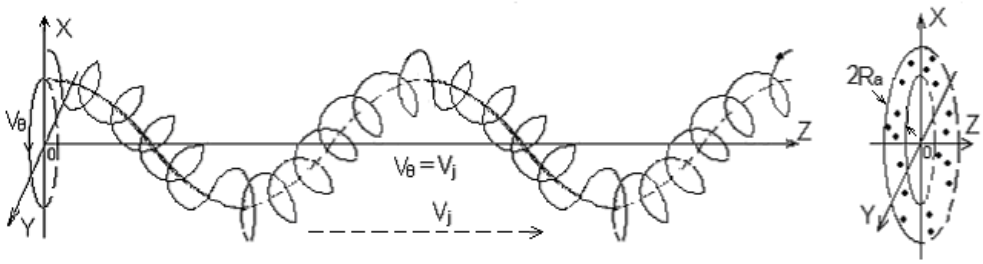

Figure 1.2 elementary particles along fluctuations, the spin precession of the orbital motion characteristics of the formation of wave-particle duality diagram

2 Elementary particle internal structure, the energy of Formation of the principles and parameters calculation

2.1 Elementary particle internal structure and energy origin

2.1.1 Elementary particle internal structure and the nature of charge Quantization

Scientific community are identified in all of the experiments from 1902 to 1990: all the free particles of free particles of the intermediate product, the spontaneous decay process of the energy radiation is electromagnetic energy; final product is the (proton) electrons, photons, neutrinos; allexperiments all particles decay process and all the transition, the final product of all baryons, mesons, leptons, charged nature can only be divided into three categories: a unit with a positive charge, with a unit negative charge, electrically neutral particles. When we will not consider the quality and the kinetic energy of the protons, neutrinos can be determined: all particle energy mc^2 are the electric and magnetic field energy, because the photons of electromagnetic energy radiation meson leptonic decay process and the final product, the electronic as electromagnetic energy ball "is beyond reproach. So, the book is the first of the elementary particles defined as follows: unit charge as one can no longer divided, basic, stable point particles, hereinafter referred to as "charged particles", in fact, the body radius tends to 0; All elementary particles, including all mesons, leptons and baryons core, when present them to electrically neutral, by n is positive, charged Particle electric dipole consisting of aggregates; when they are charged, additional charged particles; still elementary particle energy, the state of motion, and all parameters characterized by (1.2) orbit equations and (1.3) (1.5) (1.6) solutions; composed of baryons, the basic unit of the atoms (detailed proof, see the follow-up).

Photons have cyclical changes in the characteristics of electromagnetic waves; to form two photon pair of positive and negative electrons can collide annihilation; a photon can not be directly split into a pair of positive and negative electrons; neutrino production of charged mesons, leptons;$\pi^{\pm}$ mesoneventually split decaying into two neutrino and an antineutrino and an electron. The characteristics, we can make the most direct inference: photons and neutrinos are composed by a pair of electric dipole, is the most simple of elementary particles. Because neutrino properties, it can be spread as evenly as gas molecules in the vast space of the universe, the constitute a

omnipresent neutrino background field. The 2.7K blackbody microwave background radiation in the universe formed only by the neutrino field (see Chapter 5 demonstration). Electronics is composed by a pair of electric dipole and a charged particle, when a pair of electron collisions Specter, in addition to generating two photons, should be associated with a low-energy neutrino. If it is a negative electron and a positively to charged particles collide, it happens to the formation of two photons. A photon collision near the nucleus, to the simultaneous excitation of two neutrinos or two pairs of electric dipole, split, combine into two (one pair) electronic. Similarly, the chargedπ± meson is composed by two pairs of electric dipole and a charged particle. Because the moment the law of conservation of momentum and momentum, launch an anti-neutrino and absorption neutrino a neutrino are equivalent. All other mesons, leptons, including baryon core, can be determined: the electrically neutral elementary particles are composed of n electric dipole assembly; the different particle n is a natural number, one more of the charged particles Charge charged particles. Under the internal structure of elementary particles, as long as enough analysis to calculated charged elementary particles, electrically neutral elementary particles, photons and neutrinos energy forming principle and related parameters.

2.1.2 Charged particle energy origin

By classical electrodynamics, shown as in Figure 2.1, charged particle energy relativistic speed Ava straight uniform motion, electrical, magnetic field strength is:

$$\vec{E}_\alpha = \frac{e(1-\beta_\alpha^2)\vec{R}_\alpha}{4\pi\varepsilon_0 R_\alpha^3 (1-\beta_\alpha^2 \sin^2\alpha)^{1.5}} \qquad (\beta_\alpha = \frac{v_\alpha}{c}) \qquad (2.1)$$

$$\vec{B}_\alpha = \frac{\vec{v}_\alpha \times \vec{E}_\alpha}{c^2} \quad (\text{the } \alpha \text{ is the angle between } \vec{v}_\alpha \text{ and } \vec{R}_\alpha) \qquad (2.2)$$

When the circumferential fluctuation motion of the charged particles nearly the speed of light c, due to The fluctuations orbital radius R_a the entity radius much larger than the charged particles R_a., we can track the circumferential fluctuation motion simplified as the linear movement of each short circumferentially tangent. At this time, the electromagnetic waves "squeezed" only distributed within the plane of the vertical fluctuations movement $\vec{v}_\alpha$ direction to form a planar shock, as shown in Figure 2.1. Non-occurrence of electromagnetic energy radiation of charged particles stream packet rounded plane forward. By classical electrodynamics, the energy flux density

distribution of glass Poynting vector $\vec{S}_\alpha$ is:

$$\vec{S}_\alpha = \vec{E}_\alpha \times \vec{H}_\alpha = \varepsilon_0 \left[\vec{v}_\alpha E_\alpha^2 - \vec{E}_\alpha \left(\vec{E}_\alpha \cdot \vec{v}_\alpha \right) \right] \qquad (2.3)$$

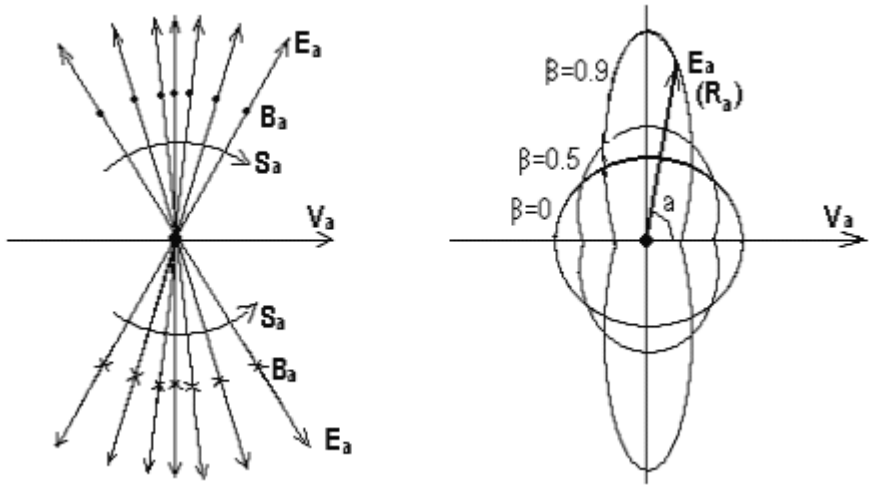

Figure 2.1 energy relativistic velocities v_a uniform linear motion of charged particles in electric and magnetic field strength characteristics Figure

By (2.3) that: $\vec{S} \cdot \vec{R} / R = 0$ (at the microscopic field, charge along the circumference to the speed of light c fluctuations movement does not occur cyclotron electromagnetic wave energy radiation, see the end of Chapter 5 supplemental argument).

Note: Because the orbit is elliptical orbit fluctuations, $\vec{v}_\alpha \to c$ and completely non-linear motion, energy flux density should take positive, so this is not simply take $\vec{S}_\alpha = \varepsilon_0 \vec{v}_\alpha E_\alpha^2$ value. But take the $\vec{S}_\alpha = \varepsilon_0 \left[\vec{v}_\alpha \vec{E}_\alpha^2 - \vec{E}_\alpha \left(\vec{E}_\alpha \cdot \vec{v}_\alpha \right) \right]$ value vector synthesis. The former when the equivalent electromagnetic field energy ball "volume should take $2\pi \overline{R}_\alpha^3$, $\beta_\alpha = 0.9981773259$ which is equivalent to the volume of the electromagnetic field" energy ball "should be taken as $\sqrt{2}\pi \overline{R}_\alpha^3$, $\beta_\alpha = 0.9987108301$. The systematic error is minimal.

The electromagnetic field of a charged particle energy for W_e, the the equivalent electromagnetic fields "energy ball" volume $\sqrt{2}\pi \overline{R}_\alpha^3$, the $\sqrt{2}$ coefficient enables electromagnetic field energy equation (2.4), transition from energy relativistic speed toward the stationary state. By the equation (2.3), due to $v_a \to c$ is a constant, so the

direct electric field intensity $\vec{E}_\alpha$ take a = 0, π/2, the synthesis of two vectors:

$$W_e = \frac{\sqrt{2}\pi \overline{R}_\alpha^3 S_\alpha}{v_\alpha} = \frac{\sqrt{2}e^2}{16\pi\varepsilon_0 \overline{R}_\alpha} \frac{\sqrt{1+(1-\beta_\alpha^2)^3}}{1-\beta_\alpha^2} \qquad (2.4)$$

When $\beta_a \to 0$, it should be equal to the average radius $\overline{R}_\alpha$ spherical shell uniform distribution of the electrostatic field energy charged particles along W_e:

$$W_e = \frac{e^2}{8\pi\varepsilon_0 \overline{R}_\alpha} \qquad (2.5)$$

Make to (2.4) of charged particles electromagnetic field energy representative (1.2-1) type of elementary particles along the circumference of the wave motion of particle energy mc^2, too:

$$\frac{\beta_\alpha \sqrt{1+(1-\beta_\alpha^2)^3}}{1-\beta_\alpha^2} = 2\sqrt{2}\left(\frac{2h\varepsilon_0 c}{e^2}\right) \qquad (2.6)$$

Solution (2.6): βa =0.9987108301. It is charged elementary particles when a fluctuation in quantum N_a limit fluctuations in speed coefficient tends to infinity, see (2.16) where.

The fine structure constant (2.6), the right to export is the origin of elementary particle energy, the initial indications of the quantum steady state orbital motion, strong, and weak, electrical, magnetic interactions unity principle. Seen from (2.6): v_a single charged particles because the speed of the waves, the orbital radius R_a is a constant electromagnetic field energy mc^2 must be a constant, and is unable to meet the (1.2) the equations of elementary particles along fluctuations, spin-orbit movement conditions. Therefore, directly by probing all experiments to all the particles split decay process Corollary: charged elementary particles must be composed by n to the electric dipole and a charged particle aggregates.

2.2 Charged elementary particles energy forming Principle and parameters calculation

2.2.1 Charged particle energy forming principle

A electric dipole is, load electric particle spacing of L_r, the $K_r = L_r / 2\overline{R}_\alpha$. The

fluctuation of electric dipole along the orbital motion while, also should be around the wobbled track rotation. On a charged elementary particles, the rotation speed and fluctuation of angular velocity of complete synchronization! In order toπ^+ meson as an example, when π^+ meson along the fluctuation orbits, if the start position a=0°, excess positive charged particle tracks just in fluctuation of polar axis R_α lateral, see Figure 2.2, (or spin orbit $R_{\theta 0}$ medial). Now, load electric particle fluctuations, rotation speed v_+, v_- and fluctuation velocity v_a relationship:

(Positive, load electric particle in fluctuating, spin orbit within the lateral distribution, readers can make a model of the rotating verification)

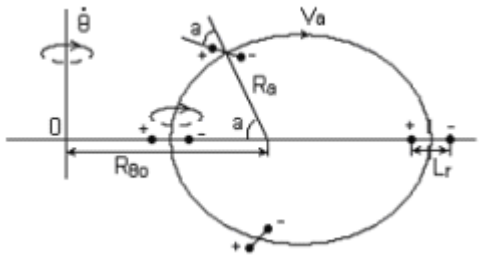

Fig 2.2 charged particle rotation speed fluctuation sketch map

$$\begin{cases} v_+ = v_\alpha (1 + K_r \cos\alpha) & (2.7-1) \\ v_- = v_\alpha (1 - K_r \cos\alpha) & (2.7-2) \end{cases}$$

And at the beginning of the last century Planck founded the ideas of quantum mechanics. As long as we make the electric dipole within Lr as capable of telescopic change electromagneticenergy vibrator, the telescopic change cause the charged particles along the wave track motion tends to speed v_+, v_- periodic variation; lead to the synthesis of electromagnetic field intensity varies periodically, to determine the periodic changes of the energy, and (1.2-1) type of elementary particle in fluctuation, spin orbit periodic variations in the instantaneous energy equal to mc^2, a, R_a and N_a function. Thus, elementary particle in steady state within the orbit motion, will not appear in cyclotron, moving direction of electromagnetic wave radiation energy, momentum, and in line with the instant energy and average momentum, the law of conservation of energy. As long as we derive electromagneticenergy vibrator in the energy equation of N_a and a, K_r presents the continuous change of the relation, be equal to that book of charged particle internal structure, energy principle and calculation of related parameters of physical model.

By (1.3-1), (1.5), (1.6), elementary particles along the instant fluctuation fluctuation orbit orbit radius R_a and the average radius of $\overline{R}_\alpha$ respectively:

$$\begin{cases} R_\alpha = \dfrac{R_{\theta 0}}{\sqrt{N_\alpha} + \cos\alpha} & (2.8-1) \\ \overline{R}_\alpha = \dfrac{R_{\theta 0}}{\sqrt{N_\alpha - 1}} & (2.8-2) \end{cases}$$

Will (2.8) equations into (2.4), (2.5), (2.6) type, because β→1, so:

Because $\sqrt{1+(1-\beta_\alpha^2)^3} \to 1$, therefore, each charged particles along the orbital motion of the instantaneous fluctuation of energy equation N_a, a, β_a relationship:

$$\frac{\beta_\alpha}{1-\beta_\alpha^2} = 2\sqrt{2}\left(\frac{2h\varepsilon_0 c}{e^2}\right)\frac{\sqrt{N_\alpha}+\cos\alpha}{\sqrt{N_\alpha - 1}} \qquad (2.9)$$

2.2.2 Charged particle energy parameter calculation

A charged particle by a pair of n electric dipole and a positively charged particle composition, and positive, load electric particles each occupy a common wave, consisting of spin orbit, as biological gene as chain-like structure, (see Figure 3.3). Then the basic particle instantaneous electrical, magnetic field strength should be each charged particle instantaneous electrical, magnetic field intensity vector and. By (2.1), (2.4), (2.9) and (2.7) equation:

$$\beta_\alpha\left[\frac{n+1}{\sqrt{1-\beta_\alpha^2(1+K_r\cos\alpha)^2}} - \frac{n}{\sqrt{1-\beta_\alpha^2(1-K_r\cos\alpha)^2}}\right]^2$$

$$= 2\sqrt{2}\left(\frac{2h\varepsilon_0 c}{e^2}\right)\frac{\sqrt{N_\alpha}+\cos\alpha}{\sqrt{N_\alpha - 1}} \qquad (2.10)$$

So (2.10) type of α=π/2 or 3π/2, too:

$$\frac{\beta_\alpha}{1-\beta_\alpha^2} = 2\sqrt{2}\left(\frac{2h\varepsilon_0 c}{e^2}\right)\frac{\sqrt{N_\alpha}}{\sqrt{N_\alpha - 1}} \qquad (2.11)$$

On the show, for a certain value of N_a, v_a, β_a are constant, is a function of N_a, and the fluctuation of electric dipole motion track position independent. As long as we at different N_a values into (2.11) type for β_a value, n value together with different substitution (2.10) type, we can calculate the different charged particle internal K_r value change tendency, see table 2.1.

From Table 2.1 calculating results can be seen: K_r is a continuous gradient of the function, and the particle internal dipole numbers n inversely proportional, with fluctuations in quantum number N_a increases. Please note: unpaired residual charged particles are distributed in spin orbital medial, and general electric, magnetic field intensity, were greater than the spin orbit of charged particles, illustrate the basic energy of mc^2 focused on spin orbital medial embodiment.

The different charged particle internal K_r value trend Table 2.1

α°		0 °	30°	60°	80°	100°	120°	150 °	180°
N_a	n	$K_r \times 10^{-5}$							
2	1	17.4001	17.8604	19.2474	20.6731	22.4384	24.4076	27.1746	28.4420
	2	10.9000	11.1214	11.7909	12.4890	13.3802	14.4297	16.0509	16.8650
	3	7.88645	8.03130	8.47239	8.93784	9.54125	10.2662	11.4169	12.0079
2.5	1	17.4035	17.8223	19.0732	20.3417	21.8883	3.5797	25.8749	26.8757
	2	10.8507	11.0523	11.6572	12.2797	13.0601	13.9547	15.2669	15.8834
	3	7.83898	7.79120	8.37056	8.78613	9.31455	9.93101	10.8563	11.2994
3	1	17.0074	17.3858	18.5084	19.6353	20.9936	22.4581	24.4003	25.2240
	2	10.5667	10.7491	11.2928	11.8467	12.5320	13.3024	14.3947	14.8881
	3	7.62548	7.74529	8.10489	8.47507	8.93901	9.46894	10.2357	10.5879
31	1	7.17710	7.23191	7.38592	7.52881	7.68703	7.84192	8.02339	8.09200
	2	4.35031	4.37730	4.45357	4.52490	4.60465	4.68357	4.77725	4.81304
	3	3.11626	3.13432	3.18550	3.23358	3.28755	3.34121	3.40522	3.42977
151	1	3.39991	3.41199	3.44543	3.47580	3.50870	3.54020	3.57621	3.58958
	2	2.04910	2.05512	2.07182	2.08706	2.10364	2.11959	2.13792	2.14475
	3	1.46546	1.46951	1.48078	1.49107	1.50229	1.51311	1.52556	1.53021
500	1	1.89531	1.89905	1.90934	1.91860	1.92856	1.93802	1.94873	1.95269
	2	1.13995	1.14182	1.14698	1.15164	1.15666	1.16143	1.16686	1.16887
	3	0.81480	0.81606	0.81955	0.82270	0.82609	0.82933	0.83301	0.83437

Further simulation calculation results show: the charged particle in the electric dipole rotation speed fluctuation of angular velocity and only fully synchronous, if it >1 natural number, then K_r values are not continuous positive solution. These

characteristics of charged elementary particles, nuclei are behind the internal structure of the design, parameters calculation based on.

2.3 Electrically neutral elementary particle energy Principle and parameter calculation

2.3.1 Electrically neutral elementary particle energy formation Principle

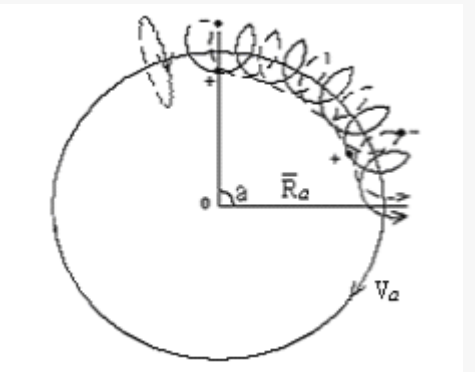

Fig 2.3 proton nuclear core electric dipole rotation diagram

In the next chapter, basic particle internal interaction analysis showed that: all the charged particles must travel at the speed of c motion can exist. The nature and even the entire universe, all charged particles along the fluctuation, spin orbit motion velocity vector and shall be $\sqrt{v_\theta^2 + v_\alpha^2} \geq c$, only such, within any charged particle along the fluctuation, spin two velocity vector superposition in a given direction, including rotation speed synthesis ability in the speed of light.

In addition to photons, neutrinos of all electrically neutral elementary particle, due to the internal structure is special, electric dipole center along the wave track wave motion velocity v_a, rotation caused all charged particle motion velocity of $N_rK_rv_a$ (N_r rotation frequency number), all two must be vector and in a direction is equal to the speed of light c, shown in figure 2.3. We have,

$$\sqrt{v_\alpha^2 + (N_r K_r v_\alpha)^2} = c \qquad (2.12)$$

By (2.12) type, too:

$$N_r = \frac{\sqrt{1-\beta_\alpha^2}}{K_r \beta_\alpha} \qquad (2.13)$$

From (2.1)to(2.6) compare the:electrically neutral elementary particle field energy is positive,on equal load electric particle electric, magnetic field intensity vector synthesis to achieve. When we consider the K_r value is very small electric dipole can be large enough to form the electromagnetic field energy, the wave speed must be very close to the speed of light c. We take the v_a= (1-10^{9})c, both in the scientific community are capable of accurately measuring the hands and the calculator to calculate the error range. By (2.3), when β_a=1-10^{-9}, can be simplified to:

$$\vec{S}_\alpha = \varepsilon_0 \vec{v}_\alpha E_\alpha^2 = \frac{e^2 \vec{v}_\alpha}{16\pi^2 \varepsilon_0 R_\alpha^4 (1-\beta_\alpha^2)} \qquad (2.14)$$

As long as the electric dipole within each charged particle fluctuation velocity of v_+, v_- and (2.7) equations as a periodic variation, it can make the electrically neutral elementary particle electric dipole in the wave track fluctuations, rotation of synthesis electromagnetic field strength also shows periodic change, thereby forming the periodic variations of the energy mc^2, this periodic variations of the frequency must be charged particle and photon N_r times.

2.3.2 Electrically neutral elementary particle energy parameter Calculation

The actual simulation, K_r changes only with a values,by (2.13): $K_r N_r = \sqrt{1-\beta_\alpha^2} \Big/ \beta_\alpha$ type, is constant, as can be seen from the table 2.2 electric dipole rotation frequency of N_r wave changes along the track. By (2.14), reference (2.9), (2.10) type inference process, electrically neutral elementary particle of β_a, N_a, K_r, a parameter relation can be expressed as:

$$n\beta_\alpha \left[\frac{1}{\sqrt{1-\beta_\alpha^2 (1+K_r \cos\alpha)^2}} - \frac{1}{\sqrt{1-\beta_\alpha^2 (1-K_r \cos\alpha)^2}} \right]^2$$

$$= 2\sqrt{2} \left(\frac{2h\varepsilon_0 c}{e^2} \right) \frac{\sqrt{N_\alpha} + \cos\alpha}{\sqrt{N_\alpha - 1}} \qquad (2.15)$$

A electric dipole numbers n=2, β_a=1-10^{-9}, N_a=3, the simulation results are shown in table 2.2.

Proton nuclear core is an electrically neutral elementary particle, fluctuations in quantum number $N_a \to \infty$, forming a circular orbit spin speed fluctuation, $v_\theta = 0$. From the atomic nucleus inner structure calculation, it is 6 on the electric dipole. n=6, $N_a \to \infty$, substitution (2.15), the simulation results are shown in table 2.2.

Electrically neutral elementary particle internal K_r value analog computation results table 2.2

α°	0°	30°	60°	80°	89°	100°	120°	150°	180°
Partide parameters	$K_r \times 10^{-13}$								
Electrically neutral particles $n=2N_a=3$	6.14	6.92	11.13	29.55	280.78	26.78	8.25	4.04	3.19
Proton nuclear core $n=6N_a=\infty$	1.499	1.732	2.999	8.638	85.948	8.638	2.999	1.732	1.499
Neutrino $n=1N_a=1$	1303	1504	2605	7501	74637.3	7501	2605	1504	1302

Similarly, the neutrino, as n=1, N_a=1, c precession rate is the speed of light. Fluctuation, precession track is cylindrical helical line. Considering the precession direction energy relativistic effects, by (2.15) type, too:

$$\beta_\alpha \left[\frac{1}{\sqrt{1-\beta_\alpha^2(1+K_r\cos\alpha)^2}} - \frac{1}{\sqrt{1-\beta_\alpha^2(1-K_r\cos\alpha)^2}} \right]^2 = \frac{2\sqrt{2}}{\sqrt{1-\beta_\alpha^2}} \left(\frac{2h\varepsilon_0 c}{e^2} \right) \tag{2.16}$$

The simulation results are shown in table 2.2. The neutrino in a=0～89° K_r values into (2.13) type, too: 343323≥ N_r ≥ 5991. Similarly, the proton core, 2.9834 x10^8 ≥ Nr≥5.2033 ×10^6.

From table 2.2 shows： that in addition to a=π /2、3π /2, K_r value is also a continuous gradient function a; in a=π/2, 3π/2, K_r value increases rapidly, but with Kr=$10^{-10\sim-13}$ orders of magnitude more, still microscopic little. From n on the electric dipole formed of electrically neutral particles, because of their a=π/2 3π/2, through when there is a tiny distance, the variation of K_r value range is much smaller than the neutrino. If we consider the electric dipole rotation frequency number N_r, then every fluctuation cycle, the electric dipole of the telescopic oscillation frequency is N_r times.

Of course, we can also make the proton nuclear core of electric dipole within 6 a values are equal, rotation angle Nra interval of 60°, 6 pairs of dipole occupy 6 wave track perfectly synchronized motion, so that the variation of K_r value with minimum amplitude, but also the most special, the most stable structure. In addition, all photons neutrino electrically neutral elementary particle, this structure may be proton core can stabilize the only reason.

2.4 Photon of electromagnetic wave, energy principle And parameter calculation

Photon only by a pair of electrical dipole component, and neutrinos, fluctuation, precession track is cylindrical spiral line, see figure 2.4.

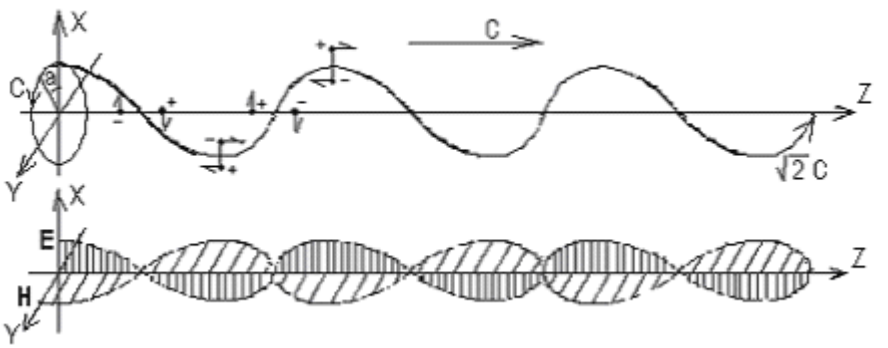

Fig 2.4 photon along the wave, cylindrical spiral orbit precession formed in the electromagnetic wave principle diagram

Orbit equation:

$$\begin{cases} X = R_\alpha \cos(\dot{\alpha}\ t + \alpha_0) & (2.17-1) \\ Y = R_\alpha \sin(\dot{\alpha}\ t + \alpha_0) & (2.17-2) \\ Z = R_\alpha (\dot{\alpha}\ t + \alpha_0) & (2.17-3) \end{cases}$$

The photon is composed of neutrino by high frequency alternating electromagnetic field excited after the formation of the. When the photon energy is greater than the excitation of the neutrino background field average energy, electric is dipole polarization, positive, load fluctuation particles around the track rotation frequency N_r to 1.Rotation plane by excitation of the alternating electromagnetic field plane control, naturally formed in a direction perpendicular to the polarization and the electromagnetic wave oscillation. Now load electric particle fluctuations, rotation speed is composed of (2.7) equation to express. Reference (2.16) type, photonic Kr value in

the calculation results, the same as in table 2.2. Kr values are equal. Photon fluctuation, precession motion along the electric dipole rotation formed by electromagnetic Potter syndrome is shown in figure 2.4.

From this chapter analysis shows: the neutrino and photon, is only one, only the energy difference. To distinguish the antineutrinos, the photon, can only be fluctuations in movement direction, the electric dipole rotation direction opposite to it, or photons in 0 for a,π,2π, office, load electric particle in fluctuation, precession of orbit.

3 Elementary particles within the outer Interaction strength

3.1 Charged particles within the outer interaction strength

3.1.1 With in the charged particles interaction strength calculation

Single charged particles along the orbital motion of the fluctuations, not only to the formation of a strong centrifugal force of the $F_{n\bullet}$, but also form a stronger electric, magnetic force $\triangle F_{e\bullet}$ $\triangle F_{b\bullet}$. Charged Particles entity as a small sphere, diameter $2R_{\bullet}$, it should be smaller than the electric dipoles within the positive the load charged particles spacing $2K_{r\bullet}\overline{R}_{\alpha}$. The $K_{r\bullet}=R_{\bullet}/\overline{R}_{\alpha}$ formed in the orbital motion of charged particles along fluctuations electricity, magnetic energy mc^2. When the orbital motion of charged particles along the volatility, the centrifugal force should be less than the fluctuation orbital motion of charged particles along the outside of the two hemispheres of their own electricity, magnetic force $\triangle F_{e\bullet}$ $\triangle F_{b\bullet}$ difference. Figure 3.1, we will average orbital radius of each charged particle along fluctuations $\overline{R}_{\alpha}$ radial divided into inner and outer side of the two hemispheres. "A" is omitted, the same below) by the equations of (2.7), $v_{\alpha 1}=\beta(1+K_{r\bullet})c$, $v_{\alpha 2}=\beta(1-K_{r\bullet})c$ (The β_{α} The subscript "α" omitted, the same below) Still exist tends to the speed of light is poor, resulting in each of the charged particles inside and outside are formed in the fluctuating movement power, the magnetic field force intensity differences. Newtonian mechanics and (1.2-1), (2.1), (2.2), (2.7), Figure 3.1 we have:

$$F_{n\bullet}=\frac{mv_{\alpha}^2}{\overline{R}_{\alpha}}=\frac{\beta hc}{2\pi R_{\alpha}^2} \qquad (3.1)$$

$$\Delta F_{e\bullet}=\frac{(0.5e)^2}{4\pi\varepsilon_0(K_{r\bullet}\overline{R}_{\alpha})^2}\left[\frac{1}{\sqrt{1-\beta^2(1+K_{r\bullet})^2}}-\frac{1}{\sqrt{1-\beta^2(1-K_{r\bullet})^2}}\right]$$

(3.2)

$$\Delta F_{b\bullet}=\frac{(0.5e)^2\beta^2(1-K_{r\bullet}^2)}{4\pi\varepsilon_0(K_{r\bullet}\overline{R}_{\alpha})^2}\left[\frac{1}{\sqrt{1-\beta^2(1+K_{r\bullet})^2}}-\frac{1}{\sqrt{1-\beta^2(1-K_{r\bullet})^2}}\right]$$

(3.3)

Compare $\triangle F_{e\bullet}$ - ($\triangle F_{b\bullet}$ + $F_{n\bullet}$) values , simultaneous (3.1) to (3.3), we have:

$$\frac{e^2}{4\pi\varepsilon_0 \overline{R}_\alpha^2}\left\{\begin{array}{l}\dfrac{\left[1-\beta^2(1-K_{r\bullet}^2)\right]}{4K_{r\bullet}^2}\left[\dfrac{1}{\sqrt{1-\beta^2(1+K_{r\bullet})^2}}-\dfrac{1}{\sqrt{1-\beta^2(1-K_{r\bullet})^2}}\right] \\ -\beta\left(\dfrac{2h\varepsilon_0 c}{e^2}\right)\end{array}\right\}=0$$

（3.4）

Make to $\beta=1-10^{9}$, $K_{r\bullet}<1/\beta-1=10^{-9}$, by table 2.2: $K_{r\bullet}<1.499\times10^{-13}$. By the simulation we find that: (3.4) type: $1.499 \times 10^{-13} > K_{r\bullet} + 8.0 \times 10^{-15}$, is the reasonable scope. $K_{r\bullet} = 8.0 \times 10^{-15}$ is charged particles entity radius coefficient lower limit, and in (3.4), to: $\triangle F_{e\bullet} - (\triangle F_{b\bullet} + F_{n\bullet}) = 0$. Have their own electric and magnetic field strength of for: maintenance $\triangle F_{e\bullet} - \triangle F_{b\bullet} >> 0$, $\triangle F_{e\bullet} - \triangle F_{b\bullet}$ processed maintenance train to fluctuations in the strength of the inside of the track, is the centrifugal force $F_{n\bullet}$ the multiple astronomy!

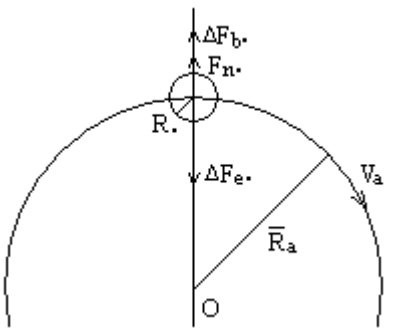

Figure 3.1 charged particles inside the interactions

3.1.2 Charged particles lateral force each other parameters are Calculated

When we will be charged particles tends to zero as a radius small sphere of view, and the lateral force electric and magnetic field will be to infinite. Magnetic field force charged particles could be overcome their own electric field repelling force, prevent occurrence blowout phenomenon? Become the scientific community for many years searching for the mixed number charge of quark?

A charged particle bursts into n pieces of debris, the initial moment of each fragment itself electric and magnetic field strength respectively for: $\triangle F_{e\bullet/n}$、 $\triangle F_{b\bullet/n}$, processed maintenance, processed, we also as long as the maximum of electric and

magnetic field force direction, perpendicular to the $\vec{v}_\alpha$ speed position is enough, (the same below). By (3.2), (3.3), to:

$$\begin{cases} \Delta F_{\frac{e_\bullet}{n}} = \dfrac{\dfrac{e}{n}\left[\dfrac{e(n-1)}{n}\right]}{4\pi\varepsilon_0 (K_{r\bullet}\overline{R}_\alpha)^2}\left[\dfrac{1}{\sqrt{1-\beta^2(1+K_{r\bullet})^2}} - \dfrac{1}{\sqrt{1-\beta^2(1-K_{r\bullet})^2}}\right] \\ \qquad\qquad (3.5-1) \\ \Delta F_{\frac{b_\bullet}{n}} = \dfrac{\dfrac{e}{n}\left[\dfrac{e(n-1)}{n}\right]\beta^2(1-K_{r\bullet}^2)}{4\pi\varepsilon_0 (K_{r\bullet}\overline{R}_\alpha)^2}\left[\dfrac{1}{\sqrt{1-\beta^2(1+K_{r\bullet})^2}} - \dfrac{1}{\sqrt{1-\beta^2(1-K_{r\bullet})^2}}\right] \\ \qquad\qquad (3.5-2) \end{cases}$$

Obviously, only the beta $\beta\to 1$、$K_{r\bullet}\to 0$, both force to infinite, effect radius is only charged particle sentity radius（$K_{r\bullet}\overline{R}_\alpha$）, and two kinds of force just equal size, direction, on the other hand, can be in equilibrium. Neutral and charged elementary particles, the wave speed coefficient beta for $1-10^{-9}>\beta\geq 0.9987108301$, that: $\triangle F_{e\bullet/n}/\triangle F_{b\bullet/n}\geq 1$

By analogy, charged particles will instantly blowout, completely disappear, but the fact is not the case. Reason from elementary particle internal structure, charged particles fluctuation, the spin velocity v_a、v_θ, theta, electric dipole $N_rK_rv_a$ rotating speed, etc. As long as we make $\sqrt{v_\alpha^2+v_\theta^2+(N_rK_rv_\alpha)^2}\geq c$, one will be the direction of the speed just for c, can make $\triangle F_{e\bullet/n}/\triangle F_{b\bullet/n}=1$ processed maintenance train. Rotation, fluctuation, spin motion orbit of charged particles oneself electric and magnetic field strength can be charged particles firmly bound within their own orbit, equal and opposite direction, just to be in equilibrium, the force is charged particles themselves electric and magnetic fields form the strong force.

The rail to tend to the speed of light wave motion is micro particles inherent characteristics. Because $1.499\times10^{-13} > K_{r\bullet}\geq 8.0\times10^{-15}$, charged particles should be an infinitesimal point of geometry. Want to rely on particle collision directly hit a moving at the speed of geometric point, by (1.2 1) type, particle collision energy want to infinite, hit probability of will is an infinitesimal. So, charged particles will is the most basic component in the whole process of the evolution and structure unit (see infinite and eternal cosmology). Within the scientific community in the cosmic rays and high-energy particle accelerators collision experiment, explore decades still cannot be

called mixed number charge "quark" particles steadily separated alone, why is this.

Which classical electrodynamics theory in the point of energy "divergence" difficult to beed solved at the same time. Charged particles as a particle will not stationary in a certain space geometry point; It never to tend to the speed of light v_a v_θ theta and energy relativistic velocities along the fluctuation, the movement of the spin track; So, charged particles and electric dipole is composed of elementary particles energy, strength, fluctuation orbit radius beta R_a、β、K_r、K_r parameters such as, only determined by the physical model and equations (1.2) this book; The energy mc^2 nature is limited. By R_a、R_θ、β、K_r theta, beta, Kr parameters such as relationships, fluctuation, the spin track movement characteristics, all the elementary particle and wave particle duality of atoms and molecules to form nature and all settled (see chapter 1, 5).

3.2 Electrically neutral elementary particle, the outer Interaction strength

3.2.1 Electrically neutral elementary particle interaction strength Within the computing

Is to set up a pair of electric dipole Charged Particle spacing of L_r, mutual electrical, magnetic force for $F_{e\pm}$, $F_{b\pm}$, by (2.1), (2.2), was:

$$\begin{cases} F_{e\pm} = \dfrac{e^2}{4\pi\varepsilon_0 L_r^2\sqrt{1-\beta^2(1+K_r\cos\alpha)^2}} & (3.6-1) \\ F_{b\pm} = \dfrac{e^2(1-K_r^2\cos^2\alpha)\beta^2}{4\pi\varepsilon_0 L_r^2\sqrt{1-\beta^2(1+K_r\cos\alpha)^2}} & (3.6-2) \end{cases}$$

Simultaneous get:

$$\frac{F_{e\pm}}{F_{b\pm}} = \frac{1}{(1-K_r^2\cos^2\alpha)\beta^2} \qquad (3.7)$$

$\beta\to1$、$K_r\to0$ above formula established conditions, field gravitational slightly larger than the magnetic field repulsion, just plays to overcome the electric dipole rotation movement periodic energy exchange between the centrifugal force generated by the charged Particle role.

Electrically neutral elementary particle composed by the n pairs of the electric

dipole between the electric and magnetic fields between each pair of electrical dipole or charged particles interaction force Figure 3.2 shows. By (2.1), (2.2), (3.6-1), (3.6-2), as long as we compare the electric force v_a direction interaction can. Positive load electric particle spacing disposed electric dipole spacing for the $2\Delta\overline{R}_\alpha$, the staggered L_x, the relationship with the other parameters:

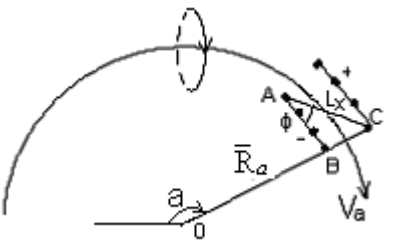

Figure 3.2 electrically neutral elementary particles within
Charged particles in an electric field force diagram

$$\begin{cases} L_x = \sqrt{(2K_r\overline{R}_\alpha)^2 + \left[2(n-1)\Delta\overline{R}_\alpha\right]^2} & (3.8\text{-}1) \\ \sin\phi = \dfrac{2K_r\overline{R}_\alpha}{L_x} & (3.8-2) \\ \cos\phi = \dfrac{2(n-1)\Delta\overline{R}_\alpha}{L_x} & (3.8-3) \end{cases}$$

By (2.1), (3.6-1), located either on the electrostatic force between the charged particles of charged particles with homosexual F_{ex1}, as F_{ex2} heterosexual the electrostatic force between the charged particles, when we calculate the points A andthat B, C between the electric field interaction, we have:

$$\begin{cases} F_{ex1} = \dfrac{e^2\left[1-\beta^2(1+K_r\cos\alpha)^2\right]}{4\pi\varepsilon_0\left[2(n-1)\Delta\overline{R}_\alpha\right]^2} & (\sin\phi = 0) \quad (3.9-1) \\ F_{ex2} = \dfrac{-e^2\left[1-\beta^2(1+K_r\cos\alpha)^2\right]\cos\phi}{4\pi\varepsilon_0 L_x^2\left[1-\beta^2(1+K_r\cos\alpha)^2\sin^2\phi\right]^{1.5}} & (3.9-2) \end{cases}$$

Simultaneous get:

$$\frac{F_{ex2}}{F_{ex1}} = \frac{-\left[2(n-1)\Delta\overline{R}_\alpha\right]^3}{\left\{(2K_r\overline{R}_\alpha)^2 + \left[2(n-1)\Delta\overline{R}_\alpha\right]^2 - \beta^2(1+K_r\cos\alpha)^2(2K_r\overline{R}_\alpha)^2\right\}^{1.5}}$$

（3.10）

Clearly, the equilibrium conditions of the two directions of the electric force is beta β→1、K_r→0.

If we (3.6-1) (3.9-1), two formulas were compared and set $L_x = 10\Delta\overline{R}_\alpha$, n = 2, then: $\frac{F_{e\pm}}{F_{ex1}} \approx \frac{(n-1)^2}{25(1-\beta^2)^{1.5}}$.

Because β=1-10^{-9}、n=2, substituting too: $F_{e\pm} / F_{ex1}=4.4721\times10^{11}$. By the previous result: electricity, electric dipole magnetic field interaction force between the electric dipole 4.4721×10^{11} times! So, when the electric and magnetic fields within the electric dipole interaction force $F_{e\pm}$ $F_{b\pm}$ as a super force, the electric and magnetic field force between the electric dipole F_{ex1} F_{bx1} naturally become weak interaction force. This proves the strong and weak interactions are actually electrical, magnetic interactions.

3.2.2 Electrically neutral elementary particle surface interaction Strength calculations

Provided an electrically neutral elementary particle has n pairs of electric dipole, electric dipoles along the radius of rotation of the vertical fluctuations in the direction of movement of the n $K_r\overline{R}_\alpha$ as elementary particles surface radius. For calculation purposes, we analyzed the calculation of fluctuations, the outside of the spin-orbit a=π at the electric dipole rotation orbit, the outer surface of the electric and magnetic field force size, you can understand the whole picture. Its surface force refers to the orbit of rotation of the electric dipoles within the elementary particles, the outer surface of the integrated power, the difference of magnetic force△F_e,△F_b. By (2.1), (2.2),△F_e, △F_b:

$$\begin{cases} \Delta F_e = \dfrac{(ne)^2}{4\pi\varepsilon_0(2K_r\overline{R}_\alpha)^2}\left[\dfrac{1}{\sqrt{1-\beta^2(1+K_r)^2}}-\dfrac{1}{\sqrt{1-\beta^2(1-K_r)^2}}\right] & (3.11-1) \\ \Delta F_b = \dfrac{(ne)^2\beta^2(1-K_r^2)}{4\pi\varepsilon_0(2K_r\overline{R}_\alpha)^2}\left[\dfrac{1}{\sqrt{1-\beta^2(1+K_r)^2}}-\dfrac{1}{\sqrt{1-\beta^2(1-K_r)^2}}\right] & (3.11-2) \end{cases}$$

Simultaneous equations (3.11) have:

$$\Delta F_e - \Delta F_b = \frac{(ne)^2}{4\pi\varepsilon_0 (2K_r \overline{R}_\alpha)^2}\left[\frac{1-\beta^2+K_r^2\beta^2}{\sqrt{1-\beta^2(1+K_r)^2}} - \frac{1-\beta^2+K_r^2\beta^2}{\sqrt{1-\beta^2(1-K_r)^2}}\right] \quad (3.12)$$

The Table 2.2, of N_a=1、n=1、β=1-10^{-9}、K_r=1302.6×10^{-13} value (3.1) into (3.12), we have:

$$\Delta F_e - \Delta F_b + F_{n\alpha} = \frac{e^2}{4\pi\varepsilon_0 \overline{R}_\alpha^2}\left[8.675331\times 10^{13} n^2 + \beta\left(\frac{2h\varepsilon_0 c}{e^2}\right)\right] >> 0 \quad (3.13)$$

Which, together electric force outward from elementary particle fluctuations inside track, or magnetic forces inward, comprehensive electrical, magnetic force point fluctuations outside the orbit. The centrifugal force F_{na} electricity, magnetic force △F_e, △F_b compared clearly insignificant. Similarly, if let a = 0, the integrated electricity, magnetic forces also point to the fluctuations outside the orbit, but point to the inside of the spin-orbit. Therefore, the entire elementary particle surface along fluctuations, spin-orbit motion, integrated electric and magnetic field force in the spin-orbit direction of changes. By (3.4), we know that the entire the elementary particle surface electric and magnetic field force is much smaller than the charged particles outside of electric and magnetic forces. The overall synthesis characteristics of electric and magnetic forces capable of elementary particles firmly constrained fluctuations, spin-orbit. The chapter concludes with a comparative demonstration will feature in Table 3.1.

3.3 Charged elementary particles outside The interaction strength

3.3.1 Charged elementary particle interaction strength within Computing

By figure 3.3 shows, set in the elementary particles by n of electric dipole and a positive charged particles. When we calculated at point A and point B, and C of the electric force between charged particles F_{ex1}, F_{ex2}, make AC = L_x, the interval between two of electric dipole in2 $\Delta\overline{R}_\alpha$, because:

Reference (3.6-1), (3.9) equations have to:

$$\begin{cases} EC = 2K_r\overline{R}_\alpha & (3.14-1) \\ AE = (2n-1)\Delta\overline{R}_\alpha & (3.14-2) \\ L_x = \sqrt{(2K_r\overline{R}_\alpha)^2 + \left[(2n-1)\Delta\overline{R}_\alpha\right]^2} & (3.14-3) \end{cases}$$

$$\begin{cases} F_{ex1} = \dfrac{e^2\left[1-\beta^2(1+K_r\cos\alpha)^2\right]}{4\pi\varepsilon_0\left[2n\Delta\overline{R}_\alpha\right]^2} \quad (\sin\phi = 0) & (3.15-1) \\ F_{ex2} = \dfrac{-e^2\left[1-\beta^2(1+K_r\cos\alpha)^2\right]\cos\phi}{4\pi\varepsilon_0 L_x^2\left[1-\beta^2(1+K_r\cos\alpha)^2\sin^2\phi\right]^{1.5}} & (3.15-2) \end{cases}$$

Will make F_{ex1}/F_{ex2}=-1, equations (3.14) into (3.15) equations were checking:

$$\Delta\overline{R}_\alpha = K_r\overline{R}_\alpha\sqrt{\frac{1-\beta^2(1+K_r\cos\alpha)^2}{\left[n^2(n-0.5)\right]^{2/3}-(n-0.5)^2}} \qquad (3.16)$$

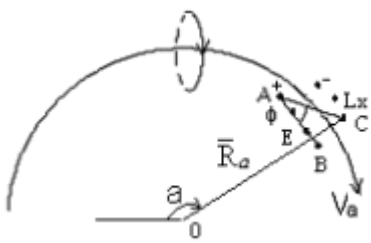

Figure 3.3 charged basic internal charged particles electric field force diagram

Make N_a = 3, into (2.11), to: β = 0.9989472725. For n = 3, table 2.1 to: K_r = 10.5879 x 10^{-5}. Generation into (3.16), to: $\Delta\overline{R}_\alpha \Big/ K_r\overline{R}_\alpha = 0.0366927$. That stagger the interval between the electric dipole is far less than the inside of the electric dipole is, load power distance between particles.

By the same token, if make n = 1, look-up table 2.2: K_r = 25.224 x 10^{-5}, substituting (3.16), type: $\Delta\overline{R}_\alpha \Big/ K_r\overline{R}_\alpha = 0.082844$, explain with electric dipole number n decrease, interval increases.

3.3.2 Charged particle surface force strength calculation

Set in the elementary particles by n of electric dipole and a surplus of charged particles, because of the excess unpaired distribution of charged particles is always in the inside of the spin track, and $\Delta\overline{R}_\alpha << K_r\overline{R}_\alpha$, we can carry on the simplified

calculation. In a=π, the inside of the n+1 charged particles on the lateral n a charged particle synthesis of electric field attractive processed $\triangle F_e$ maintenance, integrated magnetic repelling force processed $\triangle F_b$, respectively:

$$\begin{cases} \Delta F_e = \dfrac{n(n+1)e^2}{4\pi\varepsilon_0(2K_r\overline{R}_\alpha)^2}\left[\dfrac{1}{\sqrt{1-\beta^2(1+K_r)^2}}-\dfrac{1}{\sqrt{1-\beta^2(1-K_r)^2}}\right] & (3.17-1) \\ \Delta F_b = \dfrac{n(n+1)e^2\beta^2(1-K_r^2)}{4\pi\varepsilon_0(2K_r\overline{R}_\alpha)^2}\left[\dfrac{1}{\sqrt{1-\beta^2(1+K_r)^2}}-\dfrac{1}{\sqrt{1-\beta^2(1-K_r)^2}}\right] & (3.17-2) \end{cases}$$

Movement of elementary particles along the track motion of centrifugal force F_{na} is:

$$F_{n\alpha} = \frac{mv_\alpha^2}{\overline{R}_\alpha} = \frac{h\beta c(\sqrt{N_\alpha}+\cos\alpha)^2}{2\pi\overline{R}_\alpha^2(N_\alpha-1)} \qquad (3.18)$$

The equations (3.17) and (3.18) - united stand:

$$\Delta F_e - \Delta F_b + F_{n\alpha} =$$
$$\frac{e^2}{4\pi\varepsilon_0\overline{R}_\alpha^2}\left\{\begin{array}{l}\dfrac{n(n+1)(1-\beta^2+K_r^2\beta^2)}{(2K_r)^2}\left[\dfrac{1}{\sqrt{1-\beta^2(1+K_r)^2}}-\dfrac{1}{\sqrt{1-\beta^2(1-K_r)^2}}\right] \\ +\left(\dfrac{2h\varepsilon_0 c}{e^2}\right)\beta\dfrac{(\sqrt{N_\alpha}+\cos\alpha)^2}{N_\alpha-1}\end{array}\right\}$$

(3.19)

Make n = 2, N_a=3、β=0.9989472725、a=π, from table 2.1 to: K_r = 1.48881 x 10^{-4}, generation into (3.19), to:

$$\Delta F_e - \Delta F_b + F_{n\alpha} = \frac{e^2}{4\pi\varepsilon_0\overline{R}_\alpha^2}\left[\begin{array}{l}4.4389849\times10^5 \\ +0.2679492\beta\left(\dfrac{2h\varepsilon_0 c}{e^2}\right)\end{array}\right] >> 0 \qquad (3.20)$$

With equations (3.11), (3.12) and (3.13) - similar to charged elementary particles comprehensive electric and magnetic field strength in a=0、π is pointing in the direction of wave rail lateral, but strength is much smaller than neutral particles. Also change in the direction of the resultant force along the spin track, also is far less than that of (3.4) - calculation of charged particles inside and outside comprehensive

electric and magnetic field strength. The whole electric and magnetic field force synthesis characteristics can also be charged elementary particles firmly constraints in the fluctuation, the spin track.

3.4 The basic particles in internal wave direction other Position and spin direction orbit inner side and outside Of the interaction force strength calculation

3.4.1 Elementary particle internal interactions in the wave direction Other position strength calculation

Set a neutral elementary particles composed of n to the electric dipole. According to (3.1), each pair of electric dipole along the wave produced by the orbital motions centrifugal force F_{na} is:

$$F_{n\alpha} = \frac{m v_\alpha^2}{n\overline{R}_\alpha} = \frac{h\beta c}{2\pi n \overline{R}_\alpha^2} \qquad (3.21)$$

By table 2.2, $K_r < 10^{-8}$ and (3.4) results to: $1.4991\times10^{-13} \geq K_{r\bullet} \geq 8.0\times10^{-15}$, Because $K_r\cos a \to 0$, $K_{r\bullet}\cos a \to 0$. We can put each pair of electric dipole in positive and load fluctuation rate charged particles are v_a, has nothing to do with position in wave a. Each charged particles along the orbit radius fluctuation $\overline{R}_\alpha$ Aradial are divided into inner and outside two hemispheres, by (2.7) equations: $v_{\alpha 1} = \beta(1+K_{r\bullet})c$, $v_{\alpha 2} = \beta(1-K_{r\bullet})c$ is still poor speed, leading to each charged particles, and the lateral formed in the wave motion of electric and magnetic field force intensity difference. By (3.2) ~ (3.4) and (3.11) equations, n of electric dipole in 2n a charged particle inside and outside comprehensive electric and magnetic field force $\triangle F_{eb\bullet}$ processed for:

$$\Delta F_{eb\bullet} = \frac{2n(0.5e)^2\left[1-\beta^2(1-K_{r\bullet}^2)\right]}{4\pi\varepsilon_0(K_{r\bullet}\overline{R}_\alpha)^2}\left[\frac{1}{\sqrt{1-\beta^2(1+K_{r\bullet})^2}} - \frac{1}{\sqrt{1-\beta^2(1-K_{r\bullet})^2}}\right]$$

(3.22)

Will (1.2 1) into (3.21), to $\beta=1\text{-}10^{-9}$, $\triangle F_{eb\bullet} - F_{na} >> 0$, simultaneous (3.21) and (3.22), to:

$$\frac{e^2}{4\pi\varepsilon_0\overline{R}_\alpha^2}\left\{\frac{2n\left[1-\beta^2(1-K_{r\bullet}^2)\right]}{4K_{r\bullet}^2}\left[\begin{array}{c}\dfrac{1}{\sqrt{1-\beta^2(1+K_{r\bullet})^2}}\\ -\dfrac{1}{\sqrt{1-\beta^2(1-K_{r\bullet})^2}}\end{array}\right]-\beta\left(\frac{2h\varepsilon_0 c}{ne^2}\right)\right\}>>0 \quad (3.23)$$

The conditions of (3.23) - is $1/\beta\text{-}1 > K_{r\bullet}\geq 8.0\times10^{-15}$. Will $K_{r\bullet}=8.0\times10^{-15}$ generations into (3.23), for n=1, a: processed:$\triangle F_{eb\bullet}/F_{na}>>1$, the results are shown in table 3.1. These results show that neutral elementary particles within each charged particles comprehensive electric and magnetic field force direction along the R_a to fluctuations in the inside of the track, is a multiple centrifugal force in the direction of the wave astronomy.

Similarly, the charged particle, because most of the energy is reflected on the remaining charged particles, so:

$$F_{n\alpha}=\frac{mv_\alpha^2}{\overline{R}_\alpha} \quad (3.24)$$

$$\Delta F_{eb\bullet}=\frac{(2n+1)(0.5e)^2\left[1-\beta^2(1-K_{r\bullet}^2)\right]}{4\pi\varepsilon_0(K_{r\bullet}\overline{R}_\alpha)^2}\left[\frac{1}{\sqrt{1-\beta^2(1+K_{r\bullet})^2}}-\frac{1}{\sqrt{1-\beta^2(1-K_{r\bullet})^2}}\right]$$

(3.25)

Simultaneous (3.24) and (3.25), to $\triangle F_{eb\bullet}-F_{na}>>0$, to:

$$\frac{e^2}{4\pi\varepsilon_0\overline{R}_\alpha^2}\left\{\frac{(2n+1)\left[1-\beta^2(1-K_{r\bullet}^2)\right]}{4K_{r\bullet}^2}\left[\begin{array}{c}\dfrac{1}{\sqrt{1-\beta^2(1+K_{r\bullet})^2}}\\ -\dfrac{1}{\sqrt{1-\beta^2(1-K_{r\bullet})^2}}\end{array}\right]-\beta\left(\frac{2h\varepsilon_0 c}{e^2}\right)\right\}>>0$$

(3.26)

Make $\beta=0.9987108301$、（$N_a=\infty$）、n=2、$K_{r\bullet}=8.0\times10^{-15}$, into(3.26), to:

$$\frac{e^2}{4\pi\varepsilon_0\overline{R}_\alpha^2}\left[3.078125\times10^{15}-\beta\left(\frac{2h\varepsilon_0 c}{e^2}\right)\right]>>0 \quad (3.27)$$

Make$\beta=1\text{-}10^{-9}$、n=2、$K_r=8.0\times10^{-15}$, andinto（3.26）to:

$$\frac{e^2}{4\pi\varepsilon_0 \overline{R}_\alpha^2}\left[3.493835\times10^{18}-\beta\left(\frac{2h\varepsilon_0 c}{e^2}\right)\right]>>0 \qquad (3.28)$$

3.4.2 Elementary particle movement of internal and external spin track Motion the e and h field force strength calculation results

To charged particles inside and outside surface and the basic particle surface comprehensive electric and magnetic field, the results shown in table 3.1. To see that all the elementary particles, charged particles, only fluctuation, spin, rotation speed is $\vec{\nu}\geq c$ to stable; Elementary particles within each charged particles along the fluctuation, the movement of the spin track, inside and outside the two hemispheres of electric and magnetic field force $\triangle F_{eb}$. processed Feb ▪ always pointing in the direction of wave orbital medial, size is fundamental particles along the fluctuation track movement form centrifugal F_{na} astronomy multiples; And far outweigh its fluctuation track along the surface of the whole elementary particles movement form comprehensive electric and magnetic field strength of $\triangle F_{eb}$, (because $K_r >> K_{r\text{-}}$); The latter always pointing in the direction of wave rail lateral; So, the entire elementary particles can be firmly constraints in the fluctuation, the spin track.

Charged particles, the basic particle surface comprehensive electric and magnetic field force strength comparison table 3.1

Particlecategory	v_a	K_r $K_{r\text{-}}$	$\triangle F_{eb(r)}/F_{na}$	Calculation formula
Charged particles	（1-10^{-9}）c	$K_{r\text{-}}=8.0\times10^{-15}$	5.0991×10^{15}	（3.4）
Electrically neutral elementary particles	（1-10^{-9}）c	$K_r=1.306\times10^{-10}$	6.3307×10^{11}	（3.13）
		$K_{r\text{-}}=8.0\times10^{-15}$	1.0198×10^{16}	（3.23）
Charged elementary particles	0.998947273c	$K_r=1.4888\times10^{-4}$	1.20996×10^{4}	（3.20）
	0.998710830c	$K_{r\text{-}}=8.0\times10^{-15}$	2.2504×10^{13}	（3.27）
n =2	（1-10^{-9}）c	$K_{r\text{-}}=8.0\times10^{-15}$	2.5496×10^{16}	（3.28）

So, each charged particle far outweigh the elementary particles on the surface of the comprehensive electric and magnetic field strength can be unlimited to wave orbital medial shrinkage? The answer is: not! First, different elementary particles fluctuation orbit radius R_a lpha represent different energy, should be the elementary particles inside the inherent characteristics. Inward contraction means that energy increases self into infinite, violation of the law of conservation of energy. Secondly, all

of the charged particles, the fluctuation, spin, rotation orbit, can stable existence is the precondition of its speed is $\vec{v} \geq c$. We cut the ball every charged particles entity into 2n, see figure 3.4.

By (2.1), (2.2), too: when speed is $\vec{v} = c$, integrated electric and magnetic field interactions only occurs in the vertical direction the speed, the lateral plane of two small pieces, each other between adjacent plane electricity, magnetic force is zero. So, by (3.4), each charged particles internal comprehensive electric and magnetic field force as $\Delta F_{eb\bullet}$, as follows:

$$\Delta F_{eb\bullet} = \frac{e^2\left[1-\beta^2(1-K_{r\bullet}^2)\right]}{4\pi\varepsilon_0 \overline{R}_\alpha^2 (4K_{r\bullet}^2 \times 4n)} \times \left[\frac{1}{\sqrt{1-\beta^2(1+K_{r\bullet})^2}} - \frac{1}{\sqrt{1-\beta^2(1-K_{r\bullet})^2}}\right] \tag{3.29}$$

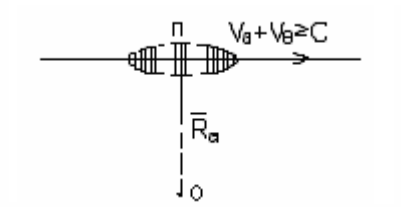

Figure 3.4 charged particles inside the subdivision schemes

Theoretically, slice the n value size there is no limit, but it can reflect the basic particle of the charged particles in the different combination structure, can normal environment, the orbit of wave motion position of deformation degree of stretch. It must adjust instantly, always meet in table 3.1 $\triangle F_{eb\bullet} \geq \triangle F_{eb}$, elementary particles can be properly, firmly constraints in the fluctuation, the spin track. Provide the self adjusting, the tensile deformation and from can state the conditions of the environment around other charged particles of the opposite sex, charged particles between electric field. This is for elementary particles, nuclei, atomic units must be positive and load all the micro particle charged particles, with positive and negative, the basic particle of symbiosis. (See chapter 7 nucleus structure model and the nuclear force forming principle).

Photons, neutrinos only consists of a pair of electric dipole, can no longer separation, and the same, rotate speed, track is cylindrical helical, and so is stable. Electronic more than only a charged particle, also can no longer separation, so also is stable. By (3.16), charged elementary particles along the fluctuation track movement

direction, internal each distance between charged particles with the number of electric dipole n laid great decreases and the interval between big and small beside. The electric and magnetic field inside the natural cause interactions imbalance, split decays either. To $\pi^{\pm}$ can only be protons, within the nucleus. The reason for this is internal only 2 of electric dipole and charged particles. Each charged particles interval symmetrical on both sides are equal, just show the internal comprehensive electric and magnetic field force between the charged particles is just balance, and a corresponding stable around the external "state" of the environment, both protons, nuclei formed special structure within the nuclear force, see chapter 6 and nuclear physics. On the proton core, composed of 6 to the electric dipole, for 6 to electric dipole just in same fluctuations orbital plane synchronous movement, spacing stagger 60 DHS, charged particles positive and negative switch position, this special structure to make proton has a special stability characteristics of the core. In addition to the above five kinds of particles can be concluded that: all other elementary particles, because of the electromagnetic force between internal charged particles are equilibrium state, so is not stable.

4 Elementary particle, strong and weak electricity, Magnetic interaction unity

4.1 The uncertainty relation

4.1.1 Unity the principle of set upon the basis

Existing statistical theory of quantum mechanics theory of elementary particles and conditions within the nucleus, strong and weak electricity, magnetic interaction is the characteristic length, whether to have produced neutrinos, role to distinguish the distance from the surface phenomenon. Has been proved in front of the book, the elementary particles energy origin is electromagnetic field energy.Internal super function and division decay is the weak interaction of charged particles and electric dipole along the fluctuation track movement of electric and magnetic field force acting between themselves and each other. So, we have every reason to further corollary: elementary particles inside the super function, along with the weak interaction of neutrino formation, interaction with electric and magnetic field is the same; Is the basic of particles with different energy fluctuation, spin quantization in the process of transition between the stationary orbit, n of electric dipole (charged particles and a surplus) collection divided, electricity, magnetic energy release of radiation process.

As long as we can from this book elementary particles quantization stationary vertical double elliptical orbit model, using classical electrodynamics and energy relativity principle, from an average of energy and momentum conservation, momentum, charge number, baryonic number are the basic laws of physics, according to the basic particles along the orbit of the distance, speed, time, the relevance of the derived four functions are the basic particles, split the decay product changes life, energy and the motion state equation, is strict prove the above argument.

4.1.2 The uncertainty relation

According to the basic particles moving along the orbit model, from all the elementary particles sprayed out of a particle accelerator, shall have volatility, spin, and went into the quantization of cylindrical helical compound movement track. Precession speed AAv_j and spin speed v_θ, mutually perpendicular direction, movement track as shown in figure 1.2 and figure 4.1.

Chart description: spray type basic particle track is not from the point source to

the collision between a straight line, but a piano, the thickness of the cylinder to the diameter of the fluctuation track $2R_a$, see figure 1.2 and figure 4.2, which indicated that the micro particle wave particle duality nature. Hybrid orbital motion equations (1.2) and (2.17) equation should be extended to:

$$\begin{cases} R_\alpha = \dfrac{h}{2\pi m v_\alpha} & (4.1-1) \\ R_\theta = \dfrac{h}{2\pi m v_\theta} & (4.1-2) \\ R_\theta = R_{\theta 0} - R_\alpha \cos\alpha & (4.1-3) \\ \alpha = N_\alpha \theta & (4.1-4) \\ \int_0^{2\pi} R_\theta d\theta = \sqrt{N_\alpha} \int_0^{2\pi} R_\alpha d\alpha & (4.1-5) \\ v_j = v_\theta & (4.1-6) \\ Z = v_j t & (4.1-7) \end{cases}$$

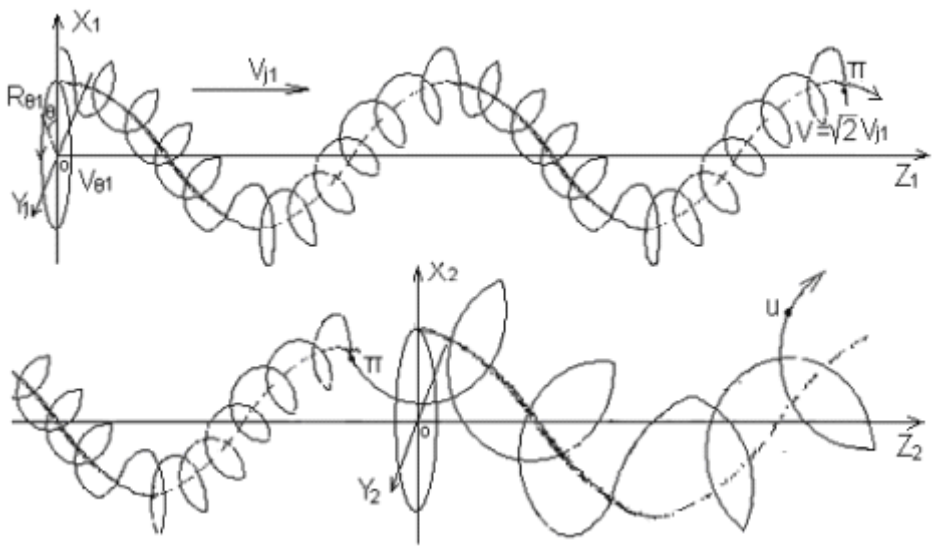

Figure 4.1 elementary particles along the fluctuation, spin, move into the compound orbit in split, decay principle diagram

Front has been proved: static fundamental particles speed fluctuation $v_a \rightarrow c$, along the fluctuation, the spin quantization stationary vertical double.

Moving in elliptical orbit, because of the fluctuation, the speed of the spin direction, and to follow the law of conservation of momentum and the average momentum, energy, will not happens electromagnetic energy radiation. So, only in the injection

type fluctuations, spin, the motion of the complex motion in orbit, the chapter 3 of the analysis shows that the fluctuation, spin, precession direction, a=π/2， 3π/2, electric dipole vibration coefficient K_r value is uncertain, elementary particle energy only in a=π/2 ， 3π/2, to discontinuous changes, and appeared precession direction of electromagnetic energy radiation. (of course, also can produce ionization collisions in environmental media, such as energy loss). Such as electromagnetic wave radiation of energy loss, the fluctuations of elementary particle track N_a quantum number increasing, spin, precession direction speed v_θ 、 v_j decreases gradually, the basic particle energy will gradually reduced. When the N_a 、 v_θ and v_j after changes to a certain degree, the basic particle decay; Split the decay product number of the quantum fluctuations of N_a decrescent, v_θ、v_j, another the next level of electromagnetic radiation and energy loss and split the decay process; Until its internal structure, energy, motion to adapt to the environment.

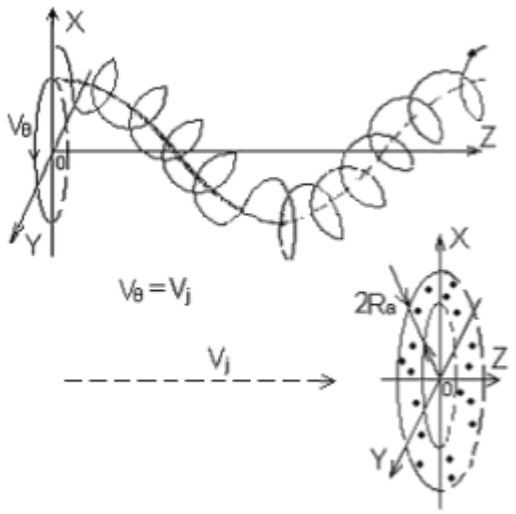

Figure 4.2 basic particle formation wave particle duality principle diagrams

In $\pi^{\pm}$, for example, by the energy principle of relativity, the injection hybrid orbital motion of the moving average quality $\overline{m}_\pi$ and static average quality $\overline{m}_{\pi 0}$ for the relationship between:

$$\overline{m}_\pi = \frac{\overline{m}_{\pi 0}}{\sqrt{1-\beta^2/N_\alpha}} \qquad (4.2)$$

When it is in moving into electromagnetic waves or other forms of energy radiation loss occurs, the quantum fluctuations interest and interest of N_{ai} and N_{ai+1}

track transition motion when the energy difference between $\Delta\overline{m}_{\pi i}c^2$ for:

$$\Delta m_{\pi i}c^2 = m_{\pi 0}c^2\left(\frac{1}{\sqrt{1-\beta_i^2/N_{\alpha i}}}-\frac{1}{\sqrt{1-\beta_{i+1}^2/N_{\alpha i+1}}}\right) \qquad (4.3)$$

By classical electrodynamics principle, fundamental particles in the moving direction for speed v_j changes lead to electromagnetic field energy radiation power $P_{e\|}$ for:

$$P_{e\|} = \frac{e^2\left|\dot{v}_j\right|^2}{6\pi\varepsilon_0 c^3\left[1-\left(v_j/c\right)^2\right]^3} \qquad (4.4)$$

Fundamental particles along the spin, the motion orbit of each cycle for the $T_{\theta i}$ by (1.4-2) type:

$$T_{\theta i} = \frac{L_{\theta i}}{v_{\theta i}} = \frac{2\pi R_{\theta i0}N_{\alpha i}}{\beta_i c\sqrt{N_{\alpha i}-1}} = \frac{hN_{\alpha i}}{m_{\pi 0}(\beta_i c)^2}\sqrt{1-\frac{\beta_i^2}{N_{\alpha i}}} \qquad (4.5)$$

Its average acceleration $\dot{v}_j$ should be the average rate of change of the spin precession direction speed v_j cycle, too:

$$\dot{v}_j = \frac{c\left(\frac{\beta_i}{\sqrt{N_{\alpha i}}}-\frac{\beta_{i+1}}{\sqrt{N_{\alpha i+1}}}\right)}{\frac{1}{2}\left(T_{\theta i}+T_{\theta i+1}\right)} \qquad (4.6)$$

By (1.6), (4.2), we have:

$$R_{\theta 0i} = \frac{h\sqrt{N_{\alpha i}-1}}{2\pi m_{\pi 0}\beta_i c}\sqrt{1-\frac{\beta_i^2}{N_{\alpha i}}} \qquad (4.7)$$

Similarly, β_i value is calculated by the formula (2.11) can be simplified as:

$$\frac{\beta_i}{1-\beta_i^2} = 2\sqrt{2}\left(\frac{2h\varepsilon_0 c}{e^2}\right)\frac{\sqrt{N_{\alpha i}}}{\sqrt{N_{\alpha i}-1}} \qquad (4.8)$$

To $\frac{2h\varepsilon_0 c}{e^2} = \frac{1}{a_c}$, generation into (4.8), to:

$$\beta_i = \frac{\sqrt{32N_{\alpha i} + a_c^2(N_{\alpha i} - 1)} - a_c\sqrt{N_{\alpha i} - 1}}{4\sqrt{2N_{\alpha i}}} \qquad (4.9)$$

A fundamental particles each spin, electromagnetic wave radiation energy into dynamic cycle for $W_{e\|i}$, by (4.4) ~ (4.9), to:

$$W_{e\|i} = \frac{1}{2}P_{e\|i}(T_{\theta i} + T_{\theta i+1})$$

$$= \frac{e^2 c\overline{m}_{\pi 0}\left(\frac{\beta_i}{\sqrt{N_{\alpha i}}} - \frac{\beta_{i+1}}{\sqrt{N_{\alpha i+1}}}\right)^2}{1.5\pi\varepsilon_0 h\left[\left(1 - \frac{\beta_i^2}{N_{\alpha i}}\right)^3 + \left(1 - \frac{\beta_{i+1}^2}{N_{\alpha i+1}}\right)^3\right]\left(\frac{N_{\alpha i}}{\beta_i^2}\sqrt{1 - \frac{\beta_i^2}{N_{\alpha i}}} + \frac{N_{\alpha i+1}}{\beta_{i+1}^2}\sqrt{1 - \frac{\beta_{i+1}^2}{N_{\alpha i+1}}}\right)}$$

（4.10）

A K_{ti} for time coefficient, make $K_{ti} = \Delta\overline{m}_{\pi i}c^2 / W_{e\|i}$. Because $K_{ti} >> 1$, jet type elementary particles should be N_{ai} and N_{ai+1} quantization stationary orbit passes between K_{ti} time step transition radiation, the energy of the oscillation will $\Delta\overline{m}_{\pi i}c^2$ all out, and then turn to the next level track; Or in N_{ai} and N_{ai+1} fluctuations between quantum number still exist K_{ti} the fluctuations of the transition of a mixed number quantum number; So, the life of the fundamental particles T should be:

$$T = \sum_{i=1}^{Nai}\frac{K_{ti}}{2}(T_{\theta i} + T_{\theta i+1}) \qquad (4.11)$$

To (4.3) ~ (4.10) - integrated into (4.11), and the determination of the equation, too:

$$W_{e\|i}T = \frac{K_i h}{8} \qquad (4.12)$$

The K_i value change with fluctuating interest quantum number N_{ai} calculation results shown in table 4.1.

The change of the calculation results show that K_i value only associated with N_{ai} value, actually has nothing to do with particle rest mass m_0 completely, that is to say: (4.12) - the basic particles of any quality calculation results are the same. This chapter main consideration particle into the moving direction of electromagnetic radiation

energy, the particle collisions with medium, ionization, and other forms of energy loss is not consideration. Obviously, the latter's influence can be neglected. So, this chapter not only reveals the uncertainty relation between forming principle, but also changes with fluctuations N_{ai} quantum number of accurate value.

The K_i value change with fluctuating interest quantum number N_{ai} the results table 4.1

N_{ai}	2	5	10	50
K_i	2.926064	1.536049	1.239385	1.044161
N_{ai}	100	500	1000	5000
K_i	1.021870	1.004341	1.002168	1.000433

By mathematical simulation results and comparison, we can use (4.13) - instead of table 4.1 the results:

$$W_{e\|_i}T = \frac{h}{8}\left(1+\frac{2.16}{N_{\alpha i}}+\frac{3.35}{N_{\alpha i}^2}\right) \qquad (4.13)$$

To basic particles are electrically neutral, there are still changes periodically of the electric and magnetic field, and the same energy origin, follow energy relativity formula (4.2), so the same applies to the above analysis results, the difference only lies in $\beta = 1\text{-}10^{-9}$ is constant.

4.2 Elementary particle life, split the decay product relates To the law of conservation of energy, and momentum

4.2.1 Elementary particles split the decay product service life and the Law of conservation of energy, and momentum equation

Elementary particle energy originated from internal electric dipole magnetic energy oscillations. By (2.9) ~ (2.16) - the results indicated that electric dipole coefficient K_r value, mainly with the basic particle internal electric dipole log n; Electrically neutral basic particles and charged particles K_r value size difference is quite wide, and fluctuations quantum interest of N_{ai} and track the position of a also to have certain relations; In $a=\pi/2$、$3\pi/2$ position, all of the neutral or charged elementary particles, K_r values are uncertain value; At this time, the internal each charged

particles between the electric and magnetic field force is perpendicular to the wave, the spin track radius, the resultant force tends to zero. So in elementary particles under the action of centrifugal force, the fluctuation track the movement of the position of the decay of split occurred only in a=π/2、3π/2. Only in this way, particles and matrix division within the plasma particles decay coefficient of all the electric dipole of K_r can get; And matrix and the plasma particles in a=π/2 location or near the moment when the sum of energy and momentum is still should follow the law of conservation of energy, momentum and energy gradually reduce spontaneous split the decay law of.

Movement of elementary particles along the orbital motion of the average quality of $\overline{m}_i$ and instant quality m_i relationship, by (1.2-1), (1.3-1), (1.5) and (2.8) equations have to:

$$m_i = \frac{\overline{m}_i\left(\sqrt{N_{\alpha i}} + \cos\alpha\right)}{\sqrt{N_{\alpha i} - 1}} \qquad (4.14)$$

Still in $\pi^+ \rightarrow u^+ + \upsilon$ (neutrino) hormone called tau was decay process, for example, in the direction of the wave motion, by (4.2), (4.14), we have:

$$\begin{cases} \dfrac{\overline{m}_{\pi 0}\left(\sqrt{N_{\alpha\pi}} + \cos\alpha\right)}{\sqrt{\left(1-\beta_\pi^2/N_{\alpha\pi}\right)\left(N_{\alpha\pi}-1\right)}} = \dfrac{\overline{m}_{u0}\left(\sqrt{N_{\alpha u}} + \cos\alpha\right)}{\sqrt{\left(1-\beta_u^2/N_{\alpha u}\right)\left(N_{\alpha u}-1\right)}} + m_\nu & (4.15-1) \\ \dfrac{\overline{m}_{\pi 0}\left(\sqrt{N_{\alpha\pi}} + \cos\alpha\right)\beta_\pi c}{\sqrt{\left(1-\beta_\pi^2/N_{\alpha\pi}\right)\left(N_{\alpha\pi}-1\right)}} = \dfrac{\overline{m}_{u0}\left(\sqrt{N_{\alpha u}} + \cos\alpha\right)\beta_u c}{\sqrt{\left(1-\beta_u^2/N_{\alpha u}\right)\left(N_{\alpha u}-1\right)}} - m_\nu c & (4.15-2) \end{cases}$$

Because charged elementary particles wave speed vθi theta I decreases with increasing number of quantum fluctuations N_{ai}, so split decay, quality very small neutrino wave speed direction should be contrary to maternal particles, the jet recoil role to improve the quality of the plasma particles u^+ the sons of light wave velocity. Interactions by chapter 3 basic particle internal structure and analysis can be seen: elementary particles stability condition is various, load interaction of charged particles, electricity, magnetic repelling force, attraction vector and must be far outweigh the centrifugal force. Split decay in a=π/2、（3π/2）, by the charged particle interactions between K_r、$\Delta\overline{R}_\alpha$ change caused by imbalance. By equations (4.15):

$$m_\nu = \frac{\overline{m}_{\pi 0}\left(\sqrt{N_{\alpha\pi}} + \cos\alpha\right)}{\sqrt{\left(1-\beta_\pi^2/N_{\alpha\pi}\right)\left(N_{\alpha\pi}-1\right)}}\left(\frac{\beta_u - \beta_\pi}{1+\beta_u}\right) \qquad (4.16)$$

4.2.2 Parameters of the simulation results

If parent π^+ mesons, plasma u^+ light and electrical dipole moment coefficient in hormone called neutrinos m_υ tau were K_{ri} value, N_{ai}、$\Delta\overline{R}_{\alpha i}$、$\beta_i$ parameters change, is in the Angle of wave $Aa=90^o\sim91^o$ within the interval of the moment, by (4.14), (4.15-1), (4.16), the moment of matrix and plasma particles energy changes with fluctuations N_{ai} quantum number shown in table 4.2. From visible: when N_{au} = 4, π^+ split muon decay into u^+ light quantum number changes when fluctuation range of corresponding: $1242\geq N_{a\pi}\geq110$. The $N_{a\pi}$ value generation into (4.10), (4.13), to π^+ violation of life range for: $4.579289\times10^{-8}\geq T\geq2.832698\times10^{-12}$ (seconds).

Similarly, a range and $N_{a\pi}$、T, the relationship between see table 4.3.

therefore, the life of the fundamental particles directly with particles in internal fluctuation track Angle parameter a=90°~91° interval change of division of speed, although this chapter only to a few a Angle value interval type calculation comparison, readers can see the change trend of calculation and the experimental results perfectly.

The π^+ mesons in a=90°~91° interval split decay instantly energy changes the results table table 4.2

$N_{\alpha\pi}$	$(m_\pi - m_u)\times10^{-28}$ Kg	$N_{\alpha\mu}$	$m_\mu\times10^{-28}$ Kg
2	4.971994843~9106368 72		
3	3.730167878~6925821 41	2	3.763675139~3.717228697
4	3.316109467~3.287172421		
5	3.109056233~3.084790194		
6	2.984816239~2.963549677		
7	2.901986125~2.882843494		
8	2.842820036~2.825278 82		
9	2.798444514~2.782164 65	3	2.823842472~2.795389007
10	2.763929647~2.748675 98		
11	2.736317391~2.721918619		
..	..		
50	2.538513845~2.532248 43		
..	..		
100	2.512896999~2.508511389		
..	..		
110	2.510593818~2.506416136	4	2.510468711~2.488561851
111	2.510386532~2.506228054		

112	2.510 182 98~2.506 043 444		
..	..		
200	2.500 281 559~2.497 196 033		
..	..		
300	2.496 104 525~2.493 589 412		
..	..		
500	2.492 772 936~2.490 827 339		
..	..		
1000	2.490 280 078~2.488 905 709		
..	..		
1242	2.489 794 933~2.488 561 947		
1243	2.489 793 32~2.488 560 831	5	2.353 761 653~2.335 390 653
1244	2.489 791 71~2.488 559 718	6	2.259 730 608 ~ 2.243 630 22
..	..	..	..
2000..	2.489 035 519~2.488 064 178	.	..
	..	..	..
3000	2.488 620 942~2.487 827 978	∞	1.883 551 778~1.883 551 778
..	..		
5000	2.488 289 38~2.487 675 235	note	Values are hormone called m_υ were by $N_{a\mu} = 4$ in the results of calculation, and $N_{a\mu}$ =2、3、……Compared to the error is negligible
..	..		
10000	2.488 040 767~2.487 606 544		
...	..		
∞	2.487 792 203~2.487 792 203		

The $\pi^{\pm}$ muon a value range and $N_{a\pi}$,T the relationship between the calculation result table table 4.3

a value range	$N_{a\pi}$ Constituting range	Partide life range (seconds)
90°~90.5°	$187 \geq N_{a\pi} \geq 110$	$2.360281\times10^{-12} \geq T \geq 2.83270\times10^{-12}$
90°~90.75°	$307 \geq N_{a\pi} \geq 110$	$1.712236\times10^{-10} \geq T \geq 2.83270\times10^{-12}$
90°~90.95°	$734 \geq N_{a\pi} \geq 110$	$5.587989\times10^{-9} \geq T \geq 2.83270\times10^{-12}$
90°~90.99°	$1083 \geq N_{a\pi} \geq 110$	$2.647643\times10^{-8} \geq T \geq 2.83270\times10^{-12}$

5 Microwave field characteristics of the transmission Principle and parameter calculation

5.1 Microwave field characteristics and parameters Are calculated

5.1.1 Microwave field characteristics

In the scientific community existing on the stability of the particle detection technology and knowledge level, combined with this theoretical model, can be determined for stable particle in the universe detection task has been finished. So, evenly distributed in space, the long-term stability of 2.73 K bold background of microwave radiation is caused by what? In protons, electrons and photons (electromagnetic waves), and choose between neutrinos, can only be electromagnetic waves.

Front has been proved that electromagnetic waves and photons are similar, when electromagnetic wave energy big light when it is photons, only consists of a pair of electric dipole, the fluctuation, the velocity is the speed of light c, orbit for cylindrical helical. When the electromagnetic wave energy small light when it becomes neutrino campaign to medium electromagnetic field shock wave. Because neutrinos are electrically neutral appearance elementary particles, low quality, and other particles, and atomic and molecular interaction is very weak, so have the special characteristics of penetration and diffusion. Inevitable in a similar gas molecular motion state evenly spread in the vast space, the physical characteristics can be reference to analysis and calculation of gas molecules kinematics law of thermodynamics.

5.1. 2 Microwave field parameters are calculated

By molecular dynamics and the universe space 2.73 K in bold background microwave radiation characteristics of a microwave average energy for $\overline{W_v}$:

$$\overline{W_v} = 1.5KT \quad \text{（K is the Boltzmann constant）} \qquad (5.1)$$

Will the AAT = 2.73 value generation into (5.1), to: $\overline{W_v}$=5.65379451×10^{-23}J, By the energy theory of relativity to: $\overline{W_v} = \overline{m_v}c^2$, $\overline{m_v}$=$6.290694778\times10^{-40}$Kg, root mean square velocity is:

$$\overline{v} = \sqrt{\frac{3KT}{\overline{m}_v}} = \sqrt{2}c \qquad (5.2)$$

Will to $\overline{m}_v$, T = 2.73 value generation into (5.2), to: $\overline{v} = \sqrt{2}c$, (directly (5.1), $\overline{W}_v = \overline{m}_v c^2$ generation into (5.2), the result is the same, and the temperature T.) That microwave fluctuations, rotate speed and photon exactly the same, all is the speed of light. Because of fluctuation, the velocity is constant c, so for microwave, the speed of gas molecules in different temperature distribution curve should be changed to microwave energy distribution curve. Thus, microwave and photon neutrinos are only one, only energy size difference.

We by the surface of the earth, the sun for microwave, hydrogen molecular kinetic energy, and gravitational potential energy compared with gravity density change, analyze the characteristics of the microwave diffusion, the results shown in table 5.1.

Hydrogen molecules, microwave kinetic energy, gravitational potential energy and diffusion characteristics calculation results table 5.1

category	Kinetic energy (J)	Gravitational potential energy (J)	Gravity density distribution
Using the formula	$\overline{W}_d$ =1.5KT	$\overline{W}_g$ =GM$_1$ $\overline{m}_2$ / R	N_f=N_0e $^{-mgHi/kT}$
microwave The earth	5.653794 51×10^{-23}		H_f=1m,H_2=50000m
		3.944365837 ×10^{-32}	N_f=N_0, N_2=N_0
Thesun		1.189891687 ×10^{-28}	N_f=N_0, N_2=N_0
hydrogen The earth	6.1715413×10^{-21}	2.09866509×10^{-19}	N_f=N_0, N_2=0.671N_0
Thesun	1.299130 15×10^{-19}	6.33101556×10^{-16}	N_f=N_0, N_2=0.591N_0
Note	Microwave temperature take 2.73 K, and the earth's surface hydrogen take 298 K, the surface of 6273 K. Assume that hydrogen without decomposition, ionization, temperature is constant.		

Comparing the calculation results can be seen, the earth, the sun gravitational potential energy of hydrogen are far outweigh the kinetic energy, gravitational density distribution in $N_1 > N_2$, can prevent hydrogen molecules spread into space. To the gravitational potential energy is far less than the kinetic energy of the microwave. Is the sun that belongs to medium quality of stars in the universe, the microwave gravitational potential energy only kinetic energy of the 2.105 x 10^{-6} times!!!! Have no

influence gravity density distribution changes with height. Moreover, at the speed of light wave and move into the neutrino has extremely strong penetration performance. Any substance composed of atoms, molecules container or planets, stars, in the presence of the neutrino is "transparent". So, unless the supermassive stars or black holes on the edge of the strong gravity field can't stop neutrino internal evenly spread in the whole universe space and stars, forming the omnipresent neutrino field and space evenly distributed in the 2.73 K bold microwave background radiation field.

5.2 Electromagnetic wave propagation theory and Parameter calculation

We know from the fluctuation of the laws of physics: any energy wave must have a media of communication, early have not yet found that neutrinos, think is a transverse wave; electromagnetic wave is only transmitted in solid medium. Michelson use optical methods and measure to earth absolute movement of historical conditions, the scientific community media of propagation of electromagnetic waves will temporarily leave out also can understand.

Now, the book has proved the photon and neutrinos are composed of a pair of electric dipole, all at the speed of the wave, the cylindrical helical orbit; Photons in the electric dipole rotation angular velocity and angular velocity fluctuation is same, can show in the fluctuation, the motion characteristics of electromagnetic wave, see figure 2.4; Neutrino because of electric dipole in rotation angular velocity is the photon, hormone called N_u were $343323 \geq N_\upsilon \geq 5991$, hormone called N_u were (see chapter 2); The electromagnetic wave frequency is the same times, hormone called energy photon N_υ were to show the variation characteristics of transient electromagnetic field in the scientific community is still not aware of; The omnipresent, uniform distribution of magnetic dipole of neutrino and early people think "etheric field" how similar!

By molecular dynamics and gas elastic medium wave propagation theory, the gas molecules adiabatic index r for:

$$r=C_p/C_v=1+2/i \qquad (5.3)$$

(C_p type is the gas constant pressure heat capacity, C_v constant heat capacity, i for molecular translational and rotational degrees of freedom). Neutrinos, into the dynamic track can be regarded as piano, translational degree of freedom for 2, the rotation of the electric dipole of freedom is 2, generation of (5.3) in type, too: r = 1.5.

According to the section of neutrino uniform diffusion distribution characteristics, can use ideal gas of the propagation of logitudinal wave velocity formula:

$$v_i = \sqrt{\frac{rRT}{u}} = c \qquad (5.4)$$

Will r=1.5, R for the universal gas constant, T=2.73K, u= $\overline{m}_\nu$, $\overline{m}_\nu = \overline{W}_\nu / c^2$, N_A=3.746712×10^{-16}Kg/mol, and in (5.4), to: v_j=2.99792436×10^8m/s, it is the speed of light c! And has nothing to do with the temperature of the blackbody microwave radiation! Experiments have determination; maxwell's equations of electromagnetic field also have been proved theoretically, the electromagnetic wave is transmitted at the speed of light. But how can is a transverse wave, electromagnetic wave in gas state distribution of neutrino field spread? And neutrino field propagation speed of longitudinal wave and happens to be the speed of light, it can't be coincidence?

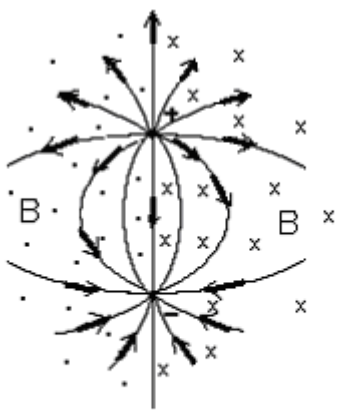

图5.1 电磁振荡源形成的电力线
与被极化的中微子电偶极矩定向
排列示意图 "→"代表电偶极矩

Figure 5.1 electromagnetic oscillation source formation of power line and the polarization of the neutrino electric dipole moment directional arrangement plan ″→"on behalf of the electric dipole moment

Detailed analysis of the mechanism of electromagnetic wave propagation in the neutrino field, it is not hard to find, it with solid material principle of transverse shear deformation of the spread in different. When an electromagnetic vibration source, we can simplify it for magnetic dipole oscillation, in neutrino field generated by the electric and magnetic fields as shown in figure 5.1, in high frequency low magnetic field, the electric dipole part of the neutrino will be formed orientation polarization photons, namely a hormone called N_u were gamma $N_\gamma = 1$. Be directional polarization of photons

in the original direction of rail current shown in figure 5.2. Obviously, this is the polarization within the photonic form of electric dipole moment directional arrangement should be completely with electromagnetic vibration source of power lines coincide, see figure 5.1, but just the opposite directions.

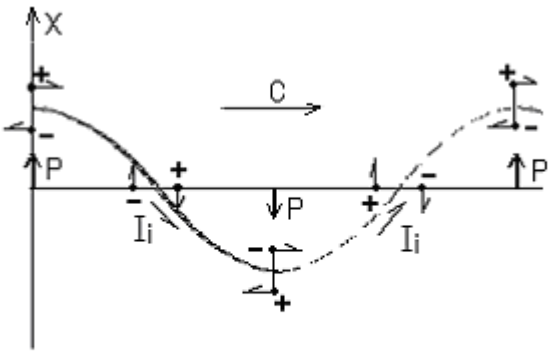

图5.2 被极化定向排列的中微子内部
位移电流I_i形成示意图
"→"代表电偶极矩

Figure 5.2 is polarized directional arrangement of neutrino internal displacement current Ii formation schematic diagram "→"on behalf of the electric dipole moment

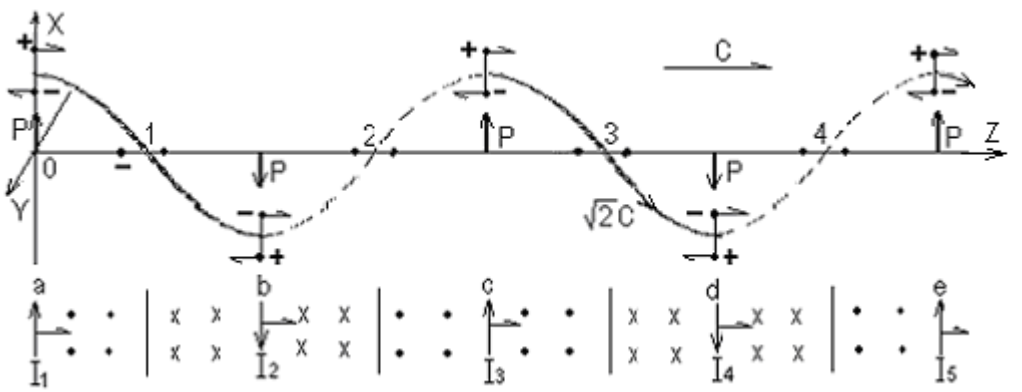

Figure 5.3 is the polarization direction of the photons in the exciting field of you moving force analysis of the current

By polarization direction of the photon along the original track movement direction displacement current generated, the exciting field forming principle is shown in figure 5.3. Since the displacement current in the exciting field under the action of the Lorentz magnetic force just pointing in the direction of photon precession.

As in the Z axis 0-1 the photon wave, into orbit, the displacement current I_1 produce a section of the magnetic field; When photons run to 1-2 rail section, the I_2

displacement current in section b magnetic force under the action of the precession v_j direction advance; I_3 displacement current then generate c section of the magnetic field; ..... Similar recurrence is forming the photon, movement, the transmission of electromagnetic wave.

To sum up, part of the neutrinos were polarized orientation to keep the original orbit fluctuation, the formation of the precession movement, photons, the electric dipole moment of the directional arrangement of McNamara power lines and displacement current in the equations, the displacement current itself and induction magnetic field. So, electric and magnetic field perpendicular oscillations are caused by the electromagnetic induction electromagnetic inherent apparent physical characteristics, partly by the polarization direction of neutrino photons to keep the original of the speed of light c and movement direction longitudinal also with the speed of light c precession is microscopic nature of electromagnetic wave propagation in the form of waves.

Photon wave particle duality of also can see from this chapter and in figure 2.4 the essence: when electromagnetic vibration source frequency f_1 less than $\overline{m}_v c^2$ /h=8.532644262×10^{10}/s, electromagnetic energy is less than the average energy neutrino field of single neutrino $\overline{m}_v c^2$, it only has to polarization neutrino field medium all the neutrino, in neutrino field in the form of electromagnetic wave propagation in the medium; When frequency $f_2 > f_1$, is enough to completely polarization single neutrinos, making it the fluctuation, and went into orbit of cylindrical spiral line. Internal electric dipole of photon rotation radius $K_r \overline{R}_\alpha$, see table 2.2, it belongs to the particles; Type of photon wave, in the piano rail surface figure 1.2 and figure 2.4, it also has the volatility. In a word, no matter how big the frequency, high energy, such as x rays and γ rays wave particle duality nature will not be changed.

5.3 Michael was measured by optical methods is not the Cause of the earth's absolute motion.

As for Michelson and posterity many times by optical methods determine the absolute velocity v is the cause of the failure: the neutrino field should be still in the universe; Including the light source, optical interferometer all transmission and reflection in the lens in front of the neutrino field is completely transparent, see figure 5.4; S, T, M_1, M_2, M between five points on the optical measurement of the relative

motion of the neutrino field velocity v are offset each other, so that M_1M and M_2M two optical path length with earth or the size of the instrument and the absolute velocity v and change, there is no optical path difference, naturally don't measure the interference fringes. Light invariance principle is fundamental to the special theory of relativity, based on the physical model and shall be proved in theory. $m = m_0 \Big/ \sqrt{1-(v/c)^2}$ ... ... Such as energy relativity between not only confirmed by all previous experiments, and confirmed by all calculating examples in this book, therefore, the above content and space-time relativity is still not meeting conflict.

According to the measured results in physics and in the Milky Way, and the universe space background, the microwave radiation energy density is $0.3ev/cm^3$. Is equivalent to (5.1) type of $860/cm^3$ microwave can quantum calculation. Front has been proved: electromagnetic wave is to rely on the spread of neutrino field. In the macroscopic field, neutrino is evenly distributed, omnipresent, so charged particles along the rail as a circle, because of the radial acceleration occur naturally swing electromagnetic energy radiation. But in the micro field, per cubic an $(A°)^3$ and microwave son density only 8.6×10^{-22}, therefore, homogeneous and continuous swing electromagnetic energy radiation can't produce. High-power microwave ithream, they can only on a single particle state of direct collision, produced a random quantum particles, x-rays and gamma rays photon energy form of electromagnetic radiation. Its energy is only elementary particles with different quantum Numbers N_{ai} interest, N_{ai+1} along the fluctuation track transition between the energy of the poor. (see the back part of nuclear physics and atomic physics).

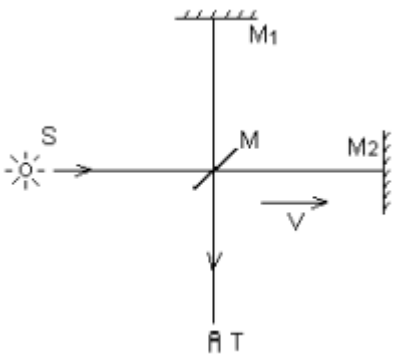

Figure 5.4 measure the absolute motion optical principle diagram

Comprehensive demonstration of this chapter, the space can be determined in the 2.73K bold microwave background radiation is caused by neutrino electromagnetic

field medium shocks. 2.73K is background temperature in the space. Because the surface of the earth including all molecules, atoms as materials of airtight container, before the neutrino field is "transparent". Neutrino velocity is the speed of light c. The reader is not difficult to imagine, in the background of the temperature and open system, the medium particles moving at the speed of light condition, local space temperature will drop to tend to 0.0K over the difficulty of this have how old?

6 Protons, neutrons internal structure and Parameter calculation

6.1 Proton internal structure and parameter calculation

6.1.1 Proton internal structure

After decades of scientific experiment and test, have been proton internal structure and charge density distribution images, see figure 6.1 and figure 6.2, ①; And accurately measured proton magnetic strength, quality, shape size, π^+ source distribution, etc. characteristics. However, the existing statistical theory of quantum mechanics model, the theory of how to calculate the above parameters, image characteristics is helpless, and the book is used to establish model and the relevant formula is but to these parameters, image features accurate simulation and validation.

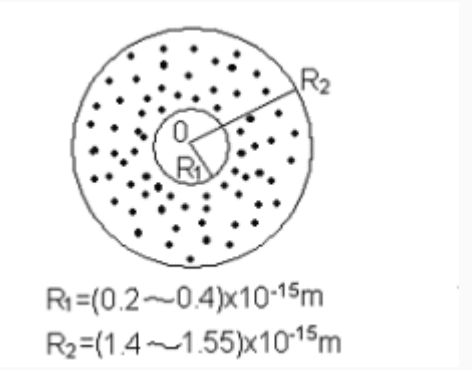

Figure 6.1 proton kernel cores and π^+ source distribution

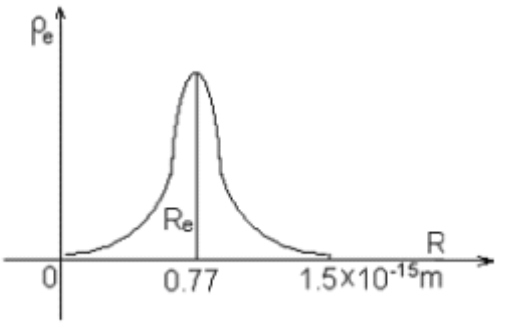

Figure 6.2 proton internal charge density distribution diagrams

According to figure 6.1 and figure 6.2 inference, proton m_p only by core m_1 and π^+ muon $\overline{m}_{\pi 2}$ of two elementary particles, the law of conservation of energy:

$$m_p = m_1 + \overline{m}_{\pi 2} \qquad (6.1)$$

Because core is a neutral elementary particles, the proton internal only to circumferential wave orbital motion, both $N_{a1}\to\infty$、$v_{a1}/c\to 1$、$v_{\theta 1}\to 0$, therefore, by (1.2-1) type, $R_{\alpha 1} = h/2\pi m_1 v_{\alpha 1}$, external display only quality characteristics. Proton most parameters by π^+ muon orbital motion. We can by (1.6), (4.9), (6.1), with different N_{a2} value and the related formula simulation proton internal structure parameters and related image features, trend compared again after revision AA and Na2 value gradually. Apparently, as long as physical model is correct, there will be a group of $\overline{m}_{\pi 2}$, and the value of N_{a2} calculated all the structural parameters, determination of image features and experimental results perfectly!

6.1.2 Proton internal structure parameters are calculated

Make N_{a2} for simpler scores or natural number, and the type (4.9) for AA beta 2. Make AA for a estimate value, value m_1 generation (6.1) in type. Will β_2, and N_{a2} value generation into (1.6), to β_2、$\overline{m}_{\pi 2}$ and N_{a2} to find π^+ muon orbit parameters of $R_{\theta o2}$. Protons in the distribution of the "π^+ muon cloud" inside and outside the radius of $R_{\theta 2(0)}$, $R_{\theta 2(\pi)}$, density and charge density distribution images, magnetic moment, all with $R_{\theta 02}$ reflected the orbit of related parameters. By (1.3) elliptical orbit equations "π^+ muon cloud" the distribution of the internal and external radius is:

$$\begin{cases} R_{\theta 2(0)} = \dfrac{R_{\theta 02}\sqrt{N_{\alpha 2}}}{\sqrt{N_{\alpha 2}} + \cos\alpha} & (\alpha = 0) \qquad (6.2-1) \\ R_{\theta 2(\pi)} = \dfrac{R_{\theta 02}\sqrt{N_{\alpha 2}}}{\sqrt{N_{\alpha 2}} + \cos\alpha} & (\alpha = \pi) \qquad (6.2-2) \end{cases}$$

By classical electrodynamics definition of magnetic moment, from elementary particles in figure 1.1 fluctuations, spin quantization stationary vertical double elliptical orbit can be seen in the model: π^+ mesons in wave direction of magnetic vector along the circumference of the $X^2 + Y^2 = R_{\theta 0}^2$ tangent, closed in internal and external not display; The spin direction of magnetic pointing in the direction of the Z axis, the magnetic moment of laboratory testing is U_p this value. By (1.2 5), (1.4-2) type, π^+ violation at the direction of the spin track length for $L_{\theta 2}$, surrounded by the area of the $S_{\theta 2}$, spin magnetic moment value U_p respectively:

$$L_{\theta 2} = N_{\alpha 2}\int_0^{2\pi/N\alpha 2} \frac{R_{\theta 02}\sqrt{N_{\alpha 2}}}{\sqrt{N_{\alpha 2}}+\cos\alpha}d\theta = \frac{2\pi R_{\theta 02}\sqrt{N_{\alpha 2}}}{\sqrt{N_{\alpha 2}-1}} \qquad (6.3)$$

$$S_{\theta 2} = \frac{N_{\alpha 2}}{2}\int_0^{2\pi/N\alpha 2}\left(\frac{R_{\theta 02}\sqrt{N_{\alpha 2}}}{\sqrt{N_{\alpha 2}}+\cos\alpha}\right)^2 d\theta \qquad (6.4)$$

$$U_p = \frac{ev_{\theta 2}S_{\theta 2}}{L_{\theta 2}} = \int_0^{2\pi/N\alpha 2} \frac{e\beta_2 cR_{\theta 02}N_{\alpha 2}\sqrt{N_{\alpha 2}-1}}{4\pi\left(\sqrt{N_{\alpha 2}}+\cos\alpha\right)^2}d\theta \qquad (6.5)$$

Make to have π^+ muon fluctuations, spin quantization stationary vertical double for L, the total length of elliptical orbit by equations (1.3) and (1.5), to:

$$L = \oint\sqrt{\left(R_{\alpha 2}d\alpha\right)^2+\left(R_{\theta 2}d\theta\right)^2} = \frac{2\pi R_{\theta 02}\sqrt{N_{\alpha 2}^2+N_{\alpha 2}}}{\sqrt{N_{\alpha 2}-1}} \qquad (6.6)$$

Because of fluctuation, the spin velocity is constant, so live π^+ muon along the line density of charge of the orbit δ=e/L is also constant. To track moving charge of electrostatic field energy and charge along the radius of $\overline{R}_e$ spherical shells on the uniform distribution of electrostatic field, the energy equivalent to:

$$\oint\frac{e^2}{8\pi\varepsilon_0 R_e L}dl = \frac{e^2}{8\pi\varepsilon_0\overline{R}_e} \qquad (6.7)$$

Among them, the $R_e = \sqrt{\left(\frac{R_{\theta 02}\sqrt{N_{\alpha 2}}}{\sqrt{N_{\alpha 2}}+\cos\alpha}\right)^2+\left(\frac{R_{\theta 02}\sin\alpha}{\sqrt{N_{\alpha 2}}+\cos\alpha}\right)^2}$ generation into (6.7), to:

$$\overline{R}_e = \left(N_{\alpha 2}\int_0^{2\pi/N\alpha 2}\frac{\sqrt{N_{\alpha 2}-1}}{2\pi R_{\theta 02}\sqrt{N_{\alpha 2}+\sin^2 N_{\alpha 2}\theta}}d\theta\right)^{-1} \qquad (6.8)$$

Different $\overline{m}_{\pi 2}$, β_i, N_{a2} value and in turn into the type of, calculated the parameters of the proton in table 6.1. The orbit of image features is shown in figure 6.3. Including $N_{a2}=22/9$、 $\overline{m}_{\pi 2}=7.7908998\times10^{-28}$Kg of this group of data calculation of $R_{\theta 2(0)}$, $R_{\theta 2(\pi)}$, U_p, $\overline{R}_e$, four data and figure 6.1 and figure 6.1 features perfectly.

Table 6.1 proton internal parameters simulation results

Anabgvalue	N_{a2}=2	N_{a2}=12/5	N_{a2}=22/9	N_{a2}= 5/2	N_{a2}=3
Parameters and Formula of Numbers	$\overline{m}_{\pi 2}\times10^{-28}$Kg				
	8.469599	7.841325	7.7908998	7.731656	7.334889
β_2 (4.9)	0.99908825	0.99901523	0.99900886	0.9990013	0.99894727
$m_1\times10^{-28}$Kg (6.1)	8.256632	8.884906	8.9353312	8.994575	9.391342
$R_{a1}\times10^{-15}$m (1.2-1)	0.426042	0.3959159	0.393682	0.391089	0.3745658
$R_{\theta02}\times10^{-15}$m (1.6)	0.4157087	0.5313226	0.54318688	0.5577799	0.6789452
$R_{\beta2(0)}\times10^{-15}$m (6.2-1)	0.243517	0.322895	0.331292	0.341682	0.430434
$R_{\beta2(\pi)}\times10^{-15}$m (6.2-2)	1.419318	1.498783	1.507187	1.517585	1.606401
$Up\times10^{-26}$J/T (6.5)	1.4106174	1.4106174	1.4106171	1.4106165	1.4106172
$\overline{R}_e\times10^{-15}$m (6.8)	0.652291	0.760395	0.771296	0.784670	0.894698

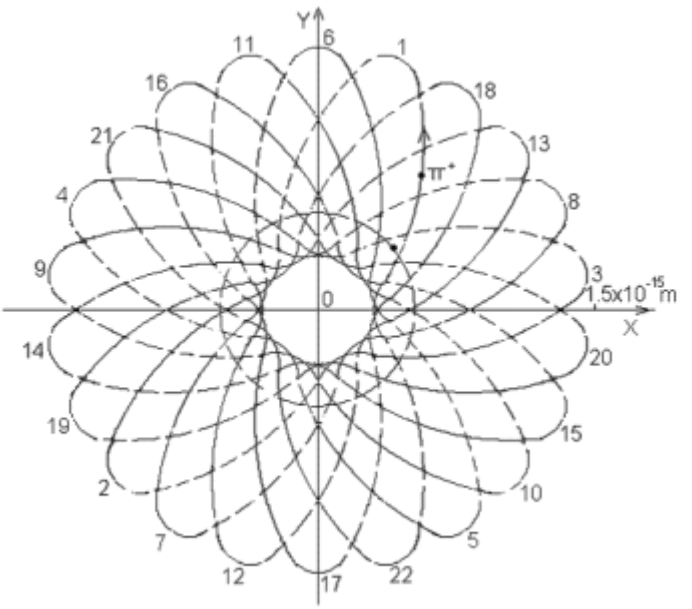

Figure 6.3 protons inside π+ mesons, core movement orbit in XOY projection in the plane of the figure

6.2 Neutron internal structure and parameter calculation

6.2.1 Neutron internal structure

Experimental determination of the neutron quality, strength, and the size of the form, the latter is the neutron internal charge density distribution, see figure 6.4. Neutron decay into protons will launch an electronic and a neutrino. Thus we can corollary: neutron core than protons core only one is charged particles and the quality is also set to m_1; Outside for a negatively charged the π^- both $\overline{m}_{\pi 2}$. When it decays into protons, core wills surplus is charged particles emitted. π^- Both absorption split after launch a load of charged particles, their split failure become positively charged of π^- violation. Load charged particles absorption environment field formed high-energy neutrinos electronic neutrinos. Because the law of conservation of momentum, absorb a neutrino and launch a neutrino is equivalent. So, according to proton internal structure, related formula and parameters of the numerical simulation method, we can also make neutron internal structure calculation formula:

$$m_n=m_1+\overline{m}_{\pi 2} \qquad (6.9)$$

Internal charge density distribution from the neutron can see 6.4: outward from the center has positive and negative, positive and negative four layer charge density distribution interval, they should be made with the positive and negative two of the fundamental particles along the integrated embodiment of wave, the movement of the spin track; Neutron the magnetic moment of the U_n should also be two basic particle magnetic U_1, U_2 vector and; So:

$$U_1=\frac{eh}{4\pi m_1} \qquad (6.10)$$

$$U_2=\int_0^{2\pi/N\alpha 2}\frac{e\beta_2 cR_{\theta 02}N_{\alpha 2}\sqrt{N_{\alpha 2}-1}}{4\pi\left(\sqrt{N_{\alpha 2}}+\cos\alpha\right)^2}d\theta \qquad (6.11)$$

$$U_n=U_1+U_2 \qquad (6.12)$$

6.2.2 Neutron internal structure parameters are calculated

Neutron internal structure parameters of the simulation results are shown in table 6.2. Because of the positive and negative charged the basic particle of the electric and magnetic field force interaction, m_1 fluctuations orbit will set the $\overline{m}_{\pi 2}$ center orbit as eccentric and random stacking, see figure 6.5. Will N_{a2} = 12/5, 22/9, 5/2 three groups

of $R_{\theta 2(0)}$, $R_{\theta 2(\pi)}$, R_{a1}, U_n data and comparison of experimental results in figure 6.4, taking into account the derivative of protons, neutrons, obviously, N_{a2} = 22/9 of the data is consistent. Figure 6.5 the neutron internal structure is draw by this group of data.

Table 6.2 neutrons internal structure parameters of the simulation results

Anabgvalue	N_{a2}=2	N_{a2}=12/5	N_{a2}=22/9	N_{a2}= 5/2	N_{a2}=3
Parameters and Formula of Numbers	$\overline{m}_{\pi 2}$ ×10^{-28}Kg				
	6.632975	6.247308	6.215628	6.178265	5.924168
β_2 (4.9)	0.99908825	0.99901523	0.99900886	0.9990013	0.99894727
m_1×10^{-28}Kg (6.1)	10.116311	10.501978	10.533658	10.571021	10.825118
$R_{\theta 20}$×10^{-15}m (1.6)	0.530816	0.666891	0.680851	0.698022	0.840622
$R_{\theta 2(0)}$×10^{-15}m (6.2-1)	0.310945	0.405282	0.415254	0.427590	0.532933
$R_{\theta 2(\pi)}$×10^{-15}m (6.2-2)	1.812317	1.881201	1.889164	1.899149	1.988934
R_{a1}×10^{-15}m (1.2-1)	0.348172	0.335386	0.334377	0.333195	0.325374
Un×10^{-26}J/T (6.12)	-0.9661143	-0.9661144	-0.9661136	-0.9661136	-0.9661143

Please note that the charged particle internal excess charged particles are distributed in the inside of the spin track, electric dipole rotation speed and direction of magnetic and charge density distribution of the calculated value is weak, the influence of this book is no longer continue to analysis and correction calculation. To core m_1 for charged particles, quantum fluctuations number $N_{\alpha 1}$ to infinite, problems of the stability of charged particles, and to be supplemented as follows: core positively charged, π^- certainly, negatively charged under the electric field force interaction, m_1 is still the core Z axial swing speed, satisfy the speed v≥c is no problem.

Behind this chapter and nucleus internal structure and parameter calculation, $\pi^{\pm}$ quality $\overline{m}_{\pi 2}$ mesons are using simulation quality, rather than by energy relativity formula:

$$\overline{m}_{\pi 2}=\frac{\overline{m}_{\pi 20}}{\sqrt{1-\beta_2^2/N_{\alpha 2}}} \qquad (6.13)$$

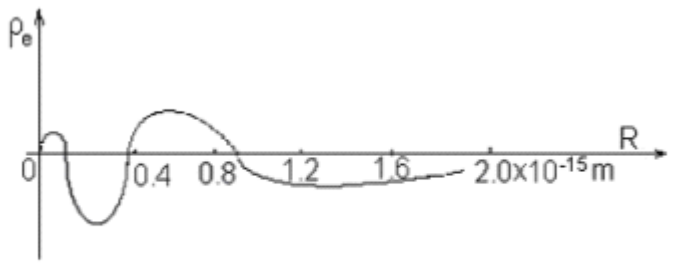

图6.4 中子内部电荷密度分布图①

Figure 6.4 neutron internal charge density profiles ①

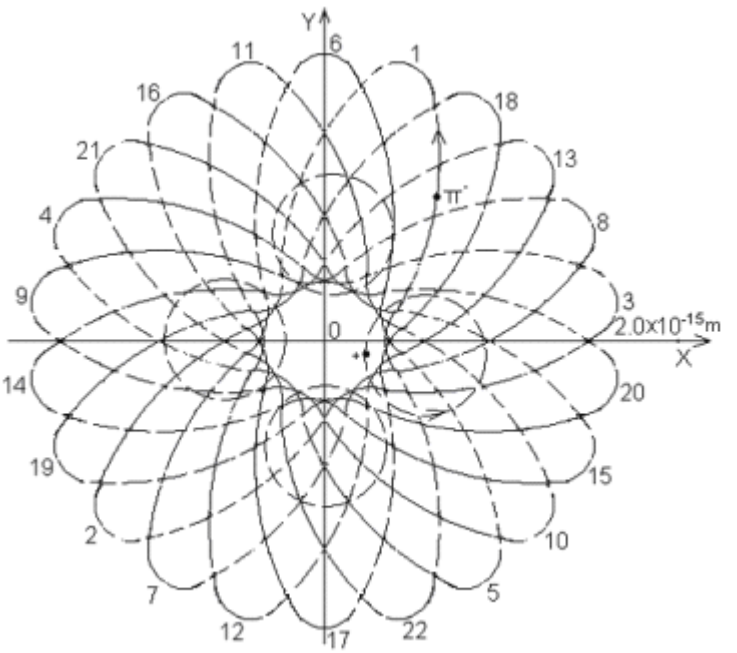

Figure 6.5 neutrons internal electrically charged particles in orbit XOY projection in the plane of the drawing

It should be from $\pi^{\pm}$ muons existence environment of "state". $\pi^{\pm}$ mesons in different environment, can stable exists, must have the energy to adapt to the environment. The energy in this book are the general law of conservation of energy and environment (1.2) ~ (1.6) elementary particles wave equations, the spin track and derivative formula simulation is obtained.

6.3 Protons, neutrons internal "quark" illusion and other Baryonic internal structure analysis

6.3.1. Protons, neutrons internal "quark" illusion

Simulation results show that this chapter protons and neutrons are only by core and $\pi^{\pm}$ source these two fundamental particles. In the experiment, then, why can detect inside protons and neutrons are three hard particles, is the so-called mixed number charge "quark", but has been unable to be separated? Reason lies in the fundamental particles along the orbit to different position with different quality, the spatial distribution of two elementary particles position changes caused by each other.

In the case of neutrons, see figure 6.5. Basic core as a positively charged particle, the fluctuation and random motion range, the quality did not change; the distribution area is in the middle of the neutron on the inside of the shell. By experimental detection will be their basic as a positively charged particle u "quark" is granted. Another stupid π^- mesons are different, the fluctuation, the spin orbit, the neutron only about one quarter of the medial, lateral of energy (protons in π^+ muon so); Plus the interval with a core of positively charged particles; In the detection of it is easy to put the π^- both for inside and outside two negatively charged particles of d "quark"; This just leads to nearly 50 years of "quark" illusion.

6.3.2 Other baryonic internal structure analysis

To other of all the baryons, according to the electric properties and can be divided into three categories: with a positive charge, with a unit negative and neutral baryonic. The average life expectancy is less than 10^{-9} seconds. The existing scientific experiments, the test means, to accurately measured as protons, neutrons its internal structure, charge density distribution and magnetic parameters such as size, shape is very difficult, also does not have the necessary

We will that baryonic general quality, magnetic data after compared with the protons and neutrons is not difficult to found that they are slightly larger than protons, neutrons, and the quality of the magnetic strength is slightly smaller than protons, neutrons; Decay of the final product is protons, electrons and photons or neutrinos. According to chapter 2, 3, and this chapter expounds the basic particle of internal structure, energy forming principle, the internal each charged particles themselves and each other force analysis and the stability principle of protons, neutrons and internal structure parameters of the simulation results; We can corollary: of all the baryons are composed of core and mesons, charged the baryonic core is a neutral elementary particles, periphery is charged source, its internal structure and proton similar;

Electrically neutral baryonic core zone of a unit charge, peripheral vision is a belt, violation of the charge, its internal structure is similar to neutrons; Core and mesons are made by n of electric dipole (and a charged particle) composed of protons, neutrons and the difference only lies in the more electric dipole. Can been deduced from all other baryonic life of much smaller than neutrons and protons. Because they are the average life expectancy is short, only as a kind of electromagnetic energy transition state of the ball, no need to further study.

7 Nucleus structure model, the nuclear force, Magnetic forming principle

7.1 Nucleus structure model, the nuclear force Forming principle

7.1.1 Nucleus structure model

The nucleus is made up of protons, neutrons. The author has been proved in the previous particle physics: protons and neutrons consist of core and $\pi^{\pm}$, these two kinds of fundamental particles by n of electric dipole (and a charged particle). To system research, precise nucleus internal structure, shape, size, charge distribution characteristics, nuclear force forming principle, the magnetic moment change rule, nuclear energy, split decay characteristics, X-ray, the relationship between γ ray energy and likely to change. According to establish the basic particle of fluctuations in particle physics, and spin quantization stationary vertical double elliptical orbit model; Electrically neutral basic particles and charged particles in the differences of the wave velocity, the former, $\beta=1-10^{-9}$, the latter when $\infty \geq N_a \geq 34/13$, by (4.9), to: $0.9987108301 \leq \beta \leq 0.9989866946$. Obviously, fluctuation, the spin velocity of different particles cannot be run in the same way. We must adopt new ideas, according to the scientific community has the total energy of the nuclide of thousands of atoms and the related parameters, the protons and neutrons all "decentralized" into a charged particle, and all of the above characteristics of the assembly with the experiments, the parameters of the nucleus. This is also for the building up of the orbit of particle physics theory of quantum physics model of comprehensive and strict inspection.

When we'll all be "decentralized" into protons and neutrons charged after elementary particles, nucleus was apparently by the large number of charged particles. Each charged elementary particles has fluctuations, spin quantization stationary vertical double elliptical orbit. We can make a moderate amount of interest, original fluctuations energy m_i, quantum number N_{ai} the same fundamental particles uniform distribution on the same wave line, the spin track, composed of particles spiral ring. According to the energy and space combination relationship into high-energy particles spiral loop and low-energy particles spiral loop. Low-energy particles spiral ring net with negatively charged of fundamental particles, the average energy and the quantum fluctuations of $\overline{m}_{di}$, N_{adi} , N_{adi} said; High-energy particles spiral ring net with the basic

particles of positively charged, their average energy and the quantum fluctuations of $\overline{m}_{gi}$, N_{agi} said.

Will more energy, and quantum fluctuations in exactly the same number of low-energy particles spiral ring side by side, make its fluctuation, spin tangent track, share on both sides. Because orbit of each charged elementary particles on the intersec ting fluctuation, the movement of the spin direction, speed is the same, spacing stagger, tangent as the radius of the same two wheels turning, composed of low-energy particles spiral ring. Total number of nuclear different nucleus skeleton by 1 ~ 5 layers the low-energy particles spiral ring, see figure 7.1 and figure 7.2. Finally make high-energy particles spiral ring also according to the energy, the number of quantum fluctuations difference is divided into five layers. Each layer of high-energy particles spiral ring respectively to "into" economical corresponding low-energy particles spiral ring wave orbital medial. So we need part of the nucleus internal structure model. According to the first layer of low-energy particles spiral ring arrangement number is odd or even, divided into A, B two types of atomic nuclei. Their electric field within the energy equation, nuclear electricity, magnetic interactions calculation method, the relevant formulas are slightly different.

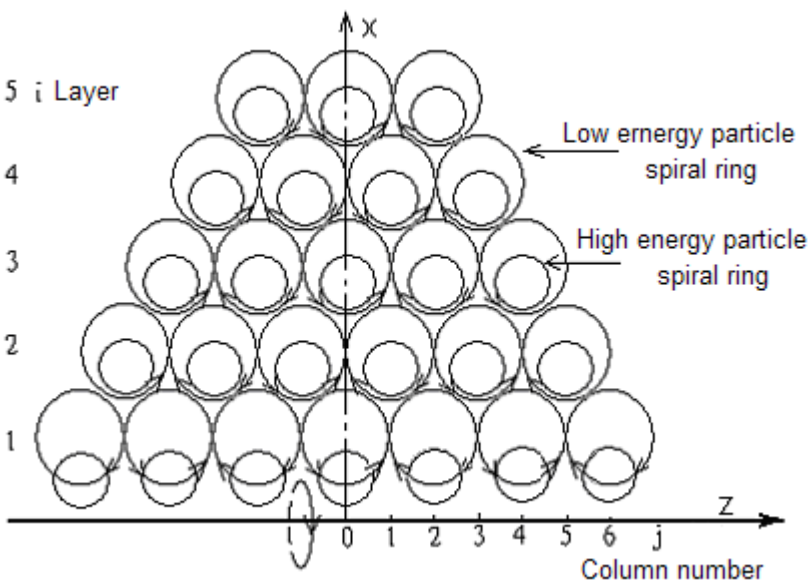

Figure 7.1 type A nucleus high internal, low-energy particles spiral rings

See from figure 7.1 and figure 7.2, the first layer low-energy particles spiral loop combination model with 2 ~ 5 layers. The author has used the same solution with 2 ~ 5 layers nucleus "assembly", but in the end of the quality of medium to heavy nuclei

energy calculation results are too big. However, for the total number of nuclear less than 56 of $^{56}_{26}F_e$ light nuclei, can consider to use. In chapter 12 12.4 and section 12.5 of the total number of nuclear less than 56 light nuclei supplement parameter calculation of $^{56}_{26}F_e$.

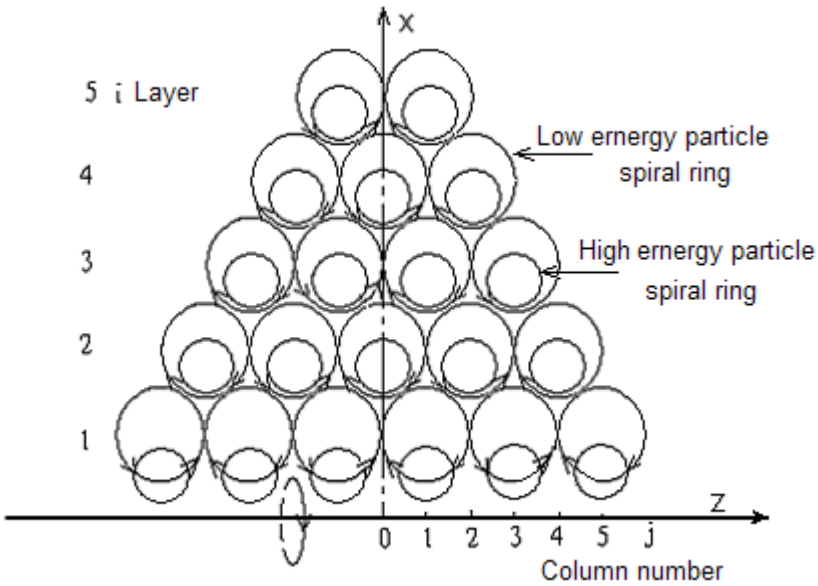

Figure 7.2 type B nucleus high internal, low-energy particles spiral rings

7.1.2 Nuclear force forming principle

By (3.23) ~ (3.26) and table 2.2 and table 3.1 has proven: as long as the radius of the charged particles entity R_α. fluctuations and the ratio of radius of $\overline{R}_\alpha$ $1.499\times10^{-13}\geq K_r\geq8.0\times10^{-15}$, charged particles along the wave motion in orbit, its comprehensive electric and magnetic field force along the fluctuations orbit radius to the inside of the track, the strength is the centrifugal force of multiple astronomy! Similarly, by (3.18), (3.19), has proven: charged elementary particles along the fluctuation orbit, except in the a = 90°, 270° and the nearby, integrated electric and magnetic field force is along the orbit radius fluctuation AARa pointing to the outside, but it is greater than all the formation of charged particles much smaller comprehensive electric and magnetic field force. In a = 90°, 270° and the nearby, although at this time the charged particle comprehensive electric and magnetic field force tends to zero, but formed by charged particles of electric and magnetic field force still exists, to wave the inside of the track, and still is a multiple wave direction form centrifugal force of astronomy! And each charged particles comprehensive electric and

magnetic field strength, see figure 3.4, (3.29), have been up and down, left and right sides opposite sex charged particles attract effect of the electric field force, will adjust tensile deformation degree, so can properly constraints fundamental particles along the fluctuation, the spin track movement.

When charged particle spin track inside there are other heterosexual charged elementary particles, with a net charge for N_e, by coulomb's law, the electric field strength $F_{e\theta}$ for:

$$F_{e\theta}=\frac{N_e e^2}{4\pi\varepsilon_0 \overline{R}_\theta^2\sqrt{1-\left(\nu_\theta/c\right)^2}} \qquad (7.1)$$

Make to charged particles electric and magnetic field comprehensive force is $\triangle F_{eb\bullet}$, it greater than the sum of $F_{n\theta}$ and $F_{e\theta}$ electric field force and centrifugal force. Simultaneous (7.1), (3.25) and (3.26), to:

$$\frac{e^2}{4\pi\varepsilon_0\overline{R}_\alpha^2}\left\{\begin{array}{l}\dfrac{(2n+1)\left[1-\beta^2\left(1-K_{r\bullet}^2\right)\right]}{4K_{r\bullet}^2}\left[\dfrac{1}{\sqrt{1-\beta^2\left(1+K_{r\bullet}\right)^2}}-\dfrac{1}{\sqrt{1-\beta^2\left(1-K_{r\bullet}\right)^2}}\right]\\ -\dfrac{N_e}{N_\alpha\sqrt{1-\beta^2/N_\alpha}}-\beta\dfrac{2h\varepsilon_0 c}{e^2}\end{array}\right\}>>0$$

(7.2)

Calculated according to (3.29) type data, the $\pi^{\pm}$ mesons, electric dipole for n=2, set N_a=50, $K_{r\bullet}=8.0\times10^{-15}$, N_e=50, by (4.9), to: β=0.9987237786, generation into (7.2), to:

$$\frac{e^2}{4\pi\varepsilon_0\overline{R}_\alpha^2}\left(3.093858\times10^{15}-1.010126-136.8611\right)>>0$$

If make N_a = 500, generation of (4.9) in type, too: β=0.9987121191. To N_e = 200, (the nucleus of human has found charge number less than 120), and other parameters are the same, and in (7.2), to:

$$\frac{e^2}{4\pi\varepsilon_0\overline{R}_\alpha^2}\left(3.076858\times10^{15}-0.4003996-136.8595\right)>>0$$

From the calculation results, table 3.1, is that charged particles inside and outside surface comprehensive electric and magnetic field force $\triangle F_{eb\bullet}$ both far outweigh the

charged particle inside and outside surface comprehensive electric and magnetic field force; Far greater than the spin track inside net with charge caused by the electric field force $F_{e\theta}$ and centrifugal force $F_{n\theta}$; So, each particle within the nucleus spiral ring along the radius of the spin direction of electric field force, centrifugal force all don't need to consider. As long as the nucleus center electric and magnetic field strength of each particle spiral ring in the spin track of axial component is enough.

Equation in (2.10) charged particle energy and N_a, β, K_r, correlation parameters such as when we found that charged elementary particle in the clean with charged particles are distributed in the inner side of the spin track. By figure 7.1 and figure 7.2 shows: the inner and outer low-energy particles spiral ring wave, the spin track although get very close, but never allow the tangent or overlap, or the inside and outside layer of elementary particles will collide. High economical, low-energy particles spiral ring on the inside of the spin track although fluctuations, the movement of the spin direction is same, but different speed; Rail adjacent side are net left are charged particles, because charged particles of electrostatic field force rejection, so orbit will not tangent, overlapping or cause collision "rear"; And low-energy particles spiral ring of high-energy particles spiral wave orbital medial part of just the spin axis space limit.

Because K_r value for 10^{-4} ~ 10^{-5} orders of magnitude, so in low economical particles spiral ring wave and spin the lateral orbital non-oil imports, the net load charged particles along the left orbit will form strong directional current attraction of ampere force. Chapter 10, 11 behind the analysis of the calculation results show that: the interaction of ampere force distance is short, have overcome the dual role of compression and tension at the same time, can effectively balance conditions within the nucleus electric field force in all the particles spiral ring the spin axis of the component, the power is nuclear force.

7.2 Nuclear magnetic forming principle

7.2.1 Nuclear magnetic forming principle

According to the experimental results: nuclear within the nucleus and excess charge is almost density distribution, such as edge are diffuse layer, see figure 7.3. Overall energy is proportional to the number of nuclear A nucleus, nucleus charge distribution within the radius of that are: R_e=（1.2～1.5）$A^{1/3}\times10^{-15}$m

Nuclear force action radius is slightly greater than nuclear power charge distribution radius, equivalent to a nucleus wrapped in a layer of "neutron skin". The

variation of the magnetic moment is: when protons and neutrons are even, with magnetic moment is zero.

Comprehensive the above data, image characteristics, through a variety of models, methods, parameters of the simulation comparison after safely draw the conclusion that we must will be positively charged protons "decentralized" into two of the fundamental particles, a negatively charged of fundamental particles; Neutron "decentralized" into four with positive and negative of two elementary particles; All charged elementary particles consists of two pairs of electric dipole and a charged particles, which are all charged $\pi^{\pm}$ violation. So that will make all the nucleus of the internal structure, composition thoroughly "democracy". Economical electric dipole in the starting rotation Angle position parameter alph a_0 and the corresponding relation of the K_r also exactly the same. Derived: the core of each proton, must be from 6 to electric dipole. To a single proton, "decentralized" redundant after an electric dipole to neutrino field release; Single neutron "decentralized", sent a electric dipole can be absorbed from the neutrino field added. Protons and neutrons "decentralized" in pairs, of course, just maintain constant total electric dipole.

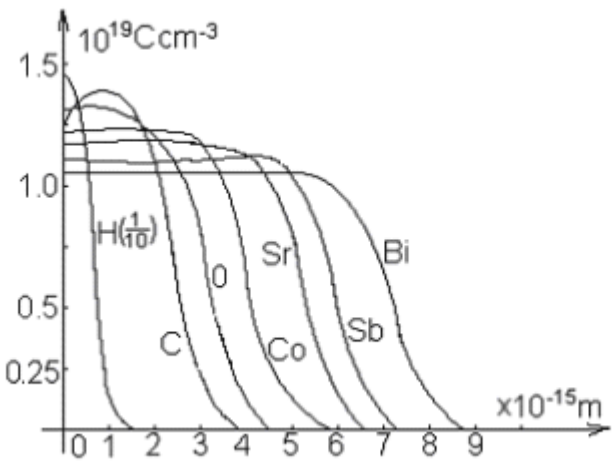

7.3 charge density distribution in nuclei (C for power unit coulomb)

In the case of a particle, two pairs of protons, neutrons were "decentralized" into eight π^{+} mesons, with "⊕", said six π^{-} violation, in "⊖" said. Of neutrons, and make a PI to $\pi^{\pm}$ mesons in high orbit, the other three $\pi^{\pm}$ mesons in low orbit; On the proton, make two $\pi^{\pm}$ mesons in high orbit, another $\pi^{\pm}$ violation into low orbit. We make high orbit of $\pi^{\pm}$ muon energy is nearly two times of low orbit, accurate values obtained by the simulation calculation in chapter 8, 9. Each proton, neutrons "decentralized" all the

$\pi^{\pm}$ mesons in high and low orbit can have only four distribution state, as shown in figure 7.4. We by a, b, c, d said the four distribution state. More protons and neutrons in the different combinations of these four states up to different high and low spiral ring particles.

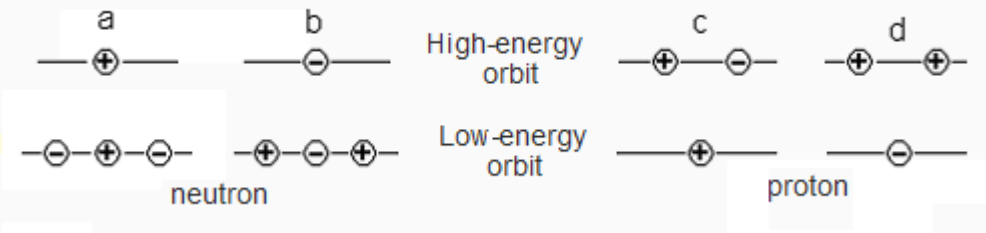

Figure 7.4 protons, neutrons "decentralized" $\pi^{\pm}$ source in the distribution of high and low orbit

By the magnetic moment of a nucleus in synthetic principle is derived: when by even protons, neutrons "decentralized" all the $\pi^{\pm}$ violation of a pair of high and low particles spiral ring, its high orbit of excess π^{+} violation number should be 2 times the number of protons, low orbit excess π^{-} violation number is equal to the number of protons. Such as a^{++} particles, when it takes a and b, 2d distribution state combination, as shown in figure 7.5. So, when is high, low $\pi^{\pm}$ muon spin movement direction, as long as high-energy $\pi^{\pm}$ both energy $\pi^{\pm}$ low-energy $\pi^{\pm}$ mesons are 2 times of $\overline{m}_{g1}$, and the $\overline{m}_{d1}$ quantum number $\pi^{\pm}$ $N_{ag1} = N_{ad1}$, by (6.5), the total magnetic is 0.

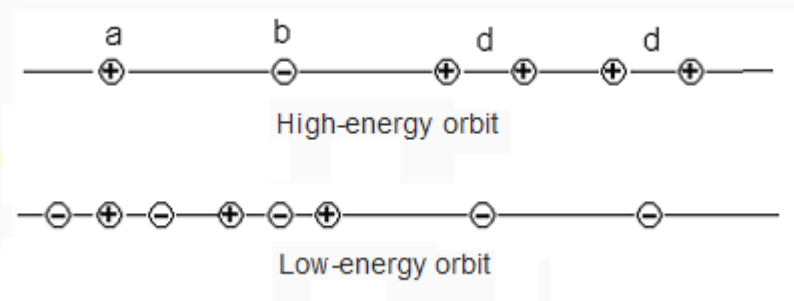

Figure 7.5 a^{++} particles within 14 $\pi^{\pm}$ mesons in high and low orbit the distribution of the portfolio

Similarly, as long as even protons, neutrons "decentralized" all the $\pi^{\pm}$ violation according to the above the same layer of the same amount of order into quantum fluctuations, low-energy particles spiral orbit, its high orbit net with π^{+} muon a total of $2P_i$, low orbit net with π^{-} both for the P_i, total (P_i for this layer, low-energy particle spiral

ring on the total number of protons). Such as ${}^{12}_{6}\mathrm{C}$ carbon nuclei, see figure 7.6. We also can make each pair of high and low particles spiral rings of the net with $\pi^{\pm}$ violation and nucleus axis X axis distribution is symmetrical. This is the nucleus kernel interaction balance necessary for the electric field force, and the results also can make the magnetic moment of 0.

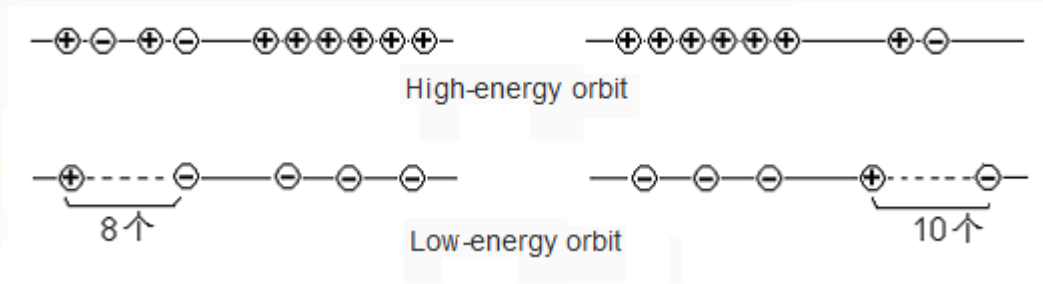

Figure 7.6 ${}^{12}_{6}\mathrm{C}$ carbon two within the nucleus on high side by side, low-energy particles spiral rings $\pi^{\pm}$ source distribution combination

To sum up, all the even nucleus composed of protons, neutrons, and as long as the number of nuclear enough, we can divide total number of protons, neutrons into 1~5, each composed of even protons, neutrons. Each of protons, neutrons Pi to all the "decentralized" $\pi^{\pm}$ violation according to the above rules into the corresponding layer N_{agi}, N_{adi}'s discretion can particles spiral ring rail inside, each corresponding layers of high-energy orbit of the net with π^{+} muon for $2P_i$, low orbit net with π^{-} both for P_i.

By (1.6), (6.3) ~ (6.5), the inside of the proton magnetic moment by π^{+} mesons are formed in the spin track motion, therefore, within the nucleus of each net of $\pi^{\pm}$ violation, the magnetic moment equations are should be:

$$U_{\pi^{\pm}} = \pm\int_0^{2\pi/N\alpha} \frac{eN_\alpha\left(N_\alpha - 1\right)\hbar}{8\pi^2 \overline{m}_{\pi^{\pm}}\left(\sqrt{N_\alpha} + \cos\alpha\right)^2} d\theta \qquad (7.3)$$

Except 1 layer, low-energy particle spiral loop N_{ag1}= N_{ad1}, $\overline{m}_{g1}$=2$\overline{m}_{d1}$, 2, 3, 4, 5 layers, high, low particles spiral ring of N_{agi}, N_{adi}, $\overline{m}_{gi}$, $\overline{m}_{di}$ values, are all through the simulation after find out, in chapter 8, 9.

7.2.2 Magnetic moment synthesis theory within the nucleus

When protons and neutrons in the nucleus is different for the even, to deduct with the even number of protons, neutrons, and the rest of the protons and neutrons there

will be an odd number of protons, neutrons; An odd number of protons, even neutrons; Even protons, an odd number of neutrons three combinations. According to each combination "decentralized" all the $\pi^{\pm}$ mesons in high and low orbit, the distribution of the nucleus of the magnetic moment can have a variety of state. Each state combination of high and low $\pi^{\pm}$ violation can respectively into the different layers of high and low particles spiral ring rail, will produce different magnetic strength. Obviously, the nucleus is the magnetic moment of each layer, high, low particles spiral ring rail of the net with $\pi^{\pm}$ formed by the violation of the algebraic sum of the magnetic moment. Are listed below:

1．Protons and neutrons are an odd number

（1）ac bd State combination

$$\sum U = \sum_{i=1}^{2} U_{gi}^{+} + U_{gi}^{-} + \sum_{i=1}^{2} U_{di}^{+} + \sum_{i=1}^{2} U_{di}^{-} \qquad (7.4\text{-}1)$$

（2）ad Statecombination

$$\sum U = \sum_{i=1}^{3} U_{gi}^{+} + 0 + U_{di}^{+} + \sum_{i=1}^{3} U_{di}^{-} \qquad (7.4\text{-}2)$$

（3）bc Statecombination

$$\sum U = U_{gi}^{+} + \sum_{i=1}^{2} U_{gi}^{-} + \sum_{i=1}^{3} U_{di}^{+} + U_{di}^{-} \qquad (7.4\text{-}3)$$

2．Proton odd, neutron even

（1）abc bbd Statecombination

$$\sum U = \sum_{i=1}^{2} U_{gi}^{+} + \sum_{i=1}^{2} U_{gi}^{-} + \sum_{i=1}^{4} U_{di}^{+} + \sum_{i=1}^{3} U_{di}^{-} \qquad (7.5\text{-}1)$$

（2）abd aacStatecombination

$$\sum U = \sum_{i=1}^{3} U_{gi}^{+} + U_{gi}^{-} + \sum_{i=1}^{3} U_{di}^{+} + \sum_{i=1}^{4} U_{di}^{-} \qquad (7.5\text{-}2)$$

（3）aad Statecombination

$$\sum U = \sum_{i=1}^{4} U_{gi}^{+} + 0 + \sum_{i=1}^{2} U_{di}^{+} + \sum_{i=1}^{5} U_{di}^{-} \qquad (7.5\text{-}3)$$

（4）bbc Statecombination

$$\sum U = U_{gi}^{+} + \sum_{i=1}^{3} U_{gi}^{-} + \sum_{i=1}^{5} U_{di}^{+} + \sum_{i=1}^{2} U_{di}^{-} \qquad (7.5\text{-}4)$$

3．Proton even, neutron odd

（1）acd bdd Statecombination

$$\sum U = \sum_{i=1}^{4} U_{gi}^{+} + U_{gi}^{-} + \sum_{i=1}^{2} U_{di}^{+} + \sum_{i=1}^{3} U_{di}^{-} \qquad (7.6\text{-}1)$$

（2）acc bcd Statecombination

$$\sum U = \sum_{i=1}^{3} U_{gi}^{+} + \sum_{i=1}^{2} U_{gi}^{-} + \sum_{i=1}^{3} U_{di}^{+} + \sum_{i=1}^{2} U_{di}^{-} \qquad (7.6\text{-}2)$$

（3）bcc Statecombination

$$\sum U = \sum_{i=1}^{2} U_{gi}^{+} + \sum_{i=1}^{3} U_{gi}^{-} + \sum_{i=1}^{4} U_{di}^{+} + U_{di}^{-} \qquad (7.6\text{-}3)$$

（4）add Statecombination

$$\sum U = \sum_{i=1}^{5} U_{gi}^{+} + 0 + U_{di}^{+} + \sum_{i=1}^{4} U_{di}^{-} \qquad (7.6\text{-}4)$$

We can by the nucleus to the magnetic moment of the experimental value analysis, numerical simulation with for even protons, neutrons "decentralized" of to the $\pi^{\pm}$ mesons in each layer height, can track the distribution state, and provide the basis for the calculation of parameters, such as nuclear energy.

8 Nucleus internal structures, the benchmark Parameters $\overline{m}_{\pi\pm}$ original energy

8.1 Nucleus inner particles spiral loop quantum Fluctuations of N_{a1}

A particles spiral ring in the direction of the spin track the outside radius of $R_{\theta(\pi)}$, by (1.3-2), (1.6), to:

$$R_{\theta(\pi)}=\frac{R_{\theta 0}\sqrt{N_\alpha}}{\sqrt{N_\alpha}+\cos\alpha}=\frac{h\sqrt{N_\alpha^2-N_\alpha}}{2\pi\overline{m}\beta c\left(\sqrt{N_\alpha}-1\right)} \qquad (8.1)$$

(7.2) type of elementary particles in the spin direction has been proved through the analysis of comprehensive force: elementary particles along the fluctuation, the spin track movement direction of the arrow diameter automatic contraction trend. The original energy $\overline{m}_1$ for value, the spin track lateral shall is minimum. Its nucleus inner particles spiral ring spin quantum is to determine the number of prerequisites.

With different number of quantum fluctuations N_{a1} generation into (4.9) is β_1 value again after together into (8.1), too: when $2.61602 \geq N_{a1} \geq 2.61589$, if use a simple points instead of, is $21/8 \geq N_{a1} \geq 34/13$, $R_{\theta(\pi)}$ has a minimum value. So, the nucleus, we take $N_{ag1}=N_{ad1}=34/13$, will it into (8.1) - the result of calculation is $N_{ad1}=21/8$ less value.

From section 7.1 and figure 7.1 and figure 7.2 and nucleus internal nuclear force forming principle, as long as 1 layer adjacent side by side of low-energy particles spiral ring wave motion in opposite directions, (one for clockwise wave motion, one for anti-clockwise wave motion); The spin direction; The high-energy particles spiral ring rail lateral and low-energy particles spiral ring rail inside adjacent interchange space orbit each other constraints and positive and negative electric field force, can overcome the high-energy particles spiral ring spin movement of the axial electric field repelling force; And the force transmitted to low-energy particles spiral ring; By low-energy particles spiral ring the spin axis orbit tangent place of ampere force to overcome.

8.2 Conditions within the nucleus π± meson spin direction electric energy equation

This book has shown in chapter 2: all the elementary particles original energy mainly is the fluctuation of electricity, the direction of the magnetic field energy, as well as the spin direction of the electric and magnetic energy. Conditions within the nucleus is made up of many protons, neutrons "decentralized" $\pi^{\pm}$ violation. In order to facilitate the calculation, we will be the nucleus general electric and magnetic energy is divided into two parts. 99.5 ~ 99.8% of them are all from $\pi^{\pm}$ muon fluctuation, the spin direction of the electric and magnetic field source energy. 1 layer within the nucleus particles spiral ring that low-energy particles spiral rings in each $\pi^{\pm}$ muon fluctuation, the spin direction original electric and magnetic field energy for $\overline{m}_{d1}c^2$, high-energy particles spiral ring each $\pi^{\pm}$ mesons in original energy for $2\,\overline{m}_{d1}c^2$. The rest of the 0.2 ~ 0.5% energy is high, low $\pi^{\pm}$ violation in the spin direction of interaction between electric and magnetic energy. It changes with different nuclear power by combination of the nucleus. Fluctuations in this way, we can use in front of the elementary particles, spin quantization stationary vertical double elliptical orbit model and proved the related formula, combined with the classical electrodynamics and energy relativity, to derive the total energy equation of the nucleus.

Basic particles are charged by (1.6) - the original average energy $\overline{m}_i c^2$, quantum fluctuations of N_{ai}, and track the relationship between the parameters of $R_{\theta 0}$ is given as:

$$R_{\theta 0} = \frac{h\sqrt{N_\alpha - 1}}{2\pi \overline{m}_i \beta c} \qquad (8.2)$$

By (6.3), particles spiral ring the spin direction of rail length L_θ for:

$$L_\theta = \oint \frac{R_{\theta 0}\sqrt{N_\alpha}}{\sqrt{N_\alpha} + \cos\alpha} d\theta = \frac{2\pi R_{\theta 0}\sqrt{N_\alpha}}{\sqrt{N_\alpha - 1}} \qquad (8.3)$$

By figure 7.1 and 7.1 (1) type, particle spiral ring wave direction elliptical orbit of short axis R_{ab} for:

$$R_{\alpha b} = \frac{R_{\theta 0}}{\sqrt{N_\alpha - 1}} \qquad (8.4)$$

By figure 8.1 shows, conditions within the nucleus of each ring particles spiral orbit $\pi^{\pm}$ mesons, relative to the radius of the nucleus center field R_{eij} is given as:

$$R_{eij}=\sqrt{R_{\theta i}^2+\left(K_{eij}R_{\alpha bi}-R_{\alpha i}\sin\alpha\right)^2}$$ (Said the subscript, $_j$ columns, same as follows)

(8.5)

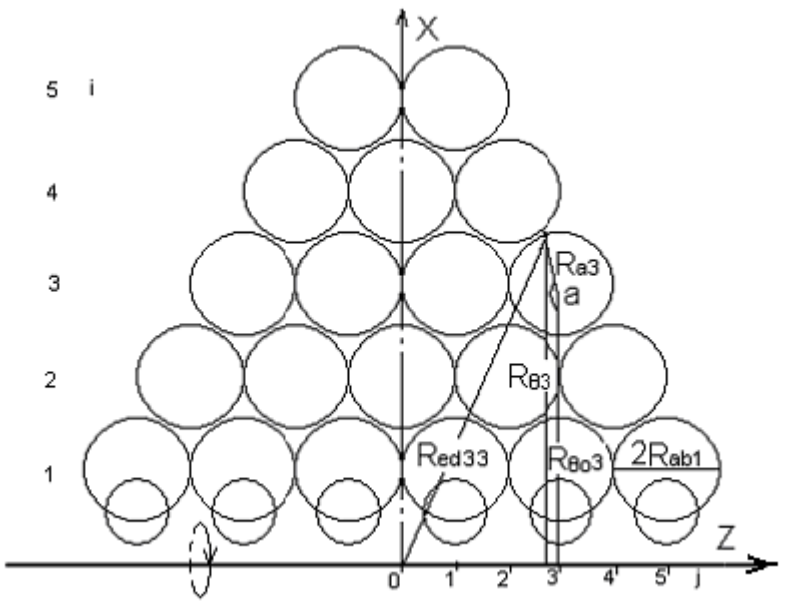

Figure 8.1 conditions within the nucleus electricity, magnetic energy equation calculation parameters

Electric field radius and divided into high-energy R_{egij}, low-energy R_{edij}. The position of the corresponding coefficient the K_{egij}, K_{edij} said, see figure 8.1 and figure 7.1 and figure 7.2. Points A and B type nucleus structure take corresponding natural number. R_{egij}, R_{edij} can specific expressed as:

$$\begin{cases} R_{egij}=\sqrt{\left(\dfrac{R_{\theta 0gi}\sqrt{N_{\alpha gi}}}{\sqrt{N_{\alpha gi}}+\cos\alpha}\right)^2+\left(\dfrac{K_{egij}R_{\theta 0di}}{\sqrt{N_{\alpha di}-1}}-\dfrac{R_{\theta 0gi}\sin\alpha}{\sqrt{N_{\alpha gi}}+\cos\alpha}\right)^2} & (8.6-1) \\ R_{edij}=\sqrt{\left(\dfrac{R_{\theta 0di}\sqrt{N_{\alpha di}}}{\sqrt{N_{\alpha di}}+\cos\alpha}\right)^2+\left(\dfrac{K_{edij}R_{\theta 0di}}{\sqrt{N_{\alpha di}-1}}-\dfrac{R_{\theta 0di}\sin\alpha}{\sqrt{N_{\alpha di}}+\cos\alpha}\right)^2} & (8.6-2) \end{cases}$$

By classical electrodynamics and (2.1), in order to spin energy relativistic velocities of each to $\pi^{\pm}$ violation, the potential can be given to:

$$V_e=\oint\frac{e}{4\pi\varepsilon_0 L_\theta R_e\sqrt{1-\beta^2/N_\alpha}}dl_\theta \qquad (8.7)$$

Will (8. 3) into (8. 7), to:

$$V_e = \frac{e}{4\pi\varepsilon_0}\oint \frac{\sqrt{N_\alpha - 1}}{2\pi R_e\left(\sqrt{N_\alpha} + \cos\alpha\right)\sqrt{1-\beta^2/N_\alpha}}\,d\theta \qquad (8.8)$$

We still will be divided into V_e high-energy V_{egij} and low-energy V_{edij} two kinds. By figure 8.1 shows: varies with the position of the particles spiral ring, they are different. Will (8.6-1), (8.6-2), respectively into (8.8), to:

$$\begin{cases} V_{egij} = \oint \dfrac{e\sqrt{N_{\alpha gi} - 1}}{8\pi^2\varepsilon_0 R_{\theta 0 gi}\sqrt{N_{\alpha gi} + \left[\dfrac{K_{egij}R_{\theta 0 di}\left(\sqrt{N_{\alpha gi}} + \cos\alpha\right)}{R_{\theta 0 gi}\sqrt{N_{\alpha di} - 1}} - \sin\alpha\right]^2}\sqrt{1 - \dfrac{\beta_{gi}^2}{N_{\alpha gi}}}}\,d\theta \qquad (8.9-1) \\ V_{edij} = \oint \dfrac{e\sqrt{N_{\alpha di} - 1}}{8\pi^2\varepsilon_0 R_{\theta 0 di}\sqrt{N_{\alpha di} + \left[\dfrac{K_{edij}\left(\sqrt{N_{\alpha di}} + \cos\alpha\right)}{\sqrt{N_{\alpha di} - 1}} - \sin\alpha\right]^2}\sqrt{1 - \dfrac{\beta_{di}^2}{N_{\alpha di}}}}\,d\theta \qquad (8.9-2) \end{cases}$$

Obviously, within the nucleus of various high and low $\pi^{\pm}$ muon spin direction of electric field energy $\sum W_e$, should be each high, low-energy particle spiral loop net with $\pi^{\pm}$ violation in the spin direction interaction between algebra and electric energy. (See the back calculating examples).

8.3 Conditions within the nucleus π± meson spin direction Magnetic field energy equation

First of all, within the nucleus of each layer, low $\pi^{\pm}$ violation, the high and low particles spiral loop composed of the orbital motion of the model, as each layer in nucleus, low-energy charged particles spiral loop combination of current solenoid layer. $\pi^{\pm}$ violation in the movement of the spin of the magnetic field as a classical electrodynamics of solenoid magnetic field. Because the conditions within the nucleus net with $\pi^{\pm}$ muon spin direction magnetic field is far less than the total energy of nuclear energy. According to the continuity of solenoid in the wind, and flux inside the solenoid and ends the basic remain unchanged, the solenoid mutual inductance between the layers of the magnetic field characteristics, with solenoid in axis at various points in the magnetic field strength instead of tube space center of the magnetic field

strength. Magnetic field intensity can be H_i simplify calculation. With the spiral ring in net charge along with the spin axis distribution density change has nothing to do.

By (8.3) type, electrodynamics, figure 8.2, the equivalent current I, radius of $\overline{R}_I$ and magnetic field strength of H is given as:

$$\overline{R}_I = \frac{R_{\theta 0}\sqrt{N_\alpha}}{\sqrt{N_\alpha - 1}} \qquad (8.10)$$

$$H = \frac{I}{2L_b}(\cos\alpha_1 + \cos\alpha_2) \qquad (8.11)$$

Will type (8.10) into (8.11), to:

$$H = \frac{I}{\sqrt{4\overline{R}_I^2 + L_b^2}} \qquad (8.12)$$

When determined by each layer particles spiral ring wave rail lateral for each layer solenoid border, from figure 7.1 and figure 7.1, (8.4) - see: make K_{bgij}, K_{bdij} for length coefficient, take the corresponding natural number, its length L_{bgij}, L_{bdij} should respectively:

$$\begin{cases} L_{bgij} = (K_{bdij} - 2)\dfrac{R_{\theta 0di}}{\sqrt{N_{\alpha di} - 1}} + \dfrac{2R_{\theta 0gi}}{\sqrt{N_{\alpha gi} - 1}} & (8.13-1) \\ L_{bdij} = K_{bdij}\dfrac{R_{\theta 0di}}{\sqrt{N_{\alpha di} - 1}} & (8.13-2) \end{cases}$$

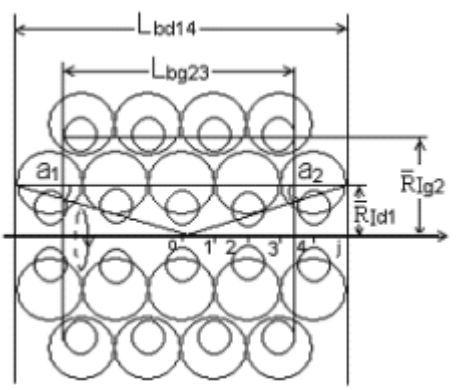

Figure 8.2 particles spiral ring layer in the magnetic energy calculation

When protons and neutrons are evens within the nucleus, (not as even when

protons, neutrons "decentralized" $\pi^{\pm}$ mesons in addition). Because high-energy particles spiral ring in net with π^{+} violation number $2P_i$, twice the number of low-energy π^{-} mesons are, (P_i for this layer, low-energy particle spiral rings of the total number of protons), therefore, by (1.5), (8.3), high and low particles spiral loop of the current intensity I_{gi}, I_{di}, respectively:

$$\begin{cases} I_{gi} = \dfrac{2P_i e\beta_{gi} c}{2\pi \overline{R}_{Igi}\sqrt{N_{\alpha gi}}} & (8.14-1) \\ I_{di} = \dfrac{-P_i e\beta_{di} c}{2\pi \overline{R}_{Idi}\sqrt{N_{\alpha di}}} & (8.14-2) \end{cases}$$

Will respectively equations (8.14) into (8.12), to each layer, low-energy particle spiral ring layer in the magnetic field strength, respectively:

$$\begin{cases} H_{gi} = \left(\dfrac{ec}{2\pi}\right)\dfrac{2P_i\beta_{gi}}{\overline{R}_{Igi}\sqrt{N_{\alpha gi}(4\overline{R}_{Igi}^2 + L_{bgi}^2)}} & (8.15-1) \\ H_{di} = \left(\dfrac{ec}{2\pi}\right)\dfrac{-P_i\beta_{di}}{\overline{R}_{Idi}\sqrt{N_{\alpha di}(4\overline{R}_{Idi}^2 + L_{bdi}^2)}} & (8.15-2) \end{cases}$$

Of each particle spiral ring layer in the magnetic energy W_{bi}, magnetic field mutual inductance between each layer should be considered. We can by the nuclear spin axis to calculate one by one. The outer to the inner have mutual inductance, inner to outer mutual inductance calculation. By classical electrodynamics principle, equations (8.13) ~ (8.15), the particles spiral ring of magnetic energy can be expressed as:

$$\begin{cases} W_{bg1} = \dfrac{u_0}{2}(H_{g1} + H_{d1} + H_{g2} + H_{d2} \cdots\cdots + H_{g5} + H_{d5})^2 \pi \overline{R}_{Ig1}^2 L_{bg1j} & (8.16-1) \\ W_{bd1} = \dfrac{u_0}{2}(H_{d1} + H_{g2} \cdots\cdots + H_{g5} + H_{d5})^2 \pi (\overline{R}_{Id1}^2 - \overline{R}_{Ig1}^2) L_{bd1j} & (8.16-2) \\ \cdots\cdots \quad \cdots\cdots \quad \cdots\cdots \quad \cdots\cdots \quad \cdots\cdots \\ \cdots\cdots \quad \cdots\cdots \quad \cdots\cdots \quad \cdots\cdots \quad \cdots\cdots \\ W_{bg5} = \dfrac{u_0}{2}(H_{g5} + H_{d5})^2 \pi (\overline{R}_{Ig5}^2 - \overline{R}_{Id4}^2) L_{bg5j} & (8.16-9) \\ W_{bd5} = \dfrac{u_0}{2} H_{d5}^2 \pi (\overline{R}_{Id5}^2 - \overline{R}_{Ig5}^2) L_{bd5j} & (8.16-10) \end{cases}$$

8.4 Basic quality $\overline{m}_{d1}$ parameters within the nucleus

In the distribution of elements of the universe, ${}_{1}^{1}\mathrm{H}$, ${}_{2}^{4}\mathrm{He}$, ${}_{6}^{12}\mathrm{C}$, ${}_{26}^{56}\mathrm{Fe}$ maintenance... Etc is the stability of the common elements. But, two ${}_{2}^{4}He$ nucleus to form stable ${}_{4}^{8}B_{e}$ nucleus, consists of two ${}_{3}^{6}Li$ nucleus can stable ${}_{6}^{12}C$ nucleus, and nuclear number is a multiple of 4. Protons and neutrons are even, magnetic moment is zero. Don't like ${}_{2}^{6}He$ nuclei have unusual magnetic moment. That ${}_{6}^{12}C$ nucleus nuclear number, proton number should be at least, meet the requirements of chapter 7 nucleus structure model, the energy equation, the most simple of the atomic nuclei. It can be used as a nucleus the basis for the calculation of $\overline{m}_{d11}$, $\overline{m}_{g11}$, benchmark model parameters.

We have ${}_{6}^{12}C$ nucleus only by two pairs of high and low particles spiral ring side by side of the simplest type B nucleus, see figure 7.2. Laboratory determination of the carbon atom energy is 12u. Because electronic itself along the spin track motion of kinetic energy, the nuclei under the action of electric field force still has certain coulomb electrostatic field energy, so the quality of the nucleus for atomic mass minus all electronic rest mass plus all the ionization energy of $\sum \Delta W_{ei}$.

By figure 7.2 and figure 7.6, ${}_{6}^{12}C$ conditions within the nucleus high-energy particles spiral ring net with π_g^+ mesons in a total of 12, its own electric field energy should be $\left(12^2/2\right)eV_{eg11}$; Two side by side of low-energy particles spiral rings net with π_d^- both for six, and both sides symmetrical distribution, its own electric field energy should be $\left(6^2/2\right)eV_{ed11}$; π_d^- both with internal high-energy π_g^+ violation the interaction of electric field energy for $-6\times 12eV_{ed11}$; So, high carbon nuclei in ${}_{6}^{12}C$, low-energy particles spiral ring in excess π_g^+, π_d^- muon spin direction interaction should be total energy of the electric field:

$$W_e = (72V_{eg11} + 18V_{ed11} - 72V_{ed11})e \qquad (8.17)$$

Similarly, in ${}_{6}^{12}C$ nuclear spin direction of the magnetic field energy calculation, K_{bd11}= 4, in equations (8.13), (8.15) equations in P_i = 6, magnetic field total energy is:

$$W_b = W_{bg11} + W_{bd11} \qquad (8.18)$$

By figure 7.6, ${}^{12}_{6}C$ conditions within the nucleus in total by 18 high-energy $\pi_g^{\pm}$ mesons, 24 low-energy $\pi_d^{\pm}$ violation, and $\overline{m}_{g1} = 2\overline{m}_{d1}$, so, ${}^{12}_{6}C$ conditions within the nucleus of low-energy $\pi_d^{\pm}$both average benchmark energy $\overline{m}_{d1}$ should be:

$$\overline{m}_{d1} = \frac{12u - 6m_{e0} + \sum_{i=1}^{6} \frac{\Delta W_{ei}}{c^2} - \frac{(W_e + W_b)}{c^2}}{24 + 18 \times 2} \qquad (8.19)$$

$\overline{m}_{d1}$ Parameters specific simulation program are as follows:

1. By (8.1), the determination of the $N_{a1}=N_{ag1}=N_{ad1}=34/13$, generation into (4.9), to: $\beta_1=0.9989866946$.

2. Estimate $\overline{m}_{d1}$ initial value, section 8.2 has been mentioned in the beginning, high in nucleus, low-energy particles spiral ring net with $\pi^{\pm}$ mesons in spin direction, each other can only nucleus of the electric and magnetic field between 0.2~0.5% of the total energy, we will take 0.3%. Measured by the laboratory carbon atoms within 6 electronics total ionization energy $\sum \Delta W_{ei} = 1030.08\,ev$ ③. Will all these parameters into (8.19), is $\overline{m}_{d1}$ initial value for 3.310209258 x 10-28 kg.

3. The β_1, N_{ag1}, N_{ad1}, $\overline{m}_{d1}$, $\overline{m}_{g1}$ and initial value generation into (8.2), calculate $R_{\theta 0g1}$, $R_{\theta 0d1}$.

4. By figure 7.2 and figure 8.1, (8.9), (8.13) equation coefficient of the position: $K_{eg11} = K_{ed11} = 1$ $K_{bd11} = 4$

5. The $R_{\theta 0g1}$, $R_{\theta 0d1}$, N_{ag1}, N_{ad1} value generation into (8.10), respectively is $\overline{R}_{Ig1}$, $\overline{R}_{Id1}$, value.

6. Will N_{ag1}, N_{ad1}, β_1, $R_{\theta 0g1}$, $R_{\theta 0d1}$, K_{eg11} …… , equivalent generation into the equations (8.9), respectively is: V_{eg11}=1251884.632v , V_{ed11}=831741.7884v

7. Make $K_{bd11} = 4$, will be N_{ag1}, N_{ad1}, $R_{\theta 0g1}$, $R_{\theta 0d1}$ generation into the equations (8.13), respectively is L_{bg11}, L_{bd11} value.

8. Makes the number of protons $P_1 = 6$, the β_1, N_{ag1}, N_{ad1}, $\overline{R}_{Ig1}$, $\overline{R}_{Id1}$, L_{bg11}, L_{bd11} value generation into the equations (8.15), calculate the magnetic field strength H_{g1}, H_{d1} value.

9. Will H_{g1}, H_{d1}, $\overline{R}_{Jg1}$, $\overline{R}_{Jd1}$, L_{bg11}, L_{bd11} value generation in equations (8.16) first two type, calculate magnetic energy $W_{bg1}=1.071369311\times10^{-12}$J, $W_{bd1}=1.688824137\times10^{-13}$J

10. Will V_{eg11}, V_{ed11} value generation into (8.17), calculate the total electric energy W_e value.

11. Will W_e, W_b and $\sum \Delta W_{ei}$ value generation into (8.19), is the transition is $\overline{m}_{d1}=3.304434003\times10^{-28}$Kg

12. Will transfer value $\overline{m}_{d1}=3.304434003\times10^{-28}$Kg instead of 3 calculation program of $\overline{m}_{d1}$ initial value, repeat 3~11 calculation procedure, until the $\overline{m}_{d1}=3.304461327\times10^{-28}$Kg for constant.

$\overline{m}_{d1}$ = 3.304461327 x 10^{-28} kg benchmark constant said: in the number of protons $P_i \geq 6$ of the nucleus, proton number = neutron number is even the first layer of particles spiral rings, the original low $\pi_d^{\pm}$ meson energy is: $\overline{m}_{d1}=3.304461327\times10^{-28}$Kg .

Original high-energy $\pi_g^{\pm}$ mesons are 2 $\overline{m}_{d1}$ energys. Residual energy is high, low-energy particle spiral loop net with $\pi^{\pm}$ violation in the spin direction of interaction between electric and magnetic energy.

9. Conditions within the nucleus

N_{adi}, N_{agi}, $\overline{m}_{di}$, $\overline{m}_{gi}$ and nuclear energy density and the electric field parameters

9.1. N_{adi}, N_{agi}, $\overline{m}_{di}$, $\overline{m}_{gi}$ parameters

By (7.2), charged elementary particles in the fluctuation, the spin track movement in the direction of comprehensive force analysis and calculation results show that charged particle in electric and magnetic field force, nuclear power field force, under the action of centrifugal force is along the wave vector rail inside diameter automatic shrinkage in the center of the trend. From figure 7.1 and figure 7.1 within the nucleus of the high and low particles spiral loop combination structure can also be seen in: each layer low-energy particles spiral ring of the spin track occupied space should be minimal, get recently, and not overlap. 2 ~ 5 layers of each pair of high and low particles spiral ring on the inside of the spin track R_{0gi0}, R_{0di0} in also is such. All high, low-energy particle spiral ring in addition to the first layer, the quantum fluctuations of N_{adi}, N_{agi} shall take natural number.

Refer to section 7.1 of the nucleus kernel forces forming principle, by figure 9.1 low-energy particles spiral ring layer combination that: the bottom low-energy particles spiral ring in excess π_d both in the spin track intersec ting in the formation of ampere force can cover the economical and the upper surplus high and low $\pi^{\pm}$ muon solenoid ring particles of the axial electric field force, should be comprehensive comparison a, b, c, d,... each boundary point, internal non-oil imports all the ampere force and comprehensive relationship between the size of the axial electric field force and. That as space limit set of geometric conditions, by figure 9.1, the first a_1< 180°, if by three same radius. Close packing of the cylinder is a_1= 150 °, so, a_1 scope is: 180° > a_1 > 150°.

According to the set position and fluctuation, the relationship between the spin track parameters, low-energy particles spiral ring of n side by side, we have:

$$\begin{cases} n\overline{R}_{\alpha b2} - R_{\alpha 2}\sin\alpha_2 = (n+1)\overline{R}_{\alpha b1} - R_{\alpha 1}\sin\alpha_1 & (9.1-1) \\ R_{\theta 02} - R_{\theta 01} = R_{\alpha 2}\cos\alpha_2 - R_{\alpha 1}\cos\alpha_1 & (9.1-2) \end{cases}$$

Will (8.1), (8.2) and (8.4) into (9.1) equations, to: $K_d = \beta_2\overline{m}_{d2} \Big/ \beta_1\overline{m}_{d1}$ Checking:

$$\begin{cases} \dfrac{\sin\alpha_2}{\sqrt{N_{\alpha d2}} + \cos\alpha_2} = \dfrac{1}{\sqrt{N_{\alpha d2}-1}}\left[n - K_d\left(n+1 - \dfrac{\sin\alpha_1\sqrt{N_{\alpha d1}-1}}{\sqrt{N_{\alpha d1}} + \cos\alpha_1} \right) \right] & (9.2-1) \\ \dfrac{\cos\alpha_2}{\sqrt{N_{\alpha d2}} + \cos\alpha_2} = 1 - \dfrac{K_d\sqrt{N_{\alpha d1}^2 - N_{\alpha d1}}}{(\sqrt{N_{\alpha d1}} + \cos\alpha_1)\sqrt{N_{\alpha d2}-1}} & (9.2-2) \end{cases}$$

By (9.2-2), to:

$$\cos\alpha_2 = \sqrt{N_{\alpha d2}}\left[\frac{\sqrt{N_{\alpha d2}-1}(\sqrt{N_{\alpha d1}} + \cos\alpha_1)}{K_d\sqrt{N_{\alpha d1}^2 - N_{\alpha d1}}} - 1 \right] \qquad (9.3)$$

Simultaneous equations (9.2) to:

$$\frac{1}{(\sqrt{N_{\alpha d2}} + \cos\alpha_2)^2} = \frac{1}{N_{\alpha d2}-1}\left\{ \left[n - K_d\left(n+1 - \frac{\sin\alpha_1\sqrt{N_{\alpha d1}-1}}{\sqrt{N_{\alpha d1}} + \cos\alpha_1} \right) \right]^2 + \left[\sqrt{N_{\alpha d2}-1} - \frac{K_d\sqrt{N_{\alpha d1}^2 - N_{\alpha d1}}}{\sqrt{N_{\alpha d1}} + \cos\alpha_1} \right]^2 \right\} \qquad (9.4)$$

Will type (9.3) into (9.4), to:

$$\frac{K_d\sqrt{N_{\alpha d1}^2 - N_{\alpha d1}}}{\sqrt{N_{\alpha d1}} + \cos\alpha_1} = \sqrt{N_{\alpha d2}}\left\{ \left[n - K_d\left(n+1 - \frac{\sin\alpha_1\sqrt{N_{\alpha d1}-1}}{\sqrt{N_{\alpha d1}} + \cos\alpha_1} \right) \right]^2 + \left[\sqrt{N_{\alpha d2}-1} - \frac{K_d\sqrt{N_{\alpha d1}^2 - N_{\alpha d1}}}{\sqrt{N_{\alpha d1}} + \cos\alpha_1} \right]^2 \right\}^{1/2} \qquad (9.5)$$

From figure 9.1, the upper and the lower low-energy particles spiral ring inlaid space relationship, equations (9.1) and (9.5) that the mathematical physics graphics

meaning is: the upper low-energy particles spiral ring should be staggered as far as possible close to the lower, but in a, b, c, d,... Each point can only as far as possible close to, can't tangent or intersection. So we must in the 180° > a_1 >150° range, solution (9.5), is on behalf of the rail tangent or position of the intersection of equations N_{ad2} the biggest natural number, add 1, make it become no equation, such ability is in recently, and not tangent or intersection, and the inner and outer rail left electric dipole rotation and axial clearance swing adjustment of space.

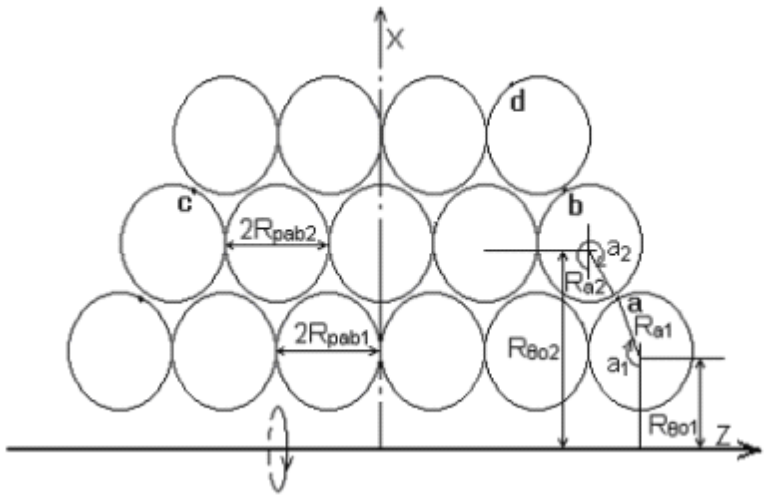

Figure 9.1 low-energy particles in the nucleus of solenoid ring inlaid portfolio

By (6.2 1), (8.1) and (8.2), a pair of high and low particles spiral ring should be on the inside of the spin track closely adjacent, but can't overlap, we have:

$$\begin{cases} R_{\theta di(0)} = \dfrac{h\sqrt{N_{\alpha di}^2 - N_{\alpha di}}}{2\pi\beta_{di}c\overline{m}_{di}(\sqrt{N_{\alpha di}}+1)} & (9.6-1) \\ R_{\theta gi(0)} = \dfrac{h\sqrt{N_{\alpha gi}^2 - N_{\alpha gi}}}{2\pi\beta_{gi}c\overline{m}_{gi}(\sqrt{N_{\alpha gi}}+1)} & (9.6-2) \end{cases}$$

Through simulation, we must make $R_{\theta gi(0)}$ is slightly larger than the $R_{\theta di(0)}$. By (7.3), each layer, low-energy particle spiral ring in the number of protons is equal to the number of neutrons are even, under the situation of the total magnetic 0 condition is:

$$K_{mui}=\frac{\overline{m}_{gi}}{\overline{m}_{di}}=\frac{2\oint\frac{N_{\alpha gi}-1}{(\sqrt{N_{\alpha gi}}+\cos\alpha)^2}d\theta}{\oint\frac{N_{\alpha di}-1}{(\sqrt{N_{\alpha di}}+\cos\alpha)^2}d\theta} \qquad (9.7)$$

Obviously, by figure 7.5, (9.7), too: when the layer, low-energy particle spiral ring number of protons equals the number of neutrons are even, high, low $\pi^{\pm}$ source energy relationship is:

$$6\overline{m}_{gi}+8\overline{m}_{di}=20\overline{m}_{d1} \qquad (9.8)$$

Will K_{mui} value generation into (9.8), to:

$$\overline{m}_{di}=\frac{20\overline{m}_{d1}}{6K_{mui}+8} \qquad (9.9)$$

By equations (9.9) and (9.2), (9.5) in K_d and can be expressed as:

$$K_d=\frac{\beta_{di+1}(6K_{mui}+8)}{\beta_{di}(6K_{mui+1}+8)} \qquad (9.10)$$

To sum up, within the nucleus N_{adi},N_{agi}, $\overline{m}_{di}$, $\overline{m}_{gi}$, parameters such as simulation program is as follows:

1. Shilling (9.5) in type K_d = 1, N_{ad1}= N_{ag1} = 34/13, n = 5, generation of (9.5) in type, too: N_{ad2}=15 is the largest natural number, at this moment: a_1 = 160.5441181 °

2. Take N_{ad2} = 16, generation of (4.9) in type, have β_{d2}. Behind a K_{mu2} = 1.95, (with the calculation results are expected to), and (9.9), (9.7) in type, have $\overline{m}_{d2}$, $\overline{m}_{g2}$ value.

3. Make N_{ag2} = 48, generation of (4.9) in type, have β_{g2}. Will N_{ad2}、β_{d2}、$\overline{m}_{d2}$, N_{ag2}, β_{g2}, $\overline{m}_{g2}$, respectively into (9.6-1), (9.6-2), to: $R_{\theta d2(0)}$=3.25289×10^{-15}m, $R_{\theta g2(0)}$=3.22557×10^{-15}m，$R_{\theta g2(0)}$<$R_{\theta d2(0)}$, obviously not appropriate.

4. Adjust N_{ag2} = 49, repeat 3 calculation procedure, to: $R_{\theta g2(0)}=3.26392\times10^{-15}$m, slightly larger than the $R_{\theta d2(0)}=3.25289\times10^{-15}$m, this is question.

5. Will N_{ad2} = 16, N_{ag2} = 49, generation of (9.7) in type, too: K_{mu2} = 1.95655948

6. Repeat 2 ~ 4 calculation program: $R_{\theta d2(0)}=3.25939\times10^{-15}$m, $R_{\theta g2(0)}=3.25948\times10^{-15}$m, the result still. According to (7.3) and the calculation procedure, may have other relevant parameters:

β_{d2}=0.998751741 $U_{\pi-}$=-2.605996272×10^{-26}J/T

$\overline{m}_{g2}$=6.550745472×10^{-28}Kg $\overline{m}_{d2}$=3.348094213×10^{-28}Kg

7. The β_{d2}, β_{g2}, $\overline{m}_{g2}$, $\overline{m}_{d2}$ value, again into (9.10), to: K_d=1.012934831. To N_{ad1}=34/13, N_{ad2}=15, generation of (9.5) in type, too: a_1=158.4362343 °, than estimated value is small. If N_{ad2} = 16 generation into the duplication in calculation, this equation is still no solution. By the same token, if for n=1~ 7 also have no solution.

8. Reference 1 ~ 7 calculation procedure, we find the other layers of N_{adi}, N_{agi}, $\overline{m}_{di}$, $\overline{m}_{gi}$ parameters, such as shown in table 9.1.

(note: the second layer of $R_{\theta g2(0)}$ is only slightly larger than the $R_{\theta d2(0)}$ value, even electric dipole rotation space is not enough, so adjust take N_{ad2} = 16, N_{ag2} = 50)

By (8.19), (9.7) ~ (9.9), table 9.1 the results see: within the nucleus, every layer, low-energy particle spiral ring of high and low $\pi^{\pm}$source energy and the formation of the spin direction magnetic moment is constant, only with the spin track quantum fluctuations in interest of N_{ai}. Each layers between the high and low $\pi^{\pm}$ both original energy and strength are not the same. Number of protons is equal to the number of neutrons and are even the nucleus of the fluctuation, the movement of the spin direction of the original total energy for $\sum 5A_i\overline{m}_{d1}$, (A_i for each layer of the nuclear), and magnetic moment is zero.

If the protons and neutrons is not even, should refer to section 7.1, first according to the actual total energy and strength of the nucleus value simulation. Determination alone protons, neutrons "decentralized" of the $\pi^{\pm}$ mesons in every particle of solenoid the distribution state of link layer, and calculated separately by the state's high and low $\pi^{\pm}$ muon accumulative total energy niv original magnetic moment. (see chapter 11, 12).

Conditions within the nucleus N_{adi}, N_{agi}, $\overline{m}_{di}$, $\overline{m}_{gi}$, parameters such as simulation results table 9.1

Spiral ring layer i	1	2	3	4	5
$N_{ad\ i}$	34/13	16	34	58	88
$N_{ag\ i}$	34/13	50	114	203	316
$\times 10^{-15}$m					
$R_{\theta d\ i\ (0)}$	0.83688	3.25899	5.19382	7.08675	8.96202
$R_{\theta g\ i\ (0)}$	0.41844	3.29768	5.20204	7.09552	8.96994
$\times 10^{-28}$Kg					
$\overline{m}_{di}$, $\overline{m}_{gi}$	3.304461327	3.348508962	3.325343178	3.316814573	3.312652282
	6.608922654	6.550192474	6.581080186	6.592451659	6.598001381
$K_{mu\ i}$	2	1.956151991	1.979067974	1.987585231	1.991757909
$\times 10^{-26}$J/T					
$U_{d\pi--}$	-3.25301628	-2.605673491	-2.578713629	-2.569286142	-2.56485582
$U_{g\pi+}$	1.626508137	1.302836745	1.289356815	1.284643071	1.282427909

9.2 Nuclear energy, the electric field parameters Within the nucleus

9.2.1 Conditions within the nucleus of each particle spiral ring of Nuclear number density

By (1.3-2), (1.6), a low-energy $\pi_d^{\pm}$ muon spin elliptical orbit, the average radius, which is elliptic half axis of $\overline{R}_{\theta di}$ for:

$$\overline{R}_{\theta di} = \frac{hN_{\alpha di}}{2\pi\beta_i c\overline{m}_{di}\sqrt{N_{\alpha di}-1}} \qquad (9.11)$$

Experiments have confirmed: nuclear and excess charge are within the nucleus of density distribution, boundary is diffuse layer, see figure 7.3. When we are in carbon conditions within the nucleus of the two side by side particles spiral ring in 12 nuclear, make layer, see figure 7.6, we can based on the average radius of $\overline{R}_{\theta di}$, related parameters according to table 9.1, to the middle of the inner particles spiral ring density for the principle, such as saturated layer, step by step, one by one particle spiral ring outside push each layer of the nucleon.

Conditions within the nucleus nucleon density, the number of each layer of nuclear should be natural, and they must all be even. Because each layer of the β_i, $\overline{m}_{di}$ value approximation, (9.11), the $h/2\pi\beta_i\overline{m}_{di}c$ can be regarded as constant. Set each layer particles spiral rings of nuclear along the spin track average perimeter of $2\pi\overline{R}_{\theta di}$ for density distribution, such as each particle spiral rings of nuclear for A_i, is:

$$A_i = \frac{6N_{\alpha di}\sqrt{N_{\alpha d1}-1}}{N_{\alpha d1}\sqrt{N_{\alpha di}-1}} \qquad (9.12)$$

To N_{adi} = 34/13, 16, 34, 58, 88 respectively into (9.12), results in the most close to the even number of each layer to particles spiral ring should fill the number of nuclear respectively: 6, 12, 18, 22, 28.

9.2.2 Within the nucleus high, low-energy particle spiral ring net with $\pi^{\pm}$ mesons in potential can parameters

Refer to section 8.2 conditions within the nucleus net with $\pi^{\pm}$ muon electric field energy equation, according to table 9.1 determine each particle of spiral rings in high and low $\pi^{\pm}$ muon quantum fluctuations of number N_{adi}, N_{agi}, original energy $\overline{m}_{di}$, $\overline{m}_{gi}$, value, high in nucleus, low-energy particles spiral ring net with $\pi^{\pm}$ mesons in potential can parameter calculation procedure is as follows:

Type A each, low-energy particles spiral ring high within the nucleus Net with $\pi^{\pm}$ mesons in potential being access (unit: v) table 9.2

j / N_{ai}	0	1	2	3	4	5	6
88	144784.2304		141618.5269				
316	y. 151861.9825		z. 148192.4244				
58		v. 177326.8464		x. 166483.1247			
203		u. 187584.5213		w. 174745.2164			
34	o. 234938.4252		q. 222384.0614		t. 194154.5797		
114	m. 252547.2638		n. 236860.6565		s. 203024.7476		
16		h. 337957.7853		k. 279802.5875		r. 219311.3930	
50		g. 366998.7106		i. 293490.8388		p. 223733.7219	
34/13	b. 978319.7079		d. 624855.4140		f. 385747.0362		l. 271894.2180
34/13	a. 1956639.416		c. 771494.0723		e. .416814.5755		j. 282481.5199

Type B each, low-energy particles spiral ring high within the nucleus Net with $\pi^{\pm}$ mesons in potential being access (unit: v) table 9.3

j / N_{ai}	0	1	2	3	4	5
88		v. 143972.9349				
316		u. 150919.0911				
58	s. 178836.7777		t. 173016.7819			
203	q. 189396.5791		r. 182445.3143			
34		n. 231601.1851		p. 209202.2517		
114		l. 248335.1566		o. 220829.7834		
16	f. 348109.8205		j. 312143.6925		m. 247821.4242	
50	e. 380656.7922		h. 333443.6084		k. 255901.5851	
34/13		b. 830297.5310		d. 481404.0368		i. 319619.5653
34/13		a. 1249710.828		c. 543788.4359		g. 336991.4616

1. Will AAN$_{adi}$, N$_{agi}$ value respectively into (4.9), calculate each layer $\pi^{\pm}$ both wave velocity coefficient β_{di}, β_{gi} value.

2. Will N$_{adi}$, N$_{agi}$, $\overline{m}_{di}$, $\overline{m}_{gi}$, β_{di}, β_{gi} generation into (8.2), respectively is $R_{\theta 0di}$, $R_{\theta 0gi}$ value.

3. According to figure 7.1 and figure 7.2, decide within the nucleus of A and B type structure, by (8.5) and (8.6) equations of each coefficient to the position of the high, low-energy particles spiral ring $K_{egij} = K_{edij} = 0 \sim 6$ of A natural number.

4. Will corresponding N_{adi}, N_{agi}, $\overline{m}_{di}$, $\overline{m}_{gi}$, β_{di}, β_{gi} and K_{egij}, K_{edij} value, respectively into (8.9-1), (8.9-2) type, you can work out A and B type all high in nucleus, low-energy particles spiral rings, each net with $\pi^{\pm}$ violation of electric parameters, see table 9.2 and table 9.3. English letters both on behalf of the potential value of parameters in table size order, also as the column parameter in subsequent analysis and calculation the location of the code used (the same below).

9.2.3 The application of the calculation parameters within the nucleus

Because conditions within the nucleus protons and neutrons are even a, its total magnetic is 0, so (9.7) ~ (9.10) and calculation of $\overline{m}_{di}$, $\overline{m}_{gi}$ in table 9.1, the original data is nuclear energy within each layer particles spiral ring of equal number of protons, neutrons and are even under the condition of only. From the nuclide commonly used data sheet (4) check: in nature can be stable in the entire nucleus, in addition to the $^{3}_{2}He$ nuclear, internal number of neutrons are greater than the number of protons. Unstable nuclei, from nuclear power charge + number 29 of $^{58}_{29}Cu$ nucleus, the internal number of neutrons are greater than the number of protons.

Extra neutron in pairs only will be the "decentralized" all of the high and low $\pi^{\pm}$ violation according to the figure 7.4 and figure 7.5 a and b solutions into the same layer particles spiral rings, and magnetic moment is zero. So, from the table 9.1 $\overline{m}_{di}$, $\overline{m}_{gi}$, original energy data, calculate each pair of extra neutron in 2, 3, 4, 5 particles spiral ring has the relative 1 layer the original energy increment of $\Delta\overline{m}_{ni}$ is: (if lack of neutron log, $\Delta\overline{m}_{ni}$ take negative, as shown in the figure 11.1) on the right side:

$$\Delta\overline{m}_{ni}=2(\overline{m}_{di}-\overline{m}_{gi})+6(\overline{m}_{di}-\overline{m}_{d1}) \qquad (9.13)$$

Similarly, without changing nuclear magnetic and nuclear power load distribution condition, when each pair of high or low $\pi^{\pm}$ violation in the particles spiral ring stimulated or transition between layers, will also lead to $\pi^{\pm}$ muon original energy changes. We with $\Delta\overline{m}_{gi}^{\pm}$, $\Delta\overline{m}_{di}^{\pm}$, said, (see chapter 11 ~ 14 calculating examples).

Comprehensive table 9.1 and table 9.2 and table 9.3 the calculation of the parameters, we can not only according to the total energy conservation, atoms, the total energy and nuclear magnetic moment, simulation, calculation of a nucleus within the particles spiral ring layer net with $\pi^{\pm}$ mesons in the distribution of state, but also can judge of extra neutron distribution level, or paired $\pi^{\pm}$ mesons, single $\pi^{\pm}$ both inspire and transition. (see chapter 11 ~ 14 calculating examples).

10. Nuclear force equation and parameter calculation

10.1. Electric field force equation and Parameter calculation within the nucleus

Conditions within the nucleus every high, low-energy particle spiral ring in excess of $\pi^{\pm}$ violation, the spin track movement, from the center of a nucleus in R_e, electric field force in spin rail axial component $F_{e\theta dij}$, is a very complex variables, we still need integral equation to calculate, see figure 10.1.

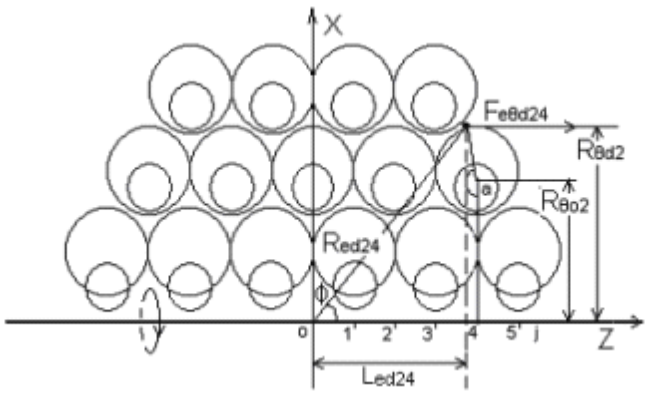

Figure 10.1 $\pi^{\pm}$ muon within the nucleus formation of electri Field force diagram

According to equations (8.9) in the nucleus in $\pi^{\pm}$ muon derivations of the equations of potential can process, by (8.3), $\pi^{\pm}$ muon spin track along the length of the spin direction $L_{\theta i}$ is given as:

$$L_{\theta i} = \frac{2\pi R_{\theta 0 i}\sqrt{N_{\alpha i}}}{\sqrt{N_{\alpha i}-1}} \qquad (10.1)$$

Each particle spiral ring each of the surplus of $\pi^{\pm}$ muon relative nuclei formed in the center of the electric field force, along the spin axis and the component of $F_{e\theta i}$, suppose particles spiral rings surrounded by excess nuclear power charge for K_{ei}, while its general for:

$$F_{e\theta i} = \frac{K_{ei}e^2}{4\pi\varepsilon_0}\oint \frac{R_{\theta i}\cos\phi}{L_{\theta i}R_{ei}^2\sqrt{1-\left(v_{\theta i}/c\right)^2}}d\theta \qquad (10.2)$$

$$\begin{cases} \cos\phi = \dfrac{L_{eij}}{R_{ei}} & (10.3-1) \\ L_{egij} = \dfrac{K_{edij}R_{\theta 0di}}{\sqrt{N_{\alpha di}-1}} - \dfrac{R_{\theta 0gi}\sin\alpha}{\sqrt{N_{\alpha gi}}+\cos\alpha} & (10.3-2) \\ L_{edij} = \dfrac{K_{edij}R_{\theta 0di}}{\sqrt{N_{\alpha di}-1}} - \dfrac{R_{\theta 0di}\sin\alpha}{\sqrt{N_{\alpha di}}+\cos\alpha} & (10.3-3) \\ R_{egij}^2 = L_{egij}^2 + R_{\theta gi}^2 & (10.3-4) \\ R_{edij}^2 = L_{edij}^2 + R_{\theta di}^2 & (10.3-5) \end{cases}$$

Similarly, by figure 10.1, (8.4), to: high and low particles spiral ring of L_{eij}, $\cos\Phi$, R_{ei}, stores to see the relationship between the equations (10.3).

Will be respectively equations (10.3) into (10.2), to:

$$\begin{cases} F_{e\theta gij} = \oint \dfrac{K_{ei}e^2\sqrt{N_{\alpha gi}-1}\left[\dfrac{K_{edij}R_{\theta 0di}\left(\sqrt{N_{\alpha gi}}+\cos\alpha\right)}{R_{\theta 0gi}\sqrt{N_{\alpha di}-1}}-\sin\alpha\right]\left(\sqrt{N_{\alpha gi}}+\cos\alpha\right)}{8\pi^2\varepsilon_0 R_{\theta 0gi}^2\left\{\left[\dfrac{K_{edij}R_{\theta 0di}\left(\sqrt{N_{\alpha gi}}+\cos\alpha\right)}{R_{\theta 0gi}\sqrt{N_{\alpha di}-1}}-\sin\alpha\right]^2+N_{\alpha gi}\right\}^{\frac{3}{2}}\sqrt{1-\dfrac{\beta_{gi}^2}{N_{\alpha gi}}}}d\theta & (10.4-1) \\ F_{e\theta dij} = \oint \dfrac{K_{ei}e^2\sqrt{N_{\alpha di}-1}\left[\dfrac{K_{edij}\left(\sqrt{N_{\alpha di}}+\cos\alpha\right)}{\sqrt{N_{\alpha di}-1}}-\sin\alpha\right]\left(\sqrt{N_{\alpha di}}+\cos\alpha\right)}{8\pi^2\varepsilon_0 R_{\theta 0di}^2\left\{\left[\dfrac{K_{edij}\left(\sqrt{N_{\alpha di}}+\cos\alpha\right)}{\sqrt{N_{\alpha di}-1}}-\sin\alpha\right]^2+N_{\alpha di}\right\}^{\frac{3}{2}}\sqrt{1-\dfrac{\beta_{di}^2}{N_{\alpha di}}}}d\theta & (10.4-2) \end{cases}$$

Refer to 9.2 electricity field energy parameters of calculation program: A and B type all high in nucleus, low-energy particles spiral rings in each net with $\pi^{\pm}$ muon along the spin track the electric field of the axial force parameters see table 10.1 and table 10.1. (K_{ei} valuesfor the time being).

Type A nucleus in all high, low-energy particle spiral loop net with $\pi^{\pm}$ violation Along the spin track the axial electric field force parameters calculation results table (unit: Newton N) table 10.1

j / N_{ai}	0	1	2	3	4	5	6
88							
316	y.		z.				
58		v. 0.4498676718		x. 1.116732986			
203		u. 0.5389700316		w. 1.307093887			
34	o.		q. 1.749312461		t. 2.327181743		
114	m.		n. 2.156310585		s. 2.715754808		
16		h. 2.957833954		k. 5.021374766		r. 4.023396124	
50		g. 3.939440164		i. 6.042344046		p. 4.460667800	
34/13	b.		d. 26.27706782		f. 11.80397946		l. 6.156321505
34/13	a.		c. 47.21591785		e. 14.76239942		j. 6.887946657

10.2. low-energy particles in the nucleus of solenoid Ring rail tangent equation and parameter calculation Of ampere force

From in figure 7.1 and figure 7.2 see: economical adjacent low-energy particles spiral ring of $\pi_d^{\pm}$ mesons, will remain fixed interval in the same wave, spin speed staggered successively by tangent track; When $v_a \to c$, the fluctuation of electricity, the direction of the magnetic field perpendicular to the wave track, despite the strength is very big, but by (2.1), (2.2), the fluctuation track the tangent direction of electric and magnetic field force is very weak; Only in the spin current direction orbit can have significant interaction, because $K_r = 10^{-4}$, $K_{r'} = 8\times10^{15}$ orders of magnitude, so can become a great track current ampere force itself.

particles spiral ring of π_g^{+} muon electric field force each other.

By (1.3 1) type, figure 10.2, the two adjacent side by side A and B low-energy particles spiral ring rail on the intersec ting, fluctuation elliptical orbit radius R_a, half axis R_{aa}, half focal length R_{ac}, half R_{ab} short axis, and a_1 value equation is as follows:

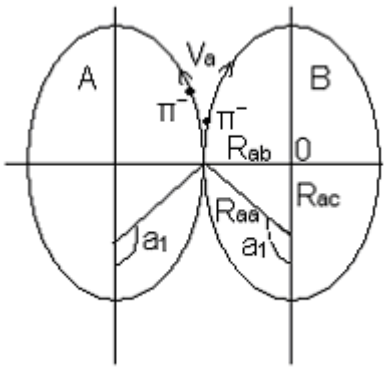

Figure 10.2 fluctuations in elliptical orbit parameters relationship

$$\begin{cases} R_{\alpha} = \dfrac{R_{\theta 0}}{\sqrt{N_{\alpha}} + \cos\alpha} & (10.5-1) \\ R_{\alpha a} = \dfrac{R_{\theta 0}\sqrt{N_{\alpha}}}{N_{\alpha} - 1} & (10.5-2) \\ R_{\alpha c} = \dfrac{R_{\theta 0}}{N_{\alpha} - 1} & (10.5-3) \\ R_{\alpha b} = \dfrac{R_{\theta 0}}{\sqrt{N_{\alpha} - 1}} & (10.5-4) \\ \alpha_1 = \arccos\dfrac{-1}{\sqrt{N_{\alpha}}} & (10.5-5) \end{cases}$$

Type B all high in nucleus, low-energy particles spiral net with $\pi^{\pm}$ mesons in ring Along the spin track the axial electric field force parameters calculation results table (unit: Newton N) table 10.2

j / Nai	0	1	2	3	4	5	6
88		v. 0.2424503354					
316		u. 0.2815204385					
58	s.	t. 0.8356753262					
203	q.	r. 0.9917450997					
34		n. 0.9881705354	p. 2.183956711				
114		l. 1.242583809	o. 2.621118729				
16	f.	j. 4.654238992		m. 4.647168885			
50	e.	h. 5.908301428		k. 5.33996127			
34/13		b. 33.60158953	d. 17.42218092		i. 8.351933465		
34/13		a. 47.21591785	c. 24.62528602		g. 9.747158235		

Note: table 10.2 a column position data for the two side by side of high-energy

In the fluctuation, the spin track tangent, side by side A and B in low-energy particle spiral ring net with π_d both electric dipole rotation diameter $2K_rR_a$ for a---a`、b----b` line, see figure 10.3. In the intersection of plane, the current forming principle as shown in figure 10.3: every π_d violation by a---a`、b----b` line intersection of plane, is equivalent to a load of charged particles from a to a ` and from b to b ` movement; Formed from a` to a from b to b's current I_a, I_b. When A and B two pairs of high and low combination of particles spiral rings, because of the spin axis of the electric field

repelling force, are in A state of tension, as shown by the figure 10.4, as long as the I_a, I_b ampere force is greater than the comprehensive electric field between repelling force, can prevent them from further stretching to disconnect. At this time:

$$\begin{cases} \phi = \alpha_1 - 90^\circ & (10.6\text{-}1) \\ L_b = 4K_r\overline{R}_\alpha \sin\phi & (10.6\text{-}2) \end{cases}$$

Principle of electrodynamics, each π_d both in tangent track along the spin direction of current strength I, magnetic field intensity B respectively:

$$\begin{cases} I = \dfrac{-e\beta c}{2\pi\overline{R}_I\sqrt{N_\alpha}} & (10.7-1) \\ B = \dfrac{Iu_0\cos 2\phi}{2\pi L_b} & (10.7-2) \end{cases}$$

Will type (8.10) into (10.7), to:

$$I = \frac{-e\beta c\sqrt{N_\alpha - 1}}{2\pi R_{\theta 0}N_\alpha} \qquad (10.8)$$

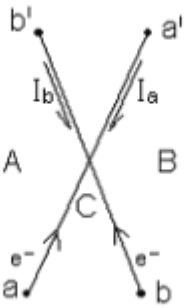

Figure 10.3 π_d both within the electric dipole rotation plane current forming principle diagram

Because a` b` point I_a and I_b current track overlap, by (3.4), calculateK_r=8.0x10^{-15}, so, each orbit between tangent I_a and I_b current F_{kb} of ampere force is:

$$F_{kb} = \int_{Kr\bullet\overline{R}\alpha}^{2Kr\overline{R}\alpha} IB\cos\phi dl = \int_{Kr\bullet\overline{R}\alpha}^{2Kr\overline{R}\alpha} \frac{u_0 I_a I_b \cos\phi\cos 2\phi}{4\pi\sin\phi(2K_r\overline{R}_\alpha)} d(2K_r\overline{R}_\alpha) \qquad (10.9)$$

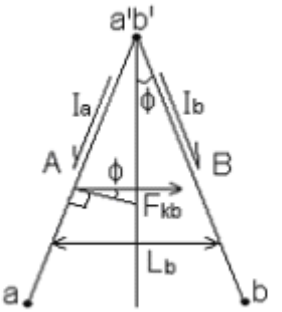

Between figure 10.4 I_a and I_b current ampere force diagram

Will (10.7-1) and (10.9) in type integral to:

$$F_{kb}=\frac{e^2\beta^2(N_\alpha-1)\cos\phi\cos 2\phi}{4\pi\varepsilon_0(2\pi R_{\theta 0})^2 N_\alpha^2\sin\phi}\ln(2K_r\overline{R}_\alpha)\Big|_{Kr\bullet\overline{R}\alpha}^{2Kr\overline{R}\alpha} \qquad (10.10)$$

For economical adjacent low-energy particles spiral rings, each spin track cycle have N_a tangent track, so:

$$F_{kb}=\frac{e^2\beta^2(N_\alpha-1)\cos\phi\cos 2\phi}{4\pi\varepsilon_0(2\pi R_{\theta 0})^2 N_\alpha\sin\phi}\ln(2K_r\overline{R}_\alpha)\Big|_{Kr\bullet\overline{R}\alpha}^{2Kr\overline{R}\alpha} \qquad (10.11)$$

From table 9.1 to determine the N_{adi}, $\overline{m}_{di}$ parameters, respectively into (4.9), (1.6), (10.5 5) type, find $\beta_i, R_{\theta 0i}, a_i$ value; The β_i, N_{adi}, a_i value generation into (2.10), respectively, for K_{ri} value; Finally by F_{kb} value (10.11), the results shown in table 10.3.

Low-energy particles spiral ring rail tangent place I_a and I_b current parameters of ampere force calculation results table table 10.3

N_{adi} / Parameters	34/13	16	34	58	88
$\overline{m}_{di}\times10^{-28}$Kg	3.304461327	3.348508962	3.325343178	3.316814573	3.312652282
β_{di}	0.9989866946	0.998751741	0.9987299178	0.9987219848	0.998718171
a°	128.1955197	104.4775122	99.87496139	97.54509259	96.11937788
$K_{ri}\times10^{-5}$	14.1733	6.36539	4.40105	3.37903	2.74688
F_{kbi}(牛)	14.26555772	26.21495095	19.10379436	14.8492151	12.09695581

10.3 Nucleus side by side in adjacent particles spiral ring the spin direction ampere force equation

For each pair of high and low particles spiral ring, the spin direction each net with $\pi^{\pm}$ muon form the current strength of AA $I_{\theta i}$, by (10.8), to:

$$I_{\theta i} = \frac{e\beta_i c\sqrt{N_{\alpha i} - 1}}{2\pi R_{\theta 0 i} N_{\alpha i}} \qquad (10.12)$$

Because the ampere force between particles spiral ring current not only stronger than the nuclear field, rail tangent of ampere force much smaller; And inversely proportional to the distance between each other, the lower level between the smaller; So, we as long as the calculation between adjacent particles spiral ring current ampere force is enough, and to simplify the calculation. First of all, to $\overline{m}_{gi} = 2\overline{m}_{di} = 2\overline{m}_{d1}$, β_i=1, the type (1.6) into (10.12), to:

$$I_{\theta i} = \frac{ec^2 \overline{m}_i}{N_{\alpha i} h} \qquad (10.13)$$

Set each of high, low-energy particle spiral loop net with π_g^+ number of mesons is N_{egij}, net with π_d^- both for N_{edij}. Each of high, low-energy particle spiral loop net current $\Delta I_{\theta ij}$, for high and low particles spiral rings contain net with $\pi^{\pm}$ muon formed in the spin direction current of algebra and:

$$\Delta I_{\theta ij} = \frac{ec^2 \overline{m}_{di}}{h}\left(\frac{2N_{egij}}{N_{\alpha gij}} - \frac{N_{edij}}{N_{\alpha dij}}\right) \qquad (10.14)$$

Side by side adjacent ampere force between two particles spiral ring current $\Delta F_{\theta bij}$, we can reference (10.7-2), (10.9) type simplifies calculation, to:

$$\begin{cases} \Delta B_{\theta ij} = \dfrac{u_0 \Delta I_{\theta ij}}{2\pi(2R_{\alpha bi})} & (10.15-1) \\ \Delta F_{\theta bij} = \Delta I_{\theta ij} \Delta B_{\theta ij}(2\pi \overline{R}_{I\,i}) & (10.15-2) \end{cases}$$

To (8.10), (10.5-4), (10.14) and (10.15) into the equations:

$$\Delta F_{\theta bij}=\frac{e^2}{2\varepsilon_0 N_{\alpha di}^{1.5}}\left(\frac{\overline{m}_{di}c}{h}\right)^2\left(2N_{egi\lambda}\frac{N_{\alpha di}}{N_{\alpha gi}}-N_{edi\lambda}\right)\left(2N_{egi2}\frac{N_{\alpha di}}{N_{\alpha gi}}-N_{edi2}\right) \quad (10.16)$$

Each pair of high and low particles spiral rings, in addition to the atomic nucleus edge, it is the left and right sides adjacent particles spiral ring of ampere force interaction, therefore, can be made by the resultant force on both sides of the $\Delta F_{\theta bij}$ said:

$$\Delta F_{\theta bij}=\frac{(e\overline{m}_{d\lambda}c)^2}{2\varepsilon_0 h^2 N_{\alpha di}^{1.5}}\left(2N_{egi2}\frac{N_{\alpha di}}{N_{\alpha gi}}-N_{edi2}\right)\left[2\frac{N_{\alpha di}}{N_{\alpha gi}}(N_{egi\lambda}-N_{egi3})-(N_{edi\lambda}-N_{edi3})\right]$$

(10.17)

By (10.17), $K_{fb}=\frac{(e\overline{m}_{di}c)^2}{2\varepsilon_0 h^2 N_{\alpha di}^{1.5}}$, N_{edi} = 34/13, 16, 34, 58, 88. Generation into, K_{fb} respectively: (unit: Newton) 7.660711103、 0.506281966、 0.1634383828、 0.07335512162、0.03925079193

Will table 10.1 ~ 10.3 compared with the corresponding data, as well as after facing the nucleus internal structure parameters integrated computation verification and nucleus radioactive decay analysis of the principle of the calculation results show that low-energy particles between spiral ring current track side by side on the intersec ting oneself ampere force, the range is limited to track tangent $K_r\overline{R}_\alpha$ within the scope of minimal, and mutual attraction is quite large, and the comprehensive electric field within the nucleus repelling force just can be composed of a pair of phase equilibrium of the nuclear force. Side by side of ampere force between particles spiral ring current, only 1 layer must attend calculation, the other can be neglected.

10.4. Same layer adjacent low-energy particles spiral Ring the spin direction ampere force equation comparing The calculation results

By (10.8), each low-energy particles spiral ring net with π_d number of d - violation is N_{ei}, the average current strength is I_i, by the (equations (10.15), (8.10), adjacent low-energy particles spiral ring the spin direction whole ampere force $\overline{F}_{bi}$ average parameter calculation equation is:

$$\overline{F}_{bi} = \frac{u_0 I_1 I_2 (2\pi R_{I\,i})}{2\pi(2R_{\alpha bi})} = \frac{e^2 \beta_i^2 N_{e1} N_{e2} (N_{\alpha i} - 1)}{8\pi^2 \varepsilon_0 R_{\theta 0 i}^2 N_{\alpha i}^{1.5}} \qquad (10.18)$$

When we use integral method to calculate the F_{bi} of ampere force, because the spin direction of current intersec ting yuan in orbit on both sides of the parallel symmetric distribution, by (10.5-4), (10.8) and (10.18), to:

$$\begin{aligned} F_{bi} &= u_0 I_1 I_2 \oint \frac{R_{\theta i}}{2\pi(2R_{\alpha bi} - 2R_{\alpha i}\sin\alpha)} d\theta \\ &= \frac{e^2 \beta_i^2 N_{e1} N_{e2}}{16\pi^3 \varepsilon_0 R_{\theta 0 i}^2 \sqrt{N_{\alpha i}}} \int_0^{2\pi/N\alpha} \frac{(\sqrt{N_{\alpha i}} + \cos\alpha)^2}{\frac{\sqrt{N_{\alpha i}} + \cos\alpha}{\sqrt{N_{\alpha i} - 1}} - \sin\alpha} d\theta \end{aligned} \qquad (10.19)$$

The ratio is:

$$\frac{F_{bi}}{\overline{F}_{bi}} = \frac{N_{\alpha i}}{2\pi(N_{\alpha i} - 1)} \int_0^{2\pi/N\alpha} \frac{(\sqrt{N_{\alpha i}} + \cos\alpha)^2}{\frac{\sqrt{N_{\alpha i}} + \cos\alpha}{\sqrt{N_{\alpha i} - 1}} - \sin\alpha} d\theta \qquad (10.20)$$

(10.19) in the fluctuation, the spin track intersec ting in the interval of two current yuan→0, a discontinuous points, point in (10.11) - ampere force have been calculated and shown in table 10.3. We by Δa_i value insert (10.20) of integral upper and lower limits for:

$$a_{i0} = 2\pi(a_i + \Delta a_i)/360^\circ N_{ai} \qquad a_{ia} = 2\pi(360^\circ + a_i - \Delta a_i)/360^\circ N_{ai}$$

Will be data generation in table 10.3 (10.20) in type, the simulation results shown in table 10.4.

Same layer adjacent low-energy particles spiral ring the spin direction ampere force equation $F_{bi}/\overline{F}_{bi}$ calculation results comparison table 10.4

N_{ai} / Δa_i	34/13	16	34	58	88
2°	无解				
	There is no solution				
5°	4.59313587	6.797401516	7.055965601	7.153204956	7.1992218355
10°	2.786828821	3.4747556	3.560352022	3.592408519	3.607980361
30°	1.464674859	1.223998448	1.204626325	1.197666272	1.194335032
60°	0.9610648229	0.6086085346	0.5779770862	0.568871121	0.5615634465
100°	0.5770989581	0.3072239687	0.2856141877	0.2778747804	0.2741756391

From table 10.4 that: when $\Delta a_i \le 30^\circ$, integral method of ampere force is greater than the overall average calculation of ampere force constants. So in (10.15-2) type of high and low particles spiral ring current overall ampere force, we take low-energy particles spiral ring current average radius of $\overline{R}_{Id1}$, and not take high, low-energy particle spiral ring of average. And, behind the readers will see: in nucleus kernel force balance verification calculation, although light conditions within the nucleus of the whole nuclear power field force, slightly greater than nuclear magnetic force, we still have plenty of reason to will them as stable nucleus.

At the same time, we also see that when $30^\circ \le \Delta a_i \le 60^\circ$, AA $F_{bi}/\overline{F}_{bi} \approx 1$, thus can speculate each layer particles spiral ring in nuclear and surplus of high and low $\pi^{\pm}$both generally allow density. Surplus of high and low $\pi^{\pm}$ mesons, especially π^- violation, in neighboring particles spiral ring motion in orbit, affirmation is the proper interval staggered through the tangent track, respectively. So in micro particles adjacent spiral ring rail and the nearby on the intersec ting, current yuan should be discrete. When $\Delta a_i \le 30^\circ$, integral method of ampere force is meaningless.

11. $^{208}_{82}$Pb, $^{232}_{90}$Th, $^{256}_{100}$Fm nucleus internal structure and Parameter calculation

11. 1 "Assembly" the principle of atomic nuclei

Pass in front of the internal structure of the nucleus, chapter 7 ~ 10 nuclear force, magnetic forming principle and parameters of calculation, we not only have "assembly" the basis of atomic nuclei, and predictable "assembly" nucleus must abide by the principle of a couple of items. At the same time also will to book model, theory of thorough and the strict proof of simulation.

11.1.1 Nuclear in nucleus, with net charge density distribution Principle, etc

According to the experimental determination results, combined with map 7.1 ~ 7.3 nucleus internal structure model, nuclear power load distribution characteristics. We will nuclear, various high, low-energy particle spiral loop net with $\pi^{\pm}$ "assembly", such as violation of density and tend to be spherical. Lining and internal each particle spiral rings, all shall be according to (9.12) is the result of saturated layer and outer layer and edge can be in a state of unsaturated. That are nucleus boundary there natural "dispersion" layer. Nuclear force action radius including low-energy particles spiral ring outside edge, slightly greater than the net with π_g^+ violation of high-energy particles spiral ring distribution radius. Outside the nucleus edge due to the low particles spiral ring net with π_d^- forces, and conditions within the nucleus edge π_g^+ mesons are weaken the effect of electric field, on the whole reflects the nucleus wrapped in a layer of "neutron skin". These characteristics are shown in figure 7.1 and figure 7.2 are clearly reflected.

11.1.2 Total energy conservation principle

Nucleus total energy is high, low-energy particle spiral ring, all the original π± muon total energy $\overline{m}_{di}, \overline{m}_{gi}$, and the high and low particles spiral rings, each net with π± muon between spin direction, electric and magnetic field of the interaction of the sum of total energy. Total energy of atoms of each element of the determination of the laboratory, should deduct outside the nucleus of all electronic rest mass $Z_i m_{eo}$, plus all of the electronic ionization energy, (book electronic ionization energy at all). Because all electronic total ionization energy is much smaller than the total energy of the nucleus, so, this book in does not affect the nucleus total energy calculation precision premise, outside the nucleus all electronic total ionization energy estimation values, (see chapter 20 atomic physics).

When protons and neutrons are even nucleus, by (9.8), (9.13), high, low particles spiral ring all π± in violation of the original total energy is: $\sum m_{\pi} = 5A_i\overline{m}_{d1} + \sum \Delta\overline{m}_{ni}$ (A_i is the sum of the number of protons and neutrons).

Nucleus of different even protons, neutrons, π± violation of the original total energy calculation should be two steps. Refer to section 7.2 the nuclear magnetic forming principle, the calculation first $5(A_i - 2)\overline{m}_{d1}$ or $5(A_i - 3)\overline{m}_{d1}$ the nucleus of the original total energy; Remaining 2 ~ 3 protons, neutrons should according to the experimental value of nuclear magnetic, analysis, simulation computation 2 ~ 3 protons, neutrons "decentralized" π± mesons, into the high, low-energy particle distribution state of spiral ring; Then on the basis of the listed in table 9.1 $\overline{m}_{di}$, $\overline{m}_{gi}$, data accumulation respectively.

When we according to the principle of article 1 will be all the protons and neutrons "decentralized" into π± mesons, filling into each layer in nucleus, various high, low-energy particle spiral ring, we can according to the list of equations (8.16), 9.2 or 9.3 to simulate calculation within the nucleus particles spiral ring, net withπ±muon spin

direction of interaction between electric and magnetic energy. Table 9.2 and table 9.3 in the high and low particles spiral rings $\pi^{\pm}$ violation of electric parameters, refers to each net with $\pi^{\pm}$ muon relative to the nucleus center for a net with unit of electric charge can parameters. In practical calculation, we can as long as potential parameters from big to small, and then in sequence one by one calculation, high in low-energy particle spiral ring net with $\pi^{\pm}$ violation of, and surrounded by the nucleus of the accumulated net charge left for interaction potential can and their own potential; They all algebra and is all the particles in the nucleus of spiral ring net with $\pi^{\pm}$ mesons in the potential of interaction.

Similarly, we can still by the "assembly" out of the nucleus structure model, by (8.15), (8.16) equations, from inside to outside, step by step calculation conditions within the nucleus layers particles spiral ring, net with $\pi^{\pm}$ violation in the spin direction of interaction between magnetic energy and accumulative total magnetic field energy.

11.1.3 Stable electric and magnetic field force balance principle

Forming principle, the parameters derived from the nuclear force, demonstration calculation process is not difficult to forecast: stable nucleus, it should be the whole inside the particles spiral ring, general electric and magnetic field force is evenly balanced; The low-energy particles spiral ring rail tangent particles and the whole spiral ring spin track current is the ampere force between the sum of all should be evenly than nuclear power field force in the nuclear spin axial force. If inside a certain position in the nuclear field force the spin axis of the repelling force is greater than the total ampere force of it, it will lead to internal excess $\pi^{\pm}$ muon adjustment, redistribution, or split the decay, until nuclear force equilibrium is stable. So, we can expect that in 1 ~ 2 principle, under the premise of $^{206}_{82}Pb$, $^{207}_{82}Pb$, $^{208}_{82}Pb$, $^{209}_{83}Bi$four kinds of natural and artificial radiation is the end of the nuclear, internal nuclear force

balance stable state of the simulation results, should be close to the critical instability. We could start the $^{208}_{82}Pb$ nucleus as validation book the nucleus internal structure, model, the nuclear force balance stable state parameters of the simulation experiment.

11.1.4 Protons, neutrons, π± muon maintain appropriate proportion Principle

Conditions within the nucleus of protons and neutrons must maintain an appropriate ratio, that is their "decentralized" all the high and low of positive and negative π± mesons in every high, low-energy particle spiral ring, must according to proper proportion of uniform distribution and orderly, make a high or low for each ring particles spiral orbit of π± violation of excess and π± between the violation of the electric field force can attract contain each other, which can satisfy various π± violation within the individual needs of charged particles expansion deformation, and can make the electric field force of each particle spiral ring can maintain the dynamic balance, the whole is in stable condition, the nucleus to ultimate stability.

11.2 $^{208}_{82}Pb$ nucleus internal structure and parameter calculation

11.2.1 Nucleus total energy verification calculation

Laboratory determination: $^{208}_{82}Pb$ atomic mass is 207.976658u④; It is the element thorium $^{232}_{90}Th$ natural radiation is the end of the nucleus. Outside the nucleus of all the electronic total ionization energy $\sum W_{me}$, we take the approximate:

$$\sum W_{me} = K_{\alpha 2} Z_i \qquad (11.1)$$

Which Z_i is nuclear charge and K_{a2} is atomic inner electronic ionization energy. Determined by laboratory to: K_{a2} = 72794 ev ④, the K_{a2} layer represents the average

atomic ionization energy of all electronic.

According to (8.19), (9.13) types $\overline{m}_{di}$, $\overline{m}_{gi}$ value in table 9.1, $^{208}_{82}$Pb nucleus total energy is:

$$\sum {}^{208}_{82}PbW_i = 208 \times 5\overline{m}_{d1} + W_e + W_b + \sum \Delta \overline{m}_{ni} \qquad (11.2)$$

By (11.1), set up atomic mass of ${}^{A}_{z}XM$, must be the original mass of the nucleus $\sum {}^{A}_{z}XW_0$ for:

$$\sum {}^{A}_{z}XW_0 = {}^{A}_{z}XM - Z_i m_{e0} + K_{\alpha 2} Z_i e / c^2 \qquad (11.3)$$

The experimental value generation into (11.3), to: $^{208}_{82}$Pb nucleus of the original total energy:

$$\sum {}^{208}_{82}PbW_0 = 3.452895452 \times 10^{-25} Kg$$

The electronic total ionization energy:

$$\sum W_{me} = 5.969108 Mev = 1.064090616 \times 10^{-29} Kg$$

With reference to the principle of figure 7.2 and section 11.1 1, 2, the design of "assembly" $^{208}_{82}$Pb nucleus structure as shown in figure 11.1, it belongs to type B nucleus. Each layer particles spiral rings layer by (9.12) - the number of nuclear calculation results were taken 6, 12, 18, 22, the outermost for unsaturated layer. Layers, various high, low-energy particles spiral ring of protons, neutrons "decentralized" all $\pi^{\pm}$ source, including the net with $\pi^{\pm}$ violation number arrangement principle and distribution status, see section 7.2. We make each layer particles spiral rings with the net high and low $\pi^{\pm}$ muon total the same, in the nuclear field force and the spin direction under the action of ampere force, position can be adjusted, symmetrical distribution, in order to maintain the balance of nuclear power, magnetic force.

Shown from figure 11.1, the $^{208}_{82}$Pb conditions within the nucleus net with $\pi^{\pm}$ violation in the moving direction spin interaction between the electric and magnetic energy calculation procedure is as follows:

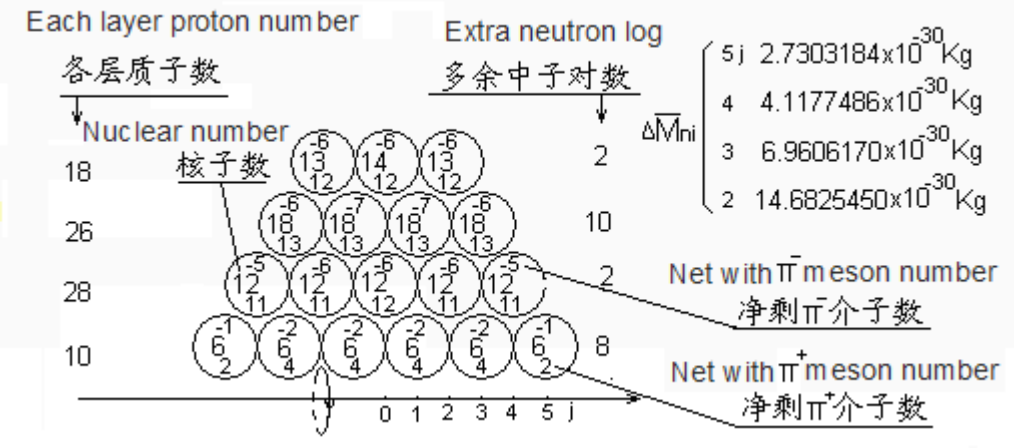

Figure 11.1 $^{208}_{82}Pb$ nuclear in nucleus, the net with $\pi^{\pm}$ source distribution

1. By electric potential, as shown in the table 9.3 can parameters, in absolute value from big to small alphabetical order in English first, it represents the net with $\pi^{\pm}$ violation by the nucleus center to the periphery of interaction potential can vary, convenient calculation, the total potential energy.

2. According to the electric potential of a system can sum method, each corresponding layer, the corresponding column of high and low particles spiral rings net with $\pi^{\pm}$ violation number accordingly, written in the letter below arrangement, π_g^+ number of mesons is positive, π_d^- number of violation is negative. To nucleus left and right sides is symmetrical distribution of two pairs of high and low particles spiral rings of the net with$\pi^{\pm}$ violation number should be peace. By (9.13), table 9.1 data: redundant excess energy for the rest of the $\Delta\overline{m}_{ni}$ value is shown in figure 11.1 on the right side.

3. (11.4) - each of the electric potential can be calculated parameters before all

the π± violation of algebra and, on behalf of the particles spiral ring inside relative nucleus surrounded by center of net with nuclear power by number, label in the upper part of the parameters of the electric potential can:

$$\begin{array}{cccccccccc} {}^{8}Va_{8} & {}^{4}Vb_{-4} & {}^{12}Vc_{8} & {}^{8}Vd_{-4} & {}^{20}Ve_{12} & {}^{14}Vf_{-6} & {}^{18}Vg_{4} & {}^{40}Vh_{22} & {}^{38}Vi_{-2} & {}^{26}Vj_{-12} \\ {}^{26}Vk_{22} & {}^{48}Vl_{26} & {}^{74}Vm_{-10} & {}^{64}Vn_{-14} & {}^{50}Vo_{26} & {}^{76}Vp_{-12} & {}^{64}Vq_{12} & {}^{76}Vr_{24} & {}^{100}Vs_{-6} & {}^{94}Vt_{-12} \end{array}$$

4. Every high, low-energy particle spiral ring net with π± both potential can, should be inside relative nucleus center surrounded by the net with total number of nuclear power by the interaction of electric potential energy and its potential. Whole high within the nucleus, low-energy particles spiral loop net with π± violation of interaction between potential energy, should be each high net, low-energy particle spiral rings with π± muon interaction potential can be combined. So, directly from the above parameters, we have:

$$W_e = \frac{e}{c^2}\left[\begin{array}{l} \frac{8^2}{2}Va-\left(8\times4-\frac{4^2}{2}\right)Vb+\left(4\times8+\frac{8^2}{2}\right)Vc-\left(12\times4-\frac{4^2}{2}\right)Vd+ \\ \cdots\cdots+\left(76\times24+\frac{24^2}{2}\right)Vr-\left(100\times6-\frac{6^2}{2}\right)Vs-\left(94\times12-\frac{12^2}{2}\right)Vt \end{array}\right] \tag{11.4}$$

The calculation table 9.3 V_{ei} value generations into (11.4), too: W_e = 1.503731485 x 10^{-27} kg

5. By each layer, as shown in the table 9.1, low-energy particle spiral loop quantum fluctuations in N_{adi}, N_{agi} value, respectively into (4.9), speed fluctuation coefficient is obtained β_{gi}, β_{di} value; Along with the generation of (1.6) in type $\overline{m}_{di}$, $\overline{m}_{gi}$ value, obtained $R_{\theta 0gi}$, $R_{\theta 0di}$ value.

6. Each particle spiral ring of N_{adi}, N_{agi}, β_{gi}, β_{di}, $R_{\theta 0gi}$, $R_{\theta 0di}$ value generation into the type (8.10), respectively, $\overline{R}_{Igi}$, $\overline{R}_{Idi}$ spiral loop current average radius, are obtained.

7. By figure 11.1 shows, the particles spiral ring layer length coefficient of $K_{bd\ l\ j}$ respectively: K_{bd15} = 12, K_{bd24} = 10, K_{bd33} = 8, K_{bd42} = 6, along with $R_{\theta 0gi}$, $R_{\theta 0di}$, N_{adi},N_{agi} value generation into the equations (8.13), obtained: L_{bgij}, L_{bdij} value.

8. By figure 11.1 shows, the particles spiral ring layer respectively: the number of protons P_1=10, P_2=28, P_3= 26 and P_4=18, along with the above obtained β_{gi}, β_{di}, $\overline{R}_{lgi}$, $\overline{R}_{ldi}$, L_{bgij}, L_{bdij} and N_{adi}, N_{agi} value generation into the equations (8.15), respectively, for magnetic field strength H_{gi}, H_{di} value.

9. The H_{gi}, H_{di}, $\overline{R}_{lgi}$, $\overline{R}_{ldi}$ and L_{bgij}, L_{bdij} value generation into the equations (8.16), respectively, for magnetic energy W_{bgi}, W_{bdi} value.

10. The W_{bgi}, W_{bdi} value accumulation, obtained the total magnetic energy, and conversion for quality, to: $W_b = 1.409748336 \times 10^{-29} kg$.

11. By (11.2), too: $\sum {}^{208}_{82}PbW_1$ = 3.452890137 x 10^{-25} kg, compared with the results of the type (11.3), 0.29815 Mev error, is only an outer electrons estimated 5.0% of the total ionization energy, precision has reached the requirement. It can turn to the next topic nuclear force balance test.

12. Figure 11.1 protons and neutrons in nucleus, the distribution of the net with $\pi^{\pm}$ muon state through variety of solutions are the result of the simulation. If default protons, neutrons, and net with $\pi^{\pm}$ source distribution A scheme after 1 ~ 11 calculation program total energy value is not consistent with the experiment, through adjusting the number of protons, neutrons, or particles spiral rings net with $\pi^{\pm}$ both axial distribution, repeated 1 ~ 11 calculation procedures, can change the total energy of the nucleus. That last until agreement with experimental value. (Behind all nuclear source parameters, calculation procedures and adjusting process are the same).

11.2.2 Nuclear force balance test

Shown by table 10.2 B type high within the nucleus, low-energy particles spiral loop net with $\pi^{\pm}$ both between the spin axis nuclear power field force parameters, we can reference potential can the method, step by step, by the calculation of the axial electric field force.

By 1 calculation program of the electric potential can parameters from big to small order, you can clearly see, each pair of high and low particles spiral ring inside relative nucleus center surrounded by the net with nuclear power charge, then itself should be unilateral net with$\pi^{\pm}$ number mesons, symmetrical should be incorporated into the other side of the total number of net with nuclear power charge within the nucleus. So, each pair of high and low particles spiral loop net with $\pi^{\pm}$ violation of A nucleus within the spin axis of the nuclear power field component should be high, low-energy particle spiral ring the axial electric field component. As shown in figure 11.1: layer 2 i= 2, 4 column j = 4 of the particles spiral rings, location code for k, m, by 1 the calculation program of arrangement parameters, we have:

$$F_{e\theta km}=11\times(26+11)F_{e\theta k}-5\times(74-5)F_{e\theta m} \qquad (11.5)$$

In the table 10.2 $F_{e\theta k}$, $F_{e\theta m}$ parameters into (11.5), to: $F_{e\theta km}$=570.0909716 (Newton).

Similarly, by (11.5), the parameters in the table 10.2, other particles spiral ring in the nuclear field force of axial component of the results shown in table 11.1.

Within the same layer side by side of low-energy particles spiral ring net with π_d^- both in the spin track tangent of ampere force, from (10.7-1) ~ (10.11) in the derivation process of the type, all is a certainly π_d^- as the basis, when they were N_{e1}, N_{e2} π_d^- violation, the strain (10.11) is:

$$F_{b\theta ij}=N_{e1}N_{e2}F_{kbi} \qquad (11.6)$$

According to the figure 11.1 shows the low-energy particles spiral ring in the net with π_d^- violation number, will each layer in the table 10.3 F_{kbi} parameters, generation into (11.6), respectively, for each track tangent place ampere force shown in table 11.1.

$^{208}_{82}$Pb nucleus kernel force balance test results list (figure 11.1, the unit: Newton)

table 11.1

j / N_a	1	2	3	4	5	Nuclear power, the total magnetic force
58 $F_{e\theta}$		t. 606.0462530				689.131672
$F_{b\theta}$		-534.5717436				
34 $F_{e\theta}$	n. 591.0889169	p.1229.43442				617.6571626
$F_{b\theta}$	-936.0859236	-802.3593631				
16 $F_{e\theta}$		j. 991.1342691	m.570.0909716			190.5821057
$F_{b\theta}$		-943.7382342	-786.4485285			
$F_{e\theta}$	b.352.235612	d.439.56555342	i.–13.81634162			359.5436277
$34/13F_{b\theta}$	-57.06223088	-57.062230 88	-28.53111544			
$\Delta F_{\theta b}$		-137.8927999	-137.8927999			

Note: table 11.1 n column redundant, lower particles on the magnetic force of the spiral ring outside nuclear power field force no set limit; do not participate in the whole nuclear force balance calculation, separated with broad, (the same below).

Adjacent 3 on the high side by side, low-energy particle spiral rings net with $\pi^{\pm}$ violation in the spin track movement direction, rail current generated interaction the overall train of ampere force $\triangle F_{\theta bij}$, by (10.17) and K_{fb} parameters, according to the figure 11.1 shows the first layer of particles spiral rings of the net with $\pi^{\pm}$ violation number, we will be the first layer of the calculated value is also listed in table 11.1.

11.2.3 Orbit tangent place ampere force analysis and whole nuclear force balance principle

From table 11.1 that: the entire $^{208}_{82}$Pb conditions within the nucleus particles spiral ring axial nuclear power field force close to the inside of the ampere force in

general; Especially the outer layer F_{e042} and inner layer F_{e022}, are close to ampere force (the same layer of electric and magnetic field force can accumulate); Overall close to unstable state of the critical limits, and the expected results. At the same time, the first layer of the edge of the particles spiral ring $F_{e015}<<F_{b0}+\triangle F_{b0}$, even negative, appear to compress the together! From 1 calculation program CLP energy parameters are top of the net with nuclear power charge number see: they are all positive, and that the high and low particles spiral ring in nuclear power, magnetic field force along axial force is not in a state of tension, but in the compressed state within the nucleus.

Further analysis low-energy particles spiral ring rail side by side on the intersec ting ampere force, we found that, it not only in tensile state phase to resist tensile, more in the compression state show the repelling force to resist the effect of compression, but also with the size of the nuclear power field force to adjust! Table 10.3 the calculation of parameters of ampere force is in tension or compression under the two states are of great value. (the characteristics of the nuclear force is also in the field of astronomy neutron stars and black holes internal resistance gravity field of the strong force, see chapter 26)

See figure 10.2 and figure 10.3 and figure 10.4, in the compression state, rail tangent place π_d^- both positive and load in the formation of charged particles is not the current a`b` some overlap, but in ab points coincide. Orbit between the tangents of ampere force to showed in figure 11.2. Even though mutual attraction, as long as the largest ampere force is still greater than nuclear power field force in axial compression force, on the whole still can prevent A and B low-energy particles spiral ring in orbit tangent place further compressed cross-border, so disconnect.

Similarly, if the rail tangent electric dipole rotation diameter line a—a`, b—-b` symmetric intersection as shown in figure 10.3, from chapter 2 elementary particle energy origin of what we already know: elementary particles energy is the wave speed

βc, radius of R_a, N_a quantum fluctuations for constituting and electric dipole rotation angle, a rotation radius $K_r\overline{R}_\alpha$, electric dipole log n key parameters comprehensive decision. So the outside of the electric and magnetic field strength unless to big enough to change its energy, otherwise can't change the key parameters, including, figure 11.2 and figure 10.4 (10.6 1) type of a, Φ value. So, current yuan a—a`、b—b` wire under the action of ampere force won't turn around the intersection, can only translation from figure 10.4 tensile state to figure 11.2 state of compression, symmetrical figure 10.3 in the middle position, ampere force general resultant force is zero. By (10.9) ~ (10.11) of integral upper and lower boundaries can be seen, the value of the ampere force in the process of translation will gradually change.

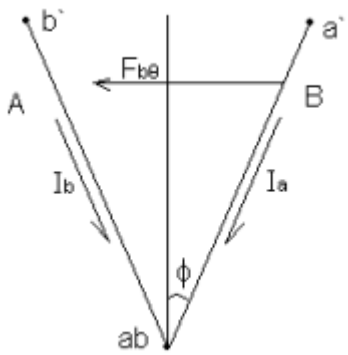

Figure 11.2 I_a and I_b current yuan between ampere force diagram

Thus safely draw the conclusion that each pair of high and low particles spiral ring by nuclear power field force in the spin axis of reality, as long as the rail on the tangent of Ampere force is less than, equal to the maximum, whether tensile force, compression force, or Ampere force will react like spring, and with a—a`, b—b` line of translation, Ampere force will adjust to with nuclear power field force is equal. When nuclear power field repelling force is greater than the left tangent of ampere force, on the tangent of Ampere force reached the maximum. If there is no other force in overcoming nuclear power field force, is where particles spiral rings net with $\pi^{\pm}$

violation will be unstable state.

Economical adjacent particles spiral rings net with $\pi^{\pm}$ overall interaction between violation of ampere force, it will be like spring series, the lateral Ampere force accumulate step by step to the inside. Similarly, inside the nuclear field of repelling force is greater than the left tangent of Ampere force; the spare part will accumulate to the outside edge.

Nucleus from figure 11.1 internal layers particles spiral ring stagger Mosaic structure that: as long as the total ampere force is greater than the total nuclear power field, the outside of the inner ring particles spiral foreign the medial layer of particles spiral ring there are space limits to maintain stability. As shown in figure 11.1 in addition to the F_{e31} and that of high, low-energy particle spiral ring outside, other particles spiral ring embedded structure can be accumulated by the electric and magnetic field force transmission from inner to outer, from outside to inside of the nucleus in general stability of nuclear force balance calculation. From table 11.1 balance accumulated as A result, the nucleus is slightly less than nuclear power of ampere force field force, so the nucleus is not stable, we must to "assemble" $^{208}_{82}$Pb nucleus.

When we adjust figure 11.1 $^{208}_{82}Pb$ within the nuclei of protons, neutrons, the distribution of the net with $\pi^{\pm}$ mesons, can "assembly" out another kind of structure of the $^{208}_{82}Pb$ nucleus, see figure 11.3. According to this section 1 ~ 11 calculation procedure, W_b, W_e, the left figure 11.3 $\sum^{208}_{82}Pb W_3$ value.

Similarly, refer to section nuclear force balance verification calculation method, the results shown in table 11.2.

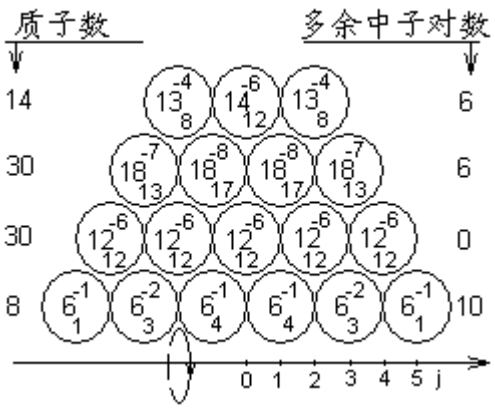

图11.3 $^{208}_{82}Pb$原子核内核子、净剩π±介子分配示意图

$$\begin{array}{cccccc} Va_{8} & Vb_{-2}^{8} & Vc_{6}^{6} & Vd_{-4}^{12} & Ve_{12}^{8} & Vf_{-6}^{20} \\ Vg_{2}^{14} & Vh_{24}^{16} & Vi_{-2}^{40} & Vj_{-12}^{38} & Vk_{24}^{26} & Vl_{34}^{50} \\ Vm_{-12}^{84} & Vn_{-16}^{72} & Vo_{26}^{56} & Vp_{-14}^{82} & Vq_{12}^{68} & Vr_{16}^{80} \\ Vs_{-6}^{96} & Vt_{-8}^{90} & & & & \end{array}$$

$$W_e = 1.549177931 \times 10^{-27}\ Kg$$

$$W_b = 9.813269321 \times 10^{-30}\ Kg$$

$$\sum {}^{208}_{82}PbW_3 = 3.452894394 \times 10^{-25}\ Kg$$

Nucleus $^{208}_{82}Pb$kernel force balance to verify results (figure 11.3, unit: N) table 11.2

j / N_a	1	2	3	4	5	nudearElectricand magneticfieldforce accumulated
58 $F_{e\theta}$		t.410.7162380				-136.2029571
$F_{b\theta}$		-356.3811624				
34 $F_{e\theta}$	n.909.3596443		p.1204.566227			-190.5380327
$F_{b\theta}$	-1222.642839		-1069.812484			
16 $F_{e\theta}$		j.1091.575393		m.260.1473009		-325.2917757
$F_{b\theta}$		-943.7382342		-943.7382342		
$F_{e\theta}$	b.520.2435589		d.316.4391041		i.–179.5180316	210.4619988
34/13$F_{b\theta}$	-14.26555772		-28.53111544		-28.53111544	
$\Delta F_{\theta b}$	-160.8749332		-183.8570665		-30.64284441	

Obviously, this kind of $^{208}_{82}Pb$ nucleus is stable, is we are looking forward to a solution, compared with the first nuclear model in figure 11.1, key in 1 ~ 2 layer net with $\pi^{\pm}$mesons are different.

11.3 $^{232}_{90}$Th nucleus internal structure and parameter Calculation

$^{232}_{90}$Th the nucleus is the natural radiation is thorium is starting, half-life 1.4 x 10^{10},

abundance of 100%. Laboratory determination $^{232}_{90}$Th atomic mass is 232.038074 u, inner electronic K_{a2} ionization energy for 89942 ev.

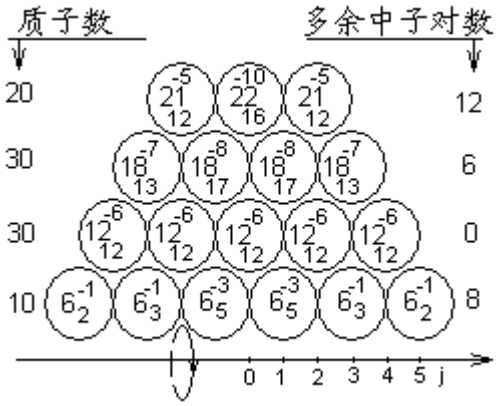

图11.4 $^{232}_{90}Th$原子核内核子、净剩π±介子分配示意图

$$\begin{array}{cccccc} {}^{10}Va_{10} & {}^{10}Vb_{-6} & {}^{4}Vc_{6} & {}^{10}Vd_{-2} & {}^{8}Ve_{12} & {}^{20}Vf_{-6} \\ {}^{14}Vg_{4} & {}^{18}Vh_{24} & {}^{42}Vi_{-2} & {}^{40}Vj_{-12} & {}^{28}Vk_{24} & {}^{52}Vl_{34} \\ {}^{86}Vm_{-12} & {}^{74}Vn_{-16} & {}^{58}Vo_{26} & {}^{84}Vp_{-14} & {}^{70}Vq_{16} & {}^{86}Vr_{24} \\ {}^{110}Vs_{-10} & {}^{100}Vt_{-10} & & & & \end{array}$$

$$W_e = 1.817530386 \times 10^{-27}\ Kg$$

$$W_b = 1.437800649 \times 10^{-29}\ Kg$$

$$\sum {}^{232}_{90}ThW_1 = 3.85240599 \times 10^{-25}\ Kg$$

$^{232}_{90}$Th nucleus kernel force balance test results list (figure 11.4, unit: N) table 11.3

j / N_a	1	2	3	4	5	nuclear Electric and magnetic field force accumulated
58 $F_{e\theta}$	t.769.3464573					65.54941594
$F_{b\theta}$	-742.460755					
34 $F_{e\theta}$	n.935.7967653	p.1242.139920				38.66371364
$F_{b\theta}$	-1222.642839	-1069.812484				
16 $F_{e\theta}$	j.1177.523760	m.332.5403448				-133.6637224
$F_{b\theta}$	-943.7382342	-943.738234 2]				
$F_{e\theta}$	b.474.7645661	d.360.3313781	i.-30.52020855			243.7486412
$34/13F_{b\theta}$	-128.3900195	-42.79667316	-14.26555772			
$\Delta F_{\theta b}$	-107.2499554	-153.2142221	-114.9106665			

By (11.3), to: $^{232}_{90}$Th nucleus total energy $\sum {}^{232}_{90}$ThW$_0$ = 3.852409956 x 10^{-25} kg, 10^{-29} kg.

According to figure 11.1 and figure 11.3, the design of $^{232}_{90}$Th nucleus internal structure is shown in figure 11.4 and figure 11.5.

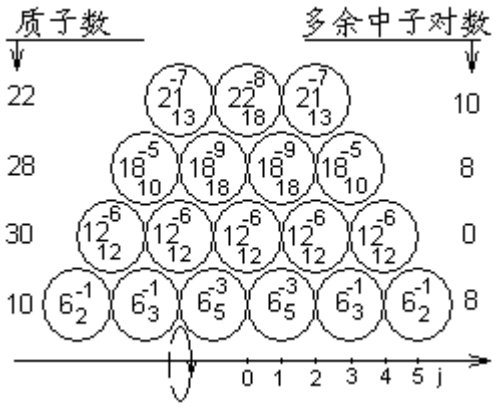

图11.5 $^{232}_{90}Th$原子核内核子、净剩π±介子分配示意图

$$Va_{10}\ Vb_{-6}^{10}\ Vc_{6}^{4}\ Vd_{-2}^{10}\ Ve_{12}^{8}\ Vf_{-6}^{20}$$

$$Vg_{4}^{14}\ Vh_{24}^{18}\ Vi_{-2}^{42}\ Vj_{-12}^{40}\ Vk_{24}^{28}\ Vl_{36}^{52}$$

$$Vm_{-12}^{88}\ Vn_{-18}^{76}\ Vo_{20}^{58}\ Vp_{-10}^{78}\ Vq_{18}^{68}\ Vr_{26}^{86}$$

$$Vs_{-8}^{112}\ Vt_{-14}^{104}$$

$$W_e = 1.812742002 \times 10^{-27} Kg$$

$$W_b = 1.434229785 \times 10^{-29} Kg$$

$$\sum {}^{232}_{90}ThW_2 = 3.852414607 \times 10^{-25} Kg$$

$^{232}_{90}Th$Nucleus kernel force balance to verify the results table (figure 11.5, the unit: Newton) table 11.4

j / N_a	1	2	3	4	5	nuclearElectricandmagnetic fieldforceaccumulated	
58 $F_{e\theta}$		t.708.9523968				↑	-186.4876078
$F_{b\theta}$		-831.5560456					
34 $F_{e\theta}$	n.969.7887665		p.985.2165362				-63.883958 96
$F_{b\theta}$	-1547.407343		-859.6707462				
16 $F_{e\theta}$		j.1177.523760		m.276.7743182			-189.429749
$F_{b\theta}$		-943.7382342		-943.7382342			
$F_{e\theta}$	b.474.7645661		d.360.3313781		i.-30.52020855		243.7486412
34/13$F_{b\theta}$	-128.3900195		-42.79667316		-14.26555772		
$\Delta F_{\theta b}$	-107.2499555		-153.2142222		-114.9106666		

According to section 11.2 of the calculation procedure and method, $^{232}_{90}$ Th nucleus kernel force balance test results see table 11.3 and table 11.4.

From table 11.3,11.4 and table 11.3， 11.4 the result shows: the first kind of nucleus near critical permanent stable state; Second nuclear although of permanent stable nuclei, but 3 ~ 4 layer between particles spiral high-energy π_g^+ mesons in ring is too concentrated, nuclear power will also lead to uneven field force throughout the nucleus are not stable.

11.4 $^{256}_{100}$Fm nucleus internal structure and parameter calculation

11.4.1 $^{256}_{100}$Fm A type nucleus internal structure and parameter calculation

Laboratory determination $^{256}_{100}$Fm atomic mass is 256.091807u, half-life is only 2.63 hours, the inner of electronic K_{a2} ionization energy for 114926 ev. By (11.3), too:

$\sum^{256}_{100}FmW_0$ = 4.251801339 x 10^{-25} kg.

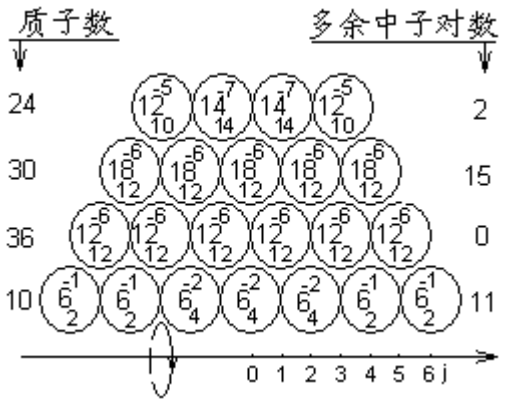

图11.6 $^{256}_{100}Fm$原子核内核子、净剩π±介子分配示意图

$$\begin{array}{cccccc} {}^{4}Va_{4} & {}^{4}Vb_{-2} & {}^{2}Vc_{8} & {}^{10}Vd_{-4} & {}^{6}Ve_{4} & {}^{10}Vf_{-2} \\ {}^{8}Vg_{24} & {}^{32}Vh_{-12} & {}^{20}Vi_{24} & {}^{44}Vj_{4} & {}^{48}Vk_{-12} & {}^{36}Vl_{-2} \\ {}^{34}Vm_{12} & {}^{46}Vn_{24} & {}^{70}Vo_{-6} & {}^{64}Vp_{24} & {}^{88}Vq_{-12} & {}^{76}Vr_{-12} \\ {}^{64}Vs_{24} & {}^{88}Vt_{-12} & {}^{76}Vu_{28} & {}^{104}Vv_{-14} & {}^{90}Vw_{20} & {}^{110}Vx_{-10} \end{array}$$

$$W_e = 2.083292346\times10^{-27}\,Kg$$

$$W_b = 1.291733144\times10^{-29}\,Kg$$

$$\sum {}^{256}_{100}FmW_1 = 4.251799043\times10^{-25}\,Kg$$

For $^{256}_{100}$Fm nucleus more nuclear, we first in 7.1 type A nucleus to the model of "assembly" $^{256}_{100}$Fm nucleus. From table 9.1 and table 10.1 types A nucleus calculation of relevant parameters, refer to section 11.2 calculation procedures and nuclear force balance verification calculation method, the result is shown in figure 11.6 and table 11.5.

$^{256}_{100}$Fm nucleus kernel force balance to verify results (figure 11.6, unit: N) table 11.5

j / N_a	1	2	3	4	5	6	nudearElectricand magnetic fieldforce accumulated
58 $F_{e\theta}$	v.373.6420907		x.720.8090694				3276.131632
$F_{b\theta}$	-727.6115399		-519.7225285				
34 $F_{e\theta}$		q.640.1304363		t.1331.794967			3075.045092
$F_{b\theta}$		-687.7365970		-687.7365970			
16 $F_{e\theta}$	h.480.0435425		k.1054.873673		r.2378.302662		2430.986722
$F_{b\theta}$	-943.7382342		-943.7382342		-943.7382342		
$F_{e\theta}$		d.712.7489433		f.1299.6257756		l.4182.198398	885.286855
$34/13F_{b\theta}$		-57.06223088		-28.53111544		-14.26555772	
$\Delta F_{\theta b}$		-137.8927999		-68.94639993		-68.94639993	

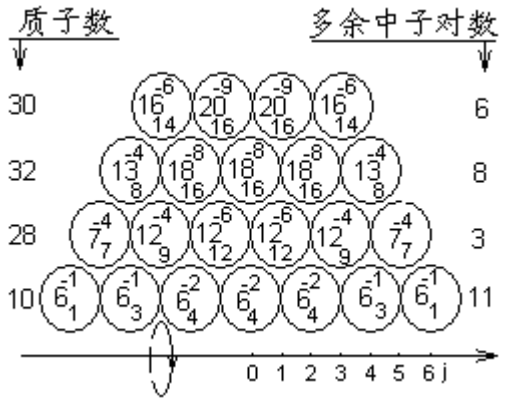

图11.7 $^{256}_{100}Fm$原子核内核子、净剩π±介子分配示意图

$$\begin{array}{cccccc}
^{4}Va_{4} & ^{2}Vb_{-2} & ^{10}Vc_{8} & ^{6}Vd_{-4} & ^{12}Ve_{6} & ^{10}Vf_{-2} \\
^{34}Vg_{24} & ^{22}Vh_{-12} & ^{40}Vi_{18} & ^{42}Vj_{2} & ^{34}Vk_{-8} & ^{32}Vl_{-2} \\
^{48}Vm_{16} & ^{80}Vn_{32} & ^{72}Vo_{-8} & ^{86}Vp_{14} & ^{70}Vq_{-16} & ^{62}Vr_{-8} \\
^{78}Vs_{16} & ^{70}Vt_{-8} & ^{102}Vu_{32} & ^{84}Vv_{-18} & ^{112}Vw_{28} & ^{96}Vx_{-12}
\end{array}$$

$$W_e = 2.072443525\times10^{-27}\,Kg$$
$$W_b = 1.231082309\times10^{-29}\,Kg$$
$$\sum {}^{256}_{100}FmW_2 = 4.251802433\times10^{-25}\,Kg$$

By data can be seen in figure 11.6 and table 11.5:2 ~ 4 layer particles spiral ring inside although magnetic force is greater than the nuclear field force, but on the inside and outside are not embedded space constraints, leading to the bottom and outside layers nuclear power field force far outweigh the magnetic field strength. The nucleus is not stable, also does not exist. We have to redesign "assembly" $^{256}_{100}$Fm nucleus. As shown in the figure 11.7 and figure 11.8. Nuclear force balance test results see table 11.6 and table 11.7.

$^{256}_{100}$Fm nucleus kernel force balance to verify the results

(Figure 11.7, unit: N) table 11.6

j / N_a	1	2	3	4	5	6	nuclearElectricand magneticfieldforce accumulated
58 $F_{e\theta}$	v.356.0835222		x.1083.090634				2465.520852
$F_{b\theta}$	-1202.786423		-801.8576154				
34 $F_{e\theta}$		q.1116.491063		t.831.9768966			2184.287834
$F_{b\theta}$		-1222.642839		-611.3214195			
16 $F_{e\theta}$	h.543.0960990		k.922.5650244		r.1404.572717		1963.632357
$F_{b\theta}$	-943.7382324		-629.1588228		-419.4392152		
$F_{e\theta}$		d.712.7489433		f.268.7410103		l.79.24720327	685.0926531
34/13 $F_{b\theta}$		-57.06223088		-28.53111544		-14.26555772	
$\Delta F_{\theta b}$		-45.96426662		-191.5177776		-38.30355552	

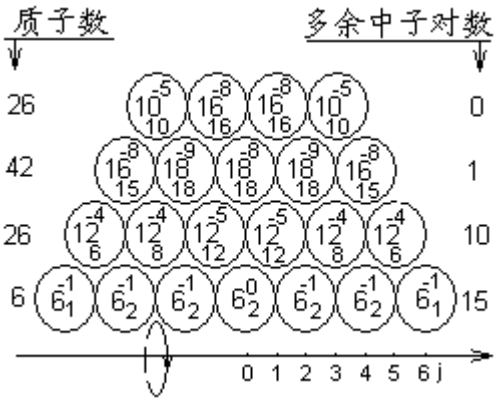

图11.8 $^{256}_{100}Fm$原子核内核子、净剩π±介子分配示意图

$$Va_{2}\ \ {}^{2}Vb_{0}\ \ {}^{2}Vc_{4}\ \ {}^{6}Vd_{-2}\ \ {}^{4}Ve_{4}\ \ {}^{8}Vf_{-2}$$

$$^{6}Vg_{24}\ \ {}^{30}Vh_{-10}\ \ {}^{20}Vi_{16}\ \ {}^{36}Vj_{2}\ \ {}^{38}Vk_{-8}\ \ {}^{30}Vl_{-2}$$

$$^{28}Vm_{18}\ \ {}^{46}Vn_{36}\ \ {}^{82}Vo_{-8}\ \ {}^{74}Vp_{12}\ \ {}^{86}Vq_{-18}\ \ {}^{68}Vr_{-8}$$

$$^{60}Vs_{30}\ \ {}^{90}Vt_{-16}\ \ {}^{74}Vu_{32}\ \ {}^{106}Vv_{-16}\ \ {}^{90}Vw_{20}\ \ {}^{110}Vx_{-10}$$

$$W_e = 2.049571000 \times 10^{-27}\ Kg$$

$$W_b = 5.584920854 \times 10^{-30}\ Kg$$

$$\sum {}^{256}_{100}FmW_3 = 4.251799918 \times 10^{-25}\ Kg$$

By figure 11.6 and figure 11.7 and figure 11.8 and table 11.5 and table 11.6 and table 11.7 the internal structure, nuclear force balance verification calculation parameters is visible, we design three kinds of the nucleus of the difference is very big, $\pi^{\pm}$ muon combination scheme, simulation calculation of type A $^{256}_{100}$Fm nucleus, the common features are: nucleus layers inside and the outside edge particles spiral ring in the nuclear field force are far outweigh the magnetic force, obviously, the three type A nucleus is very unstable, also won't exist. Further behind on quality of medium to light nuclei of the nuclear force balance test simulation analysis also showed that the number of nuclear power by $Z \geq 6$ all the nucleus, type A nucleus are unreliable, can only is type B nucleus.

$^{256}_{100}$Fm nucleus kernel force balance to verify the results (figure 11.8, unit: N) table 11.7

j / N_a	1	2	3	4	5	6	nuclear Electric and magnetic field force accumulated
58 $F_{e\theta}$	v.423.420591		x.720.8090694				1414.655202
$F_{b\theta}$	−950.3497664		−593.968604				
34 $F_{e\theta}$		q.1271.796258		t.1528.592936			1287.814736
$F_{b\theta}$		-1375.473194		-1375.473194			
16 $F_{e\theta}$	h.481.1898312		k.670.5780981		r.1111.131136		1134.694994
$F_{b\theta}$	−655.3737738		−524.299019		−419.4392152		
$F_{e\theta}$		d.246.3420037		f.94.52093682		l.76.32070266	296.7239945
34/13$F_{b\theta}$		-22.98213332		-14.26555772		-14.26555772	
$\Delta F_{\theta b}$				-45.96426665		-22.98213332	

11.4.2 $^{256}_{100}$Fm B type nucleus internal structure and parameter Calculation

$^{256}_{100}$Fm nucleus kernel force balance to verify the results (figure 11.9, unit: N) table 11.8

j / N_a	1	2	3	4	5	nuclear Electric and magnetic field force accumulated
88 $F_{e\theta}$	v.63.14830698					290.5680627
$F_{b\theta}$	-48.38782324					
58 $F_{e\theta}$		t.954.9819745				275.8075790
$F_{b\theta}$		-950.3497664				
34 $F_{e\theta}$	n.879.4710447		p.1583.763385			271.1753709
$F_{b\theta}$	-1547.407343		-1203.539045			
16 $F_{e\theta}$		j.1177.523760		m.332.5403448		-109.0489691
$F_{b\theta}$		-943.7382342		-943.7382342		
$F_{e\theta}$	b.352.2356112		d.238.3761117		i.96.19284851	268.3633945
34/13$F_{b\theta}$	-57.06223088		-57.06223088		-28.53111544	
$\Delta F_{\theta b}$	-91.92853324		-30.64284441		-153.2142221	

When we use type B nuclei model to "assemble" $^{256}_{100}$Fm nucleus, see figure 11.9 and figure 11.10, the nuclear force balance test simulation results shown in table 11.8 and table 11.9.

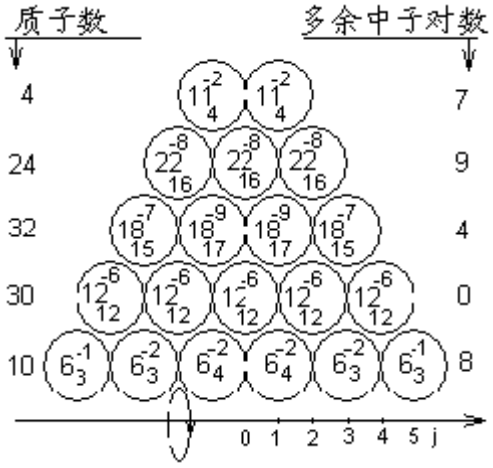

图11.9 $^{256}_{100}Fm$原子核内核子、净剩π±介子分配示意图

$^{8}_{8}Va$	$^{8}_{-4}Vb$	$^{4}_{6}Vc$	$^{10}_{-4}Vd$	$^{6}_{12}Ve$	$^{18}_{-6}Vf$
$^{12}_{6}Vg$	$^{18}_{24}Vh$	$^{42}_{-2}Vi$	$^{40}_{-12}Vj$	$^{28}_{24}Vk$	$^{52}_{34}Vl$
$^{86}_{-12}Vm$	$^{74}_{-18}Vn$	$^{56}_{30}Vo$	$^{86}_{-14}Vp$	$^{72}_{16}Vq$	$^{88}_{32}Vr$
$^{120}_{-8}Vs$	$^{112}_{-16}Vt$	$^{96}_{8}Vu$	$^{104}_{-4}Vv$		

$$W_e = 2.110556341\times10^{-27}\,Kg$$

$$W_b = 1.446182535\times10^{-29}\,Kg$$

$$\sum {}^{256}_{100}FmW_4 = 4.251800825\times10^{-25}\,Kg$$

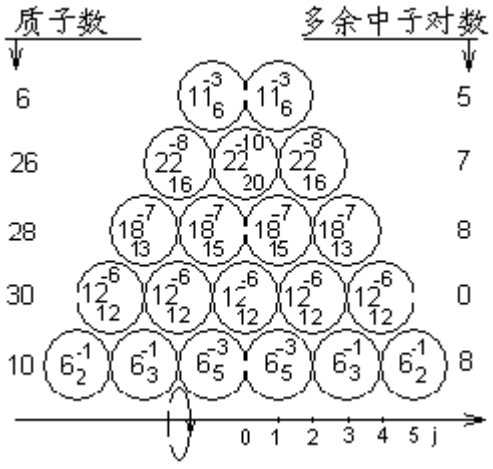

图11.8 $^{256}_{100}Fm$原子核内核子、净剩π±介子分配示意图

$^{10}_{10}Va$	$^{10}_{-6}Vb$	$^{4}_{6}Vc$	$^{10}_{-2}Vd$	$^{8}_{12}Ve$	$^{20}_{-6}Vf$
$^{14}_{4}Vg$	$^{18}_{24}Vh$	$^{42}_{-2}Vi$	$^{40}_{-12}Vj$	$^{28}_{24}Vk$	$^{52}_{30}Vl$
$^{82}_{-12}Vm$	$^{70}_{-14}Vn$	$^{56}_{26}Vo$	$^{82}_{-14}Vp$	$^{68}_{20}Vq$	$^{88}_{32}Vr$
$^{120}_{-10}Vs$	$^{110}_{-16}Vt$	$^{94}_{12}Vu$	$^{106}_{-6}Vv$		

$$W_e = 2.096575583\times10^{-27}\,Kg$$

$$W_b = 1.437941511\times10^{-29}\,Kg$$

$$\sum {}^{256}_{100}FmW_5 = 4.251801656\times10^{-25}\,Kg$$

By figure 11.9 and figure 11.10 and table 11.8 and table 11.9 the results can be seen, with both the internal structure of the nucleus $^{256}_{100}$Fm, accumulative total nuclear power field force is only slightly greater than the magnetic field strength. Such as column of table 11.9 v, t, although ampere force is greater than the nuclear field, as a result of p particles in the column spiral ring no set limit, although that is unstable nuclei, but there can temporarily.

$^{256}_{100}$Fm nucleus kernel force balance to verify results (figure 11.10, unit: N) table 11.9

j / N_a	1	2	3	4	5	nuclearElectricandmagneticfieldforceaccumulated	
88 $F_{e\theta}$	v.93.99510946					↑	11.88671131
$F_{b\theta}$	-108.87260023						
58 $F_{e\theta}$		t.968.3527797					26.76420594
$F_{b\theta}$		-1187.937208					
34 $F_{e\theta}$	n.813.0135219		p.1204.566227				246.3486342
$F_{b\theta}$	-936.08592 36		-936.0859236				
16 $F_{e\theta}$		j.1177.523760		m.444.0723980			-22.13166916
$F_{b\theta}$		-943.7382342		-943.7382342			
$F_{e\theta}$	b.474.7645661		d.360.3313781		i.-30.52020855		243.7486412
34/13$F_{b\theta}$	-128.3900195		-42.79667316		-14.26555772		
$\Delta F_{\theta b}$	-107.2499554		-153.2142221		-114.9106665		

From this chapter three atoms of $^{208}_{82}$Pb, $^{232}_{90}$Th, $^{256}_{100}$Fm the internal structure of nuclide in the design, simulation results can be seen that: in the nuclear in nucleus, net with $\pi^{\pm}$ muon uniform distribution, under the premise of to "assemble" out of accord with a stable nuclei of the total energy of only a few solutions, which can only individual with internal nuclear force balance condition, but this individual (not only) example also shows that exist with nuclear power.

12 $^{168}_{70}$Yb, $^{124}_{54}$Xe, $^{54}_{26}$Fe, $^{40}_{20}$Ca, $^{16}_{8}$O maintenance Nuclei and stable isotope internal structure And parameter Calculation

12.1 $^{168}_{70}$Yb nucleus and stable isotope internal structure And parameter calculation

12.1.1 $^{168}_{70}$Yb nucleus and stable isotopes experiment, parameters calculated value

The scientific community has been found that thousands of nuclide, of which only hundreds of stable isotopes. This chapter will purposefully selected the above five kinds of nuclei and isotope, internal structure design, analysis and parameter calculation, so as to fully verify the theoretical model.

$^{168}_{70}$Yb nucleus and stable isotopes energy parameters experiment results table 12.1

Nuclide	The determination of total energy atomic u	Abundance %	Nucleus total energy calculated value x 10^{-25} kg	Net with π± source electromagnetic field total energy x 10^{-27} kg	Magnetic moment U_P Mrison
$^{168}_{70}$Yb	167.933925	0.14	2.788036725	1.228920997	
$^{170}_{70}$Yb	169.934792	3.0	2.821261926	1.246979758	
$^{171}_{70}$Yb	170.936354	14.3	2.837893265	1.257883058	0.4919
$^{172}_{70}$Yb	171.936405	21.9	2.854499514	1.266277282	
$^{173}_{70}$Yb	172.938234	16.2	2.871135287	1.277623947	-0.678
$^{174}_{70}$Yb	173.938881	31.8	2.887751433	1.287007853	
$^{176}_{70}$Yb	175.942582	12.7	2.921023694	1.309772585	

$^{168}_{70}$ Yb nuclide is total of seven kinds of stable isotopes. In laboratory determination of atoms of each isotope total energy, deduct nucleus all electronic original total energy 70 m_{eo}, plus by (11.1) to estimate the total ionization energy of

nuclear electronic 70 x 51326 ev= 6.404786 x10^{-30} kg, obtained $^{168}_{70}$Yb nucleus and stable isotopes energy parameters experiment, the results shown in table 12.1.

Among them, the $\pi^{\pm}$ source electromagnetic field temporarily takes no account of $\overline{m}_{di}$, $\overline{m}_{gi}$ and $\overline{m}_{d1}$, $\overline{m}_{g1}$ the energy difference between (the same below).

From table 12.1 that: increases with number of neutrons in the nucleus, nucleus of the particles spiral rings net with $\pi^{\pm}$muon spin direction of the electric and magnetic energy gradually increases, it will be for us in the "assembly", adjusting and simulation nucleus total energy provides the net with $\pi^{\pm}$ source distribution state.

12.1.2 $^{172}_{70}$Yb nucleus internal structure and parameter calculation

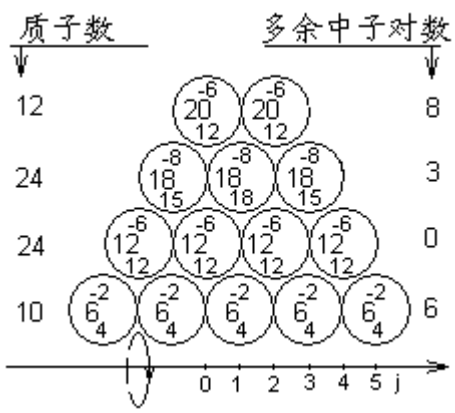

图12.1 $^{172}_{70}Yb$原子核内核子、净剩π±介子分配示意图

$$Va_{4}\quad Vb^{4}_{-2}\quad Vc^{2}_{8}\quad Vd^{10}_{-4}\quad Ve^{6}_{8}\quad Vf^{14}_{-4}$$

$$Vg^{10}_{24}\quad Vh^{34}_{-12}\quad Vi^{22}_{24}\quad Vj\quad Vk^{46}_{-12}\quad Vl$$

$$Vm^{34}_{18}\quad Vn^{52}_{30}\quad Vo^{82}_{-8}\quad Vp\quad Vq^{74}_{-16}\quad Vr$$

$$Vs\quad Vt\quad Vu^{58}_{24}\quad Vv^{82}_{-12}$$

$$W_e = 1.195446297\times10^{-27}\,Kg$$

$$W_b = 1.647200661\times10^{-29}\,Kg$$

$$\sum {}^{172}_{70}YbW_1 = 2.854494163\times10^{-25}\,Kg$$

Refer to section 11.1 ~ 2, all the particles in the nucleus of solenoid ring "assembly", with net high and low $\pi^{\pm}$ source distribution, energy simulation and fitting adjustment process. First to "assemble" $^{172}_{70}$Yb with type A nuclear nucleus, see figure 12.1. From table 9.2 type A nuclear potential energy parameters, refer to section (11.4),

11.2 5 ~ 13 calculation procedures, the net can be obtained with $\pi^{\pm}$ muon electric, magnetic energy and nuclear energy. From table 10.1 and table 10.1, (10.17) - calculation data, according to (11.5), (11.6) and (11.7), nuclear force balance test results to shown in table 12.2.

$^{172}_{70}$Yb nucleus kernel force balance test results list 12.2 (figure 12.1)

j / N_a	1	2	3	4	5	6	nuclear Electric and magnetic field force accumulated
58 $F_{e\theta}$ $F_{b\theta}$	v.247.5951682 -534.5717436						↑
34 $F_{e\theta}$ $F_{b\theta}$		q.1243.455159 -1222.642839					967.2598644
16 $F_{e\theta}$ $F_{b\theta}$	h.543.096099 -943.7382342		k.1260.146427 -943.7382342				946.4475444
$F_{e\theta}$ $34/13F_{b\theta}$ $\Delta F_{\theta b}$		d.712.7489433 -57.06223088		f.307.2004698 -57.06223088 -275.7855997			630.0393516

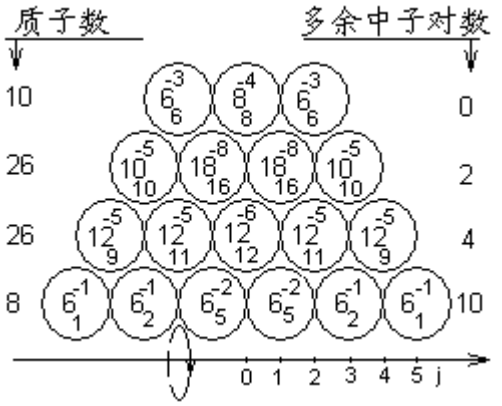

图12.2 $^{172}_{70}Yb$原子核内核子、净剩$\pi^{\pm}$介子分配示意图

$$Va_{10}\ \ Vb^{10}_{-4}\ \ Vc^{6}_{4}\ \ Vd^{10}_{-2}\ \ Ve^{8}_{12}\ \ Vf^{20}_{-6}$$
$$Vg^{14}_{2}\ \ Vh^{16}_{22}\ \ Vi^{38}_{-2}\ \ Vj^{36}_{-10}\ \ Vk^{26}_{18}\ \ Vl^{44}_{32}$$
$$Vm^{76}_{-10}\ \ Vn^{66}_{-16}\ \ Vo^{50}_{20}\ \ Vp^{70}_{-10}\ \ Vq^{60}_{8}\ \ Vr^{68}_{12}$$
$$Vs^{80}_{-4}\ \ Vt^{76}_{-6}$$

$$W_e = 1.184427299\times10^{-27}\ Kg$$
$$W_b = 9.366575355\times10^{-30}\ Kg$$
$$\sum {}^{172}_{70}YbW_2 = 2.854501194\times10^{-25}\ Kg$$

In figure 12.1 $^{172}_{70}$Yb type A nucleus structure model is after many kinds of scheme selection in the simulation of A, all the particles spiral rings net with $\pi^{\pm}$adjusted already tend to limit the distribution of the violation. From can be seen in table 12.2,

uneven size of electric and magnetic field distribution in nuclei, especially the bottom, can't set cover the edge spiral ring particles. That is to say: can't stable $^{172}_{70}$Yb "assembly" type A nucleus.

Similarly, when we use type B nuclei model, see figure 12.2:

$^{172}_{70}$Yb nucleus kernel force balance to verify results (figure 12.2, unit: N) table 12.3

j / N_a	1	2	3	4	5	nuclearElectricand magneticfieldforce accumulated
58 $F_{e\theta}$		t.257.3219278				-71.23721 54
$F_{b\theta}$		-178.1905812				
34 $F_{e\theta}$	n.734.3693282		p.862.88530 63			-150.368562
$F_{b\theta}$	-1222.642839		-764.1517744			
16 $F_{e\theta}$		j.1033.35848		m.32.34284588		-249.10209 39
$F_{b\theta}$		-786.4485285		-655.3737738		
$F_{e\theta}$	b.642.7725138		d.237.204948		i.-162.8141647	127.0188825
34/13$F_{b\theta}$	-57.06223088		-28.53111544		-14.26555744	
$\Delta F_{\theta b}$	-306.4284441		-160.8749332		-22.98213331	

From table 9.1 and table 9.1 and table 10.2 the calculated data, with reference to the above calculation method, a type B $^{172}_{70}$Yb nucleus internal structure parameters and nuclear force balance test results shown in table 12.3.

12.1.3 $^{170}_{70}$Yb nucleus internal structure and parameter calculation

Similarly, stable isotopes of $^{172}_{70}$Yb nucleus $^{170}_{70}$Yb nucleus, we can in the $^{172}_{70}$Yb nucleus, figure 12.2 model "assembly" on the basis of the protons, neutrons, $\pi^{\pm}$ source distribution adjust state for the internal structure and related parameters.

As shown in the figure 12.3, $^{170}_{70}$Yb nucleus nuclear force balance test results shown in table 12.4.

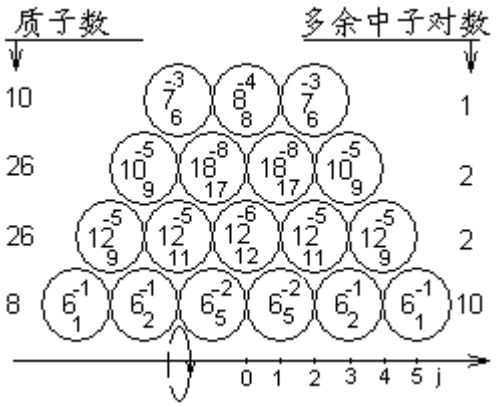

图12.3 $^{170}_{70}Yb$原子核内核子、净剩π±介子分配示意图

$$Va^{10}_{10}\quad Vb^{10}_{-4}\quad Vc^{6}_{4}\quad Vd^{10}_{-2}\quad Ve^{8}_{12}\quad Vf^{20}_{-6}$$

$$Vg^{14}_{2}\quad Vh^{16}_{22}\quad Vi^{38}_{-2}\quad Vj^{36}_{-10}\quad Vk^{26}_{18}\quad Vl^{44}_{34}$$

$$Vm^{78}_{-10}\quad Vn^{68}_{-16}\quad Vo^{52}_{18}\quad Vp^{70}_{-10}\quad Vq^{60}_{8}\quad Vr^{68}_{12}$$

$$Vs^{80}_{-4}\quad Vt^{76}_{-6}$$

$$W_e = 1.190401554\times10^{-27}\,Kg$$

$$W_b = 9.366575355\times10^{-30}\,Kg$$

$$\sum {}^{170}_{70}YbW_1 = 2.82126385\times10^{-25}\,Kg$$

$^{170}_{70}$Yb nucleus kernel force balance to verify results (figure 12.3, unit: N) table 12.4

j / N_a	1	2	3	4	5	nuclearElectricand magneticfieldforce accumulated
58 $F_{e\theta}$		t.257.3219278				-251.38595 95
$F_{b\theta}$		-178.1905812				
34 $F_{e\theta}$	n.814.2375529		p.729.2082511			-330.5173061
$F_{b\theta}$	-1222.642839		-764.1517744			
16 $F_{e\theta}$		j.1033.35848		m.-14.12884298		-295.5737828
$F_{b\theta}$		-786.4485285		-655.3737738		
$F_{e\theta}$	b.642.7725138		d.237.204948		i.-162.8141647	127.0188825
34/13$F_{b\theta}$	-57.06223088		-28.53111544		-14.26555772	
$\Delta F_{\theta b}$	-306.4284441		-160.8749332		-22.98213331	

12.1.4 $^{173}_{70}$Yb nucleus internal structure and parameter calculation

$^{173}_{70}$Yb inside protons and neutrons are not even, nuclei are U = 0.678 U_P strength. Because a single nuclear for m_n+2 m_p, according to section 7.2 magnetic moment within the nucleus formation principle, we make the m_n + 2 m_p "decentralized" all the $\pi^{\pm}$ violation, as shown in figure 7.4 a, d, d to plan in each layer, low-energy particle spiral ring rail. By (7.6-4), nuclear magnetic synthesis solution for:

$$\sum U = 5U^{+}_{g1} + U^{-}_{d1} + 2U^{-}_{d2} + U^{-}_{d3} + U^{+}_{d4} \qquad (12.1)$$

Will each to π± mesons in table 9.1 the original magnetic moment of value generation into (12.1), and converted to MRI son have to: $\sum U = -0.6756U_p$.

From table 9.1 of the π± muon $\overline{m}_{di}$, $\overline{m}_{gi}$, data quality, $m_n + 2m_p$ "decentralized" of the π± violation according to (12.1) of the scheme in the high and low particles spiral ring, the m_n+2m_p total quality, quality will be increased by:△m=1.213303744×10^{-29}Kg.

So, $^{173}_{70}$Yb total energy equation of nucleus $\sum {}^{173}_{70}YbW_1$ should be expressed as:

$$\sum {}^{173}_{70}YbW_1 = 173\times 5\overline{m}_{d1} + \Delta m + \sum N_i\overline{m}_{ni} + W_b + W_e \qquad (12.2)$$

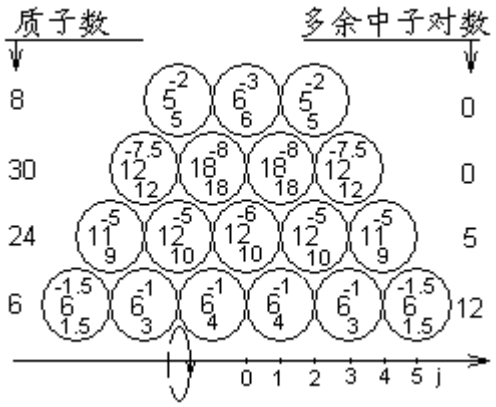

图12.4 $^{173}_{70}Yb$原子核内核子、净剩π±介子分配示意图

$$\begin{array}{cccccc}
{}^{8}Va_{8} & {}^{6}Vb_{-2} & {}^{12}Vc_{6} & {}^{10}Vd_{-2} & {}^{20}Ve_{10} & Vf_{-6} \\
{}^{14}Vg_{3} & {}^{17}Vh_{20} & {}^{37}Vi_{-3} & {}^{34}Vj_{-10} & {}^{24}Vk_{18} & {}^{42}Vl_{36} \\
{}^{78}Vm_{-10} & {}^{68}Vn_{-16} & {}^{52}Vo_{24} & {}^{76}Vp_{-15} & {}^{61}Vq_{6} & {}^{67}Vr_{10} \\
{}^{77}Vs_{-3} & {}^{74}Vt_{-4} & & & &
\end{array}$$

$$W_e = 1.182004425\times 10^{-27}\,Kg$$
$$W_b = 1.051690152\times 10^{-29}\,Kg$$
$$\sum {}^{173}_{70}YbW_1 = 2.871139719\times 10^{-25}\,Kg$$

According to the above scheme, design of $^{173}_{70}Yb$ nucleus to showed in figure 12.4. Convenient for calculating, we will be alone $\pi^{\pm}$ violation "into" two and a half to nuclear power charge number calculation. This does not mean that charged particles can "decentralized", on the contrary, $^{173}_{70}Yb$ nucleus of electric quadrupole moment love you just book the correctness of the model and charged particles cannot "disassemble. $^{173}_{70}Yb$ Nucleus kernel force balance test results shown in table 12.5.

$^{173}_{70}Yb$ Nucleus kernel force balance to verify results (figure 12.4, unit: N) table 12.5

j / N_a	1	2	3	4	5	nuclearElectricand magneticfieldforce accumulated
58 $F_{e\theta}$ $F_{b\theta}$		t.236.6909889 -89.09529 06				-389.2552892
34 $F_{e\theta}$ $F_{b\theta}$	n.867.6686567 -1222.642839		p.891.0114236 -1146.227662			-536.8509875
16 $F_{e\theta}$ $F_{b\theta}$		j.920.3767317 -786.4485285		m.-1110.2481458 -655.3737738		-281.6347491
$F_{e\theta}$ 34/13$F_{b\theta}$ $\Delta F_{\theta b}$	b.520.2435589 -14.26555772 -107.2499554		d.473.2387324 -14.26555772 -210.6695553		i.–218.119028 -21.39833658 -57.45533327	350.0589672

12.1.5 $^{168}_{70}$Yb nucleus internal structure and parameter calculation

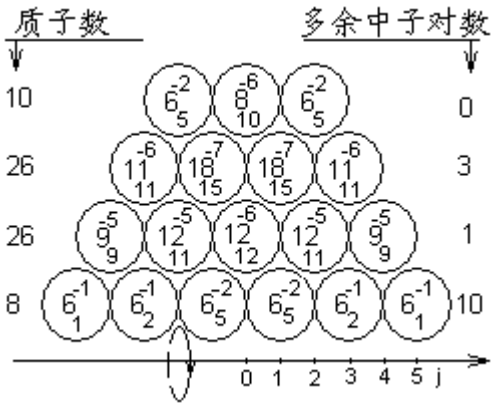

图12.5 $^{168}_{70}Yb$原子核内核子、净剩π±介子分配示意图

$$\underset{10}{Va}\ \ \underset{-4}{\overset{10}{Vb}}\ \ \underset{4}{\overset{6}{Vc}}\ \ \underset{-2}{\overset{10}{Vd}}\ \ \underset{12}{\overset{8}{Ve}}\ \ \underset{-6}{\overset{20}{Vf}}$$

$$\underset{2}{\overset{14}{Vg}}\ \ \underset{22}{\overset{16}{Vh}}\ \ \underset{-2}{\overset{38}{Vi}}\ \ \underset{-10}{\overset{36}{Vj}}\ \ \underset{18}{\overset{26}{Vk}}\ \ \underset{30}{\overset{44}{Vl}}$$

$$\underset{-10}{\overset{74}{Vm}}\ \ \underset{-14}{\overset{64}{Vn}}\ \ \underset{22}{\overset{50}{Vo}}\ \ \underset{-12}{\overset{72}{Vp}}\ \ \underset{10}{\overset{60}{Vq}}\ \ \underset{10}{\overset{70}{Vr}}$$

$$\underset{-6}{\overset{80}{Vs}}\ \ \underset{-4}{\overset{74}{Vt}}$$

$$W_e = 1.18362812 \times 10^{-27}\ Kg$$

$$W_b = 9.366575355 \times 10^{-30}\ Kg$$

$$\sum {}^{168}_{70}YbW_1 = 2.788033106 \times 10^{-25}\ Kg$$

$^{168}_{70}Yb$Nucleus kernel force balance to verify results (figure 12.5, unit: N) table 12.6

j / N_a	1	2	3	4	5	nuclearElectricand magneticfieldforce accumulated
58 $F_{e\theta}$ $F_{b\theta}$		t.251.5671654 -178.1905812				-37.68937437
34 $F_{e\theta}$ $F_{b\theta}$	n.705.4066273 -936.0859236		p.893.9238096 -802.3593631			-111.0659586

16 $F_{e\theta}$ $F_{b\theta}$		j.1033.35848 -786.4485285	m.788.81453473 -655.37377738		|	-202.6304051
$F_{e\theta}$ 34/13$F_{b\theta}$ $\Delta F_{\theta b}$	b.642.7725138 -57.06223088 -306.4284441	d.237.204948 -28.53111544 -160.8749332	i.-162.8141647 -14.26555772 -22.98213331		|	127.0188825

Similarly, refer to section 12.1.2 ~ 12.1.3, $^{168}_{70}$Yb nucleus internal structure and the nuclear force balance verification calculation is shown in figure 12.5 and table 12.6.

12.1.6 Y $^{174}_{70}$b nucleus internal structure and parameter calculation

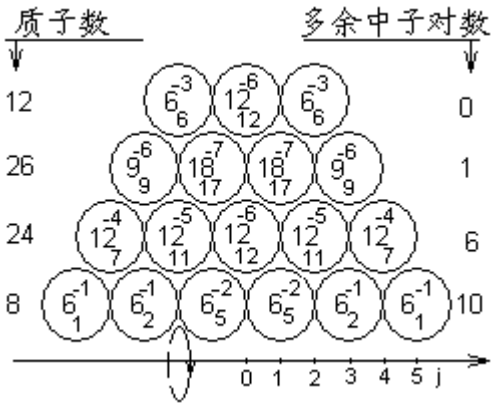

图12.6 $^{174}_{70}Yb$原子核内核子、净剩π±介子分配示意图

$$\begin{array}{cccccc} {}^{10}Va_{10} & {}^{10}Vb_{-4} & {}^{6}Vc_{4} & {}^{10}Vd_{-2} & {}^{8}Ve_{12} & {}^{20}Vf_{-6} \\ {}^{14}Vg_{2} & {}^{16}Vh_{22} & {}^{38}Vi_{-2} & {}^{36}Vj_{-10} & {}^{26}Vk_{14} & {}^{40}Vl_{34} \\ {}^{74}Vm_{-8} & {}^{66}Vn_{-14} & {}^{52}Vo_{18} & {}^{70}Vp_{-12} & {}^{58}Vq_{12} & {}^{70}Vr_{12} \\ {}^{82}Vs_{-6} & {}^{76}Vt_{-6} & & & & \end{array}$$

$$W_e = 1.182568429\times10^{-27}\,Kg$$

$$W_b = 9.223978353\times10^{-30}\,Kg$$

$$\sum {}^{174}_{70}YbW_1 = 2.887749837\times10^{-25}\,Kg$$

$^{174}_{70}Yb$Nucleus kernel force balance to verify results (figure 12.6, unit: N) table 12.7

j / N_a	1 2 3 4 5				nuclearElectricand magneticfieldforce accumulated
58 $F_{e\theta}$ $F_{b\theta}$	t.2692228690 -267.2858718			↑ |	-418.1139802
34 $F_{e\theta}$ $F_{b\theta}$	n.795.9492798 -936.0859236	p.600.3548052 -802.3593631		|	-420.0509774
16 $F_{e\theta}$ $F_{b\theta}$	j.1033.35848 -786.448285	m.-67.67623443 -524.299019		|	-218.0464195
$F_{e\theta}$ 34/13$F_{b\theta}$ $\Delta F_{\theta b}$	b.642.7725138 -57.06223088 -306.4284441	d.237.204948 -28.53111544 -160.8749332	i.-162.8141647 -14.26555772 -22.98213331	|	127.0188825

Similarly, refer to section 12.1.2 ~ 12.1.3, 12.1.5, $^{174}_{70}$Yb nucleus internal structure and the nuclear force balance verification calculation is shown in figure 12.6 and table 12.7.

12.1.7 $^{176}_{70}$Yb nucleus internal structure and parameter calculation

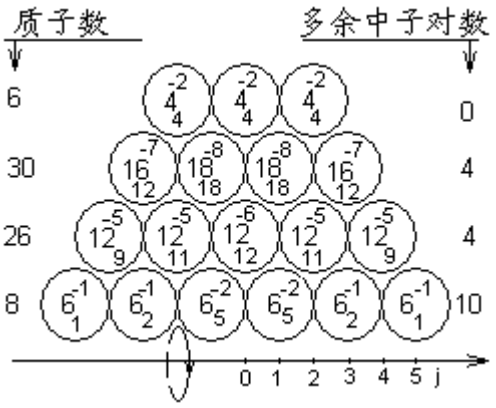

图12.7 $^{176}_{70}Yb$原子核内核子、净剩π±介子分配示意图

$$\begin{matrix} {}^{10}Va_{10} & {}^{10}Vb_{-4} & {}^{6}Vc_{4} & {}^{10}Vd_{-2} & {}^{8}Ve_{12} & {}^{20}Vf_{-6} \\ {}^{14}Vg_{2} & {}^{16}Vh_{22} & {}^{38}Vi_{-2} & {}^{36}Vj_{-10} & {}^{26}Vk_{18} & {}^{44}Vl_{36} \\ {}^{80}Vm_{-10} & {}^{70}Vn_{-16} & {}^{54}Vo_{24} & {}^{78}Vp_{-14} & {}^{64}Vq_{4} & {}^{68}Vr_{8} \\ {}^{76}Vs_{-2} & {}^{74}Vt_{-4} \end{matrix}$$

$$W_e = 1.214035693 \times 10^{-27} Kg$$

$$W_b = 9.43993031 \times 10^{-30} Kg$$

$$\sum {}^{176}_{70}YbW_1 = 2.921026450 \times 10^{-25} Kg$$

$^{176}_{70}Yb$Nucleus kernel force balance to verify results (figure 12.7, unit: N) table 12.8

j / Na	1	2	3	4	5	nuclearElectricand magnetic fieldforce accumulated
58 $F_{e\theta}$		t.1652853417				-315.4699263
$F_{b\theta}$		-59.39686 04				
34 $F_{e\theta}$	n.896.5909453		p.990.4995480			-421.3584076
$F_{b\theta}$	-1222.642839		-1069.812484			
16 $F_{e\theta}$		j.1033.35848		m.-60.600531 83		-342.0454716
$F_{b\theta}$		-786.4485285		-655.3737738		
$F_{e\theta}$	b.642.7725138		d.237.204948		i.-162.8141647	127.0188825
$34/13F_{b\theta}$	-57.06223088		-28.53111544		-14.26555772	
$\Delta F_{\theta b}$	-306.4284441		-160.8749332		-22.98213331	

Similarly, referring to the 12.1.5 ~ 12.1.6, internal structure and the $^{176}_{70}Yb$ nucleus nuclear force balance verification calculation is shown in figure 12.7 and table 12.8.

12.2 $^{130}_{54}$Xe nucleus and stable isotope internal structure and parameter calculation

12.2.1 $^{130}_{54}$Xe nucleus and stable isotopes of the calculated value

$^{130}_{54}$Xe nucleus and stable isotopes parameter experiment, the results table table 12.9

Nuclide	The determination of total energy atomic u	Abundance %	Nucleus total energy calculated value $\times 10^{-25}$Kg	Net with π± source electromagnetic field total energy $\times 10^{-28}$Kg	Magnetic moment U_P
$^{124}_{54}$Xe	123.90612	0.096	2.057047409	8.281386454	
$^{126}_{54}$Xe	125.904279	0.09	2.090227643	8.417006639	
$^{128}_{54}$Xe	127.9035323	1.92	2.123426047	8.570798115	
$^{129}_{54}$Xe	128.904784	26.44	2.140052234	8.674678462	-0.7768
$^{130}_{54}$Xe	129.9035108	4.08	2.156636494	8.736631829	
$^{131}_{54}$Xe	130.9050847	21.18	2.173268032	8.845862436	0.69066
$^{132}_{54}$Xe	131.9041568	26.89	2.189858025	8.913549648	
$^{134}_{54}$Xe	133.905398	10.44	2.22308944	9.100351003	
$^{136}_{54}$Xe	135.907222	8.9	2.256330532	9.296829987	

$^{130}_{54}$Xe isotopes and stable isotopes of nine, with reference to the section on $^{168}_{70}$Yb nucleus and table 12.1 the parameters of the calculation method of $^{130}_{54}$Xe nucleus and stable isotopes parameter experimental data, the results shown in table 12.9. Of atoms inside the K_{a2} layer of electronic ionization energy K_{a2} = 29485 ev, generation of (11.1) in type, too: $\sum W_{me}=2.838337718\times10^{-30}$Kg.

12.2.2 $^{130}_{54}$Xe nucleus internal structure and parameter calculation

Refer to section 12.1 $^{172}_{70}$Yb nucleus internal structure and parameter calculation method, the nuclear force balance verification calculation process, we are still in 7.1 type A nucleus model of the first "assembly" $^{130}_{54}$Xe nucleus, see figure 12.8. $^{130}_{54}$Xe nuclear force balance test results shown in table 12.10.

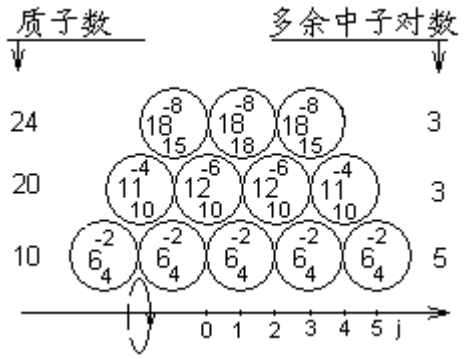

图12.8 $^{130}_{54}Xe$原子核内核子、净剩π±

介子分配示意图

$$\begin{array}{cccccc} {}^{4}Va_{4} & {}^{2}Vb_{-2} & {}^{10}Vc_{8} & {}^{6}Vd_{-4} & {}^{14}Ve_{8} & Vf_{-4} \\ {}^{10}Vg_{20} & {}^{30}Vh_{-12} & {}^{18}Vi_{20} & Vj & {}^{38}Vk_{-8} & Vl \\ {}^{30}Vm_{18} & {}^{48}Vn_{30} & {}^{78}Vo_{-8} & Vp & {}^{70}Vq_{-16} & \end{array}$$

$$W_e = 7.926277014\times10^{-28}\,Kg$$

$$W_b = 1.614707866\times10^{-29}\,Kg$$

$$\sum {}^{130}_{54}XeW_1 = 2.15663905\times10^{-25}\,Kg$$

$^{130}_{54}Xe$Nucleus kernel force balance to verify results (figure 12.8, unit: N) table 12.10

j / N_a	1	2	3	4	5	6	nuclearElectricand magnetic fieldforce accumulated	
34 $F_{e\theta}$ $F_{b\theta}$		q.1170.054522 -1222.642839					↑	
16 $F_{e\theta}$ $F_{b\theta}$	h.361.9599434 -943.7382342		k.1008.949365 -629.1588228				|	1009.829894
$F_{e\theta}$ 34/13$F_{b\theta}$ $\Delta F_{\theta b}$		d.712.7489433 -57.06223088		f.307.2004698 -57.06223088 -275.7855997			|||	630.0393516

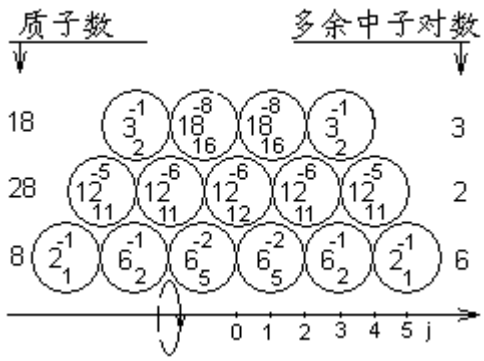

图12.9 $^{130}_{54}Xe$原子核内核子、净剩π±

介子分配示意图

$$\begin{array}{cccccc} {}^{10}Va_{10} & {}^{6}Vb_{-4} & {}^{10}Vc_{4} & {}^{8}Vd_{-2} & {}^{20}Ve_{12} & Vf_{-6} \\ {}^{14}Vg_{2} & {}^{16}Vh_{22} & {}^{38}Vi_{-2} & {}^{36}Vj_{-12} & {}^{24}Vk_{22} & {}^{46}Vl_{32} \\ {}^{78}Vm_{-10} & {}^{68}Vn_{-16} & {}^{52}Vo_{4} & {}^{56}Vp_{-2} & & \end{array}$$

$$W_e = 8.136574665\times10^{-28}\,Kg$$

$$W_b = 9.346342627\times10^{-30}\,Kg$$

$$\sum {}^{130}_{54}XeW_2 = 2.15663237\times10^{-25}\,Kg$$

With the table 12.2, uneven distribution of electric and magnetic field force in the nuclear, especially the bottom, not set edge of particles spiral ring, this kind of type A

nucleus is still not stable. So, we should adopt the type B nuclei model to "assemble" $^{130}_{54}Xe$ series nuclide atom, see figure 12.9 and table 12.11.

$^{130}_{54}$Xe nucleus kernel force balance to verify results (figure 12.9, unit: N) table 12.11

j / N_a	1	2	3	4	5		nuclearElectricand magneticfieldforce accumulated
34 $F_{e\theta}$	n.758.3212815		p.162.96320 36			↑	-316.36408
$F_{b\theta}$	-1222.642839		-152.8303549				
16 $F_{e\theta}$		j.917.00250 56		m.359.6684459			-326.49692 87
$F_{b\theta}$		-943.738234 2		-786.448285			
$F_{e\theta}$	b.642.7725138		d.237.204948		i.-162.8141647		127.0188825
34/13$F_{b\theta}$	-57.06223088		-28.53111544		-14.26555772		
$\Delta F_{\theta b}$	-306.428444 1		-160.874933 2		-22.982133 31		

12.2.3 $^{131}_{54}$Xe nucleus internal structure and parameter calculation

$^{131}_{54}$Xe nucleus, the experiment measured strength value of 0.69066 U_p, electric quadrupole moment for $-0.12\times10^{-24}cm^2$. Refer to section 7.2 (12.1) and type of magnetic synthesis principle. By figure 7.4 shows, still take a, d, d, its magnetic synthesis formula is:

$$\sum U = 5U^{+}_{g1} + U^{+}_{d2} + 3U^{-}_{d2} + U^{-}_{d3} \qquad (12.3)$$

$^{131}_{54}$Xe nucleus kernel force balance to verify results (figure 12.10, unit: N) table 12.12

j / Na	1	2	3	4	5		nuclearElectricand magneticfieldforce accumulated
34 Feθ	n. 663.5682269		p. 294.3919560			↑	-160.79181 13
Fbθ	-687.736597 0		-401.179681 6				
16 Feθ		j. 1028.200151		m.308.1758925			-54.004085 74
Fbθ		-943.738234 2		-943.738234 2			
Feθ	b.520.2435589		d.473.2387324		i.–782.1443493		497.0963392
34/13Fbθ	-14.26555772		-14.26555772		-14.26555772		
$\Delta F\theta b$	-107.249955 4		-191.517777 6		-76.607111 03		

Will each layer in the table 9.1 net with $\pi^{\pm}$ muon original strength value generation

into (12.3), too: $\sum U = 0.67806U_p$.

Similarly, according to this kind of alone $m_n + 2\ m_p$ "decentralized" $\pi^{\pm}$ mesons in (12.3) of the scheme, the $\overline{m}_{di}$, $\overline{m}_{gi}$, in table 9.1, alone the $m_n + 2m_p$ its total quality increment is: $\triangle m=1.9707240905\times 10^{-29}Kg$. So, according to (12.2), $^{173}_{70}$Yb nuclear magnetic moment, internal structure and parameter calculation, assembly of type B $^{131}_{54}$Xe nucleus is shown in figure 12.10, the nuclear force balance test results shown in table 12.12.

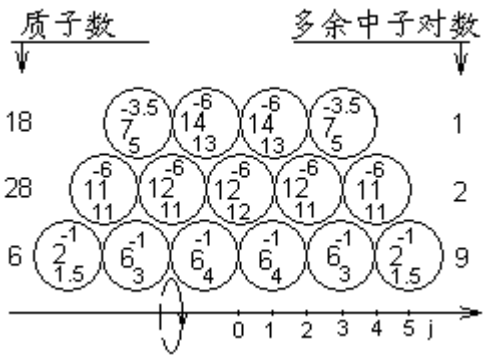

图12.10 $^{131}_{54}Xe$原子核内核子、净剩π±介子分配示意图

$$\begin{array}{cccccc} {\scriptstyle 8} & {\scriptstyle 6} & {\scriptstyle 12} & {\scriptstyle 10} & {\scriptstyle 22} \\ Va & Vb & Vc & Vd & Ve & Vf \\ {\scriptstyle 8} & {\scriptstyle -2} & {\scriptstyle 6} & {\scriptstyle -2} & {\scriptstyle 12} & {\scriptstyle -6} \\ {\scriptstyle 16} & {\scriptstyle 19} & {\scriptstyle 41} & {\scriptstyle 39} & {\scriptstyle 27} & {\scriptstyle 49} \\ Vg & Vh & Vi & Vj & Vk & Vl \\ {\scriptstyle 3} & {\scriptstyle 22} & {\scriptstyle -2} & {\scriptstyle -12} & {\scriptstyle 22} & {\scriptstyle 26} \\ {\scriptstyle 75} & {\scriptstyle 63} & {\scriptstyle 51} & {\scriptstyle 61} \\ Vm & Vn & Vo & Vp \\ {\scriptstyle -12} & {\scriptstyle -12} & {\scriptstyle 10} & {\scriptstyle -7} \end{array}$$

$$W_e = 8.186479798\times 10^{-28}\ Kg$$
$$W_b = 1.086864991\times 10^{-29}\ Kg$$
$$\sum {}^{131}_{54}XeW_1 = 2.173277665\times 10^{-25}\ Kg$$

12.2.4 $^{124}_{54}$Xe nucleus internal structure and parameter calculation

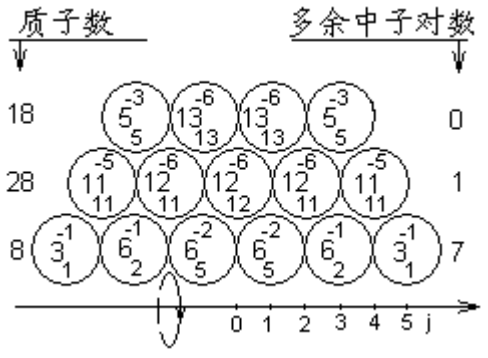

图12.11 $^{124}_{54}Xe$原子核内核子、净剩π±介子分配示意图

$$\begin{array}{cccccc} {\scriptstyle 10} & {\scriptstyle 6} & {\scriptstyle 10} & {\scriptstyle 8} & {\scriptstyle 20} \\ Va & Vb & Vc & Vd & Ve & Vf \\ {\scriptstyle 10} & {\scriptstyle -4} & {\scriptstyle 4} & {\scriptstyle -2} & {\scriptstyle 12} & {\scriptstyle -6} \\ {\scriptstyle 14} & {\scriptstyle 16} & {\scriptstyle 38} & {\scriptstyle 36} & {\scriptstyle 24} & {\scriptstyle 46} \\ Vg & Vh & Vi & Vj & Vk & Vl \\ {\scriptstyle 2} & {\scriptstyle 22} & {\scriptstyle -2} & {\scriptstyle -12} & {\scriptstyle 22} & {\scriptstyle 26} \\ {\scriptstyle 72} & {\scriptstyle 62} & {\scriptstyle 50} & {\scriptstyle 60} \\ Vm & Vn & Vo & Vp \\ {\scriptstyle -10} & {\scriptstyle -12} & {\scriptstyle 10} & {\scriptstyle -6} \end{array}$$

$$W_e = 8.048187241\times 10^{-28}\ Kg$$
$$W_b = 9.346342627\times 10^{-30}\ Kg$$
$$\sum {}^{124}_{54}XeW_1 = 2.057054499\times 10^{-25}\ Kg$$

$^{124}_{54}Xe$Nucleus kernel force balance to verify results (Figure12.11 units: N) table 12.13

j / N_a	1	2	3	4	5	nuclearElectricand magneticfieldforce accumulated
34 Feθ	n.621.0364816		p.347.35105 29			-183.59910 77
Fbθ	-687.736597 0		-343.8682985			
16 Feθ		j.917.00250 56		m.499.0835125		-187.08186 21
Fbθ		-943.738234 2		-786.4485285		
Feθ	b.642.7725138		d.237.204948		i.-162.8141647	127.0188825
34/13Fbθ	-57.0622308 8		-28.5311154 4		-14.265557 72	
ΔFθb	-306.428444 1		-160.8749332		-22.982133 31	

12.2.5 $^{136}_{54}$Xe nucleus internal structure and parameter calculation

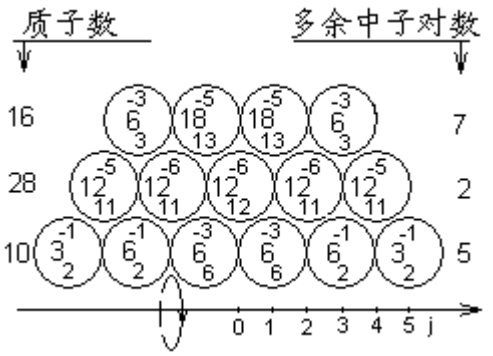

图12.12 $^{136}_{54}Xe$原子核内核子、净剩π±介子分配示意图

$$\overset{12}{Va}_{12}\ \overset{6}{Vb}_{-6}\ \overset{10}{Vc}_{4}\ \overset{8}{Vd}_{-2}\ \overset{20}{Ve}_{12}\ \overset{14}{Vf}_{-6}$$

$$\overset{18}{Vg}_{4}\ \overset{40}{Vh}_{22}\ \overset{38}{Vi}_{-2}\ \overset{26}{Vj}_{-12}\ \overset{48}{Vk}_{22}\ \overset{74}{Vl}_{26}$$

$$\overset{64}{Vm}_{-10}\ \overset{54}{Vn}_{-10}\ \overset{60}{Vo}_{6}\ Vp_{-6}$$

$$W_e = 8.384428902 \times 10^{-28}\ Kg$$

$$W_b = 1.384307482 \times 10^{-29}\ Kg$$

$$\sum {}^{136}_{54}XeW_1 = 2.256337456 \times 10^{-25}\ Kg$$

$^{136}_{54}Xe$Nucleus kernel force balance to verify results (Figure12.12 units: N) table 12.14

j / N_a	1	2	3	4	5	nuclearElectricand magneticfieldforce accumulated
34 $F_{e\theta}$	n.693.8586526		p.74.754705 08			45.44894326
$F_{b\theta}$	-477.594859 0		-286.5569154			
16 $F_{e\theta}$		j.991.1342691		m.570.0909716		40.98735998
$F_{b\theta}$		-943.738234 2		-786.4485285		
$F_{e\theta}$	b.792.5301253		d.237.204948		i.-13.81634162	209.948882
34/13$F_{b\theta}$	-128.390019 5		-42.79667316		-14.265557 72	
$\Delta F_{\theta b}$	-413.678399 6		-137.8927999		-68.946399 93	

See from the table above, the lateral force in general is slightly less than nuclear power. When we consider the first layer side by side low-energy particles spiral ring rail tangent and near because of the spin direction current yuan interval is small, with the integral method to calculate the overall ampere force will increase, as shown in the (10.20), table 10.4, may be affirmed, the nucleus is still stable, (the same below).

12.3 $^{56}_{26}$Fe, $^{40}_{20}$Ca, $^{16}_{8}$O The nucleus and stable isotopes

The internal structure and parameter calculation

12.3.1 $^{56}_{26}$Fe nucleus and stable isotope internal structure and parameter calculation

$^{56}_{26}$ Fe nuclide and stable isotopes of 5 kinds of K_{a2} layer electronic ionization energy K_{a2} = 6390 ev, generation of (11.1) in type, too: $\sum W_{me}=2.961715803\times10^{-31}$Kg . According to the atomic energy, computing parameters to showed in table 12.15.

$^{56}_{26}Fe$Nucleus and stable isotopes parameter experimental data results table 12.15

Nuclide	The determination of total energy atomic u	Abundance %	Nucleus total energy calculated value ×10^{-26}Kg	Net with π± source electromagnetic field total energy ×10^{-28}Kg	Magnetic moment UP
$^{54}_{26}$Fe	53.9396120	5.8	8.954550586	3.250500278	
$^{56}_{26}$Fe	55.9349339	91.7	9.285881808	3.339009277	
$^{57}_{26}$Fe	56.9353907	2.19	9.452011682	3.429689989	0.0902
$^{58}_{26}$Fe	57.9332745	0.31	9.617714298	3.477645002	

We first to type A nucleus model to "assemble" $^{56}_{26}$Fe nucleus, see figure 12.13, $^{56}_{26}$Fe nuclear force balance verification calculation shown in table 12.16. From figure 12.13 shows: in nuclear magnetic moment = 0, under the premise of nuclear in net with $\pi^{\pm}$ mesons, each layer nuclear number no further can be adjusted. At this time, we can adjust the pairs of high or low $\pi^{\pm}$ mesons in each layer of particles spiral ring

number of distribution. According to table 9.1 each layer $\overline{m}_{di}, \overline{m}_{gi}$, differences in values, see table 13.3 the calculated value of also can rise to adjust the nucleus of the total energy of function.

$^{56}_{26}$Fe maintenance nucleus kernel force balance to verify the results table (figure 12.13, the unit: Newton) table 12.16

j / N_a	1	2	3	4	5	nuclearElectricand magneticfieldforce accumulated	
16 $F_{e\theta}$ $F_{b\theta}$	h. 484.0435425 -943.7382342						
$F_{e\theta}$ 34/13$F_{b\theta}$ $\Delta F_{\theta b}$		d. 1257.573065 -85.59334632 -536.2497772				↑ |	635.7299415

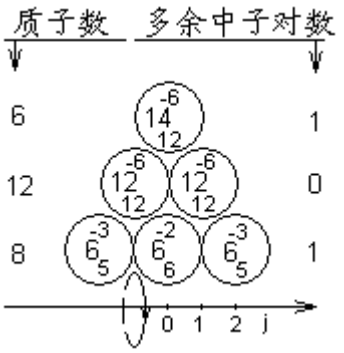

图12.13 $^{56}_{24}Fe$原子核内核子、净剩π±介子分配示意图

$$Va_{6}\quad Vb_{-2}^{6}\quad Vc_{10}^{4}\quad Vd_{-6}^{14}\quad Ve\quad Vf$$

$$Vg_{24}^{8}\quad Vh_{-12}^{32}\quad Vi\quad Vj\quad Vk\quad Vl$$

$$Vm_{12}^{20}\quad Vn\quad Vo_{-6}^{32}$$

$$W_e = 2.892590098\times10^{-28}\,Kg$$

$$W_b = 1.700296422\times10^{-29}\,Kg$$

$$\sum {}^{56}_{26}FeW_1 = 9.283813975\times10^{-26}\,Kg$$

Train to $\overline{m}^{\pm}_{d1}\rightarrow\overline{m}^{\pm}_{d2}$, $\overline{m}^{\pm}_{g2}\rightarrow\overline{m}^{\pm}_{g1}$, the∑△m = 2.05555632 x 10^{-29} kg. After adjusting $^{56}_{26}$Fe nucleus total energy for $\sum {}^{56}_{26}$Fe W_2 =9.285869531×10^{-26}Kg, coincided with experimental value. But by shown in table 12.16, 1 layer particles spiral ring in the nuclear field force far outweigh the magnetic field, the second layer of the magnetic field strength is big, but the first layer of the lateral particle spiral ring doesn't set stability, so the nucleus is also does not exist.

When we use type B nuclei model to "assemble" $^{56}_{26}$Fe nucleus, see figure 12.14 and table 12.17. Although nuclear power field force is greater than the nuclear magnetic force, but it's better than figure 12.13 and table 12.16 shows the type A much more stable nucleus.

Of course, we also can consider to increase the layer 3 particles spiral rings, and the first layer of particles spiral ring number of protons to 10. Interested readers can do it yourself "assembly", simulated calculation exercises.

To make AA $2\overline{m}^{\pm}_{d1} \rightarrow 2\overline{m}^{\pm}_{d2}$, the π± source energy increment processed △m = 1.76190544×10^{-29}Kg, for type B nucleus $^{56}_{26}$Fe after the adjustment the total energy $\sum^{56}_{26}$Fe W_4=9.285944876×10^{-26}Kg.

If maintain figure 12.14, $^{56}_{26}$ Fe within the nucleus of the net with $\pi^{\pm}$ muon distribution state, the nuclear net with $\pi^{\pm}$muon electric and magnetic field total energy and nuclear force equilibrium constant, as shown in the table 12.17. $^{58}_{26}$Fe nucleus, shillings a neutron into the first layer particles spiral ring, then to:

$\overline{m}^{\pm}_{g2} \rightarrow \overline{m}^{\pm}_{g1}$，则$\sum^{58}_{26}FeW_1$=9.617565612×10^{-26}Kg。

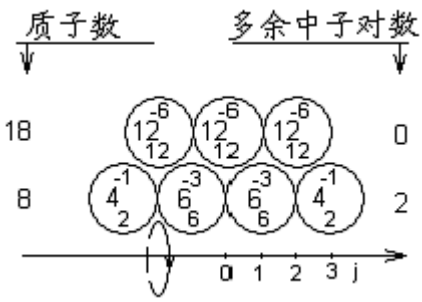

图12.14 $^{56}_{26}Fe$原子核内核子、净剩

π±介子分配示意图

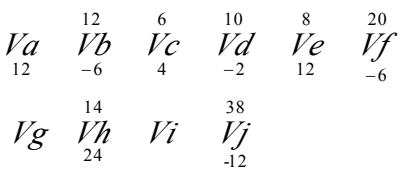

$W_e = 3.039936250 \times 10^{-28}\ Kg$

$W_b = 1.291892102 \times 10^{-29}\ Kg$

$\sum^{56}_{26} FeW_3 = 9.28418297 \times 10^{-26}\ Kg$

$^{56}_{26}$Fe nucleus kernel force balance to verify results (figure 12.14, unit: N) table 12.17

j / N_a	1	2	3	4	5	nuclearElectricand magneticfieldforce accumulated	
16 $F_{e\theta}$ $F_{b\theta}$		j.949.7761591 -943.73824 32				↑	244.0687062
$F_{e\theta}$ 34/13 $F_{b\theta}$ $\Delta F_{\theta b}$	b.792.5301253 -128.3900195 -413.6783998		d. 237.204948 -42.79667316 -206.8391998			|	238.0307813

Similarly, $^{54}_{26}$Fe nucleus, as long as in the figure 12.14 1 layer particles spiral ring in the edge of the two neutron take out, then to $\overline{m}^{\pm}_{d2} \rightarrow \overline{m}^{\pm}_{d1}$, the $\sum {}^{54}_{26}$Fe W_1 =8.95461779×10 $^{-26}$Kg . These parameters and the experimental results are very close.

12.3. 2 $^{40}_{20}$Ca nucleus and stable isotope internal structure and parameter calculation

$^{40}_{20}$Ca nuclide and stable isotopes are 5 kinds of atoms. K_{a2} layer electronic ionization energy K_{a2}=3688 ev, generation of (11.1) in type, too: $\sum W_{me}$=1.314892005×10^{-31}Kg. According to the atomic energy, computing parameters to showed in table 12.18.

$^{40}_{20}$Ca nucleus and stable isotopes parameter experimental data results table 12.18

Nuclide	The determination of total energy atomic u	Abundance %	Nucleus total energy calculated value ×10^{-26}Kg	Net with π± source electromagnetic field total energy ×10^{-28}Kg	Magnetic moment UP
$^{40}_{20}Ca$	39.9625921	96.94	6.634140339	2.521768481	
$^{42}_{20}Ca$	41.9586281	0.65	6.965590141	2.622135397	
$^{43}_{20}Ca$	42.9587774	0.14	7.131668953	2.707709949	-1.31721
$^{44}_{20}Ca$	43.9554875	2.08	7.297176671	2.736175201	
$^{46}_{20}Ca$	45.953689	0.003	7.628986063	2.872501116	

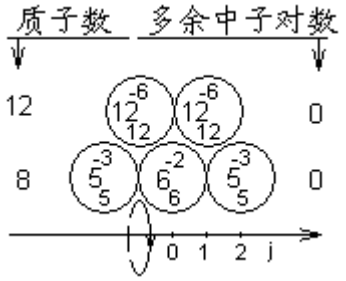

图12.15 $^{40}_{20}Ca$ 原子核内核子、净剩π±介子分配示意图

$$\overset{6}{Va}_{6}\quad \overset{4}{Vb}_{-2}\quad \overset{14}{Vc}_{10}\quad \overset{}{Vd}_{-6}\quad Ve\quad Vf$$

$$\overset{8}{Vg}_{24}\quad \overset{32}{Vh}_{-12}$$

$$W_e = 2.216685332\times10^{-28}\,Kg$$

$$W_b = 1.698237985\times10^{-29}\,Kg$$

$$\sum {}^{40}_{20}CaW_1 = 6.632787745\times10^{-26}\,Kg$$

We use first type A nucleus model to "assemble" $^{40}_{20}Ca$ nucleus. Because of equal number of protons, neutrons, we have no choice, only in 12.15 "assembly" $^{40}_{20}Ca$ nucleus, and make $2\overline{m}^{\pm}_{g2} \to 2\overline{m}^{\pm}_{g1}$, $\overline{m}^{\pm}_{d2} \to \overline{m}^{\pm}_{d1}$, to: $\sum {}^{40}_{20}Ca$W$_2$ = 6.634256 x 10^{-26} kg.

Although agreement with experimental data, and figure 12.13 and table 12.16 types A $^{56}_{26}$Fe nucleus, 1, 2 layer particles spiral ring nuclear force parameters in exactly the same, so the nucleus is still unstable or does not exist.

When we use type B "assembly" $^{40}_{20}Ca$ nucleus, nucleus model is shown in figure 12.16 and table 12.19.

To make $3\overline{m}^{\pm}_{d1} \to 3\overline{m}^{\pm}_{d2}$, too: $\sum {}^{40}_{20}Ca$W$_3$ = 6.634091126 x 10^{-26} kg

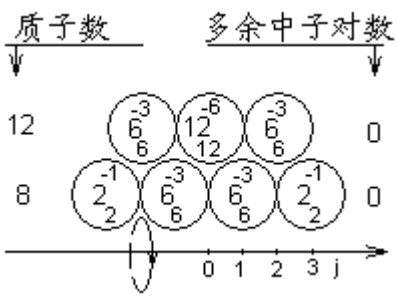

图12.16 $^{40}_{16}Ca$ 原子核内核子、净剩π±介子分配示意图

$$\overset{12}{Va}_{12}\quad \overset{12}{Vb}_{-6}\quad \overset{6}{Vc}_{4}\quad \overset{10}{Vd}_{-2}\quad \overset{8}{Ve}_{12}\quad \overset{20}{Vf}_{-6}$$

$$Vg\quad \overset{14}{Vh}_{12}\quad Vi\quad \overset{26}{Vj}_{-6}$$

$$W_e = 2.126232534\times10^{-28}\,Kg$$

$$W_b = 1.263288342\times10^{-29}\,Kg$$

$$\sum {}^{40}_{20}CaW_2 = 6.631448268\times10^{-26}\,Kg$$

To maintain figure 12.16, the net in $^{40}_{20}Ca$ nucleus with $\pi^{\pm}$ both scheme is changeless, adjust new neutron and high in pairs, low-energy $\pi^{\pm}$ violation to the distribution of the levels, we can make the simulation $^{40}_{20}Ca$ isotopes, the internal structure and parameters of at this time, the nuclear spin direction of electric and magnetic energy, the nuclear force equilibrium state is unchanged.

$^{40}_{20}Ca$ Nucleus kernel force balance to verify results (figure 12.16, unit: N) table 12.19

j / N_a	1	2	3	4	5	nudearElectricand magneticfieldforce accumulated
16 $F_{e\theta}$		j.387.85368609			↑	154.0153451
$F_{b\theta}$		-471.8691171				
$F_{e\theta}$	b.792.5301253	d.237.204948				238.0307813
34/13$F_{b\theta}$	-128.3900195	-42.79667316				
$\Delta F_{\theta b}$	-413.6783996	-206.8391998				

To $^{42}_{20}$Ca atomic nuclide, make a new pair of neutron into the layer 2 particles spiral ring, is:

$$\sum {}^{42}_{20}CaW_1=6.963362655\times10^{-26}Kg$$

To $2\overline{m}^{\pm}_{g2} \rightarrow 2\overline{m}^{\pm}_{g1}$, to: $\sum {}^{42}_{20}CaW_2$ = 6.965711862 x 10^{-26} kg

To $^{44}_{20}$Ca atomic nuclide, make 2 to new neutrons are into the layer 2 particles spiral ring, is:

$$\sum {}^{44}_{20}CaW_1=7.295277042\times10^{-26}Kg$$

To $\overline{m}^{\pm}_{d1} \rightarrow \overline{m}^{\pm}_{d2}$, $\overline{m}^{\pm}_{g2} \rightarrow \overline{m}^{\pm}_{g1}$, the $\sum {}^{44}_{20}CaW_2=7.297332599\times10^{-26}Kg$

To $^{46}_{20}$Ca atomic nuclide, make 3 to add neutron full into the layer 2 particles spiral ring, is:

$\sum_{20}^{46}$CaW$_1$=7.62719143×10^{-26}Kg

And then to $2\overline{m}_{d1}^{\pm} \rightarrow 2\overline{m}_{d2}^{\pm}$, to : $\sum_{20}^{46}\mathrm{CaW}_2$ = 7.628953335 x 10^{-26} kg

Synthesis of $^{43}_{20}$Ca nucleus, magnetic or in figure 7.4 a, c, d or b, d, d, by (7.6 1) type, to:

$$\sum U = U_{g1}^{+} + U_{g1}^{-} + 3U_{g2}^{+} + 2U_{d2}^{+} + 3U_{d1}^{-} \qquad (12.4)$$

$^{43}_{20}$Ca nucleus kernel force balance to verify results (figure 12.17, unit: N) table 12.20

j / N_a	1	2	3	4	5	nuclearElectricandmagnetic fieldforceaccumulated	
16 $F_{e\theta}$		j.433.3100386				↑	227.5599386
$F_{b\theta}$		-209.7196076					
$F_{e\theta}$	b.792.5301253		d.67.33868407				3.969507647
34/13$F_{b\theta}$	-128.3900195		-106.9916829				
$\Delta F_{\theta b}$	-517.0979995		-103.4195999				

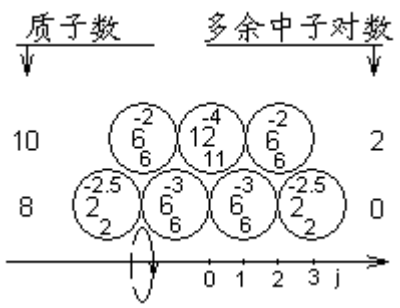

图12.17 $^{43}_{16}Ca$原子核内核子、净剩

π$^{\pm}$介子分配示意图

Va_{12} Vb_{-6}^{12} Vc_{4}^{6} Vd_{-5}^{10} Ve_{11}^{5} Vf_{-4}^{16}

Vg Vh_{12}^{12} Vi Vj_{-4}^{24}

$W_e = 2.023653299\times10^{-28}Kg$

$W_b = 1.263917481\times10^{-29}Kg$

$\sum_{20}^{43}CaW_1 = 7.12814786\times10^{-26}Kg$

Will the original magnetic strength values in table 9.1 generation into (12.4), too: $\sum U$=-1.26551U$_p$.

Similarly, quality increment is: train △m = -8.80952673 x 10^{-30} kg

"Assembly" $^{43}_{16}Ca$nucleus figure 12.17, the nuclear force balance test results

shown in table 12.20.

To $3\overline{m}_{g2}^{\pm} \rightarrow 3\overline{m}_{g1}^{\pm}$,to: $\sum {}_{20}^{43}CaW_2$ = 7.131671671 x 10^{-26} kg

12.3.3 $^{16}_{8}O$ nuclei and stable isotope internal structure and parameter calculation

$^{16}_{8}O$ atom nuclide is only 3 and stable isotopes. K_{a2} layer electronic ionization energy K_{a2}=523 ev, generation of (11.1) in type, to:$\sum W_{me}$=41804ev=7.45866×10^{-33}Kg. Calculated according to the atomic energy, energy parameters to showed in table 12.21.

$^{16}_{8}O$ nuclei and stable isotopes energy parameters experimental data,

the results table table 12.21

Nuclide	The determination of total energy atomic u	Abundance %	Nucleus total energy calculated value ×10 $^{-26}$Kg	Net with π± source electromagnetic field total energy ×10^{-28}Kg	Magnetic moment U_P
$^{16}_{8}O$	15.99491502	99.76	2.655291933	1.172287172	
$^{17}_{8}O$	16.9991333	0.039	2.822046416	1.325428772	-1.89371
$^{18}_{8}O$	17.99915996	0.205	2.988104863	1.408966837	

We first to type A nucleus model "assembly" $^{16}_{8}O$ nuclei, see figure 12.18 and table 12.22.

$^{16}_{8}O$ nuclei kernel force balance test results list (figure 12.18, unit: N) table 12.22

j / N_a	1	2	3	4	5	nuclear Electric and magnetic field force accumulated
$F_{e\theta}$		d. 1257.573065			↑	635.7299417
$34/13F_{b\theta}$		-85.59334632			|	
$\Delta F_{\theta b}$		-536.24977762			|	

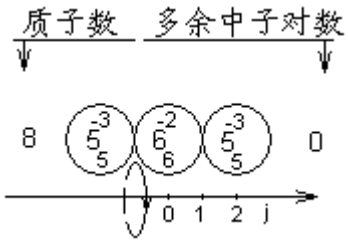

图12.18 ${}^{16}_{8}O$原子核内核子、净剩

π±介子分配示意图

$$Va_{6}\quad Vb^{6}_{-2}\quad Vc^{4}_{10}\quad Vd^{14}_{-6}$$

$$W_e = 9.560477373\times10^{-29}\,Kg$$
$$W_b = 1.689408034\times10^{-29}\,Kg$$
$$\sum {}^{16}_{8}OW_1 = 2.654818947\times10^{-26}\,Kg$$

Can be seen from the above results is that ${}^{16}_{8}$O conditions within the nucleus net with $\pi^{\pm}$violation can such distribution, and nuclear power, magnetic field is a maximum total energy, nuclear energy, but still less than the value, the nuclear force is also unable to balance. So, A type ${}^{16}_{8}$ O nuclear model also cannot exist. Similarly, "assembly" type B ${}^{16}_{8}$O nucleus figure 12.19, the nuclear force balance verification calculation shown in table 12.23.

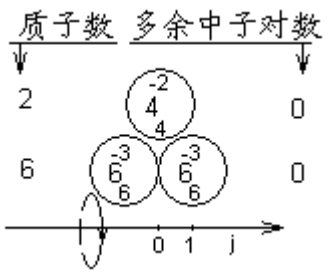

图12.19 ${}^{16}_{8}O$原子核内核子、净剩

π±介子分配示意图

$$Va_{12}\quad Vb^{12}_{-6}\quad Vc\quad Vd\quad Ve^{6}_{4}\quad Vf^{10}_{-2}$$

$$W_e = 9.10194656\times10^{-29}\,Kg$$
$$W_b = 1.379237908\times10^{-29}\,Kg$$
$$\sum {}^{16}_{8}OW_1 = 2.654050246\times10^{-26}\,Kg$$

${}^{16}_{8}$O nuclei kernel force balance test results list (figure 12.19, unit: N) table 12.23

j / N_a	1	2	3	4	5	nuclear Electric and magnetic field force accumulated	
$F_{e\theta}$		b.792.5301253				↑	43.62250648
$34/13F_{b\theta}$		-128.3900195				|	
$\Delta F_{\theta b}$		-620.5175993				|	

Make to $\overline{m}_{g2}^{\pm} \rightarrow \overline{m}_{g1}^{\pm}$, to: $\sum {}_{8}^{16}OW_2$=2.65522486×10^{-26}Kg

To ${}_{8}^{18}O$ nuclei, and make a pair of neutron into layer, layer 2 particles spiral ring:

$$\sum {}_{8}^{18}OW_1=2.985964633\times10^{-26}Kg$$

Tomake $\overline{m}_{g2}^{\pm} \rightarrow \overline{m}_{g1}^{\pm}$, $\overline{m}_{d1}^{\pm} \rightarrow \overline{m}_{d2}^{\pm}$, to: $\sum {}_{8}^{18}OW_2$=2.98802019×10^{-26}Kg

Synthesis of ${}_{8}^{17}O$ nuclei, magnetic take in figure 7.4 a, d, d, by (7.6-4) and table 9.1 data:

$$\sum U = 5U_{g1}^{+} + 2U_{d1}^{-} + U_{d2}^{+} + 2U_{d2}^{-} = -1.93864U_{p} \qquad (12.5)$$

$$\Delta m = 1.321429084\times10^{-29}Kg$$

Its internal structure and the calculation result is shown in figure 12.20 and table 12.24.

Tomake $\overline{m}_{g1}^{\pm} \rightarrow \overline{m}_{g2}^{\pm}$, $\overline{m}_{d1}^{\pm} \rightarrow \overline{m}_{d2}^{\pm}$, to: $\sum {}_{8}^{17}OW_2$=2.82206546×10^{-26}Kg

${}_{8}^{17}O$ nuclei kernel force balance test results list (figure 12.20, unit: N) table 12.24

j / N_a	1	2	3	4	5	nuclearElectricand magneticfieldforce accumulated	
$F_{e\theta}$		b.986.8248433				↑	92.36371348
$34/13F_{b\theta}$		-128.3900195				|	
$\Delta F_{\theta b}$		-766.0711103				|	

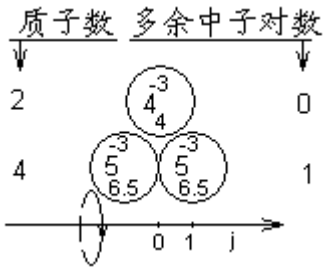

图12.20 ${}_{8}^{17}O$原子核内核子、净剩

π±介子分配示意图

$$Va_{13} \quad {}^{13}Vb_{-6} \quad Vc \quad Vd \quad {}^{7}Ve_{4} \quad {}^{11}Vf_{-3}$$

$$W_e = 1.061847095\times10^{-28}\,Kg$$
$$W_b = 1.62708268\times10^{-29}\,Kg$$
$$\sum {}_{8}^{17}OW_1 = 2.822359111\times10^{-26}\,Kg$$

Through the chapter 11, 12 of several nuclei and isotope internal model design, the nuclear force balance test simulation results, we can see that: the number of nuclear A≥12 all the nucleus, nucleus is B, internal nuclear force to balance. Because each layer particles spiral ring high and low $\pi^{\pm}$ violation of, neutron energy fluctuation in the original slightly difference, in neighbouring particles spiral ring in motivating, transition does not affect the distribution of nuclear power, but it can reflect the total energy of the nucleus, it is without the γ rays, x rays, formation conditions, nuclear small changes in the internal energy and nuclear power.

12.4 Light nuclei supplement internal structure and Parameter calculation

12.4.1 Light $N_{\alpha di}$、$N_{\alpha gi}$、$\overline{M}_{di}$、$\overline{M}_{gi}$ added calculation parameters within the nucleus

Front chapter 7 of section 7.1 shown in figure 7.1 and figure 7.2, the first layer, low-energy particle spiral loop combination model with 2 ~ 5 layers. But this scheme is applicable to the quality of medium to heavy nuclei. To light nuclei and the simulation results can be seen from the previous section: common small total energy and nuclear electric field in repelling force slants big; therefore, to light nuclei, we can consider to use the first layer and 2 ~ 5 layer, low-energy particle spiral rings set combination model of the same.

Refer to chapter 8 ${}^{12}_{6}C$ $\overline{M}_{\pi d1}$ forces within the nucleus of the benchmark constant calculation method. Shilling $N_{\alpha d1} = 34/13$, and (4.9) in type $\beta_{\alpha d1}$ are obtained. Refer to chapter 9 $N_{\alpha di}$、$N_{\alpha gi}$、$\overline{M}_{di}$、$\overline{M}_{gi}$ parameter simulation calculation method, the $N_{\alpha gi}$ = 4, 5, 6 of a natural number. Respectively into (9.7) and (9.9) and (9.6)

equations, get $N_{\alpha gi}$ = 5. Finally by chapter 8 section 8.4 the last 1 ~ 12 simulation procedures, simulation is obtained:

$$\overline{M}_{\pi d1} = 3.572742815\times10^{-28}\text{Kg}$$

$^{56}_{26}Fe$、$^{40}_{20}Ca$、$^{16}_{8}O$Uclei original energy simulation results ratio table table 12.25

Atomic nuclide / The project	$^{56}_{26}Fe$	$^{40}_{20}Ca$	$^{16}_{8}O$
Experimental value (10^{-26}kg)	9.285881808	6.634140339	2.655291933
Type B the simulation predicted value of the nucleus	9.28418297	6.631448286	2.654050246
The ratio of experimental data and the simulation value	1.000182982	1.000405952	1.000467846
Electromagnetic field the ratio of total energy and nuclear energy	0.0034135	0.0033968	0.0039491

Us from in front of all the particles in the nucleus of solenoid ring of surplus high and low $\pi^{\pm}$ violation, the spin direction of electromagnetic field energy accumulated in the already know, the electromagnetic field energy is always positive. Accounted for the nucleus of the total energy of 0.003 ~ 0.004, see table 12.25.

When we take $N_{\alpha g1}$ = 5, $N_{\alpha d1}$ = 34/13, and figure 7.1 and figure 7.2 2 ~ 5 layers of particles spiral ring of the same set of ring structure, simulation results $\overline{M}_{\pi d1}$ values being beyond 8%! Far outweigh the electromagnetic field energy, clearly obvious. So, further simulation and comparison, see table 12.26, the appropriate value is: $N_{\alpha d1} = N_{\alpha g1}$ = 17/6. It can properly increase the quality of the light nuclei, and may be appropriate to reduce nuclear power field force, make the internal nuclear force equilibrium.

The first layer of particles spiral ring different quantum fluctuations benchmark constant changes $\overline{M}_{\pi d1}$ simulation result table table 12.26

$N_{\alpha d1}$ $N_{\alpha g1}$	34/13 34/13	21/8 21/8	17/6 17/6	34/13 17/6	34/13 5
$\overline{M}_{\pi d1}\times$ 10^{-28}Kg	3.304461327	3.304486416	3.304966183	3.351764984	3.572742815
与原基准常数的比值	1	1.000007592	1.00015278	1.014315089	1.081187662

Table 9.1 similarly, refer to chapter 9 nucleus of internal related parameters calculation method of the added calculation, and calculate the result of light conditions within the nucleus $N_{\alpha di}$、$N_{\alpha gi}$、$\overline{M}_{di}$、$\overline{M}_{gi}$ parameters shown in table 12.27.

Light conditions within the nucleus $N_{\alpha di}$、$N_{\alpha gi}$、$\overline{M}_{di}$、$\overline{M}_{gi}$ parameters complement the results table table 12.27

Particless pirallinklayer		1	2	3
波动量子数 Quantumfluctuationsnumber	$N_{\alpha di}$	17/6	16	34
	$N_{\alpha gi}$	17/6	50	114
$R_{\theta di(0)}/R_{\theta gi(0)}$		2	0.9882663482	0.9984184964
$\overline{M}_{di}\times10^{-28}Kg$		3.304966183	3.349020548	3.325851224
$\overline{M}_{gi}\times10^{-28}Kg$		6.609932366	6.551193213	6.582085645
K_{mui}		2	1.956151991	1.979067974
$U^{-}_{\pi di}\times10^{-26}$ J/T		3.177738798	2.605275456	2.578319713
$U^{+}_{\pi gi}\times10^{-26}$ J/T		1.588869399	1.302637728	1.289159857
Neutronsurplusenergy$\times10^{-30}Kg$		0.0	14.6847884	6.9616804
$\pi^{\pm}$ Violation of transition energy $\Delta\overline{M}^{\pm}_{di}\times10^{-30}Kg$ $\Delta\overline{M}^{\pm}_{gi}\times10^{-30}Kg$			8.810873 11.7478306	4.6338648 6.1784864

Obtained by the same token, by (9.12), light nucleus layers particles spiral ring number of nuclear density respectively: 6, 12, 18 and 24.

12.4.2. Light nuclei internal parameters of the nuclear power field Energy supplement

Similarly, refer to section 9.2 and chapter 10 conditions within the nucleus electric energy parameters and the analysis of the electromagnetic force calculation method,

added calculation for light conditions within the nucleus electric energy, the parameters of the electromagnetic force results see table 12.28 ~ 12.28.

Type A high light within the nucleus, low-energy particles spiral ring net with to $\pi^{\pm}$ mesons in potential can supplement parameter calculation table (unit: V) 12.28

$N_{\alpha di} N_{\alpha gi}$ / $\overline{M}_{dgi} \times 10^{-28} Kg$		0	1	2	3	4
34	3.325851224	m.234974.3191		n.222418.0372		
114	6.582085645	k.252585.8481		l.236896.8441		
16	3.349020548		h.338009.4186		j.279845.3358	
50	6.551193213		g.367054.7807		i.293535.6784	
17/6	3.304966183	b.923649.0682		d.604437.8209		f.375758.6618
17/6	6.609932366	a.1847298.136		c.751517.3235		e.406970.8136

Type B high light within the nucleus, low-energy particles spiral ring net with to $\pi^{\pm}$ mesons in potential can supplement parameter calculation table (unit: V) 12.29

$N_{\alpha di} N_{\alpha gi}$ / $\overline{M}_{dgi} \times 10^{-28} Kg$		0	1	2	3	4
34	3.325851224		j.231636.5691			
114	6.582085645		i.248373.0973			
16	3.349020548	f.348163.0047		h.312191.3818		
50	6.551193213	e.380714.9489		g.333494.552		
17/6	3.304966183		b.793951.3881		c.467932.561	
17/6	6.609932366		a.1208875.642		d.530611.8724	

Type A high light within the nucleus, low-energy particles spiral ring net with to $\pi^{\pm}$ mesons in electric field force parameters added calculation (unit: N) table 12.30

$N_{\alpha di} N_{\alpha gi}$ / $\overline{M}_{dgi} \times 10^{-28} Kg$		0	1	2	3	4
34	3.325851224	m		n.1.749847022		
114	6.582085645	k		l.2.156969519		
16	3.349020548		h.2.958737819		j.5.022909216	
50	6.551193213		g 3.940643992		i.6.044190487	
17/6	3.304966183	b		d.24.75830452		f.11.41675181
17/6	6.609932366	a		c.45.667007 26		e.14.39055243

Type B high light within the nucleus, low-energy particles spiral ring net with to $\pi^{\pm}$ mesons in electric field force parameters added calculation (unit: N) table 12.31

$N_{\alpha di}\ N_{\alpha gi}$ / $\overline{M}_{dsi}\times10^{-28}Kg$		0	1	2	3	4
34	3.325851224		j.0.988472504			
114	6.582085645		i.1.242963523			
16	3.349020548	f		h.4.655661251		
50	6.551193213	e		g.5.910106907		
17/6	3.304966183		b.30.20475342		c.16.72091553	
17/6	6.609932366		a.45.66700726		d.23.95612641	

12.4.3. Light nuclei internal ring particles spiral magnetic force parameters calculation

Light conditions within the nucleus low-energy particles spiral ring current magnetic field force parameters complement the results table table 12.32

$N_{\alpha di}$ 参数（公式）	17/6	16	34
$M_{di}\times10^{-28}Kg$	3.304966183	3.349020548	3.325851224
β_i (4.9)	0.998962861 2	0.998751741	0.998729917 8
α_1° (10.5-5)	126.4476824	104.4775122	99.87496 14
$K_{ri}\times10^{-5}$（2.10）	13.7902	6.36539	4.40105
$F_{kbi}(N)$ (10.11)	17.51945005	26.22296182	19.10963214
$K_{fbi}(N)$ (10.17)	6.796082125	0.52002800 83	0.16556111 59

Similarly, refer to section 9.2 and chapter 10 section 10.2 conditions within the nucleus particles spiral ring the analysis of the magnetic field strength calculation method, added calculation for light nuclei within the parameters of the magnetic field strength results shown in table 12.30.

12.5 $^{56}_{26}$Fe, $^{40}_{20}$Ca, $^{16}_{8}$O nuclei and stable isotope internal Structure and parameters calculation

12.5.1 $^{56}_{26}$Fe nucleus and stable isotope internal structure and Parameters calculation

$^{56}_{26}$Fe nucleus kernel added calculation result is proved force balance table (figure 12.21 units: Newton) of 12.33

j / N_a	1	2	3	nuclearElectricandmagneticfieldforceaccumulated（originalNuclearforceparameters）	
16 $F_{e\theta}$	h.484.1914583				
$F_{b\theta}$	-944.0266255				
$F_{e\theta}$		d.1237.991278		↑	657.148829
17/6 $F_{b\theta}$		−105.1167003		|	（635.7299415）
$\Delta F_{\theta b}$		−475.7257488			

By in front of the results of table 12.15, we first to type A nucleus model to add "assembly" $^{56}_{26}$Fe nucleus, see figure 12.21, $^{56}_{26}$Fe nuclear force balance verification calculation shown in table 12.33.

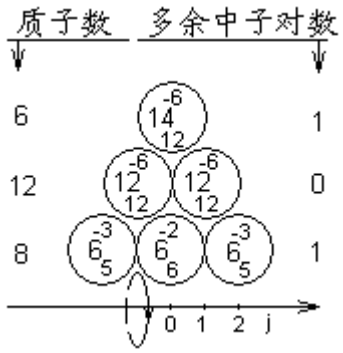

图12.21 $^{56}_{24}Fe$原子核内核子、净剩π±介子分配补充示意图

$$\overset{6}{Va}_{6}\quad \overset{6}{Vb}_{-2}\quad \overset{4}{Vc}_{10}\quad \overset{14}{Vd}_{-6}\quad Ve\quad Vf$$

$$\overset{8}{Vg}_{24}\quad \overset{32}{Vh}_{-12}\quad Vi\quad Vj\quad \overset{20}{Vk}_{12}\quad Vl$$

$$\overset{32}{Vm}_{-6}\quad Vn$$

$$W_e = 2.859518388\times10^{-28}\,Kg$$

$$W_b = 1.560541023\times10^{-29}\,Kg$$

$$\sum {}^{56}_{26}FeW_1 = 9.284757205\times10^{-26}\,Kg$$

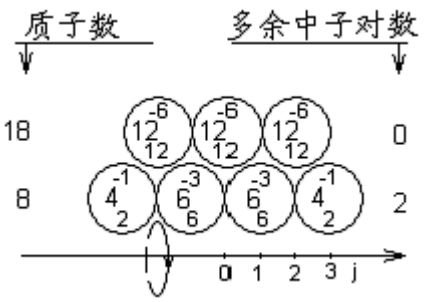

图12.22 $^{56}_{26}Fe$原子核内核子、净剩π±介子补充分配示意图

$$\overset{12}{Va}_{12}\quad \overset{12}{Vb}_{-6}\quad \overset{6}{Vc}_{4}\quad \overset{10}{Vd}_{-2}\quad \overset{8}{Ve}_{12}\quad \overset{20}{Vf}_{-6}$$

$$\overset{14}{Vg}_{24}\quad \overset{38}{Vh}_{-12}$$

$$W_e = 3.019635581\times10^{-28}\,Kg$$

$$W_b = 1.192644484\times10^{-29}\,Kg$$

$$\sum {}^{56}_{26}FeW_3 = 9.285294313\times10^{-26}\,Kg$$

To $\overline{m}_{g2}^{\pm} \rightarrow \overline{m}_{g1}^{\pm}$, accidents are ∑△m = 11.7478306 x 10^{-30} kg. After adjusting $^{56}_{26}$Fe nucleus total energy for -$\sum {}^{56}_{26}$FeW₂ = 9.285931988 x 10^{-26} kg, with experimental value

ratio of 1.0000054, is also very consistent. Shown by table 12.33, however, nuclear power magnetic field force of value is slightly larger than the original.

$^{56}_{26}$Fe nucleus kernel added calculation result is proved force balance table (figure 12.22 units: Newton) of 12.34

j / N_a	1	2	3	4	5	nuclear Electric and magnetic field force accumulated	
16 $F_{e\theta}$		h.950.0663948				↑	306.6174184
$F_{b\theta}$		-944.0266255				|	（244.0687062）
$F_{e\theta}$	b.828.4839 19		d.232.8097828			|	300.5776491
17/6 $F_{b\theta}$	-157.6750505		-52.55835015			|	（238.0307813）
$\Delta F_{\theta b}$	-366.9884348		-183.4942174				

When we use type B nuclei model to add "assembly" $^{56}_{26}$Fe nucleus, see figure 12.22 and table 12.34.

To make $\overline{m}^{\pm}_{d1} \rightarrow \overline{m}^{\pm}_{d2}$, the π±source energy increment △m = 8.810873 x 10^{-30} kg, for type B nucleus $^{56}_{26}$Fe after the adjustment the total energy $\sum^{56}_{26}$FeW4 = 9.2861754 x 10^{-26} kg.

Of course, we also can consider to increase the layer 3 particles spiral rings, and the first layer of particles spiral ring number of protons to 10. Interested readers can do it yourself "assembly", simulated calculation exercises.

If maintain figure 12.22, $^{56}_{26}$ Fe within the nucleus of the net with π± muon distribution state, the nuclear net with π±muon electric and magnetic field total energy and nuclear force equilibrium constant, as shown in the table 12.34. $^{58}_{26}$Fe nucleus, shillings a neutron into the first layer particles spiral ring, then make: $\overline{m}^{\pm}_{g2} \rightarrow \overline{m}^{\pm}_{g1}$, then $\sum^{58}_{26}$FeW1=9.617846802 x 10^{-26} kg.

Similarly, $^{54}_{26}$Fe nucleus, as long as in the figure 12.22 1 layer particles spiral ring in the edge of the two neutron, then $\sum {}^{54}_{26}$FeW$_1$ = 8.954797695 x 10^{-26} kg. These parameters and the experimental results are very close.

12.5.2 $^{40}_{20}$Ca nucleus supplement internal structure and parameter calculation

We first use type A nucleus model to add "assembly" $^{40}_{20}Ca$ nucleus. Because of the equal number of protons, neutrons, we have no choice, only in 12.23 "assembly" $^{40}_{20}Ca$ nucleus, and order: $\overline{m}^{\pm}_{d1} \rightarrow \overline{m}^{\pm}_{d2}$, to: $\sum {}^{40}_{20}Ca$ W$_2$=6.63420698 x 10^{-26} kg.

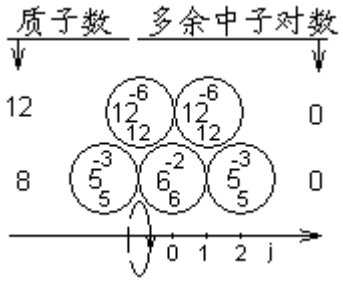

图12.23 $^{40}_{20}Ca$原子核内核子、净剩π±介子分配补充示意图

$$Va_{6} \quad Vb^{6}_{-2} \quad Vc^{4}_{10} \quad Vd^{14}_{-6} \quad Ve \quad Vf$$

$$Vg^{8}_{24} \quad Vh^{32}_{-12}$$

$$W_e = 2.183510355\times10^{-28}\,Kg$$

$$W_b = 1.5584234\times10^{-29}\,Kg$$

$$\sum {}^{40}_{20}CaW_1 = 6.633325893\times10^{-26}\,Kg$$

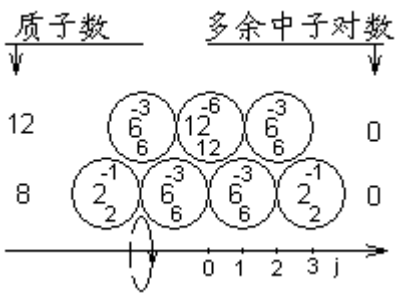

图12.24 $^{40}_{20}Ca$原子核内核子、净剩π±介子分配补充示意图

$$Va_{12} \quad Vb^{12}_{-6} \quad Vc^{6}_{4} \quad Vd^{10}_{-2} \quad Ve^{8}_{12} \quad Vf^{20}_{-6}$$

$$Vg^{14}_{12} \quad Vh^{26}_{-6} \quad Vi \quad Vj$$

$$W_e = 2.105792269\times10^{-28}\,Kg$$

$$W_b = 1.163840951\times10^{-29}\,Kg$$

$$\sum {}^{40}_{20}CaW_2 = 6.63215413\times10^{-26}\,Kg$$

Although agreement with experimental data, and figure 12.21 and table 12.33

type A $^{56}_{26}$Fe nucleus, 1, 2 layer particles spiral ring nuclear force parameters in exactly the same, so the nucleus is still unstable or does not exist.

When we use type B nuclei model added "assembly" $^{40}_{20}Ca$ nucleus, see figure 12.24 and table 12.35.

$^{40}_{20}Ca$ Added calculation result is proved nucleus kernel force balance table (figure 12.24 units: Newton) of 12.35

j / N_a	1	2	3	4	5	nuclearElectricandmagnetic fieldforceaccumulated	
16 $F_{e\theta}$		j.3879722025				↑	216.5365388
$F_{b\theta}$		−472.0133128				|	（154.0153451）
$F_{e\theta}$	b.828.4839 19		d.232.8097828			|	300.5776491
17/6 $F_{b\theta}$	-157.6750505		-52.55835015			|	（238.0307813）
$\Delta F_{\theta b}$	-366.9884348		-183.4942174			|	

To $\overline{m}^{\pm}_{d1} \rightarrow \overline{m}^{\pm}_{d2}$ $\overline{m}^{\pm}_{g2} \rightarrow \overline{m}^{\pm}_{g1}$, to: $\sum {}^{40}_{20}Ca W_3$=6.63421×10^{-26}Kg.

12.5.3 $^{16}_{8}$O nuclei supplement internal structure and parameter calculation

We first to type A nucleus model "assembly" $^{16}_{8}$O nuclei, see figure 12.25 and table 12.36.

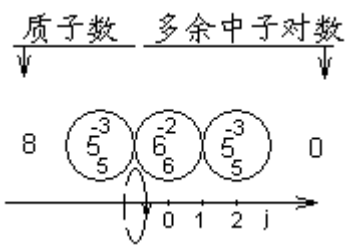

图12.25 $^{16}_{8}O$原子核内核子、净剩

π±介子分配补充示意图

$$\underset{6}{Va} \quad \underset{-2}{Vb} \quad \underset{10}{Vc} \quad \underset{-6}{Vd}$$

$$W_e = 9.226801614 \times 10^{-29} Kg$$
$$W_b = 1.532931683 \times 10^{-29} Kg$$
$$\sum {}^{16}_{8}OW_1 = 2.65473268 \times 10^{-26} Kg$$

$^{16}_{8}$O nuclei kernel added calculation result is proved force balance table (figure

12.25 units: Newton) of 12.36

j / N_θ	1	2	3	4	5	nuclearElectricandmagneticfield forceaccumulated	
$F_{e\theta}$		d.1237.991278				↑	657.1488285
$17/6\,F_{b\theta}$		−105.1167003				|	（635.7299417）
$\Delta F_{\theta b}$		−475.7257488				|	

Can be seen from the above results is that $^{16}_{8}O$ conditions within the nucleus net with $\pi^{\pm}$violation can such distribution, and nuclear power, magnetic field is a maximum total energy, nuclear energy, but still less than the value, the nuclear force is also unable to balance. So, A type $^{16}_{8}O$ nuclear model also cannot exist.

Similarly, "assembly" type B $^{16}_{8}O$ nucleus figure 12.26, the nuclear force balance verification calculation shown in table 12.37.

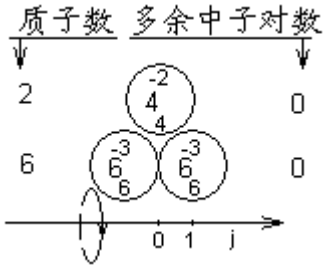

图12.26 $^{16}_{8}O$原子核内核子、净剩

$$Va_{12}\quad Vb^{12}_{-6}\quad Vc\quad Vd\quad Ve^{6}_{4}\quad Vf^{10}_{-2}$$

$$W_e = 8.927862779\times10^{-29}\,Kg$$
$$W_b = 1.250605562\times10^{-29}\,Kg$$
$$\sum {}^{16}_{8}OW_1 = 2.654151415\times10^{-26}\,Kg$$

π±介子分配补充示意图

Tomake $\overline{m}^{\pm}_{g2} \rightarrow \overline{m}^{\pm}_{g1}$, to: $\sum {}^{16}_{8}OW_2$=2.655326198×10-26Kg

Front has stressed that the parameters of the simulation in nucleus, energy conservation and nuclear force balance is two important principles. From the 12.4 and 12.5 of this chapter two within the nucleus of the related parameters of simulation results is to see that by the law of conservation of energy only allowed particles spiral loop quantum fluctuations of the first layer of $N_{\alpha g1} = N_{\alpha d1} = 17/6$, but nuclear force balance

simulation results of the system increases, so, the original of the parameters of the conditions within the nucleus is the best choice.

$^{16}_{8}O$ nuclei kernel added calculation result is proved force balance table (figure 12.26 units: Newton) of 12.37

j / N_a	1	2	3	4	5	nuclearElectricandmagnetic field forceaccumulated	
$F_{e\theta}$		b.828.4839 19				↑	120.3262164
$17/6F_{b\theta}$		−157.6750505				|	（43.62250648）
$\Delta F_{\theta b}$		−550.4826521				|	

13 γ Rays in nucleus forming principle and Parameter calculation

13.1 Conditions within the nucleus formation Principle of γ rays

13.1.1 $\beta^{\pm}$ Electronics and photon, neutrino associated principle

Conditions within the nucleus only have high and low $\pi^{\pm}$ violation of spiral ring particles. When a $\pi^{\pm}$ split muon decay, internal 2 of charged particles and a charged particle collection divided, can be generated by a pair of charged particles and a charged particles composed of electrons, left a pair of charged particles formed neutrinos or photons. With nuclear power by the number of the same isotopes, less number of neutrons, main show is β^{+} positron emission. Along with the increased number of neutrons, transition to stable isotopes. If the neutron number to continues increase, the performance of β^{-} electron emission.

Both β^{+} or β^{-} electron emission, the total number of nuclear are the parent nucleus remain unchanged. When launching a β^{+} electronic, number of nuclear power by reducing 1, within a proton nuclear will be transformed into neutrons. By figure 7.4, protons, neutrons "decentralized" $\pi^{\pm}$ source distribution graph to: particles spiral rings a high-energy π_g^{+} source must be continuously absorbs neutrinos in game 4 of neutrinos, then split decay into a pair of low-energy $\pi_d^{\pm}$ mesons, an electronic β^{+}; A low-energy $\pi_d^{\pm}$ muon to low-energy particles spiral ring rail, β^{+} positron emission form β^{+} rays, complete the protons and neutrons transformation process. Similarly, if the diffusion β^{-} launch, the mother will have a neutron nuclear into protons. At this time, as long as A low-energy π_d^{-} violation will be their most primitive wave motion direction of electromagnetic field energy transfer to another low π_d^{+} after mesons, its direct split

into a $\beta^{\cdot}$ electronics and A photon or neutrinos emission; Another low π_{d}^{+} muon after absorbing energy is emitted into the high-energy π_{g}^{+} muon orbit, complete the neutrons and protons.

13.1.2 γ Rays forming principle

Conditions within the nucleus does not exist, electrons and photons neutrinos, but is a nucleus in the ubiquity of neutrino field, the neutrino through at any moment. When conditions within the nucleus by net with $\pi^{\pm}$ muon electric and magnetic field, the formation of nuclear force and energy distribution is uniform, do not need to adjust, stable, even more neutrino through nucleus, also won't produce.

When nucleus kernel force balance, not nuclear power, nuclear power by uneven distribution, to adjust itself to nuclear power, nuclear force distribution, make whole nuclei tend to be stable, the particles spiral ring net with to $\pi^{\pm}$ mesons in the state of the distribution adjustment is inevitable. Net with $\pi^{\pm}$ mesons in each particle spiral loop adjustment, redistribution will cause the change of electric and magnetic energy in nuclear. When it is reduces the surplus electricity, magnetic energy through stimulating through nucleus formation of neutrino photons. Such already can transfer surplus energy, and can produce γ rays. Neutron or in pairs, of course, $\pi^{\pm}$ violation in the particles spiral ring layer between the adjustment, redistribution, residual energy can also produce γ rays.

13.1.3 γ Ray spectrum energy form model

From chapter 11, 12 nucleus structure calculation and analysis in the know, nature can stability of nuclide atom, the number of nuclear power by $Z_i \leq 83$. All the nucleus of $Z_i \geq 6$, nuclear power charge can be evenly distributed, the nuclear force balance without splitting the moment of the nucleus is type B nucleus. When the first

layer is 6 to particles spiral ring side by side, 4 ring particles spiral layer composed of nearly spherical nuclei, saturated when the total number of nuclear is 234, and the department of radiation starting nuclear quite; When after the first layer of 4, 3 layers particles spiral loop composed of the nearly spherical nuclei saturated when the total number of nuclear is 96. So, the nuclear of $234 \geq A \geq 96$ all the nucleus, may think they have A combination of particles spiral ring structure shown in figure 13.1. The difference is that with the increase of the nuclear number, nuclear power by number, nucleus layers and the lateral particle spiral rings filling nuclear number increase, gradually saturated, nuclear power load distribution of the edge of the diffusion layer gradually thinning.

If a pair of particles spiral rings, high low $\pi^{\pm}$ muon same direction of the wave motion, see figure 7.2; High and low $\pi^{\pm}$ violation can only in the direction of the adjacent particles spiral wave motion transition in the ring. By the relationship of the space, the same layer, low-energy particle spiral rings π_g^+, π_d^- or π_g^-, π_d^+ combination of lateral migration. Due to the symmetry, the first floor there are 12 seating arrangement, 2, 3, 4 layer respectively in 12, 6, 6 seating arrangement, a total of 36 seating arrangement. By figure 13.1 shows, between the upper and the lower migration, 1 ~ 2 layer particles spiral ring in five transitions. 2 ~ 3, 3 ~ 4 layer between respectively have four, three, a total of 12 channel. If each channel is π_g^+, π_d^- or π_g^-, π_d^+ combination of transition, it also have 36 seating arrangement.

To the nucleus internal excess $\pi^{\pm}$ violation of saturated layer, unable to increase; Adjust some of the seating arrangement will make mother nuclear total energy increases, it can only be achieved under the external energy to participate in; Most minor adjustment in the edge of the nucleus, will make the nuclear energy is reduced, to get through the formation of neutrino γ rays. Due to the different positions within the

nucleus of the excess $\pi^{\pm}$ muon distribution, lateral migration, the lower level migration, transition to another position, the electric and magnetic energy change value is not the same. The table 9.1 shows that transition between adjacent layers will lead to high, low $\pi^{\pm}$ muon original the slight variations of wave energy. So, different size of nuclei formation energy spectrum of the γ rays, combination and different features, these can only through the calculation of concrete examples to illustrate.

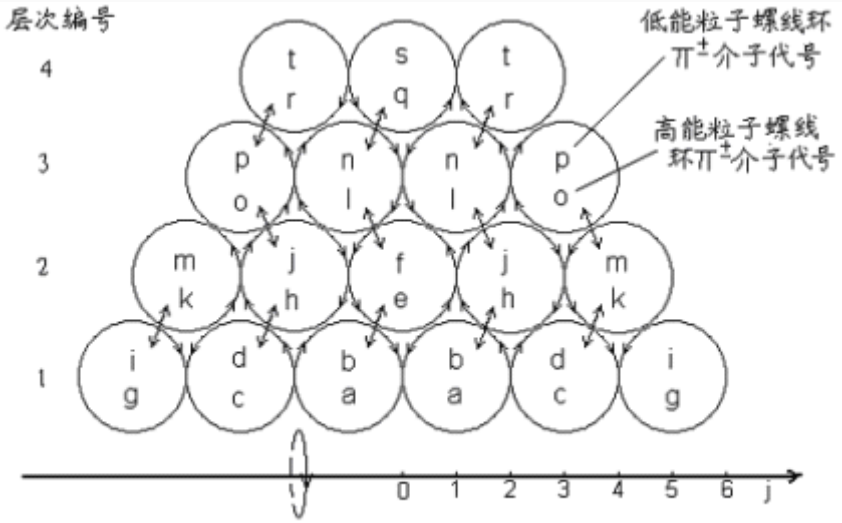

图13.1 原子核内净剩 $\pi^{\pm}$ 介子跃迁通道示意图

13.2 γ Ray energy parameters calculation model

13.2.1 $^{194}_{79}$Au, $^{194}_{78}$Pt nucleus internal structure and parameter Calculation

$^{194}_{79}$Au nuclide atomic energy is 193.965406 u, 39.5 hours half-life, and magnetic $\pm 0.074U_p$. Launch β^+ rays, electron kinetic energy is 1.487, 1.230, 0.950 Mev three groups. Decay into $^{194}_{78}$Pt nucleus in the process of the communist party of China launch 49 level of γ rays, energy distribution range of 0.20291 ~ 2.1142 Mev ④, eventually become a stable $^{194}_{78}$Pt nucleus. So, we could start from decay and the

internal structure of two nuclei model, calculation and analysis to γ rays forming principle and energy.

For $^{194}_{79}$Au nucleus, refer to section 12.1 for the magnetic moment of a nucleus simulation method. Make protons, neutrons according to figure 7.4 a, c, or b, d scheme "decentralized", from table 9.1, 7.4 (1) type, $^{194}_{79}$Au nucleus combined magnetic and can be expressed as:

$$\sum U = U^{+}_{g1} + U^{-}_{g1} + U^{+}_{g4} + 2U^{-}_{d1} + U^{+}_{d2} + U^{+}_{d3} = -0.07325U_p \quad (13.1)$$

Take a and d state combination, by (7.4-2) type:

$$\sum U = 2U^{+}_{g1} + U^{+}_{g4} + U^{+}_{d1} + U^{-}_{d2} + U^{-}_{d3} + U^{-}_{d4} = 0.07325U_p \quad (13.2)$$

If according to (13.2) type magnetic combination of calculation model, haveπ± both original energy increment: $\Delta\overline{m}$ =6.081173925×10 $^{-30}$Kg.

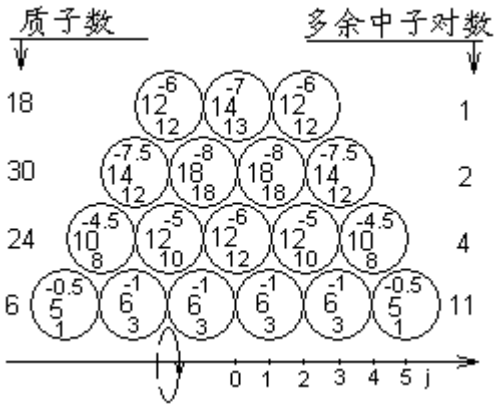

图13.2 $^{194}_{79}Au$原子核内核子、净剩π± 介子分配示意图

$$Va_{6}\ \ Vb^{6}_{-2}\ \ Vc^{4}_{6}\ \ Vd^{10}_{-2}\ \ Ve^{8}_{12}\ \ Vf^{20}_{-6}$$
$$Vg^{14}_{2}\ \ Vh^{16}_{20}\ \ Vi^{36}_{-1}\ \ Vj^{35}_{-10}\ \ Vk^{25}_{16}\ \ Vl^{41}_{36}$$
$$Vm^{77}_{-9}\ \ Vn^{68}_{-16}\ \ Vo^{52}_{24}\ \ Vp^{76}_{-15}\ \ Vq^{61}_{13}\ \ Vr^{74}_{24}$$
$$Vs^{98}_{-7}\ \ Vt^{91}_{-12}$$

$$W_e = 1.401321064\times10^{-27}\,Kg$$
$$W_b = 7.827518402\times10^{-30}\,Kg$$
$$\sum {}^{194}_{79}AuW_1 = 3.220247476\times10^{-25}\,Kg$$

Refer to section 11.2 of the nucleus structure model, design and energy balance calculation procedures, the nuclear force numerical comparison results. The design of the $^{194}_{79}$Au, $^{194}_{78}$Pt nucleus internal structure is shown in figure 13.2 and figure 13.3; nuclear force balance test results see table 13.1 and table 13.2. $^{194}_{79}$Au, $^{194}_{78}$Pt of the

experimental value of nuclear energy, respectively:

$$\sum {}^{194}_{79}AuW_0 = 3.220244434\times10^{-25}Kg$$

$$\sum {}^{194}_{78}PtW_0 = 3.220208825\times10^{-25}Kg$$

$^{194}_{79}$Au nucleus nuclear force balance to verify the results table (figure 13.2, the unit: Newton) table 13.1

j / N_a	1	2	3	4	5	nuclearElectricand magneticfieldforce accumulated
58 $F_{e\theta}$ $F_{b\theta}$		t.597.2865265 -623.6670342				-538.2026478
34 $F_{e\theta}$ $F_{b\theta}$	n.845.3021482 -1222.642839		p.891.0114236 -1146.227662			-511.8221401
16 $F_{e\theta}$ $F_{b\theta}$		j.838.0225225 -786.4485285		m.106.3890735 -598.8363964		-256.6059021
$F_{e\theta}$ 34/13$F_{b\theta}$ $\Delta F_{\theta b}$	b.256.935313 -14.26555772		d.360.3313781 -14.26555772 -134.0624443		i.–2.039445479 -7.132778786 -57.45533327	388.0455737

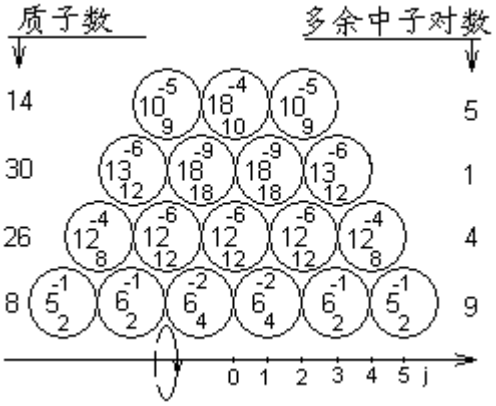

图13.3 $^{194}_{78}Pt$原子核内核子、净剩π±介子分配示意图

$$Va_{8}\quad Vb^{8}_{-4}\quad Vc^{4}_{4}\quad Vd^{8}_{-2}\quad Ve^{6}_{12}\quad Vf^{18}_{-6}$$

$$Vg^{12}_{4}\quad Vh^{16}_{24}\quad Vi^{40}_{-2}\quad Vj^{38}_{-12}\quad Vk^{26}_{16}\quad Vl^{42}_{36}$$

$$Vm^{78}_{-8}\quad Vn^{70}_{-18}\quad Vo^{52}_{24}\quad Vp^{76}_{-12}\quad Vq^{64}_{10}\quad Vr^{74}_{18}$$

$$Vs^{92}_{-4}\quad Vt^{88}_{-10}$$

$$W_e = 1.392890861\times10^{-27}Kg$$

$$W_b = 9.474618808\times10^{-30}Kg$$

$$\sum {}^{194}_{79}PtW_1 = 3.220213937\times10^{-25}Kg$$

To mother nuclear $^{194}_{79}$Au, $^{194}_{78}$Pt internal structure comparison, can see mother son become nuclear fission failure when net with high and low π± muon and extra neutron to adjust the migration trend. By the law of conservation of energy, we can

calculate $^{194}_{79}Au$ every position in nucleus, each net with high and low π± violation or to each pair of π± violation adjustment migration when launching the γ ray energy. It must be pointed out that this is just our ideal model. By this model, we can see by the numerous nuclides $^{194}_{79}Au \rightarrow {}^{194}_{78}Pt$, γ rays in the process of energy spectrum, the trend of the chance.

$^{194}_{78}Pt$ nucleus nuclear force balance test results see (figure 13.3, unit: N) table 13.2

j / N_a	1	2	3	4	5	nuclear Electric and magnetic field force accumulated
58 $F_{e\theta}$		t. 394.0283291				-145.88339332
$F_{b\theta}$		-296.98430 2				
34 $F_{e\theta}$	n. 799.4848898		p. 1095.757365			-242.92742 03
$F_{b\theta}$	-1547.407343		-1031.604895			
16 $F_{e\theta}$		j. 1091.575393		m. 76.90747548		-307.07988 98
$F_{b\theta}$		-943.738234 2		-629.1588228		
$F_{e\theta}$	b. 352.2356112		d. 173.5481658		i. –52.80497456	97.33429869
34/13 $F_{b\theta}$	-57.06223088		-28.53111544		-14.26555772	
$\Delta F_{\theta b}$	-137.8927999		-68.94639993		-68.94639993	

13.2.2 γ ray spectrum simulation principle

The data in the table 9.1 shows that the net with high and low $\pi^{\pm}$ mesons in different particles spiral ring transition between layer, due to the high and low $\pi^{\pm}$ muon original wave motion direction of the original energy $\overline{m}_{\mathrm{gi}}$, $\overline{m}_{di}$, a slight differences, so the total energy a little influence. Behind us in order to convenient calculation, first the energy difference between the value of $\Delta\overline{m}_{gi}$, $\Delta\overline{m}_{di}$, direct conversion into Mev, shown in table 13.3.

Each layer particles spiral rings are made by the original PI to wave energy is the same as π± violation, in addition to the net with π± violation of migration, antiparticle π±

both migration is also exist. Position as shown in figure 13.1, p a low-energy π_d^- both migrated to m position, and can be expressed as $p\pi_d^- \rightarrow m\pi_d^-$. If antiparticle migration, the m position a low-energy π_d^+ muon migrated to p for nuclear power charge distribution adjustment effect is the same, only difference is calculated in table 13.3 nucleus total energy, $\Delta\overline{m}_{di}$ school when is take the positive or negative. It is in the law of conservation of energy, under the premise of judgment with net high and low $\pi^{\pm}$ muon migration channel can be formed an important basis for adjustment.

Different particles spiral ring between $\pi^{\pm}$muon original energy

Differences $\Delta\overline{m}_{gi}$, $\Delta\overline{m}_{di}$, table 13.3

$N_{\alpha d,g}$ / $\overline{m}_{di.gi}$	$\frac{34}{13}$、$\frac{34}{13}$	16 50	34 114	58 203	88 316
$\overline{m}_{di}$	3.304461327	3.348508963	3.325343178	3.316814573	3.312652281
$\overline{m}_{gi}$	6.608922653	6.550192473	6.581080185	6.592451659	6.598001381
$\times 10^{-28} Kg$					
$\Delta\overline{m}_{d(i\sim i+1)}$		4.4047636	2.3165785	0.8528605	0.4162292
$\times 10^{-30} Kg$					
MeV		2.470890	1.299505	0.478419	0.233487
$\Delta\overline{m}_{g(i\sim i+1)}$		5.873018	3.0887712	1.1371474	0.5549722
$\times 10^{-30} Kg$					
Mev		3.294520	1.732673	0.637893	0.311316

By know in chapter 11, 12, to split the decay naturally mother nucleus and the stability of the son, and there is a variety of meat with nuclear power. Laboratory detection to launch out 49 in the process of the decay of nuclear fission energy levels of γ rays is lucky and rock atomic number N_A constituting for coefficient of $^{194}_{79}Au$ nuclei with nuclear power, in the process of decay released all the comprehensive results of γ ray spectrum. Most of the energy level of the γ rays appear less risk of poor, but also do not eliminate the energy behind the data error range is composed of several level is

close to the results of the comprehensive reflection of γ rays. With existing experimental detection technology level, we can't separate detection to the whole process of the decay, with a particular internal structure, energy of $^{194}_{79}Au$ nuclei with nuclear power, completely failure become stable another has certain internal structure, the level of $^{194}_{78}Pt$ nuclei with nuclear power, in the whole process of all the γ ray energy spectrum and time sequence. In fact also doesn't exist the physical condition of the external environment. Because and thermodynamics of the statistical laws of gas molecules thermal motion completely, the entire field of neutrinos, one neutrino one at a time through the nucleus of a particular position, is completely random, unpredictable.

therefore, can think of: laboratory detected a γ ray energy levels and the risk of appear, is a large number of nuclei with nuclear power, $^{194}_{79}Au \rightarrow {}^{194}_{78}Pt$ during the whole process of split decay, a particular internal structure adjustment, specific energy of nuclide $^{194}_{79}Au$ atoms, one of the characteristics of the location of the high and low $\pi^{\pm}$ muon migration, adjust to another level of nuclide $^{194}_{79}Au$ atoms, or change to another $^{194}_{78}Pt$ atoms nuclide characteristics of a certain position, excess energy release in the form of γ rays. Nuclide in gram atom coefficient as the unit of atoms, this process can only be the two $^{194}_{79}Au$, $^{194}_{78}Pt$ atoms of two particular nuclides with nuclear power risk existing in the process of transformation, only statistical significance. We can't figure out, is the parent nucleus transformation before or after transformation launch γ rays.

So, we can use a kind of as shown in figure 13.2 $^{194}_{79}Au$ the parent nucleus with nuclear power, as the reference standard. When its internal structure, nuclear and clean with $\pi^{\pm}$ mesons in total energy conservation under the premise of to the son, as

shown in the figure 13.3 nuclear $^{194}_{78}Pt$ with nuclear power, adjust the transformation, each γ ray energy that is released in the adjustment process, as the reference value of the γ ray energy spectrum. Obviously, it is only a small part of the actual γ ray spectrum of possible.

13.2.3 γ ray energy spectrum of applications

According to the principle of γ rays in the above form, design of γ ray spectrum calculation procedure is as follows:

1. According to section 11.2 nucleus total energy calculation procedure, we repeated computation as shown in the figure 13.2 $^{194}_{79}Au$ nuclei with nuclear power of total energy $\sum^{194}_{79}AuW_1=3.220247476\times10^{-25}Kg$

2. According to the figure 13.1, high, low $\pi^{\pm}$ muon possible migration channel, make $f\pi^-\rightarrow b\pi^-$, into another with nuclear power, 2, and the power, and nuclear energy calculation parameters of Vb ~ Vf of coefficient table 13.4 line 4; Other coefficient remain unchanged. Similarly, nucleus total magnetic energy will also change. Repeating section 11.2 1 ~ 12 calculation program: power, total energy 2 $\sum^{194}_{79}AuW_2=3.220192308\times10^{-25}Kg$

3. Make two states with nuclear power, the energy difference as $\triangle W_e$:

$$\triangle W_e=\sum^{194}_{79}AuW_1-\sum^{194}_{79}AuW_2=3.094686Mev$$

For laboratory detects γ rays energy spectrum is the range of 0.20291_6 ~ 2.1142_2 Mev, (subscript for terminal error range). $\Delta\overline{m}_{gi}$、$\Delta\overline{m}_{di}$ Data from table 13.3, the total of the law of conservation of energy, is a particle transition, $f\pi^-\rightarrow b\pi^-$, the γ ray energy W_γ is:

$$W_\gamma=\sum {}^{194}_{79}AuW_1-\sum {}^{194}_{79}AuW_2+\Delta\overline{m}_{d(1\sim2)}=5.565576Mev;$$

Similarly, if the antiparticle transition, $b\pi^+\rightarrow f\pi^+$ to W_γ is:

$$W_\gamma=\sum {}^{194}_{79}AuW_1-\sum {}^{194}_{79}AuW_2-\Delta\overline{m}_{d(1\sim2)}=0.623796Mev;$$

The former far outweigh the laboratory value 2.1142 Mev, obviously does not exist, the latter is one of our expectations.

13.3 γ ray spectrum calculation example

To calculated according the above program, ${}^{194}_{79}Au\rightarrow {}^{194}_{78}Pt$ nucleus of γ ray spectrum simulation in table 13.4.

${}^{194}_{79}Au$ conditions within the nucleus on the lower π± muon warp gamma ray spectrum simulation table table 13.4

π±Muon transition position	Electric energy coefficient changes	∑Wi×10-25Kg ∑W0-∑W(Mev)	π±Muontransition way （Wγ=Mev）
$e\pi^+\rightarrow a\pi^+$	$\underset{7}{Va}\ \underset{-2}{\overset{7}{Vb}}\ \underset{6}{\overset{5}{Vc}}\ \underset{-2}{\overset{11}{Vd}}\ \underset{11}{\overset{9}{Ve}}$	3.220355938 -6.084245	
$e\pi^+\rightarrow a\pi^+$ $f\pi^-\rightarrow b\pi^-$	$\underset{7}{Va}\ \underset{-3}{\overset{7}{Vb}}\ \underset{6}{\overset{4}{Vc}}\ \underset{-2}{\overset{10}{Vd}}\ \underset{11}{\overset{8}{Ve}}\ \underset{-5}{\overset{19}{Vf}}$	3.220292476 -2.524305	
$f\pi^-\rightarrow b\pi^-$	$\underset{-3}{\overset{6}{Vb}}\ \underset{6}{\overset{3}{Vc}}\ \underset{-2}{\overset{9}{Vd}}\ \underset{12}{\overset{7}{Ve}}\ \underset{-5}{\overset{19}{Vf}}$	3.220192308 3.094736	$b\pi^+\rightarrow f\pi^+$ 0.623796
$h\pi^+\rightarrow a\pi^+$	$\underset{7}{Va}\ \underset{-2}{\overset{7}{Vb}}\ \underset{6}{\overset{5}{Vc}}\ \underset{-2}{\overset{11}{Vd}}\ \underset{12}{\overset{9}{Ve}}\ \underset{-6}{\overset{21}{Vf}}\ \underset{2}{\overset{15}{Vg}}\ \underset{19}{\overset{17}{Vh}}$	3.220371749 -6.971214	
$.j\pi^-\rightarrow b\pi^-$ $h\pi^+\rightarrow a\pi^+$	$\underset{7}{Va}\ \underset{-3}{\overset{7}{Vb}}\ \underset{6}{\overset{4}{Vc}}\ \underset{-2}{\overset{10}{Vd}}\ \underset{12}{\overset{8}{Ve}}\ \underset{-6}{\overset{20}{Vf}}\ \underset{2}{\overset{14}{Vg}}\ \underset{19}{\overset{16}{Vh}}\ \underset{-1}{\overset{35}{Vi}}\ \underset{-9}{\overset{34}{Vj}}$	3.220290444 -2.410299	
$.j\pi^-\rightarrow b\pi^-$	$\underset{-3}{\overset{6}{Vb}}\ \underset{6}{\overset{3}{Vc}}\ \underset{-2}{\overset{9}{Vd}}\ \underset{12}{\overset{7}{Ve}}\ \underset{-6}{\overset{19}{Vf}}\ \underset{2}{\overset{13}{Vg}}\ \underset{20}{\overset{15}{Vh}}\ \underset{-1}{\overset{35}{Vi}}\ \underset{-9}{\overset{34}{Vj}}$	3.220175306 4.048447	$b\pi^+\rightarrow j\pi^+$ 1.577557
$h\pi^+\rightarrow c\pi^+$	$\underset{7}{Vc}\ \underset{-2}{\overset{11}{Vd}}\ \underset{12}{\overset{9}{Ve}}\ \underset{-6}{\overset{21}{Vf}}\ \underset{2}{\overset{15}{Vg}}\ \underset{19}{\overset{17}{Vh}}$	3.220300167 -2.955736	$c\pi^-\rightarrow h\pi^-$ 0.338784
$.j\pi^-\rightarrow d\pi^-$ $h\pi^+\rightarrow c\pi^+$	$\underset{7}{Vc}\ \underset{-3}{\overset{11}{Vd}}\ \underset{12}{\overset{8}{Ve}}\ \underset{-6}{\overset{20}{Vf}}\ \underset{2}{\overset{14}{Vg}}\ \underset{19}{\overset{16}{Vh}}\ \underset{-1}{\overset{35}{Vi}}\ \underset{-9}{\overset{34}{Vj}}$	3.220253522 -0.339149	$c\pi^-\rightarrow h\pi^-$ $d\pi^+\rightarrow j\pi^+$ 0.484481

.jπ⁻→dπ⁻	10 7 19 13 15 35 34 *Vd Ve Vf Vg Vh Vi Vj* −3 12 −6 2 20 −1 −9	3.220203747 2.453013	
kπ⁺→cπ⁺	4 11 9 21 15 17 37 36 26 *Vc Vd Ve Vf Vg Vh Vi Vj Vk* 7 −2 12 −6 2 20 −1 −10 15	3.220339459 -5.159881	
kπ⁺→cπ⁺. mπ⁻→dπ⁻	4 11 8 20 14 16 36 35 25 *Vc Vd Ve Vf Vg Vh Vi Vj Vk* 7 −3 12 −6 2 20 −1 −10 15 40 76 *Vl Vm* 36 −8	3.220260705 -0.7420794	dπ⁺→mπ⁺. cπ⁻→kπ⁻ 0.081551
mπ⁻→dπ⁻	10 7 19 13 15 35 34 24 40 76 *Vd Ve Vf Vg Vh Vi Vj Vk Vl Vm* −3 12 −6 2 20 −1 −10 16 36 −8	3.22017302 4.176686	dπ⁺→mπ⁺. 1.705796
kπ⁺→gπ⁺	14 17 37 36 26 *Vg Vh Vi Vj Vk* 3 20 −1 −10 15	3.220297748 -2.820064	gπ⁻→kπ⁻ 0.474456
kπ⁺→gπ⁺ mπ⁻→iπ⁻	14 17 37 35 25 40 76 *Vg Vh Vi Vj Vk Vl Vm* 3 20 −2 −10 15 36 −8	3.220259066 -0.650160	iπ⁺→mπ⁺. gπ⁻→kπ⁻ 0.173470
mπ⁻→iπ⁻	36 34 24 40 76 *Vi Vj Vk Vl Vm* −2 −10 16 36 −8	3.22021208 2.090572	
lπ⁺→eπ⁺	8 21 15 17 37 36 26 42 *Ve Vf Vg Vh Vi Vj Vk Vl* 13 −6 2 20 −1 −10 16 35	3.220308713 -3.435152	
lπ⁺→eπ⁺ nπ⁻→fπ⁻	8 21 14 16 36 35 25 41 76 67 *Ve Vf Vg Vh Vi Vj Vk Vl Vm Vn* 13 −7 2 20 −1 −10 16 35 −9 −15	3.220239193 0.464617	fπ⁺→nπ⁺ eπ⁻→lπ⁻ 0.031449 lπ⁺→eπ⁺ nπ⁻→fπ⁻ 0.897785
nπ⁻→fπ⁻	20 13 15 35 34 24 40 76 67 *Vf Vg Vh Vi Vj Vk Vl Vm Vn* −7 2 20 −1 −10 16 36 −9 −15	3.220179757 3.798768	nπ⁻→fπ⁻ 2.499263
lπ⁺→hπ⁺	16 37 36 26 42 *Vh Vi Vj Vk Vl* 21 −1 −10 16 35	3.220292902 -2.548183	
lπ⁺→hπ⁺ nπ⁻→jπ⁻	16 37 36 25 41 76 67 *Vh Vi Vj Vk Vl Vm Vn* 21 −1 −11 16 35 −9 −15	3.220241025 0.361859	lπ⁺→hπ⁺ nπ⁻→jπ⁻ 0.795027
nπ⁻→jπ⁻	35 24 40 76 67 *Vj Vk Vl Vm Vn* −11 16 36 −9 −15	3.220196759 2.845007	nπ⁻→jπ⁻ 1.545502
oπ⁺→hπ⁺	16 37 36 26 42 78 69 53 *Vh Vi Vj Vk Vl Vm Vn Vo* 21 −1 −10 16 36 −9 −16 23	3.220323499 -4.264582	
oπ⁺→hπ⁺ pπ⁻→jπ⁻	16 37 36 25 41 77 68 52 75 *Vh Vi Vj Vk Vl Vm Vn Vo Vp* 21 −1 −11 16 36 −9 −16 23 −14	3.220245594 0.105570	oπ⁺→hπ⁺ pπ⁻→jπ⁻ 0.538738
pπ⁻→jπ⁻	35 24 40 76 67 51 75 *Vj Vk Vl Vm Vn Vo Vp* −11 16 36 −9 −16 24 −14	3.220171221 4.277613	

$o\pi^+ \rightarrow k\pi^+$	$\underset{17}{25}Vk\ \underset{36}{42}Vl\ \underset{-9}{78}Vm\ \underset{-16}{69}Vn\ \underset{23}{53}Vo$	3.220284207 -2.060437	
$o\pi^+ \rightarrow k\pi^+$ $p\pi^- \rightarrow m\pi^-$	$\underset{17}{25}Vk\ \underset{36}{42}Vl\ \underset{-10}{78}Vm\ \underset{-16}{68}Vn\ \underset{23}{52}Vo\ \underset{-14}{75}Vp$	3.220238175 0.521720	$m\pi^+ \rightarrow p\pi^+$ $k\pi^- \rightarrow o\pi^-$ 0.088522 $o\pi^+ \rightarrow k\pi^+$ $p\pi^- \rightarrow m\pi^-$ 0.954888
$p\pi^- \rightarrow m\pi^-$	$\underset{-10}{77}Vm\ \underset{-16}{67}Vn\ \underset{24}{51}Vo\ \underset{-14}{75}Vp$	3.220201948 2.553941	$p\pi^- \rightarrow m\pi^-$ 1.254436
$q\pi^+ \rightarrow l\pi^+$	$\underset{37}{41}Vl\ \underset{-9}{78}Vm\ \underset{-16}{69}Vn\ \underset{24}{53}Vo\ \underset{-15}{77}Vp\ \underset{12}{62}Vq$	3.220315827 -3.834195	
$q\pi^+ \rightarrow l\pi^+$ $s\pi^- \rightarrow n\pi^-$	$\underset{37}{41}Vl\ \underset{-9}{78}Vm\ \underset{-17}{69}Vn\ \underset{24}{52}Vo\ \underset{-15}{76}Vp\ \underset{12}{61}Vq\ \underset{24}{73}Vr\ \underset{-6}{97}Vs$	3.220252627 -0.288933	$q\pi^+ \rightarrow l\pi^+$ $n\pi^+ \rightarrow s\pi^+$ 0.827379
$s\pi^- \rightarrow n\pi^-$	$\underset{-17}{68}Vn\ \underset{24}{51}Vo\ \underset{-15}{75}Vp\ \underset{13}{60}Vq\ \underset{24}{73}Vr\ \underset{-6}{97}Vs$	3.220185034 3.502738	
$r\pi^+ \rightarrow l\pi^+$ $t\pi^- \rightarrow n\pi^-$	$\underset{37}{41}Vl\ \underset{-9}{78}Vm\ \underset{-17}{69}Vn\ \underset{24}{52}Vo\ \underset{-15}{76}Vp\ \underset{13}{61}Vq\ \underset{23}{74}Vr\ \underset{-7}{97}Vs\ \underset{-11}{90}Vt$	3.220252345 -0.273141	$r\pi^+ \rightarrow l\pi^+$ $n\pi^+ \rightarrow t\pi^+$ 0.843171
$t\pi^- \rightarrow n\pi^-$	$\underset{-17}{68}Vn\ \underset{24}{51}Vo\ \underset{-15}{75}Vp\ \underset{13}{60}Vq\ \underset{24}{73}Vr\ \underset{-7}{97}Vs\ \underset{-11}{90}Vt$	3.220175644 4.029504	
$r\pi^+ \rightarrow o\pi^+$	$\underset{25}{52}Vo\ \underset{-15}{77}Vp\ \underset{13}{62}Vq\ \underset{23}{75}Vr$	3.220294461 -2.635665	
$r\pi^+ \rightarrow o\pi^+$ $t\pi^- \rightarrow p\pi^-$	$\underset{25}{52}Vo\ \underset{-16}{77}Vp\ \underset{13}{61}Vq\ \underset{23}{74}Vr\ \underset{-7}{97}Vs\ \underset{-11}{90}Vt$	3.220247685 -0.011747	$r\pi^+ \rightarrow o\pi^+$ $t\pi^- \rightarrow p\pi^-$ 0.147727 $r\pi^+ \rightarrow o\pi^+$ $p\pi^+ \rightarrow t\pi^+$ 1.104565
$t\pi^- \rightarrow p\pi^-$	$\underset{-16}{76}Vp\ \underset{13}{60}Vq\ \underset{24}{73}Vr\ \underset{-7}{97}Vs\ \underset{-11}{90}Vt$	3.220201183 2.596849	$t\pi^- \rightarrow p\pi^-$ 2.118430
note	W_γ field, part of the γ ray energy spectrum calculation result is negative, the part beyond the experimental range, are no longer to calculate.		

14 nuclear stability, particle beam forming

Principle and parameter calculation

14.1 nuclear stability analyses

14.1.1 Particles spiral ring of π± mesons in stability analysis

From 7 to 13 chapters nucleus internal structure, the formation of the nuclear force, principle and parameter simulation of already know: nuclear power charge number Z≥ 6 all conditions within the nucleus of the high and low positive and negative π± violation. Both high, low-energy particle spiral ring, which take different number π± muon to the charge. So, under what conditions, the same particles spiral ring, the same fluctuation, spin elliptical orbit in the movement of the positive and negative π± muon to stability, not as positive, antimatter merge, annihilation, huge burst of energy?

To formed from chapter 2, 3 elementary particle energy principles and the internal and external interactions analysis: high, low positive and negativeπ± mesons are made by 2 to the electric dipole and a charged particles. By (3.5-1), (3.5-2) - the results compared to: each charged particles around v_a fluctuations rail $K_r v_a$ rotating speed, speed, spin velocity v_θ and speed of the vz must be higher than the speed of light $v_z \geq c$, charged particles can be stable. By (2.1), (2.2), in order to speed $v_z \geq c$ motion of charged particles, high voltage, the formation of magnetic field distribution in vertical speed is completely $v_z=c$ movement orbit plane, along the track the tangent direction of the electric and magnetic field strength are tending to o! The spin direction, the same particles spiral ring ofπ± muon fully equal to the speed of the spin, interval, often in different wave track loop, and the same particles spiral ring and other particles spiral ring ofπ± muon contain attract effect of the electric field force, between each other internal will automatically adjust to balance. So, to:

$$v_z = \sqrt{v_\alpha^2 + v_\theta^2 + (K_r v_\alpha)^2} \geq c \qquad (14.1)$$

By equations (1.2), (1.5), (2.1), (2.12), (2.13), make fluctuation velocity for $\dot{\alpha}$, too:

$v_a=\beta c$, $v_\theta = \beta c \Big/ \sqrt{N_\alpha}$, $K_r v_\alpha = K_r R_\alpha \dot{\alpha} = K_r R_\alpha \beta c \Big/ 2\pi R_\alpha = K_r \beta c \Big/ 2\pi$, generation into (14.1), to:

$$v_z = \beta c \sqrt{1 + \frac{1}{N_\alpha} + \left(\frac{K_r}{2\pi}\right)^2} \geq c \qquad (14.2)$$

When $2.5 \leq N_a \leq 500$, by the table2.1, the $\pi^{\pm}$ mesons, because $1.13995\times10^{-5} \leq K_r \leq 16.8629\times10^{-5}$, so:

$$v_z \approx \beta c \sqrt{1 + \frac{1}{N_\alpha}} \geq c \qquad (14.3)$$

By (4.9), (14.3), the numerical simulation to:

$N_a \geq 388 \quad v_z \leq 0.9999986639c$

$N_a \leq 387 \quad v_z \geq 1.000001989c$

By figure 7.1 and figure 7.2 nucleus internal structure, hypothesis 5 layers of high and low of high-energy particles spiral ring positive and negative $\pi^{\pm}$ mesons in low-energy particles spiral rings continue to peripheral transition, and in the process of transition, if the layer of particles spiral ring inside protons and neutrons are even a, and magnetic moment always is 0, then to: $N_{ad5}=88$，$N_{ag5}=388\sim391$.

Conditions within the nucleus stability parameter calculation results comparison table 14.1

N_{ad5}	N_{ag5}	$R_{\theta d5(\pi)}\times10^{-14}$m	$R_{\theta g5(\pi)}\times10^{-14}$m
88	388	1.109875689	1.106463483
	390	1.109871285	1.109169534
	391	1.109869099	1.110519962

Refer to section 9.1 2 ~ 6 calculation program, by (8.1), we calculate is higher, low-energy particle spiral ring and negative $\pi^{\pm}$ violation of $R_{\theta g5(\pi)}$, $R_{\theta d5(\pi)}$ of space tolerance relation, the results shown in table 14.1.

By (14.3), table 14.1 the results to: $388 \le N_{ag5} \le 390$, is the fifth ring particles spiral layer within the nucleus of high-energy $\pi_g^{\pm}$ to positive and negative mesons in unstable interval. So, particles within the nucleus spiral ring layer is composed of five layers can be at most. If bottom side by side, low-energy particles spiral ring for up to 6 prevailed, by (9.12), atomic nuclei saturated when most can only accommodate 290 nuclear, and 6 layer is not stable, If the 4 layer, the saturated as 234 nuclear, and natural radiation is starting nuclear $^{232}_{90}Th$, $^{235}_{92}U$, $^{238}_{92}U$, (behind will prove, separate a^{++} high, low-energy particles spiral ring in heavy nuclei the spin axis on the proper position can long-term stable existence).

Scientists predicted that nuclear power charge number for 114 a stable island, near their corresponding to the total number of nuclear also is around 290. According to the analysis of this section: nucleus can consist of 6 particles spiral ring, saturated when can accommodate 290 nuclear; Beyond will lead to high and low to $\pi_g^{\pm}$ to positive and negative violation of unstable; So, the prophecy is bound to fail.

14.1.2 Nucleus kernel force stability analysis

By (7.2) - the results and chapter 11 ~ 13 nucleus internal structure, the nuclear force balance verification comprehensive comparison of the calculated results can be seen that: each individual charged particles spiral ring, the spin elliptical orbit radius in the direction of integrated electrical, magnetic force, the centrifugal force of interaction between don't need to consider. Is located in the nucleus spin of charged particles in the plane of the equator spiral ring, as long as nuclear charge distribution on the equator plane symmetric on both sides, also need not consider nuclear power, the magnetic field strength. Most B type structure of the nucleus, as a result of the adjacent low-energy particles spiral ring layer on the whole of the medial low-energy particles spiral ring, have set, to overcome the stability of the nuclear power field force. Except for the bottom layer 1, other layers inside the particles spiral ring spin elliptical

orbit non-oil imports of ampere force general field force is greater than nuclear power. At the bottom, especially the bottom inside the particles spiral ring spin elliptical orbit non-oil imports most of ampere force is less than the nuclear field force, rely on particles spiral ring side by side the whole current of ampere force $\triangle F_{\theta bj}$ added to maintain nuclear force balance. By (10.17) and chapter 11 ~ 13 nucleus internal structure, the nuclear force balance comparative test results: as long as the bottom side by side particles spiral loop net with high and low π^+ violation to the lateral migration, nuclear power field force $F_{e\theta j}$ will increase greatly, and the whole $\triangle F_{\theta bj}$ accidents of ampere force is greatly reduced, and even as a negative value, the original is squeezed into a upcountry outward expansion, the bottom of the nucleus particles spiral ring nuclear force can't balance. So, along the spin of the elliptical orbit axial positively charged electronic β^+, a^{++} particle, p^+ proton injection decay is unable to avoid. See section 14.3 and 14.4 calculation example.

14.2 particle beam forming principle within the nucleus

14.2.1 Particle radiation type and develop trend within the nucleus

Laboratory has detected particle emission in the process of the decay of nuclear fission rays are: a^{++} particle, p^+ protons, n neutrons, positive and negative $\beta^{\pm}$. Otherwise epsilon ε orbit electronic capture, is equivalent to the antiparticle positron β^+ emission, this chapter boils down to study together.

Common law is the formation of this particle ray: with the same number of nuclear power by isotope, neutron numbers less or, at least equivalent to nuclear net with high-energy π_g^+ muon comparatively much, mainly produce a^{++} particle, p^+positron protons, β^+ rays and ε epsilon track electronic capture. Along with the increased number of neutrons, mainly produce β^- diffusion and n neutron rays. During the whole process of nuclear fission decay, most with γ rays, the conservation of energy is always, always in the direction of energy gradually reduce the parent nucleus occur

spontaneously. Section 14.1.1 same particles spiral rings $\pi^{\pm}$ mesons in stability analysis has been mentioned, $\pi^{\pm}$ muon must maintain proper ratio, internal, electric attraction between each other mutual contain to maintain balance. Therefore, only protons, neutrons to maintain the proper proportion, the relative excess of high and low $\pi^{\pm}$ muon rejection, nucleus can maintain stable finally.

14.2.2 a^{++} Particle internal structure and parameter calculation

The a^{++} particles is ${}_{2}^{4}He$ nucleus, the atomic energy measured 4.00260326u, two electronic total ionization energy of 79.003 ev③. By (11.3), too:

$$\sum {}_{2}^{4}HeW_0 = 6.644661599\times10^{-27}\text{Kg}$$

By figure 7.5: a^{++} particles within the 6 high-energy $\pi_g^{\pm}$ muons (including the net with 4 π_g^{+} violation), 8 low $\pi_d^{\pm}$muons (including the net with 2 π_d^{-}). Refer to section 11.2 calculation procedures, if we will a^{++} particles designed to type B nucleus, as shown in figure 14.1, the data from table 9.1 and table 9.1:

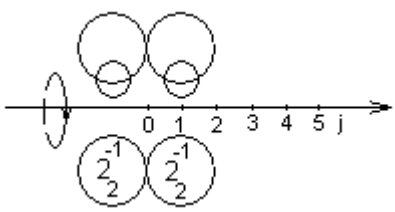

图14.1 ${}_{2}^{4}He$原子核内核子、净剩$\pi^{\pm}$介子分配示意图

$$Va \quad {}_{4}^{4}Vb_{-2}$$

$$W_e = 8.941660379\times10^{-30}Kg$$
$$W_b = 1.53063327\times10^{-30}Kg$$
$$\sum {}_{2}^{4}HeW_{\text{b}} = 6.619394948\times10^{-27}Kg$$

If a^{++} particle design into type A nucleus, as shown in the figure 7.1, only A pair of particles spiral ring, see figure 14.2. By (7.2), the nucleus do not exist the spin axis electric and magnetic field strength. From table 9.1 and table 9.1 data, obtained a^{++} particle energy figure 14.2 on the right.

$^{4}_{2}$He nucleus kernel force balance verification results table (figure 14.1 units: Newton) of 14.2

N \ j / Nai	0	1	2	3	4	5	核电、磁场力累计
Feθ		b 88.05890278					4.846944828
$\frac{34}{13}$ Fbθ		-14.26555798					
ΔFθb		-68.94639997					

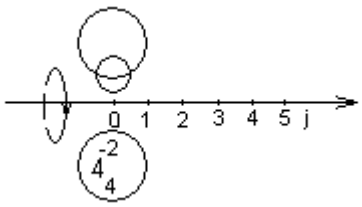

图14.2 $^{4}_{2}He$原子核内核子、净剩π±介子分配示意图

$$^{4}_{4}Va \qquad ^{4}_{-2}Vb$$

$$W_e = 1.744014049\times10^{-29}Kg$$

$$W_b = 1.747945042\times10^{-30}Kg$$

$$\sum {}^{4}_{2}HeW_a = 6.62811074\times10^{-27}Kg$$

Compare the above two kinds of type A and B a^{++} particle nucleus, are obviously is stable, but has reached the maximum total energy, there is no room for further increase. Because nuclear power charge number $2 \le Z_i < 6$ of the nucleus may be by A pair of high and low among particles spiral ring and edge "sticky" not "decentralized" composed of protons, neutrons, and axial nuclear power field force by the overall current ampere force to maintain balance, so, we can make a^{++} particles in type A nuclear, quantum fluctuations of N_{a1}=34/13 is changeless, and to: $\overline{m}_{d\alpha} = \overline{m}_{d1}\sum {}^{4}_{2}HeW_0 \Big/ \sum {}^{4}_{2}HeW_\alpha$,In the analysis of the follow-up, a^{++} particles directly take the energy of the experimental value:

$$\sum {}^{4}_{2}HeW_0 = 6.644661599\times10^{27}Kg$$

14.2.3 a^{++} particles and P^{+}protons in nuclei of emission mechanism

Nucleus, a^{++} particles are made by high and low in π±violation. When the bottom

of the high and low positive and negative $\pi^{\pm}$ violation by the nuclear spin axial injection out in figure 14.3 relative position, as long as we avoid relatively small interactions of the magnetic field, the electric field force each other to make them in a stable equilibrium state. A nucleus with N_e nuclear power, to a^{++} particles, high-energy particles spiral ring net with 4 π_g^+ mesons, low net with 2 π_d^- violations. The Coulomb's law:

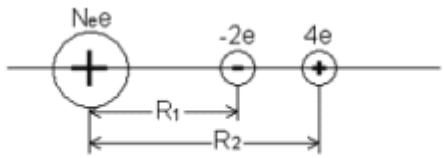

图14.3 原子核与外边带电粒子电场力平衡示意图

Figure 14.3 nuclear and outside charged particle electric field force Equilibrium diagram

$$\begin{cases} \dfrac{2N_e e^2}{4\pi\varepsilon_0 R_1^2\sqrt{1-\dfrac{\beta^2}{N_\alpha}}} = \dfrac{8e^2}{4\pi\varepsilon_0 (R_2-R_1)^2\sqrt{1-\dfrac{\beta^2}{N_\alpha}}} & (14.4-1) \\ \dfrac{4N_e e^2}{4\pi\varepsilon_0 R_2^2\sqrt{1-\dfrac{\beta^2}{N_\alpha}}} = \dfrac{8e^2}{4\pi\varepsilon_0 (R_2-R_1)^2\sqrt{1-\dfrac{\beta^2}{N_\alpha}}} & (14.4-2) \end{cases}$$

Solution (14.4) equations to: $R_2/R_1 = \sqrt{2}$. That is to say, as long as the component a^{++} a pair of high and low particles spiral ring outside the nuclear spin axis and nucleus maintain the relative distance of $R_2/R_1 = \sqrt{2}$, can smoothly from the nucleus, or with a nucleus in the spin axis to balance a long position in a stable state. When high, low-energy particle spiral ring close to combine into a^{++} particles, this equilibrium is destroyed, because nuclear power field force rejection, will lead to a^{++} particle emission.

Similarly, by figure 7.4, we have in the design of the "assembly" nuclear protons p^+ split into two energy π_g^+ mesons, a low-energy π_d^- violation, a pair of electric dipole in

neutrino or remaining photons released form. According to equations (14.4) of the solution, as long as two high-energy π_g^+ violation, a low-energy π_d^- both of a pair of high and low particles spiral ring, the nuclear spin axis and maintain the relative distance of $R_2/R_1 = \sqrt{2}$, it also can keep balance with the nucleus, or smoothly from the nucleus. High when the nucleus, low-energy particles spiral ring close to, as long as high-energy particles spiral ring in the 2 π_g^+ muon neutrino adsorption field a neutrino, at the same time release a are charged particles, and low-energy particle spiral ring of π_d^- muon exchange a load charged particles, from the figure 6.3, section 6.1 shows that the proton p^+ is formed. In the nuclear field force under to actioned of proton p^+ rays. Because proton launch mainly in proton number is greater than the number of neutrons unstable light nuclei, despite the launch principle similar to the above a^{++} particles, but the launch process should not only absorbs neutrinos, and exchange, load charged particles, the transformation process is more complicated, so that the appear of proton emission energy, total energy conservation alone simulation unable to reveal the detailed process, behind no longer research.

In addition, the total number of more than 234 nuclear heavy nuclei, the fifth layer of particles spiral rings, high low $\pi_g^{\pm}$ to positive and negative source of instability caused by fluctuation of quantum number N_{ag5}, N_{ad5} change also can produce a^{++} particle ray, see section 14.3 calculation example.

14.2.4 $\beta^{\pm}$ electron beam forming principle

Nucleus each launch a negativeβ^- electronics, total number of nuclear remain unchanged, the parent nucleus nuclear charge will increase the number 1, equivalent to a neutron should be transformed into protons within the parent nucleus. By figure 7.4 that there will be a pair of low-energy $\pi_d^{\pm}$ violation of the π_d^- muon split into β^- electronics and a neutrino or photons, and most of the energy transfer will originally

inspired another π_d^+ to low-energy mesons, make its become high-energy $\pi_g^{\pm}$ mesons, enter the high-energy muon orbit, β^- electronic depend on residual energy to overcome their own nuclear power field force constraint the launch.

Similarly, nucleus each launch a β^+ positron, total number of nuclear also remain unchanged, the parent nucleus nuclear power by several reduced by 1, equivalent to a proton in the parent nucleus into neutrons. Consist of figure 7.4, $\pi^{\pm}$muon principle, electric dipole number n increased from 2.5 to 2.5, and then, one of the high-energy π_g^+ source must be continuous adsorption four neutrinos, eventually split, into a pair of low-energy $\pi_d^{\pm}$positron emission source and a β^+.

ε epsilon orbit electronic capture and launch a positron effect, the difference is only 1 high-energy π_g^+ violation as long as adsorption neutrino field in a neutrino, and the adsorption of electronic β^- together into a pair of low-energy $\pi_d^{\pm}$ muon to enter the low-energy particles spiral ring rail is ok.

14.3 conditions within the nucleus a^{++}

Particle ray energy calculation example

14.3.1 Nuclear number $A \geq 234$ Heavy nucleus a^{++} particle ray energy Calculation example

Nuclear total $A_i \geq 234$ and $A_i < 234$ within the nucleus of the a^{++} different particle beam forming principle. Under the calculation example, respectively, in the case of $^{236}_{92}U \rightarrow {}^{232}_{90}Th + \alpha^{++}$:

$^{236}_{92}U$ Atomic total energy experimental value is 236.045582 u, K_{a2} layer electronic ionization energy for 94648 ev, generation into (11.3), to:

$$\sum {}^{236}_{92}UW_0 = 3.918948943 \times 10^{25}\text{Kg}$$

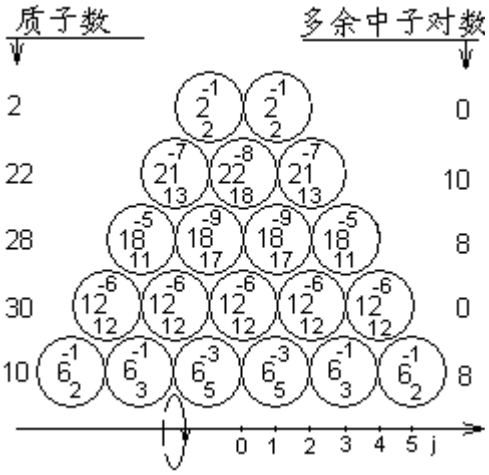

图14.4 $^{236}_{92}U$原子核内核子、净剩π±

介子分配示意图

$$\begin{array}{cccccc} {}^{10}_{Va}_{10} & {}^{10}_{Vb}_{-6} & {}^{4}_{Vc}_{6} & {}^{10}_{Vd}_{-2} & {}^{8}_{Ve}_{12} & {}^{20}_{Vf}_{-6} \\ {}^{14}_{Vg}_{4} & {}^{18}_{Vh}_{24} & {}^{42}_{Vi}_{-2} & {}^{40}_{Vj}_{-12} & {}^{28}_{Vk}_{24} & {}^{52}_{Vl}_{34} \\ {}^{86}_{Vm}_{-12} & {}^{74}_{Vn}_{-18} & {}^{56}_{Vo}_{22} & {}^{78}_{Vp}_{-10} & {}^{68}_{Vq}_{18} & {}^{86}_{Vr}_{26} \\ {}^{112}_{Vs}_{-8} & {}^{104}_{Vt}_{-14} & {}^{90}_{Vu}_{4} & {}^{94}_{Vv}_{2} & & \end{array}$$

$$W_e = 1.857324426 \times 10^{-27}\ Kg$$

$$W_b = 1.43454811 \times 10^{-29}\ Kg$$

$$\sum {}^{236}_{92}UW_1 = 3.918949689 \times 10^{-25}\ Kg$$

$^{236}_{92}U$ Nucleus kernel force balance to verify the results table (figure 14.4, the unit: Newton) table 14.3

j / N_a	1	2	3	4	5	nuclear Electric and magnetic field force cumulated
$88F_{e\theta}$	v.29.25187949					35.83711032
$F_{b\theta}$	-12.09695 58					
$58F_{e\theta}$		t.708.9523968				18.68218664
$F_{b\theta}$		-831.5560456				
$34F_{e\theta}$	n.879.4710447		p.1134.620304			141.2858354
$F_{b\theta}$	-1547.407343		-859.67 07462			
$16F_{e\theta}$		j.1177.523760		m.332.5403448		-133.6637224
$F_{b\theta}$		-943.7382342		-943.7382342		
$F_{e\theta}$	b.474.7645661		d.360.3313781		i.-30.52020855	243.7486412
$34/13F_{b\theta}$	-128.3900195		-42.79667316		-14.26555772	
$\Delta F_{\theta b}$	-107.2499554		-153.2142221		-114.9106665	

In 11.5 the $^{232}_{90}Th$ nucleus internal structure, the calculation results as the reference standard. Make redundant four nuclear "decentralized" of high and low $\pi^{\pm}$ muon all into 5 levels, low-energy particles spiral ring; see figure 14.4, the total energy figure on the left, the nuclear force balance test results shown in table 14.3.

Make a^{++} γ rays in the kinetic energy of the particles and total energy for $W_{γa}$, by the law of conservation of energy:

$$W_{r\alpha} = \sum {}^{236}_{92}UW_1 - \sum {}^{232}_{90}ThW_2 - \sum {}^{4}_{2}HeW_0 \qquad (14.5)$$

Will the correlation value generation into (14.5), to:

$W_{γa1}$=8.847259384×10^{-30}Kg=4.962946Mev

Laboratory determination a^{++} particle kinetic energy has three groups, respectively, 4.494 (73.7%), 4.445 (26%), 4.331 (0.26%) of the Mev (strength). Otherwise γ rays in the 2 groups, energy is: 0.1716, 0.2232 Mev.

Obviously, a^{++} particle kinetic energy of the weighted average of 4.4790386 Mev, and γ rays total energy $W_{γa0}$=4.8738386Mev. And the model calculation value $W_{γa1}$=4.962946Mev error only 0.08911 Mev. We have reason to speculate that this is the nucleus of magnetic energy simplified simulation of small error, the experimental error or by with nuclear power, and the inner electronic energy caused by the error.

14.3.2 Nuclear number $A_i < 234$ nucleus a^{++} particle ray energy calculation example

In the case of ${}^{174}_{72}Hf \rightarrow {}^{170}_{70}Yb + \alpha^{++}$:

${}^{174}_{72}Hf$ Atomic experimental determination of the total energy is 173.940140u, K_{a2} layer electronic ionization energy for 54579 ev, generation of (11.3) in type, to:

$$\sum {}^{174}_{72}HfW_0 = 2.887760126 \times 10^{25}\text{Kg}$$

We are shown in 12.3 ${}^{170}_{70}Yb$ nucleus of the internal structure, calculation of energy parameters for reference standards. Make four nuclear "decentralized" all of the high and low $\pi^{\pm}$ mesons are into 4 layer, low-energy particle spiral ring rail, see figure 14.5, nucleus kernel force balance verification calculation shown in table 14.4.

By the solution of equations (14.4), we can see that: as long as the fourth layer of high and low $\pi^{\pm}$muon particles spiral ring local concentration, it is not stable state; Can the $R_2/R_1=\sqrt{2}$ the relative distance of smoothly along the spin axis from the nucleus. By (7.2), particles spiral ring itself with shrinkage properties. When high, low-energy particle spiral ring once along the edge of the spin axis to slip out of the nucleus, internal support, he will rapidly shrinking to N_{a1} = 34/13 of the limit state, into a^{++} particle type spiral rings, transfer to a certain position after composition a^{++} particles. Throughout the decay in the process of transformation, by (14.5), a^{++} the kinetic energy of the particles W_{a1} for:

$$W_{a1}=4.571712894\times10^{-30}Kg=2.564542Mev$$

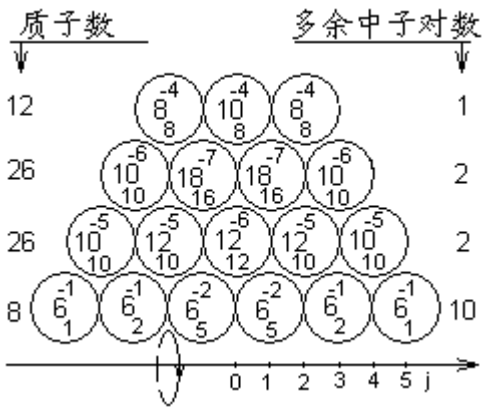

图14.5 $^{174}_{72}Hf$ 原子核内核子、净剩$\pi^{\pm}$介子分配示意图

$$\begin{array}{cccccc}
\overset{10}{Va}_{10} & \overset{10}{Vb}_{-4} & \overset{6}{Vc}_{4} & \overset{10}{Vd}_{-2} & \overset{8}{Ve}_{12} & \overset{20}{Vf}_{-6} \\
\overset{14}{Vg}_{2} & \overset{16}{Vh}_{20} & \overset{36}{Vi}_{-2} & \overset{34}{Vj}_{-10} & \overset{24}{Vk}_{20} & \overset{44}{Vl}_{32} \\
\overset{76}{Vm}_{-10} & \overset{66}{Vn}_{-14} & \overset{52}{Vo}_{20} & \overset{72}{Vp}_{-12} & \overset{60}{Vq}_{8} & \overset{68}{Vr}_{16} \\
\overset{84}{Vs}_{-4} & \overset{80}{Vt}_{-8} & & & &
\end{array}$$

$$W_e=1.230703829\times10^{-27}\,Kg$$

$$W_b=9.375240045\times10^{-30}\,Kg$$

$$\sum {}^{174}_{72}HfW_1=2.887756186\times10^{-25}\,Kg$$

The experiment measured a^{++} the kinetic energy of the particles of 2.50 Mev, results are very well.

If we fine tune $^{174}_{74}Hf$ nucleus shown in figure 14.5 4 layer particles spiral ring of $\pi^{\pm}$ source distribution condition, can be seen from table 14.4, $^{174}_{74}Hf$ nucleus is still stable, a nucleus electric energy coefficient is:

$\overset{60}{\underset{10}{Vq}}\ \overset{70}{\underset{14}{Vr}}\ \overset{84}{\underset{-6}{Vs}}\ \overset{78}{\underset{-6}{Vt}}$ $\sum {}^{174}_{72}HfW_2 = 2.887756894 \times 10^{-25} Kg$

${}^{174}_{74}Hf$ Nucleus kernel force balance test results list 14.4 (figure 14.5)

j / N_a	1	2	3	4	5	nuclear Electric and magnetic field force cccumulated
$58F_{e\theta}$	t. 348.9357215					-201.7282867
$F_{b\theta}$	-237.5874416					
$34F_{e\theta}$	n. 784.7660255	p. 760.2467544				-313.0765666
$F_{b\theta}$	-936.0859236	-802.3593631				
$16F_{e\theta}$	j. 861.2937174	m. 165.8418776				-270.9639579
$F_{b\theta}$	-786.4485285	-655.3737738				
$F_{e\theta}$	b. 642.7725138	d. 237.204948	i. -146.1102978			143.7227494
$34/13F_{t\theta}$	-57.06223088	-28.53111544	-14.26555772			
$\Delta F_{\theta b}$	-306.4284441	-160.8749332	-22.98213331			

Obviously, this is a nuclide with nuclear power. Readers may ask: table 14.4 shows that ${}^{174}_{74}Hf$ nucleus kernel forces are balanced stable, why will decay? Section 14.1.1 of this chapter is that only the protons and neutrons to maintain the proper proportion, remove the excess of high and low $\pi^{\pm}$ muon rejection, nucleus to ultimate stability.

14.4 $\beta^{\pm}$ Electron beam energy calculation example Within the nucleus

14.4.1 β^- electronic rays

β^- Electronic rays appear more number of neutrons in the isotope. Nucleus each to launch a β^- electronics, nuclear power charge increases the number 1. We in ${}^{208}_{81}Tl \rightarrow {}^{208}_{82}Pb + \beta^- + \gamma$, for example, because the author did not refer to the relevant ${}^{208}_{81}Tl$ magnetic moment of a nucleus value, and the number of protons and ${}^{194}_{79}Au$ nucleus, neutron is an odd number, so, according to figure 13.2, ${}^{208}_{81}Tl$ magnetic

moment of a nucleus, also take 0.07325 U_p.

$^{208}_{81}Tl$ Atomic experimental determination of total energy is 207.982019 u, K_{a2} layer electronic ionization energy 70820 ev. By (11.3), to: $\sum {}^{208}_{81}TlW_0$ = 3.452989435 x 10^{-25} kg. Magnetic moment synthesis scheme see (13.2), the energy increment for $\Delta\overline{m}$ = 6.0811736 x 10^{-30} kg. Design $^{208}_{81}Tl$ nucleus internal structure is shown in figure 14.6, the nuclear force balance test results shown in table 14.5.

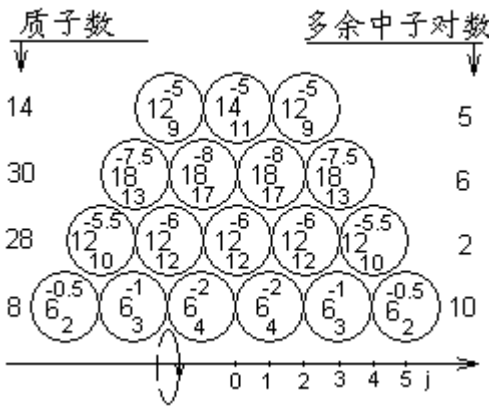

图14.6 $^{208}_{81}Tl$原子核内核子、净剩π± 介子分配示意图

$^{8}_{8}Va$	$^{8}_{-4}Vb$	$^{4}_{6}Vc$	$^{10}_{-2}Vd$	$^{8}_{12}Ve$	$^{20}_{-6}Vf$
$^{14}_{4}Vg$	$^{18}_{24}Vh$	$^{42}_{-1}Vi$	$^{41}_{-12}Vj$	$^{29}_{20}Vk$	$^{49}_{34}Vl$
$^{83}_{-11}Vm$	$^{72}_{-16}Vn$	$^{56}_{26}Vo$	$^{82}_{-15}Vp$	$^{67}_{11}Vq$	$^{78}_{18}Vr$
$^{96}_{-5}Vs$	$^{91}_{-10}Vt$				

$$W_e = 1.524426978\times10^{-27}\,Kg$$
$$W_b = 1.218929001\times10^{-29}\,Kg$$
$$\sum {}^{208}_{81}TlW_1 = 3.45298393\times10^{-25}\,Kg$$

According to section 14.2 β^- electronic ray emission mechanism is discussed. Set up as shown in figure 14.6, the parent nucleus by $^{208}_{81}Tl$ state began to β^- decay, and by the lowest energy of $t\pi^{\pm}$ in the launch. Starting from a low-energy $t\pi_{d4}^{\pm}\rightarrow r\pi_{g4}^{+}+\beta^-+\gamma(\upsilon)$, if we don't consider electron kinetic energy, neutrino(υ) hormone called or photon γ energy, while the table 13.3 to: $\Delta\overline{M}$ =3.20680973 x 10^{-30} kg. Electric and magnetic energy parameters are as follows:

$$\ldots\ldots {}^{78}_{19}Vr\ \ {}^{97}_{-5}Vs\ \ {}^{92}_{-10}Vt \qquad W_e = 1.551134156\times10^{-27}\,Kg$$

$$W_b = 1.219994669\times10^{-29}\,Kg$$

$$\sum {}^{208}_{82}PbW_3 = 3.45321904 \times 10^{-25} Kg$$

$^{208}_{81}Tl$ Nucleus kernel force balance test results list 14.5 (14.6)

j / N_a	1	2	3	4	5	nuclear Electric and magnetic field force cccumulated
$58F_{e\theta}$		t. 417.1960228				-44.24675164
$F_{b\theta}$		-371.2303775				
$34F_{e\theta}$	n. 888.23571196		p. 1130.857688			-90.21239694
$F_{b\theta}$	-1222.642839		-1146.227662			
$16F_{e\theta}$		j. 1149.598326		m. 101.72915 81		-74.84242294
$F_{b\theta}$		-943.7382342		-865.0933814		
$F_{e\theta}$	b. 352.23561 12		d. 360.3313781		i. 138.6064441	482.66 17085
$34/13F_{b\theta}$	-57.06223088		-28.53111544		-7.13277886	
$\Delta F_{\theta b}$	-45.96426662		-95.75888879		-134.0624443	

To compared to: son nuclear mother and decay products total energy is greater than 3.246461415 x 10^{-29} kg, violation of the law of conservation of total energy, so won't happen.

If by $^{208}_{81}Tl$, as shown in the figure 14.6, the parent nucleus through internal $\pi^{\pm}$ mesons, neutron comprehensive adjustment to $^{208}_{(82)}Pb$ nuclear excited states, to launch a β electronic after completely into $^{208}_{82}Pb$ nucleus, as shown in the figure 11.3, is the fourth layer of particles spiral loop:

$$t\,\pi^{\pm} \rightarrow r\,\pi^{+} + \beta^{-} + \gamma(\upsilon)$$

By figure 11.3 shows, excited states of electric and magnetic energy parameters are as follows:

$$\ldots\ldots {}^{80}_{15}Vr \quad {}^{95}_{-6}Vs \quad {}^{89}_{-8}Vt$$

$$W_e = 1.522497937 \times 10^{-27} Kg$$

$$W_b = 9.803396807 \times 10^{-30} Kg$$

$$\sum {}^{208}_{(82)}PbW = 3.452627495 \times 10^{-25} Kg$$

Compared to: $\sum {}^{208}_{(82)}PbW$ state of total energy less than the total energy of the

ultimate stability of the sub nuclear $\sum {}^{208}_{82}PbW_3$, △W=2.66898609×10^{-29}Kg, so, this split decay also won't happen.

To sum up, the nucleus of the particle ray is not limited to the initial state of the parent nucleus or nuclear excited states to launch. It should be in the female nuclear sub nuclear transformation to decay, internal π± mesons, neutron distribution state fully adjust some process with nuclear power, interval to launch. Particle emission and total energy $\sum W_i$ should be equal, and in between mother and son kernel total energy, this is the book chapter 13 γ ray spectrum calculations using mother nuclear energy for the cause of the reference standard.

According to the experimental determination of the β- ray's energy and stability of nuclear energy state of ${}^{208}_{82}PbW$ as shown in figure 11.3, the simulation calculation was: as shown in the figure 14.7 ${}^{208}_{81}Tl$ nuclei with nuclear power in the process of decay, is the ideal firing interval.

To: $\overline{m}^{\pm}_{g2} \rightarrow \overline{m}^{\pm}_{g1}$**, to:** $\sum {}^{208}_{81}TlW_3$ =3.45294119×10^{-25}Kg

When it s position to launch a β- electronic, through:

$$s\pi^{\pm} \rightarrow q\pi^{+} + \beta^{-} + \gamma(\upsilon); \quad \overline{m}^{\pm}_{g1} \rightarrow \overline{m}^{\pm}_{g2};$$

Certainly a to c position high-energy π_{g1}^{+} diffusion adjustment: $2a\pi^{+} \rightarrow 2c\pi^{+}$;

Three process coordination at the same time, we can finish the β- electron emission, ${}^{208}_{81}Tl$ with nuclear power, it is converted into the stability of the sub nuclear ${}^{208}_{82}Pb$, as shown in figure 11.3. Please note: if we will $s\pi^{\pm} \rightarrow q\pi^{+} + \beta^{-} + \gamma$ (υ) hormone called were closed up alone, the resulting electron kinetic energy is:

$$\Delta\overline{m} = 3.20680973 \times 10^{-30} Kg = 1.798888 Mev$$

If regardless of neutrinos or photon energy, with the experimental value 1.7950 Mev (50%) of the energy level are consistent.

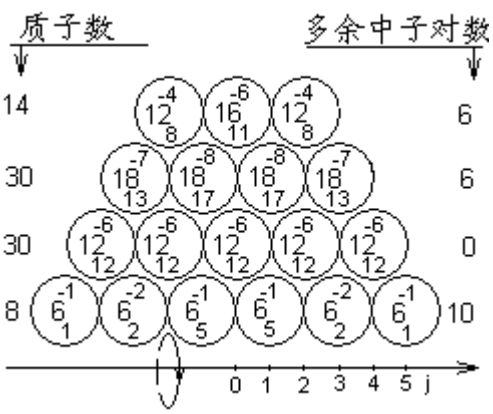

$$\begin{array}{cccccc} {}^{10}_{Va}_{10} & {}^{8}_{Vb}_{-2} & {}^{12}_{Vc}_{4} & {}^{8}_{Vd}_{-4} & {}^{20}_{Ve}_{12} & {}^{}_{Vf}_{-6} \\ {}^{14}_{Vg}_{2} & {}^{16}_{Vh}_{24} & {}^{40}_{Vi}_{-2} & {}^{38}_{Vj}_{-12} & {}^{26}_{Vk}_{24} & {}^{50}_{Vl}_{34} \\ {}^{84}_{Vm}_{-12} & {}^{72}_{Vn}_{-16} & {}^{56}_{Vo}_{26} & {}^{82}_{Vp}_{-14} & {}^{68}_{Vq}_{11} & {}^{79}_{Vr}_{16} \\ {}^{95}_{Vs}_{-6} & {}^{89}_{Vt}_{-8} & & & & \end{array}$$

$$W_e = 1.542121382 \times 10^{-27}\ Kg$$

$$W_b = 9.803396811 \times 10^{-30}\ Kg$$

$$\sum {}^{208}_{81}Tl W_2 = 3.45282373 \times 10^{-25}\ Kg$$

图14.7 ${}^{208}_{81}Tl$原子核内核子、净剩π±介子分配示意图

Because the nucleus is a whole consists of electric and magnetic field of the total energy system. Within a particu lar location of π± mesons, neutron distribution state of adjustment will lead to energy change. This adjustment is not limited to a certain location, a certain steps; multiple steps can be more than one location, at the same time. It is lead to particle γ ray, the diversification and complication of the rays.

Book on nuclear spin direction of magnetic energy is using simplified way solenoid magnetic field calculation, not considering the spin axis charge density changes in the current intensity and magnetic field strength of the change. Electronic total energy in the atomic lining also is too. Although magnetic field total energy generally accounts for only a nucleus total energy enough of a few, do not affect the nucleus of the total energy of the precision, but it can affect particle γ rays, the radiation energy simulation precision, please forgive me.

14.4.2 β^+ electronics and ε track electronic capture

β^+ Electronics and ε track electronic capture of the role of nucleus, as this is quite

a part of the nucleus at the same time with these two phenomena decay. The total number of nuclear remain unchanged, the parent nucleus nuclear power charge number 1. Equivalent nuclear within a proton into neutrons, decay reaction equation of particles can be expressed as:

$$\begin{cases} \beta^+: \quad \pi_g^+ + 4\nu \rightarrow \pi_d^\pm + \beta^+ & (14.6-1) \\ \varepsilon: \quad \pi_g^+ + \nu + \beta^- \rightarrow \pi_d^\pm & (14.6-2) \end{cases}$$

To $^{194}_{79}Au \rightarrow ^{194}_{78}Pt + \beta^+$ decay process as an example, the mother nuclear, internal structure, energy, parameter calculation value is shown in figure 13.2, table 13.1 and figure 13.3 and table 13.2. If decay is in energy change at least 4 layer particles spiral ring outside r, t happen, by table 13.3 of each layer, low $\pi^\pm$ muon original wave energy, and the equations (14.6), calculate particle decay energy increment in the process of transformation, respectively:

$\Delta\overline{m}_{\beta 4}$=5.02868767×10^{-30}Kg $\Delta\overline{m}_{\varepsilon 4}$=3.20680973×10^{-30}Kg

(Temporary not consider electron kinetic energy, the photon or neutrino energy)

If directly from $^{194}_{79}Au$ nucleus, as shown in the figure 13.2 r, t location β^+ electronic decay, the electric and magnetic energy parameters are:

$$.....^{74}_{23}Vr \quad ^{97}_{-7}Vs \quad ^{90}_{-12}Vt$$

$$W_e = 1.375543122 \times 10^{-27}\,Kg$$

$$W_b = 7.817404549 \times 10^{-30}\,Kg$$

$$\sum {}^{194}_{78}PtW_2 = 3.220039883 \times 10^{-25}\,Kg$$

Less than the son, as shown in the figure 13.3 nuclear $\sum {}^{194}_{78}PtW_1$ values to 1.7405427 x 10^{-29} kg, so, the decay phenomenon won't happen.

Similarly, if by radiation in the $^{194}_{(78)}Pt$ excited states, as shown in the figure 13.3, electricity, magnetic energy parameters is:

$$\cdots\cdots\overset{74}{\underset{19}{Vr}}\quad\overset{93}{\underset{-4}{Vs}}\quad\overset{89}{\underset{-10}{Vt}}$$

$$W_e = 1.418615891\times10^{-27}\,Kg$$

$$W_b = 9.484283676\times10^{-30}\,Kg$$

$$\sum{}^{194}_{(78)}PtW_3 = 3.220521571\times10^{-25}\,Kg$$

Greater than mother nuclear energy $\sum{}^{194}_{79}AuW_1$ values 2.74095268 x 10^{-29} kg, obviously, this until finally excited states radiation β⁺ electronic phenomenon won't happen.

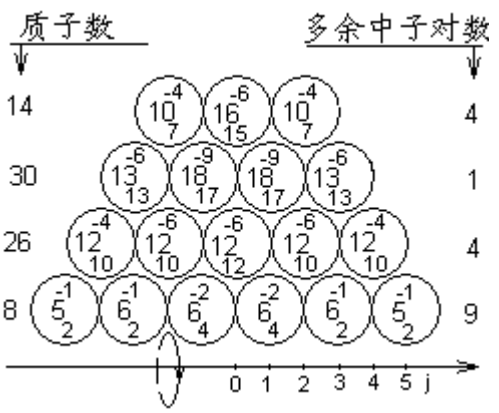

图14.8 $^{194}_{79}Au$原子核内核子、净剩π±介子分配示意图

$$\overset{8}{\underset{8}{Va}}\quad\overset{8}{\underset{-4}{Vb}}\quad\overset{4}{\underset{4}{Vc}}\quad\overset{8}{\underset{-2}{Vd}}\quad\overset{6}{\underset{12}{Ve}}\quad\overset{18}{\underset{-6}{Vf}}$$

$$\overset{12}{\underset{4}{Vg}}\quad\overset{16}{\underset{20}{Vh}}\quad\overset{36}{\underset{-2}{Vi}}\quad\overset{34}{\underset{-12}{Vj}}\quad\overset{22}{\underset{20}{Vk}}\quad\overset{42}{\underset{34}{Vl}}$$

$$\overset{76}{\underset{-8}{Vm}}\quad\overset{68}{\underset{-18}{Vn}}\quad\overset{50}{\underset{26}{Vo}}\quad\overset{76}{\underset{-12}{Vp}}\quad\overset{64}{\underset{15}{Vq}}\quad\overset{79}{\underset{14}{Vr}}$$

$$\overset{93}{\underset{-6}{Vs}}\quad\overset{87}{\underset{-8}{Vt}}$$

$$W_e = 1.400149869\times10^{-27}\,Kg$$

$$W_b = 9.484283679\times10^{-30}\,Kg$$

$$\sum{}^{194}_{79}AuW_3 = 3.220245447\times10^{-25}\,Kg$$

So, we should still in the process of $^{194}_{79}Au\rightarrow{}^{194}_{78}Pt+\beta^+$ nucleus decays with nuclear power, in the transition of β⁺ electron emission of the mother. With experimental determination of β⁺ electron kinetic energy and stability of the internal structure of nuclear as shown in figure 13.3, energy as reference standard, the simulation calculation of $^{194}_{79}Au$, launch β⁺ electronic before and after the parent nucleus with the structure of the nuclear power, see figure 14.8 and figure 14.9.

β⁺ the high-energy electron emission process and related π_9^+ muon change adjustment process is as follows:

qπ⁺+4ν→sπ±+β⁺、4kπ⁺→4hπ⁺、2oπ⁺→2lπ⁺、2qπ⁺→2rπ⁺

Because β^+ positron emission process to continuously absorb four neutrinos, nature must have a process, so the back three high-energy π_g^+ violation adjustment procedures can be carried out together. By the total energy conservation, electron kinetic energy is W_{ev}, to:

$$W_{ev} = \sum {}^{194}_{79}AuW_3 - \sum {}^{194}_{78}PtW_3 - m_{e0} = 1.226553Mev$$

Experimental value is 1.230 Mev, agreement is very good.

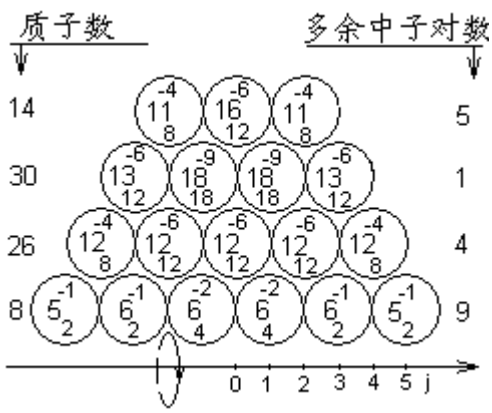

图14.9 ${}^{194}_{78}Pt$ 原子核内核子、净剩$\pi^{\pm}$介子分配示意图

$$\begin{array}{cccccc} {}^{8}Va_{8} & {}^{8}Vb_{-4} & {}^{4}Vc_{4} & {}^{8}Vd_{-2} & {}^{6}Ve_{12} & {}^{18}Vf_{-6} \\ {}^{12}Vg_{4} & {}^{16}Vh_{24} & {}^{40}Vi_{-2} & {}^{38}Vj_{-12} & {}^{26}Vk_{16} & {}^{42}Vl_{36} \\ {}^{78}Vm_{-8} & {}^{70}Vn_{-18} & {}^{52}Vo_{24} & {}^{76}Vp_{-12} & {}^{64}Vq_{12} & {}^{76}Vr_{16} \\ {}^{92}Vs_{-6} & {}^{86}Vt_{-8} & & & & \end{array}$$

$$W_e = 1.392944360 \times 10^{-27} Kg$$

$$W_b = 9.474618808 \times 10^{-30} Kg$$

$$\sum {}^{194}_{78}PtW_3 = 3.220214472 \times 10^{-25} Kg$$

Can be seen from the above analysis and calculation, we through the simulation although only find a group of electronic kinetic parameters, and there are small error, but in the current level of knowledge, have enough problems. If $\sum {}^{194}_{79}AuW_0$、$\sum {}^{194}_{78}PtW_0$ laboratory in section 13.2 the energy calculation, the difference between, minus the static energy m_{eo}, maximum 1.3336 Mev electron kinetic energy, still less than the largest 1.487 Mev electron kinetic energy experimental value, it is regardless of the γ ray energy. Obviously, it is mainly composed of with nuclear power, solenoid magnetic energy simplified calculation and atomic inner electronic total energy caused by the change of the error.

15 the energy under the condition of the relativistic electron spin elliptical orbit equations of motion

15.1 Is far lower than the speed of light under the condition of electron spin elliptical orbit equations of motion

15.1.1 Electron spin elliptical orbit characteristics

Electronics in the nucleus as the center under the action of electric field force along the spin elliptical orbit characteristics, which is similar to Newton's mechanics in the sun, the earth is the center of gravity field under the action of the elliptical orbit, and has the following features:

1. The interactions between the planets in the solar system are still the gravity, so the planets can distribution in almost the same spin elliptical orbit plane. Electronic is the interaction between electric field repelling force, make every electronic in nucleus and electronic integrated under the action of electric field force between different spin elliptical orbit plane respectively. Nucleus is located in the same focus of each electron spin elliptical orbit. Each electron spin elliptical orbit as repelling force between electric field, magnetic field lateral force, there will always be around their respective spin axis elliptical orbit additional rotation, rotating ellipsoid surface formation, which is the scientific community has been observed by experiment "s, p, d, f type electron hull shell".

2. Earth or other planets along the spin elliptical orbit around the sun when there is no spin quantum number $N_{\theta i}$ value problem, $N_{\theta i}$ value is 1. Each electron around the nucleus along the spin elliptical orbit, $N_{\theta i} \geq 1$ of is natural number or simple points.

3. Earth around the sun along the spin elliptical orbit, the speed is far less than the speed of light c, need not consider speed caused by the energy relativity quality effect. Electronic itself the wave speed of v_a to the speed of light, the spin velocity $v_{\theta i}$

also is much bigger than the planet, especially heavy atoms of inner electrons, the spin velocity $v_{\theta i}$ most close to 0.7 c. The spin velocity of its quality and electric field strength has significant energy relativistic effects.

4. Sun to the earth's gravity, for both qualities is the same, other planets influence each other lesser, and gravity size only with spin movement orbit of the earth around the sun is inversely proportional to the square of the radius. Nucleus of each electronic the nuclear field of gravity, because of the numerous electronic shielding effect, the comprehensive strength of electric field the charge coefficient Z_i is a fairly complex variables. Range between 1 ~ 5 times, will make the electric field force of multivariable functions.

Comprehensive the above features, will make the electron spin elliptical orbit is quite complicated, even serious deformation. Because of this, we have to atomic physics is divided into two parts: the first part discuss the energy under the condition of the relativistic electron spin elliptical orbit equations of motion, it can solve the atomic outer, outer electron spin elliptical orbit characteristics of atoms form, size, electronic gradually ionization or warp absorption and emission spectra of each level. "S, p, d, f type electron hull shell" forming principle; The second part discuss the energy under the condition of the relativistic electron spin elliptic orbit characteristics, the corresponding each level of X-ray energy calculation; It can solve the atomic inner K, L layer many combination electron orbital motion characteristics.

15.1.2 Is far lower than the speed of light under the condition of Electron spin elliptical orbit equations of motion

For light and heavy atoms of outer, outer single electronics, because spin speed is far less than the speed of light, so don't consider energy under the premise of the theory of relativity, to simplify the analysis. Pay by electronic rest mass m_{eo} on behalf of the low speed spin of electrons movement quality of m_e; At the same time, we

assume that the electronic integrated intensity of the electric charge coefficient Z_i is the same, or change is very small, within the permitted error; Don't consider the wave motion of electronic, when the electronic wave radius R_a and radius of nuclei are far smaller than the electron spin elliptical orbit radius R_θ, we could bring the electron and the nucleus as a two particles.

When electron around the nucleus along the elliptical orbit for spin, due to the effect of electric field force between attracts each other, the nucleus will be relatively electronic for weak movement. By theoretical mechanics that: electron spin movement should be equal to the quality of the quality $m_{eo}K_m$ said. $m_{eo}K_m=Mm_{eo}/(M+ m_{eo})$, M for the quality of the nucleus. K_m only the outer single atom electronic makes sense. In this paper, only the three kinds of hydrogen, helium and lithium atoms consider correction coefficient:

^1_1H：Km= 0.9994556793 ^4_2He：Km= 0.9998629254 ^7_3Li：Km= 0.9999218102

Other atoms or economical paired electrons K_m=1.

By book equations (1.2) and Newton's mechanics, coulomb's law, see figure 15.1, electron around the nucleus along the spin elliptical orbit equations of motion for:

$$\begin{cases} R_\theta = \dfrac{N_{\theta i} h}{2\pi m_{e0} K_m v_\theta} & (15.1-1) \\ m_{e0} K_m (\ddot{R}_\theta - R_\theta \dot{\theta}^2) = \dfrac{-Z_i e^2}{4\pi\varepsilon_0 R_\theta^2} & (15.1-2) \\ m_{e0} K_m (R_\theta \ddot{\theta} + 2\dot{R}_\theta \dot{\theta}) = 0 & (15.1-3) \end{cases}$$

To compared with equations (1.2), (15.1-1) - more than just a spin quantum number $N_{\theta i}$. Was neils Bohr atom spectrum model derived from the application of the quantum number in neutral departments, won the Nobel Prize for physics in 1922, its significance self-evident, here no longer. (15.1-2), (15.1 3) two type of learned

Newtonian mechanics and classical electrodynamics people know that law of universal gravitation is quoted to the coulomb's law within the atoms. (15.1-1) is the electronic in the nucleus and all other electronic integrated under the action of electric field force along the spin elliptical orbit, the quantization of momentum conservation equation. When momentum is constant, electronic and atomic nuclei, other electronic integrated electric field force along the spin of the resultant force will orbit radius pointing to the center of the nucleus. Equations is proved by the law of universal gravitation and (1.2), (15.1-1) type of momentum $N_\theta h$ for constant, so, (15.1-2), (15.1 3) type.

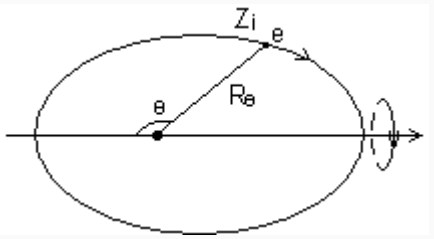

Figure 15.1 electron spin orbit around the nucleus

By (15.1 1), the electronic movement of the spin angular velocity $\dot{\theta}$ for:

$$\dot{\theta} = \frac{v_\theta}{R_\theta} = \frac{N_{\theta i} h}{2\pi m_{e0} K_m R_\theta^2} \qquad (15.2)$$

Make $R_\theta=1/u$, to $dR_\theta=-du/u^2$, generation into (15.2), to:

$$\dot{\theta} = \frac{N_{\theta i} h}{2\pi m_{e0} K_m} u^2 \qquad (15.3)$$

By figure 15.1, (15.3), electronic v_r ($\dot{R}_\theta$) of the radial velocity and acceleration a_r ($\ddot{R}_\theta$), respectively:

$$v_r = \frac{dR_\theta}{d\theta}\dot{\theta} = -\frac{N_{\theta i} h}{2\pi m_{e0} K_m}\frac{du}{d\theta} \qquad (15.4)$$

$$\alpha_r = -\frac{N_{\theta i} h}{2\pi m_{e0} K_m} \frac{du^2}{d\theta^2}\dot{\theta} = -\left(\frac{N_{\theta i} h}{2\pi m_{e0} K_m}\right)^2 u^2 \frac{du^2}{d\theta^2} \qquad (15.5)$$

To (15.4), (15.5) into (15.1-2) type checking:

$$\frac{du^2}{d\theta^2} + u = \frac{Z_i K_m}{N_{\theta i}^2 r_0} \quad (r_0 = \frac{h}{2\pi m_{e0} a_c c} \quad a_c = \frac{e^2}{2h\varepsilon_0 c}) \qquad (15.6)$$

Solution (15.6) decays differential equations:

$$R_\theta = \frac{N_{\theta i}^2 r_0}{Z_i K_m (1 + E_\theta \cos\theta)} \qquad (15.7)$$

This is everyone acquaint with of conical section line orbital motion equation. In all atoms, electronic by comprehensive electric field force is attractive, electronic ionization energy is negative, so,$0 \le E_\theta \le 1$, the equation says electronic along the spin elliptical orbits around the nucleus of the elliptic equations.

By (15.1 1), (15.2) and (15.7), electronic along radius direction, the spin direction and the tangent velocity v_{ri}, v_θ, v_{ei} respectively:

$$\begin{cases} v_{ri} = \dfrac{Z_i a_c c}{N_{\theta i}} E_{\theta i} \sin\theta & (15.8-1) \\ v_{\theta i} = \dfrac{Z_i a_c c}{N_{\theta i}} (1 + E_{\theta i} \cos\theta) & (15.8-2) \\ v_{ei} = \dfrac{Z_i a_c c}{N_{\theta i}} \sqrt{1 + 2E_{\theta i}\cos\theta + E_{\theta i}^2} & (15.8-3) \end{cases}$$

Subscript "$_i$" said electronic along different spin elliptical orbit, (the same below). Electronic along different spin elliptical orbit the kinetic energy of W_{mi}, from equations (15.8) and Newton's mechanics have to:

$$W_{mi} = \frac{m_{e0} K_m}{2}\left(\frac{Z_i a_c c}{N_{\theta i}}\right)^2 (1 + 2E_{\theta i}\cos\theta + E_{\theta i}^2) \qquad (15.9)$$

Electronic along the spin elliptical orbit, the nucleus and other electronic

integrated under the action of electric potential can W_{ei}, by Coulomb's law and (15.7), to:

$$W_{ei} = \frac{-Z_i e^2}{4\pi\varepsilon_0 R_{\theta i}} = -\left(\frac{Z_i a_c c}{N_{\theta i}}\right)^2 m_{e0} K_m (1 + E_{\theta i}\cos\theta) \qquad (15.10)$$

Atomic electric field outside or foreign energy under the action of an electronic ionization energy $\triangle W_{ei}$, apparently because of its kinetic energy and potential can be combined. By (15.9), (15.10), may (after convenient for calculation, we all take positive)

$$\Delta W_{ei} = \frac{m_{e0} K_m}{2}\left(\frac{Z_i a_c c}{N_{\theta i}}\right)^2 (E_{\theta i}^2 - 1) \qquad (15.11)$$

By (15.11), can see: electronic ionization energy only with spin comprehensive electric field of elliptic orbit charge intensity coefficient Z_i, spin quantum number of $N_{\theta i}$ and elliptical orbit parameters eccentricity of $E_{\theta i}$, and its position in orbit $R_{\theta i(\theta)}$ has nothing to do.

If we change a way of expression, by (15.7), to $\theta = 0, \pi$, the spin axis elliptical orbit A_θ is:

$$A_{\theta i} = \frac{N_{\theta i}^2 r_0}{\overline{Z}_i K_{mi}(1 - E_{\theta i}^2)} \quad (\overline{Z}_i \text{ for the spin track on the average}) \qquad (15.12)$$

Will type (15.12) into (15.11), to:

$$\Delta W_{ei} = m_{e0}(a_c c)^2 \frac{r_0 \overline{Z}_i}{2A_{\theta i}} \qquad (15.13)$$

Type shows that electronic ionization energy and comprehensive strength of electric field the charge only average coefficient of $\overline{Z}_i$ and elliptical orbit long axis $A_{\theta i}$, the nature of the law of universal gravitation and the same is familiar to most readers.

15.2 Rate of elliptical orbit centrifugal $E_{\theta i}$ solution

15.2.1 An electron transition in the process of energy conservation Principle

From particle physics sections in the book we have proved that the fluctuations of the photon, spin velocity is the speed of light. The photon wave particle duality characteristic, we can write P_γ photon momentum, energy and W_γ wavelength of λ formula:

$$\begin{cases} P_\gamma = \dfrac{h}{\lambda} & (15.14-1) \\ W_\gamma = \dfrac{hc}{\lambda} & (15.14-2) \end{cases}$$

In light of the characteristics of man-made earth satellite launch vehicles and orbit transfer, electronic by low-energy spin elliptical orbit to high orbit transfer must be along as shown in figure 15.2 the abc transfer of elliptical orbit, the energy utilization efficiency can be the biggest. In photonic and electronic collision point a, $\theta=0, Z_1=Z_a$, the spin velocity increment $\triangle v_e=\triangle v_\theta$. By the law of conservation of momentum, momentum and energy increment, (15.11) and (15.14) equations, we have:

$$\begin{cases} \dfrac{h}{\lambda} = m_{e0} K_m \Delta v_{\theta a} & (15.15-1) \\ \dfrac{h}{\lambda} R_{\theta a} = m_{e0} K_m (R_{\theta a} v_{\theta a} - R_{\theta 1} v_{\theta 1}) & (15.15-2) \\ \dfrac{hc}{\lambda} = \dfrac{1}{2} m_{e0} K_m (v_{\theta a}^2 - v_{\theta 1}^2) & (15.15-3) \\ \dfrac{hc}{\lambda} = \dfrac{m_{e0} K_m (Z_1 a_c c)^2}{2} \left(\dfrac{E_{\theta ac}^2 - 1}{N_{\theta ac}^2} - \dfrac{E_{\theta 1}^2 - 1}{N_{\theta 1}^2} \right) & (15.15-4) \end{cases}$$

Respectively simultaneous (15.15-1), (15.15-2) and (15.15 3), (15.15-4), (15.7) and (15.8) will be equations into, get the same results:

$$\frac{N_{\theta ac}^2}{1+E_{\theta ac}}=\frac{N_{\theta 1}^2}{1+E_{\theta 1}} \qquad (15.16)$$

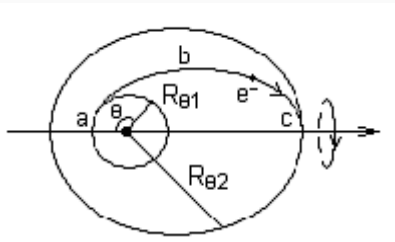

Figure 15.2 electronic excitation of transfer orbit

Along the abc electronic transfer orbit, to spin quantum number $N_{\theta abc}$ and centrifugal rate $E_{\theta abc}$ values are remain the same, at point c and orbit transfer, $\theta=\pi$, $Z_2=Z_c$ spin elliptical orbit radius should be equal, by (15.7), to:

$$\frac{N_{\theta ac}^2}{1-E_{\theta ac}}=\frac{N_{\theta 2}^2}{1-E_{\theta 2}} \qquad (15.17)$$

Simultaneous (15.16) and (15.17), to:

$$N_{\theta ac}=\frac{\sqrt{2}N_{\theta 1}N_{\theta 2}}{\sqrt{N_{\theta 1}^2(1-E_{\theta 2})+N_{\theta 2}^2(1+E_{\theta 1})}} \qquad (15.18)$$

Chapter 2 elementary particle formation principle of the internal structure and energy we have proved that the photon and neutrinos are composed of a pair of charged particles; Fluctuations, into orbit are cylindrical helical, velocity is the speed of light c; The difference is neutrinos are uhf electromagnetic field excitation is transformed into the photon. Electronic e^- consists of a pair of charged particles and a load of charged particles. In the process of stimulating step by step, only absorbs photon energy, not eventually increase their number of charged particles. When photons and electrons transfer orbit starting point in a collision, the photon will be not only their own momentum transfer to electronics, can adsorption on electronic, will own most of the energy transmitted to the electric and magnetic field, to increase the electron kinetic energy, into orbit transfer. When electronic run to orbit position c point

of instant, the residual energy photons will transfer again to electronics, their own at a very low energy of the photon or neutrinos form reverse jet leave, to keep the original number of charged particles. These two kinds of combination can improve the electronic spin speed, again to e- final orbit.

Below to hydrogen atoms in the electronic inspired by $N_{\theta 1} \rightarrow N_{\theta 2}$ process as an example, detailed analysis and orbit transfer in the process of spin elliptical orbit parameters change, do it more intuitive and clear.

15.2.2 Electronic excitation, transition in the energy Conservation calculation example

If the electrons within the atoms of hydrogen in the $N_{\theta 1}=1$ ground spin moving in elliptical orbit, the eccentricity of $E_{\theta 1}=0$, $Z_1=Z_l=1$ is constant. When electrons are high energy photon collision, one-time ionization, the spin track a parabola, the $N_{\theta 2}=\infty$, $E_{\theta 2}=1$, electronic ionization energy $\triangle W_e$, by (15.11), to:

$$\Delta W_{ei} = \frac{m_{e0} K_m}{2} (Z_l a_c c)^2 \left(\frac{E_{\theta 2}^2 - 1}{N_{\theta 2}^2} - \frac{E_{\theta 1}^2 - 1}{N_{\theta 1}^2} \right) \qquad (15.19)$$

The Km = 0.9994556793... Equivalent generation into (15.19), to $\triangle W_{ei}$ = 13.59829196 ev.

If electronic, between $N_{\theta l}=1 \sim 2$ first assume that $E_{\theta 1}=E_{\theta 2}=0$, by (15.15-4), electronic should absorption wavelength of the photon λ is:

$$\lambda = \frac{2hc}{m_{e0} K_m (Z_1 a_c c)^2 \left(\frac{E_{\theta 2}^2 - 1}{N_{\theta 2}^2} - \frac{E_{\theta 1}^2 - 1}{N_{\theta 1}^2} \right)} \qquad (15.20)$$

The $N_{\theta 1}=1$, $N_{\theta 2}=2$... ...Equivalent generation into (15.20), to: λ=1215.684489A°. The λ values into (15.14-2), the photon energy is obtained: W_γ=10.19871898 ev.

Will be λ value generation (15.15 1) in type, obtained the collision point of the electron spin velocity

increment:

$\triangle v_{\theta a}$=5986.633654m/s

By $N_{\theta 1}$=1, $N_{\theta 2}$=2，$E_{\theta 1}=E_{\theta 2}$=0, generation of (15.18) in type, too: $N_{\theta abc}$=1.264911064.

The $N_{\theta abc}$ values into (15.16), to: $E_{\theta abc}$=0.6.

From (15.8-2), electron spin in the collision point a speed increment for $\triangle v_{\theta a}$:

$$\Delta v_{\theta a} = Z_1 a_c c\left(\frac{1+E_{\theta ac}}{N_{\theta ac}} - \frac{1+E_{\theta 1}}{N_{\theta 1}}\right) \qquad (15.21)$$

The $E_{\theta abc}$, $N_{\theta abc}$ equivalent generation into (15.21), to $\triangle v_{\theta a}$ = 579543.6558 m/s.

It is (15.15 1) of the law of conservation of momentum and the velocity increment of 96.8 times. Similarly, by (15.15 3) type, too: electronic new kinetic energy $\triangle W_{ma}$ = 8.158975179 ev, is 1.5913 times of the former!

When electronic along the abc transfer orbit to point c, θ=π. By (15.8-2), the spin velocity $v_{\theta c}$ for:

$$v_{\theta c} = Z_1 a_c c\left(\frac{1-E_{\theta ac}}{N_{\theta ac}}\right) \qquad (15.22)$$

Will $E_{\theta abc}$=0.6, $N_{\theta abc}$=1.264911064 generation into (15.22), to: $v_{\theta c}$=691808.7631m/s. Similarly, by (15.22), to: orbit in the speed at point c $v_{\theta 2}$=1093845.698m/s, is $v_{\theta c}$ 1.58 times. So, electronic at point c to orbit transfer, still need to provide residual energy photon. By (15.15 3) type, is c at orbit transfer need energy for $\triangle W_{mc}$:

$$\Delta W_{mc} = \frac{1}{2} m_{e0} K_m (v_{\theta 2}^2 - v_{\theta c}^2) \qquad (15.22)$$

The $v_{\theta 2}$, $v_{\theta c}$ data into (15.23), to: $\triangle W_{mc}$=2.039743792ev, and was equal to the sum of the $\triangle W_{ma}$ (15.14-2) type in all the photon energy W_r. That the abc transfer orbit

energy utilization rate is 100%. (In the c of photons or neutrinos reverse jet out remaining low energy ignored).

Through analyzing the above calculation results, we have to the photon energy is divided into two parts: the first part is the kinetic energy of the photons, and electronic collision followed the momentum and the law of momentum conservation, behind the calculation that it will increase the electron spin elliptical orbit of centrifugal rate; Second part for electric and magnetic energy photon itself, most of the total energy, it will be attached to the electronic form, quality to provide an electron transfer process in the orbit at a, c and orbit transfer moment for the main kinetic energy.

(This section the following content of electronic spin elliptical orbit of centrifugal rate $E_{\theta i}$ derivation and calculation process is very complicated, relationship with the main content is not big, and readers can jump over it.)

In the scientific community existing experiment, testing level, also cannot be directly measured atomic internal each electron spin elliptical orbit radius of eccentricity of $E_{\theta i}$ and $R_{\theta i}$ ... ... Parameters such as. Book, therefore, at present only from electronic ground ionization energy $\triangle W_{eo}$ test value or absorption, emission spectrum energy W_{γ} , and by the law of conservation of energy, (15.11), (15.14-2), (15.15-4), to simulate calculation of each electron spin movement elliptical orbit of eccentricity of $E_{\theta i}$:

$$E_{\theta i}=\sqrt{1+N_{\theta i}^{2}\left[\frac{2h}{m_{e0}K_{mi}\lambda(Z_{t}a_{c})^{2}c}+\frac{E_{\theta 1}^{2}-1}{N_{\theta 1}^{2}}\right]} \qquad (15.24)$$

$N_{\theta 2}=2$ in the hydrogen atoms of $E_{\theta 2}$ value, the experimental value of λ=1215.68 A° generation in (15.24), to $E_{\theta 1}=0$, to, $E_{\theta 2}$= 0.003328476546

If the electronic transfer along the rail abc stimulated or Z_i a tiny change in the process of transition, is still by (15.11), (15.14-2), (15.15-4), the spin of electrons shillings quantum number $N_{\theta abc}$ is constant, only eccentricity of $E_{\theta a}\rightarrow E_{\theta c}$ tiny changes:

$$\begin{cases} \dfrac{hc}{\lambda} = \dfrac{1}{2} m_{e0} K_m (Z_1 a_c c)^2 \left[\dfrac{E_{\theta a}^2 - 1}{N_{\theta ac}^2} - \dfrac{E_{\theta 1}^2 - 1}{N_{\theta 1}^2} \right] & (15.25-1) \\ \dfrac{hc}{\lambda} = \dfrac{1}{2} m_{e0} K_m (a_c c)^2 \left[\left(\dfrac{Z_2}{N_{\theta ac}} \right)^2 (E_{\theta ac}^2 - 1) - \left(\dfrac{Z_1}{N_{\theta 1}} \right)^2 (E_{\theta 1}^2 - 1) \right] & (15.25-2) \end{cases}$$

Solution (15.25) equations have to:

$$E_{\theta c} = \sqrt{\left(\frac{Z_1}{Z_2} \right)^2 (E_{\theta a}^2 - 1) + 1} \qquad (15.26)$$

In transfer orbit at point a, photonic and electronic collision, by (15.16), (15.21), electron spins velocity increment $\triangle v_{\theta a}$ for:

$$\Delta v_{\theta a} = Z_1 a_c c \left(\frac{1 + E_{\theta 1}}{N_{\theta 1}} \right) \left(\frac{N_{\theta a}}{N_{\theta 1}} - 1 \right) \qquad (15.27)$$

By (15.15-1), (15.15-4) type, only the photon momentum collision impact on electron spin speed for:

$$\begin{cases} \dfrac{hc}{\lambda} = m_{e0} K_m \Delta v_{\theta a} c & (15.28-1) \\ \dfrac{hc}{\lambda} = \dfrac{1}{2} m_{e0} K_m (a_c c)^2 \left[\left(\dfrac{Z_2}{N_{\theta 2}} \right)^2 (E_{\theta 2}^2 - 1) - \left(\dfrac{Z_1}{N_{\theta 1}} \right)^2 (E_{\theta 1}^2 - 1) \right] & (15.28-2) \end{cases}$$

Simplified as:

$$\Delta v_{\theta a} = \frac{a_c^2 c}{2} \left[\left(\frac{Z_2}{N_{\theta 2}} \right)^2 (E_{\theta 2}^2 - 1) - \left(\frac{Z_1}{N_{\theta 1}} \right)^2 (E_{\theta 1}^2 - 1) \right] \qquad (15.29)$$

Simultaneous (15.27) and (15.29), to $\triangle N_{\theta a} = N_{\theta a} - N_{\theta}$, too:

$$\Delta N_{\theta a} = \frac{a_c \left[\left(\dfrac{Z_2 N_{\theta 1}}{N_{\theta 2}} \right)^2 (E_{\theta 2}^2 - 1) - Z_1^2 (E_{\theta 1}^2 - 1) \right]}{2 Z_1 (1 + E_{\theta 1})} \qquad (15.30)$$

Similarly, when the electron orbit at c, $\theta_2 = \pi$, a photon residual energy of electron spin elliptical orbit quantum number incremental $\triangle N_{\theta c}$, according to equations (15.28),

(15.27), to:

$$\begin{cases} \Delta v_{\theta c} = \dfrac{a_c^2 c}{2}\left[\left(\dfrac{Z_2}{N_{\theta 2}}\right)^2 (E_{\theta 2}^2 - 1) - \left(\dfrac{Z_1}{N_{\theta ac}}\right)^2 (E_{\theta ac}^2 - 1)\right] & (15.31-1) \\ \Delta v_{\theta c} = Z_2 a_c c\left(\dfrac{1-E_{\theta 2}}{N_{\theta 2}}\right)\left(1 - \dfrac{N_{\theta c}}{N_{\theta 2}}\right) & (15.31-2) \end{cases}$$

Solution (15.31) equations, the $\triangle N_{\theta c}=N_{\theta 2}-N_{\theta c}$ to:

$$\Delta N_{\theta c} = \frac{a_c\left[Z_2^2 (E_{\theta 2}^2 - 1) - \left(\dfrac{Z_1 N_{\theta 2}}{N_{\theta ac}}\right)^2 (E_{\theta ac}^2 - 1)\right]}{2Z_2(1-E_{\theta 2})} \qquad (15.32)$$

By (15.16), (15.17), because of the electron spin quantum number incremental $\triangle N_{\theta a}$, $\triangle N_{\theta c}$ to spin elliptical orbit centrifugal rate increment $\triangle E_{\theta a}$, $\triangle E_{\theta c}$ for:

$$\begin{cases} \Delta E_{\theta a} = \left[\left(\dfrac{N_{\theta a}}{N_{\theta 1}}\right)^2 - 1\right](1 + E_{\theta 1}) & (15.33-1) \\ \Delta E_{\theta c} = \left[1 - \left(\dfrac{N_{\theta c}}{N_{\theta 2}}\right)^2\right](1 - E_{\theta 2}) & (15.33-2) \end{cases}$$

Clearly:

$$E_{\theta 2}=E_{\theta 1}+\triangle E_{\theta a}+\triangle E_{\theta c} \qquad (15.34)$$

Detailed calculation procedure is as follows:

1. Shillings $N_{\theta 1}=1$, $N_{\theta 2}=2$, $E_{\theta 1}=E_{\theta 2}=0$, generation of (15.18) in type, find $N_{\theta abc}$values.

2. Will $N_{\theta abc}$ equivalent generation into (15.16), and $E_{\theta abc}$ values. When Z_a, Z_c change, by (15.26), respectively for $E_{\theta a}$, $E_{\theta c}$ values.

3. The related parameter generation into (15.30), (15.32), respectively, for $\triangle N_{\theta a}$, $\triangle N_{\theta c}$ values.

4. The values of $\triangle N_{\theta a}$, $\triangle N_{\theta c}$ generation in equations (15.33), and $\triangle E_{\theta a}$, $\triangle E_{\theta c}$,

again into (15.34), and $E_{\theta 2}$ values.

5. With $E_{\theta 2}$ values into (15.18), 1 ~ 4 calculation procedure, until the $E_{\theta 2}$ is constant value: $E_{\theta 2}$=0.00330554, and (15.24) by the experimental spectrum wavelength λ, direct calculation values of $E_{\theta 2}$.

By the incremental $E_{\theta 2}$, we can find a hydrogen atom stimulate the process step by step changes in the rate of spin elliptical orbit centrifugal, see section 16.1 calculation example. And we also see that a single electronic stimulate step by step in the process of changes in the rate of spin elliptical orbit centrifugal is quite complicated. We are all in the future to avoid such complicated calculations, directly through the experimental determination of the atoms in each level changes, by (15.11), (15.24), directly to find out the level of the elliptical orbit centrifugal rate.

15.3 atomic outer electron spin cycle

Correlation of elliptical orbit

By (15.12), electron spin elliptical orbit the half axis $A_{\theta i}$, short axis of $B_{\theta i}$, respectively:

$$\begin{cases} A_{\theta i} = \dfrac{N_{\theta i}^2 r_0}{\overline{Z}_i K_{mi}(1-E_{\theta i}^2)} & (15.35-1) \\ B_{\theta i} = \dfrac{N_{\theta i}^2 r_0}{\overline{Z}_i K_{mi}\sqrt{1-E_{\theta i}^2}} & (15.35-2) \end{cases}$$

The area of the elliptic S for:

$$S = \frac{1}{2}\oint R_{\theta i}^2 d\theta = \pi A_{\theta i} B_{\theta i} = \pi\left(\frac{N_{\theta i}^2 r_0}{\overline{Z}_i K_{mi}}\right)^2 (1-E_{\theta i}^2)^{-1.5} \qquad (15.36)$$

Electronic along the spin elliptical orbit the cycle of $T_{\theta i}$, by (15.1-1), (15.7), to:

$$T_{\theta i}=\frac{\oint R_{\theta i}d\theta}{v_{\theta i}}=\oint\frac{2\pi m_{e0}K_{mi}R_{\theta i}^2}{N_{\theta i}h}d\theta=\frac{4\pi m_{e0}K_{mi}}{2N_{\theta i}h}\oint R_{\theta i}^2d\theta \quad (15.37)$$

Will type (15.36) into (15.37), to:

$$T_{\theta i}=\frac{N_{\theta i}^3h}{(\overline{Z}_i a_c c)^2 m_{e0}K_{mi}(1-E_{\theta i}^2)^{1.5}} \quad (15.38)$$

Some adjacent two atoms in the outermost electrons along the orbit parameters of different orbits, the distance between their relative position, space is changing and will inevitably lead to their respective rotating elliptical orbit parameter changes of Z_i, $E_{\theta i}$, $R_{\theta i}$. In order to simplify the analysis and calculation, we can only work out their respective rotating elliptical orbit, the parameters of average. And assumptions, $\overline{Z}_i$, $\overline{E}_{\theta i}$, $\overline{R}_{\theta i}$ values are the same. Due to comprehensive interaction of electric field force, similar to particle fluctuations, spin elliptical orbit, maintain the condition of moving along the orbit between them is: the spin of electrons inside the elliptical orbit cycle $\overline{Z}_i$, $\overline{E}_{\theta i}N_{\theta i}$ must be outer electronic $T_{\theta 1}$ of $N_{1,2}$ times! $N_{1,2}$ for natural number or simple points.

By (15.38), to:

$$N_{1,2}=\left(\frac{N_{\theta 2}}{N_{\theta 1}}\right)^3\left(\frac{\overline{Z}_1}{\overline{Z}_2}\right)^2\frac{K_{m1}}{K_{m2}}\left(\frac{1-E_{\theta 1}^2}{1-E_{\theta 2}^2}\right)^{1.5} \quad (15.39)$$

To spin elliptical orbit half axis of $A_{\theta i}=\overline{R}_{\theta i}$, by (15.12), (15.39), to:

$$\begin{cases}\dfrac{\overline{Z}_2}{\overline{Z}_1}=\left(\dfrac{N_{\theta 2}}{N_{\theta 1}}\right)^2\dfrac{\overline{R}_{\theta 1}K_{m1}}{\overline{R}_{\theta 2}K_{m2}}\left(\dfrac{1-E_{\theta 1}^2}{1-E_{\theta 2}^2}\right) & (15.40-1)\\ \left(\dfrac{\overline{Z}_2}{\overline{Z}_1}\right)^2=\left(\dfrac{N_{\theta 2}}{N_{\theta 1}}\right)^3\dfrac{K_{m1}}{K_{m2}N_{1,2}}\left(\dfrac{1-E_{\theta 1}^2}{1-E_{\theta 2}^2}\right)^{1.5} & (15.40-2)\end{cases}$$

Solution (15.40) equations have to:

$$N_{1,2} = \left(\frac{\overline{R}_{\theta 2}}{\overline{R}_{\theta 1}} \right)^{1.5} \sqrt{\frac{\overline{Z}_1 K_{m2}}{\overline{Z}_2 K_{m1}}} \qquad (15.41)$$

$N_{1,2}$ is the key of the boundary constraints, the adjacent layer between electron spin elliptical orbit a quantization, is behind the atomic energy level and energy spectrum provides the basis for the key.

16 hydrogen, helium and lithium atoms internal structure model, the parameters, and the spectral energy calculation

16.1 hydrogen internal structure model, the spectrum level

16.1.1 Internal structure model of the hydrogen atom

Hydrogen atoms within only one electron, electronic integrated electric charge intensity coefficient Z_i = 1 is not a variable. Laboratory determination of hydrogen atom ionization energy $\triangle W_{e1}$=13.599ev, electronic form in proton peripheral "s type ball shell electron cloud".

By (15.7), (15.12), "s type ball shell electron cloud" the average radius of electron spin elliptical orbit of long axis $A_{\theta i}$ for:

$$A_{\theta i} = \frac{N_{\theta i}^2 r_0}{\overline{Z}_i K_{mi}(1 - E_{\theta i}^2)} \qquad (16.1)$$

To $N_{\theta 1}$=1, $\overline{Z}_1$=1, $E_{\theta 1}$=0, generation of (16.1) in type, too: $A_{\theta 1}$=5.294655×10^{-11}m .

Electronic protons along the spin elliptical orbit around the formation of magnetic U_h, by the principle of electrodynamics, (15.1-1) and (15.7), (15.8-2), to:

$$U_h = IS = \frac{eh}{4\pi m_{e0} K_{mi}} \qquad (16.2)$$

The K_{mi}... ...Equivalent generation goes into: U_h = 9.279066276 x10^{-24} j/T.

Under the action of hydrogen atom or external electric field outside the photon collision, electron spin quantum number $N_{\theta i}$= 1, 2, 3, 4... Stimulate increase gradually, electronic gradually absorb certain wavelengths of energy photon gradually inspire ionization, by (15.20), to each level of the spin elliptical orbit of eccentricity of $E_{\theta i}$ = 0,

we can export was neils Bohr hydrogen atom absorption spectrum model:

$$\lambda = \frac{2h}{m_{e0} K_{mi} a_c^2 c \left(\frac{1}{N_{\theta 1}^2} - \frac{1}{N_{\theta 2}^2} \right)} \qquad (16.3)$$

The $\frac{1}{\lambda} = 10967758.04 \left(\frac{1}{N_{\theta 1}^2} - \frac{1}{N_{\theta 2}^2} \right) m^{-1}$, is everyone acquaint with of Rydberg constant ".

16.1.2 Hydrogen atom spectrum energy calculation

By (16.3), to $N_{\theta i}$ = 1, 2, 3, 4... , we can find out a hydrogen atom in electronic between each level spin elliptical orbit gradually stimulated and transition when the wavelength of the absorption and emission spectrum, see table 16.1 B.

Hydrogen wavelength spectrum calculation results comparison (A °) table 16.1

$N_{\theta i}$	λ_{1-i}	λ_{2-i}	λ_{3-i}	λ_{4-i}	λ_{5-i}
2	A：1215.68 B：1215.684 C：1215.680				
3	A：1025.73 B：1025.734 C：1025.728	6562.79 6564.696 6562.760			
4	A：972.54 B：972.548 C：972.541	4861.33 4862.738 4861.374	18751.1 18756.275 18751.562		
5	A: B: C:	4340.47 4341.730 4340.486	12818.1 12821.672 12818.687	40500 40522.816 40505.555	
6	A: B: C:	4101.74 4102.935 4101.725	10938 10941.160 10938.571	26250 26258.785 26248.747	74000 74598.821 74045.421
7	A: B: C:	3970.07 3971.236 3970.034			

From the data in table 16.1 compared to: Neils Bohr atom spectrum model has

high accuracy, but on the whole is greater than the determination of the wavelength. By section 15.2 of the hydrogen atoms in the electronic and orbit transfer process parameter calculation and analysis can be seen that: small errors are caused by changes in the rate of spin elliptical orbit centrifugal.

Explanation: A line is the determination of wavelength; B was Neils Bohr model calculated value, C line model to calculate the book value.

By (15.24) and the experimental determination of the hydrogen atoms in the λ_i level spectral wavelengths, we can directly get the electronic stimulate ionization step by step in the process of spin elliptical orbit eccentricity of $E_{\theta i}$ values, in table 16.2 A. With section 15.2 the last out of the hydrogen atoms in the original eccentricity of incremental $\triangle E_{\theta i}$ in the following relationship: see table 16.2 C.

Hydrogen atoms in the electron spin elliptical orbit changes in the rate of centrifugal table ($E_{\theta 1} = 0$) table 16.2

$N_{\theta i}$	$E_{\theta i}$				
	$(N_{\theta i}-1)\triangle E_\theta$	$3(N_{\theta i}-1)\triangle E_\theta$	$(2N_{\theta i}-3)\triangle E_\theta$	$2N_{\theta i}-4)\triangle E_\theta$	$3N_{\theta i}\triangle E_\theta$
2	A：0.003328476 5 B: C：0.003305540 3				
3	A：0.005435379 5 B: C：0.006611080 6	0.019697843 0.019833242			
4	A：0.010820727 B: C：0.009916621	0.030218982 0.029749863	0.016345480 0.016527701		
5	A: B: C：0.013222161	0.039920633 0.039666483	0.024031726 0.023138782	0.02235718 0.019833242	
6	A: B: C:	0.049302363 0.049583 10	0.031384513 0.029749863	0.02611092 0.026444322	0.061743872 0.059499725
7	A: B: C:	0.058649886 0.059499725			

By the C line as shown in the table 16.2 $E_{\theta i}$ a revised, and the type (15.20), and a hydrogen atom in electronic stimulate step by step in the process of absorption wavelength, see table 16.1 C, its precision is higher than neils Bohr atom spectrum model.

In fact, like nuclear internal parameter calculation, the hydrogen atom electronic magnetic energy continues to exist. So in the electronic energy level transition should be considered in the process of the change of magnetic energy. For interested readers simulated calculation.

16.2 Helium atoms in internal structure model

The spectrum level

16.2.1 Helium atoms in internal structure model

According to the results of laboratory detection of helium atoms, there are two helium atoms in electronics, forming a layer "s type ball shell electron cloud". The primary and secondary ionization energy are only one, $\triangle W_{e1}$ = 24.587ev, $\triangle W_{e2}$ = 54.416ev. Electronic in each level track stimulated or transition in the process of absorption and emission spectra of wavelength in table 16.3 to 6, (3) (the same below).

Through comparative analysis, helium atoms in the spatial distribution of two electron spin elliptical orbit must be shown in figure 16.1. To maintain two electrons between the nucleus and comprehensive electric field force, centrifugal force balance, they must each take a level, and the parameters are the same and nuclear symmetry in the center of the spin, lateral rotation ellipsoid surface of orbit. While two paired electrons into the quality coefficient K_m=1. By coulomb's law, every electron in another electronic and atomic nucleus under the action of electric field force, the average

charge intensity coefficient $\overline{Z}_i$ is:

$$\frac{\overline{Z}_i e^2}{4\pi\varepsilon_0 \overline{R}_{\theta i}^2} = \frac{2e^2}{4\pi\varepsilon_0 \overline{R}_{\theta i}^2} - \frac{e^2}{4\pi\varepsilon_0 (2\overline{R}_{\theta i})^2} \tag{16.4}$$

Solution (16.4), to: $\overline{Z}_i$ = 1.75. When an electron completely, remaining another electronic, $\overline{Z}_i$ = 2.

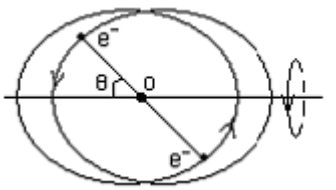

Figure 16.1 helium atoms in paired electron spin orbit constitution diagram

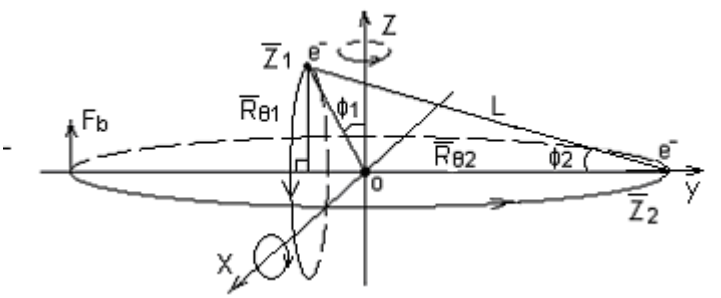

Figure 16.2 helium atom excitation process electron spin orbit constitution diagram

When helium atoms in the first electronic gradually ionization, because another electronic and atomic nucleus the interaction of electric field force and two electron spin elliptical orbit must be shown in 16.2 the spatial distribution of orbit to maintain balance. (Spatial distribution of the electron, shown in figure 16.2 is based on the determination of atomic outer "probability" a "s, p, d, f" type of the specific shape to speculate, same as follows.) Z_1 electron spin momentum vector pointing in the direction of the Y axis, the Z_2 electronics, nucleus under the action of electric field force, spin elliptical orbit plane attach around the Z axis rotation. Similarly, Z_2 electronic in Z_1, nuclear electric power, electron spin elliptical orbit form under the magnetic force,

attach of lateral movement and the XOY orbital plane, swinging. Combination to make Z_1, Z_2 electron spin elliptical orbit plane in vertical condition each other and rotates on the X axis additional together. Superposition movement result is two layer "s type ball shell electron cloud". By (15.41), two layers of electron spin elliptical orbit cycle $T_{\theta 1}$, $T_{\theta 2}$ should also exist between multiple $N_{1,2}$ the relationship between.

When helium atoms in the first electronic gradually ionization, because another electron and the nucleus of the electric field force based on the analysis of the above, if we consider the original wave motion; Inner and outer two electrons along their respective elliptical orbit to different position, the spin track radius change, each other space position change; Due to their comprehensive electric charge strength coefficient of Z_1, Z_2 complex changes and the periodicity of elliptical orbit deformation. The reader imagine not hard, electronic movement track, complex to what extent! So, we can only seize the main electronic along the motion law of elliptical orbit, the spin elliptical orbit cycle $T_{\theta 1}$, $T_{\theta 2}$ between multiple $N_{1,2}$ relationship, with average parameters $\overline{Z}_i$, $\overline{R}_{\theta i}$, $E_{\theta i}$, simplify the value simulation analysis and calculation. Back to all of the illustrations in chapter 18, for drawing convenient, intuitive, on the chart we paired electrons to $R_{\theta i(\pi)}$ value for $\overline{R}_{\theta i}$ value, please pay attention to identify readers.

By (15.7), (15.12), electron spin elliptical orbit the average radius of $\overline{R}_{\theta i}$ and average charge strength coefficient of $\overline{Z}_i$, relationship is:

$$\overline{R}_{\theta i} = \frac{N_{\theta i}^2 r_0}{\overline{Z}_i K_{mi}(1 - E_{\theta i}^2)} \qquad (16.5)$$

According to Newton's mechanics, coulomb's law, as shown in figure 16.2, two electrons between the nucleus and the balance of the electric field force interaction relationship, we have:

$$\begin{cases} L=\sqrt{\overline{R}_{\theta 1}^2+(\overline{R}_{\theta 2}+\overline{R}_{\theta 1}tg\phi_1)^2} & (16.6-1) \\ \dfrac{\overline{Z}_1e^2}{4\pi\varepsilon_0\overline{R}_{\theta 1}^2}=\dfrac{2e^2\cos^3\phi_1}{4\pi\varepsilon_0\overline{R}_{\theta 1}^2}-\dfrac{e^2\sin\phi_2}{4\pi\varepsilon_0L^2} & (16.6-2) \\ \dfrac{\overline{Z}_2e^2}{4\pi\varepsilon_0\overline{R}_{\theta 2}^2}=\dfrac{2e^2}{4\pi\varepsilon_0\overline{R}_{\theta 2}^2}-\dfrac{e^2\cos\phi_2}{4\pi\varepsilon_0L^2} & (16.6-3) \\ \dfrac{2e^2\cos^2\phi_1}{4\pi\varepsilon_0\overline{R}_{\theta 1}^2}\sin\phi_1=\dfrac{2e^2}{4\pi\varepsilon_0\overline{R}_{\theta 2}^2} & (16.6-4) \end{cases}$$

Of simplifying the equations (16.6):

$$\begin{cases} \overline{Z}_1=2\cos^3\phi_1-\left[1+\left(\dfrac{\overline{R}_{\theta 2}}{\overline{R}_{\theta 1}}+tg\phi_1\right)^2\right]^{-1.5} & (16.7-1) \\ \overline{Z}_2=2-\left(1+\dfrac{\overline{R}_{\theta 1}}{\overline{R}_{\theta 2}}tg\phi_1\right)\left[\left(\dfrac{\overline{R}_{\theta 1}}{\overline{R}_{\theta 2}}\right)^2+\left(1+\dfrac{\overline{R}_{\theta 1}}{\overline{R}_{\theta 2}}tg\phi_1\right)^2\right]^{-1.5} & (16.7-2) \\ \dfrac{\overline{R}_{\theta 2}}{\overline{R}_{\theta 1}}=\dfrac{1}{\cos\phi_1\sqrt{\sin\phi_1}} & (16.7-3) \end{cases}$$

Will type (15.41) and (16.7) into the equations:

$$\frac{1}{(\sin\phi_1)^{1.5}N_{1,2}^2}=\frac{2\left[1+\sin\phi_1+2(\sin\phi_1)^{1.5}\right]^{1.5}-\left[1+(\sin\phi_1)^{1.5}\right]}{2\left[1+\sin\phi_1+2(\sin\phi_1)^{1.5}\right]^{1.5}-(\sin\phi_1)^{1.5}} \quad (16.8)$$

By (16.5), the adjacent two electrons spin elliptical orbit average radius ratio of $\overline{R}_{\theta 2}/\overline{R}_{\theta 1}$ for:

$$\frac{\overline{R}_{\theta 2}}{\overline{R}_{\theta 1}}=\left(\frac{N_{\theta 2}}{N_{\theta 1}}\right)^2\frac{\overline{Z}_1K_{m1}}{\overline{Z}_2K_{m2}}\left(\frac{1-E_{\theta 1}^2}{1-E_{\theta 2}^2}\right) \quad (16.9)$$

Combined with equations (16.7), we can estimate (16.8) - the $N_{1,2}$ value scope, to prepare for the subsequent simulation. Similarly, by (16.9), but also can be used to deduce $E_{\theta 2}$ and $N_{\theta 2}$ would equation parameters such as:

$$E_{\theta 2}=\sqrt{1-\left(\frac{N_{\theta 2}}{N_{\theta 1}}\right)^2\frac{\overline{Z}_1K_{m1}}{\overline{Z}_2K_{m2}}\frac{\overline{R}_{\theta 1}}{\overline{R}_{\theta 2}}(1-E_{\theta 1}^2)} \quad (16.10)$$

By the law of conservation of energy, (15.11), (15.25-2), (16.3), an electron spin quantum number from $N_{\theta a} \rightarrow N_{\theta c}$ would inspire change process, absorb the energy of the photon $\triangle W_\gamma$ should be equal to the two each electronic total ionization energy in the atomic energy level of the poor:

$$\Delta W_\gamma = \sum \Delta W_{eia} - \sum \Delta W_{eic} \qquad (16.11)$$

Absorb the wavelength of the photon $\lambda_{a\sim c}$ for:

$$\lambda_{a-c} = \frac{hc}{e\left(\sum \Delta W_{eia} - \sum \Delta W_{eic}\right)} \qquad (16.12)$$

16.2.2 Helium atom spectrum energy calculation

To sum up, the helium atoms in electron spin elliptical orbit parameters and absorption wavelength calculation procedure is as follows:

1 Determined by the laboratory of helium atoms in the first and second sum of ionization energy, as the original total ionization energy: $\sum \Delta W_{e0}$ = 79.003ev. Make K_{m1} = 1, $\overline{Z}_1$ = 1.75, $N_{\theta 1}$ = 1, see figure 16.1, the generation of (15.11) in type, calculate electron spin elliptical orbit of original centrifugal rate: $E_{\theta 0}$= 0.227995205.

2. Will the above parameters in (15.7) and (15.12), to θ=0, π, have "s type ball shell electron cloud" the inner and outer radius of $R_{\theta 1(0)}$, $R_{\theta 1(\pi)}$, average radius $\overline{R}_{\theta 1}$ and the thickness of the $\triangle R_{\theta 1}=R_{\theta 1(\pi)} - R_{\theta 1(0)}$is respectively:

$R_{\theta 1(0)}$=0.2462A° $R_{\theta 1(\pi)}$=0.3917A° $\overline{R}_{\theta 1}$=0.3190A° $\triangle R_{\theta 1}$=0.1455A°

(the data significantly less than the value $R_{\theta 1(\pi)}$=1~ 1.1 A°, its reason is that most of the atomic radius is compound or mass calculation of the proportion of liquid or solid, atoms between outer electron spin elliptical orbit or "probability" has different degree of overlap, helium atoms are inert gases, not combined with other atoms, and is in cryogenic liquid state, "s type ball shell electron cloud" the edge of the display with the

number of the negative electric field can also prevent between helium atoms in near further, to the experimental value bigger).

3. When an electron from the start to completely ionization, the average charge intensity coefficient for inner electronic $\overline{Z}_1$ =1.75→2. Make K_{m1} = 0.9998629254, $N_{\theta 1}$=1, $\overline{Z}_1$ =2, $E_{\theta 1}$=0, generation into (15.11), is the inner electronic ionization energy for: $\triangle W_{e1}$ = 54.41533133 ev, still less than the value of 54.416 ev. So, in helium atoms in outer electronic ionization process step by step, the inner electron spin elliptical orbit changes in the rate of the centrifugal by $E_{\theta 0}$→0.

(4) From (16.9), (15.41), to $E_{\theta 1}$=$E_{\theta 2}$=0 , $N_{\theta 1}$=1, $N_{\theta 2}$=2, $\overline{Z}_1$ =1.95, $\overline{Z}_2$ =1, generation to estimate are: $N_{1,2}$ = 30.42, by the same token, if to $\overline{Z}_1$ =2, $\overline{Z}_2$ =1, the $N_{1,2}$ = 32.

5. Take the $N_{1,2}$ = 31, generation of (16.8) in type, too: Φ_1= 0.916733834°, the value generation to equations (16.7) are: $\overline{Z}_1$ = 1.997268498, $\overline{Z}_2$ = 1.027369561.

6. Will $\overline{R}_{\theta 2}/\overline{R}_{\theta 1}$, $\overline{Z}_i$, $N_{\theta i}$ equivalent generation into (16.10), calculate $E_{\theta 2}$ = 0.1285330284.

7. Will, NAA would, $\overline{Z}_i$, $N_{\theta i}$, E_{θ} equivalent generation into (15.11), calculates the helium atoms excited states of the atomic energy level always ionization energy:

$$\sum \Delta W_{eic} = 57.79716452 ev$$

8. Make $\sum \Delta W_{eia}$ =79.003ev, will $\sum \Delta W_{eic}$ = 57.79716452ev together into (16.12), to: λ_{a-c} = 584.670A°, 584.3A° comparison with experimental data, A little big.

9. Adjust the scope of the $E_{\theta 1}$ repeat 6 ~ 8 calculation procedure, finally: when the $E_{\theta 1}$= 0.01525,

$E_{\theta 2}$=0.129419704 $\sum \Delta W_{eic}$ =57.78372307ev λ_{a-c}=584.300A°

10. Similarly, to $N_{\theta 2}$= 1.5,2.5,3,4,5,6,N1,2 = 11,62,108,256,500and864,respectively, repeat4 ~ 9calculationprocedure,wecan findoutthe heliumatomsallfarultravioletspectralwavelengths,shownin table16.3.

Helium atoms far ultraviolet wavelength spectrum calculation results table (A°) 16.3

$N_{\theta 1}$	$N_{\theta 2}$	$N_{1,2}$	$E_{\theta 1}$	$E_{\theta 2}$	$\sum \Delta W_{eic}$ ev	calculated λa -- cA°	Experimental λ_{a-c}A°
	1.5	11	0.198890	0.2350068249	58.03846134	591.400	591.4
1	2	31	0.01525	0.129419704	57.78372307	584.300	584.3
	2.5	62	0.101903	0.1390334447	55.99608629	538.900	538.9
	3	108	0.0105	0.08235517544	55.91469054	537.000	537.0
1	4	256	0.0088	0.04610406155	55.26032413	522.200	522.2
	5	500	0.0072	0.02962118787	54.95639484	515.600	515.6
	6	864	0.005	0.02048134594	54.79176748	512.094	

Note: due to limited experimental data collected $N_{\theta 2}$ > 6 of calculation (same below).

Helium atoms in part of the visible spectrum wavelength the results table (A°) 16.4

$N_{\theta 1}$	$N_{\theta 2}$	$N_{1,2}$	$E_{\theta 1}$	$E_{\theta 2}$	$\sum \Delta W_{eic}$ ev	calculated λa -- cA°	Experimental λ_{a-c}A°
	1.5	11	0.19889	0.2350068249	58.03846134		
1	3	107	0.0057	0.02474674815	55.92832058	5875.639	5875.6
	4	256	0	0.04525818282	55.26460382	4469.741	4471.6
	5	500	0	0.02873356175	54.95924392	4026.486	4026.2
	2	31	0.01525	0.129419704	57.78372307		
1	3	107	0.00732	0.02516906259	55.92714088	6678.091	6678.1
	4	256	0	0.04525818282	55.26460382	4921.730	4921.9
	5	500	0	0.02873356175	54.95924392	4389.632	

11. The table 16.3, respectively to: $N_{\theta 2a}$ = 1.5, 2, $\sum \Delta W_{eia}$ =58.03846134 ev, 57.78372307 ev, $N_{\theta 2}$ = 3, 4, and 5, respectively, repeat 4 ~ 9 calculation procedures, can be a part of the visible spectrum, shown in table 16.4.

Helium atoms in a couple of far infrared wavelength spectrum calculation results table (A°) in table 16.5

$N_{\theta 1}$	$N_{\theta 2}$	$N_{1,2}$	$E_{\theta 1}$	$E_{\theta 2}$	$\sum \Delta W_{eic}$ ev	calculated λa -- cA°	Experimental λ_{a-c}A°

	2.5	62	0.101903	0.139033447	55.99608629		
	3	107	0.00448	0.024494675 88	55.92901521	184854.99	184859.06
1	3	107	0.01078	0.026383164 95	55.92363819	171135.27	171129.148
	3	107	0.01149	0.026680965 56	55.92275384	169071.47	169082.189
	3	107	0.01241	0.027089650 64	55.92152405	166282.89	166271.70
	3	107	0.01441	0.028061683 21	55.91852396	159851.11	159850.318

Helium atoms in surplus visible spectroscopy and infrared wavelength calculation results table (A°) 16.6

$N_{\theta 1}$	$N_{\theta 2}$	$N_{1,2}$	$E_{\theta 1}$	$E_{\theta 2}$	$\sum \Delta W_{eic}$ ev	calculated λa -- cA°	Experimental λ_{a--o}A°
	2	31	0.015 25	0.129 419 704	57.78372303		
	2	42	0.0205	0.431 957 741 9	57.18142959	20585.354	20582.0
	2	59	0.0168	0.587 643 035	56.6389549	10830.511	10830.3
1	2	92	0.0119	0.713 861 862	56.08096694	7281.386	7281.3
	2	97	0.0067	0.725 447 722	56.02899709	7065.733	7065.7
	3	229	0.0066	0.628 954 029 2	55.32752142	5047.804	5047.7
	4	316	0.0024	0.363 745 375	55.15327507	4713.427	4713.4
	7	1694	0	0.362 294 421 9	54.65653834	3964.724	3964.7
	8	2628	0	0.391 448 121 5	54.59532809	3888.610	3888.6

12. The table 16.3, the $N_{\theta 2a}$=2.5, $N_{\theta 2}$=3, $N_{1,2}$=107, $\sum \Delta W_{eia}$ =55.99608629ev, repeat 5 ~ 9 calculation procedures, can get the helium atoms in a few far infrared spectral wavelengths, shown in table 16.5.

13. The table 16.4, the $N_{\theta 2a}$=2, $\sum \Delta W_{eia}$ = 57.78372307 ev, $N_{\theta 2}$= 2, 3, 4, 7, 8, $N_{1,2}$=42, 59, 92, 97, 229, 316, 1694, 2628, respectively, repeat 4 ~ 9 calculation procedures, can get the helium atoms surplus visible spectroscopy and infrared wavelength, shown in table 16.6.

16.3 lithium atoms internal structure model

The spectrum level

16.3.1 Lithium atoms internal structure model

By experimental detection: lithium atoms by two layer "s type ball shell electron

cloud". A total of three electronics, level 3 ionization energy, respectively, 5.392, 75.638 and 122.451 ev. Atomic radius of 1.5 ~ 1.6 A°, atomic absorption and emission spectra of the two-level wave table 16.8 ~ 16.11.

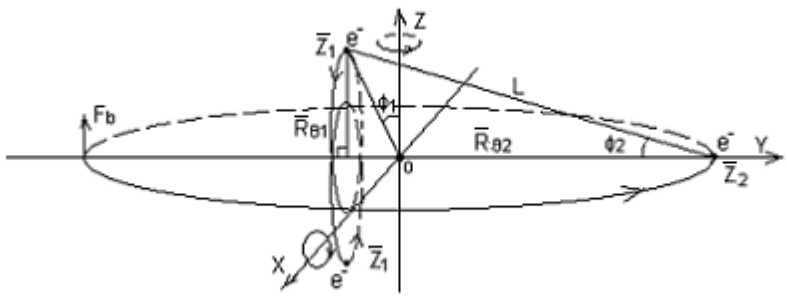

Figure 16.3 of lithium atom in electron spin combination with elliptical orbit

According to figure 16.2 helium atoms ionization step by step in the process of electron spin elliptical orbit combination model of lithium atom in three electronic should be in 16.3 the spin of the elliptical orbit combination model can be in a state of stable movement. Similarly, various electric and magnetic field between the electronic interactions will lead to additional rotation and lateral movement, comprehensive superposition result is rotating ellipsoid surface combination of two layer "s type ball shell electron cloud".

According to Newton's mechanics and Coulomb's law, we have:

$$\begin{cases} L = \sqrt{\overline{R}_{\theta 1}^2 + (\overline{R}_{\theta 2} + \overline{R}_{\theta 1} tg\phi_1)^2} & (16.13-1) \\ \dfrac{\overline{Z}_1 e^2}{4\pi\varepsilon_0 \overline{R}_{\theta 1}^2} = \dfrac{3e^2 \cos^3\phi_1}{4\pi\varepsilon_0 \overline{R}_{\theta 1}^2} - \dfrac{e^2}{4\pi\varepsilon_0 (2\overline{R}_{\theta 1})^2} - \dfrac{e^2 \sin\phi_2}{4\pi\varepsilon_0 L^2} & (16.13-2) \\ \dfrac{\overline{Z}_2 e^2}{4\pi\varepsilon_0 \overline{R}_{\theta 2}^2} = \dfrac{3e^2}{4\pi\varepsilon_0 \overline{R}_{\theta 2}^2} - \dfrac{2e^2 \cos\phi_2}{4\pi\varepsilon_0 L^2} & (16.13-3) \\ \dfrac{2\times 3e^2 \cos^2\phi_1}{4\pi\varepsilon_0 \overline{R}_{\theta 1}^2} \sin\phi_1 = \dfrac{3e^2}{4\pi\varepsilon_0 \overline{R}_{\theta 2}^2} & (16.13-4) \end{cases}$$

Simplified as:

$$\begin{cases} \overline{Z}_1 = 3\cos^3\phi_1 - \dfrac{1}{4} - \left[1+\left(\dfrac{\overline{R}_{\theta 2}}{\overline{R}_{\theta 1}} + tg\phi_1\right)^2\right]^{-1.5} & (16.14-1) \\ \overline{Z}_2 = 3 - 2\left(1+\dfrac{\overline{R}_{\theta 1}}{\overline{R}_{\theta 2}}tg\phi_1\right)\left[\left(\dfrac{\overline{R}_{\theta 1}}{\overline{R}_{\theta 2}}\right)^2 + \left(1+\dfrac{\overline{R}_{\theta 1}}{\overline{R}_{\theta 2}}tg\phi_1\right)^2\right]^{-1.5} & (16.14-2) \\ \dfrac{\overline{R}_{\theta 2}}{\overline{R}_{\theta 1}} = \dfrac{1}{\cos\phi_1\sqrt{2\sin\phi_1}} & (16.14-3) \end{cases}$$

Will type (15.41) and (16.14) into the equations, because of $K_{m1} = 1$, so:

$$\frac{K_{m2}}{(2\sin\phi_1)^{1.5}N_{1,2}^2} = \frac{3\left[1+2\sin\phi_1+(2\sin\phi_1)^{1.5}\right]^{1.5} - \left[2+(2\sin\phi_1)^{1.5}\right]}{\left(3-\dfrac{1}{4\cos^3\phi_1}\right)\left[1+2\sin\phi_1+(2\sin\phi_1)^{1.5}\right]^{1.5} - (2\sin\phi_1)^{1.5}}$$

(16.15)

By (16.9), (15.41), inside and outside two layers adjacent electron spin elliptical orbit cycle multiple $N_{1,2}$ the relationship between is:

$$N_{1,2} = \left(\frac{N_{\theta 2}}{N_{\theta 1}}\right)^3\left(\frac{\overline{Z}_1}{\overline{Z}_2}\right)^2\frac{K_{m1}}{K_{m2}}\left(\frac{1-E_{\theta 1}^2}{1-E_{\theta 2}^2}\right)^{1.5} \quad (16.16)$$

16.3.2 Lithium atom spectrum energy calculation

To sum up, with reference to the helium atoms in electron spin elliptical orbit parameters and spectrum energy wave calculation method of lithium atom in the spectrum level wavelength calculation procedure is as follows:

1. When lithium atoms outer electrons completely, the inner two electron spin elliptical orbit combination with helium atoms. By (16.4): $\overline{Z}_1 = 2.75$.

2. By the second and third electronic ionization energy sum $\sum \Delta W_e = 198.089$ ev, to $N_{\theta 1} = 1$, $K_{m1} = 1$, $\overline{Z}_1 = 2.75$, and into the (15.11), to: $E_{\theta 1} = 0.1934005519$.

3. The outer electronic ionization process, step by step to the inner of electron

spin elliptical orbit parameters influence is small; we can put them as the basis for proper adjustment.

4. Make $N_{\theta 1}$= 1, $N_{\theta 2}$= 1.5, $E_{\theta 1}$= 0.1934005519, $E_{\theta 2}$=0, $\overline{Z}_1$ =2.75, $\overline{Z}_2$ =1, K_{m1}=1, K_{m2}=0.9999218102, generation of (16.16) in type, too: $N_{1,2}$= 24.1068.

5. Take the $N_{1,2}$ = 24, generation of (16.15) in type, too: Φ_1 = 0.768043708°. Will Φ_1 value generation to equations (16.14) is: $\overline{R}_{\theta 2}/\overline{R}_{\theta 1}$ =6.107997833. $\overline{Z}_1$=2.745000742, $\overline{Z}_2$ =1.085882032.

6. Will $N_{\theta i}$, $E_{\theta 1}$, $\overline{Z}_i$, K_{mi} equivalent generation into (16.10), to: $E_{\theta 2}$ = 0.321806274.

7. Will $N_{\theta i}$, $E_{\theta i}$, $\overline{Z}_i$ and K_{mi} parameters respectively into (15.11) is the total ionization energy: $\sum \Delta W_{eia}$ = 203.7607675 ev, compared with the experimental value $\sum \Delta W_{eia}$ = 203.481 ev, slightly bigger.

8. The fine-tuning $E_{\theta 1}$ scope, repeat 6 ~ 7 calculation procedure, finally: when $E_{\theta 1}$=0.1967877968, $E_{\theta 2}$= 0.3237130035, $\sum \Delta W_{eia}$ =203.481 ev.

9. By (15.7), (15.12), respectively to θ=0, π, lithium atoms in electron spin elliptical orbit inside and outside radius and average radius, respectively:

$R_{\theta 1(0)}$=0.1611A° $R_{\theta 1(\pi)}$=0.2400A° $\overline{R}_{\theta 1}$ =0.2005A°

$R_{\theta 2(0)}$=0.8284A° $R_{\theta 2(\pi)}$=1.6215A° $\overline{R}_{\theta 2}$ =1.2249A°

Of course, if we change $N_{1,2}$ the scope of, also can find the corresponding spin elliptical orbit parameters, but atomic radius with the experimental value difference is bigger, shown in table 16.7.

Lithium atoms in electron spin elliptical orbit parameters calculation results table (R_θ units: A°) table 16.7

$N_{1,2}$	20	22	23	24	27
$E_{\theta 1}$	0.2039826921	0.200206942	0.198456041	0.1967877968	0.1922230755
$E_{\theta 2}$	0.1416428756	0.2542468475	0.2919388194	0.3237130035	0.3975299812
$\overline{Z}_1$	2.742886747	2.744081026	2.7445696	2.745000742	2.746028199
$\overline{Z}_2$	1.108166703	1.09592591	1.090665912	1.085882032	1.073844193
$R_{\theta 2(0)}$	0.9412	0.8663	0.8451	0.8284	0.7934
$R_{\theta 2(\pi)}$	1.2518	1.4569	1.5419	1.6215	1.8405
$\overline{R}_{\theta 2}$	1.0965	1.1616	1.1935	1.2249	1.3170
Note	The experiment $R_{\theta 2(\pi)}$ = 1.5-1.6A°. So, $N_{1,2}$ = 23,24 the two groups data can be used				

10. The $N_{\theta 2}$=2, $\overline{Z}_1/\overline{Z}_2$ =2.75, $E_{\theta 2}$=0, $E_{\theta 1}$=0.1935, the generation of (16.16) in type, too: $N_{1,2}$=57.134, take $N_{1,2}$=57, repeat 5~7 applications: $\sum \Delta W_{eic}$ = 201.4193956 ev.

11. To $\sum \Delta W_{eia}$ = 203.481 ev, with $\sum \Delta W_{eic}$ = 201.4193956 ev into (16.12), to: λ_{a-c} = 6013.969 A°.

Lithium atoms line of spectrum calculation results table (A°) 16.8

$N_{\theta 1}$	$N_{\theta 2}$	$N_{1,2}$	$E_{\theta 1}$	$E_{\theta 2}$	$\sum \Delta W_{eic}$ ev	calculated λa -- cA°	Experimental λ_{a-0}A°
	1.5	23	0.198456041	0.2919388194	203.481		
	2	57	0.190848437	0.1832293863	201.6326517	6707.840	6707.84
	3	193	0.19276	0.08619620946	199.6454801	3232.528	3232.61
1	4	457	0.19315	0.04432574063	198.958488	2741.491	2741.31
	5	892	0.19328	0.01566138316	198.6428922	2562.660	2562.50
	6	1543	0.19333	0.02206354654	198.4724202	2475.437	2475.30
	7	2450	0.19340	0.01576806866	198.3666534	2424.244	
	8	3657	0.19340	0.01111312169	198.3016049	2393.798	

12. Fine-tuning $E_{\theta 1}$ scope, repeat 6 ~ 7, 11 calculation procedure, finally have to:

$E_{\theta 1}$=0.190848437 $E_{\theta 2}$=0.1832293863

$\sum \Delta W_{eic}$ =201.6326517ev λ_{a-c}=6707.840A°

13. Make $N_{\theta 2}$= 2, 3, 4, 5, 6, 7, 8, $\overline{Z}_1/\overline{Z}_2$ =2.75, $E_{\theta 2}$ = 0, $E_{\theta 1}$=0.1935, respectively into (16.16), to: $N_{1,2}$ = 57, 193, 457, 892, 1543, 2450, 3657.

Lithium atoms "crazy" - line spectrum calculation results table (A°) 16.9

$N_{\theta 1}$	$N_{\theta 2}$	$N_{1,2}$	$E_{\theta 1}$	$E_{\theta 2}$	$\sum \Delta W_{eic}$ ev	calculated λa -- cA°	Experimental λ_{a-c}A°
1	2	57	0.190848	0.183229386 3	201.6326517		
	3	193	0.19331	0.08745673627	199.6014517	6103.990	6103.53
	4	457	0.19339	0.04539764991	198.9393154	4603.370	4603.0
	5	892	0.19341	0.01724780055	198.6325189	4132.625	4132.3
1	6	1543	0.19341	0.02277992403	198.4660412	3915.361	3915.0
1	7	2450	0.19342	0.01602083031	198.3650591	3794.361	3794.7
	8	3657	0.19343	0.01164284397	198.2992142	3719.411	

14. In different $N_{1,2}$ value, respectively into (16.15), repeat 5~7, 11~12 calculation procedures, can be derived lithium atoms all lines of spectrum, it is equivalent to the hydrogen atom line is "crazy", shown in table 16.8.

15. Similarly, to $N_{\theta 2}$=3, 4, 5, 6, 7, 8, from the table, 16.8, $\sum \Delta W_{eia}$ =201.6326517 ev, with $N_{\theta 2}$ value corresponding to the $N_{1,2}$ value, respectively into (16.15), repeat the 14 calculation procedures, can calculate lithium atoms "overflow line is" full spectrum, equivalent to the hydrogen atom "Baal line is not", shown in table 16.9.

16. By table 16.8, make $\sum \Delta W_{eia}$ = 199.6454801 ev, $N_{\theta 2}$= 4, 5, $N_{1,2}$ = 457, 892, respectively, and the type (16.15), repeat the 14 calculation procedures, can calculate lithium atoms baseline of spectrum, equivalent to the hydrogen atom line is "Xing", shown in table 16.10.

17. Make $N_{\theta 2}$ = 2.5, 3.5, 4.5, 5.5, 6.5, 7.5, $\overline{Z}_1 / \overline{Z}_2$ =2.75, $E_{\theta 2}$ = 0, $E_{\theta 1}$= 0.1935, respectively into (16.16), to: $N_{1,2}$ = 112, 306, 651, 1188, 1961, 3013.

18. Make $\sum \Delta W_{eia}$ = 201.6326517 ev, $N_{1,2}$ = 112 equivalent generation into the type (16.15) respectively, repetition 14 calculation procedures, can be derived lithium atoms "sharp line is" full spectrum, shown in table 16.11.

Lithium atoms baseline of wavelength spectrum calculation results table (A°) 6.10

$N_{\theta 1}$	$N_{\theta 2}$	$N_{1,2}$	$E_{\theta 1}$	$E_{\theta 2}$	$\sum \Delta W_{eic}$ ev	calculated λa -- cA°	Experimental λ_{a-c}A°
	3	193	0.19276	0.086196209 46	199.6454801		
1	4	457	0.19285	0.042950204 44	198.9824202	18698.801	18697.0
	5	892	0.19287	0.00899187 41	198.675562	12782.961	12782.2
	6	1543	0.19289	0.01761678 07	198.5074576	10894.709	

Line is lithium atoms "sharp" wavelength spectrum calculation results table (A°) 6.11

$N_{\theta 1}$	$N_{\theta 2}$	$N_{1,2}$	$E_{\theta 1}$	$E_{\theta 2}$	$\sum \Delta W_{eic}$ ev	calculated λa -- cA°	Experimental λ_{a-c}A°
	2	57	0.190848437	0.18322 938 63	201.6326517		
	2.5	112	0.19509	0.13357 642 77	200.1068834	8126.020	8126.52
1	3.5	306	0.19414	0.06032 338 54	199.1386 51	4971.299	4971.90
	4.5	651	0.19376	0.04089 456 26	198.7315359	4273.674	4273.3
	5.5	1188	0.19361	0.02243 049 31	198.5219727	3985.761	3985.8
	6.5	1961	0.1935	0.01285 992 717	198.4030833	3839.035	

Through this chapter to three kinds of hydrogen, helium and lithium atoms wavelength spectrum simulation, can see: the inner electron spin elliptical orbit of centrifugal rate scope, $0 \leq E_{\theta 1} \leq 1$ can be used as the boundary constraints consideration; $E_{\theta 1}$ value from the atoms of the original state transition to electronic completely after ionization ion condition; As long as further fine-tuning $E_{\theta 1}$ value, can make the wavelength spectrum calculation value and experimental value equal, but have no the necessary.

Atomic spectrum or level is based on atomic energy group as a whole. When an electron in the ionization process, step by step it and economical, lining surplus electronic integrated the average electric charge the strength coefficient of $\overline{Z}_i$ and the rail, and energy parameters will be gradually changed. And conditions within the nucleus of the γ ray forming principle, is under the condition of total energy conservation, repeated simulation of the whole system accumulate.

17 Beryllium, boron and carbon atoms internal structure, parameters and the atomic energy level

17.1 beryllium atomic internal structure, parameters and the atomic energy level

17.1.1 Beryllium atomic internal structure and parameter calculation

Beryllium atoms there were four electronics, composition inside and outside two layer "s type ball shell electron cloud". Experimental determination of four electronic ionization energy, respectively, 9.322, 18.211, 153.893, 217.713 ev, the atom radius of 1.0-1.1 A°.

Beryllium atomic outer first electronic ionization front, inner and outer electron spin elliptical orbit combination are helium atoms. After the first electronic completely ionization of beryllium ion B + electron spin elliptical orbit combination of lithium atoms, so relevant parameters calculation should be 3 steps.

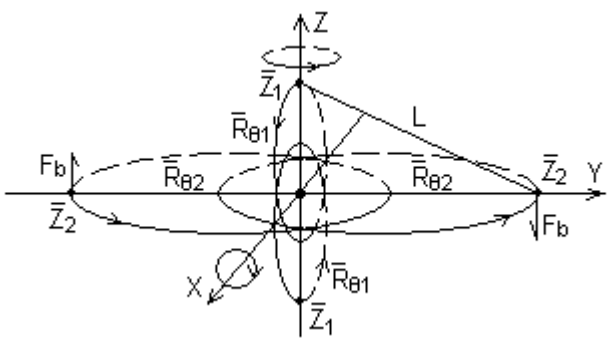

Figure 17.1 beryllium atoms in the electron spin, lateral additional movement track combination model

According to figure 16.2, beryllium atoms within four electron spin elliptical orbit combination shall be as shown in figure 17.1, to maintain stability. Inner electron spin elliptical orbit plane in outer electronic electric and magnetic field strength under the action of spin elliptical orbit will be additional rotation axis, form two symmetrical

rotating ellipsoid surface and outer electronic, electronic electric and magnetic field strength under the action of spin elliptical orbit will appear lateral additional movement. The mutual influence the forms inside and outside two layer "s type ball shell electron cloud". According to Newton's mechanics, coulomb's law, we have:

$$\begin{cases} L=\sqrt{\overline{R}_{\theta 1}^2+\overline{R}_{\theta 2}^2} & (17.1-1) \\ \dfrac{\overline{Z}_1 e^2}{4\pi\varepsilon_0\overline{R}_{\theta 1}^2}=\dfrac{4e^2}{4\pi\varepsilon_0\overline{R}_{\theta 1}^2}-\dfrac{e^2}{4\pi\varepsilon_0(2\overline{R}_{\theta 1})^2}-\dfrac{2e^2\overline{R}_{\theta 1}}{4\pi\varepsilon_0 L^3} & (17.1-2) \\ \dfrac{\overline{Z}_2 e^2}{4\pi\varepsilon_0\overline{R}_{\theta 2}^2}=\dfrac{4e^2}{4\pi\varepsilon_0\overline{R}_{\theta 2}^2}-\dfrac{e^2}{4\pi\varepsilon_0(2\overline{R}_{\theta 2})^2}-\dfrac{2e^2\overline{R}_{\theta 2}}{4\pi\varepsilon_0 L^3} & (17.1-3) \end{cases}$$

Simplified to:

$$\begin{cases} \overline{Z}_1=3.75-2\left[1+\left(\dfrac{\overline{R}_{\theta 2}}{\overline{R}_{\theta 1}}\right)^2\right]^{-1.5} & (17.2-1) \\ \overline{Z}_2=3.75-2\left[1+\left(\dfrac{\overline{R}_{\theta 1}}{\overline{R}_{\theta 2}}\right)^2\right]^{-1.5} & (17.2-2) \end{cases}$$

By (15.41), (16.16), because K_m=1, to:

$$\begin{cases} \dfrac{\overline{Z}_2}{\overline{Z}_1}=\dfrac{1}{N_{1,2}^2}\left(\dfrac{\overline{R}_{\theta 2}}{\overline{R}_{\theta 1}}\right)^3 & (17.3-1) \\ N_{1,2}=\left(\dfrac{N_{\theta 2}}{N_{\theta 1}}\right)^3\left(\dfrac{\overline{Z}_1}{\overline{Z}_2}\right)^2\left(\dfrac{1-E_{\theta 1}^2}{1-E_{\theta 2}^2}\right)^{1.5} & (17.3-2) \end{cases}$$

Simultaneous equations (17.2), (17.3) to:

$$\frac{1}{N_{1,2}^2}\left(\frac{\overline{R}_{\theta 2}}{\overline{R}_{\theta 1}}\right)^3=\frac{3.75-2\left[1+\left(\overline{R}_{\theta 1}/\overline{R}_{\theta 2}\right)^2\right]^{-1.5}}{3.75-2\left[1+\left(\overline{R}_{\theta 2}/\overline{R}_{\theta 1}\right)^2\right]^{-1.5}} \qquad (17.4)$$

By (15.11), inside and outside two layers of electron spin elliptical orbit of eccentricity $E_{\theta i}$ for:

$$E_{\theta i} = \sqrt{1 - \frac{\Delta W_{ei} e N_{\theta i}^2}{(\overline{Z}_i a_c c)^2 m_{e0}}} \qquad (17.5)$$

Beryllium atoms in electron spin elliptical orbit parameters simulation program are as follows:

1. By beryllium atoms inside and outside two layer of ionization energy, make $\sum \Delta W_{e2}$ =27.533 ev, $\sum \Delta W_{e1}$ =371.606 ev, $N_{\theta 1}$=1 , $N_{\theta 2}$=1.5. Type, by (16.4) $\overline{Z}_1$ = 3.75, $\overline{Z}_2$ =1.75, respectively into (17.5), to: $E_{\theta 1}$=0.1699644106, $E_{\theta 2}$=0.5065796762.

2. Will the above parameters into (17.3-2), to: $N_{1,2}$ = 23.139, take 23.

3. The $N_{1,2}$ = 23 into (17.4), to: $\overline{R}_{\theta 2} / \overline{R}_{\theta 1}$ = 6.3621652, generation to equations (17.2) are: $\overline{Z}_1$ = 3.742512847, $\overline{Z}_2$ = 1.821891263.

4. Make $E_{\theta 1}$= 0.1699644106, will the $N_{\theta i}$, $\overline{Z}_i$, $\overline{R}_{\theta 2} / \overline{R}_{\theta 1}$, together into (16.10), to: $E_{\theta 2}$= 0.5426923566.

5. Will $N_{\theta i}$, $\overline{Z}_i$, $E_{\theta i}$ value generation into (15.11), respectively, for beryllium atomic original state of ionization energy: $\sum \Delta W_{eia}$ = 398.4441085 ev, compared with the experimental value $\sum \Delta W_{ei0}$ = 399.139 ev, is a little small.

6. Fine-tuning $E_{\theta 1}$ value, repeat 4 ~ 5 applications, finally to: when the $E_{\theta 1}$= 0.16490685, $E_{\theta 2}$=0.541557586 3, $\sum \Delta W_{eia}$ =399.139ev.

7. Make θ_i=0, π, the above parameters respectively into (15.7), (15.12), is beryllium atomic outer "s type electronic cloud" inside and outside radius and average radius.

8. Similarly, to $N_{1,2}$ = 17, 18, 19, 20, 21, repeat 3 ~ 7 applications, respectively, the results shown in table 17.1.

Beryllium atom Be internal structure, parameter calculation results table (the radius of the unit A °) 17.1

$N_{1,2}$	17	18	19	20	21
$E_{\theta 1}$	0.2012983478	0.194591632	0.188181261	0.1820344636	0.1761226983
$E_{\theta 2}$	0.4112049615	0.4398212558	0.4648951917	0.4871497652	0.5071027948
$\overline{Z}_1$	3.736786778	3.738120189	3.739262476	3.740248373	3.741105084
$\overline{Z}_2$	1.85469143	1.847584016	1.84127354	1.83563886	1.830581641
$R_{\theta 2(0)}$	0.4549	0.4476	0.4414	0.4362	0.4316
$R_{\theta 2(\pi)}$	1.090	1.1504	1.2084	1.2648	1.3196
$\overline{R}_{\theta 2}$	0.7726	0.7990	0.8249	0.8505	0.8756

Can be seen from table 17.1 calculated results that $N_{1,2}$ = 17, 18, "s type ball shell electron cloud" outside the radius of the atomic radius of 1.0-1.1 A° with experimental data very close, they will be as the following calculation according to the atomic energy level.

17.1.2. Beryllium ion Be^{+} internal structure and parameter calculation

Beryllium atomic outer first electronic completely, after the electron spin combination with lithium atoms with elliptical orbit is same, but the number of nuclear power charge shall be 4. According to figure 16.3, equations (16.13), (16.14) and (16.15), to:

$$\begin{cases} \overline{Z}_1 = 4\cos^3\phi_1 - \dfrac{1}{4} - \left[1+\left(\dfrac{\overline{R}_{\theta 2}}{\overline{R}_{\theta 1}} + tg\phi_1\right)^2\right]^{-1.5} & (17.6-1) \\ \overline{Z}_2 = 4 - 2\left(1+\dfrac{\overline{R}_{\theta 1}}{\overline{R}_{\theta 2}}tg\phi_1\right)\left[\left(\dfrac{\overline{R}_{\theta 1}}{\overline{R}_{\theta 2}}\right)^2 + \left(1+\dfrac{\overline{R}_{\theta 1}}{\overline{R}_{\theta 2}}tg\phi_1\right)^2\right]^{-1.5} & (17.6-2) \\ \dfrac{\overline{R}_{\theta 2}}{\overline{R}_{\theta 1}} = \dfrac{1}{\cos\phi_1\sqrt{2\sin\phi_1}} & (17.6-3) \\ \dfrac{1}{N_{1,2}^2(2\sin\phi_1)^{1.5}} = \dfrac{4\left[1+2\sin\phi_1+(2\sin\phi_1)^{1.5}\right]^{1.5} - \left[2+(2\sin\phi_1)^{1.5}\right]}{\left(4-1/4\cos^3\phi_1\right)\left[1+2\sin\phi_1+(2\sin\phi_1)^{1.5}\right]^{1.5} - (2\sin\phi_1)^{1.5}} & \end{cases}$$

（17.6-4）

Refer to section 1 ~ 8 calculation program, make $N_{\theta 1}$=1, $N_{\theta 2}$=1.5, $\sum \Delta W_{eia}$ =

389.817 ev, $N_{1,2}$ = 16, 17, 18, 19, can a beryllium ion Be^+ each electron spin elliptical orbit parameters, see table 17.2.

Beryllium ion Be^+ electron spin in elliptical orbit parameters calculation results table table 17.2

$N_{1,2}$	Φ_1°	$E_{\theta 1}$	$E_{\theta 2}$	$\overline{Z}_1$	$\overline{Z}_2$
16	1.039281	0.170251801	0.5142742949	3.741544867	2.116412676
17	0.9613	0.165470325	0.5369154899	3.742515504	2.107660264
18	0.89306	0.1609317267	0.5570420175	3.743330151	2.099977322
19	0.832814	0.1566126991	0.5750910309	3.744020279	2.09318866

17.1.3. Beryllium atomic energy level

Beryllium atomic outer first electron in the process of gradually ionization, due to the nucleus and various electronic interactions between the electric field intensity, with each electron spin elliptical orbit position change, calculate difficult, we must first be simplified to it. Figure 17.2, the inner electronic outer $\overline{Z}_i$ has an impact on the value, the outermost electron in the innermost electron $\overline{Z}_i$ values influence can be neglected. See the equations (17.7).

$$\begin{cases} \dfrac{\overline{Z}_1 e^2}{4\pi\varepsilon_0 \overline{R}_{\theta 1}^2} = \dfrac{4e^2}{4\pi\varepsilon_0 \overline{R}_{\theta 1}^2} - \dfrac{e^2}{4\pi\varepsilon_0 (2\overline{R}_{\theta 1})^2} - \dfrac{e^2 \overline{R}_{\theta 1}}{4\pi\varepsilon_0 L_{1,2}^3} & (17.7-1) \\ \dfrac{\overline{Z}_2 e^2}{4\pi\varepsilon_0 \overline{R}_{\theta 2}^2} = \dfrac{4e^2}{4\pi\varepsilon_0 \overline{R}_{\theta 2}^2} - \dfrac{2e^2 \overline{R}_{\theta 2}}{4\pi\varepsilon_0 L_{1.2}^3} - \dfrac{e^2 \overline{R}_{\theta 2}}{4\pi\varepsilon_0 L_{2,3}^3} & (17.7-2) \\ \dfrac{\overline{Z}_3 e^2}{4\pi\varepsilon_0 \overline{R}_{\theta 3}^2} = \dfrac{4e^2}{4\pi\varepsilon_0 \overline{R}_{\theta 3}^2} - \dfrac{e^2}{4\pi\varepsilon_0 (\overline{R}_{\theta 3} + \overline{R}_{\theta 1})^2} - \dfrac{e^2}{4\pi\varepsilon_0 (\overline{R}_{\theta 3} - \overline{R}_{\theta 1})^2} - \dfrac{e^2 \overline{R}_{\theta 3}}{4\pi\varepsilon_0 L_{2,3}^3} \end{cases}$$

（17.7-3）

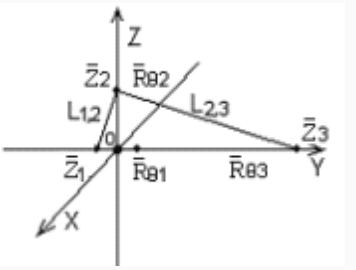

Figure 17.2 beryllium atomic internal electron relative location plans

Simplified to:

$$\begin{cases} \bar{Z}_1 = 3.75 - \left[1+\left(\dfrac{\bar{R}_{\theta 2}}{\bar{R}_{\theta 1}}\right)^2\right]^{-1.5} & (17.8\text{-}1) \\ \bar{Z}_2 = 4 - 2\left[1+\left(\dfrac{\bar{R}_{\theta 1}}{\bar{R}_{\theta 2}}\right)^2\right]^{-1.5} - \left[1+\left(\dfrac{\bar{R}_{\theta 3}}{\bar{R}_{\theta 2}}\right)^2\right]^{-1.5} & (17.8-2) \\ \bar{Z}_3 = 4 - \left(1+\dfrac{\bar{R}_{\theta 1}}{\bar{R}_{\theta 3}}\right)^{-2} - \left(1-\dfrac{\bar{R}_{\theta 1}}{\bar{R}_{\theta 3}}\right)^{-2} - \left[1+\left(\dfrac{\bar{R}_{\theta 2}}{\bar{R}_{\theta 3}}\right)^2\right]^{-1.5} & (17.8-3) \end{cases}$$

By equations (17.3), (17.8) to:

$$\frac{1}{N_{2,3}^2}\left(\frac{\bar{R}_{\theta 3}}{\bar{R}_{\theta 2}}\right)^3 = \frac{4 - \left(1+\dfrac{\bar{R}_{\theta 1}}{\bar{R}_{\theta 3}}\right)^{-2} - \left(1-\dfrac{\bar{R}_{\theta 1}}{\bar{R}_{\theta 3}}\right)^{-2} - \left[1+\left(\dfrac{\bar{R}_{\theta 2}}{\bar{R}_{\theta 3}}\right)^2\right]^{-1.5}}{4 - 2\left[1+\left(\dfrac{\bar{R}_{\theta 1}}{\bar{R}_{\theta 2}}\right)^2\right]^{-1.5} - \left[1+\left(\dfrac{\bar{R}_{\theta 3}}{\bar{R}_{\theta 2}}\right)^2\right]^{-1.5}} \quad (17.9)$$

Beryllium atoms in the original state, $N_{1,2}$ and take what value? By experimental detection beryllium atomic radius is: 1.0 ~ 1.1 A°, if we consider gold attribute of the element mass outer, can form "free electrons clouds", compound atom outer "probability" have overlapping phenomenon, from table 17.1, $R_{\theta 2(\pi)}$ value, we shall be more than $17 \leq N_{1,2} \leq 20$. By chapter 16 that: in the calculation of atomic spectrum energy, inner electronic $E_{\theta 1}$, $E_{\theta 2}$ values from atomic state transition to electronic completely after ionization ion condition, therefore, should be through several solutions to the atomic

energy level results after comparison and analysis, to determine. We choose the following beryllium atomic energy level simulation of subsequent program:

9. Make beryllium atomic original state $N_{1,2}$ = 19, $N_{\theta 1}$=1、 $N_{\theta 2}$=$N_{\theta 3}$=1.5; Ion state $N_{1,2}$= 18, look-up table 17.2 to: $E_{\theta 1}$= 0.1609317267. Electronic ionization in the early stage by stage, $N_{1,2}$ = 19, make $\overline{Z}_1$ = 3.75, $\overline{Z}_2$ =2, $\overline{Z}_3$ =1, $E_{\theta 3}$=0, the related value respectively into (17.3-1), (16.9), to:

$\overline{R}_{\theta 2}/\overline{R}_{\theta 1}$ = 5.774335008, $\overline{R}_{\theta 1}/\overline{R}_{\theta 3}$ = 0.1216696431

10. The $N_{2,3}$ = 2, together generation with $\overline{R}_{\theta 2}/\overline{R}_{\theta 1}$ and $\overline{R}_{\theta 1}/\overline{R}_{\theta 3}$ into (17.9), to: $\overline{R}_{\theta 3}/\overline{R}_{\theta 2}$ = 1.421541032.

11. The $\overline{R}_{\theta 2}/\overline{R}_{\theta 1}$, $\overline{R}_{\theta 1}/\overline{R}_{\theta 3}$ and $\overline{R}_{\theta 3}/\overline{R}_{\theta 2}$, together generation into equations (17.8) is: $\overline{Z}_1$ =1.896247359, $\overline{Z}_2$ = 3.745031289, $\overline{Z}_3$ = 1.361799586.

12. Will $\overline{Z}_i$, $N_{1,2}$ = 19 value generation into (17.3-1), a new value: $\overline{R}_{\theta 2}/\overline{R}_{\theta 1}$ = 5.675214056, together into (16.10), to: $E_{\theta 2}$= 0.48711471. Similarly, will $\overline{Z}_2$, $\overline{Z}_3$, $E_{\theta 2}$, $\overline{R}_{\theta 3}/\overline{R}_{\theta 2}$, $N_{\theta i}$ values generation into (16.10), to: $E_{\theta 3}$= 0.5028773261.

13. The corresponding $\overline{Z}_i$, $E_{\theta i}$, $N_{\theta i}$, values generation into (15.11), respectively, to atomic ionization energy always: $\sum \Delta W_{eib}$ = 396.7249634 ev.

14. Will in the new $\overline{Z}_i$, $E_{\theta i}$ values equivalent repeat 9 ~ 13 calculation procedure, until $\sum \Delta W_{eic}$ = 396.6746814 ev is constant.

15. Because $\sum \Delta W_{ei0}$ = 399.139 ev, by (16.11), to the atomic energy level: △Wei== 2.464318621 ev

16. Appropriate fine-tuning $E_{\theta 1}$, repeated 9 ~ 15 calculation program, finally to: when the $E_{\theta 1}$=0.16291, $\sum \Delta W_{eic}$ =396.4137961ev, the atomic energy level $\triangle W_{ei}$ = 2.7252 ev.

17. Similarly, to $N_{1,\ 2}$ = 19, $N_{\theta 1}$=1, $N_{\theta 2}$=1.5， $E_{\theta 1}$= 0.1609317267 are invariable values, $N_{2,3}$ = 3, 4, 5,... 17, $N_{\theta 3}$= 1.5, 2, 3, respectively, repeat 9 ~ 15 calculation procedures, the atomic energy level is obtained data in table 17.3.

Beryllium atomic energy level the results table table 17.3

$N_{\theta 3}$	$N_{2,3}$	$E_{\theta 2}$	$E_{\theta 3}$	$\sum \Delta W_{eib}$ ev	$\triangle W_{ei}$ev	实验值ev
	2	0.488510297	0.500718702	396.6746814	2.464318 62	
1.5	2	0.489022518 6	0.501210558 8	396.4137961	2.7252	2.7252
				($E_{\theta 1}$=0.16291)		
	3	0.525774324 8	0.614642384	394.8973346	4.241665 42	
	4	0.542398057 2	0.170348002 7	393.9081965	5.230803 46	5.277
	5	0.551404368 8	0.353488821 7	393.2697172	5.869282 78	
	6	0.556865831 5	0.445819113 3	392.8190209	6.319979 07	6.457
	7	0.560436538 9	0.508134878 4	392.4813773	6.657622 67	6.779
	8	0.562901735 3	0.554563693 1	392.2174938	6.921506 21	6.997
	9	0.564675866 4	0.591080353 6	392.0046365	7.134363 50	7.289
2	10	0.565995314 6	0.620828499 3	391.8286858	7.310314 22	7.401
	11	0.567003191 8	0.645677859	391.6803794	7.458620 57	7.462
	12	0.567790361 2	0.666833045 2	391.5533719	7.585628 06	
	13	0.568416802 8	0.685115423 8	391.4431596	7.695840 41	7.694
	14	0.568923419 6	0.701109350 4	391.3464508	7.792549 16	
	15	0.569338887 1	0.715244572 1	391.2607798	7.878220 17	
	16	0.569683793	0.727845676 3	391.1842599	7.954740 11	7.988
	17	0.569973228 2	0.739163273 2	391.1154209	8.023579 09	7.998
3	18	0.5702184581	0.1165424905	391.053099	8.085901 00	8.089

Beryllium atomic energy level the results table table 17.4

$N_{\theta 3}$	$N_{2,3}$	$E_{\theta 2}$	$E_{\theta 3}$	$\sum \Delta W_{eib}$ ev	$\triangle W_{ei}$ev	实验值ev
3	19	0.560895744 8	0.167064620 9	391.3062219	7.832778 07	
4	46	0.562540115 7	0.087117648 0	390.6100692	8.528930 79	8.335
5	91	0.562808128 4	0.078378469 8	390.2953222	8.843677 77	8.865

18. Make $N_{1,2}$=18.5、$N_{\theta 1}$=1、$N_{\theta 2}$=1.5，$E_{\theta 1}$=0.1609317267 all are constants, $N_{\theta 3}$=3, 4, 5, $N_{2,3}$ = 19, 20, 46, 91... (46, 91 values is by simulation in equation (17.3 2) find out), repeat calculation procedure, 9 to 15 respectively corresponding to the atomic energy level in table 17.4.

19. Make $N_{1,2}$=20、$N_{\theta 1}$=1、$N_{\theta 2}$=1.5; Ion state $N_{1,2}$ = 19, look-up table 17.2: $E_{\theta 1}$= 0.1566126991 are constants, $N_{\theta 3}$=1.5, 2, 3, $N_{2,3}$ = 2, 3,.....17, repeated 9 ~ 17 calculation procedure, respectively, to beryllium atoms and ions to another state, the outer electronic ionization step by step in the process of atomic energy level, see table 17.5.

Beryllium atomic energy level the results table table 17.5

$N_{\theta 3}$	$N_{2,3}$	$E_{\theta 2}$	$E_{\theta 3}$	$\sum \Delta W_{eib}$ ev	△W_{ei}ev	实验值ev
1.5	2	0.5105035709	0.5278616424	396.4879154	2.65108456	2.725
	3	0.5452401981	0.632230023	394.7520959	4.38690412	
	4	0.5608293013	0.2497425916	393.7890729	5.34992714	5.277
	5	0.5692968151	0.393149501	393.1683692	5.97063081	
	6	0.5744387584	0.4749794477	392.7306094	6.40839063	6.457
	7	0.5778034894	0.531872743	392.4028537	6.73614630	6.779
	8	0.5801278393	0.5748638351	392.1468091	6.99219089	6.997
2	9	0.5818013026	0.608960831	391.9403429	7.19865711	7.289
	10	0.5830462663	0.6368931379	391.7697191	7.36928086	7.401
	11	0.583997472	0.6603191363	391.6259327	7.51306734	7.462
	12	0.5847405177	0.680322739	391.5028169	7.63618312	7.694
	13	0.5853319329	0.6976506922	391.3959968	7.74300320	
	14	0.5858102814	0.7128384159	391.302276	7.83672404	
	15	0.586202606	0.7262820654	391.2192604	7.91973963	7.988
	16	0.5865283271	0.7382823124	391.1451188	7.99388120	7.998
3	17	0.5868016826	0.1117841642	391.0784246	8.06057538	8.089

20. Similarly, to $N_{1,2}$ = 19.5, $N_{\theta 1}$=1, $N_{\theta 2}$=1.5, $E_{\theta 1}$= 0.1566126991 are constants, $N_{\theta 3}$= 3, 4, 5, 6, $N_{2,3}$ =, 44, 86, 86, 18 ($N_{2,3}$ values are from (17.3 2) equation obtained in simulation), repeat calculation program 9 ~15, respectively, to find out the corresponding beryllium atoms in each level, see table 17.6.

Beryllium atomic energy level the results table table 17.6

$N_{\theta 3}$	$N_{2,3}$	$E_{\theta 2}$	$E_{\theta 3}$	$\sum \Delta W_{eib}$ ev	△Weiev	实验值ev
3	18	0.57844195 44	0.17107587 22	391.3049719	7.83402811	7.988
4	44	0.58016396 69	0.11210712 97	390.6006239	8.53837613	
5	86	0.58043716 61	0.05093087 79	390.2913574	8.84764257	8.865
6	149	0.58050304 62	0.02164567 88	390.1232882	9.01571181	

By comparing table 17.3 ~ 17.6 calculated results can be seen: beryllium atomic original state, $N_{1, 2}$ = 20, ionic state $N_{1, 2}$ = 19 calculation results with the experimental value more, as long as we fine tune $E_{\theta 1}$ value, can with the experimental values are equal, but have no the necessary.

21. To $N_{1,2}$=19.5, $N_{\theta 1}$=1, $N_{\theta 2}$=1.5, $N_{\theta 3}$=5，$N_{2,3}$=86, 87, …… 92，$E_{\theta 1}$=0.1566126991, respectively, repeat 9 ~ 15 calculation procedures, can work out another group of beryllium atomic energy level data, including $N_{2, 3}$ doesn't have to take continuous natural number, it can be 2, 3, 4,... Multiple of, depending on specific experimental data, see table 17.7.

Beryllium atomic energy level the results table table 17.7

$N_{\theta 3}$	$N_{2,3}$	$E_{\theta 2}$	$E_{\theta 3}$	$\sum \Delta W_{eib}$ ev	△Weiev	实验值ev
	86	0.58043716 61	0.05093087 79	390.2913574	8.84764257	
	87	0.58043941 37	0.10069318 01	390.2871485	8.85185147	
	88	0.58044158 57	0.13245217 88	390.2830196	8.8559804	
5	89	0.58044368 55	0.15751662 42	390.2789684	8.86003163	
	90	0.58044571 63	0.17873672 17	390.2749924	8.86400762	8.865
	91	0.580447681	0.19736612 21	390.2710895	8.86791052	
	92	0.58044958 25	0.21409079 61	390.2672575	8.87174246	

To sum up, to more than the atomic energy level, according to the model of the book, the choice of appropriate $N_{1,2}$ and $N_{2,3}$ quantum number, fine-tuning $E_{\theta 1}$ parameters, we can calculate all the atomic energy level. Deficiency is laboratory is not directly determining electron spin elliptical orbit parameters, we can only from the atomic energy level or spectra experiment energy to reverse simulation.

17.2 Boron atom internal structure, parameters And the atomic energy level

17.2.1. Boron atom internal structure and parameter calculation

According to the experimental determination, the boron atom within five electronic ionization energy, respectively, 8.298, 25.154, 37.930, 259.368 and 340.217 ev, total ionization energy $\sum \Delta W_{ei0}$ = 670.967 ev. Atomic radius are 0.8 ~ 1.0 A °, the atomic energy level in table 17.10 and table 17.11. Refer to section 17.1 and figure 17.2, boron atoms in electron spin elliptical orbit combination shall be as shown in figure 17.3, to stability. We cut out Φ_1 Angle offset effects, by Newtonian mechanics; Coulomb's law (17.10) is derived equations.

$$\begin{cases} \dfrac{\overline{Z}_1 e^2}{4\pi\varepsilon_0 \overline{R}_{\theta 1}^2} = \dfrac{5e^2}{4\pi\varepsilon_0 \overline{R}_{\theta 1}^2} - \dfrac{e^2}{4\pi\varepsilon_0 (2\overline{R}_{\theta 1})^2} - \dfrac{2e^2 \overline{R}_{\theta 1}}{4\pi\varepsilon_0 L_{1,2}^3} & (17.10-1) \\ \dfrac{\overline{Z}_2 e^2}{4\pi\varepsilon_0 \overline{R}_{\theta 2}^2} = \dfrac{5e^2}{4\pi\varepsilon_0 \overline{R}_{\theta 2}^2} - \dfrac{e^2}{4\pi\varepsilon_0 (2\overline{R}_{\theta 2})^2} - \dfrac{2e^2 \overline{R}_{\theta 2}}{4\pi\varepsilon_0 L_{1,2}^3} - \dfrac{e^2 \overline{R}_{\theta 2}}{4\pi\varepsilon_0 L_{2,3}^3} & (17.10-2) \\ \dfrac{\overline{Z}_3 e^2}{4\pi\varepsilon_0 \overline{R}_{\theta 3}^2} = \dfrac{e^2}{4\pi\varepsilon_0} \left[\dfrac{5}{\overline{R}_{\theta 3}^2} - \dfrac{2\overline{R}_{\theta 3}}{L_{2,3}^3} - \dfrac{1}{(\overline{R}_{\theta 3} + \overline{R}_{\theta 1})^2} - \dfrac{1}{(\overline{R}_{\theta 3} - \overline{R}_{\theta 1})^2} \right] & (17.10\text{-}3) \end{cases}$$

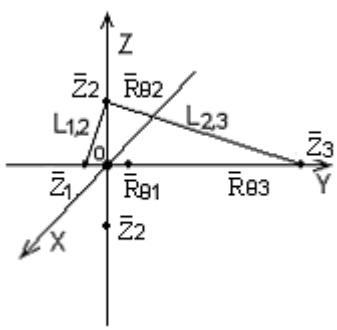

Figure 17.3 in boron atom electronic relative location plan

Simplified to:

$$\begin{cases} \overline{Z}_1 = 4.75 - 2\left[1+\left(\dfrac{\overline{R}_{\theta 2}}{\overline{R}_{\theta 1}}\right)^2\right]^{-1.5} & (17.11-1) \\ \overline{Z}_2 = 4.75 - 2\left[1+\left(\dfrac{\overline{R}_{\theta 1}}{\overline{R}_{\theta 2}}\right)^2\right]^{-1.5} - \left[1+\left(\dfrac{\overline{R}_{\theta 3}}{\overline{R}_{\theta 2}}\right)^2\right]^{-1.5} & (17.11-2) \\ \overline{Z}_3 = 5 - \left(1+\dfrac{\overline{R}_{\theta 1}}{\overline{R}_{\theta 3}}\right)^{-2} - \left(1-\dfrac{\overline{R}_{\theta 1}}{\overline{R}_{\theta 3}}\right)^{-2} - 2\left[1+\left(\dfrac{\overline{R}_{\theta 2}}{\overline{R}_{\theta 3}}\right)^2\right]^{-1.5} & (17.11-3) \end{cases}$$

Will (15.41) into (17.11-2), (17.11-3), to:

$$\frac{1}{N_{2,3}^2}\left(\frac{\overline{R}_{\theta 3}}{\overline{R}_{\theta 2}}\right)^3 = \frac{5 - \dfrac{1}{\left(1+\dfrac{\overline{R}_{\theta 1}}{\overline{R}_{\theta 3}}\right)^2} - \dfrac{1}{\left(1-\dfrac{\overline{R}_{\theta 1}}{\overline{R}_{\theta 3}}\right)^2} - \dfrac{2}{\left[1+\left(\dfrac{\overline{R}_{\theta 2}}{\overline{R}_{\theta 3}}\right)^2\right]^{1.5}}}{4.75 - \dfrac{2}{\left[1+\left(\dfrac{\overline{R}_{\theta 1}}{\overline{R}_{\theta 2}}\right)^2\right]^{1.5}} - \dfrac{1}{\left[1+\left(\dfrac{\overline{R}_{\theta 3}}{\overline{R}_{\theta 2}}\right)^2\right]^{1.5}}} \quad (17.12)$$

By (15.41), (15.12):

$$\begin{cases} \dfrac{\overline{R}_{\theta 2}}{\overline{R}_{\theta 1}} = \sqrt[3]{N_{1,2}^2 \dfrac{\overline{Z}_2}{\overline{Z}_1}} & (17.13-1) \\ E_{\theta 2} = \sqrt{1-\left(N_{\theta 2}/N_{\theta 1}\right)^2 (1-E_{\theta 1}^2)\dfrac{\overline{Z}_1 \overline{R}_{\theta 1}}{\overline{Z}_2 \overline{R}_{\theta 2}}} & (17.13-2) \\ E_{\theta 3} = \sqrt{1-\left(N_{\theta 3}/N_{\theta 2}\right)^2 (1-E_{\theta 2}^2)\dfrac{\overline{Z}_2 \overline{R}_{\theta 2}}{\overline{Z}_3 \overline{R}_{\theta 3}}} & (17.13-3) \\ \dfrac{\overline{R}_{\theta 1}}{\overline{R}_{\theta 3}} = \dfrac{\overline{Z}_3 (1-E_{\theta 3}^2) N_{\theta 1}^2}{\overline{Z}_1 (1-E_{\theta 1}^2) N_{\theta 3}^2} & (17.13-4) \end{cases}$$

Boron atom internal structure, each electron spin elliptical orbit parameters simulation program is as follows:

1. Make $N_{\theta 1}=1$, $N_{\theta 2}=N_{\theta 3}=1.5$, $N_{1,2}=17$, $\overline{Z}_1=4.75$, $\overline{Z}_2=2.75$, $\overline{Z}_3=1$, $E_{\theta 1}=0.1$, $E_{\theta 3}=0$, respectively into (17.13-1), (17.13-4), to: $\overline{R}_{\theta 2}/\overline{R}_{\theta 1}$ = 5.510347347, $\overline{R}_{\theta 1}/\overline{R}_{\theta 3}$ =

0.09451237521.

2. Make the $N_{2,3}$ = 1, will be together $\overline{R}_{\theta 2}/\overline{R}_{\theta 1}$, and $\overline{R}_{\theta 1}/\overline{R}_{\theta 3}$ in to (17.12), to: $\overline{R}_{\theta 3}/\overline{R}_{\theta 2}$ = 0.971354264.

3. Will $\overline{R}_{\theta 2}/\overline{R}_{\theta 1}$, $\overline{R}_{\theta 1}/\overline{R}_{\theta 3}$, and $\overline{R}_{\theta 3}/\overline{R}_{\theta 2}$ value respectively generation into equations (17.11) is: $\overline{Z}_1$=4.738613655, $\overline{Z}_2$=2.475810775, $\overline{Z}_3$ = 2.269083104.

4. Will $\overline{Z}_i$, $N_{\theta i}$, $N_{1,2}$=17, $\overline{R}_{\theta 2}/\overline{R}_{\theta 1}$, $\overline{R}_{\theta 1}/\overline{R}_{\theta 3}$, $E_{\theta 1}$=0.1, value generation to equations (17.13) are respectively: $\overline{R}_{\theta 2}/\overline{R}_{\theta 1}$ =5.325021063, $\overline{R}_{\theta 1}/\overline{R}_{\theta 3}$ =0.2135021, $E_{\theta 2}$=0.4465120303, $E_{\theta 3}$ =0.3172835642.

5. Will $\overline{Z}_i$, $N_{\theta i}$, $E_{\theta i}$ values generation into (15.11), respectively is five electronic total ionization energy: $\sum \Delta W_{ei0}$ = 692.2587889 ev.

Boron atom internal structure, parameter calculation results table (the radius of the unit A°) 17.8

$N_{1,2}$	16	17	18	19	20
$\overline{Z}_1$	4.735866103	4.737393859	4.738687511	4.739792467	4.740743642
$\overline{Z}_2$	2.474483909	2.468725932	2.463593351	2.458999284	2.454870288
$\overline{Z}_3$	2.076414537	2.097001777	2.114482795	2.12949919	2.142527476
$E_{\theta 1}$	0.2049905362	0.1944862044	0.1841990858	0.1740809	0.1640807263
$E_{\theta 2}$	0.4397305292	0.4681501595	0.4928926473	0.514732940	0.5342219851
$E_{\theta 3}$	0.138390543i	0.1713469525	0.2680612289	0.330936171	0.3784422718
$R_{\theta 2(0)}$	0.334210	0.328504	0.323732	0.319661	0.316131
$R_{\theta 2(\pi)}$	0.858820	0.906821	0.953048	0.997802	1.041301
$\overline{R}_{\theta 2}$	0.596514	0.617663	0.638390	0.658731	0.678716
$R_{\theta 3(0)}$		0.484729	0.444058	0.420096	0.403152
$R_{\theta 3(\pi)}$		0.685192	0.769316	0.835677	0.894079
$\overline{R}_{\theta 3}$	0.562640	0.584961	0.606687	0.627887	0.648615

6. With a new $\overline{Z}_i$ and $E_{\theta 3}$ values, generation into the (17.13-1), (17.13-4) type, repeated calculation procedure, 1 ~ 5 until $\sum \Delta W_{eia}$ = 690.3705144 ev is constant,

slightly greater than the value $\sum \Delta W_{ei0}$ = 670.967 ev.

7. Adjust $E_{\theta 1}$ scope, repeated 1 ~ 6 calculation procedures, the last to: when the $E_{\theta 1}$= 0.1944862044, $\sum \Delta W_{eia}$ =670.967 ev.

8. Similarly, to $N_{1,2}$ = 16, 18, 19, 20, repeated 1 ~ 7 applications, to electronic $\overline{Z}_i$, $E_{\theta i}$ are obtained.

9. Will each, $\overline{Z}_i$, $E_{\theta i}$, $N_{\theta i}$ value generation into (15.7), (15.12), respectively, make to θ_i=0, π, can get the electron spin elliptical orbit parameters, see table 17.8.

17.2.2, boron ions B^+ internal structure and parameter calculation

Refer to section 17.1 figure 17.1 and figure 17.4 beryllium atomic internal structure calculation model, because the number of nuclear power load is 5, we have:

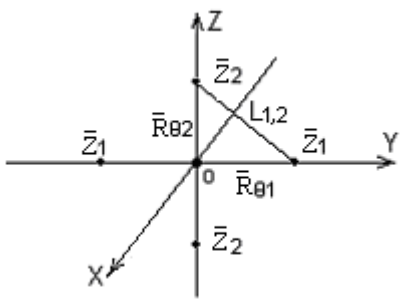

Figure 17.4 boron ion in electronic relative location plan

Simplified to:

$$\begin{cases} \dfrac{\overline{Z}_1 e^2}{4\pi\varepsilon_0 \overline{R}_{\theta 1}^2} = \dfrac{5e^2}{4\pi\varepsilon_0 \overline{R}_{\theta 1}^2} - \dfrac{e^2}{4\pi\varepsilon_0 (2\overline{R}_{\theta 1})^2} - \dfrac{2e^2 \overline{R}_{\theta 1}}{4\pi\varepsilon_0 L_{1,2}^3} & (17.14-1) \\ \dfrac{\overline{Z}_2 e^2}{4\pi\varepsilon_0 \overline{R}_{\theta 2}^2} = \dfrac{5e^2}{4\pi\varepsilon_0 \overline{R}_{\theta 2}^2} - \dfrac{e^2}{4\pi\varepsilon_0 (2\overline{R}_{\theta 2})^2} - \dfrac{2e^2 \overline{R}_{\theta 2}}{4\pi\varepsilon_0 L_{1,2}^3} & (17.14-2) \end{cases}$$

By the simplified equation (17.14), to:

$$\begin{cases} \overline{Z}_1 = 4.75 - 2\left[1 + \left(\overline{R}_{\theta 2} / \overline{R}_{\theta 1}\right)^2\right]^{-1.5} & (17.15-1) \\ \overline{Z}_2 = 4.75 - 2\left[1 + \left(\overline{R}_{\theta 1} / \overline{R}_{\theta 2}\right)^2\right]^{-1.5} & (17.15-2) \end{cases}$$

By (17.3 1) type, simultaneous equations (17.15):

$$\frac{1}{N_{1,2}^2}\left(\frac{\overline{R}_{\theta 2}}{\overline{R}_{\theta 1}}\right)^3 = \frac{4.75 - 2\left[1 + \left(\overline{R}_{\theta 1} / \overline{R}_{\theta 2}\right)^2\right]^{-1.5}}{4.75 - 2\left[1 + \left(\overline{R}_{\theta 2} / \overline{R}_{\theta 1}\right)^2\right]^{-1.5}} \qquad (17.16)$$

According to equations (17.13), (17.15), (17.16), (15.7) and (15.12), refer to section 17.1 beryllium atomic 1 ~ 9 calculation procedures, make $\sum \Delta W_{ei0}$ = 662.669 ev, obtained boron ions B + inner structure parameters, see table 17.9).

Boron B^+ inner structure parameters calculation results table (radius nit A°) 17.9

$N_{1,2}$	17	18	19	20	21
$\overline{Z}_1$	4.738998376	4.740129133	4.741094833	4.741926007	4.742646456
$\overline{Z}_2$	2.842752291	2.83633042	2.830643113	2.825576514	2.821038609
$E_{\theta 1}$	0.1448008043	0.1330941967	0.1213038073	0.1092638506	0.0967493541
$E_{\theta 2}$	0.5843090113	0.6015065491	0.6170099394	0.6310771482	0.643913695
$R_{\theta 1(0)}$	0.0975404	0.098525	0.099540	0.100603	0.101736
$R_{\theta 1(\pi)}$	0.130571	0.128777	0.127023	0.125284	0.123530
$\overline{R}_{\theta 1}$	0.114056	0.113651	0.113282	0.112944	0.112633
$R_{\theta 2(0)}$	0.264366	0.262119	0.260127	0.258346	0.256741
$R_{\theta 2(\pi)}$	1.007567	1.053430	1.098275	1.142197	1.185276
$\overline{R}_{\theta 2}$	0.635966	0.657774	0.679201	0.700272	0.721008

17.2.3. Boron atomic energy level

A boron atom the outermost electrons in the process of gradually ionization, inner $N_{\theta 1}$, $N_{\theta 2}$, $N_{1,2}$ values will remain unchanged. Make to: $\sum \Delta W_{ei0}$ = 670.967 ev, $N_{1,2}$=17、$N_{\theta 1}$=1、$N_{\theta 2}$=1.5、$N_{\theta 3}$=1.5、2、2.5、3、4、5 and 10^5, $E_{\theta 1}$=0.1944862044 ~ 0.1448008043, $N_{2,3}$ value from (17.3-2) insertion 1~7 simulation calculation procedure, condition is: 0 ≤ $E_{\theta 3}$ ≤ 1. Reference 1 ~ 7 calculation procedure, calculate boron atoms in outer electrons ionization the $\sum \Delta W_{eic}$ value in each step by step, and then from (16.11) - is the atomic energy level △W_{ei} value, as shown in the table 17.10.

Boron atomic energy level the results table table 17.10

$N_{\theta 3}$	$N_{2,3}$	$E_{\theta 1}$	$E_{\theta 2}$	$E_{\theta 3}$	$\sum \Delta W_{eib}$ ev	$\triangle W_{e}$ev	实验值ev
1.5	4	0.144801	0.56149478	0.621531	669.674	1.29299995	
	5	0.144801	0.56786633	0.653430	668.598496	2.36850389	
	6	0.144801	0.57185724	0.201196	667.852777	3.11422315	
	6	0.147100	0.57226043	0.202824	667.395	3.572	3.572
2	7	0.144801	0.57453711	0.301624	667.301818	3.66518230	
	11	0.144801	0.57968227	0.490741	666.022431	4.94456875	4.9642
	12	0.144801	0.58032630	0.519210	665.823213	5.14378664	
2.5	18	0.144801	0.58237156	0.248970	665.048042	5.91895780	5.9335
	19	0.144801	0.58255340	0.296526	664.961054	6.00594614	
3	32	0.144801	0.58364601	0.128716	664.274596	6.69240384	6.7900
	36	0.144801	0.58377951	0.287142	664.151456	6.81554380	6.8202
4	80	0.144801	0.58419703	0.074386	663.535165	7.43183530	7.4377
	84	0.144801	0.57420729	0.190009	663.507301	7.45969898	7.4572
5	158	0.144801	0.58427989	0.021236	663.218348	7.74865180	7.7467
	162	0.144801	0.58428130	0.129211	663.209248	7.75775188	
10^5		0.144801	0.58430901	1.2×10^{-7}	662.669	8.298	8.2983

Similarly, make: $\sum \Delta W_{ei0}$ = 670.967 ev, $N_{1,2}$ = 19, $E_{\theta 1}$= 0.1740809-0.1213038073, repeat the above calculation procedure, we can find another series of boron atoms each level value, as shown in the table 17.11.

Boron atomic energy level the results table table 17.11

$N_{\theta 3}$	$N_{2,3}$	$E_{\theta 1}$	$E_{\theta 2}$	$E_{\theta 3}$	$\sum \Delta W_{eib}$ ev	$\triangle W_{e}$ev	实验值ev
	5	0.12130381	0.60237754	0.224922	668.232679	2.73432124	
	6	0.12130381	0.60592103	0.324466	667.530163	3.43683736	3.572
2	7	0.12130381	0.60830322	0.389918	667.011653	3.95534718	
	10	0.12130381	0.61215807	0.511650	666.028987	4.93801256	4.9642
	11	0.12130381	0.61288327	0.539633	665.809381	5.15761938	
2.5	16	0.12130381	0.61487097	0.264517	665.084565	5.88243464	
	17	0.12130381	0.61509214	0.312709	664.985160	5.98184009	5.9335
3	28	0.12130381	0.61624762	0.085725	664.313641	6.65335869	6.7900
4	72	0.12130381	0.61688692	0.075813	663.538296	7.42870380	7.4377
5	143	0.12130381	0.61697823	0.049277	663.218088	7.74891189	7.7467
10^5		0.12130381	0.61700994	0.0	662.669	8.298	8.2983

As can be seen in table 17.10 and table 17.11: $N_{1,2}$ = 17, 19 two series of parameters in $E_{\theta 1}$ changes extremely hours, are consistent with experimental data.

17.3 Carbon atoms internal structure, parameters And the atomic energy level

17.3.1. Carbon atoms internal structure, parameters are calculated

Experimental determination of carbon atoms outer four electronic ionization energy, respectively, 11.260, 24.383, 47.887 and 64.492 ev. Atomic radius are 0.7 ~ 0.8 A°.

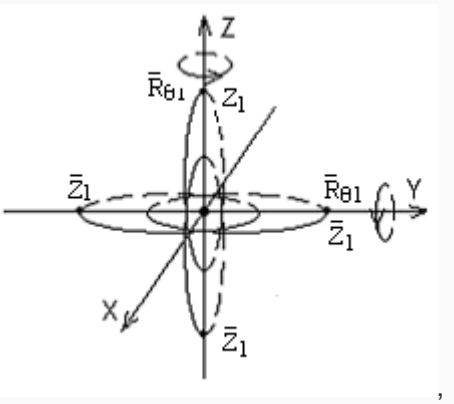

Figure 17.5 carbon atoms outer four electron spin track group

Because carbon atoms outer four electron spin elliptical orbit parameters are the same, "cloud" of two rotating ellipsoid surface, see figure 17.5, we have:

$$\frac{\overline{Z}_1 e^2}{4\pi\varepsilon_0 \overline{R}_{\theta 1}^2} = \frac{3.75e^2}{4\pi\varepsilon_0 \overline{R}_{\theta 1}^2} - \frac{2e^2 \overline{R}_{\theta 1}}{4\pi\varepsilon_0 (2\overline{R}_{\theta 1}^2)^{1.5}} \qquad (17.17)$$

By (17.17), to: $\overline{Z}_1 = 3.75 - 1/\sqrt{2} = 3.0428932$, to:

$$E_{\theta i}=\sqrt{1-\frac{2\sum\Delta W_{eia}N_{\theta i}^{2}e}{m_{e0}N_{e}(\overline{Z}_{i}a_{c}c)^{2}}} \qquad (17.18)$$

By (15.11), make to economical electronic number of N_e, obtained:

Make $N_{\theta 1}$=1.5, $\sum\Delta W_{ei0}$ =148.022ev, N_e=4，will $\overline{Z}_1$ value generation into (17.18), to: $E_{\theta 1}$= 0.5822983738. By (15.7), (15.12), make the θ_1=0, π, obtained carbon atoms outer four electrons spin elliptical orbit parameters are: $R_{\theta 1(0)}$=0.247291A°, $R_{\theta 1(\pi)}$=0.936765A°, $\overline{R}_{\theta 1}$=0.592028A°.

17.3.2. Carbon ion internal structure, parameters are calculated

Carbon atoms outer an electronic completely after ionization, electron spin elliptical orbit combination similar lithium atoms, but $N_{\theta 1}$=1.5, $N_{1,2}$=1, nuclear power charge for 4, see figure 17.6. Because the inner electronic external layer of symmetry electric repelling force balances effect, $\overline{Z}_1$ electronic translation angle Φ_1 negligible, we have:

$$\begin{cases}\dfrac{\overline{Z}_1e^2}{4\pi\varepsilon_0\overline{R}_{\theta 1}^2}=\dfrac{3.75e^2}{4\pi\varepsilon_0\overline{R}_{\theta 1}^2}-\dfrac{e^2\overline{R}_{\theta 1}}{4\pi\varepsilon_0 L_{1,2}^3} & (17.19-1)\\ \dfrac{\overline{Z}_2e^2}{4\pi\varepsilon_0\overline{R}_{\theta 2}^2}=\dfrac{4e^2}{4\pi\varepsilon_0\overline{R}_{\theta 2}^2}-\dfrac{2e^2\overline{R}_{\theta 2}}{4\pi\varepsilon_0 L_{1,2}^3} & (17.19-2)\end{cases}$$

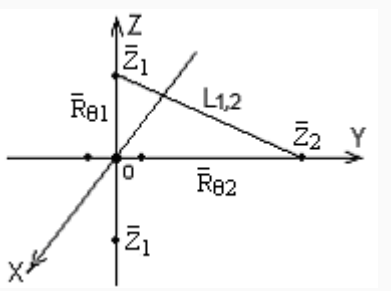

Figure 17.6 carbon ions within C^+ 5 electronic relative locations

Simplified to:

$$\begin{cases} \overline{Z}_1 = 3.75 - \left[1 + \left(\overline{R}_{\theta 2} \big/ \overline{R}_{\theta 1}\right)^2\right]^{-1.5} & (17.20-1) \\ \overline{Z}_2 = 4 - 2\left[1 + \left(\overline{R}_{\theta 1} \big/ \overline{R}_{\theta 2}\right)^2\right]^{-1.5} & (17.20-1) \end{cases}$$

By (15.12), (16.9) - (17.20) and equations united stand:

$$\frac{1}{N_{1,2}^2}\left(\frac{\overline{R}_{\theta 2}}{\overline{R}_{\theta 1}}\right)^3 = \frac{4 - 2\left[1 + \left(\dfrac{\overline{R}_{\theta 1}}{\overline{R}_{\theta 2}}\right)^2\right]^{-1.5}}{3.75 - \left[1 + \left(\dfrac{\overline{R}_{\theta 2}}{\overline{R}_{\theta 1}}\right)^2\right]^{-1.5}} \qquad (17.21)$$

By equations (17.13) to:

$$E_{\theta 2} = \sqrt{1 - \left(\frac{N_{\theta 2}}{N_{\theta 1}}\right)^2 \frac{\overline{Z}_1 \overline{R}_{\theta 1}}{\overline{Z}_2 \overline{R}_{\theta 2}}(1 - E_{\theta 1}^2)} \qquad (17.22)$$

Carbon ion internal structure, parameters of the simulation program are as follows:

1. Make the $N_{1,2}$ = 1, generation of (17.21) in type, too: $\overline{R}_{\theta 2}/\overline{R}_{\theta 1}$ = 0.9911356941.

2. Will $\overline{R}_{\theta 2}/\overline{R}_{\theta 1}$ = 0.9911356941value generation into (17.20) equations to: $\overline{Z}_1$ = 3.391714272 and $\overline{Z}_2$ =3.302315853.

3. Make $N_{\theta 1}=N_{\theta 2}=1.5$, $E_{\theta 1}=0.5$, and $\overline{Z}_1$, $\overline{Z}_2$, $\overline{R}_{\theta 2}/\overline{R}_{\theta 1}$ generation into (17.22) with, to: $E_{\theta 2}$= 0.4720245236.

4. The above all kinds of generation into (15.11), respectively is general ionization energy $\sum \Delta W_{ei0}$ = 155.5953768 ev, with carbon ion outer 3 electronic total ionization energy $\sum \Delta W_{ei0}$ = 136.762 ev, slightly bigger.

5. Adjust $E_{\theta 1}$ value, repeat 2 ~ 4 calculation procedure, finally to: when the $E_{\theta 1}$=0.583764115, $\sum \Delta W_{ei0}$ = 136.762 ev.

6. By (15.7), (15.12), make theθ_i =0, π, obtained carbon ion electron spin elliptical orbit parameters are:

$E_{\theta 1}$=0.583764115 $E_{\theta 2}$=0.5629201852

$R_{\theta 1(0)}$=0.221653A° $R_{\theta 1(\pi)}$=0.843383A° $\overline{R}_{\theta 1}$=0.532518A°

$R_{\theta 2(0)}$=0.230690A° $R_{\theta 2(\pi)}$=0.824906A° $\overline{R}_{\theta 2}$=0.527798A°

17.3.4. Carbon atomic energy level

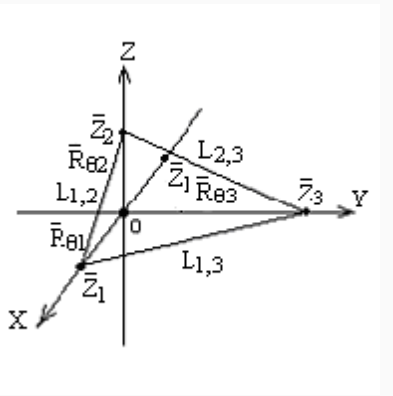

Figure 17.7 carbon ions in the electron iclocation plan

Carbon atoms outer an electron in the process of gradually ionization, the electron spin elliptical orbit combination model as shown in figure 17.7, we have:

$$\begin{cases} \dfrac{\overline{Z}_1 e^2}{4\pi\varepsilon_0 \overline{R}_{\theta 1}^2} = \dfrac{3.75e^2}{4\pi\varepsilon_0 \overline{R}_{\theta 1}^2} - \dfrac{e^2 \overline{R}_{\theta 1}}{4\pi\varepsilon_0 L_{1,2}^3} - \dfrac{e^2 \overline{R}_{\theta 1}}{4\pi\varepsilon_0 L_{1,3}^3} & (17.23-1) \\ \dfrac{\overline{Z}_2 e^2}{4\pi\varepsilon\ \overline{R}_{\theta 2}^2} = \dfrac{4e^2}{4\pi\varepsilon_0 \overline{R}_{\theta 2}^2} - \dfrac{2e^2 \overline{R}_{\theta 2}}{4\pi\varepsilon_0 L_{1,2}^3} - \dfrac{e^2 \overline{R}_{\theta 2}}{4\pi\varepsilon_0 L_{2,3}^3} & (17.23-2) \\ \dfrac{\overline{Z}_3 e^2}{4\pi\varepsilon_0 \overline{R}_{\theta 3}^2} = \dfrac{4e^2}{4\pi\varepsilon_0 \overline{R}_{\theta 3}^2} - \dfrac{2e^2 \overline{R}_{\theta 3}}{4\pi\varepsilon_0 L_{1,.3}^3} - \dfrac{e^2 \overline{R}_{\theta 3}}{4\pi\varepsilon_0 L_{2,3}^3} & (17.23-3) \end{cases}$$

Simplifiedas:

$$\begin{cases} \overline{Z}_1 = 3.75 - \left[1+\left(\dfrac{\overline{R}_{\theta 2}}{\overline{R}_{\theta 1}}\right)^2\right]^{-1.5} - \left[1+\left(\dfrac{\overline{R}_{\theta 3}}{\overline{R}_{\theta 1}}\right)^2\right]^{-1.5} & (17.24-1) \\ \overline{Z}_2 = 4 - 2\left[1+\left(\dfrac{\overline{R}_{\theta 1}}{\overline{R}_{\theta 2}}\right)^2\right]^{-1.5} - \left[1+\left(\dfrac{\overline{R}_{\theta 3}}{\overline{R}_{\theta 2}}\right)^2\right]^{-1.5} & (17.24-2) \\ \overline{Z}_3 = 4 - 2\left[1+\left(\dfrac{\overline{R}_{\theta 1}}{\overline{R}_{\theta 3}}\right)^2\right]^{-1.5} - \left[1+\left(\dfrac{\overline{R}_{\theta 2}}{\overline{R}_{\theta 3}}\right)^2\right]^{-1.5} & (17.24-3) \end{cases}$$

Simultaneous (15.41), (17.24-2), (17.24 3) type, obtained:

$$\frac{1}{N_{2,3}^2}\left(\frac{\overline{R}_{\theta 3}}{\overline{R}_{\theta 2}}\right)^3 - \frac{4 - 2\left[1+\left(\dfrac{\overline{R}_{\theta 1}}{\overline{R}_{\theta 3}}\right)^2\right]^{-1.5} - \left[1+\left(\dfrac{\overline{R}_{\theta 2}}{\overline{R}_{\theta 3}}\right)^2\right]^{-1.5}}{4 - 2\left[1+\left(\dfrac{\overline{R}_{\theta 1}}{\overline{R}_{\theta 2}}\right)^2\right]^{-1.5} - \left[1+\left(\dfrac{\overline{R}_{\theta 3}}{\overline{R}_{\theta 2}}\right)^2\right]^{-1.5}} \qquad (17.25)$$

By (15.41), (15.12), to:

$$N_{2,3} = \left(\frac{N_{\theta 3}}{N_{\theta 2}}\right)^3 \left(\frac{\overline{Z}_2}{\overline{Z}_3}\right)^2 \left(\frac{1-E_{\theta 2}^2}{1-E_{\theta 3}^2}\right)^{1.5} \qquad (17.26)$$

Carbon atomic energy level simulation procedure is as follows:

7. Make $N_{\theta 1}=N_{\theta 2}=N_{\theta 3}=1.5$, $N_{1,2}=N_{2,3}=1$, $E_{\theta 1}=0.58$, $E_{\theta 2}=E_{\theta 3}=0$, $\overline{Z}_1=3.4$, $\overline{Z}_2=3.3$, $\overline{Z}_3=1$, and in turn into (17.13-4), (17.13-1) type, to: $\overline{R}_{\theta 1}/\overline{R}_{\theta 3}$ = 0.4432152608, $\overline{R}_{\theta 2}/\overline{R}_{\theta 1}$ = 0.9900983595.

8. Will the $N_{2,3}$, $\overline{R}_{\theta 1}/\overline{R}_{\theta 3}$, $\overline{R}_{\theta 2}/\overline{R}_{\theta 1}$, together into (17.25), to: $\overline{R}_{\theta 3}/\overline{R}_{\theta 2}$ = 0.907849102.

9. Will the $\overline{R}_{\theta 1}/\overline{R}_{\theta 3}$, $\overline{R}_{\theta 2}/\overline{R}_{\theta 1}$ and $\overline{R}_{\theta 3}/\overline{R}_{\theta 2}$ values generation to equations (17.24) are respectively: $\overline{Z}_1$=3.32462785, $\overline{Z}_2$ = 2.897543763, $\overline{Z}_3$= 2.168058568.

10. Will the $N_{\theta i}$, $\overline{R}_{\theta 2}/\overline{R}_{\theta 1}$, $\overline{R}_{\theta 3}/\overline{R}_{\theta 2}$, $E_{\theta 1}$ value and new $\overline{Z}_i$ value respectively into (17.13-2), (17.13 3) type, too: $E_{\theta 2}$ = 0.4504219205, $E_{\theta 3}$= 0.416487862i imaginary (appear).

Table 17.12 carbon atomic energy level calculation results

$N_{\theta 3}$	$N_{2,3}$	$E_{\theta 1}$	$E_{\theta 2}$	$E_{\theta 3}$	$\sum \Delta W_{eib}$ ev	△Wev	实验值ev
	1	0.5781556	0.5558214	0.555821	146.758	1.264	1.264
1.5	1	0.5836997	0.5618043	0.561804	145.338	2.684	2.684
	2	0.5801173	0.5586506	0.604947	143.839	4.183	4.183
	8	0.5837641	0.5629032	0.295976	140.6249309	7.397 0690 6	7.480
2	12	0.5837641	0.5629144	0.435772	139.9865155	8.0354 8455	8.537
	18	0.5837641	0.5629183	0.553313	139.3881452	8.6338 5476	8.771
	22	0.5837641	0.5629192	0.092219	139.1157914	8.9062 0856	
2.5	24	0.5837641	0.5629194	0.220092	139.003486	9.0185 1404	9.003
	30	0.5837641	0.5629198	0.385714	138.7325458	9.2894 5424	9.172
3	44	0.5837641	0.5629201	0.069410	138.326576	9.6954 2398	9.713
	59	0.5837641	0.5629201	0.401584	138.0650824	9.9569 1758	
4	113	0.5837641	0.5629202	0.047909	137.6206096	10.401 3904	
	128	0.5837641	0.5629202	0.280214	137.5535977	10.468 4023	
5	225	0.5837641	0.56292018	0.028301	137.3084413	10.713 5588	
	240	0.5837641	0.56292018	0.205222	137.2856393	10.736 3607	
10^8		0.5837641	0.56292019	1.2×10^{-5}	136.7620136	11.259 9864	11.268
Note		This is only the $N_{2,3}$ interval value sand experimental value, from the trend can be seen level distribution					

11. Will $N_{\theta i}$, $\overline{Z}_i$, $E_{\theta i}$ value generation into (15.11), respectively, have four electronic total ionization energy: $\sum \Delta W_{eic}$ = 162.5306605 ev.

12. Will $N_{\theta i}$、$\overline{Z}_i$、$E_{\theta i}$ value again into (17.13-4), (17.13-1), 7 ~ 11 repeated calculation procedures, and finally to: $\sum \Delta W_{eic}$ = 146.2870955ev is constant.

13. Because of the determination of carbon atoms outer four electronic original total ionization energy of $\sum \Delta W_{ei0}$ = 148.022ev, adjust $E_{\theta 1}$ scope, repeat 7 ~ 12 calculation procedure, finally have to: When $E_{\theta 1}$=0.5731753467, $\sum \Delta W_{ei0}$ =148.022

ev.

Can be seen from the above results that carbon atoms outer first electronic ionization process, step by step with $N_{2,3}$, $N_{\theta 3}$, quantum number increases gradually, the inner electron spin elliptical orbit centrifugal rate will be critical state $E_{\theta 1}$= 0.5731753467 tends to ionic state $E_{\theta 1}$ = 0.583764115 transition. So that $N_{\theta 1}$=$N_{\theta 2}$=1.5, $N_{1,2}$=1, $N_{\theta 3}$=1.5, 2, 2.5, 3, 4, 5, …… 1000，$N_{2,3}$=1, 2, 3, ……∞， $E_{\theta 1}$ in tend to adjust values between 0.5731753467 ~ 0.583764115, repeat 7 to 13 calculation program, we can find out the carbon atoms all level, as shown in the table 17.12. After calculation is also know: $\overline{Z}_i$ only with $N_{2,3}$ values, has nothing to do with the value $N_{\theta 3}$, $E_{\theta 1}$; $\sum \Delta W_{eic}$ Only with $N_{2,3}$, $E_{\theta 1}$ value, has nothing to do with the value $N_{\theta 3}$; $N_{\theta 3}$ values reflect only the electron spin elliptical orbit centrifugal rate must be $E_{\theta 3}\rightarrow 0$.

19The theory of relativity and energy under the condition of electron spin elliptic orbit equation of motion

19.1 Energy under the condition of the theory of relativity electronic wave, spin orbital motion characteristics

The book section 1.1 (1.2) equations, the theory of relativity energy under the condition of electronic wave, spin orbital motion equations should be expanded to:

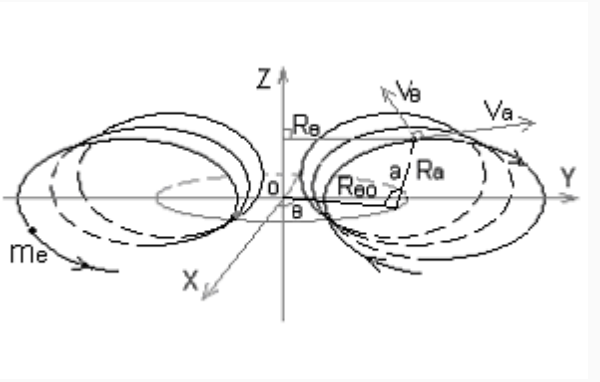

Figure 19.1 electronic waves, spin orbital motion characteristics schematic diagram

$$\begin{cases} R_\alpha = \dfrac{h}{2\pi m_e v_\alpha} & (19.1-1) \\ R_\theta = \dfrac{hN_\theta}{2\pi m_e v_\theta} & (19.1-2) \\ R_\theta = R_{\theta 0} - R_\alpha \cos\alpha & (19.1-3) \\ \alpha = N_\alpha \theta & (19.1-4) \\ v_e = \sqrt{v_\theta^2 + v_r^2} & (19.1-5) \\ \int_{\theta 0}^{\theta 0 + \frac{2\pi}{N\alpha}} \dfrac{1}{v_e} dl = \int_0^{2\pi} \dfrac{R_\alpha}{v_\alpha} d\alpha & (19.1-6) \end{cases}$$

And (1.2) equations is different (19.1-2) type in a spin quantum number N_θ, (19.1-5), (19.1-6) type of spin track length and spin speed will R_θ radial length dR_θ, speed v_r are included in the. Because of the fluctuation quantum number N_a, eccentricity E_a, speed v_a and electronic movement quality parameters such as m_e will be as comprehensive charge strength coefficient Z_i, spin angle θ position and change, therefore, (19.1-6) type said electronic in each wave orbit with the corresponding spin

orbit $d\theta = 2\pi/N_a$ on the parameters of the mean value. Simultaneous (19.1-1) ~ (19.1-3) type, reference (1.2) equations solution, make to the $R_a/R_\theta = v_\theta/v_a N_\theta = E_{a\theta}$, to:

$$\begin{cases} R_\alpha = \dfrac{R_{\theta 0} E_{\alpha\theta}}{1 + E_{\alpha\theta}\cos\alpha} & (19.2-1) \\ R_\theta = \dfrac{R_{\theta 0}}{1 + E_{\alpha\theta}\cos\alpha} & (19.2-2) \end{cases}$$

Both are still for mutual vertical wave, spin elliptic orbit equation. By (19.1) and (19.2) equations, reference (15.8) equations solution must:

$$\begin{cases} dl = \dfrac{R_{\theta 0}}{1 + E_{\alpha\theta}\cos N_\alpha\theta}\sqrt{1 + \left(\dfrac{N_\alpha E_{\alpha\theta}\sin N_\alpha\theta}{1 + E_{\alpha\theta}\cos N_\alpha\theta}\right)^2}\, d\theta & (19.3-1) \\ v_\theta = \dfrac{N_\theta h(1 + E_{\alpha\theta}\cos N_\alpha\theta)}{2\pi m_e R_{\theta 0}} & (19.3-2) \\ v_r = \dfrac{N_\theta h(N_\alpha E_{\alpha\theta}\sin N_\alpha\theta)}{2\pi m_e R_{\theta 0}} & (19.3-3) \\ v_e = v_\theta\sqrt{1 + \left(\dfrac{N_\alpha E_{\alpha\theta}\sin N_\alpha\theta}{1 + E_{\alpha\theta}\cos N_\alpha\theta}\right)^2} & (19.3-4) \end{cases}$$

Will (19.3) equations substitution (19.1-6) type, have to:

$$E_{\alpha\theta} = \frac{1}{\sqrt{N_\alpha N_\theta}} \qquad (19.4)$$

The type that: electronic wave, spin elliptic orbit eccentricity $E_{a\theta}$ and the conditions within the nucleus phenomen $\pi^{\pm}$ meson fluctuation, spin vertical double elliptic orbit movement of the eccentricity are similar, but the electron spin movement should be resultant velocity v_e said. By the energy theory of relativity, the electron spins direction of the movement quality m_e should be expressed as:

$$m_e = \frac{m_{e0}}{\sqrt{1 - (v_e/c)^2}} \qquad (19.5)$$

And electronic average quality $\overline{m}_e$ corresponding average fluctuations radius $\overline{R}_\alpha$, the average wave Angle $\overline{\alpha}$ ... Parameters, it is derived the electron spin orbital motion of the reference parameter. By (19.1-1), (19.2-1) and (19.5) type, a wave length of the orbit for L_a, reference (1.6) type solution must:

$$L_\alpha = \int_0^{2\pi} R_\alpha \, d\alpha = \int_0^{2\pi} \frac{R_{\theta 0} E_{\alpha\theta}}{1 + E_{\alpha\theta} \cos\alpha} d\alpha = \frac{2\pi R_{\theta 0}}{\sqrt{N_\alpha N_\theta - 1}} \qquad (19.6)$$

$$\overline{m}_e = \int_0^{2\pi} \frac{m_e}{L_\alpha} dl_\alpha = \int_0^{2\pi} \frac{hR_\alpha}{2\pi R_\alpha v_\alpha L_\alpha} d\alpha = \frac{h\sqrt{N_\alpha N_\theta - 1}}{2\pi R_{\theta 0} v_\alpha} \qquad (19.7)$$

Make $\overline{R}_\alpha$ = $R_{\theta o}$ $E_{a\theta}$/ (1 + $E_{a\theta}$ cos $\overline{\alpha}$), by the figure 19.2, (19.1-1) and (19.4), (19.5) and (19.7) type, we have:

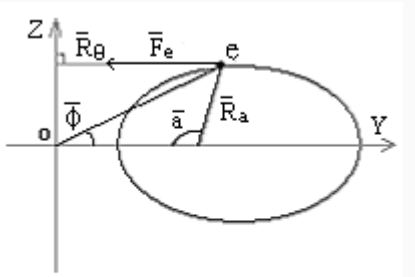

图19.2 电子波动、自旋轨道平均半径示意图

Figure 19.2 electronic waves, spin orbit mean radius schematic diagram

$$\begin{cases} R_{\theta 0} = \dfrac{r_0 a_c}{\beta_\alpha} \sqrt{(N_\alpha N_\theta - 1)\left[1 - \left(\dfrac{v_e}{c}\right)^2\right]} & (19.8-1) \\ \cos\overline{\alpha} = \sqrt{N_\alpha N_\theta - 1} - \sqrt{N_\alpha N_\theta} & (19.8-2) \\ \overline{R}_\theta = \dfrac{R_{\theta 0}\sqrt{N_\alpha N_\theta}}{\sqrt{N_\alpha N_\theta - 1}} & (19.8-3) \\ \sin\overline{\alpha} = \sqrt{1 - cos^2\overline{\alpha}} & (19.8-4) \end{cases}$$

The figure 19.2 shows, the electron spin orbit each fluctuation in orbit by comprehensive field average force $\overline{F}_e$ for:

$$\overline{F}_e = \frac{-Ze^2 \cos^3\overline{\phi}}{4\pi\varepsilon_0 \overline{R}_\theta^2 \sqrt{1 - \left(v_\theta / c\right)^2}} \qquad (19.9)$$

Among them, by (19.8) equations:

$$\cos\overline{\phi} = \frac{\overline{R}_\theta}{\sqrt{\overline{R}_\theta^2 + (\overline{R}_\alpha \sin\overline{\alpha})^2}} = \frac{1}{\sqrt{2\sqrt{1-\frac{1}{N_\alpha N_\theta}} - 1 + \frac{2}{N_\alpha N_\theta}}} \quad (19.10)$$

19.2 The theory of relativity energy under the condition Of electron spins elliptic orbit equation of motion

In the multilayer, multiple atom lining, each electron in nuclear and other electronic integrated electric field under the action of charge strength factor Z_i is a variable. When the electron spins orbital motion their quality and electric field force strength will appear energy relativity speed effect. Along the electron spin orbital motion of the moment of momentum conservation law, (19.5), (19.9) and (15.1) equations, the electron spin orbital motion equations should be expanded to:

$$\begin{cases} R_\theta = \dfrac{N_\theta h}{2\pi m_e v_\theta} & (19.11-1) \\ m_e(\ddot{R}_\theta - R_\theta\dot{\theta}^2) = \dfrac{-Z_i e^2\cos^3\overline{\phi}}{4\pi\varepsilon_0 R_\theta^2\sqrt{1-\left(v_\theta/c\right)^2}} & (19.11-2) \\ m_e(R_\theta\ddot{\theta} + 2\dot{R}_\theta\dot{\theta}) = \dfrac{m_e}{R_\theta}\dfrac{d(R_\theta^2\theta)}{dt} = 0 & (19.11-3) \\ m_e = \dfrac{m_{e0}}{\sqrt{1-\left(v_e/c\right)^2}} & (19.11-4) \end{cases}$$

Reference (15.1) ~ (15.7) and all kinds of equations is derived, and the solution. We first assume that m_e, v_θ, v_e, $\cos\overline{\phi}$, Z_i, five parameters in the electronic spin orbit within a short period of dl_θ each are remain unchanged.

Make $R_\theta = \dfrac{1}{u}$, to: $\dfrac{dR_\theta}{dt} = \dfrac{dR_\theta}{d\theta}\dot{\theta}$, $dR_\theta = -\dfrac{du}{u^2}$, $\dot{\theta} = \left(\dfrac{N_\theta h}{2\pi m_e}\right)u^2$ $\dot{R}_\theta = -\left(\dfrac{N_\theta h}{2\pi m_e}\right)\dfrac{du}{d\theta}$,

$$\ddot{R}_\theta = -\left(\frac{N_\theta h}{2\pi m_e}\right)^2 u^2\frac{du^2}{d\theta^2}$$

Will these transition results are substituting (19.11) equations:

$$\frac{du^2}{d\theta^2}+u=\frac{Z_i\cos^3\overline{\phi}}{r_0N_\theta^2\sqrt{\left[1-\left(v_\theta/c\right)^2\right]\left[1-\left(v_e/c\right)^2\right]}}=\frac{1}{R_{\theta 0}} \qquad (19.12)$$

The (19.12) decline point's equation solution for: $u=C_1\cos\theta+C_2$

Because: $\frac{du}{d\theta}=-C_1\sin\theta$, $\frac{du^2}{d\theta^2}=-C_1\cos\theta$, substituting (19.12) to: $C_2=\frac{1}{R_{\theta 0}}$.

And because: $R_\theta=\frac{1}{u}$, so, the electron spin elliptic orbit equation of motion for:

$$R_\theta=\frac{1}{C_2+C_1\cos\theta}=\frac{R_{\theta 0}}{1+E_\theta\cos\theta} \qquad (19.13)$$

Including:

$$R_{\theta 0}=\frac{r_0N_\theta^2\sqrt{\left[1-\left(v_\theta/c\right)^2\right]\left[1-\left(v_e/c\right)^2\right]}}{Z_i\cos^3\overline{\phi}} \qquad (19.14)$$

By (19.13) and (19.14) type known: the electronic each a short spin motion track dl_θ speaking, electron spin motion track is still ellipse, but it and the earth's orbit around the sun movement of the elliptic orbit is different, R_θ is m_e, v_θ, v_e, $\overline{\phi}$, Z_i parameter functions; These parameters are variable and, without doubt than many planets revolve around the sun movement is more complicated. In the energy under the condition of the theory of relativity, the electron spin elliptic orbit equation of motion, should be called variable elliptic orbit equation.

19.3 electrons spin variable elliptic orbit equation eccentricity E_θ change analysis

By (19.11-1) and (19.13) and (19.14) type, electronic along the variable elliptic orbit spin movement speed v_θ for:

$$v_\theta=\frac{Z_ia_cc\cos^3\overline{\phi}(1+E_\theta\cos\theta)}{N_\theta\sqrt{1-\left(v_\theta/c\right)^2}} \qquad (19.15)$$

Because $v_\theta = \beta_\alpha c\sqrt{N_\theta / N_\alpha}$, from (19.10) type, substituting (19.15) type, get electronic wave velocity coefficient β_a for:

$$\beta_\alpha = \sqrt{\frac{N_\alpha}{2N_\theta}\left\{1-\sqrt{1-\frac{4}{N_\theta^2}\left[Z_i a_c(1+E_\theta\cos\theta)\right]^2\left(2\sqrt{1-\frac{1}{N_\alpha N_\theta}}-1+\frac{2}{N_\alpha N_\theta}\right)^{-3}}\right\}}$$

（19.16）

Make (19.16) type of N_θ, θ, E_θ, Z_i for a known determine value, substituting (19.16) type, and with (4.9) type simultaneous, can find out the location of the electron wave quantum number N_a, as the basis for subsequent accurate calculation.

Reference (19.3) of the equations is derived, the electron spin orbital motion of the two velocity v_θ, v_r, niv speed v_e respectively is:

$$\begin{cases} v_\theta = \dfrac{N_\theta h(1+E_\theta\cos\theta)}{2\pi m_e R_{\theta 0}} & (19.17-1) \\ v_r = \dfrac{N_\theta h E_\theta \sin\theta}{2\pi m_e R_{\theta 0}} & (19.17-2) \\ v_e = v_\theta\sqrt{1+\left(\dfrac{E_\theta\sin\theta}{1+E_\theta\cos\theta}\right)^2} & (19.17-3) \end{cases}$$

Theoretical mechanics has already proved, the planets in the solar system in the sun under the action of gravity field around the sun, the elliptic orbit movement, each planet on the track of any point, its kinetic energy and potential energy of the sun to its gravity is the same value; The value and elliptic orbit eccentricity or long shaft related, and is not to track the position. This book (15.9) ~ (15.13) type show that when Z_i for constant, electron spin velocity $v_\theta << c$, regardless of the energy theory of relativity speed effect. Electronic in nucleus as the center of gravity field, the spin around the nucleus ellipse, its kinetic energy and potential can also the sum of the same value. Only with elliptic orbit eccentricity or long shaft related, and is not to track the position. Both the theory of relativity is energy under the condition of the law of conservation of energy of the specific forms.

We just can use the law of conservation of energy, derived electronic in different N_θ, θ, E_θ, Z_i condition, to the energy theory of relativity speed along the spin variable elliptic

orbit movement of energy change, and then determine the change rule of eccentricity. Calculation procedure is as follows:

1. The first set a electronic along the spin variable elliptic orbit movement N_θ, E_θ, Z_i each for a constant value, and they make θ_i = 0, π/3,... π, rhapsodize about it, substituting (19.16) type, and (4.9) type simultaneous, respectively and the electron in the several position fluctuations quantum number $N_{a(0)}$, $N_{a(\pi/3)}$,... $N_{a(\pi)}$ values.

2. Will $N_{a(0)}$, $N_{a(\pi/3)}$,... $N_{a(\pi)}$ respectively equivalent substitution (4.9) type, and the electronic wave velocity ratio$\beta_{a(0)}$, $\beta_{a(\pi/3)}$, …… $\beta_{a(\pi)}$ values.

3. By the $v_\theta = \beta_a c\sqrt{N_\theta / N_\alpha}$, (19.17), respectively, and the equations of the electron $\theta_i = 0, \pi/3, \ldots\ldots \pi$ position of the spin velocity v_θ, v_e values.

4. The electron spin orbit each position kinetic energy $W_{m(0)}$, $W_{m(\pi/3)}$,... $W_{m(\pi)}$, the energy theory of relativity, (19.11-4) type, have to:

$$W_{m(\theta)} = \frac{m_{e0}c^2}{e}\left[\frac{1}{\sqrt{1-\left(v_{\theta(\theta)}/c\right)^2}}-1\right] \qquad (19.18)$$

5. The electron spin orbit a position θ = 0, π/3, π, the potential can $W_{e(\theta)}$, by the (19.9) and (19.10), (19.13) and (19.14), type to:

$$W_{e(\theta)} = \frac{-Z_i e^2\cos\bar{\phi}}{4\pi\varepsilon_0 R_\theta\sqrt{1-\left(v_{\theta(\theta)}/c\right)^2}} = \frac{-Z_i^2 e^2\cos^4\bar{\phi}(1+E_\theta\cos\theta)}{4\pi\varepsilon_0 r_0 N_\theta^2\left[1-\left(v_{\theta(\theta)}/c\right)^2\right]\sqrt{1-\left(v_{e(\theta)}/c\right)^2}}$$

(19.19)

6. Reference (15.9) ~ (15.13) type the deduced, electronic in the orbit position of ionization energy $\triangle W_{e(\theta)}$ should be constant:

$$\triangle W_{e(\theta)} = W_{m(\theta)} + W_{e(\theta)} \qquad (19.20)$$

Make $N_{\theta 1}$ = 1, Zi are 1, 10, 30, 50, 70, 90, in each group set point, then make E_θ, θ for a set of values, in turn, substituting 1 ~ 6 calculation procedure, the result see table 19.1.

Electron spin variable elliptic orbit eccentricity, ionization energy change results table table 19.1

$E_{\theta i}$	0	π/3	2π/3	π
	Z_i=1		N_θ =1	
0.0	13.6058	13.6058	13.6058	13.6058
0.1	13.4700	13.4699	13.4698	13.4697
0.5	10.2064	10.2053	10.2044	10.2042
Z_i=10		N_θ =1		
0. 0	1362.38	1362.38	1362.38	1362.38
0.1	1350.55	1349.66	1348.21	1347.63
0.5	1041.08	1030.73	1021.44	1020.09
Z_i=30		N_θ =1		
0.0	12401.5	12401.5	12401.5	12401.5
0.1	12409.5	12344.4	12235.2	12190.3
0.5	10550.1	9916.19	9268.97	9158.87
Z_i=50		N_θ =1		
0.0	35385.9	35385.9	35385.9	35385.9
0.1	35972.5	35510.1	34713.3	34374.7
0.5	34522.6	30543.0	26213.4	25354.3
Z_i=70		N_θ =1		
0.0	72997.0	72997.0	72997.0	72997.0
0.1	76013.9	74146.7	70954.0	69595.9
0.5	87961.3	69487.8	52980.3	49576.5
Z_i=90		N_θ =1		
0.0	132556	132556	132556	132556
0.1	144762	137691	126666	122266
0.5		155929	91931	82024
Note	The blank space part can't solve, energy units：ev			

By table 19.1 see: E_θ=0 is the only solution, so, in multilayer, multiple electronic atomic internal, Z_i space change rule will determine electron spin orbit parameters change. To $Z_i \leq 10$ atomic electrons to the energy theory of relativity condition calculation error is very small. Electron spin elliptic orbit of eccentricity is allowed to have certain value range. But the total energy must be completely conservation, (front electron spin movement and lateral rotary motion of the magnetic field energy were not involved in

calculation).

Comprehensive analysis of the chapter 15 ~ 19 and the calculated results are compared, can see the atomic internal electronic spin orbit parameters change rule: 1. Spin quantum number $N_{\theta i}$ surface take 1, 1.5, and gradually ionization process, $N_{\theta i}$= $1 \rightarrow \infty$, internal all take $N_{\theta i}$ = 1, 2. Atomic inner electron spin elliptic orbit eccentricity E_θ= 0, time and energy in the outer surface of the theory of relativity spin movement similar premise condition E_θ can be in between 0 ~ 1 move; 3. Atomic layer within the electronic must be synchronous spin movement, only in this way, each layer inside each electronic, $\overline{Z}_i$, E_θ values in the lining of the electronic shielding effect to maintain constant, spin ellipse to set up, each electronic integrated electric field force of the force to the spin orbital motion of the radius vector pointing to nuclear center, conservation of angular momentum of the quantization fluctuation, spin orbital motion can be established; 4. Atomic surface electron pair inner electron electric field force can be neglected, the inner surface of the electronic to electronic field stress shielding effect can make the surface electron spin elliptic orbit surface of revolution into small in the large flow line surface of revolution "electron clouds". Before 3 rules for subsequent atomic inner electron spin orbit parameter calculation and provides a convenient.

20 Atom in K, L layer electronic wave, spin orbital motion characteristics and parameters are calculated

20.1 Atoms in K, L layer electronic X ray properties and characteristics

The laboratory has accurate determination of the atom in K, L layer electronic X-ray critical absorption and emission energy. To $_{100}$Fm, $_{40}$Zr element, for example, see table 20.1.

Atom in K, L layer electronic X-ray critical absorption and emission can scale (ev) table 20.1

$_{100}$Fm	L layer level		K layer level	K layer within the layer electronic ionization energy level difference			
K_{ab}			141510				
$K_{\beta 2}$			140122	1388			
$K_{\beta 1}$			136075	5435	4047		
K_{a1}			120598	20912	19524	15477	
K_{a2}			114926	26584	25196	21149	5672
L layer				20912	19879	16113	
level	27503	16379		26584	25475	21785	
$_{40}$Zr	L layer level		K layer level	K layer within the layer electronic ionization energy level difference			
K_{ab}			17998				
$K_{\beta 2}$			17969	29			
$K_{\beta 1}$			17666	332	303		
K_{a1}			15774	2224	2195	1892	
K_{a2}			15690	2308	2279	1976	84
L layer				2220	2219	2040	
level	2547	2042		2305	2302	2124	

Similar to the hydrogen atom spectrum calculation and atomic energy level characteristics, temporary not consider nucleus and each layer between the various electronic electric and magnetic fields interaction on the influence of various electronic ionization energy level. Atomic inner electron X-ray critical absorption and emission energy should be regarded as directly from high energy X-ray photons will K, L layer electronic one-time collision excitation emission to atomic outside energy, or external

static electronic direct transition to K, L layers of electron spin orbit emit a photon energy. On behalf of the K, L layer in each layer of the electron spin orbital motion of their original ionization energy. Table 20.1 right L layer 6 X-ray level is K layer in each layer of the electron spin orbit stimulated or transition between the absorption and emission X-ray energy. The left 2 energy value, almost equal, the other 4 smaller, the system of $(1 \sim 7)/100$, obviously, they should be the electron excitation, transition process exists in other forms of energy conversion and mutual electric, magnetic field effects on the level of influence. The left column of table 20.1 2 L layer electronic ray level should be truly representative of the intraformational 2 electronic original ionization energy.

20.2 Atoms in K, L layer electronic wave, spin rbital motion characteristics and parameters are calculated

20.2.1 Atomic inner K, L layer electronic wave, spin orbit parameters are calculated

Because the whole atom in each layer, various electronic and electric and magnetic fields between nuclear interaction, and to make every layer, each layer of each electronic along the fluctuation, spin orbital motion of charge strength coefficient value Z_i is always a fairly complex variable. The author have not collected within the atom each electronic integrated magnetic moment of the experimental value of parameters, the calculation of magnetic energy also lack basis, so, this chapter will not enter all along the electron spin orbital motion interaction of the magnetic field energy, inside and outside layer electronic shielding effect. First by the atomic K, L layer in the layer of the electronic spin orbit excitation, transition when absorption or emission X-ray photon energy to simulation the layer electronic charge function average strength factor $\overline{Z}_i$, corresponding the fluctuation, spin orbit parameters.

Because the atoms in K, L layer electronic spin orbit, $N_\theta = 1$, $v_\theta = v_e$, $E_\theta = 0$, so relevant parameters calculation formula can be simplified. By (9.16) type, electronic wave velocity ratio β_a is:

$$\beta_\alpha = \sqrt{\frac{N_\alpha}{2}\left\{1-\sqrt{1-(2\overline{Z}_i a_c)^2\left(2\sqrt{1-\frac{1}{N_\alpha}}-1+\frac{2}{N_\alpha}\right)^{-3}}\right\}} \qquad (20.1)$$

Will (20.1) and (4.9) type group stand:

$$\sqrt{\frac{N_\alpha}{2}\left[1-\sqrt{1-(2\overline{Z}_i a_c)^2\left(2\sqrt{1-1/N_\alpha}-1+\frac{2}{N_\alpha}\right)^{-3}}\right]} = \frac{\sqrt{32N_\alpha+a_c^2(N_\alpha-1)}-a_c\sqrt{N_\alpha-1}}{4\sqrt{2N_\alpha}} \quad (20.2)$$

The theory of relativity and energy (19.5) type, electronic along the spin orbital motion of the kinetic energy $\overline{W}_m$ for:

$$\overline{W}_m = \frac{m_{e0}c^2}{e}\left\{\left[1-\left(\frac{v_\theta}{c}\right)^2\right]^{-0.5}-1\right\} \quad (20.3)$$

The diagram (19.2) and (19.10) type:

$$\cos\overline{\phi} = \left(2\sqrt{1-\frac{1}{N_\alpha}}-1+\frac{2}{N_\alpha}\right)^{-0.5} \quad (20.4)$$

By (19.19) type, electronic spin orbital motion along the average potential can $\overline{W}_e$ for:

$$\overline{W}_e = \frac{\overline{Z}_i^2 e^2\cos^4\overline{\phi}}{4\pi\varepsilon_0 r_0\left[1-\left(v_\theta/c\right)^2\right]^{1.5}} \quad (20.5)$$

Electronic ionization energy $\Delta\overline{W}_e$ for:

$$\Delta\overline{W}_e = \overline{W}_e - \overline{W}_m \quad (20.6)$$

By (19.8-1) type, electronic wave, spin orbit parameter $R_{\theta 0}$ for:

$$R_{\theta 0} = \frac{a_c r_0}{\beta_\alpha}\sqrt{(N_\alpha-1)\left[1-\left(\frac{v_\theta}{c}\right)^2\right]} \quad (20.7)$$

By (19.2) equations, make $a=0,\pi$, rhapsodize about it, electronic wave, spin orbit radius of inner and outer side are:

$$\begin{cases} R_\theta = \dfrac{R_{\theta 0}\sqrt{N_\alpha}}{\sqrt{N_\alpha} \pm 1} & (20.8-1) \\ R_\alpha = \dfrac{R_{\theta 0}}{\sqrt{N_\alpha} \pm 1} & (20.8-2) \end{cases}$$

With $_{100}$Fm atom, for example, the atom in K, L layer electronic wave, spin orbit parameter calculation program is as follows:

1. Set $\overline{Z}_i$ = 95, substituting (20.2) type, to: N_a = 3.038122032.

2. Will N_a value substitution (4.9) type, β_a = 0.998943977.

3. For $v_\theta/c = \beta_\alpha \Big/ \sqrt{N_\alpha}$, will $\overline{Z}_i$, N_a, β_a, $\beta_\alpha \Big/ \sqrt{N_\alpha}$ values respectively substitution (20.3) ~ (20.6) type, get electronic ionization energy $\Delta\overline{W}_e$= 152955.3887ev, than the experimental value 141510ev slightly big.

4. Adjust $\overline{Z}_i$ value range, repeat 1 ~ 3 calculation procedure until $\Delta\overline{W}_e$=141510 ev so far.

$_{100}$Fm atomic inner K, L layer electronic wave, spin orbit parameter calculation results table (unit: ev, A°) table 20.2

level / parameters	K_{ab}	$K_{\beta 2}$	$K_{\beta 1}$	K_{a1}	K_{a2}	$L_{I\,ab}$	L_{a1}
$\Delta\overline{W}_{ei}$	141510	140122	136075	120598	114926	27503	16379
$\overline{Z}_i$	92.28574	91.94110	90.91620	86.70329	85.03313	44.29352	34.40190
N_a	3.200082	3.221373	3.285732	3.568394	3.689546	11.17994	17.58303
$R_{\theta(0)}$	0.003051	0.003074	0.003143	0.003438	0.003561	0.009062	0.012347
$R_{\theta(\pi)}$	0.010786	0.010809	0.010878	0.011173	0.011296	0.016796	0.020081
$R_{a(0)}$	0.001706	0.001713	0.001734	0.001820	0.001854	0.002710	0.002946
$R_{a(\pi)}$	0.006030	0.006022	0.006001	0.005915	0.005881	0.005023	0.004789

5. Will the final, $\overline{Z}_i$, N_a, β_a, $\beta_\alpha \Big/ \sqrt{N_\alpha}$ values respectively substitution (20.7) type and (20.8) equations, get electronic wave, spin orbit parameter table 20.2. Other atoms simulation instance sees table 20.3, table 20.4, and table 20.5.

$_{80}$Hg atomic inner K, L layer electronic wave, spin orbit parameter calculation results table (unit: ev, A°) table 20.3

level / parameters	K_{ab}	$K_{\beta 2}$	$K_{\beta 1}$	K_{a1}	K_{a2}	$L_{I\,ab}$	L_{a1}
$\Delta\overline{W}_{ei}$	83106	82526	80258	70821	68894	14841	9987
$\overline{Z}_i$	74.13319	73.90621	73.00723	69.057804	68.20656	32.77473	26.95634
N_a	4.650707	4.674640	4.771362	5.236431	5.346212	19.21285	27.61807
$R_{\theta(0)}$	0.004473	0.004494	0.004580	0.004982	0.005074	0.013082	0.016454
$R_{\theta(\pi)}$	0.012207	0.012228	0.012314	0.012716	0.012809	0.020815	0.024187
$R_{a(0)}$	0.002074	0.002079	0.002097	0.002177	0.002195	0.002985	0.003131
$R_{a(\pi)}$	0.005660	0.005656	0.005638	0.005557	0.005540	0.004749	0.004602

If the reference to the conditions within the nucleus $\pi^{\pm}$ meson fluctuation quantum number value scope of N_a, N_a also should be simple fraction or natural number. Table 20.2 ~ in table 20.5, $\overline{Z}_i$, N_a value is regardless of the electron spin direction integrated magnetic field energy, each layer of many electronic integrated functions of the value. Because of the magnetic field energy than electric energy, electronic kinetic energy much smaller, so table 20.2 ~ table 20.5 the $\overline{Z}_i$ value is close to the real value.

$_{60}$Nd atomic inner K, L layer electronic wave, spin orbit parameter calculation results table (unit: ev, A°) table 20.4

level / parameters	K_{ab}	$K_{\beta 2}$	$K_{\beta 1}$	K_{a1}	K_{a2}	$L_{I\,ab}$	L_{a1}
$\Delta\overline{W}_{ei}$	43571	43298	42269	37359	36845	7144	5230
$\overline{Z}_i$	55.19302	55.02962	54.40810	51.31143	50.97375	22.83278	19.55529
N_a	7.639382	7.678098	7.828379	8.655758	8.754746	37.81120	50.89352
$R_{\theta(0)}$	0.006821	0.006848	0.006952	0.007510	0.007575	0.019910	0.023718
$R_{\theta(\pi)}$	0.014555	0.014582	0.014686	0.015244	0.015308	0.027643	0.031451
$R_{a(0)}$	0.002468	0.002471	0.002485	0.002553	0.002560	0.003238	0.003325
$R_{a(\pi)}$	0.005266	0.005262	0.005249	0.005181	0.005174	0.004495	0.004409

From table 20.2 to table 20.5 K, L layer electronic spin orbit space distribution range, we can see that: 1. When nuclear charge number $Z_i \leq 80$, K layer and L layer electronic wave, spin orbit no overlap, there are certain interval; 2. K, L layer and layer within the electronic wave, spin orbit of spiral ring surrounding space most overlap, staggered together. The former side reflects the stable nuclide $Z_i \leq 83$; The latter shows in the electronic electric dipole rotation radius coefficient K_r is 10^{-4} order of magnitude to $K_r\overline{R}_\alpha$ value as electron particle radius, plus with the charge phase rejection effect, each sublayer electronic symmetric synchronous movement, so, in the electronic tiny fluctuation, spin orbit overlap zone, dozens of electronic can still like highway overpass the same flow separately, never collide each other.

20.2.2 Electron spin elliptic orbit motion characteristics summary

Atomic inner electron should be paired movement, spin direction completely symmetrical same, fluctuation in opposite directions. That is, each pair of electronic wave, spin orbital motion are made by two waves, spin relative nuclear center completely symmetrical, spin cycle are T/2 (phase difference of π) of the orbit. In this way, we can be sure, paired electron wave motion direction magnetic field should cancel each other out.

By the law of conservation of energy and energy under the condition of the theory of relativity derived electron spin elliptic orbit equation of motion, elliptic orbit of eccentricity $E_\theta = 0$, into circular orbit. It is actually the conditions within the nucleus to the particle spiral ring orbit characteristics regression, should be fully established, correct. The energy theory of relativity is derived under the condition of the electron spin elliptic orbit equation, although $0 \leq E_\theta \leq 1$, relative total law of conservation of energy, it is only a result of approximation. When we will electronic along the elliptic orbit revolved additional lateral movement speed, kinetic energy, magnetic energy is taken into account, we have every reason to believe that: electronic energy relativity kinetic energy, relative nuclear power field, integrated the electric potential energy, magnetic energy summation also fully conform to the general law of conservation of energy.

Decided to atomic, molecular chemical properties, physical characteristics are atomic outer electron spin, additional lateral ellipsoid surface of revolution of the orbital motion characteristics. Inner X fluorescence ray spectrum feature only as a measurement of the atomic spectrum identification. Rail internal conversion in nuclear physics has been discussed. Table 20.2 ~ 20.5 table data in each sublayer is electronic

integrated action of simulation parameters. Make sure all the layers of electronic number, wave quantum number; it is necessary to consider mutual shielding effect, and simultaneous equations using simulation method. Because of the time and the author hand calculation tool limit, no longer continue to study.

21 Infinite eternal cosmology summaries

21.1 Hot big bang cosmology question form

21.1.1 Thermal explosion according to the formation of cosmology

The universe is how to form evolution? How is the end? Modern international day literati agree that the universe was created by a super high temperature, high density, and high can mathematical singularity in the formation of hot big bang. I support this theory based on observation are:

1. The spectrum red shift of Hubble's law think the universe is still in a state of inflation.

2. The existing same-sex 2.73 K blackbody spectrum cosmic background radiation.

3. Observation to helium, deuterium elements of the cosmic abundance than star internal reaction formation rate.

4. The age of the universe no more than 20 billion years.

21.1.2 Problems

The evolution of the universe is essentially stars, black holes, galaxy formation, evolution process, main performance for nuclear reaction evolution process. By the statistical theory of quantum mechanics theory system, cannot provide particle reaction and evolution of the basic physical model and theoretical support. It is hard to imagine, in order to looking for fifty years is still missing of so-called mixed number charge "quark" as the universe is the leading role of 0 ~ 7×10^{-5} seconds according to what? Before the big bang mathematical singularity physical meaning, model features what look? Our research is a catch-all in the universe of the most basic, real physical model, the motion characteristics and evolution law, not abstract mathematics new concept. The latter can only as help us to carry on the analysis and calculation of the auxiliary tool. This is the quantum statistical theory, the universe academic force physics and relativity in the field of widespread, in violation of the basic laws of physics, conventional and philosophy the common sense. Inevitably leads to the observation, sorting, research material, data selection, analysis and interpretation in the process of human bias. Control the Hubble's law before and after the advent of galaxy, the universe form

evolution theory, the literature of stars, the galaxy's actual observation data analysis, and interpretation and choice of difference will understand.

Observations show that the amount of dark matter in the universe for visual Ming 10 times more than the amount of matter, the general cluster, up to 100 ~ 300 times. What they with kind of state of matter there? How in the universe space distribution and evolution? We have observed from various types of galaxy formation and evolution to death the whole process, is gradually expansion or contraction of gradually? Active galactic nuclei, quasars huge energy radiation is how form? Spectrum red shift, especially whether high-redshift is cosmology sex...? The nature of the universal problems are not effectively resolved, the universe was formed in the evolution of research will be hot big bang form cosmology identified as the standard model and from any talk about?

Moreover, the thermal explosion formation cosmological 4 points according to the observation is worth questioning:

1. Spectrum red shift can only show the photon in the propagation of energy loss, Doppler redshift is not the only explanation, especially the quasar supernormal value red shift, some scholars have put forward question.

2. Isotropic 2.73 K blackbody spectrum cosmic background microwave radiation is the challenge Hubble red shift law, denial of the universe's expansion strong evidence. Because the blackbody spectrum background in the microwave radiation energy is lossed from other aspects necessary to obtain the supplementary to maintaining the balance. Since as black body, it can radiation all frequency, energy electromagnetic wave, of course, also can part absorbed all frequency, energy of electromagnetic energy, and the photon is the electromagnetic wave. By the law of conservation of energy can corollary: it will inevitably lead to spectrum red shift with distance into direct ratio increases, (see the next chapter).

3. Observation to helium, deuterium two elements of the cosmic abundance than star internal reaction formation rate also can be used as the basis. Helium, deuterium two elements in the evolution of stars process abundance is constantly changing and increasing. At present the scientific community about galaxy formation and evolution process of the knowledge level, who can determine the formation of the sun or other stars of the nebula, is after several generation of stars after combustion evolution explosion left residual nebula? We are now in the solar system; only know meteorites

nearby galaxy, stars, nebulae visual Ming material general composition. Don't know stellar debris neutron star, a White Dwarf, brown dwarfs, black dwarf and black hole content, distribution range. More do not know which accounts for more than 90% of the universe for dark matter, now and in the future, the composition of the internal structure is how formation, evolution. At the present level of understanding will detect helium, deuterium element abundance as the big bang universe form the original abundance based on reliability and have how old?

4. Age of the universe not more than 20 billion years, recently more unusual academic reports, he said after observation research that age of the universe for 13.6 billion years, the error of 0.2%.

At present academia that age of the universe basically has 3 kinds of methods, respectively the evaluation:

A. by "Hubble's law" certain constant H_o, calculate age of the universe, both the Hubble age T, such as:

H_o=50	T=19.7 billionyears
H_o=75	T=14.8 billionyears
H_o=100	T=9.8 billionyears

First of all, the Hubble constant is artificial difficult to determine value, review again the Hubble constant change history, to evaluate the Hubble's law and the reliability of the age of the universe is helpful:

In 1929, the Hubble I first given Ho = 500 km/sMpc (behind the unit is abbreviated).

In 1936, the Hubble considering the interstellar extinction influence, will be constant to Ho = 526. Since then, the number has been considered to be correct. The reason is the age of the universe is H_o^{-1} = 1.84 billion, and when using radioactive method determination in the crust of ancient rock age 1.8 billion years is consistent.

1945 years later, my American journey astronomers (Baade), observed M31 and neighboring galaxy, there are two kinds of cepheid variable stars, both classical cepheid variable and Lyra "RR type made father" variable. The former light than the latter, thus derived Magellanic cloud distance from 750000 light years to 1.5 million light-years away, the Hubble constant is to H_o= 260.

In 1956, Humasion Mayall and Sandege have summarized the 620 galaxy redshift

data, maximum Z = 0.202, think: H_o = 180.

Since 1956, Sandege in the system measurement Hubble constant, the first found Hubble used bright stars in the spiral galaxy is actually "H Ⅱ area", not a single star, both differ $1.^m8$. magnitude. The correction, the Hubble constant into H_o = 75.

The Hubble constant recently a number of observations

Table 21.1 (5) (the same below)

H_o(Km / sMpc)	Measuring method	献 literature
86±18	Virgin group of planetary nebula	Mende`z et al.(1993)
84±4	F—T method	Ford et al.(1996)
81±8	The virgin group cepheid variable stars	Van den Bergh (1995a)
80±12	SB Ups and downs	Jacoby et al. (1992)
78±11	In M87 globular clusters	Whitmore et al. (1995)
75±8	Day furnace and planetary nebula	McMillan et al. (1993)
70±13	Virgin group of supernova	Della Valle & Livio (1995)
60 或 82	Lens 0957+561	Grogin & Narayan (1995)
55±17	S – Z method	Birkinshaw & Hughes (1994)
55 ～ 60	SNe Ia (In theory)	Van den Bergh (1995b)
52±9	SNe Ia (1937C)	Saha et al. (1994)
52±8	SNe Ia (1972E)	Saha et al. (1995)
43±11	Galaxy diameter	Sandage (1993)
70±10	Cepheid variable	Freedman (1996)
55±10	Cepheid variable	Tamman (1996)
64±13	Gravitational lens	Tumer (1997)

In 1961, Sandege in the United States at the Berkeley IAU conference announced that summarizes all kinds of measurement results, H_o should be 75~113, the most

probable value $H_o = 98 \pm 15$. Since then, generally take H_o = 100.

1970 years later, led by the United States Sandege measuring group after more system, precise measurement confirmed $H_o = 50.3 \pm 4.3$. In France DE, Vacualear led another observation that the $H_o = 100 \pm 10$. The two groups at day on behalf of the literati observation Hubble constant of the highest level value are still nearly doubled.

1990 years later, with the Hubble space telescope to heaven, and further improve the measurement method, and then define H_o=75±8, equal to compromise in take value.

1990 years later representative measurement results see table 21.1.

By the Hubble constant ten times as many as in the process of change within it is not difficult to see that it is the scientific community based on measurement, prediction of rock, meteorites and stars age continuously revised, although day literati finally tend to take the Hubble constant H_o=75±8, still can't explain age of the universe. Because of the age of the globular clusters in the Milky Way galaxy in 12 billion, individual 17 billion years, still more for the present flat universe, the age of only $2/3H_o$ = 9.87 billion. This description: Hubble's law and the contradiction between the age of the universe has not harmonic.

B. the "solar system" within the rock, meteorites determination of radioactive element age

The half-life of radioactive elements by determination of elements of the age, first of all have a condition assumptions: rock just generation, mother nuclear element content is 100%, the son nuclear element content is 0.0%. Through the determination of radioactive decay after the mother nucleus, daughter nucleus related elements content ratio, again by determination of this element radioactive decay process the half-life of calculation. So, this age should is maximum. If use uranium - lead method:

$$\frac{Pb^{206}}{U^{238}} = e^{\lambda t} - 1 \qquad (21.1)$$

This measured the earth, moon rocks in the solar system, the oldest meteorites are over the age of 4.5 billion years.

If the supernova explosion by rich neutron conditions U_o^{235} formation, U_o^{238} theory ratio is 1.24, now measure for 1/140, according to the ratio of the two elements of the

radioactive half-life must:

$$\frac{U^{235}}{U^{238}} = \frac{U_0^{235}}{U_0^{238}} e^{-(\lambda 235 - \lambda 238)\, t} \qquad (212)$$

This is the age for 8.9 billion years.

We must face the fact that in the Milky Way galaxy slewing has great quality and the blue stars are forming. The famous Taurus crab nebula, A.D. that 1054 a supernova explosion formation. We are sure the inner solar system meteorites mainly from 8.9 billion years ago a supernova explosion residual fragments thing, but, as a spiral galaxy's disk family stars, 8.9 billion years ago the supernova explosion is the Milky Way in the family of double stars which generation of stars? The 8.9 billion years in the Milky Way or the age of the universe should belong to which time? Modern day literati can give confirmation?

C. the globular clusters LuoHe diagram decision age of the universe

Use of globular cluster LuoHe diagram method to get the most ancient globular cluster age of 17 billion years, see figure 21.1. If the globular cluster overall dynamics process is also taken into consideration, both globular cluster from formation to collapse, total about 20 billion years of age. This has been seen as a globular clusters in the universe of $<<10\%$ only visual Ming material composition, 17 billion more than the Hubble's law and the age of the universe, 13.6 billion more than the universe as a flat in 9.87 billion.

From LuoHe diagram, (21.2) type, the solar system: the meteorite formation age of 8.9 billion years, as the life of the star is about 13 billion years. At present the sun about 4.5 billion years of age. From the nebula material, meteorites origin to end the nuclear burning stars form a White Dwarf, total life of about 17.4 billion years. Therefore, we can make the reasoning: if in the Milky Way to see the sun in the quality and close to the White Dwarf, the age should be more than 17 billion years. If meet the quality for the mass of the sun only half of the White Dwarf, the age should be more than 24 billion years. Along with the White Dwarf energy radiation gradually cooling becomes invisible black dwarf or dark matter, then, these stars are remains of the age and should be how to calculate?

To sum up, the Hubble's law to determine the age of the universe has no meaning. By the evolution of stars LuoHe chart to determine the most ancient of globular clusters

age also represents only the visible surface of the cluster of stars age. Also not globular cluster center plays a main role the gravitational field of the black hole age, more is not the galaxy's age. You can be sure: the universe accounts for more than 90% of the dark matter is death star, globular cluster wreckage, even older or dead the whole galaxy remains.

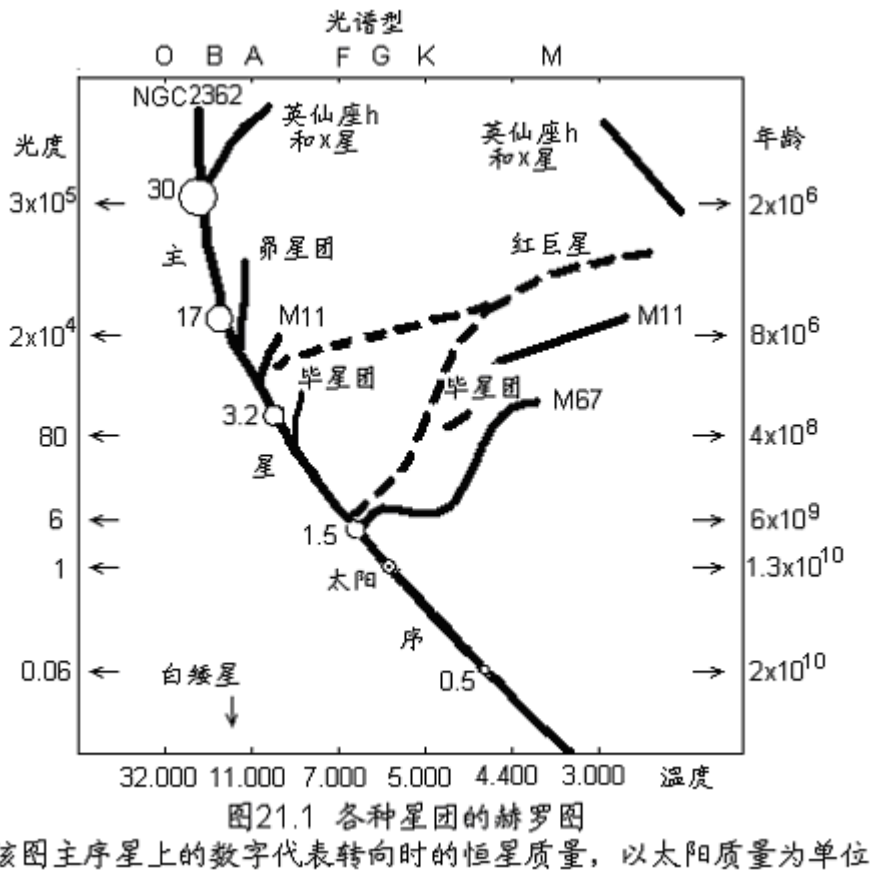

图21.1 各种星团的赫罗图

该图主序星上的数字代表转向时的恒星质量，以太阳质量为单位

Figure 21.1 all kinds of cluster of Hector ROM diagram

(The main sequence star on the figure of the representative to the star quality to the mass of the sun as the unit)

History has such lessons:

In 1922, Kapteyn for the first time found in the Milky Way there is dark matter. In 1933, Zwicky with system photometry and virial movement law of balance to cluster the galaxy motion law of comparative study found: virgo cluster of the quality of light than for 200 times, 400 times as much as the base cluster. With the improvement of observation technology, found that the more a waning galaxy, but quality than light still reach 10 times above. The young galaxy blue strong, qualitative light than small, old galaxy tend

to reddening, dark and light quality than the big, this law is recognized. This corollary: 18 mag galaxies is old galaxy, invisible galaxy or black dwarf, black holes, should be death galaxy or star debris (if galaxy scale, and the distance from the earth are almost). So, we must reiterate: at present academia popular age of the universe is only visible optical keep the stars within the age, not globular cluster center plays a main role the gravitational field of the black hole age, more is not the galaxy's age. The universe of 90% more dark matter is dead stars, globular cluster wreckage, even older or dead the whole galaxy remains. At present already observed most galaxy have spherical outer halo. Since the galaxy are made by mass of nebula shrinkage formation, then, halo inside of globular cluster or disk family star, when they die into a White Dwarf, black dwarf, neutron stars and black holes, we can see? The death of the stellar debris age is how old? The entire universe to account for more than 90% of the dark matter age is how old?

21.2 infinite eternal cosmological bases And model

21.2.1 Infinite, eternal cosmological basis

Infinite eternal cosmology is the Newton out, because can't explain Mr Bers paradox, spectral red shift to be abandoned. Now reverts the model and on the basis of as follows:

1. We observed cosmic space is Europe's 3 d flat space to cluster of large scale in the universe the uniform distribution is the same. (This model has started and Einstein's theory of relativity, time and space 27 ~ and chapter give system demonstration.

2. Mr Bers paradox, spectral red shift, blackbody cosmic background microwave radiation in the total energy conservation conditions whole into infinite eternal cosmological key basis. The relative motion between stars, galaxy is still there, but the cause with respect to the earth's observer Doppler red shift is only a minimum value, speed even reach 10^6 m/s, the red shift $Z \leq 0.0033$.

3. Active galactic nuclei, quasars internal structure, huge energy conversion model mechanism have been solved successfully.

4. In the study of neutron stars, black holes, the dark matter of the composition, structure, formation and evolution of the entire process, have overcome gravitational collapse, mathematical singularity difficulties. System can solve the stars, all kinds of

galaxy formation and evolution, death, into a black hole, dark matter, a black hole collision big bang, or black hole through the accretion disk accretion, polar axis injection, radio process, and nebula regeneration of the whole is material nebula, galaxy evolution process cycle.

5. Orbital theory of quantum physics and the infinite, eternal cosmology is microscopic and macroscopic, yu view field and unified whole. All according to all experiments have confirmed that the classical physics, energy relativity theory model set up. No new, without experiments, human imagination, abstract physics, mathematics new concepts, new model to participate in. Have been able to successfully solve Newton the infinite eternal cosmology and modern hot big bang cosmology cannot solve all the problems. Therefore, the basic physical model, theoretical basis and have already obtained results is of no doubt.

21.2.2 Infinite eternal cosmology summary

Modern astronomy observation research of different quality star material origin, formation, evolution to nova, supernovae, the big bang after the death of a White Dwarf, neutron stars, black holes, the stellar debris for electromagnetic pulse radiation and heat radiation to kinetic energy and heat energy completely exhausted, become we are unable to see brown dwarfs, black dwarf, black holes, the entire process, has been quite clear. Gravitational field are act the leading role. The author here only added 2: no longer emission electromagnetic pulse neutron stars and black dwarf, stars Level of black holes and globular cluster the central black hole and the dead large, medium and small galaxy, even galaxy group, all to the dark matter. Dark energy is the big bang universe acceleration model people guess out, this book is ignored.

In the present can be observed, within the scope of the countless nebula, various types of large and small different galaxy, including the initial formation of irregular small galaxy. The origin, formation and evolution of the whole process of to death with stars similar: the mass of nebula began, in the last round of residual small galaxy, stars debris respectively under the action of gravity field, Or floating in the space of the mass of nebula met along the rail passing other galaxy or galaxy group, also in gravitational field effect; Mass of nebula is the residue of small and medium-sized galaxy, stars debris, or passing other galaxy clusters, their formation of gravitational field, attract or tear; Each contraction respectively into size, type of galaxy or globular cluster. The original has entered the old state quality medium galaxy, gravitational field strength and gravity

range is larger, can attract the more new nebula substances, rapid development into large galaxy. The original has entered the middle-aged state of small galaxy, get part of the new nebula supplementation will become medium galaxy. As for the original galaxy edge or medium and small galaxy peripheral residual stars, stars debris, globular cluster, in limited within the scope of the gravitational field receive a small nebula material added renewable form small galaxy or globular cluster, even is the massive stars.

With the evolution of the various types of galaxy, the central galaxy nuclear quality increase gradually, gravitational field strengthen gradually, the galaxy visible stars distribution optical scope gradually shrink. Has detected the all kinds of elliptical galaxy, spiral galaxy peripheral all sizes spherical halo, is contraction after the residual traces. Keep the stars within the in formation, the nuclear burning, death, the explosion of replacement process, residual nebula gradually reduce the star formation rate and quality also gradually decreases, and star life but then extended. So, in the rest of the galaxy are reddening, quality smaller stars. The whole galaxy optical visual range also gradually contraction, qualitative light than increase gradually. If later not to get new nebula supplementation, and ultimately the galaxy or the entire galaxy group, even the small cluster will have become high density ball death galaxy, and the core of a galaxy, peripheral stellar debris neutron stars and black dwarf a, into the dark matter.

And the stars are similar, the quality of the galaxy, the central galaxy nuclear quality and gravitational field strength increase faster, the whole galaxy contraction also faster. The internal star formation rate and the star quality is bigger also, the entire galaxy's life is shorter. Especially the elliptical and giant elliptical galaxy, lack of spiral galaxy slewing that rotary orbital motion of the centrifugal force to maintain, its life is shorter.

Only when the two big, medium-sized, quality close galaxy nuclear or dead galactic nucleus in under the action of gravity collide head-on, will the big bang to form large group nebula, the diffusion range should be the whole galaxy group or larger. Not near death or dead of small and medium-sized galaxy or original galactic nucleus edge stellar debris, each become mass of new nebula split, gravitational contraction center. (such as a CD cluster center giant elliptical galaxy inside sometimes visible multiple galactic nucleus is not surprising that). And will start a new round of galaxy group of the origin, formation and evolution process. Due to the quality of the larger galaxy nuclear central black hole distance between, conflict of the "big bang" opportunity seldom.

Common is mutual winding movement has the attraction devour phenomenon, and with the polar axis injection and symmetry compact source radio disc, also can produce mass of new nebula. The two series can be repeated and eternal, infinite.

In the galaxy group, within the scope of the local gravitational field is located in the center of the galaxy group of quality center. With two galaxy nuclear collision big bang and change, local gravitational field center moved to a new round of galaxy group of quality center. Observations show that cluster in the large scale distribution is uniform, the gay, the scientific community has failed to determine, and will never be able to establish the boundary. Explain gravitation field, for each cluster is the overall to balance, uniform. Newton's law of universal gravitation mechanics early has already proved, in uniform, infinite, and density of material distribution in the space, infinite eternal universe, if cluster of large scale to measure, by each direction of gravitational force will tend to zero; Cluster within and around can exist position, strength changing gravitational field shrinkage center and mutual winding along certain orbital motion.

At the back, will the model of the main aspects of the argument.

22 Spectrum redshift is range scale

22.1 Spectrum redshift principle

22.1.1 2.73K blackbody cosmic background microwave radiation principle

Book particle physics part and the fifth chapter has already proved, photon, neutrinos are only charged particles by a pair of electric dipole, fluctuation, precession orbit are cylindrical helix; Fluctuation, precession speed are the speed of light, the fluctuation, precession orbital motion velocity vector and are $\sqrt{2}$ c. In the whole universe, photon and neutrino, are only a (regardless of the antiparticle), only the size of energy and wave, precession the length of the track, and different. Two kinds of particles all have wave-particle duality, fluctuation radius R_a and electric dipole rotation radius ratio K_r=(1.3026~74.637) x 10^{-10}, (a=0°~89°). Wave-particle duality can also understand directly for the cylindrical spiral wave, precession orbital motion of the wavelength of $\lambda = 2\pi\overline{R}_\alpha$, particle radius of entity for $R_{\alpha\bullet} = K_r\overline{R}_\alpha$. The only difference is in the neutrino electric dipole rotation frequency is photon N_U times, N_U=5991~343323. Neutrino along the fluctuation, precession orbital motion shows that the electromagnetic wave is like a continuous frequency, amplitude modulation wave series.

The universe 2.73 K microwave blackbody background radiation field is in the neutrino field medium of the shock wave. Neutrinos, photon under certain conditions can transform into each other. Neutrinos field of neutrino was high frequency electromagnetic field excitation can turn into the photon (frequency is greater than the $\overline{m}_\nu c^2 / h \geq photon$ conditions). Neutrinos field is electromagnetic and gravitational field of the media, in the space of neutrino velocity is the speed of light.

The basic laws of physics know: any wave propagation should have media, and any energy wave in the media will spread for medium vibration, temperature and friction loss of energy. To the electromagnetic wave and the photon, because of the fluctuation, precession speed are fixed to the speed of light, the energy loss can only lead to wavelength increase, not only cause red shift; Of course, and the light propagation direction opposite movement also can produce frequency smaller red shift; But as stars, galaxy speaking, this kind of red shift quantity is limited; General relative visual acuities to speed 1000 Km/s, Individual such as M31 and light propagation direction of the

movement of the blue shift also however 119 Km/s. The back section 26.4 we will prove, only different material component composition, can achieve different movement speed.

So, the universe blackbody microwave radiation background fields since the frequency of electromagnetic can to radiation, for added loss of energy, maintain long-term stable energy radiation balance, it's necessary to absorb energy. As a medium of electromagnetic wave propagation of neutrino field, neutrino and photon with similar and the essential characteristics of absorbing energy, the first choice of object nature is electromagnetic wave and the photon, Moreover, spectrum red shift and blackbody radiation the established overall energy balance system and rightly explains Mr Bers detailed Hubble's law and Samuel. Of course, all kinds of cosmic rays of neutrino field also provide any part of the energy function.

22.2 Spectrum red shift parameter calculation

The calculation results by chapter 5: neutrino floor neutrino average density of 860/cm^3. Set each microwave energy levels of neutrino average quality for: $\overline{m}_\nu$ = 6.221566264 x10^{-40} kg. By (1.2-1) type, the average wave radius $\overline{R}_\nu$ for:

$$\overline{R}_\nu = \frac{h}{2\pi \overline{m}_\nu c} = 5.654 \times 10^{-4}\, m \qquad (22.1)$$

To neutrino, photon inside electric dipole rotation radius coefficient K_r, we unified take mean: K_r = 2.6052 x 10^{-10}. Because of neutrino within the electric dipole rotation frequency N_u is extremely high, equivalent to the fluctuation, precession cylindrical spiral orbit are beaded electric dipole ball; If we to electric dipole rotation by rail ring for volume, as a blackbody radiation absorption, the volume of V_l, we have:

$$V_l = 2\pi \overline{R}_\nu \sqrt{2}\pi (K_r \overline{R}_\nu)^2 = 2\sqrt{2}\overline{R}_\nu (\pi K_r \overline{R}_\nu)^2 \qquad (22.2)$$

With electric dipole each rotation frequency electromagnetic field by ball volume, as a photon through energy target area V_0, we have:

$$V_0 = \frac{4}{3}\pi (K_r \overline{R}_\nu)^3 \qquad (22.3)$$

A neutrino inside electric dipole rotation by rail ring volume in neutrino field of space density ratio for $K_{\nu l}$:

$$K_{vl} = V_l \times 860 \times 10^6 / m^3 \qquad (22.4)$$

Because of the photon energy far outweigh the neutrino background field of microwave level of neutrino average energy, so wavelength, wave radius is far less than the wavelength of neutrinos, volatility radius. To simplify the photons to point particle, it along the fluctuation, precession cylindrical spiral orbital motion stroke T time, can impact the neutrino electromagnetic field ball number N_{mu} for:

$$N_{mv} = \frac{\sqrt{2} c T \pi (K_r \overline{R}_v)^2 K_{vl}}{V_0} \qquad (22.5)$$

Will (22.1), (22.3) and (22.4) type results substitution (22.5) type, to: N_{mu} = 635.7595T. Both photon in space operation, along the way to a second through the 635.7595T microwave level neutrino inside electric dipole rotation formation of electromagnetic field goals, and photon operation time, is proportional to the distance. Because of the photon energy far outweigh the neutrino background field of microwave level neutrino average energy, a photon every through a neutrino electromagnetic field on the ball will loss K_w coefficient of energy, $K_w \to 0$, so, can make the photon energy m_γ for constant. By (1.2-1) type, through the $n=N_{mu}$ a neutrino electromagnetic field after the ball photon wavelength λ_i into:

$$\lambda_i = \frac{h}{m_r (1 - K_w)^n c} \qquad (22.6)$$

Make light just for the photons emitted by a wavelength λ_0, then through the first neutrino electromagnetic field ball, wavelength for λ_1, red shift for K_{z1}, through the first n a neutrino electromagnetic field the ball wavelength λ_n available sequence said:

$$\begin{cases} \lambda_1 = \dfrac{h}{m_r (1 - K_w) c} & K_{z1} = \dfrac{\lambda_1}{\lambda_0} - 1 = \dfrac{1}{1 - K_w} - 1 & (27.7-1) \\ \lambda_2 = \dfrac{h}{m_r (1 - K_w)^2 c} & K_{z2} = \dfrac{\lambda_2}{\lambda_1} - 1 = \dfrac{1}{1 - K_w} - 1 & (27.7-2) \\ \cdots\cdots \quad \cdots\cdots & \cdots\cdots \quad \cdots\cdots & \cdots\cdots \\ \lambda_n = \dfrac{h}{m_r (1 - K_w)^n c} & K_{zn} = \dfrac{\lambda_n}{\lambda_{n-1}} - 1 = \dfrac{1}{1 - K_w} - 1 & (27.7-n) \end{cases}$$

The photon operation the red shift $Z = \sum K_{zi}$ for:

$$\sum K_{zi} = \frac{N_{mv} K_w}{1 - K_w} \qquad (22.8)$$

The equations (22.7) and (22.8) type, for n= N_{mu}, we have:

$$K_w = \frac{\sum K_{zi}}{\sum K_{zi} + N_{mv}} \qquad (22.9)$$

The Hubble's law, spectrum red shift $\sum K_{zi}$ and distance R relationship for:

$$R = \frac{\sum K_{zi}}{H_0} \qquad (22.10)$$

H_o takes 75 km/sMpc, conversion: H_o = 1/13031 x 10^6 light years away.

In different red shift value, respectively substitution (22.10), (22.5) and (22.9) type, get R, N_{mu}, K_w parameter table 22.1.

Spectrum red shift ΣK_{zi} and distance R relation calculation results table table 22.1

ΣK_{zi}	R (light-years)	N_{mu}	K_w
0.01	1.3031×10^{8}	2.6126×10^{18}	3.827×10^{-21}
0.1	1.3031×10^{9}	2.6126×10^{19}	3.827×10^{-21}
1	1.3031×10^{10}	2.6126×10^{20}	3.827×10^{-21}
10	1.3031×10^{11}	2.6126×10^{21}	3.827×10^{-21}
100	1.3031×10^{12}	2.6126×10^{22}	3.827×10^{-21}

From the above derivation calculation result: photon and microwave energy levels of neutrino electromagnetic field ball collision frequency N_{mu} and operation distance R, time T is proportional to the; Energy loss coefficient K_w for constant, not with the photon energy, wavelength, red shift value change and change; So, from (22.10) type, Hubble's law and spectrum red shift value, just can be used as a range scale, and will be astronomy field only reliable scale.

Because the wavelength of visible light for 7000~4000 A°, from purple light to red light, the red shift of AA, substituting (22.10) type, : we can see the furthest visible light optical galaxy for 24.4 billion light-years.

22.3 spectrum red shift formula of correction

This section is 2005 years ago have not yet found and complete chapter 29 《the graviton and mystery of the dark matter》 of the paper writing. Thought the universe space is mainly homogeneous, isotropic in microwave energy levels of neutrino field; regardless of the chapter 29 in the discussion of the universal gravitation can form the electron neutrino field. The reader can ignore this section of the spectrum red shift formula of correction.

The last section spectrum red shift formula derivation, we will photon as point particle processing. When the photon energy close to microwave level neutrino background field energy; Or red shift value is bigger, make the photon energy, wavelength down to close to the neutrino background field far infrared area; Photon entity radius should be considered, it will increase with the neutrino electromagnetic field ball collision frequency N_{mu}. Below, we'll assume that photon energy loss coefficient K_w the same, only the photon and neutrino collision frequency N_{mu} amended.

By (22.1) type, far infrared photon average fluctuations radius $\overline{R}_{\alpha r}$ for:

$$\overline{R}_{\alpha r}=\frac{h}{2\pi m_r(1-K_w)^n c} \qquad (22.11)$$

By (22.2) ~ (22.4) type, (22.5) type rewritten for:

$$N_{mv}=\sqrt{2}cT\pi\left[K_r(\overline{R}_{\alpha r}+\overline{R}_{\alpha v})\right]^2\frac{V_t}{V_0}\times 860\times 10^6 \qquad (22.12)$$

Will K_r value, (22.1) and (22.3) type calculation results substitution (22.12) type, have to:

$$N_{mv}=635.7595T\left(\frac{\overline{R}_{\alpha r}}{\overline{R}_{\alpha v}}+1\right)^2 \qquad (22.13)$$

By (22.1) and (22.11) type, (22.13) type should be expressed as:

$$N_{mv}=635.7595T\left[\frac{m_v}{m_r(1-K_w)^n}+1\right]^2 \qquad (22.14)$$

Because of the photon energy will eventually tend to neutrino background field

energy, so (22.14) type simplified to:

$$N_{mv} = 635.7595T\left[1+2\frac{m_v}{m_r}+\left(\frac{m_v}{m_r}\right)^2\right] \qquad (22.15)$$

And (22.5) type, compared to the photon in the operation process, and neutrino electromagnetic field ball collision frequency N_{mu} will increase, but each time collision energy loss coefficient is constant, (K_w value whether changes should eventually by observation results to determine); So, in the far infrared, red shift K_{zi} get bigger, its limit area is photon and microwave energy levels of neutrino background field energy is same, photon into neutrino. When the electromagnetic wave energy is less than the neutrino average energy, in the nature of the electromagnetic wave propagation, the energy loss of media medium energy loss, this paper will not discuss.

By (22.15) type known: N_{mu} is variable, so we have to use integral method for calculating the mean $\overline{N}_{mv}$:

$$\overline{N}_{mv} = \int_{m_v}^{m_\gamma} 635.7595T\left[1+2\frac{m_v}{m_r}+\left(\frac{m_v}{m_r}\right)^2\right]\frac{dm}{\Delta m} = 635.7595T\left[1+2\frac{m_v}{\Delta m}\ln\frac{m_r}{m_v}+\frac{m_v}{m_r}\right]$$

Among them:

$$\Delta m = (m_r - m_v) \qquad (22.16)$$

Because $\sum K_{zi}+1=\frac{m_r}{m_v}$, substituting (22.16), type to:

$$\overline{N}_{mv} = 635.7595\left[1+\frac{2}{\sum K_{zi}+1}\ln\left(\sum K_{zi}+1\right)+\frac{1}{\sum K_{zi}+1}\right] \qquad (22.17)$$

By (22.17) type, when the photon energy close to microwave level neutrino background field energy:

Make $\sum K_{zi} \to 0 \sim 2.5 \sim 10$, to the: $\overline{N}_{mv}$=(2~2.0016~1.5269)×635.7595/s

When photons travel infinity and energy is neutrino fields all absorption:

Make $\sum K_{zi} \to \infty$, to: $\overline{N}_{mv}$=635.7595/s.

23 Neutron star total energy and gravitational potential energy, rotation kinetic energy equation

This chapter, by default the function of the neutron star density changes, simulation calculations prove: the massive solid spherical structure of the neutron star gravitational collapse will inevitably lead to the total energy, the spatial extent of the gravitational field strength; the force of gravity tends to infinity "divergence" phenomenon. Which will inevitably lead to entire galaxies, clusters of galaxies, clusters of galaxies, and even the entire universe at the speed of light contraction, and in fact this astronomical phenomenon does not occur, so readers do not have to care about in this chapter the default neutron star density changes as a function of the accuracy, as long as the understanding of solid spherical structure of the neutron star is bound to lead to this trend.

23.1 Densities, the total energy of the neutron star, The gravitational potential energy, rotation Kinetic energy equation

23.1.1 The internal structure of neutron stars

The general quality of large stellar fusion burn late, the middle of the wreckage of the rest of the neutron star was a supernova explosion; the quality will not be much, much smaller than the speed of light along the equatorial edge of the rotation speed, rotation of the total kinetic energy thus formed to increase energy relativistic mass negligible. We can in density, its mass, gravitational potential energy; non-energy relativistic conditions simplify research rotation kinetic energy.

Assume that the neutron star for a spin round sphere. The book particle, nuclear physics know: a neutron star internal structure should be similar with the nucleus, the high and low energy particle spiral ring close accumulation and become. We will each neutron "broken down into"2 high energy is π_g^+ meson, 2 low energy negative π_d^- meson, (electronic is compressed and proton combination into neutron time a pair of electric dipole field by neutrino absorb added). Make high energy is π_g^+ meson quality for low energy negative π_d^- meson two times; By (1.2-1) type, each neutron rest mass for m_{n0}, low energy negative π_d^- meson average fluctuations radius $\overline{R}_\alpha$ for:

$$\overline{R}_{\alpha} = \frac{h}{2\pi\left(m_{n0}/6\right)c} = 1.2601\times10^{-15}\,m \qquad (23.1)$$

To everyone neutron occupied volume are $V_{n0} = \frac{4}{3}\pi\overline{R}_{\alpha}^{3}$, the neutron star of the original density $\overline{\rho}_0$ for:

$$\overline{\rho}_0 = \frac{m_{n0}}{V_{n0}} = 1.9984\times10^{17}\,Kgm^{-3} \qquad (23.2)$$

Make a rigid body rotating neutron star whole, (the conditions within the nucleus of each layer particle spiral ring layer for difference spin motion). By the law of conservation of energy, the neutron star gravitational potential energy and rotational kinetic energy will all into particle energy relativity quality, the result is narrow particle fluctuation radius, resulting in the increase of density, neutron star reduced in size.

23.1.2 Etc density conditions neutron star total energy and gravitational potential energy equation

A neutron star first for isotropic body, density of constant ρ_0 (ρ_0 is slightly bigger than $\overline{\rho}_0$) total quality as the M_{n0}, and radius R_0, density ρ_0 relationship for:

$$M_{n0} = \frac{4}{3}\pi R_0^3\rho_0 \qquad (23.3)$$

$$\rho_0 = \frac{3M_{n0}}{4\pi R_0^3} \qquad (23.4)$$

The neutron star internal quality M_{nr} and star body radius R_r relationship for:

$$M_{nr} = \frac{4}{3}\pi R_r^3\rho_0 = M_{n0}\left(R_r/R_0\right)^3 \qquad (23.5)$$

Neutron star in total energy, gravitational potential energy will increase attracted the kinetic energy of a material body. Gravitational field potential energy of an object, particle compression results will all into high and low energy $\pi^{\pm}$ meson energy relativity quality, so this book gravitational potential energy is all take value.

By Gauss theorem, gravitational field strength E_{nr} for:

$$E_{nr}=\frac{GM_{nr}}{R_r^2} \qquad E_{nr}=\begin{cases}\dfrac{4}{3}\pi R_r\rho_0 G & (R_r\le R_0)\\ \dfrac{4}{3}\pi\rho_0 G\dfrac{R_0^3}{R_r^2} & (R_r>R_0)\end{cases} \tag{23.6}$$

By (23.3), (23.5) and (23.6) type,, gravitational potential U_{nr} for:

$$U_{nr}=\int_{Rr}^{Ro}E_{nr}dR_r+\int_{Ro}^{\infty}E_{nr}dR_r=\frac{4}{3}\pi\rho_0 G\left[\int_{Rr}^{Ro}R_r dR_r+\int_{Ro}^{\infty}\frac{R_0^3}{R_r^2}dR_r\right]=\frac{M_{n0}G}{2R_0}\left[3-\left(\frac{R_r}{R_0}\right)^2\right] \tag{23.7}$$

By (23.7) type, each layer in the spherical shell of neutron dW_{nu} gravitational potential energy can be expressed as:

$$dW_{nu}=\frac{M_{n0}G}{2R_0}\left[3-\left(\frac{R_r}{R_0}\right)^2\right]\times 4\pi R_r^2 dR_r\rho_0 \tag{23.8}$$

By (23.3), (23.7) and (23.8) type, the neutron star gravitational potential energy W_{nu} for:

$$\begin{aligned}W_{nu}&=\int_0^{Ro}4\pi R_r^2\rho_0 U_{nr}dR_r=\int_0^{Ro}\frac{M_{n0}G}{2R_0}\left[3-\left(\frac{R_r}{R_0}\right)^2\right]\times 4\pi R_r^2\rho_0 dR_r\\ &=\frac{2\pi M_{n0}G\rho_0}{R_0}\left[R_r^3-\frac{R_r^5}{5R_0^2}\right]_0^{Ro}=\frac{6M_{n0}^2G}{5R_0}\end{aligned} \tag{23.9}$$

23.1.3 Rotational kinetic energy equation

Make a neutron star is a rigid ball, rotation angular velocity is the $\dot{\theta}$, see figure 23.1, since the rotation for W_{nv}:

Because $X=R_r\cos\phi,...Y=R_r\sin\phi,...dS=R_r d\phi\cdot dR_r$, and by the figure 23.1 shows:

$$\begin{cases}dM_{nr}=2\pi R_r\cos\phi\ dS\rho_0 & (23.10-1)\\ dW_{nv}=\dfrac{1}{2}dM_{nr}(\dot{\theta}R_r\cos\phi)^2 & (23.10-2)\end{cases}$$

By (23.10) equations, the neutron star in the rotation movement the total kinetic

energy W_{nv} for:

$$W_{nv} = \frac{1}{2}\int 2\pi R_r \cos\phi \rho_0 (\dot{\theta} R_r \cos\phi)^2 dS$$

$$= 2\pi\rho_0 \int_0^{Ro} \dot{\theta}^2 \int_0^{\pi/2} R_r^4 \cos^3\phi dR_r d\phi = 2\pi\rho_0 \frac{R_0^5 \dot{\theta}^2}{5} \int_0^{\pi/2} (1-\sin^2\phi) d\sin\phi$$

$$= \frac{4}{15}\pi R_0^5 \dot{\theta}^2 \rho_0 = \frac{1}{5} M_{n0} \dot{\theta}^2 R_0^2 \qquad (23.11)$$

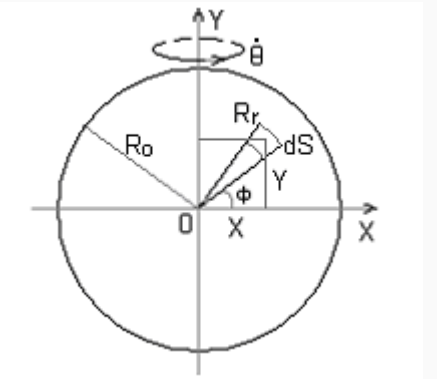

Figure 23.1 the neutron star rotation characteristic diagram

By Virial theorem, the neutron star took office a circle neutron material ring rotates, centrifugal force and gravity should be equal, to balance, the figure 23.1:

$$\frac{dM_{nr}(\dot{\theta} R_r \cos\phi)^2}{R_r \cos\phi} = \frac{GM_{nr} dM_{nr}}{R_r^2} \cos\phi \qquad (23.12)$$

$$(\dot{\theta} R_r)^2 = \frac{GM_{nr}}{R_r} \qquad \dot{\theta}^2 = \frac{4}{3}\pi\rho_0 G$$

Will (23.12) type substitution (23.11) type, have to:

$$W_{nv} = \frac{GM_{n0}^2}{5R_0} \qquad (23.13)$$

Comparison (23.9) and (23.13) type, such as density, neutron stars: in the energy theory of relativity speed rotation condition, the neutron star gravitational potential energy is 6 times of rotation kinetic energy.

If in accordance with the virial theorem the neutron star rotation kinetic energy deducted from the gravitational potential energy, and the gravitational potential energy

into energy theory of relativity the quality ΔM_{n0}, by (23.9) and (23.13), type:

$$\Delta M_{n0} = \frac{GM_{n0}^2}{R_0 c^2} \qquad (23.14)$$

Quality increase coefficient K_{m0} for:

$$K_{m0} = \frac{\Delta M_{n0}}{M_{n0}} = \frac{GM_{n0}}{R_0 c^2} \qquad (23.15)$$

Make $K_{m0} = 1$, R_0 value represents the black hole of the Schwarzschild radius.

23.2 variable density conditions neutron star total energy, Gravitational potential energy and rotational kinetic energy equation

23.2.1 Variable density conditions neutron star total energy and gravitational potential energy equation

When a neutron m_{n0} from the static state from infinity are attracted to the neutron star surface, make whole neutron star quality as the M_{n0}, from (23.15) type, its gravitational potential energy quality increase coefficient K_{m0} for:

$$K_{m0} = \frac{GM_{nr0}}{R_0 c^2} \qquad (23.16)$$

When introduced into the neutron star center, the (23.7) type, its gravitational potential energy quality increase coefficient K_{m1} for:

$$K_{m1} = \frac{3GM_{nr0}}{2R_0 c^2} \qquad (23.17)$$

By the wave equation (1.2-1) type, particle spiral ring average fluctuations radius $\overline{R}_{\alpha i}$ into:

$$\overline{R}_{\alpha i} = \frac{h}{2\pi(1+K_{mi})\left(m_{n0}/6\right)c} \qquad (23.18)$$

Because each a neutron occupy the volume of the particles spiral ring for $\frac{4}{3}\pi\overline{R}_{\alpha i}^3$, so the neutron star surface density function ρ_0 should be:

$$\rho_0 = \overline{\rho}_0 (1 + K_{m0})^4 \qquad (23.19)$$

The gravitational potential function (23.7) type, the center of gravitational potential energy surface is 1.5 times, because it is derived under the condition of such as density, if variable density conditions, the center of gravity potential bigger, so we first design center gravitational potential energy surface for 3 times, the center density ρ_1 for surface ρ_0 27 times, the neutron star internal density function ρ_r can be designed for:

$$\rho_r = \rho_0 \left[27 - 26 \left(\frac{R_r}{R_0} \right)^2 \right] \qquad (23.20)$$

By (23.20) type, the neutron star internal quality M_{nr} and total quality M_{nr} for:

$$M_{nr} = \int_0^{Rr} 4\pi R_r^2 \rho_r dR_r = 4\pi\rho_0 \int_0^{Rr} R_r^2 \left[27 - 26 \left(\frac{R_r}{R_0} \right)^2 \right] dR_r$$

$$= 4\pi\rho_0 \left(9R_r^3 - \frac{26R_r^5}{5R_0^2} \right) \qquad (23.21)$$

$$M_{nr0} = \frac{57}{5} \times \frac{4}{3}\pi R_0^3 \rho_0 = 11.4 M_{n0} \qquad \left(M_{n0} = \frac{4}{3}\pi R_0^3 \rho_0 \right) \qquad (23.22)$$

By (23.6) type, gravitational field strength E_{nr} for:

$$E_{nr} = \frac{GM_{nr}}{R_r^2} \qquad E_{nr} = \begin{cases} 4\pi\rho_0 G \left(9R_r - \frac{26R_r^3}{5R_0^2} \right) & (R_r \le R_0) \\ 4\pi\rho_0 G \times \frac{19R_0^3}{5R_r^2} & (R_r > R_0) \end{cases} \qquad (23.23)$$

By (23.7) type, gravitational potential U_{nr} for:

$$U_{nr} = \int_{Rr}^{Ro} E_{nr} dR_r + \int_{Ro}^{\infty} E_{nr} dR_r$$

$$= 4\pi\rho_0 G\left[\int_{Rr}^{Ro}\left(9R_r - \frac{26R_r^3}{5R_0^2}\right)dR_r + \int_{Ro}^{\infty}\frac{19R_0^3}{5R_r^2}dR_r\right]$$

$$= 4\pi\rho_0 G\left(7R_0^2 - \frac{9}{2}R_r^2 + \frac{13R_r^4}{10R_0^2}\right) \qquad (23.24)$$

The neutron star gravitational potential energy W_{nu}, by (23.9) and (23.20), (23.21) and (23.24), type:

$$W_{nu} = \int_0^{Ro} 4\pi R_r^2 \rho_r U_{nr} dR_r$$

$$= (4\pi\rho_0)^2 G\int_o^{Ro}\left(7R_0^2 - \frac{9}{2}R_r^2 + \frac{13R_r^4}{10R_0^2}\right)R_r^2\left[27 - 26\left(\frac{R_r}{R_0}\right)^2\right]dR_r$$

$$= (4\pi\rho_0)^2 GR_0^5\left[63\left(\frac{R_r}{R_0}\right)^3 - \frac{607}{10}\left(\frac{R_r}{R_0}\right)^5 + \frac{1521}{70}\left(\frac{R_r}{R_0}\right)^7 - \frac{338}{90}\left(\frac{R_r}{R_0}\right)^9\right]_0^{Ro}$$

$$= 182.4571 M_{n0}\left(\frac{M_{n0}G}{R_0c^2}\right) \qquad (23.25)$$

23.2.2 Neutron star rotation total kinetic energy equation

When the neutron star quality is bigger, the center gravity field compressive force is bigger also, lead to intermediate density change, due to the rotation speed is bigger, and then you should consider rotation speed energy relativistic effects. By (23.16) ~ (23.20) type, figure 23.1, a neutron star rotation angular velocity is the $\dot{\theta}$, because of the rotation direction along the X axis density change for ρ_x:

$$\rho_x = \rho_0\left[27 - 26\left(\frac{R_r}{R_0}\right)^2\right]\left[1 - \left(\frac{\dot{\theta}R_r\cos\phi}{c}\right)^2\right]^{-2} \qquad (23.26)$$

The energy theory of relativity and figure 23.1, (23.6) type, each material ring the total energy of the dM_n for:

$$dM_n = \frac{dM_{n0}}{\sqrt{1 - \left(\dot{\theta}R_r\cos\phi\Big/c\right)^2}} = 2\pi R_r\cos\phi\rho_x dS \qquad (23.27)$$

By (23.26) and (23.27) type, the neutron star M_{nr} total energy for:

$$M_{nr}=2\int_0^{Rr}\int_0^{\pi/2}2\pi R_r\cos\phi\rho_0\left[27-26\left(\frac{R_r}{R_0}\right)^2\right]R_r\left[1-\left(\frac{\dot{\theta}R_r\cos\phi}{c}\right)^2\right]^{-2}d\phi dR_r$$

$$=4\pi\rho_0\int_0^{Rr}\int_0^{\pi/2}R_r^2\left[27-26\left(\frac{R_r}{R_0}\right)^2\right]\left[1-\left(\frac{\dot{\theta}R_r}{c}\right)^2+\left(\frac{\dot{\theta}R_r\cos\phi}{c}\right)^2\right]^{-2}dR_r d\sin\phi$$

$$=2\pi\rho_0R_0^3\int_0^{Ro}\left\{\begin{array}{l}\left(\frac{R_r}{R_0}\right)^2\left[27-26\left(\frac{R_r}{R_0}\right)^2\right]\left[1-\left(\frac{\dot{\theta}R_r}{c}\right)^2\right]^{-1}\\ \left[1+arctg\frac{\dot{\theta}R_r}{c\sqrt{1-\left(\dot{\theta}R_r/c\right)^2}}\left(\frac{\dot{\theta}R_r}{c}\sqrt{1-\left(\dot{\theta}R_r/c\right)^2}\right)^{-1}\right]\end{array}\right\}d\left(\frac{R_r}{R_0}\right)$$

（23.28）

Because the neutron stars equatorial edge rotational velocity $v_\theta < c$, $\dot{\theta}R_0/c < 1$, so, make the $R_r/R_0 = \dot{\theta}R_r/c = 0 \rightarrow < 1$, the starting point $R_r/R_0 = 10^{-6}$, get variable density neutron star total energy parameter table 23.1:

Variable density neutron star total energy parameter simulation results table table 23.1

$\dot{\theta}R_0/c$	$M_{nro}= K_m \times 4\pi R_0^3\rho_0/3$ (K_m)
0.001	11.400006
0.01	11.400675
0.1	11.467896
0.3	12.047244
0.5	13.444395
0.7	16.501857
0.9	25.74513
0.99	52.269
0.998	79.8

By Virial theorem, a neutron star equatorial surface, rotation speed is still should be less than the speed of light, by (23.12), type:

$$\frac{dM_n(\dot{\theta}R_0)^2}{R_0} = \frac{GM_{nr0}dM_n}{R_0^2}, \quad (\dot{\theta}R_0)^2 = \frac{GM_{nr0}}{R_0}$$

Because:$(\dot{\theta}R_0) < c$, so:

$$R_0 > \frac{GM_{nr0}}{c^2} \qquad (23.29)$$

By (23.22), (23.25) and (23.28) type calculation results is to:

Variable density neutron star rest mass is 11.4 times of the neutron star and density. In general the center of the core of a galaxy the black hole, because $GM_{n0} / R_0c^2 > > 1$, so the gravitational potential energy far outweigh the 182.4571 times. When the neutron star high-speed rotation, due to the equatorial surface by the speed of light limit, including kinetic energy, the energy theory of relativity total quality most can only achieve static quality 79.8 times, is far less than the gravitational potential energy of the increment of the > > 182.4571 times.

By (23.16) and (23.17) type, the gravitational potential energy increment coefficient K_{mi}, when $GM_{n0} / R_0c^2 > > 1$, the total energy will tend to infinity, such as in the core of a galaxy, in the middle of the huge black hole, the gravitational potential energy will far outweigh the neutron star surface at the speed of light when motion can hold by the energy law of relativity and the total energy. The gravitational collapse phenomenon will make the total energy is skyrocketing geometric series, led directly to the gravitational field strength and gravity range also shows geometric series increase, The end result is that the entire galaxy, clusters, cluster, and even the entire universe contraction at the speed of light, Form the so-called space infinitesimal, energy and density are the infinity of mathematical singularity. To be sure, all have been forming large, medium and small galaxy central galaxy nuclear black holes, even globular cluster at the center of the black hole, are completely satisfy this condition, but in the observation of 200 light-years in sight, all of the galaxy clusters are not seen this kind of singularity shrinkage phenomenon; So, great quality galaxy nuclear central black hole, the internal structure of state should reconsider.

24 The interior of a black hole structure and total energy equation

24.1 The interior of a black hole structure and gravitational field equation

24.1.1 Black hole internal structure and the general law of conservation of energy

From the front have discussion of the basic particle, electromagnetic wave, the neutrino field, the energy of the gravitational field of origin can be deduced that energy is the only form of material existence; Neither is created out of thin air, also cannot off for no reason at all; It can only be converted from one form into another kind of form; And no matter what the state of matter, form transformation process, even in microscopic and macroscopic, yu view field, all kinds of material between the state transition process, the total energy must be fully conservation.

In classical electrodynamics, we have to "point charge" energy divergent difficult, through the wave equation of wave orbit radius smoothly solve; At the same time proves charged particle in a certain direction of the wave, spin motion resultant velocity must $\geq c$ to stability.

Similarly, in section 23.2 has been proved: quality large neutron star in variable density condition gravitational field, but the total potential energy than energy relativistic rotation movement of the total energy. Gravitational collapse also tend to be singular point in total energy, gravitational field strength, gravity to infinity space range all the whole "divergence" difficult; And with the point charge, in microscopic and macroscopic, yu view field, in reality the "divergence" phenomenon is not exist; Just reflect our basic law of physics is not comprehensive and perfect; Therefore, since we have wave equation and electronic wave motion orbit radius fix the point charge energy "divergence" difficult; Why can't use this method to solve the interior of a black hole structure and total energy, gravitational field strength, gravity space range of overall "divergence" difficult?

In the macroscopic field, we already know, a high speed rotation of globular star, polar axis ends because no rotation speed formation of centrifugal force, in under the action of gravity field will shrink or even dent. The centrifugal force of the equator the

congress inflation, will eventually make round ball, become rotating flat ellipsoid. If the quality of the neutron star is larger, rotation speed is large enough, the polar axis ends in strong gravitational field will be under the action of shrinkage, depression and even scored; The equator in strong centrifugal force under the action of continuous inflation, it would form a circular ring of neutron spiral ring aggregation, see figure 24.1, (behind referred to as neutron material ring). Each neutron material ring every small piece, should follow the general law of conservation of energy and the virial theorem.

Design the internal structure of the black hole, it does not exist total energy, gravitational field strength, gravity space range of overall "divergence" difficulties, and can realize smoothly collision big bang, accretion disk material to polar axis injection, make the neutron decay into protons, electrons and neutrino, produce symmetrical radio disc, form is material nebula regeneration cycle.

Moreover, when material from accretion disk edge of high-speed rotary motion to polar axis injection, accretion disk edge of the moment of momentum energy will be transformed into a shaft injection kinetic energy. Just like in the basin high-speed rotation movement of water, the moment of momentum energy will eventually because of friction into heat energy. Similarly, solar nebula began to shrink from the early stages of the edge of the moment of momentum; most of the material energy eventually is converted to the heat of the sun.

24.1.2 Neutron material ring gravitational field equation

Each neutron material ring itself, lateral and different direction of the gravitational field strength are a little different, we first study respectively, and finally makes a comprehensive comparison between.

1. Each neutron material ring itself gravitational field equation

See figure 24.1 and figure 24.2, make the neutron material ring for circular ring aggregate, density ρ_0 for constant, rotation angular velocity is the $\dot{\phi}$. Particle spiral ring structure and nuclear similar, because both side's symmetry, a universal gravitation for F_i, we have:

$$dl = R_1 d\phi, \quad dM_{ni} = \pi R_2^2 dl_i \rho_0, \quad dF_1 = \frac{G dM_{n1} dM_{ni}}{\left(2R_1 \cos\frac{\phi}{2}\right)^2} \cos\frac{\phi}{2}$$

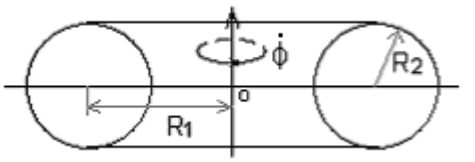

Figure 24.1 neutron material ring structure diagrams

$$F_i = \int_0^{\phi} \frac{2GdM_{n1}\pi R_2^2 \rho_0}{\left(2R_1 \cos\frac{\phi}{2}\right)^2} \cos\frac{\phi}{2} R_1 d\phi = \int_0^{\phi} \frac{GdM_{n1}\pi R_2^2 \rho_0}{2R_1 \cos\frac{\phi}{2}} d\phi$$

$$= \frac{GdM_{n1}\pi R_2^2 \rho_0}{R_1} \left(\ln\ tg\frac{\phi}{2} - \ln\ tg\frac{\phi}{4} \right) \quad \text{.....(24.1)}$$

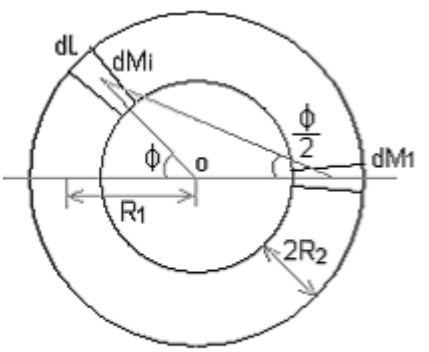

图24.2 中子物质环自身
引力场示意图

Figure 24.1 neutron material ring structure diagrams

Because of $\phi = \pi - d\phi/2$, so, $\ln\ tg(\phi/2) \approx 2\pi$, $M_{n1} = 2\pi R_1 \times \pi R_2^2 \rho_0$ substitution (24.1), type to:

$$F_i = \frac{GM_{n1}dM_{n1}}{R_1^2} \qquad (24.2)$$

2. Each neutron material ring plane the outside of the gravitational field equation

See figure 24.3, make A place for A neutron material ring dM_{n1}, in ΔAOB:

$$\begin{cases} AB^2 = OA^2 + R_1^2 + 2OA\ R_1 \cos\phi & (24.3-1) \\ R_1^2 = AB^2 + OA^2 - 2OA\ AB\cos\alpha & (24.3-2) \end{cases}$$

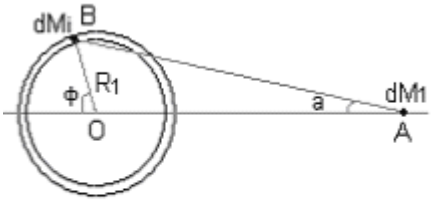

图24.3 中子物质环平面外侧
引力场示意图

Figure 24.3 neutron material ring plane lateral gravitational field schematic diagram

By (24.3) equations to:

$$\cos\alpha = \frac{OA + R_1\cos\phi}{AB} \qquad (24.4)$$

$$dF_i = \frac{GdM_{n1}dM_{ni}}{AB^2}\cos\alpha \qquad (24.5)$$

By (24.3-1) and (24.4) and (24.5) type, have to:

$$F_i = \int_0^{\pi} \frac{2GdM_{n1}\pi R_2^2\rho_0 R_1\cos\alpha}{AB^2}d\phi$$

$$= \frac{GdM_{n1}M_{n2}}{OA^2}\int_0^{\pi} \frac{\left(1+\frac{R_1}{OA}\cos\phi\right)}{\pi\left[1+\left(\frac{R_1}{OA}\right)^2+2\left(\frac{R_1}{OA}\right)\cos\phi\right]^{1.5}}d\phi \qquad (24.6)$$

(24.6) type behind the integral value simulation results are as follows:

$$\frac{R_1}{OA}=0.5 \qquad \int_0^{\pi} \frac{\left(1+\frac{R_1}{OA}\cos\phi\right)}{\pi\left[1+\left(\frac{R_1}{OA}\right)^2+2\left(\frac{R_1}{OA}\right)\cos\phi\right]^{1.5}}d\phi = 1.24562$$

$=0.1$ … … … $=1.00757$

$=0.01$ … … $=1.000075$

3. Vertical each neutron material on the ring of the gravitational field equation

See figure 24.4, reference (24.6), type:

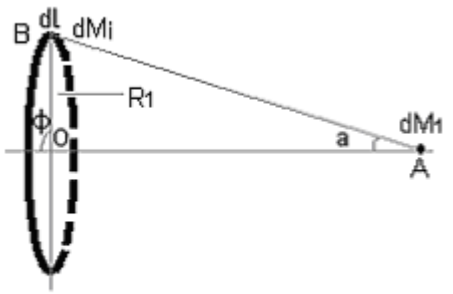

图24.4 中子物质环轴线上
引力场方程示意图

Figure 24.4 neutron material rings on the axis of gravitational field

Equation schematic diagram

$$F=\int_0^{2\pi}\frac{GdM_{n1}\pi R_2^2\rho_0 R_1\cos\alpha}{AB^2}d\phi$$
$$=\int_0^{2\pi}\frac{GdM_{n1}\pi R_2^2\rho_0 R_1 OA}{\left(R_1^2+OA^2\right)^{1.5}}d\phi$$
$$=\frac{GdM_{n1}M_{n1}}{OA^2\left[1+\left(\frac{R_1}{OA}\right)^2\right]^{1.5}} \qquad (24.7)$$

Similarly, as: $\frac{R_1}{OA}\to 0$, $\left[1+\left(R_1/OA\right)^2\right]^{-1.5}\to 1$, and (24.6) type calculation results can mutual away, make comprehensive results more close to 1. Of course, we can also in figure 24.3 and figure 24.4 between simulation results find transition ring, make comprehensive value is 1.

4. Inner neutron material ring combination foreign layer neutron material ring comprehensive gravitational field equation

When the inner each neutron material ring all alone occupy a ball shell rail surface, multilayer neutron material ring is equivalent to their uniform distribution in each layer on

the spherical shell. The Gauss theorem of symmetry, the inner all neutron material ring foreign layer neutron material ring dM_i gravitational fields can be expressed as:

$$F_m = \frac{G(M_{n1} + M_{n2} \ldots\ldots + M_{nn}) dM_{ni}}{R_{1n}^2} \qquad (24.8)$$

24.2 The interior of a black hole of the virial equilibrium theorem and total energy equation

24.2.1 Black hole internal Virial equilibrium theorem

According to the Virial movement balance theorem, a neutron material ring spin the energy of motion theory of relativity speed coefficient for K_v, to the center of the black hole first neutron material ring M_{n1}, make the orbit radius for $R_{1,1}$, cross section radius for $R_{2,1}$, (both to subscript difference, the same below), the average density of ρ_{01}. By (24.2) and (23.29) type:

$$\frac{2\pi R_{1,1}\pi R_{2,1}^2 \rho_{01} G dM_{ni}}{R_{1,1}^2} = \frac{dM_{ni}(K_v c)^2}{R_{1,1}}$$

$$R_{2,1} = \frac{K_v c}{\sqrt{2\pi^2 G\rho_{01}}} \qquad (24.9)$$

The theory of relativity and energy (23.19) type, the neutron material ring density ρ_{0n} and original neutron spiral ring density $\overline{\rho}_0$ relationship for:

$$\rho_{0n} = \frac{\overline{\rho}_0}{(1 - K_v^2)^2} \qquad (24.10)$$

Will (24.10) type substitution (24.9) type, have to:

$$R_{2,1} = \frac{K_v c(1 - K_v^2)}{\sqrt{2\pi^2 G\overline{\rho}_0}} \qquad (24.11)$$

Because K_v for undetermined coefficient, other is constant, the (24.11) type and derivative take very worth:

When $K_v = \frac{1}{\sqrt{3}}$, $R_{2,1} = \frac{2\sqrt{3}c}{9\sqrt{2\pi^2 G\overline{\rho}_0}}$=7112.39 m is great value

Front section 21.2 has been mentioned, galaxy in the formation, evolution process, as the core of a galaxy quality increase gradually, under the action of the gravitational field, optical galaxy is gradually contraction. We now consider the galaxy's shrinkage speed: if the whole galaxy in the evolution process, the total number of protons, neutrons remain unchanged; So, by energy theory of relativity, suction galaxy nuclear central black hole formation of neutron material ring of total quality depends on the energy relativistic spin speed $K_v c$; If $K_v \to 0$, cannot form a neutron material ring structure, will form a solid ball supermassive neutron star, in under the action of gravity rapid collapse into a so-called mathematical singularity, leading to the total energy and gravitational field "divergence", the result is the universe at the speed of light contraction; If $K_v \to 1$, from (23.28) type, it is known that a black hole total energy also will be hundreds of thousands of multiplication, also will cause the entire galaxy rapid contraction; But the observed universe within the scope of this phenomenon are not seen. In our Milky Way galaxy speaking, visual optical galaxy scale genera - large, still have more complex vortex structure; Video of the oldest globular cluster surface stars age has more than 17 billion years. Silver spiral arm and blue young massive star formation; the whole galaxy's mass light than ten to twenty; the galaxy that is young galaxy, this visual optical galaxy life should be more than 80 billion years.

Therefore, the core of a galaxy, inside a black hole neutron material ring spin speed should try to take the little value to meet both neither can form solid spherical neutron star cause gravitational collapse form singularity, and won't make energy relativity quality increase too much, so the whole galaxy can extend life. Take $K_\nu = 1/\sqrt{3}$, $R_{2,1}$ has great value, it is neutron material ring cross section of great value.

24.2.2 Black hole total energy equation

In order to simplify the calculation behind the study, we make the whole inside a black hole or edge each neutron material ring total energy all are M_{ni}, rotation speed $K_v c$ are equal. Because $M_{ni} = 2\pi R_{1,I} \times \pi (R_{2,i})^2 \rho_{0n}$, as long as $R_{1,i} \cong R_{2,i}$, can think the neutron material ring in $\pi (R_{2,i})^2$ cross section on the particle spiral ring spin speed $K_v c$ unchanged.

By (24.10) type, to: in $\pi (R_{2,i})^2$ section on the density and the ρ_{0n} density of each neutron material ring are equal. By (24.8) type and Virial law, from center to outside, the

first N_i a neutron material ring circular motion equilibrium condition is:

$$\frac{GdM_{ni}N_iM_{ni}}{R_{1,i}^2}=\frac{dM_{ni}(K_vc)^2}{R_{1,i}}$$

$$M_{ni}=\frac{(K_vc)^2R_{1,i}}{GN_i} \qquad (24.12)$$

Make $K_v=1/\sqrt{3}$, $R_{1,1}$ = $R_{2,1}$ = 7112.39 m, N_1 = 1, substituting (24.12) type, the center of the black hole first neutron material ring quality M_{n1} = 3.1933 x 10^{30} kg = 1.6055 $M_\odot$ ($M_\odot$= 1.989 x 10^{30} kg for the mass of the sun).

By (24.12) type, black hole total quality N_iM_{n1} and outer neutron material ring distribution radius $R_{1,i}$ relationship for:

$$R_{1,i}=\frac{GN_iM_{n1}}{(K_vc)^2} \qquad (24.13)$$

By (24.13) type see: each neutron material ring distribution of spherical shell spacing are: $\Delta R_{1,1}$ = 7112.39 m. A total mass of black hole for N_iM_{n1} = 10^{12} $M_\odot$, substituting (24.13) type, : $R_{1,n}$ = 4.41 x 10^{15} m = 0.466 light years.

Make (24.13) type of K_v = 1, then the Schwarzschild radius R_s for:

$$R_s=\frac{GN_iM_{n1}}{c^2}=1.47\times10^{15}\,m=0.155\ (\text{lightyears}) \qquad (24.14)$$

Comparison: outer neutron material ring radius is the Schwarzschild radius 3 times. By (24.9) and (24.10), (24.11) and (24.13) type:

$$M_{n1}=2\pi R_{1,i}\pi R_{2,i}^2\rho_{0n}$$

$$R_{2,i}=\sqrt{\frac{M_{n1}}{2\pi^2R_{1,i}\rho_{0n}}}=\frac{K_v(1-K_v^2)c}{\sqrt{2\pi^2GN_i\overline{\rho}_0}}=\frac{7112.39}{\sqrt{N_i}}m \qquad (24.15)$$

Will the $N_i=\frac{1.98\times10^{42}}{M_{n1}}$ substitution (24.15) type, to: $R_{2,i}$ = 9.03 x 10^{-3} m, is far less than the center.

The above all is only a simplified ideal structure model. In each neutron material ring centrifugal force and gravity center under the premise of fully balance, Virial

theorem, it is known that the quality of each neutron material ring from inside to outside can press a series rules distribution, which each layer spherical shell spacing should also by Virial law to determine.

A combination of the calculation results comparison shows: if neutron material ring cross section radius $R_{2,i}$ went from the center to the outer (24.15) type narrowing. Thus it is not difficult to imagine: elliptical galaxy spherical and contraction, the central black hole inside and outside all neutron material ring, whole is spherical symmetric distribution; Spiral galaxy black hole in the middle part is quite a spherical symmetric distribution, edge inherit part of angular momentum, like galaxy edge as a disk distribution; Now already observed spiral galaxy active galactic nuclei and part of HengXingJi black holes in the disk accretion disk is obviously edge neutron material ring level and dust, gas mixed transition zone.

24.2.3 Each neutron material ring internal force analysis

By the virial theorem, each a neutron material ring occupies the whole ball shell thickness within the orbit of fixed space, black hole from center to outside, each a neutron material ring in spin orbit radial only by gravity and centrifugal force F_m and F_n effect, the equal and opposite, complete balance, see figure 24.5. Vertical spin radius direction of each neutron material ring cross section from the shell of various neutron material ring their gravitation F_m and force F_b (see chapter 11 ~ 10 track point of contact in current ampere force) interaction and, in general, also should be in balance.

Neutron material ring is made from high and low energy $\pi^{\pm}$ meson composed of particles spiral ring; it is designed to be curved cylindrical spiral. Refer to section 10.2 ampere force parameter calculation model, side by side the same layer particle spiral ring rail point of tangency place ampere force can be simplified calculation.

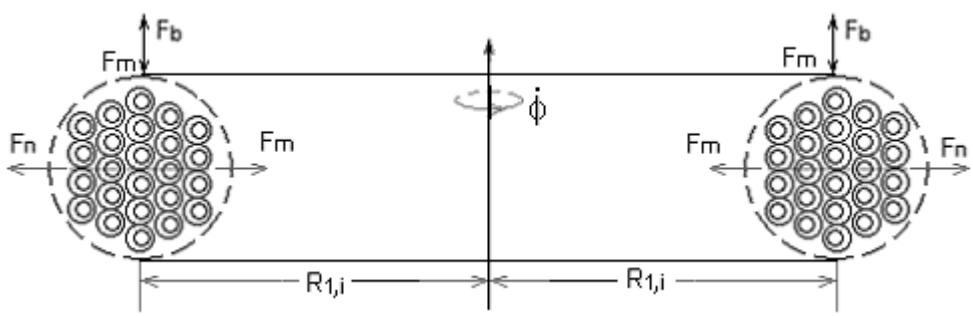

Figure 24.5 neutron material ring internal force diagram

By (10.11) type nuclear internal force forming principle: the same layer low-energy particle spiral ring rail point of tangency place has great ampere force, in figure 24.5 neutron material ring spin motion conditions for the performance of the repulsive force to overcome the compression function of the universal gravitation, see figure 11.2.

Because each neutron "disassemble" there are two low-energy π_d^- mesons, so, each particle spiral ring contains a number of negative N_e, by (23.1) and (23.2) type and energy theory of relativity, to:

$$N_e = 2 \times \frac{2\pi R_{1,i} \pi \overline{R}_\alpha^2}{\frac{4}{3}\pi \overline{R}_\alpha^3} = \frac{3\pi R_{1,i}}{\overline{R}_\alpha} \qquad (24.16)$$

$$(\overline{R}_\alpha = 1.0289 \times 10^{-15}\, m) \qquad (24.16)$$

By (10.7-1) and (24.11) type, the spin direction of low-energy particle spiral ring rail current I_θ for:

$$I_\theta = \frac{eK_\nu c}{2\pi R_{1,i}} N_e \qquad (24.17)$$

By (10.7-2), track point of contact in the magnetic field strength B:

$$B = \frac{u_0 I_\theta}{2\pi K_r \overline{R}_\alpha} \qquad (24.18)$$

By (10.9) and (24.16) ~ (24.18) type, each spin orbit point of tangency place ampere force F_b is:

$$F_b = \int_{Kr \bullet \overline{R}\alpha}^{2Kr\overline{R}\alpha} I_\theta B dl = \int_{Kr \bullet \overline{R}\alpha}^{2Kr\overline{R}\alpha} \frac{u_0 I_\theta^2}{2\pi K_r \overline{R}_\alpha} dl = \frac{u_0 I_\theta^2}{2\pi} \ln \frac{2K_r}{K_{r\bullet}}$$

$$= \frac{u_0}{2\pi} \left(\frac{3eK_\nu c}{2\overline{R}_\alpha} \right)^2 \ln \frac{2K_r}{K_{r\bullet}} \qquad (24.19)$$

Table 2.1 an estimated: $2K_r/K_{r\bullet} = 2 \times 10^9$, then $\ln \frac{2K_r}{K_{r\bullet}} = 20.72$. Substituting (24.19) type, the maximum force: $F_b = 6773.2523$ (Newton).

For neutron material ring cross section on gravitation strength solution, it should be as infinite long cylinder, the gaussian symmetry principle, in the cross section in the

gravitational field intensity E_{mr} for:

$$E_{mr} = 2\pi G\rho_{0n} R_{2j} \qquad (24.20)$$

And the nuclear core force balance verification calculation method similar to each layer particle spiral ring, we as long as the calculation on the cross section width of a layer of particle spiral ring lateral interaction force. A neutron material ring cross section center gravitation accumulated F_{mr}, see figure 24.5, because each particle spiral ring wave orbital diameter for $2\overline{R}_{\alpha}$, reference (24.20), type to:

$$F_{mr} = \int_1^{Nn} 2\pi G\rho_{0n} R_2 dm_n = 2\pi G\rho_{0n} \int_1^{Nn} 2N_n \overline{R}_{\alpha} \times \frac{4}{3}\pi \overline{R}_{\alpha}^3 \rho_{0n} dN_n$$

$$= \frac{8\pi^2 G\rho_{0n}^2 \overline{R}_{\alpha}^4 (N_n^2 - 1)}{3} = 3.9794 \times 10^{-34} N_n^2 \text{ (Newton)} \qquad (24.21)$$

By (24.19) type, the calculated results and (24.21) values range league stand: neutron material ring cross section radius value range allows for: R_{2i} = 8489.7126 m, more than (24.11) and (24.15) type calculation value range.

And the conditions within the nucleus of the nuclear force forming principle similar, F_b force can also with the external force size, tensile, compression state adjust; So, for each neutron material ring cross sectional area size should be a black hole total energy, space distribution and force balance, and virial equilibrium theorem 4 aspects comprehensive consideration. For instance, we can balance from the nuclear force is preferred, with reference to the conditions within the nucleus of the force balance simulation calculation method, suppose that each neutron material ring cross sectional area are equal, took R_{2i} = 7112.39 m of great value. In this way, it is in the interior of a black hole gravitational field and electromagnetic force formed completely in balance and unity state. Of course, strong, weak interaction is actually electromagnetic interaction, so this is the interior of a black hole in the gravitational field and strong, the weak interaction, and electricity, magnetic interaction completely unified balance. Because the international day literati of the black hole the internal structure of the observation study also is basically blank, this paper is given here only black hole total energy, size, internal structure, avoid the gravitational collapse of the whole simplified model. Further analysis of the structure of the inside black holes, quasars spectrum supernormal value red shift, super star fusion physical evolution model and detailed calculation example see chapter 27.

24.2.4 Black hole accretion rate K_{mx}

When a black hole from accretion disk continuous accretion increases, it's the radius of the black hole R_1 will gradually increase. By (24.11) type, make black hole neutron material ring radius of the maximum R_2 = 7112.39 m for constant, also is the only black hole by a neutron material of ring.

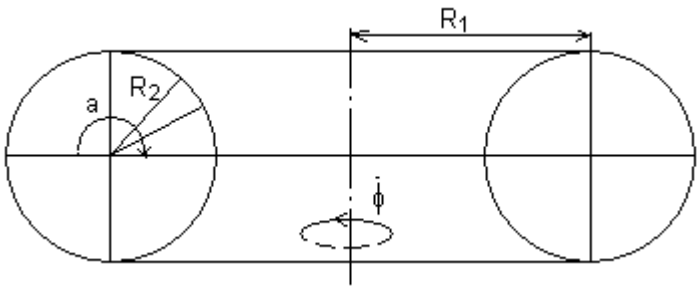

Figure 24.6 black hole accretion rates Kmx calculation principle diagram

At this point, if the idea, neutron material outside ring by high energy particles spiral ring composed of each layer neutron surface are such as crystal from accretion disk adsorption after growth step by step. Because the black hole neutron material ring radius R_2 = 7112.39 m for constant, so the inside of each layer neutron surface can only from the polar axis injection forming radio disc. So, by shown in figure 24.6, make each layer neutron particle spiral ring layer thickness of d_n, black hole accretion rate K_{mx} can be expressed as:

$$K_{mx} = 1 - \frac{\int_0^{2\pi}\int_{\pi/2}^{\pi}(R_1 + R_2\cos\alpha)R_2 d\alpha \cdot d\phi \cdot d_n}{\int_0^{2\pi}\int_0^{\pi/2}(R_1 + R_2\cos\alpha)R_2 d\alpha \cdot d\phi \cdot d_n} \qquad (24.22)$$

$$= 1 - \frac{\int_{\pi/2}^{\pi}(R_1 + R_2\cos\alpha)d\alpha}{\int_0^{\pi/2}(R_1 + R_2\cos\alpha)d\alpha} = \frac{2R_2}{\frac{\pi}{2}R_1 + R_2}$$

By (24.22) type: when $R_1 = R_2$, namely the mass of a black hole for minimum value, $K_{mx} = 0.7779690593$; With $\frac{R_1}{R_2} = 10、100、1000、10000\ldots\ldots$ is geometric series increases, the K_{mx} also are: 0.1197033994, 0.01265185126, 1.272429491 x 10^{-3},

1.273158493 x 10^{-4} a geometric series reduced.

The calculation result shows: the quality of smaller HengXingJi black hole, just formed accretion rate is bigger, like this is advantageous to the accretion new nebula formation quasars, (see chapter 27). The quality of the large XingXiJi central black hole, accretion rate is very small, almost tending to zero, so that the middle of the galaxy black hole quality increase very slow, it is beneficial to the whole galaxy, especially with small star ball shell galactic nucleus, which can maintain the longer optical galaxy's life, at the same time will be most galaxy disk material to polar axis radio disc way to polar axis ends radiation form new nebula. So as to change the whole galaxy original moment of momentum, (see chapter 25 ~ 27).

The middle of the galaxy to normal nuclear ball, polar axis ends with ball shell distribution of stars and nebulae, must by polar axis ends neutron material ring inner radiation form "jacking force", can effectively support balance and overcome black hole at the center of gravity of the stars and nebulae. And the core of a galaxy, a black hole is peripheral small star ball shell layer, and constantly to get polar axis injection forming new nebula supplements. The galactic nucleus internal shade material automatic transition cycle results will make the galaxy nuclear ball shell layer stars in life, far outweigh the galaxy nuclear peripheral star life.

We can thus further reasoning: the whole galaxy formation to death from all into large and small black holes, the total mass increase is limited. Make $K_{\nu} = \frac{1}{\sqrt{3}}$, the energy theory of relativity, increment ratio, $\frac{\Delta M}{M} = \sqrt{\frac{3}{2}} - 1$.

The above shows that the entire universe total quality should be a constant, the universe is eternal.

25 Galaxy nuclear early characteristics and energy conversion, radiation mechanism

25.1. The core of a galaxy, early characteristics

Section 21.2 of galaxy formation and evolution has been reviewed. Day literati observed many violent activities of the galactic nucleus, quasars and Seyfert galaxy central star shape light nuclei are galaxy formation at the early stage of the galactic nucleus characteristics, we will all kinds of characteristic points above are as follows:

25.1.1 Quasars

It is often and active galactic nuclei share the name of, these kind of spherical main features are:

1. Highlights of

A quasar total photometric for 10^{43} ~ 10^{48} erg/s, equivalent to 10^{3} ~ 10^{4} ordinary galaxy's total photometric, each band radiation energy comparison table 25.1.

Ordinary galaxy and active galactic nuclei photometric comparative

List (unit: erg/s) table 25.1

Type	Radio	Infrared	Optical	X-ray
Spiral galaxy	5×10^{38}	3×10^{42}	4×10^{43}	3×10^{39}
Radio galaxy	$10^{42}\sim10^{45}$	2×10^{42}	1×10^{44}	3×10^{41}
Seyfert	$10^{40}\sim10^{45}$	3×10^{46}	5×10^{43}	$10^{42}\sim10^{45}$
quasars	$10^{44}\sim10^{48}$	4×10^{47}	$10^{45}\sim10^{47}$	10^{46}

2. Small scale

A quasar photometric change cycle is usually only a few hours or a few days, if the speed of light through the quasar time needed for meter that YuGuangCheng small diameter, D<0.2PC.

3. The core for black holes

Chapter 24 have reasoning, to form the first condition of the galaxy is necessary to have a strong gravitational field, and have this condition can be massive black holes.

Back then argument: huge energy conversion and the thermal radiation can only by the black hole gravitational potential energy and accretion content of total energy transformation to achieve.

4. Non thermal radiation spectrum

Quasars main energy in the form of non thermal radiation spectrum emission, spectrum flow strength F_u, on frequency u a power law distribution:

$$F_\nu \propto \frac{1}{\nu} \qquad (25.1)$$

Some in optical and infrared band the thermal emission primarily continuous spectrum.

5. Light change phenomenon

Active galactic nuclei have some light is obviously change phenomenon, and light change cycle is irregular, optical variable time scale only a few hours to a few days of the order of magnitude of the longest, in a few years.

6. Injection phenomenon

From a radius less than 0.1pc nuclear area, can emit continuous energy $W>10^{38}$erg/s, spectrum from 1 Mev ~ 100 um (λ), most of the power law distribution of the electromagnetic spectrum.

25.1.2 Seyfert galaxy

The main features are:

1. The spectrum has obvious line of fire, including allows line, half forbidden line and forbidden line. Allow line width is wide, such as Baltimore not line Doppler width can reach 500 ~ 1000 km/s. According to the Buddha's galaxy line width is divided into Seyfert1, Seyfert2 two kinds, the former Ha full width > 3000 km/s, the latter width of 500 ~ 1000 km/s.

2. Mother galaxy is generally spiral galaxy or Sa, Sb type, active galactic nuclei are star shaped dense nuclear, its size is only about 1 pc.

3. Continuous spectrum is blue or UV super, is a thermal spectrum or incomplete is thermal spectrum.

4. Absolute magnitude M_v >-24^m.

25.1.3 BL, Lac object (also called flash partial body)

The main features are:

1. The thermal type continuous spectrum: from the radio, infrared and optical even extended to X-ray band are performance is a hot type power law spectrum.

2. Quick light change phenomenon: the light change cycle is irregular, time scale from a few hours to a few months. Optical variable amplitude for magnitude, individual or even disastrous, and optical variable in the infrared and X-ray band also occur. Optical variable timing and band related, optical band is often hours or day's magnitude, radio band is on level to achieve.

3. High polarization, often 30%, polarization degree with the same wavelength, it the wavelength increase to decrease.

4 only very weak emission lines, explain that from the source to the observer, and the dust between lacks of nebula.

25.1.4 N galaxy

The main feature is the center has a bright star nuclear around low light extension nebula surrounded, the center on the color of the nuclear and quasars similar.

25.1.5 Star detonation galaxy

It is to point to have massive stars that exploded or are formed galaxy. Observation shows that: in the close spiral galaxy and irregular galaxy, about 10% of the galaxy with a strong infrared radiation, X-rays, and radio radiation, and shows strong nebula line of fire, all of these show that in the galaxy with a large number of stars explosive forming process. Star detonation galaxy formation time scale only about 10^7 years, mainly in the core region, scale is only about 1 Kpc and ordinary galaxy star forming region is in the galaxy disk or spiral arms.

According to hydrogen, helium line strength analysis, star detonation galaxy's effective temperature range is 38500 ~ 47000 k; According to the quality in 30 ~ 60$M_\odot$ of O7 ~ O5 type star line, that age is only 10^7 ~ 10^8 years.

Usually think star detonation galaxy is active galactic nuclei evolution predecessor, as the evolution of the initial stage, the star detonation galaxy and Seyfert2 are very

similar, in great quality hot main sequence star formation stage.

25.1.6 Active galactic nuclei characteristics comprehensive comparison

A combination of the five types of active galactic nuclei characteristics, with a preliminary comprehensive physical model generalization, according to the active galactic nuclei integral structure dimension from the outgoing every ten times as many as in the difference of the physical structure is as follows:

1Mpc Radio show source observed range

100Kpc Radio injection phenomenon, in the radio injection around sometimes accompanied by satelite galaxy

10Kpc Mother Galaxy, radio galaxy is generally an elliptical galaxy, Seyfert galaxy is generally spiral galaxy, quasars mother galaxy has not yet been forming, so generally not clear

1Kpc the core part of the galaxy

100pc Narrow line area

10pc Star distribution of critical point, the outward injection also often start from here (injection are polar axis)

1pc Wide line area

100mpc dense radio nuclear, VLBI observable limit

10mpc Continuous spectrum form area, accretion disk appeared

1mpc UV radiation forming region

100upc X-ray form area

10upc Black hole

This chapter mainly discusses the content is limited to 1 Kpc within the scope of the galactic nucleus formation initial internal structure characteristics.

25.2 Galaxy nuclear energy conversion mechanism

Astronomers already know, a supernova release huge energy comes from gravitational field potential energy. Last chapter has been proved: formation neutron star or black hole, it's necessary to release the redundant gravitational field potential energy, can appear otherwise gravitational collapse, form the singular point; Moreover,

according to the virial law, (24.11) type, the interior of a black hole neutron material ring spin speed and the ratio of the speed of light is constant, $K_v = 1/\sqrt{3}$. The available: black holes and neutron material outer ring peripheral nebula, dust accretion ring, also as long as meet the virial law, can form a stable accretion disk structure. Set accretion ring material for dm, surrounded by a black hole of the material and the inside of the amount of matter of accretion disks for N_iM_1, around black holes circular motion velocity v_θ, $v_\theta \le c/\sqrt{3}$, the:

$$\frac{GdmN_iM_{n1}}{R_{1,n}^2} = \frac{dmv_\theta^2}{R_{1,n}}$$

$$v_\theta = \sqrt{\frac{GN_iM_{n1}}{R_{1,n}}} \qquad (25.2)$$

The type description: from the accretion disk outer inward, spin velocity v_θ increase gradually, into a neutron material ring critical radius for $R_{1,n}$. Make nebula, dust rest energy for m_0c^2, when the accretion disk peripheral enter inside the outer ring to neutron material, spin speed to $v_\theta = c/\sqrt{3}$. The energy theory of relativity, increase the kinetic energy of W_v for:

$$W_v = m_0c^2\left[\frac{1}{\sqrt{1-(v_\theta/c)^2}} - 1\right] \qquad (25.3)$$

A nebula, dust was accretion process black holes in the gravitational field work for W_u, from (24.13) differentiate type:

$$dR_{1,n} = \frac{-2GN_iM_{n1}}{K_v^3c^2}dK_v \qquad (25.4)$$

$$W_u = \int_\infty^{R1,n} \frac{GN_iM_{n1}m_0}{R_{1,n}^2\sqrt{1-K_v^2}}dR_{1,n} \qquad (25.5)$$

Will (24.13) and (25.4) type substitution (25.5) type, have to:

$$W_u = \int_0^{Kv} \frac{2m_0K_vc^2}{\sqrt{1-K_v^2}}dK_v = 2m_0c^2\left(1-\sqrt{1-K_v^2}\right) \qquad (25.6)$$

Gravitational field potential energy and accretion disk material kinetic energy ratio for:

$$\frac{W_u}{W_v} = 2\sqrt{1-K_v^2} \qquad (25.7)$$

When $K_v = 1/\sqrt{3}$, W_u/W_v = 1.63299 times greater than that gravitational field potential new inside a black hole, the kinetic energy of the poor, is a black hole in accretion process should be the energy release of the $\triangle W_{uv}$ train. By (25.3) and (25.6) type, have to:

$$\Delta W_{uv} = m_0 c^2 \left(3 - \frac{3-2K_v^2}{\sqrt{1-K_v^2}} \right) = 0.14226 m_0 c^2 \qquad (25.8)$$

As shown in figure 25.1 shows, nebula, dust was accretion process in the position of the energy change is as follows:

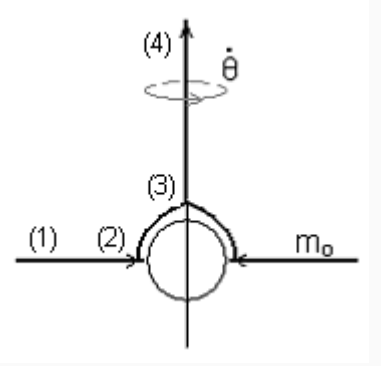

Figure 25.1 black hole peripheral accretion disk energy conversion plans

In the accretion disk starting point, set $v_\theta = 0$:

$$(1) \quad m_0 c^2 \qquad (25.9)$$

$$(2) \quad \frac{m_0 c^2}{\sqrt{1-K_v^2}} + 2m_0 c^2 \left(1 - \sqrt{1-K_v^2}\right) \qquad (25.10)$$

In the neutron material ring edge, the total energy to kinetic energy, potential energy and its own energy $m_0 c^2$ combined.

(3) $\frac{m_0c^2(1-K_{mx})}{\sqrt{1-K_v^2}}+2m_0c^2\left(1-\sqrt{1-K_v^2}\right)$ （25.11）

（$0 \le K_{mx} \le 1$ Said accretion rate)

(4) $\frac{m_0c^2(1-K_{mx})}{\sqrt{1-K_v^2}}+2m_0c^2\left(1-\sqrt{1-K_v^2}\right)-2m_0c^2(1-K_{mx})\left(1-\sqrt{1-K_v^2}\right)$

（25.12）

(25.12) type the last item for polar axis injection to overcome the central black hole gravitational field potential loss of energy, and ultimately the total energy released $\triangle W_{uv}$ for:

$$\Delta W_{uv}=\frac{m_0c^2(1-K_{mx})}{\sqrt{1-K_v^2}}+2m_0c^2\left(1-\sqrt{1-K_v^2}\right)K_{mx} \quad （25.13）$$

By (25.13) type see:

When K_{mx}= 0, no accretion, and final K_v = 0, $\triangle Wuv = m_0c^2$, accretion content from the accretion disk outer transferred to polar axis injection direction.

When K_{mx} = 1, are all accretion, release the gravitational potential energy $\Delta W_u = 2m_0c^2\left[1-\sqrt{1-K_v^2}\right]$.

When we make $K_v = 1/\sqrt{3}$ for constant, black holes in the entire galaxy life period, total quality, radius smoothly increases, the release of gravitational potential energy and the central black hole size, the quality has nothing to do with the accretion rate only K_{mx} relevant. When we by the law of conservation of energy deducted black hole kinetic energy increment, the (25.8) type, : $\triangle W_{uv}/m_0c^2$ = 0.14226 for constant that massive black holes accretion disk to the material energy conversion rate is 14.226% of the energy theory of relativity rest mass, which is about the fusion of stars burn conversion 20 times! This is the core of a galaxy, quasars huge capacity mechanism of reason.

25.3 The core of a galaxy spectral radiation mechanism

25.3.1 Galaxy nuclear each ring area structure, the combination of the characteristics and the forming principle

Comprehensive day literati observations and physical model in this paper see figure 25.2, we first to dust YunHuan, accretion disk and the central black hole composition, physical characteristics description:

1. Dust YunHuan: including peripheral neutral hydrogen cloud, ionization hydrogen cloud area, form the galaxy's early residual nebula or peripheral stars and debris by the central galaxy nuclear strong gravitational field suction; Because orbit radius reduced, spin speed increase to thousands of kilometers per second, star or debris was tearing into nebula or meteorite fragments; Be accretion disk radiation photon energy heating, gasification, the temperature can reach 10^4~4x10^4k, forming high temperature excitation radiation dust YunHuan; Peripheral for thin neutral hydrogen cloud, or is ionized hydrogen cloud diffusion zone.

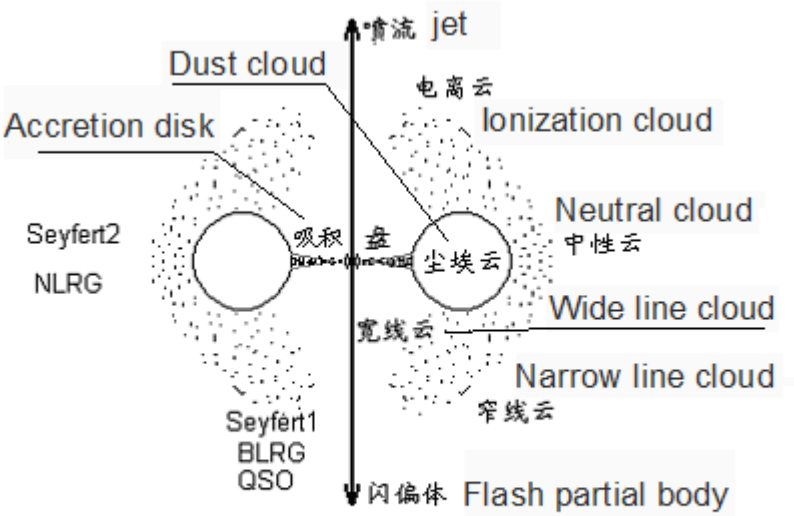

图25.2 活动星系核的统一模型示意图、图周围标出的是天体所在的观测方向

Figure 25.2 active galactic nuclei unified model diagram, drawing around the mark is the observation direction objects

2. Accretion disk: YunHuan dust in a small amount of material continuously by the central black hole accretion; In the accretion, spin motion process due to the radius reduced, the speed increase, all kinds of complex molecules, atoms has been torn into similar nuclear the internal structure of the particle spiral ring; Due to the negative and positive role to attract each other, each particle spin velocity v_θ must be equal, they form

from inside to outside of the high-energy π_g^+ meson, low-energy π_d^- meson and high energy electron e^- three trap close synchronization spin motion of particles spiral ring. In the accretion process, the kinetic energy increase gradually, residual gravitational potential energy is constantly stimulating neutrino field of neutrino, forming a continuous non thermal radiation spectrum. Finally, when the accretion of particles spiral ring to neutron material ring near or on the surface, and high and low energy π_g^+, π_d^- meson particle spiral ring and the nucleus, similar to happen ε decay, high energy electron adsorption a neutrino into low energy π_d^- meson into low energy π_d^- meson orbit, finish $2\pi_g^+ + \pi_d^- +$ electronic + neutrino $\rightarrow$ $2\pi_g^+ + 2\pi_d^-$ conversion process. In the last stage, the residual gravitational potential energy and decay in redundant energy all stimulate neutrino field of neutrino into X- rays or gamma radiation.

(3) From the virial theorem can see: dust YunHuan spin speed is 500 ~ 1000 Km/s, accretion disk spin speed should be from outside to is (1000 ~ 3000 Km/s $\rightarrow$ $c/\sqrt{3}$).

25.3.2 Accretion disk residual gravitational potential energy radiation mechanism

By (25.8) type, make K_v for variables, $K_v = 0.0033 \rightarrow 1/\sqrt{3}$, to $\triangle W_{uv}$ to differentiate:

$$\Delta W_{uv}^{'} = \frac{m_0 c^2 K_v}{\sqrt{1-K_v^2}}\left(\frac{1-2K_v^2}{1-K_v^2}\right) \qquad (25.14)$$

Every small ring accretion disk m_0 spin speed change area $\triangle K_v$ residual gravitational potential energy $\triangle W_{uvi}$ for:

$$\Delta W_{uvi} = \frac{m_0 c^2 K_v}{\sqrt{1-K_v^2}}\left(\frac{1-2K_v^2}{1-K_v^2}\right)\Delta K_v \qquad (25.15)$$

By the quantum physics, each photon energy $W_{\gamma i}$, and frequency υ_i, PuLang g constant h relationship for:

$$W_{\gamma i} = h\upsilon_i \qquad (25.16)$$

Obviously, a band F_{vi} total emission and photon energy $W_{\gamma i}$, residual gravitational potential energy train W_{uvi} relationship for:

$$F_{vi} W_{ri} = \Delta W_{uvi}$$

$$F_{vi} = \frac{m_0 c^2 K_{vi}}{\sqrt{1-K_{vi}^2}} \left(\frac{1-2K_{vi}^2}{1-K_{vi}^2} \right) \frac{\Delta K_{vi}}{h\nu_i} \qquad (25.17)$$

By (25.17) type see: F_{vi} and frequency u_i not only show the relationship between the power law (25.1) type relationship, but also with the spin velocity coefficient K_{vi} and speed factor interval ΔK_{vi} relevant.

25.3.3 Active galactic nuclei unified model, wide line, and narrow pattern formation mechanism

First of all, to active galactic nuclei, can confirm is optical galaxy formation of early central galaxy nuclear. According to the characteristics of the type of difference nature evolution sequence according to the arrangement for:

1.N Galaxy.→2.BL、Lac（Flash partialobjects）.→3.Quasars.→4.Stardetonationgalaxy.→5.Seyfert1→ 6. Seyfert2→7.Normalgalaxy nuclear。

From section 21.2 infinite eternal cosmological bases and the model has been preliminary description: a large galaxy formation, general from globular cluster→small galaxy, → medium galaxy →large galaxy after many times regeneration nebula supplementation, just gradually by their own gravitational field of the development of accretion. Of course, this also includes an elliptical galaxy, barred galaxy and spiral galaxy their original spin total angular momentum adaptive development.

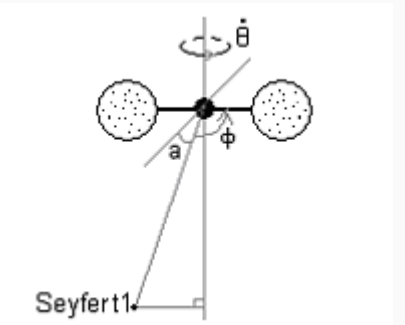

Figure 25.3 Seyfert1 observation spectral broadening schematic diagram

So, the above 6 kinds of active galactic nuclei from the given the quality of the stellar debris through the accretion other renewable nebula, peripheral residual nebula, dust in the process, the central black hole original quality gradually change, the nucleus of galaxy formation and evolution process of each period should appear from different types and our observation Angle should see characteristics.

By (25.15) type, figure 25.1 can see: Annular dust cloud medial spin speed of 1000 Km/s, speed coefficient K_{va} = 0.0033, in the accretion disk inside into neutron material ring, speed coefficient $K_{vb} = 1/\sqrt{3}$ to mean respectively substitution (25.15), type:

$$\Delta W_{uvi} = \left(\frac{1+0.5}{2}\right)\frac{m_0 c^2 K_v}{\sqrt{1-K_v^2}}\Delta K_v$$

$$= 0.75\frac{m_0 c^2 K_v}{\sqrt{1-K_v^2}}\Delta K_v \qquad (25.18)$$

Make accretion rate K_{mx}, speed interval ΔK_{vi} for constant, from (25.18) type known: the accretion disk edge to medial spin velocity increases, the total energy photon radiation also increase, Because the whole universe 2.73 K blackbody radiation is isotropic, so, the accretion disk per unit area on the launch of the photon number should also be the same.

By inference: accretion disks inside radiation each photon energy bigger, shorter wavelength. The figure 25.2 and figure 25.3 see, without the dust ring stop, we observed from the accretion disk directly on emission Seyfert1 type spectral Doppler broadening should be:

$$\Delta Z = \pm\left(0.0033 \to \frac{1}{\sqrt{3}}\right)\cos\alpha \sin\phi \qquad (25.19)$$

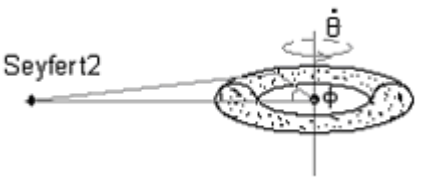

Figure 25.4 Seyfert2 observation spectral broadening location plan

The α is observation position and accretion disk plane Angle, Φ for accretion disk spectral radiation position and observer, polar axis plane constitute a Angle. Moreover, the photon energy is higher, accretion disk spin greater speed, the greater the Doppler broadening.

Similarly, we observed the narrow line spectrum is mainly composed of dust ring outer launch out, see figure 25.4. If dust ring outer spin speed of 500 km/s, inside for

1000 km/s, the different observation Angle can see Doppler apparent to speed difference, observed broadening should be:

$$\Delta Z = \pm(0.0017 \to 0.0033)\sin\ \phi \qquad (25.20)$$

25.3.4 Normal galaxy nuclear internal structure and energy conversion mechanism

Normal galaxy nuclear show by the active galactic nuclei further evolution, make the dust YunHuan, neutral hydrogen cloud, ionized hydrogen cloud (hereinafter referred to as the dust gas clouds) a ball shell enclosed encase black holes and accretion disk, the appearance of the entire galaxy nuclear spherical. Peripheral along the spherical shell uniform distribution of stars are rigid motion. With the evolution of the galaxy contraction, the central galaxy nuclear volume, quality relative peripheral visual optical galaxy proportion increase gradually. Early active galactic nuclei of dust gas cloud ball shell unfinished totally enclosed, initial black holes, the size of the accretion disks are small, accretion disk on the band spectral radiation and optical variable can be directly observed. Middle aged and elderly galaxy nuclear dust gas cloud ball shell is completely closed, and has considerable thickness, the foregoing band electromagnetic radiation and light change cannot be observed.

Dust gas cloud of black holes surrounded by ball shell is isolation layer, but also energy absorption layer. In order to overcome the central black hole strong gravitation, to maintain balance, in addition to their own part of the rotary motion of the centrifugal force, internal accretion disk on accretion content gravitational potential energy release into high energy photon radiation form the great light pressure, its strength should be enough to hold and hold dust gas cloud ball shell; (front has been proved that the core of a galaxy, a black hole center by the accretion disk accretion content release of gravitational potential energy, is the star of the nuclear fusion within twenty times! . At the same time, most of the photon energy is absorbed, make its transformation to visible light and infrared band, and dust gas cloud shell of gaseous atomic, molecular stimulated, transition produce new visible and infrared electromagnetic wave together to form strong infrared emission source; Also make the old galaxy nuclear central black hole accretion disk spectral radiation due to the effect of strong gravitational field generates a large red shift.

By (25.8) type, figure 25.1 can see: the accretion disks angular momentum loss, gravitational potential energy release will inevitably result in polar axis direction of the

radio and injection. As for the polar axis of symmetry radio disc forming principle, the figure 25.1 shows that is residual accretion thing, along the time axis direction injection to a certain position, kinetic energy after running; And again the ion, protons, electrons recombining into neutral hydrogen clouds and dust gas cloud process, electronic transition is generated when.

The elliptical galaxy galaxy nuclear, internal structure and spiral galaxy similar, the difference only lies in the accretion disk and disk family stars of the moment of momentum more small; So, their radio and reddening is comprehensive, the polar axis injection characteristics was not significant.

26 All kinds of galaxy, cluster characteristics and formation, evolution principle

26.1 All kinds of galaxy characteristics

26.1.1 Galaxy classification

At present day literati with Hubble classification will galaxy according to morphological characteristics in three categories, see figure 26.1. The author only added a optical galaxy evolution, the contraction in the direction of the line.

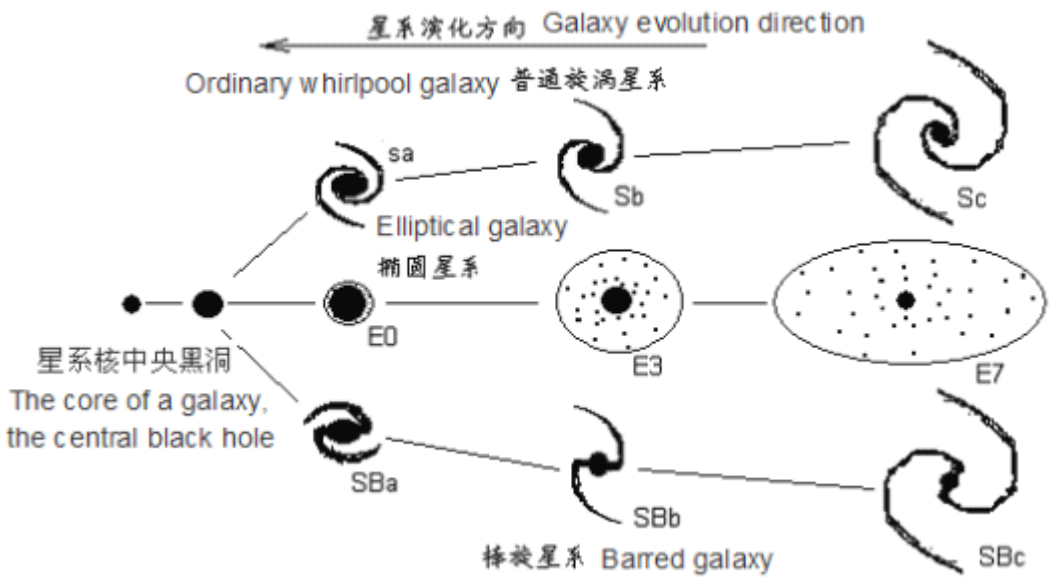

Figure 26.1 the galaxy's Hubble classification, evolution diagram

1. The elliptical galaxy: code E, often is flat scale in the back. Definition of flat for: $n = 10(a-b)/a$, a and b is half long shaft and half short shaft. The n is divided into eight grade 0, 1, 2,... 7. Please note that we see is only apparent flat degrees, really flat degree due to the short shaft orientation not clear not sure.

2. Spiral galaxy: segmentation ordinary spiral galaxy and barred galaxy, code for S, SB. According to the galaxy nuclear size and slewing closure degree in turn into So, Sa, Sb, Sc and SBa and SBb, SBc type.

3. Irregular galaxy: irregular galaxy and divided into two kinds, code Irr Ⅰ, Irr Ⅱ. The former shows that tear shape, surface brightness is low; there is no obvious

slewing or nuclear structure, the latter completely irregular.

4. Other types: in recent years to classic Hubble classification added some other types, such as:

（1）Sd or SBd type, nuclear small, slewing intermittently, belong to a shapeless vortex or barred galaxy

(2) The Sm type: MaiZheLun cloud type galaxy

(3) DE type: short elliptical galaxy, quality is very small, some with globular cluster almost

(4) CE type: special giant elliptical galaxy

(5) CD type: for super giant diffuse galaxy, often have several galactic nucleus, whole looks elliptical galaxy

(6) Radio galaxy: there is obvious radio radiation, the galaxy shapes

(7) Active galactic: including the Buddha's galaxy, radio galaxy and quasars

All kinds of galaxy number according to the Vandenberg statistical results see table 26.1:

The number of all kinds of galaxy statistical results distribution table table 26.1

kind	E+SO	Sa+SBa	Sb+SBb	Sc+SBc	Irr	Other kinds
百分比%	22.9	7.7	27.5	27.3	2.1	12.5

26.1.2 The main characteristics of all kinds of galaxy

1. The galaxy's mass light than M/L

All kinds of the galaxy's mass light than M/L, which shows the galaxy physical property, the dark matter content; evolution process is an important parameter. You can be sure: type, size the same visual optical galaxy, qualitative light, and the greater than this optical galaxy of the age. As shown in the figure 26.1, table 26. 2.

In the same galaxy different position, qualitative light ratio is not the same. Such as the Milky Way, in the sun position orbit radius $R_{\odot}$ inside, M/L = 10; In the 2 $R_{\odot}$ inside, M/L = 15 ~ twenty; In the ten $R_{\odot}$ inside, M/L = 30. Shows the distribution of dark matter

is not uniform, the visible light in the edge of the galaxy and peripheral galactic halo of dark matter, a much higher percentage.

All kinds of the galaxy's mass light than table table 26. 2

galaxy kind	mass light than	galaxy kind	mass light than	galaxy kind	mass light than
E	20～40	Sa、SBa	10～13	Sc、SBc	＜10
SO	10～15	Sb、SBb	about 10	Irr	about 3

3. The rotation of the galaxy

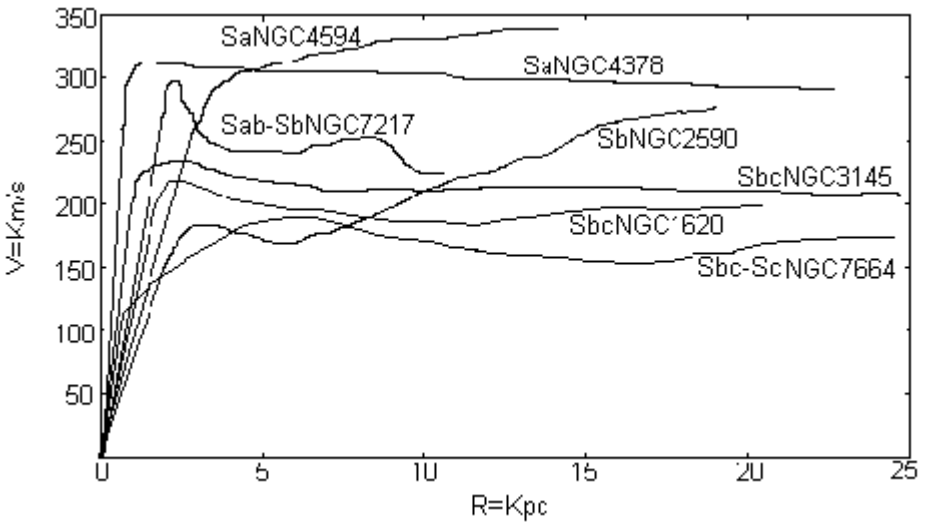

Figure 26.2 7 spiral galaxy rotation speed curve

X axis is to center distance, R, ordinate is rotational velocity

Observation results show that the general spiral galaxy are obvious rotation movement, see figure 26.2. The center of a galaxy is rigid rotation; speed is proportional to the distance to the rotation. From the slewing began to outside, speed is gradual change. In the outer part of the galaxy, Kepler's rotational speed, inverse ratio to the square root of orbit radius. This peculiar rotation movement, is dark matter distribution has certain law, followed by further analysis.

26.1.3 All kinds of galaxy feature comparison

Generally speaking, the quality of the elliptical galaxy is the largest, spiral galaxy is the second smallest, and irregular galaxy minimum. Evolution rate the fastest is elliptical galaxy, due to the nebula, stars around the galaxy nuclear spin speed is very small, the

lack of centrifugal force to balance gravitation; When an elliptical galaxy preliminary formed, almost all nebula gases into stars at the same time, little interstellar medium; Therefore, elliptical galaxy almost all of the stars, the stars belong to the family of star Ⅱ. Round optical galaxy life, star replacement may only have a few generation, from massive stars evolve rapidly to the quality of the small stars. On the structure, the center of the elliptical galaxy density is high, its density change and to center distance is inversely proportional to the vertical $\rho \propto R^{-3}$ that shrinkage soon.

Spiral galaxy mainly by the nuclear and slewing is composition, the core part and elliptical galaxy similar, mainly by the old stars form. Slewing in part by the stars and interstellar medium gas is composition, including common young and massive stars.

British astronomer Rees 1977 think there Ⅲ family of stars, star family Ⅲ answered in arthritic galaxy peripheral halo; Especially spiral galaxy, peripheral there is a spherical structure of the big halo shell; The early formation of star family Ⅲ, (most has become a neutron star, a White Dwarf, black dwarf) distribution in the halo of. This kind of speculation book model would have to be sure. In all optical galaxy peripheral halo, even halo peripheral already dim the nebula group area, should exist in the early formation of star family Ⅲ and globular cluster; Optical galaxy (such as the Milky Way) from the peripheral and central and edge and center of the quality of light than in turn reduce is valid proof.

Galaxy optical color reflects the quality of the stars and the temperature of the surface by Hector ROM diagram can also calculate the age of the stars. The observation comparison, general elliptical galaxy than spiral galaxy are more red, irregular galaxy partial blue. Spiral galaxy the outer part and nuclear ball area is different, when nuclear ball area bigger or slewing crimple, color red.

Comprehensive this section of galaxy characteristics and discusses previous chapters, we can preliminary inference is as follows:

1. The irregular galaxy quality small, qualitative light, star than small slant blue color, it is the embryo of the galaxy.

2. The size of the galaxy in batch by batch accretion new nebula group's development and growth process, the total moment of momentum has inherited and conservativeness. It is spiral galaxy, get new nebula supplements after growth is still spiral galaxy, originally is elliptical galaxy further development is still an elliptical galaxy,

(assuming new nebula group's moment of momentum are small).

3. All optical galaxy in every stage of the evolution process, the nebula, stars and visual optical galaxy range is gradually shrinking, the core of a galaxy, gradually change, slewing gradually tightening spiral galaxy, in the middle of the optical part eventually evolved into dense elliptical galaxy.

4. All optical galaxy in every period in the process of evolution, with the age change, qualitative light than bigger star color red.

26.2 All kinds of cluster characteristics

26.2.1 Cluster classification

Galaxy lumps sex can and stars in the Milky Way clouds sex than similar. According to the rich degree points 5 levels, see table 26.3.

Galaxy lumps of rich level meter table 26.3

Rich degree level	Galaxy number	North days of cluster number
0	30～49	10
1	50～79	1224
2	80～129	283
3	130～199	68
4	200～299	6
5	300～	1
Note	Statistical scope of north day red shift value Z = 0.02 ~ 0.2 range	

Cluster form, can be generally divided into regular and irregular, the former form is symmetrical round or quasi circular distribution; the latter have no obvious center and symmetrical shape boundary. Leave our recent and the largest Virgo cluster is a typical irregular cluster.

If according to the cluster member classification, can be divided into:

1. CD cluster, CD type galaxy refers to some cluster found supersized elliptical

galaxy, its star cladding may extend 100 Kpc, general distribution in the dense type cluster (a galaxy/Mpc^3). Part of the CD type galaxy and multiple galactic are nucleus. In CD cluster, the proportion of all kinds of galaxy is about E: So: S = 3:4:2, spiral galaxy accounted for only 20%, galaxy distribution regularly to center intensive.

2. Rich spiral galaxy type, the proportion of members of the galaxy for E: So: S = 1:2:3, members of the spiral galaxy is 50%, galaxy distribution is irregular, and center density is very low.

3. Lean spiral galaxy type, the rest of the cluster can be referred to as lean spiral galaxy type, its members ratio for E: So: S = 1:2:1, members galaxy clusters in the distribution between between 1 to 2.

The members of the galaxy distribution also have obvious difference, CD type and lean spiral galaxy type, spiral galaxy most distribution in the peripheral and central part mainly is the elliptical galaxy and So galaxy. Rich spiral galaxy type, all kinds of galaxy distribution is consistent with the basic.

26.2.2 Cluster quality and dark matter

The quality of the cluster can directly use dynamics method, from the virial theorem and out. A detailed study of the Coma cluster is its members about 800. If the R = 16 Mpc/h, it is concluded that the total quality:

$$\sum M = 1.79 \times 10^{15} \, M_{\Theta} / h$$

And the center part of the radius R less than 1Mpc ball area, quality have $\sum M = 6.1 \times 10^{14} \, M_{\Theta} / h$. The central part of the quality of light than for 350 $M_{\odot}/L_{\odot}h$. In general, the cluster of the quality of light than are 100 ~ 300 that exist in the cluster of dark matter more than ten times more than a single galaxy. Mentioned before, we will star debris neutron stars, black holes, a White Dwarf, black dwarf and dead galaxy, galaxy group, all too dark matter. So, cluster middle light than far outweigh the each galaxy internal quality light ratio, is enough to indicate that there has been a considerable proportion of death and the whole galaxy galaxy group remains there.

26.3 galaxy formation and evolution principle

26.3.1 Nebula regeneration

Front has already proved, the universe has more than 90% of the dark matter, they are dead the whole galaxy group, galaxy or star debris, and some meteorite fragments, dust and nebula residual.

Among them was part or most of the dark matter concentrated in the center of the galaxy nuclear neutron material universal huge black hole. All the bright, dark matter in their bodies under the action of gravity field attracts each other, moving around.

When the quality of similar galaxy nuclear center massive black hole, the neutron star or black hole HengXingJi in under the action of gravity field attract each other conflict, it will destroy the balance of the neutron material stable structure, and lead to complete the big bang. All the gravitational potential energy and kinetic energy and its own energy all into neutron, high, low energy $\pi^{\pm}$ meson energy relativity kinetic energy, and overcome the gravitational potential energy explosion diffusion into neutron cloud, high can $\pi^{\pm}$ meson clouds. Then quickly decay, regroup into protons, electrons and photons or neutrino, the formation of a hydrogen element is given priority to, rich in d, helium two elements of new nebula group. If it is two galaxies nuclear center massive black hole to conflict big bang, the total energy is it can be imagined. The big bang formation of very large scale, large energy new nebula group, and the particle energy andγ -ray energy must follow the probability curve distribution. At this time, high energy happenedγ-ray bursts and proton ray is not surprising. See figure 26.3 two black holes conflict big bang form new nebula schematic diagram. Because most of the galaxy, the dark m atter objects have mutual winding motion, and the distance between the larger, so this can collide less likely. This is the dark matter celestial far more than the root cause of the Ming material objects.

Common quality is similar or greater difference between galaxy nuclear center hole, neutron star or black hole in the gravitational field Quality as stars Level of black holes attracted to each other under the action of a close winding motion, this will inevitably occur the phenomenon of the law of the jungle. Moreover, the structure, density, the same quality, is stronger of the gravity. Quality small galaxy nuclear and even the whole galaxy will gradually be massive galactic nucleus all swallowed. Be out of the neutron material ring will be along the accretion disk transfer, in part, by adsorption, part of the polar axis jet formation neutron flow injection and symmetrical radio disc. Valve area is neutron decay, protons, electrons with the formation of hydrogen cloud area, see figure 25.1 and figure 26.3.

This kind of compact source devouring, injection phenomenon also can form new

nebula group, and is the common phenomenon. Have many scholars pay attention to the density of the huge source radio area often satellite galaxy distribution. The main galaxy engulfed in weak growing in the galaxy, until the two quality similar galaxy check thoroughly into the big bang, all into a super new nebula group so far. Please note: dark matter conflict completely big bang into bright material new nebula group's process, can cause the regional gravitational potential energy is reduced, the surrounding objects of the gravitational field strength become smaller, it will lead to the galaxy around objects of the orbits of the original large adjustment. The above two kinds of produce new nebula group way process will not rule out some d, the synthesis of helium. Of course, also does not exclude the nebula group of other small galaxy, dark matter and residual stars.

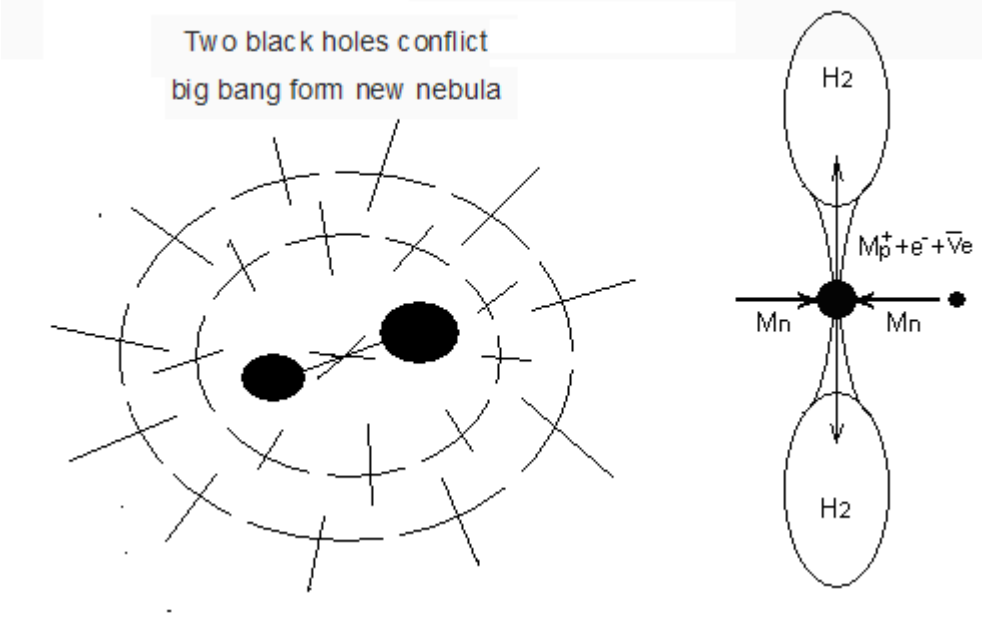

Figure 26.3 Two black holes conflict big bang form new nebula and
Devour process polar axis radio nebula group forming principle diagram

The universe is not death galactic nucleus, stars or its wreckage White Dwarf, brown dwarfs are also will appear conflict explosion or close up the phenomenon. Also can produce radio and injection, but they have not the nebula is completely hydrogen cloud, still can clip some residual stellar gas cloud, meteorites, dust and other impurities.

26.3.2 Galaxy the formation and evolution of the principle

For each new nebula group, regardless of their size, to be sure, are in a large

number of local uneven distribution of dark matter and not death galaxy, stars of the gravitational field attracted to each other to contain the role. Just like the surface of the earth's atmosphere as the clouds, floating in the space. So, the dark matter in the universe or not death galaxy, stars sometimes just through the nebula group also becomes possible.

If new nebula group gravitational field around a radial uniform distribution, the lack of a clear direction; So, in the nebula cluster centre some residual stars, galaxy and remains under the action of the gravitational field, can form a sphere, a spherical symmetry of the galaxy. If nebula group is big enough, it also has the potential to develop CD type cluster. Of course, if the nebula group is bigger, center residual galaxy and remains more than one, so, forming super huge dispersion type elliptical galaxy contains multiple galactic nucleus is not surprising. If the nebula group around the bright, dark matter total gravitational field have a obvious directivity, nebula group is located in two galaxy or two main gravitational field between center, or there are a certain direction of mutual winding rotary motion. The nebula group will be stretching and rotating, form the original vortex nebula group, in the center gravity field or small galaxy under the action of the gravitational field, may directly formed spiral galaxy. For any a galaxy or spherical form evolution, as long as not from accretion disk to polar axis injection, so, the original galaxy or objects, and accretion of the nebula total moment of momentum should exist inheritance and conservativeness.

To sum up, decided to form spiral galaxy or elliptical galaxy conditions mainly new nebula group and within the scope of the original Ming and dark matter the total moment of momentum. This is also different cluster in different space position distribution of different types of the main reasons for the galaxy. Moreover, galaxy, dark matter and nebula group is the relationship between the evolution of batch by batch, has formed the optical galaxy gradually contraction, nebula batch by batch adsorption added, the whole galaxy is one period development process. Eventually the two large and superlarge galactic nucleus and will in the universal gravitation field under the action of gravity collide into super big bang all new nebula groups.

26.3.3 Galaxy internal structure forming principle

Whether elliptical galaxy or spiral galaxy, composed of stars can be divided into star family Ⅰ, star family Ⅱ and galactic halo of star Ⅲ family. The difference between them is just before the different proportion of. For all the middle aged and

elderly galaxy galaxy nuclear, in chapter 25 have argument, there is a layer of completely closed the central black hole dust gas cloud ball shell and stars form ball shell. Similar inside a black hole neutron material ring spin motion combination, we can will dust gas clouds, star family Ⅱ, star Ⅰ into the family along the different spin orbital motion direction, to the central black hole formation totally enclosed spherical shell combination. As for the Milky Way, the family Ⅰ spin motion axial main point to spiral galaxy nuclear polar axis, globular cluster and star family Ⅱ spin motion axial were radial symmetry distribution.

The figure 26.2 shows, the core of a galaxy, a ball star main is rigid motion. A nuclear ball in the layer of stars, black holes, total quality, the average density of ρ_0, the star around the galactic nucleus movement orbit radius in the total quality is surrounded by $4\pi R^3\rho_0/3$. By the virial theorem, each of the mass of the sun star balance spin movement condition is:

$$\frac{\frac{4}{3}\pi R^3\rho_0 GM_\Theta}{R^2}=\frac{M_\Theta(\dot{\theta}R)^2}{R}\qquad \dot{\theta}=\sqrt{\frac{4}{3}\pi\rho_0 G}\qquad (26.1)$$

By (26.1) type, that the nuclear ball rotation movements in angular velocity $\dot{\theta}$ are constant, maintain rigid body motion, ρ_0 has to be constant, also is the nuclear ball in each layer of the star quality, life, interval, density must tend to be consistent. Stars along the spin orbital motion of the radial force is 0, vertical radial direction of the spherical between stars gravitational attraction force must contain zero. To meet this condition can be close to the quality of the formation of small, and a long life and small stars.

26.3.4 Spiral galaxy's spiral arm forming principle

Front has reasoning, original spiral galaxy's spiral arm has been initially formed. When galaxy each absorption a period after the nebula is gradually evolving process, because the arms of the original Ming, the initial concentration, the dark matter in the gravitational field long-term interaction effect, can make the original Ming, dark matter and new absorption of the nebula further to galactic nucleus and slewing center focus; Plus galaxy ends slewing in spin movement will automatically adjust make both ends slewing total mass, angular momentum tend to be more symmetrical; So, with the evolution of the galaxy, slewing will tend to clear by fuzzy, the complex tend to be simple, the asymmetry tend to complete symmetry. It also for the next period continues

to absorb nebula forms with clearer spiral galaxy provides conditions. Thus we can speculate: in spiral galaxy, star family Ⅱ, globular cluster, halo star family Ⅲ and remains largely tend to globular distribution. And star family Ⅰ and slewing of residual nebula, tend to be in a line along the radial distribution.

To radial internal and external stars spin motion along the rotary arm of stars, stars debris, residual nebula along the spiral arm in a circular cross section radius R_2 range is tend to and density distribution of ρ_0. A star around the galactic nucleus in the spin motion orbit radius R_1 range total quality can approximate expressed as: $\sum M = 2R_1\pi R_2^2\rho_0$, by the virial theorem:

$$\frac{2R_1\pi R_2^2\rho_0 GM_\Theta}{R_1^2} = \frac{M_\Theta v_\theta^2}{R_1}$$

$$v_\theta = \sqrt{2\pi R_2^2\rho_0 G} \qquad (26.2)$$

(R_2 for radial cross section radius of a circle)

By (26.2) type, : as long as rotary arm $R_2^2\rho_0$ for constant, the rotary arm stars spin velocity v_θ is constant, and distance galaxy nuclear size has nothing to do, this is shown in figure 26.2 is poor movement characteristics.

As for barred galaxy and ordinary spiral galaxy, the relationship between the two series: the author thinks that is one thing, and the difference is only spiral galaxy evolution different stages to get new nebula supplements. If the spiral galaxy, early get new nebula complement, then slewing is loose, a new round of the galaxy evolution can be more fully inherited the original galaxy appearance; If spiral galaxy to medium, old age to get new nebula complement, because the original galaxy's spiral arm has been tightening, internal spin speed is bigger, peripheral new nebula total angular momentum is lesser, lead to internal and external rotation speed difference bigger, naturally formed barred galaxy.

26.4 gravitational fields in the cosmic evolution in the leading role

26.4.1 Different gravitational field strength which is dominated by celestial existence type

According to various objects form the strength of the gravitational field, from big to small into the type?

1. Cluster → 2. Galaxy galaxy →3. Galaxy galaxy nuclear → 4. The core of a galaxy, the central black hole → 5. Stars → 6. Quality and star quite black holes → 7. The remains of the neutron star and dwarf stars →8. Planet →9. Meteorites →10. clouds.

Modern astronomy observations have shown that: if the cluster for the unit in the whole universe, in all directions of the density distribution is very uniform. We each cluster including peripheral two clusters half the distance between surrounded huge ball spaces, as Newton's universal gravitation field of quality unit. This can be concluded that the cluster surrounded the entire surface of the great ball space, in the infinite, eternal the whole universe in all directions of the gravitational field function, its overall force is 0, (assuming the cluster and the cluster around does not exist between gravity field around each other sports). This can also be further inference: in this huge spherical surface spaces every limited area unit, even infinitesimal area unit, this cluster and outside cluster, and even the entire universe of gravitational field between the role of resultant force is zero. As for cluster each other between winding motion, granted to each cluster quality, size, density distribution of local caused by uneven.

Similarly, in each cluster internal, for each galaxy, including all become dark matter has died of the galaxy. If we to each galaxy including peripheral two galaxys half the distance between to surrounded ball space, as Newton's universal gravitation field of quality unit. The same can be concluded that the galaxy surrounded the entire surface of the spherical space, in the whole cluster in all directions of the gravitational field function, its overall force must be tending to zero. The different is, galaxy the each other between winding motion, each galaxy clusters around the center of the overall quality of the relative movement and the obvious just.

From the above can corollary: local gravitational field strength determines the cluster of total quality size, type, distribution and the distance between each cluster. By (24.11) and (25.3) that the type, the cluster in all the core of a galaxy, the central black hole, and its quality is the core of a galaxy, two of the central black hole conflict completely big bang form large group nebula quality 1.2247448714 times. So, each cluster of the gravitational field of the overall strength and the center of the gravitational field is as cluster within the galaxy evolution in a constantly changing.

This will inevitably lead to cluster the total quality size, type, distribution and the distance between each cluster with the constant change. Of course, the each other between adjacent clusters around movement also must be in constant change. Even on the surrounding neutrino field gravitation effect, also can appear change. As the earth's atmosphere air local flow, the whole universe space of neutrino field are not absolutely still remains the same, we are hard to find, sleep is far less than the speed of light sport.

To galaxy, galactic nucleus and galactic nucleus in the middle of the huge black hole, the author in chapter 24 ~ 26 already was systematically discussed. Here is only that the 2 features please reader's attention:

1. The galaxy is in its own gravitational field, under the action of one stage attract along the orbital motion into nebula material to gradually grow up. So, galaxy original gravitational field strength and to determine the moment of momentum can absorb nebula share, which determines the quality of the galaxy size and type.

2. According to the size of the galaxy and galaxy nuclear development degree, section 25.3 25.3.3 section is the core of a galaxy, the evolution of the morning and evening order: 1. Cluster → 2. Galaxy galaxy →3. Galaxy galaxy nuclear → 4. The core of a galaxy, the central black hole → 5. Stars → 6. Quality and star quite black holes →7. The remains of the neutron star and dwarf stars. The（flash partial body）on the periphery of the lack of nebula and dust. N galaxy and quasar has a star shape light nuclear, some quasars in infrared and optical band to heat the continuous spectrum is given priority to. Thus we can speculate: N galaxy should be small galaxy of the embryo, the middle of the bright nucleus may be a super star, the center will not rule out a globular cluster level of a black hole. Part of the quasars in infrared and optical band to heat the continuous spectrum is given priority to, the surface that there are still star shaped thermonuclear reactions. The edge of the black hole existing star shaped thermonuclear reaction showed that, from the black hole accretion disk radiation photon formation of light pressure, is enough to hold and hold edge nebula ball shell, and can resist internal black holes and the entire nebula ball shell powerful gravitation, inside and outside the top pressure two force on the top, under the action of the nebula spherical shell lining to happen thermonuclear fusion reaction. This new speculative astronomical phenomenon, can explain part quasars in infrared and optical band to heat the continuous spectrum based super, super strength of star shape thermonuclear reaction (see chapter 27). As the shell in the nebula

thermonuclear reaction, by the central black hole accretion, peripheral a large number of stars explosive terrain paired nebula split adsorption. Make the ball in the shell of the nebula gradually dilute, finally and peripheral stars together nebula - star mixed ball shell. So far, the black hole surface thermonuclear reaction natural stopped.

Different quality of stars in the gravitational field under the action of formation from →the nebula, thermonuclear reaction →nuclear fuel most run out of death into black holes, neutron stars, dwarf the entire process, the scientific community that has done detailed research. Here only repeat 1: star quality, thermonuclear reaction speed, life and death remains of the type, still by the strength of the gravitational field decision.

Planets and meteorites clouds, most in spiral galaxy's spiral arms, basically and star company was born. It is a generation of stars thermonuclear fusion reaction before death after explosion, astral surface shot out of the fusion reaction after the residue. Its composition is mainly for the nuclear charge number $Z_{ie} > 2$ atoms, shot after cooling solidification often into various sulfide, silicate and rich in carbon, nitrogen and mineral elements of meteorites.

The star surface explosion, the meteorite quality, inertia far outweigh the gas, so meteorite shot distance must be higher than gas state of the nebula distribution of a much wider range. If you include the whirlpool galaxy globular cluster center early large and superlarge stars exploded projectile meteorites clouds, to be sure, meteorites can spherical and widely distributed throughout the galaxy and peripheral halo in the. For spiral galaxy, for radial and disk has many spherical gravitational field long-term effects, meteorites cloud will eventually tend to be along the area distribution. This is the late disk family star formation provides rich material sources of the planet. It can be speculated that: most of the disk family stars may be accompanying the planet. Obviously, the death star before the explosion, meteorites cloud migration, disk family star formation, accompanying the whole process of planet, and gravitational field still plays a leading role.

In 26.1.1 ~ 3 sections, has been to the formation of the nebula, dark matter by other celestial bodies, galaxy and adsorption process makes a detailed discussion. Readers it is not overly difficult to see: only by radio and black hole conflict completely big bang severe inflation, mainly for the formation of hydrogen, helium elements thin single nebula, if no other celestial bodies, dark matter galaxy gravitational field more adsorption, it is very difficult to rely on their own are gas molecular uniform state, from

their own weak gravitational field from the mass of nebula division contraction form new galaxy and spherical.

26.4.2 High-speed motion object state of being

On the earth, we can observe meteorites movement speed of general per second to hundreds of kilometers. The figure 26.2 shows that seven spiral galaxy's spiral arm rotation speeds are 150 ~ 350 km/s. The figure 25.2 and figure 26.2 shows, active galactic nuclei peripheral annular dust clouds spin speed, outer ring 500 ~ 1000 Km/s, inner ring 1000 ~ 3000 Km/s. Active galactic nuclei the edge of the accretion disk spin speed, (chapter 25 has been discussed, accretion disk from outside to inside, along with the spin velocity increases, the material from molecular and atomic state gradually transition to being torn shown in figure 1.2 the fluctuation, spin and precession orbit combination of particle spiral ring orbital motion state, finally and neutron material ring height can particle spiral ring track speed. From outside to inside is:

$$500Km/s \rightarrow 1000Km/s \rightarrow 3000Km/s \rightarrow c/\sqrt{3}$$

As for the galaxy and cluster of relative motion between, the virial law and spectral Doppler frequency shift difference (deducting the neutrino field of spectral energy absorption produce red shift) prediction, the movement speed in hundreds of kilometers per second range.

Table 6.1, table 6.2, and calculates the protons, neutrons $\pi^{\pm}$ meson spin orbit quantum number N_{α} = 22/9; Table 9.3 determined within the nucleus height low-energy particle spiral ring of discretion can $\pi^{\pm}$ meson spin orbit quantum number $N_{\alpha i}$; By (1.5) type, figure 1.2 certain particle spin and precession speed for:

$$v_{\theta} = v_{j} = v_{\alpha}/\sqrt{N_{\alpha}} = \beta c/\sqrt{N_{\alpha}} \approx c/\sqrt{N_{\alpha}}$$

According to chapter 16 hydrogen, helium and lithium atom surface electron orbit calculation parameters, we find out the three atoms along the surface electron spin orbital motion of the average velocity $v_{\theta i}$ respectively is: 2187.7 Km/s, 3828.5 Km/s, 143.8 Km/s.

According to chapter 20 table 20.2 ~ to table 20.5, $_{100}Fm$, $_{80}Hg$, $_{60}Nd$ and $_{40}Zr$ four atomic internal K layer electronic spin orbit quantum number $N_{\alpha i}$ calculation

results, $N_{\alpha i}$ value is between 3.2 and 18.3, by (1.5) type can be inferred, K layer electronic spin speed $v_{\theta i} = 167589.1 \sim 70080.2 Km/s$.

All kinds of particle spin, precession speed calculation results see table 26.4.

Particle type	Spin quantum number $N_{\alpha i}$		Spin or precession speed Units (Km/s)	
Proton	22/9		191747.9	
Neutron	22/9		191747.9	
Conditions within the nucleus	Nαdi	Nαgi	low-energy π±、	High energy π±
First layer	34/13	34/13	185375.7	185375.7
Layer 2	16	50	74948.1	42397.1
Layer 3	34	114	51414.0	28078.1
Tier 4	58	203	39364.7	21041.3
Fifth layer	88	316	31958.0	16864.6

A combination of the astronomical observation data and particle, electrons within the atoms spin speed parameters, it can be deduced: this section beginning list of ten kinds of molecules, atoms or by the aggregation of objects, the overall total kinetic rate generally in hundreds of kilometers per second range. As the earth's equator surface rotation speed of about 464 m/s, revolves around the sun in spin speed is about 29.8 Km/s, the solar system is located in the Milky Way in the arms, the silver heart around the rotation speed of about 300 Km/s. The molecules, atoms or its aggregate composition bodies and meteorites, in great quality, black hole edge will be evaporation, cracking or ionization, form shown in figure 25.2 gas clouds of dust or ionization cloud.

When the particle's spin or precession speed gradually increase $v_\theta = v_j = 3000 \sim 10000 Km/s \to c/\sqrt{3}$, the black hole edge of the annular gas dust and accretion disk medial particle spiral ring motion track, the last will and neutron material ring height can particle spiral ring track speed. Heavy nucleus is internal, 5 layers of low-energy particle spiral ring spin speed will also from 31958.0

Km/s $\rightarrow c/\sqrt{3}$, the first layer particle spiral ring spin orbit and axle. So, the future spacecraft as molecules, atoms aggregation, when it travels thousands of kilometers to nearly the speed of light c flight, what is the disintegration of the critical speed? I'm afraid or a large group of unknown!

26.4.3 Gravitational field in the cosmic evolution in the leading role

From the beginning of this section lists ten kinds of celestial bodies, 8. Planet →9. Meteorites clouds →nebula is the most weak gravitational field strength and the amount of matter at least 3 class objects. In these objects to atomic surface electronic electromagnetic force interaction is given priority to, can form various compounds or the structure is quite complicate organism. Gravitational field only determine their condensation degree and overall movement track.

5. Stars → **6.** Quality and star quite black holes → 7. Stellar debris neutron star, dwarf that three kinds of celestial gravitational field strength medium. This book has been proved: the conditions within the nucleus, neutron stars and black holes inside the strength of the interaction force is the force, also is the electromagnetic force. The electromagnetic force is slightly less than or equal to the universal gravitation, which determines the stars internal thermonuclear reaction speed, strength and the type of stellar debris.

3. The core of a galaxy → 4. The core of a galaxy, the central black hole, if local space they are when the gravitational field strength biggest 2 class objects. Here because the gravitational field strength far outweigh the electromagnetic force, forcing the interior of a black hole into hollow neutron material ring structure, make universal gravitation and electromagnetic force finally realize the complete balance equal big unification, and become all objects of the nebula of samsara, the area.

1. Cluster → 2. Galaxy, can saying is the basic unit of the celestial bodies. Front have argument: cluster size, type, overall density, all by gravitational field strength decided. Similarly, the galaxy's size, type, life, overall density, also all by gravitational field strength decided.

To sum up, the universe by all the heavenly body is composed, all of the celestial being determines the gravitation field strength, the strength of the gravitational field and determine the object of the type, composition, movement and evolution, therefore, gravitational field in the infinite, eternal universe model evolution is worthy of the name

"God".

27 quasar spectral supernormal value red shift of the gravitational field formation mechanism

27.1. Quasar spectral supernormal value Red shift principle

27.1.1. Quasar spectral supernormal value red shift paradox

Chapter 25 galaxy nuclear early characteristics and energy conversion, radiation, this paper discusses the mechanism of already know: N galaxy center and quasar has a star shape light nuclear, or less in 0.2pc in the tiny space, a quasar total luminosity is equivalent to 10^3 ~ 10^4 ordinary galaxy's total luminosity. Quite a number of quasars have spectrum supernormal value red shift phenomenon. Individual spectrum red shift of Z value have up to 3 ~ 5! The theory of relativity by spectral Doppler frequency shift effect

$$\frac{v}{c}=\frac{Z^2-1}{1+Z^2}=\frac{4}{5}\sim\frac{12}{13}\geq 1/\sqrt{3}$$

It is hard to imagine, to v≧0.8c speed movement of the celestial black hole accretion disks, than the edge of the neutron material ring limit rotation movement speed is fast. The object is to molecules, atoms aggregation state exist? If the (22.10) type Hubble's cosmic expansion model to calculate the distance of quasars, hypothesis H_0=75, the R = (3 ~ 5) x14.8 billion light-years in! It also made the universe hot big bang form theorists can't end. It is no wonder that many astronomical scholars to the quasar spectra supernormal value red shift repeatedly doubt whether it is truly cosmology sex.

27.1.2. Quasars stars form bright nucleus and spectral supernormal value red shift form physical model

The section 26.4 gravitational field has analysied to 1. N galaxy. → 2. BL, Lac (flash partial celestial) → 3. The quasar gravity, we speculated that N galaxy and quasars core exist a fairly massive black holes. N galaxy should be small galaxy of the embryo, the middle of the bright nucleus may be a very large hollow ball shell of stars, the center will not rule out a globular cluster level of a black hole. These quasars in infrared and optical band to heat the continuous spectrum are given priority to, the surface that there are still star shaped thermonuclear reactions. By (25.8) type, it is known that the edge of the black hole existing star shaped thermonuclear reaction

showed that, from the black hole accretion disk by the effect of gravitational field radiation that the total energy of the photon, equivalent to star thermonuclear fusion reactions release total energy twenty times! It shows that: the accretion disk radiation formation of light pressure, is enough to hold and hold edge nebula ball shell, and can resist internal black holes and the entire nebula ball shell powerful gravitation, inside and outside the top pressure two forces on the top, under the action of the nebula spherical shell lining to happened thermonuclear reaction. This new speculate stars fusion model that can explain part quasars in infrared and optical band formation to heat the continuous spectrum based super, super strength of star shape thermonuclear reaction, and can explain part the quasar supernormal value red shift. It is to break the gravitational potential energy must pay the price, see figure 27.1. At the same time, also to Einstein's theory of relativity put forward severe question time and space.

27.1.3. The interior of a black hole neutron material ring structure model

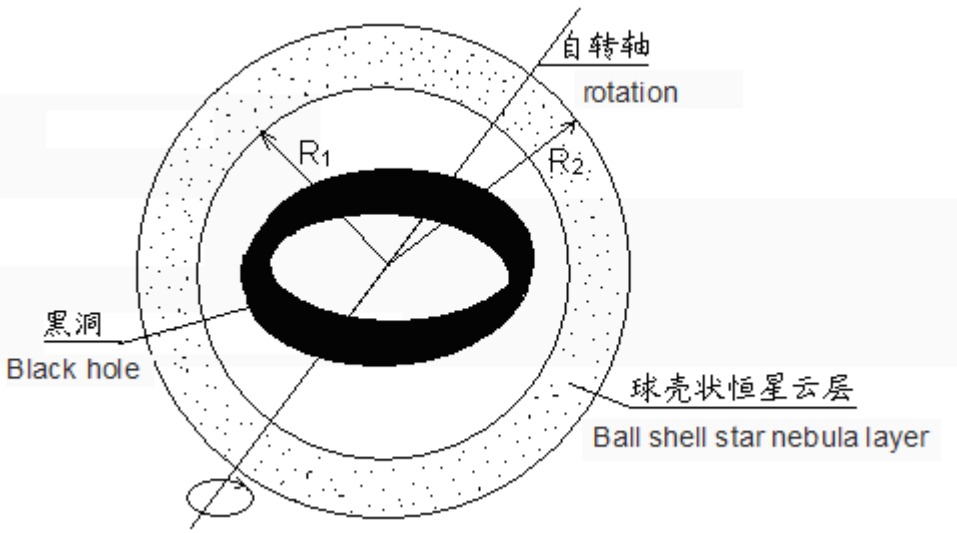

Figure 27.1 quasars internal neutron material ring

And ball shell star cloud structure model

Take the $R_{1,i}$ = 7112.39 m great value is constant. A black hole from center to outside the reason N a neutron material of ring. Make $R_{1,1}$= $R_{2,0}$, $v_\theta = c/\sqrt{3}$ is constant. The black hole in the neutron material ring aggregate total quality as $\sum M_i$.

By Newton's law of universal gravitation and the virial theorem, the black hole is the most outer neutron material on the ring as a segment neutron aggregate dM_i, we have:

$$\frac{G\sum M_i \cdot dM_i}{R_{1,i}^2} = \frac{dM_i \cdot v_\theta^2}{R_{1,i}}, \quad \text{Simplified to:}$$

$$\frac{G\sum M_i}{R_{1,i}} = v_\theta^2 \qquad (27.1)$$

Because each a neutron material ring quality M_i for: $M_i = 2\pi R_{1,i} \cdot \pi R_{2,0}^2 \rho_{0n}$, so:

$\sum M_i = 2\pi^2 R_{2,0}^2 \rho_{0n}\left(R_{1,1} + R_{1,2} + \cdots\cdots R_{1,i}\right)$. Substituting (27.1) type to:

$$\frac{2\pi^2 G R_{2,0}^2 \rho_{0n}\left(R_{1,1} + R_{1,2} + \cdots\cdots + R_{1,i}\right)}{R_{1,i}} = v_\theta^2 \qquad (27.2)$$

Will $R_{2,0}$ = 7112.39 m, $v_\theta = c/\sqrt{3}$, $\rho_0 = 1.9984 \times 10^{17}\ Kg/m^3$, substituting (24.10) type: $\rho_{0n} = \frac{\rho_0}{\left(1 - K_v^2\right)^2} = 4.4964 \times 10^{17}\ Kg/m^3$. Will these values are substitution (27.2) type to:

$$\frac{R_{1,1} + R_{1,2} + \cdots\cdots + R_{1,i}}{R_{1,i}} = 1 \qquad (27.3)$$

The type results show that: all the black hole, no matter size, internal quality of neutron material ring can steadily there is a lower limit, the quality is 1.6055 $M_\odot$. And, with the increase of the black hole quality, the spin radius $R_{1,i}$ will directly proportional increase. The back, we will directly with $M_{\bullet,1}$ symbol quasars center the mass of a black hole.

27.2. Quasars internal structure model and the relevant parameters of the simulation

27.2.1. Quasars internal structure model and the relevant parameters collection

In the light of the stars internal fusion energy conversion process study, what we already know: light between nuclear fusion reaction must overcome coulomb field repulsive force of the barrier, so, nuclear energy, also is the plasma temperature T_c will play the leading role. To pressure P_c and density ρ_c reaction are not sensitive. According to the scientific community to long-term research in magnetic field constraint controlled thermonuclear fusion reaction, mainly based on ultra high temperature, low pressure and density conditions. So, to figure 27.1 shows the outer shell of the black hole ball star cloud fusion physical conditions, as long as we take the sun center temperature T_c =1.5x10^{7}k, the average density of $\overline{\rho}_{\Theta}=1.4084\times10^3\ Kg/m^3$ and appropriate pressure parameters is enough.

At present the scientific community about the black hole edge accretion disk on the release of a large number of photon energy, their ball shell star cloud bottom support pressure, heating and thermal convection of the back pressure effect, is still not clear. But you can speculate that the hole edge ball shell star clouds, from the black hole edge accretion disk on the release of a large number of photon energy, at the bottom of the nebula heating and thermal convection of the pressure gradient is bigger, the nebula density change smaller. We can use Newton mechanics gravitational field to the top of the ball shell star clouds solving gravitational potential energy.

27.2.2. Quasars stars form bright nucleus and spectral supernormal value red shift simulation results

The figure 27.1 shows, a quasar the central black hole quality for $M_{•1}$, and peripheral ball shell star cloud overall quality of M_2 ball shell star cloud surface photon m_r of the gravitational field potential for $\triangle W_r$. From the front of the particle physics in figure 2.4 we already know, photon and neutrino fluctuations, precession orbit is circular helix, fluctuation and precession speed is the speed of light, along the track of the resultant velocity for $\sqrt{2}c$; So, by quantum mechanics, each photon actual kinetic energy should be expressed as $W_r = m_rc^2$, rather than Newtonian mechanics that $W_r = 0.5\ m_rc^2$. So, the calculation of photon and gravitational field of neutrinos gravitational potential energy or force, gravitational constant G remain unchanged, but the photon energy should instead be $W_r=m_rc^2$. (see section 28.2 further analysis of the derivation and verify the calculation results.

Make $R_{\bullet,i}$= $C_1R_{2,0}$、$M_{\bullet 1}$=1.6055$C_1M_{\odot}$、R_1=$C_1C_2R_{2,0}$、C_3= R_1/R_2、$R_2=\dfrac{C_1C_2R_{2,0}}{C_3}$, average density $\overline{\rho}_{\Theta}=1.4084\times10^3\ Kg/m^3$.（$C_1\geq1$ $C_2\geq1$ $0<C_3\leq1$）. We have:

$$\Delta W_r=\frac{2G\left[M_{\bullet 1}+\frac{4}{3}\pi\overline{\rho}_{\Theta}\left(R_2^3-R_1^3\right)\right]m_r}{R_2}$$

The above hypothesis factor substitution (27.4) type, have to:

$$\Delta W_r=2G\frac{\left[1.6055C_1M_{\Theta}+\frac{4}{3}\pi\overline{\rho}_{\Theta}\left(C_1C_2R_{2,0}\right)^3\left(\frac{1-C_3^3}{C_3^3}\right)\right]m_rC_3}{C_1C_2R_{2,0}} \qquad (27.4)$$

By quantum mechanics, the law of conservation of energy and (27.4) type, photon in the gravitational field under the action of the spectrum gravitational red shift value $\sum K_z$ can be expressed as:

$$\begin{aligned}\sum K_z&=\frac{m_rc^2}{m_rc^2-\Delta W_r}-1\\&=\frac{\Delta W_r}{c^2-\Delta W_r}\end{aligned} \qquad (27.5)$$

By (27.5) type that can be seen: when $\Delta W_r\to c^2$, the spectrum gravitational red shift value $\sum K_z\to\pm\infty$ will have infinite value.

Make the ball shell star cloud thickness of ΔR_{1-2} from the above C_1 and C_2 and C_3 set:

$$\Delta R_{1-2}=\frac{R_1}{C_3}-R_1=C_1C_2R_{2,0}\left(\frac{1}{C_3}-1\right) \qquad (27.6)$$

Make the ball shell star cloud total quality as the M_2, is the mass of the sun $M_{\odot}$ of C_m times, we have:

$$C_m=\frac{4}{3}\pi\overline{\rho}_{\Theta}\frac{\left(R_2^3-R_1^3\right)}{M_{\Theta}}=\frac{4}{3}\pi\overline{\rho}_{\Theta}\left(C_1C_2R_{2,0}\right)^3\left(\frac{1-C_3^3}{C_3^3M_{\Theta}}\right) \qquad (27.7)$$

Make the ball shell star cloud bottom pressure P_c support by the central black hole accretion disk release of photon momentum impulse to provide, the accretion disk per second need radiation photon total quality Δm_r, by Newtonian mechanics and quantum mechanics have to:

$$\Delta m_r = 4\pi R_1^2 \frac{P_c}{c} = 4\pi \left(C_1 C_2 R_{2,0}\right)^2 \frac{P_c}{c} \qquad (27.8)$$

Make the central black hole every accretion rate is $\sum \Delta m_r$, is the mass of the sun $M_\odot$ times of $C_{m\odot}$. By (25.8) type, the central black hole from accretion disk release of photon total energy is accretion amount of 14.226%, therefore, by (27.8) type, total accretion rate $\sum \Delta m_r$ is equivalent to the mass of the sun $M_\odot$ multiples of $C_{m\odot}$ for:

$$C_{m\Theta} = \frac{\sum \Delta m_r}{M_\Theta} = \frac{\Delta m_r \times 3600 \times 24 \times 365}{0.14226 M_\Theta} \qquad (27.9)$$

The quasar light change time scale, the figure 27.1, it can see with neutron pulsar as emission mechanism. The interior of a black hole neutron material ring and edge of accretion disks produce strong electromagnetic fields, will decide quasars inside and outside of the spectrum polarization direction. By (24.11) type for the interior of a black hole neutron material ring spin speed $v = c/\sqrt{3}$, timing days T can be expressed as:

$$T = \frac{\left(2\pi C_1 R_{2,0}\right)\sqrt{3}}{3600 \times 24 c} \qquad (27.10)$$

To sum up, the internal structure of quasars each parameter simulation program is as follows:

By(27.4)~ (27.10)type,we make sure C_2=2, C_3=0.5, $\overline{\rho}_\Theta = 1.4084 \times 10^3\ Kg/m^3$, $P_c = 10^6$ （N/m^2）,belong to the reasonable value range. Then the default C_1 value for a reasonable determine constant,respectively substitution(27.4)~ (27.10)type,simulation calculated quasars internal structure, parameters and spectrum red shift equivalent see table 27.1.

Quasars internal structure, parameters and spectrum red shift equivalent simulation results table 27.1

C_1	△W_r (J)	$\sum K_z$	ΔR_{1-2} (m)	C_m（$M_\odot$）	$C_{m\odot}$($M_\odot$)	T(day 天)

10^8	5.5907×10^{18}	-1.0163	1.422×10^{12}	5.976×10^{10}	9.4530	0.298
5×10^7	1.4089×10^{18}	-1.0681	7.112×10^{11}	7.470×10^9	2.363	0.149
2×10^7	2.3801×10^{17}	-1.6067	2.845×10^{11}	4.781×10^8	0.3781	0.060
1.5×10^7	1.4043×10^{17}	-2.7777	2.134×10^{11}	2.017×10^8	0.2127	0.045
1.2×10^7	9.5269×10^{16}	-17.6630	1.707×10^{11}	1.033×10^8	0.1361	0.036
1.1×10^7	8.2445×10^{16}	11.0957	1.565×10^{11}	7.954×10^7	0.1144	0.033
1.05×10^7	7.6451×10^{16}	5.6950	1.494×10^{11}	6.918×10^7	0.1042	0.031
1.025×10^7	7.3559×10^{16}	4.5082	1.458×10^{11}	6.436×10^7	0.0993	0.031
1.01×10^7	7.1857×10^{16}	3.9879	1.437×10^{11}	6.157×10^7	0.0964	0.030
10^7	7.0736×10^{16}	3.6959	1.422×10^{11}	5.976×10^7	0.0945	0.030
5×10^6	2.8919×10^{16}	0.4744	7.112×10^{10}	7.470×10^6	0.0236	0.015
10^6	1.5537×10^{16}	0.2090	1.422×10^{10}	5.976×10^4	0.0009	0.003
5×10^5	1.5119×10^{16}	0.2022	7.112×10^9	7470.07	2.4×10^{-4}	1.49×10^{-3}
10^4	1.4979×10^{16}	0.2000	1.422×10^8	5.976×10^{-2}	9.5×10^{-5}	2.99×10^{-5}
10^3	1.4979×10^{16}	0.2000	1.422×10^7	5.976×10^{-5}	9.5×10^{-10}	2.99×10^{-6}

Table 27.1 the results can be seen: in $C_1 = 1.2 \times 10^7 \sim 1.1 \times 10^7$ of the interval of a certain value, the spectrum gravitational red shift value $\sum K_z \to \pm\infty$ will have infinite value. The $\sum K_z$ is negative in the whole quasars schwarzschild black holes within the radius. (Does not exist completely black holes, even if gravitational field's largest neutron material ring surface, there are from accretion disks not so hot in the continuous spectrum emission). When $C_1 > 5 \times 10^5$, ball shell star cloud total quality $M_2 > 5.976 \times 10^7 M_\odot$, these quasars should belong to the galaxy nuclear embryos.

When $C_1 < 5 \times 10^5$, we can greatly improve the values of C_2, such as make $C_2 = 10^5$, other parameters constant, simulation results see table 27.2.

Quasars internal structure, parameters and spectrum red shift equivalent simulation results table 27.2

C_1	$\triangle W_r$ (J)	$\sum K_z$	ΔR_{1-2} (m)	C_m（$M_\odot$）	$C_{m\odot}(M_\odot)$	T(天)
10^5	1.3939×10^{22}	-1.0000	7.112×10^{13}	7.470×10^{15}	23632.5	2.99×10^{-4}
5×10^4	3.4848×10^{21}	-1.0000	3.556×10^{13}	9.338×10^{14}	5908.12	1.49×10^{-4}
10^4	1.3939×10^{20}	-1.0006	7.112×10^{12}	7.470×10^{12}	236.325	2.99×10^{-5}
5×10^3	3.4848×10^{19}	-1.0026	3.556×10^{12}	9.338×10^{11}	59.0812	1.49×10^{-5}
10^3	1.3939×10^{18}	-1.0689	7.112×10^{11}	7.470×10^{9}	2.36324	2.99×10^{-6}
500	3.4848×10^{17}	-1.3475	3.556×10^{11}	9.338×10^{8}	0.59081	1.49×10^{-6}
260	9.4229×10^{16}	-21.642	1.849×10^{11}	1.313×10^{8}	0.15976	7.77×10^{-7}
250	8.7120×10^{16}	31.6210	1.778×10^{11}	1.167×10^{8}	0.14770	7.47×10^{-7}
200	5.5757×10^{16}	1.63422	1.422×10^{11}	5.976×10^{7}	0.09453	5.98×10^{-7}
100	1.3940×10^{16}	0.18357	7.112×10^{10}	7.470×10^{6}	0.02363	2.99×10^{-7}
10	1.3969×10^{14}	1.557×10^{-3}	7.112×10^{9}	7470.07	2.36×10^{-4}	2.99×10^{-8}
1	1.6935×10^{14}	1.884×10^{-5}	7.112×10^{8}	7.47007	2.36×10^{-6}	2.99×10^{-9}

Table 27.2 the results that: when $C_1 < 250$ range, there are also great spectrum red shift value. When $C_1 < 200$, within the scope of the ball shell star cloud total quality $M_2 < 5.976 \times 10^7 M_\odot$, it is equivalent to the dwarf nuclear embryonic little quasars or globular cluster center early formation supermassive stars.

A combination of the simulation show that quasars supernormal value spectrum red shift is the central black hole gravitation place to; Can't use the hot big bang expansion Hubble's law is to distance; More can't use Einstein's theory of relativity time and space of the Doppler frequency shift law to inference quasars away from our movement speed tends to the speed of light; Even in superluminal movement speed far from us.

As for the quasar unimaginable so-called super energy radiation problem, when we in their actual distance analysis, then consider the central black hole accretion disk to accretion content up to twenty times the energy release of the light fusion, natural all problems lead edge and the solution.

In the universe, common two stars close mutual winding motion form the light of the periodic change phenomenon. Table 27.1 and table 27.2 simulation quasar light change cycle is obvious small. To this, we might as well to speculate that quasars as galactic nucleus of the embryo, the scale although far outweigh the stars, but it sure is far less than the quality of secondary normal galactic nucleus; With our relative distances, and two stars quasars close around each other sports can also form the light of the periodic change phenomenon.

28. Newton and Einstein's absolute time-space relative concept of space-time relationship

28.1 Einstein's relative the birth of space-time physics history background

28.1.1 Einstein's relative the birth of space-time physics history background

What are the light particles or wave? To Newton as a representative of school think just particles, and his contemporary Dutch physicist cost more, (1629-1695), and other scholars believe that light is a wave. Two school debate competition for 100 years. Until 1801, the British doctor and physicists Young (1733-1829) completed the interference of light experiment, just make physical scholars tend to believe that light is a wave.

In 1842, Doppler was first put forward: the movement of light source may affect the position of the line. In 1868, Huggins in far away from the earth stars emits spectral line the first observed spectral Doppler redshift phenomenon. Later, the use of the earth's motion light source experiment also confirmed this phenomenon.

In 1864, maxwell electromagnetic field equations is derived, and predicted the existence of electromagnetic wave, and calculates the electromagnetic wave propagation speed is equal to the speed of light, asserting that the same properties, the light is very short wavelength of electromagnetic waves.

Until 1888 Hz with the experiment confirmed the presence of electromagnetic wave, maxwell electromagnetic fields equations to be physical scholars admit. In 1879, the United States physicists Michelson accurately measure the speed of light in a vacuum c = 299796 km/s.

1887 Michelson - Morey with optical interference method (see figure 5.4) experimental proof: can not be measured relative to the earth "ether" movement speed.

At the turn of the century New Year message, a famous British physicist Lord kelvin (1824-1907) restlessly mentioned in the calm and clear physics is in the sky there is the two a dark clouds: a and blackbody radiation experiments, a and "the etheric" drift experiments.

On December 14, 1900 in Germany at the Max Planck physics report their research results. He assumed black body is made of many tiny energy oscillator components, each a vibrator energy is a basic energy h integer times. Thus derived blackbody radiation formula and experimental results perfectly, a dark cloud be dispelled, quantum physics was born.

From the above data shows that: when the physical understanding of the academic circles light is a superficial, only know that light is very short wavelength of electromagnetic waves, and electromagnetic wave that is shear wave, can only in the solid medium propagation; "The etheric" if not solid, whether there is already doesn't matter; Vacuum of the speed of light is constant; As for the light source the movement of the Doppler frequency shift, did not give enough attention; What is the light particles or wave? Still is not final conclusion.

In 1905, Einstein from Planck blackbody radiation to explain the basic idea of the quantum energy is inspired, in the photoelectric effect study established the light wave particle duality; In the lorentz transformation formula based on to the special theory of relativity; In 1916 and completed the general theory of relativity. (Please note: theory of relativity prerequisite is the speed of light invariance, namely between the observer and the source if there is speed v < c relative motion, the speed of light is still the same.

28.1.2 Nearly 100 years in the research field of the related physics major new find

At the field of astronomy observation, since 1912, the weasley eph found that distant galaxy light emitted from earth relative is close to the light of stars, like the sound source, can happen Doppler frequency shift, there are red shift phenomenon. In 1929, the Hubble found that the red shift to follow a very simple rule: galaxy the farther the distance, the greater the red shift and red shift and is proportional to the distance.

In 1924 Hubble confirmed the presence of the outer rim river, and then measure the distance spread to hundreds of millions of ~ the last years.

In 1965, the United States telecom engineer PengJi and Wilson: in the microwave communication, accidentally found 2.73 K cosmic background blackbody microwave radiation.

In the field of particle physics, in December 1930, in Germany diagram bingen

physics at the meeting, BaoLi prophecy: nuclear beta decay process of energy loss is caused by the neutrino. Until 1956, ke lai mild to exchange with the experiment confirmed the presence of electron neutrino and then been found **μ** muon type, τ sub-type neutrino and its antiparticle.

1980 years later, some scientists found space in the neutrino oscillation phenomena existing energy.

28.2. Gravitational field to light bending effect

Of Newtonian mechanics analysis

The book (1.2) equations and Newton's mechanics, see chapter 15 electron atomic nucleus along the spin elliptic orbit motion equations derived process, see figure 28.1. Make the photon movement quality for m_γ, as a particle along the fluctuation, precession helix orbital motion, the mass of the sun for $M_\odot$. By Newton's law of gravitation:

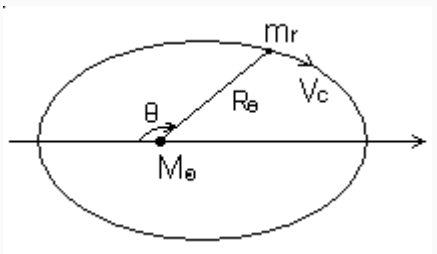

Figure 28.1 photon orbits round the sun precession

$$\begin{cases} R_\theta = \dfrac{H}{m_r v_\theta} \qquad (\dfrac{H}{m_r} = R_\theta v_\theta) & (28.1-1) \\ m_r(\ddot{R}_\theta - R_\theta \dot{\theta}^2) = \dfrac{-GM_\Theta m_r}{R_\theta^2} & (28.1-2) \\ m_r(R_\theta \ddot{\theta} + 2\dot{R}_\theta \dot{\theta}) = 0 & (28.1-3) \end{cases}$$

And (15.1) equations comparison, (28.1-1) type to remove a spin quantum number N_θ. (28.1-2), (28.1-3) two type for learned Newtonian mechanics people all know, is the law of universal gravitation expression. (28.1-1) type is photon in the sun as the center of gravity field under the action of precession of the orbital motion of moment of momentum conservation formula. We in order to make the model intuitive

and convenient analysis, first assumed cone surface cutting line for elliptic orbit. When the moment of momentum is constant, the photon by the sun's gravitational field force will be along the precession orbit radius to the center of the sun. The law of universal gravitation proof, (28.1-1) type of moment of momentum H is constant, so, (28.1-2), (28.1-3) type natural was established.

By (28.1-1) type, make the photon precession of the angular velocity $\dot{\theta}$ for:

$$\dot{\theta} = \frac{v_\theta}{R_\theta} = \frac{H}{m_\gamma R_\theta^2} \qquad (28.2)$$

Make $R_\theta = \frac{1}{u}$, the $dR_\theta = -\frac{du}{u^2}$, substituting (28.2), type to:

$$\dot{\theta} = \frac{H}{m_\gamma} u^2 \qquad (28.3)$$

The figure 28.1, (28.3) type, the photons radial velocity v_r ($\dot{R}_\theta$) and acceleration a_r ($\ddot{R}_\theta$) respectively is:

$$v_r = \frac{dR_\theta}{d\theta}\dot{\theta} = -\frac{H}{m_r}\frac{du}{d\theta} \qquad (28.4)$$

$$\alpha_r = -\frac{H}{m_r}\frac{du^2}{d\theta^2}\dot{\theta} = -\left(\frac{H}{m_r}\right)^2 u^2 \frac{du^2}{d\theta^2} \qquad (28.5)$$

Will (28.4) and (28.5) type substitution (28.1-2) type arrangement must:

$$\frac{du^2}{d\theta^2} + u = GM_\Theta \left(\frac{m_r}{H}\right)^2 \qquad (28.6)$$

Make $u = C_1 \cos\theta + C_2$, $\frac{du}{d\theta} = -C_1 \sin\theta$, $\frac{du^2}{d\theta^2} = -C_1 \cos\theta$ substituting (28.6) type, solution of differential equations (28.6) declined to:

$$R_\theta = \frac{\frac{1}{GM_\Theta}\left(\frac{H}{m_r}\right)^2}{1 + C_1 \frac{1}{GM_\Theta}\left(\frac{H}{m_r}\right)^2 \cos\theta} \qquad (28.7)$$

Make $P = \frac{1}{GM_\Theta}\left(\frac{H}{m_r}\right)^2$, $E_\theta = \frac{C_1}{GM_\Theta}\left(\frac{H}{m_r}\right)^2$, (27.7) type expressed as:

$$R_\theta = \frac{P}{1 + E_\theta \cos\theta} \qquad (28.8)$$

This is what we are familiar with conical surface cutting line track equation of motion.

The law of universal gravitation and the (28.8) type, we can see that: the photon energy $W_{\gamma m}$ will far outweigh the gravitational potential energy $W_{\gamma g}$, $W_{\gamma m} >> W_{\gamma g}$, so, $E_\theta >> 1$, the photons into dynamic track can be hyperbolic, see figure 28.2.

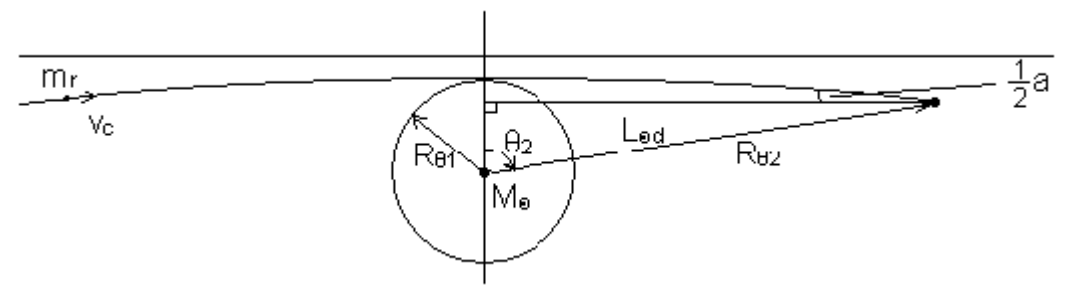

Figure 28.2 photon in the gravitational field under of the sun action of precession orbit is bending angle calculation diagram

By (28.1-1) and (28.2) and (28.7) type, make the photon along the precession direction, radius direction and orbit tangent velocity v_θ, v_r, v_c respectively is:

$$\begin{cases} v_r = GM_\Theta \frac{m_r}{H} E_\theta \sin\theta & (28.9-1) \\ v_\theta = GM_\Theta \frac{m_r}{H}(1 + E_\theta \cos\theta) & (28.9-2) \\ v_c = GM_\Theta \frac{m_r}{H}\sqrt{1 + 2E_\theta \cos\theta + E_\theta^2} & (28.9-3) \end{cases}$$

Photon along the precession of the hyperbolic orbital motion of the kinetic energy

W_{rm}, from (28.9) equations and Newtonian mechanics have to:

$$W_{rm} = \frac{m_r}{2}\left(GM_{\Theta}\frac{m_r}{H}\right)^2(1+2E_{\theta}\cos\theta+E_{\theta}^2) \qquad (28.10)$$

Photon along the precession hyperbolic orbital motion, in the sun under the action of gravity of gravitational potential energy for $W_{\gamma g}$, by the law of universal gravitation (28.1-2) type:

$$W_{rg} = \frac{-GM_{\Theta}m_r}{R_{\theta}} = -m_r\left(GM_{\Theta}\frac{m_r}{H}\right)^2(1+E_{\theta}\cos\theta) \qquad (28.11)$$

The photon in the sun under the action of the gravitational field of the total energy of the $\triangle W_{\gamma c}$, apparently for its kinetic energy and the sum of gravitational potential energy. By (28.10) and (28.11) type, have to:

$$\Delta W_{rc} = \frac{1}{2}m_r\left(GM_{\Theta}\frac{m_r}{H}\right)^2(E_{\theta}^2-1) \qquad (28.12)$$

Below, we by Newton's law of gravitation to calculate photon as a common particle, from infinity through the surface of the sun, again shot to the surface of the earth, in the sun under the action of gravity field, photon precession orbit should bend Angle α value.

The astronomical observation data, the mass of the sun $M_{\odot}$ = 1.989 x 10^{30} kg, radius $R_{\theta 1}$ = 6.9599 x 10^{8}m, the sun and the earth's distance $L_{\odot d}$ = 1.496 x 10^{11}m. Calculation model is shown in figure 28.2.

First, make the photon skim over the sun surface speed $v_{\theta} = v_c = c$, surface cutting position $\theta_1 = 0$, $R_{\theta 1}$ = 6.9599 x10^{8}m. The above data substitution (28.7) and (28.8) type to: P = 3.28033488 x10^{14}, C_1 = 1.4366799204 x10^{-9}, E_{θ} = 471318.2546.

Make $R_{\theta 2} = L_{\odot d}$ = 1.496 x 10^{11}m, the P = 3.28033488 x10^{14}, Eθ = 471318.2546 value substitution (28.8) type: θ_2 = 89.73356061°. Photon precession orbit bending of $\triangle L_{\odot d}$, bending Angle α, the figure 28.2 can see simplified calculation equation for:

$$\Delta L_{\Theta d} = R_{\theta 1} - L_{\Theta d}\cos\theta_2 = 315930.9399(m) \qquad (28.13)$$

$$\alpha=2arctg\frac{\Delta L_{\Theta d}}{L_{\Theta d}\sin\theta_2}=0.871205063''\qquad(28.14)$$

In 1911, Einstein first calculates the light over the surface of the sun happen deflection Angle is 0.83 ", in 1915, he will be the corrections for 1.73 ". Later the British total eclipse observation team confirmed the prediction, which shot to fame.

So, α bending Angle value why are close to times? Why Einstein, a second time he made correct? The reason is that the particularity of the photon itself. The quantum physics and the theory of relativity, photon orbit is circular helix; the whole speed is $\sqrt{2}c$, energy $W_{rc}=m_rc^2$. The Newtonian mechanics, see (28.10) type, the kinetic energy of the photon should be $W_{rc}=\frac{1}{2}m_rv_c^2$, both just by one time. Van and Newton mechanics quality refers to the object and the photon rest mass, the fluctuation; precession speed is constant c, no static quality. From the front orbital theory of quantum physics system demonstration, we already know, relativistic speed movement of the charge, in the vertical direction of the electromagnetic field intensity produced shall be divided by a theory of relativity factor $\sqrt{1-\left(v/c\right)^2}$. And when $v\to c$, the electromagnetic field intensity will tend to infinity. So, we direct to quantum physics and the theory of relativity, energy (27.4) type the derivation process of the Newtonian mechanics and the photon energy formula comparison must make the photon relative the sun's gravitational field strength of interaction between double, then can make the photons Newton kinetic energy doubled for $W_{rc}=m_rc^2$. Therefore, make (28.1-2) type is:

$$m_r(\ddot{R}_{\theta r}-R_{\theta r}\dot{\theta}_r^2)=-\frac{2GM_\Theta m_r}{R_{\theta r}^2}\qquad\textbf{(28.15)}$$

Similarly, will (28.4) and (28.5) type substitution (28.15) type arrangement must:

$$\frac{du_r^2}{d\theta_r^2}+u_r=2GM_\Theta\left(\frac{m_r}{H}\right)^2\qquad(28.16)$$

Make $u_r=C_1\cos\theta_r+C_2$, $\frac{du_r}{d\theta_r}=-C_1\sin\theta_r$, $\frac{du_r^2}{d\theta_r^2}=-C_1\cos\theta_r$, substituting (28.16) type, solution of differential equations (28.16) declined to:

$$R_{\theta r}=\frac{\frac{1}{2GM_{\Theta}}\left(\frac{H}{m_r}\right)^2}{1+C_1\frac{1}{2GM_{\Theta}}\left(\frac{H}{m_r}\right)^2\cos\theta_r} \qquad (28.17)$$

Make $P_r=\frac{1}{2GM_{\Theta}}\left(\frac{H}{m_r}\right)^2$, $E_{\theta r}=\frac{C_1}{2GM_{\Theta}}\left(\frac{H}{m_r}\right)^2$, (28.17) type also said:

$$R_{\theta r}=\frac{P_r}{1+E_{\theta r}\cos\theta_r} \qquad (28.18)$$

This is what we are familiar with conical surface cutting line track equation of motion.

By the same token, first of all, to the photon skim over the sun surface speed v_θ = v_c = c, surface cutting position θ_{r1} = 0, $R_{\theta r1}$ = 6.9599 x10^8 m. The above data substitution (28.17) and (28.18) type: P_r = 1.64016744 x 10^{14}, $E_{\theta r}$ = 235658.6272.

Make $R_{\theta r2}$ = $L_{\odot rd}$ = 1.496 x 10^{11} m, the above P_r = 1.64016744 x 10^{14}, $E_{\theta r}$ = 235658.6272 value substitution (28.18) type: θ_{r2} = 89.73368161°. Photon precession orbit bending of$\triangle L_{\odot rd}$, bending Angle α_r value, also can see from figure 28.2 simplified calculation equation for:

$$\Delta L_{\Theta rd}=R_{\theta r1}-L_{\Theta rd}\cos\theta_{r2}=631862.9056(m) \qquad (28.19)$$

$$\alpha_r=2arctg\frac{\Delta L_{\Theta rd}}{L_{\Theta rd}\sin\theta_{r2}}=1.742412937'' \qquad (28.20)$$

28.3 absolute time-space Newton and Einstein relative concept of space-time relationship

28.3.1 Newton and Einstein's absolute time-space relative concept of space-time relationship

In Newtonian mechanics absolute time-space readers not only are familiar with, and formula and physical model are simple, intuitive and easy to understand. According to the modern astronomy research field observation distance has been extended to tens of billions of light-years above; the author in 21 ~ 27 chapter

systematically infinite eternal cosmological model. Especially in section 26.4 summary of the gravitational field in the whole universe evolution in the leading role. This special emphasis on: Newton's absolute time and space, it is to point to infinite eternal cosmological model of all objects, from the invisible black hole to the size of the galaxy, stars, planets celestial, nebula and meteorites, and even nebula every atom, molecule, which in any moment of the corresponding space coordinate position and the corresponding space time, it is absolutely not because any other celestial bodies, atomic, molecular, and the presence of relative motion and change. Chapter 5 by electromagnetic wave physical characteristics and neutrino field as electromagnetic wave propagation medium can be demonstrated that: absolute space and time also includes all the static or beyond less than the speed of light sports bodies and meteorites, nebula, atomic, molecular relative static neutrino field of space and time.

Similarly, as physics history background condition limit, Einstein until the death of all don't know neutrino existence, more do not know neutrino field, the universe space background 2.73 K microwave radiation and the relationship between the electromagnetic wave propagation. And ignore the moving light source will occur Doppler frequency shift phenomenon. Directly from the speed of light invariance principle and lorentz transformation formula of founded the special theory of relativity, which refers to the relative time and space, we now can see: the relative space and time is to point to in neutrino field movement of the object relative neutrino field relative space and light or electromagnetic wave in the relative neutrino field relative space (wavelength) to spread the relative time (cycle). When the movement of the object from the static began to accelerated motion and final reduction to static, it corresponds to the space coordinates and time should be infinite eternal cosmological model, including the static neutrino field, the absolute space and time. In other words, the relative theory of relativity of time and space, only is for to tend to the speed of light body in motion is relatively neutrino field along the direction it is moving in. And other objects exist or not, whether the relative motion completely irrelevant!

28.3.2 Relative time and space scope

Since Albert Einstein in the photoelectric effect research put forward the photon with wave-particle duality argument since, can confirm, 100 years, the international scientific community in all experimental study, are confirmed. Now, we have to face such a sensitive problem: photon after journey form light is must take it as a representative including neutrino field around the space, right? Should represent the

photon as a particle of precession orbit more appropriate??? Even if neutrino it is particle, its fluctuation, precession orbit and photon completely the same, in the sun under the action of gravity field is also happen precession orbital bending phenomenon, can represent the space around bend??? Similarly, all the objects, no matter quality and gravitational field strength size, the photon, the neutrino and all other celestial gravity effect, also can only produce particles and other objects into dynamic track bending phenomenon, but is not the so-called space and time bending!!!

Today, we already know sports light source will occur doppler frequency shift of physical essence. Photons into dynamic wavelength and frequency of the product the speed of light c, is for constant. (Photon wave and precession orbit wavelength completely equal, in order to more intuitive reasoning relative nature of space and time, here specially discuss photons precession direction orbit wavelength). See figure 28.3, if moving objects in A, B, C between two points on the attachment, AB line and X axis parallel, moving objects C to B movement. At any moment from the object to A, B two out of light, when it into A point, reduce the frequency, wave length, growth; When it into B, the frequency increases, the wavelength shorten. The precession and the photon orbit wavelength and frequency of the product is the speed of light c, still is constant. Put the object C movement speed of v, frequency shift of the frequency spectrum for ν' , because $\nu' = c/\lambda'$, $\nu = c/\lambda$, make $t' = \lambda'/c$ $t = \lambda/c$, the electromagnetic wave theory of relativity Doppler frequency shift effect:

$$\nu' = \frac{1 + v/c}{\sqrt{1 - (v/c)^2}}\nu \qquad (2821)$$

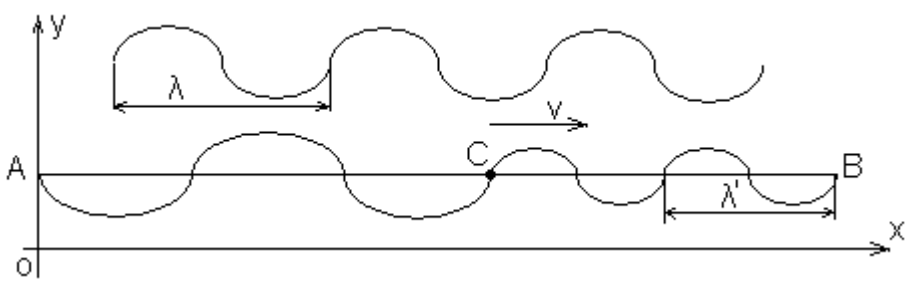

Figure 28.3. Movement of the light source spectral Doppler frequency shift and wavelength λ', frequency ν' change schematic diagram

By (28.21) type, frequency shift of spectral wavelength λ' for:

$$\lambda' = \frac{c}{\nu'} = \frac{c\sqrt{1-\left(\nu/c\right)^2}}{\nu\left(1+\nu/c\right)} = \lambda\frac{\sqrt{1-\left(\nu/c\right)^2}}{1+\nu/c} = \frac{\lambda-\nu t}{\sqrt{1-\left(\nu/c\right)^2}} \qquad (28.22)$$

Similarly, the speed of light c through the frequency shift of photon precession direction each wavelength λ' needs time t' for:

$$t' = \frac{\lambda'}{c} = \frac{\lambda-\nu t}{c\sqrt{1-\left(\nu/c\right)^2}} = \frac{t-\frac{\nu}{c^2}\lambda}{\sqrt{1-\left(\nu/c\right)^2}} \qquad (28.23)$$

Will (28.22) and (28.23) two type of photon relative precession orbit wavelength λ', time t' and relativity of the relative space and relative time relation is:

$$x' = \frac{x-\nu t}{\sqrt{1-\left(\nu/c\right)^2}}, \qquad t' = \frac{t-\frac{\nu}{c^2}x}{\sqrt{1-\left(\nu/c\right)^2}}$$

Obviously, they are identical. This can be concluded that Einstein's relative space, light is movement to occurred Doppler frequency shift change after the photon in the precession direction orbit wavelength λ'. Relative time is the speed of light c through each orbit wavelength λ' needed for the relative time t', namely cycle. We come again analysis chart 28.3 shows the high speed motion object C, no matter in A and B between any position, as long as it can the instantaneous static, or slow to rest, by (28.22) and (28.23) type can see: it between two points A and B of absolute space and time relationship, is still Newton's absolute time and space. And, still can further see: static this A, B two if we are to high speed movement of the C point the light, no matter C point in A and B between any position, when light to C point period, are not happen doppler frequency shift; (as long as the reader to understand is as follows: if A and B does not exist between high speed motion object C, then from the rest of the A, B two light from each other in A and B the transmission between is not going to happen doppler frequency shift. When A and B between the high speed motion object C, then from the rest of the A, B two light from each other in C object side through and into C object before, also won't happen doppler frequency shift) The space between AC and

CB and the speed of light through the need of the time Newton's absolute space and time. So, Einstein's theory of relativity nature of the problem space and time in the high speed motion object a light doppler frequency shift change of photon precession direction after the length of the track, λ', the speed of light c through each track length λ' needs time t', also is the cycle, and Newton objects when static absolute space and time confuse STH with STH else!!!

Integrated the inference, the relativity of the twin paradox, the clock problem and relative time, space and Newton's absolute time, space relationship between all are lead edge and the solution.

Front section 26.4 it has been proved that able to tend to the speed of light motion objects, can only be particle. Any in atomic and molecular composition of FeiHangTi, when it to tend to the speed of light movement, all in the atomic and molecular electronics and the conditions within the nucleus of high and low energy $\pi^{\pm}$ spin precession direction, will turn to the object movement direction, which will be like the high temperature thermal motion vaporizing, will be completely collapse. The consequences of which are between atoms, molecules by the electron cloud "linked to chemical and physical mechanics of materials, electromagnetic properties are qualitative change will happen. Ultimately burst into nuclear or particle, become as shown in figure 1.2 shows the fluctuation, the spin and precession orbit combination of particle track motion state. The core of a galaxy, the quality of the huge black hole edge accretion disk atomic, molecular are all destroyed, and the last in the gravitational field and under the action of neutron material ring is a very good example. In human existing science and technology level, to be in the near future will be able to build a spacecraft flight tends to the speed of light, especially to overcome all materials will be thoroughly burst into nuclear or particle difficulty, also is only fantasy.

What is our universe by a super density, super high temperature, and high can so-called mathematical singularity cuhk explosion form? Or the author in chapter 21 ~ and reasoning, our universe is Newton's absolute time and space under the condition of the infinite and eternal universe. Believe that the reader now know fairly well.

Besides, the modern civilized men out of town on a plane are now common. Excuse me: we will have all mankind have the habit of the time, London Greenwich observatory and Beijing, Moscow and Washington... The large area of the time, all to their respective not coherent plane relative to the atmosphere in flight, in a relatively

sound velocity in the atmosphere relative space needed for spread of the relative time? As for all of the flights, the aircraft in flight their relative time and relative to the atmosphere of the relative space how to determine, estimate the modern and advanced computer are powerless. Because the atmosphere of the earth's surface and relative is not completely absolute rest, air formation of wind direction, wind speed is a common atmospheric phenomenon. Even if can mark the so-called the plane relative to somewhere in the atmosphere relative space and time, this to happen doppler frequency shift change after the acoustic wave length, and speed of sound through the wavelength need relative time, as a measure of the relative time scale in human real life and what is the point?

So, Einstein's theory of relativity of the relative time and space, only suitable for particle physics research field. We have absolutely no need now is asking for trouble, simple, intuitive classical physics law, formula all human complication. The time and space theory of relativity recklessly spread to the whole astronomy and astronautics field, even it as science knowledge on the science and technology personnel and the teachers and students. This will be Einstein's life by one of the most serious and difficult to forgive mistakes. This error will be infinite directly, eternal universe model guide hot big bang to form a cosmology, and statistical theory of quantum physics three joint caused by the research in the field of modern physics stagnant, contradictory problem, loopholes, go astray. Make broad science and technology personnel and the teachers and students to modern physics terrified, will affect their modern and future in many high-tech fields of innovative research ability. The serious consequences of mankind are directly delay of modern science and civilization development process.

28.3.3 The future of spectrum red shift parameter measurement research proposals

Chapter 5 of the book has proved neutrino field characteristics, electromagnetic wave propagation principle and parameter calculation. By using thermodynamic method rigorous proof that the neutrino field is to spread the electromagnetic wave "of the etheric field, electromagnetic wave is a longitudinal wave! In chapter 22 demonstrates spectrum red shift principle and red shift parameter calculation, and the Hubble constant as astronomy field only accurate range scale (quasars except). Now, all the debate focus all boils down to how to understand the Hubble constant, is the relative motion in Kepler's red shift? Or photon in the long the universe space

long-term operation, the energy consumption is gradually neutrino place to cause red shift? So, the accurate determination of photon or electromagnetic wave in the space of long distance transmission of red shift parameters is to solve two universities sent long-term debate reliable evidence. Because the red shift of minimum, in limited space and time, at the present level of technology, it is very difficult to measure effectively.

Therefore, from the first physical model a analogy analysis. We know, any wave propagation, whether longitudinal or transverse wave, must through the medium molecular vibrations to transfer. So, all medium molecular in vibration in the process, will be because of the friction between temperature and some of the energy consumption wave. From the system total energy conservation law can inference, any wave in the transmission process, will appear energy loss. So, we now although cannot measure electromagnetic wave red shift, but to existing technical level, determination of sound waves in a calm sea, along with the increase of the propagation distance from the red shift parameter or certain. Moreover, with the scientific community existing fluid mechanics, continuous elastic medium mechanical wave theory, and even can be directly on the sound waves in the air in the process of the propagation of the analysis of energy consumption.

29 Relationship of neutrino and graviton dark matter

Yu-Xiang Huang，Zhen-Qiang Huang

kexuetansuoze@126.com tel: 13338400718

This paper is completed in May 2012; initially to the British science journal contribution was rejected. And then to the United States scientific journals and physical review contribution, because the program is not familiar with no success. Finally had to published in Chinese paper preprints and network, and to domestic and international part of the scientific research personnel E-mail sent communication. In this book is a final chapter 29 logging.

Abstracts

This paper discusses the neutrino field in the space of the universe. According to the neutrino energy shocks in the fact that the neutrino field principle the formation of quantum gravity.According to the solar neutrino disappearance, neutrino energy density is derived. The inference neutrino field is dark matter. Use a simple and intuitive physical model to answer fortunately the four challenges.

Keyword:

Neutrino field, Neutrino energy loss, The quantum gravitational field, Graviton energy, Dark matter.

Introduction to section

The author at first just want to use neutrinos there are energy shocks, the speed of light, linear motion, the extraordinary ability to penetrate ... and other features. To a large number of neutrino flow along the radial penetration of a spherical celestial bodies, the friction loss of energy into the energy of the graviton, to explore the principle of the formation of the quantum gravitational field. Surprised to discover that quantum gravitational field, neutrino field, solar neutrino disappearance and dark matter dark energy of the physics community today is intrinsically linked. We happened to answer the five challenges.

In the future, if we can directly use the ready-made neutrino field characteristics, to development of linear penetrating confidential directional communication technology, certainly enticing. If we can further the development and utilization of the neutrino dark

matter energy in the universe in space, it is more likely to succeed than the development thermonuclear fusion reactor ITER. With the author "Cold fusion reactor" Invention patents projects is the best[1]. See the author's follow-up papers and patent applications.

Neutrino field characteristics

Modern scientific research has found that the original nebula neutron decay into protons, electrons, associated with the electron neutrino $\overline{\nu}_e$. The stars also produce a large number of electron neutrino. The average energy is

$\overline{W}_{v0} = m_v c^2 = 15 \sim 30ev = 22.5eV$[2]. since the birth of the universe gave rise to countless stars. Only the sun produces neutrinos about 10^{15} per second penetrate the human body[3]. Therefore, the space of the universe will be inevitably full of neutrinos. Neutrinos are electrically neutral elementary particles, linear motion of the neutrinos travel at the speed of light. Matter interactions with atoms, molecules and objects are very weak. Neutrinos have extraordinary penetration and diffusion characteristics. They are necessarily similar to the state of motion of the gas molecules, and evenly spread in the space of the universe, the formation of the neutrino field. The laboratory has demonstrated that the neutrino energy oscillation exists[2].

Formation principle of quantum gravity field

Figure 1 is shown, neutrino around any celestial body or the movement of objects. We will direction of motion were divided into radial, warp, weft of positive and negative direction. Along the radial second piercing or penetration of the earth, or any spherical celestial body surface per unit volume fluxes are N_{vr0}. Relationship with the objects inside and outside the flux N_{vri} is:

$$N_{vri} = \frac{N_{v0} c}{6}\left(\frac{R_2}{R_{2i}}\right)^2 \Big/ m^3 = N_{vr0}\left(\frac{R_2}{R_{2i}}\right)^2 \Big/ m^3 \qquad (1)$$

In the (1) $R_{2i} < R_2$, indicating that within the earth, $R_{2i} \geq R_2$ on the surface or external. Make the unit of volume flux N_{vr0} of the neutrino beam through the earth along the radial direction, each neutrino friction losses in the energy $\Delta\overline{W}_{v2} = k_w M_2 / 4\pi R_2^2 N_{vr0}$. It is proportional to the quality and penetration of celestial bodies, and is inversely proportional to the celestial body surface area and per unit area fluxes N_{vr0}. The k_w is quantum of the graviton energy coefficient. Make k_{wyj} for

continuous along the radial penetration j objects, the background field graviton energy $\Delta\overline{W}_{vi}$, due to the friction of the j objects coefficient of variation, in units of m/s^2 .

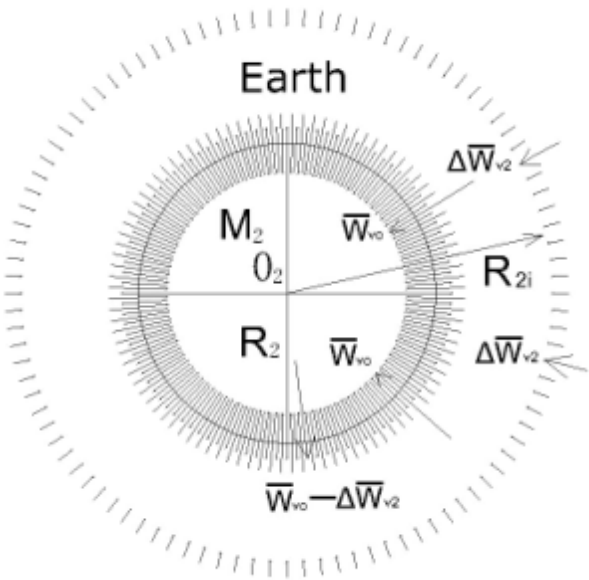

Figure1, Assumed that the solar system the vicinity of the original density is N_{v0} of the electron neutrino and average energy is $\overline{W}_{v0}$. Electron neutrino radial penetrates the earth, the friction loss of energy is $\Delta\overline{W}_{v2}$. Residual energy is $(\overline{W}_{vo}-\Delta\overline{W}_{v2})$, $\overline{W}_{v0}-(\overline{W}_{v0}-\Delta\overline{W}_{v2})=\Delta\overline{W}_{v2}$ .Equivalent to energy $\Delta\overline{W}_{v2}$ is transformed into graviton energy. On the surface of the Earth and the outer space to the center is forming shrinkage of the graviton background field.

The total energy of the graviton friction loss into $\Delta\overline{W}_{vij}$ a spherical celestial bodies or any celestial object, these all can be expressed as:

$$\Delta\overline{W}_{vij}=k_{wvj}\Delta\overline{W}_{vi}=k_{wvj}\left(\frac{k_w M_i}{4\pi R_i^2 N_{vr0}}\right) \qquad (2)$$

$$P_{ri}=\Delta\overline{W}_{vi}N_{vri} \qquad (3)$$

Shown in Figure 2, we argument all along the axis in the two-cones the O_2O_3 projection line direction. (So that treatment can simplify the calculation). From (1), (2), (3), the radial direction total flux $\vec{\Phi}_2$ and $\vec{\Phi}_3$, of neutrinos stream, the gravitational force F_{23} and F_{32} between Earth and the Moon, can be expressed as:

$$\vec{\Phi}_2 = N_{\nu r0}\int_0^{\alpha_2} 2\pi R_2^2 \sin\alpha\cos\alpha d\alpha = \pi N_{\nu r0}\left(\frac{R_2R_3}{R_{23}}\right)^2 \quad (4)$$

$$\vec{\Phi}_3 = N_{\nu r0}\int_0^{\alpha_3} 2\pi R_3^2 \sin\alpha\cos\alpha d\alpha = \pi N_{\nu r0}\left(\frac{R_2R_3}{R_{23}}\right)^2 = \vec{\Phi}_2 \quad (5)$$

$$F_{23} = \int_0^{\alpha_3} 2\pi R_3^2 \sin\alpha P_{ra}\cos\alpha d\alpha = \frac{k_{w\nu 2}k_w M_3}{4}\left(\frac{R_2}{R_{23}}\right)^2 \quad (6)$$

$$F_{32} = \int_0^{\alpha_2} 2\pi R_2^2 \sin\alpha P_{rb}\cos\alpha d\alpha = \frac{k_{w\nu 3}k_w M_2}{4}\left(\frac{R_3}{R_{23}}\right)^2 \quad (7)$$

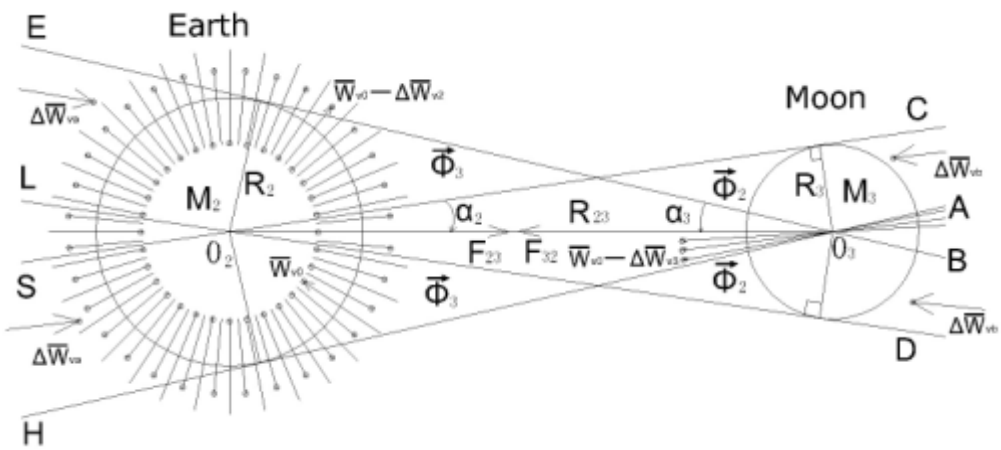

Figure 2 neutrino field formation principle of quantum gravitational field. In LO2D and SO2C segment consists of two cones, neutrino flux total flux all are $\vec{\Phi}_2$ along radial direction, In the AO3H and BO3E segments all are $\vec{\Phi}_3$. From left to right, Neutrinos along the radial penetration of Earth, friction energy loss is $\Delta\overline{W}_{\nu 2}$, it into the energy of the graviton.It formed the background field of the graviton. Continue to penetrate the Moon as the friction losses in the total energy $\Delta\overline{W}_{\nu b}$. Similarly, from right to left through the friction loss of energy is $\Delta\overline{W}_{\nu 3}$ and $\Delta\overline{W}_{\nu a}$.

Figure 3 and Newton's law of gravitation shows: $F_{23} = F_{32} = GM_2M_3/R_{23}^2$. Into (6), (7), we obtain: $k_{w\nu 2} = 4GM_2/k_wR_2^2$, $k_{w\nu 3} = 4GM_3/k_wR_3^2$. The two outside the cone, the graviton $\Delta\overline{W}_{\nu 2}$ and $\Delta\overline{W}_{\nu 3}$ forces are symmetrical with each other offset.

Energy coefficient k_{wv2} and k_{wv3} of variation and then into (2) may:

$$\begin{cases} \Delta\overline{W}_{va} = \left(\dfrac{4GM_2}{k_w R_2^2}\right)\left(\dfrac{k_w M_3}{4\pi R_3^2 N_{vr0}}\right) \quad \cdots\cdots(8-1) \\ \Delta\overline{W}_{vb} = \left(\dfrac{4GM_3}{k_w R_3^2}\right)\left(\dfrac{k_w M_2}{4\pi R_2^2 N_{vr0}}\right) = \Delta\overline{W}_{va} \quad \cdots\cdots(8-2) \end{cases}$$

From (4) (5) and (8) equations, because $\vec{\Phi}_2 = \vec{\Phi}_3$ and $\Delta\overline{W}_{va} = \Delta\overline{W}_{vb}$. Therefore, we have quantum gravitational field to prove Newton's law of universal gravitation: $\Delta\overline{W}_{vb} \cdot \vec{\Phi}_2 = F_{32} = F_{23} = GM_2 M_3 / R_{23}^2 \cdot$

The mystery of missing solar neutrinos

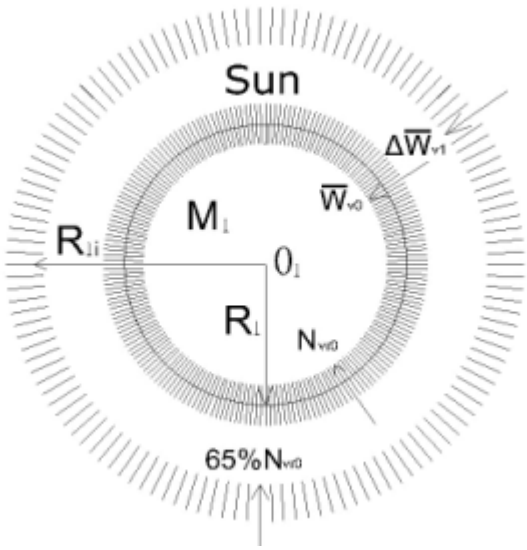

Figure3, neutrinos along the radial penetration of the sun, the friction loss of energy is $\Delta\overline{W}_{v1}$ .If most 65% of the electron neutrino energy of all the sun been intercepted absorption, the neutrino energy is absorbed into all the energy $\Delta\overline{W}_{v1}$ of the graviton. The outer space been formed a unidirectional contraction of the 65% graviton $\Delta\overline{W}_{v1}$ background field to the center of Sun.

According to the electron neutrino missing about 65% events, the penetration of solar neutrinos friction energy loss $\Delta\overline{W}_{v1} = 25eV$, And then penetrate the total energy of the neutrino friction loss after another sun $\Delta\overline{W}_{v11} = 50eV$. Into（8-1）、（1），we can obtained: $N_{vr0} = 4.407\times10^{31}/m^3$ ， $N_{v0} = 8.82\times10^{23}/\mathrm{m}^3$. As in standard condition[4],

1m^3 gas molecule number is $N_a = 1000N_{\mathrm{a}}/22.4138 = 2.6868\times10^{25}/\mathrm{m}^3$, so we can get: $N_a/N_{v0} = 30.46$. Once again making (2) $k_w M_1/4\pi R_1^2 N_{vr0} = 25eV$, get: $k_w = 544.078$.

Similarly, by (2) and (8) equations, as long as respectively $k_w = 544.078$, so that all kinds in, you can find the Earth, the moon and other celestial graviton energy $\Delta\overline{W}_{v2}$ and $\Delta\overline{W}_{v3}$ .....Various parameters in table 1.

Objects parameters and calculated in Table 1[11]

Celestial name	Quality (kg)	Radius (m)	Loss of energy $\Delta\overline{W}_{\mathrm{vi}}$ (eV)
Steel ball	2.932×10^4	1	1.8×10^{-7}
Moon	7.35×10^{22}	1.738×10^6	0.1492
Earth	5.983×10^{24}	6.3673×10^6	0.9049
Sun	1.971×10^{30}	6.953×10^8	25
White dwarf	1.971×10^{30}	6.3673×10^6	298109
Neutron star	1.971×10^{30}	1.738×10^4	4×10^{10}
Remark	In this table is neutrino density along the radial movement of the $N_{vr0} = 4.407\times10^{31}/m^3$.		

Be seen from Table 1, the neutrino loss of energy of white dwarfs, neutron stars or black holes are much larger than 25eV.This shows completely absorbed neutrino range is much larger than the actual radius of the celestial bodies. This range should be quite the solar radius, and the formation of quantum gravitation size and total flux $\vec{\Phi}_1$ vector objects independent of the radius.

The mystery dark matter

Modern cosmological observations that the visual material in the universe is only about 4%, about 23% percent dark matter, dark energy about 73%[5]. According to astronomical observations, the solar system around the center of the galaxy revolution

speed is 250km / s, the orbital radius are about 25200 lightyears[6]. From Newton's law of gravitation, we can obtain the total mass of the Milky Way in the solar system orbits about $M_{01} = 2.23 \times 10^{41} kg$ .The astronomical community can be observed and speculated to stellar, stellar wreckage of the black holes, neutron stars, white dwarfs, red dwarfs, planets, nebulae, gas and dust, meteorites ..... etc. only about the amount of material $M_0 = 5.913 \times 10^{40} kg$.

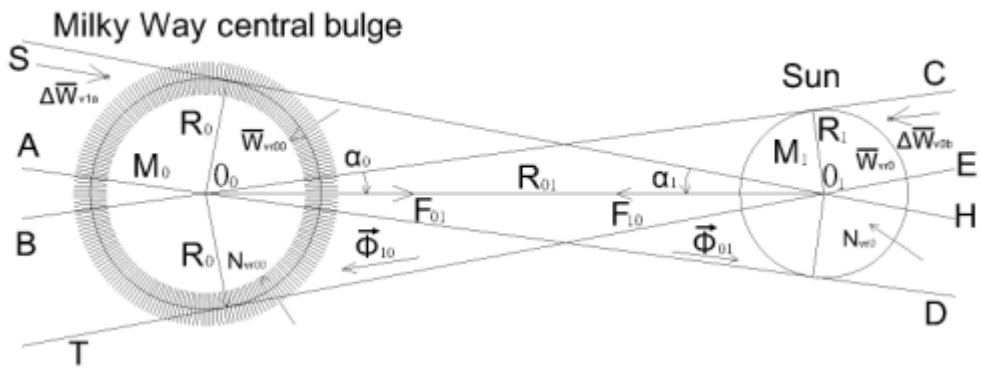

Figure4, the neutrino field density and gravitation strength are relationship. Segments constitute the AO_0D and BO_0C two conical body, the neutrino flow radial total flux within the in EO_1T and HO_1S segments are $\vec{\Phi}_{01}$, within the EO_1T and HO_1S line are $\vec{\Phi}_{10}$ .From left to right, neutrinos along the radial penetration of the Milky Way central bulge, the friction loss of energy is $\Delta\overline{W}_{\nu 0}$,it been formed of the graviton energy. Continue to penetrate the sun as the friction losses in the total energy $\Delta\overline{W}_{\nu 0b}$ .Similarly, from right to left through the friction losses in energy $\Delta\overline{W}_{\nu 1}$ and $\Delta\overline{W}_{\nu 1a}$.

Formed from the neutrino field in the principle of universal quantum gravitation field to prove, in the penetration of a variety of objects, the neutrino has a different frictional loss of energy or lack of events. Sun for example, see figure 3 and 4 and (8) equations. Because $k_{wyj} = 4GM_1 \Big/ k_w R_1^2 = 2$, so $k_{wyj}\Delta\overline{W}_{\nu 1} >> 25eV$ by Sun. They will inevitably lead to most of the absence of the sun as the center of the graviton background neutrino field divergence. Figure 4 shows the AD, BC and HS, ET conic at both ends to extend the area, the vast majority of missing events can cause a wide range of neutrino. Similarly, in the open areas outside the cluster of galaxies and the original density of the neutrino field all are the highest-energy. From the galaxy periphery, the spiral arms to the central nucleus of the ball, due to the presence of various size objects, the neutrino density and energy are in turn reduced. That

especially the central bulge area of the galaxy, the massive black holes and dense spherical shell-like distribution of stars and debris, the graviton must pass from tens to tens of thousands of years of time difference. Figure 3 and 4 shows, in many celestial gravitation cones line at both ends to extend the sweep of the airspace, will significantly reduce the original neutrino density $N_{\nu 0}$ and average energy $\overline{W}_{\nu 0}$, in particular, radial movement of the neutrino density $N_{\nu r 0}$ along the central bulge.

Figure 4, assuming that the neutrino density is $N_{\nu r 00}$ of the Milky Way central bulge area. All of us along the direction of the two cone axis O_0O_1 projection line argument. Because $N_{\nu r 00} < N_{\nu r 0}$,by (1) - (5) and (8) equations, the neutrino flow to the total radial flux $\vec{\Phi}_{01}$ and $\overline{\Phi}_{10}$,quantum gravity F_{01} and F_{10} between the Milky Way central bulge and the sun, can be expressed as follows:

$$\vec{\Phi}_{01} = N_{\nu r 00}\int_0^{\alpha_0} 2\pi R_0^2 \sin\alpha\cos\alpha d\alpha = \pi N_{\nu r 00}\left(\frac{R_0 R_1}{R_{01}}\right)^2 \quad (9)$$

$$\vec{\Phi}_{10} = N_{\nu r 0}\int_0^{\alpha_1} 2\pi R_1^2 \sin\alpha\cos\alpha d\alpha = \pi N_{\nu r 0}\left(\frac{R_0 R_1}{R_{01}}\right)^2 \quad (10)$$

$$F_{01} = \Delta\overline{W}_{\nu 1a}\cdot\vec{\Phi}_{10} = \frac{GM_0M_1N_{\nu r 0}}{R_{01}^2 N_{\nu r 0}} \quad (11)$$

$$F_{10} = \Delta\overline{W}_{\nu 0b}\cdot\vec{\Phi}_{01} = \frac{GM_{01}M_1N_{\nu r 00}}{R_{01}^2 N_{\nu r 0}} \quad (12)$$

When the neutrino density $N_{\nu r 0} = 4.407\times10^{31}/m^3$ in the vicinity of the solar system is calibration of quantum gravity constant, continuous penetrate the mass and radius of the two celestial bodies are the same, the friction losses in the total energy $\Delta\overline{W}_{\nu 1a} = \Delta\overline{W}_{\nu 0b}$ of each neutrino will remain unchanged. The two celestial quantum gravity values on the basis of Newton's law of gravitation, but also with other regions in which the neutrino density is proportional to. Such as (11) and (12) $F_{01} = GM_0M_1/R_{01}^2$ and $M_{01}N_{\nu r 00}/M_0N_{\nu r 0} = 1$ .Therefore, the neutrino density in the central bulge a significant reduction, equivalent to substantially improve their quality, leading to misjudgment of the central bulge of a large number of dark matter.

Constitute the quantum gravitational field of neutrino dark matter, dark matter is reflected by the gravitation field of non-baryonic matter. Modern cosmology speculate that the density of matter in the whole universe is $\rho_0 = 6\times10^{-27}\ kg/m^3$ [7]. We collected the derivation of the average energy and density of the electron neutrino is 22.5eV and $N_{v0} = 8.82\times10^{23}/m^3$, The neutrino field density of the nearby area of the solar system are $\rho_{ve} = 3.54\times10^{-11}\ kg/m^3$. Because $\rho_{ve}/\rho_0 = 5.9\times10^{15}$, Therefore, the neutrino particle density material quality is far greater than the quality of the visible matter universe，the dark matter than enough.

Conclusion

This paper argues that the physical characteristics of the neutrino, the establishment of the principle of quantum gravity field. According to the solar neutrino disappearance, deduced the neutrino particle density of matter. Lucky enough to answer with a simple and intuitive physical the model, be including four of the dark matter problem.

References:

1. "Cold nuclear fusion reactor" patent application

CN200910129632.7 Huang Zhenqiang 2009

2. http://baike.baidu.com/view/9474.htm

3. http://news.163.com/12/0313/09/7SFF7VIJ00014JB6.html

4. Physics at the University Manual P665 ~ 668, Shandong Science and Technology Press Pen-Wang Cheng etc 1985

5. http://www.ihep.cas.cn/kxcb/kjqy/200907/t20090723_2160257.html

6. http://www.docin.com/p-324814333.html

7. Observational cosmology Xiang-Tao He P227 Science Press 2000

Natural magazine editor Ladies and Gentlemen:

How are you!

The author at first just want to use neutrinos there are energy shocks, the speed

of light, linear motion, the extraordinary ability to penetrate ... and other features. To a large number of neutrino flow along the radial penetration of a spherical celestial bodies, the friction loss of energy into the energy of the graviton, to explore the principle of the formation of the quantum gravitational field. Surprised to discover that quantum gravitational field of the physics community today, neutrino, solar neutrino disappearance and dark matter is intrinsically linked. We lucky enough to answered the f0ur problems.

In the future, if we can directly use the ready-made neutrino field characteristics, the development of linear are penetrating confidential directional communication technology, certainly enticing. If we can further the development and utilization of the neutrino dark matter energy in the universe in space, it will more than thermonuclear fusion reactor ITER project is more likely to succeed. Even better than the author of "Cold nuclear fusion reactor" patent for invention projects. See the author's follow-up papers and patent applications.

We hope this paper can cause the majority of modern physicists and fans, and prospects interested in the development of future neutrino field.

This article about have 2000 words, 4 small charts, 1 table. To takes about 3 to 4 pages.

Thank you!

Huang Yuxiang Huang Zhenqiang

2012.7.6

Address: No. 68, Fuzhou, Fujian Province, China Jinan District West Yuan Village, West fen Road

Tel: 86- 0591-28238177 Email: kexuetansuoze@126.com

Note: We do not have a fax machines, please use your e-mail to contact us.

Conclusion

The Book review

This book will classical Newtonian mechanics, electricity dynamics, thermodynamics, energy relativity into micro field, the establishment of basic particle fluctuation, spin quantization steady state vertical double elliptic orbit motion model. It fluctuation are spin cylindrical spiral orbital motion model. Deduced basic particle related orbital motion equations. Using the simulation method, which successfully solved the statistical theory of quantum mechanics most long-term unable to solve the key problem; And in orbit theory of quantum physics theory model, the establishment of a absolute time-space conditions of infinite eternal cosmological model, so as to solve the thermal explosion formation age of the universe, dark matter in cosmology composition, structure and bright, dark matter of the transitions between circulation problem; Finally realize the neutrino field as a grand unified field medium, Newton's absolute time and space and Einstein's relative time and space, and strong, weak, electrical, magnetic and gravitational field interaction between role, and to realize the microscopic and macroscopic view field and space between the grand unified whole.

Chapter 1 ~ 6 particle physics demonstrates the basic particles are all along the fluctuation, spin quantization steady state vertical double elliptic orbit or cylindrical spiral orbital motion of the law. Sure all the basic particle are made with a unit charge "charged particle" aggregate composition, derived fine structure constant, particle internal structure, composition, energy, momentum forming principle and related parameter calculation equation. Special proof that the photon and neutrino internal are made by a pair of electric dipole. Only difference lies in the electric dipole of different rotation frequency. Proof that the strong, weak, electricity, magnetic interaction are electric, magnetic interaction. Given the basic particle inside, electric, magnetic field interaction force strength, split decay energy, average life, related parameters of the accurate solution. To solve the point charge energy "divergence" difficult to classical electrodynamics theory unconditional restrictions in microscopic particle field to provide the basis. Prove the universe space 2.73 K blackbody background microwave radiation is a medium by neutrino oscillation energy caused by electromagnetic wave, the neutrino field is that previous "ether" field. Neutrinos, photon excitation conversion process, the electromagnetic wave, the photon wave particle duality transformation critical energy and propagation characteristic, movement speed. Accurately simulated

protons, neutrons, internal structure, the electromagnetic field distribution characteristics, spin magnetic moment value. Pointed out those protons, neutrons are exist "quark" false reason.

Chapter 7 ~ 14 in nuclear physics design nuclear internal structure model, combined with particle physics research results, we have successfully resolved the nucleus internal structure, force, magnetic moment forming principle; All in nuclear particle orbital motion combination features, including nuclear force, energy, magnetic moment, each parameter calculation equation. Given a^{++} particle, p^{+} proton, $\beta^{\pm}$ electronics and γ-ray been formed principle and the energy spectrum calculation method. Introducing neutrino to electric dipole means to participate in the nucleus, protons, neutrons, and other basic particle energy, structure and split decay principle.

Chapter 15 ~ and atomic physics demonstrates the atomic outer, times of outer all electronic are fluctuating, spin, additional lateral orbital motion of ellipsoid revolved around the nucleus movement way; Reveal atomic outer, times of outer "s, p, d, f type electron cloud shell" form nature. In all atomic spectrum, level and other parameters of the simulation process, only through the small range rationally adjust the atomic internal a layer of electronic elliptic orbit centrifugal rate are all solve the problem. Proof of the chemical reaction of electronic excitation or transition, energy change of so-called virtual photon participation is actually neutrino participation.

20 ~ 26 chapter infinite eternal cosmology, the spectrum red shift, 2.73 K cosmic blackbody background microwave radiation and Mr Bers paradox in photon stroke to total energy conservation law overall argument for infinite eternal cosmological key basis. Pointed out that Hubble's law can is precise range scale. Day literati popular age of the universe is only measured star age, is not the galaxy's age. The universe accounts for more than 90% of the dark matter is dead stars, galaxy, even the remains of galaxy clusters, the dark matter about age has no meaning. The design of the interior of a black hole neutron material ring structure can avoid gravitational collapse, leading to the total energy, gravitational field strength, gravity range into infinity "divergence" difficult. To solve the accretion content of gravitational field potential energy transformation mechanism and polar axis injection, radio principle, be accretion of dark matter in certain conditions well activation regeneration, the black hole conflict big bang into bright material nebula create conditions. Proof of neutrino participate the whole process.

27 ~ 29 chapters space-time relativity in question, the design of quasars internal

structure model, solved the unimaginable quasars huge energy radiation principle and supernormal value spectrum red shift mechanism. Make absolute time-space conditions of infinite eternal universe model be fully demonstrated. Further analysis of the gravitational field in the whole universe evolution in the leading role; The theory of relativity, in the space and time the essence of bending, is photon in the gravitational field under the action of precession orbit bending! Further demonstrates the neutrino field physical characteristics, the establishment of a universal gravitation forming principle. According to the solar neutrino missing events, it to deduced neutrino field particle material density. With a simple intuitive physical model, fortunately have solutions including the graviton and dark matter of the four problems.

New modern physics meaning

The author please mainstream modern physics community and nuclear fusion engineering world calm in the face of the following facts:

1. The capital contribution by tax payers in all the natural scientific research, it is to discover the objective laws of nature, to the advancement of mankind civilization and progress of science, to create the first productivity service, and not for the maintenance of the school's subjective hypothesis of defense. The mainstream school insisted maintenance old modern physics theory system, the modern other natural scientific innovation research, especially for all mankind imminent nuclear fusion energy development research, what can have what kind of role? Don't also should not to tell?

2. This paper pointed out the mainstream school old modern physics theory system in 19 aspects problem and research status, whether all the information given is true?

3. In ancient and modern, Chinese and foreign all modern physicists, including the entire Nobel Prize winner, what a potential on the above a certain aspect problem, even if it is a difficult problem in the a small subject, which gives the qualitative reasonable explanation?

4. What a lucky enough to like the author so, only according to a set of classical particle quantization vertical double elliptic orbit motion model, and Newtonian mechanics and classical electrodynamics and particle energy relativity union, can the 19 aspects of the problem are derived all accurate mathematical physics equation

general solution?

5. Although this book shortcomings and mistakes, and inevitably, needs to be correct, however, will be Newtonian mechanics and classical electrodynamics and particle energy relativistic classical particle along the quantization vertical double ellipse model introduced modern physics, overall physical model design basis and related mathematical physics equation is derived calculus process and all the calculation results, with all the observation test data agree with the fact, at present the old modern physics the mainstream academic traditional school can find out the reason of rejection?

To sum up, in the microscopic quantum physics field, the book demonstrates strong, weak, electricity, magnetic interaction are under the control for electric and magnetic interaction. In the macroscopic field, demonstrates the electric, magnetic field, the interaction between the electric and magnetic field media is neutrino field. In the field of view of space, this paper demonstrates that the black hole gravitational field through the accretion disk and polar axis injection, radio will gravitational field potential energy into electromagnetic energy, or conflict big bang, that dark matter activation regeneration transformation ChengMing material nebula whole cycle process. This description: in microscopic and macroscopic, yu view field, in the infinite eternal universe, gravitational field leading unified the electric and magnetic interaction and bright, dark matter into circulation. Special emphasis on neutrino field as the universe space only exist, ubiquitous media field, the neutrino participate the strong, weak, electricity, magnetic interaction and gravitational interaction. Constitute the grand unified field.

Quantum physics, the physics and relativity the three pillars of the modern physics subject to hold up the building. In the preface puts forward some 19 aspects of the problem, the author with the aid of modern high performance computer finally solved all the argument. Classical particle quantization orbital motion model building, theoretical basis is the classical Newtonian mechanics, electricity dynamics, thermodynamics, energy relativity and microscopic particles along the fluctuation, spin quantization orbital motion model organically. All of the equation, the formula derivation and simulation process are not people to join the other parameters and experiment fitting correction coefficient, and finally the calculation results with the experiment, observation of the parameters and physical, astronomical phenomenon all anastomosis. Thus, three disciplines as unified whole comprehensive studies have

been a complete success. And have realized classical physics and modern physics all basic physical law between the big unification.

If the book open contribute, they do not have the whole system, and it is hard to understand and accept by modern science. The overall evaluation communication and publication will have one-time solve international three disciplines the effect of long-term debate. If you scholars can overcome school prejudice, fair to the modern physics classical particle quantization orbital motion model general solution - referred to as the new modern physics "carry on carefully, it is easy to see: the preface of the book and the generalization of the international modern physics circles facing a difficult problem of 19, the whole truth. The author only according to a classical particle quantization fluctuation, spin vertical double elliptic orbit motion model, and Newtonian mechanics and classical electrodynamics and energy relativity union, can to 19 issues can be deduced all accurate mathematical physics equation general solution. Overall physical model design and related mathematical physics equation is derived calculus process and result, and experiment and observation data anastomosis, isn't that what modern physicists nearly years dream physical model and ideal theory system?

So, the proposal should be priority academic innovation based on natural science basic theory research results fair exchange evaluation system. As long as can solve the modern natural science major problems, no matter fee, at one's own expense, the researchers degree, identity or different school, should accept, participate in communication, and fair evaluation. Can't find out the reason for rejection, shall be granted to notice. Has an important value to research results, should be given support and encouragement. The authors believe that the modern physics classical particle quantization orbital motion model general solution, "a book, stand up to scrutiny and time, the inspection.

The book was published,, is what we have found the key "hidden parameter", and through the simulation calculation of the modern physics to solve most of the problems cannot be solved for a long time when. In the face of facts, the scientific community to adhere to, maintain old ideas are not wise. Had better be hand in hand as soon as possible, and work together, so that the theory system to further improve and perfect. All mankind create a new era of scientific civilization service. It is benefit future generations and well-documented immeasurable qualities!

The research results at one's own expenses "cold fusion reactor

and new modern physics published, they show that the mainstream of nuclear fusion reactor engineering circles and modern physics circles of subsequent research has no meaning. If will continue to adhere to the school's point of view, will be spent all his life and tax payers a lot after the hard-earned money nothing. Such as dozens of years searching for quark, dark matter particles, graviton and Higgs boson are missing. Dozens of years all the nuclear fusion research, including the ITER international cooperation research progress is slow, hope is frail. Continue will increase historic jokes, in the face of the tax payers and severity of later generations' question, please let your careful consideration.

References

① B M Yauorsky A A Detlaf Modern physics manual 1982

②LinZhong koga, Early Sichuan, Symplectic male the universe physics

Science press 1978

③ Xu Kezun, Higher atomic and molecular physics

Science press 2000

④ Nuclide chart preparation group

Nuclide commonly used data sheet

Atomic energy press 1977

⑤ He Xiangtao Observation cosmology

Science press 2002